PEOPLE'S DEMOCRATIC REPUBLIC OF ALGERIA
MINISTRY OF HIGHER EDUCATION AND SCIENTIFIC RESEARCH

MENTOURI BROTHERS UNIVERSITY, CONSTANTINE 1
FACULTY OF EXACT SCIENCES
DEPARTMENT OF CHEMISTRY

N° of order : 32/D3C/2023

Series : 04/CH/2023

THESIS

PRESENTED TO OBTAIN THE 3rd CYCLE DOCTORATE DIPLOMA

Sector / OPTION

Chemistry / Synthesis and biological evaluation of new molecules

THEME

Synthesis, Characterisation, and application of new functionalized heterocyclic systems for therapeutic and catalytic purposes; Quinoline-heterocycle Hybrids and benzimidazole carbene metal complexes

By
Abd elkrim SANDELI

Presented on 26 - 06 - 2023 in front of the jury:

Examining Committee Members:

Mrs. Sabrina BICHA	Pr. At Mentouri Brothers University, Constantine1-	President
Mr. Raouf BOULCINA	Pr. Pr. At Mostefa Benboulaïd-Batna 2 University	Examiner
Mrs.Taoues BOUMOUD	Pr. At Mentouri Brothers University, Constantine1	Examiner
Mrs. Narimane SEGUENI	Pr. At Salah Boubnider University, Constantine 3	Examiner
Mrs. Naima KHIRI	Pr. At Mentouri Brothers University, Constantine1-	Rapporteur
Mrs. Saida BENZERKA	Dr. At Mentouri Brothers University, Constantine1-	Rapporteur

Dedication

I dedicate this piece of work

In honor of My Parents

May it serve as a small gesture of appreciation for all that you have done for me

Words cannot fully express the depth of my gratitude, but I simply say thank you for molding me into who I am today.

To my sisters ***Hadjer***, ***Amel***, ***Naoual***, *and* ***Sihem***

To my brother ***Yacin***

To the entire ***SANDELI*** *&* ***MESSAOUDI*** *family*

To my beloved Wife Soumia

Your unwavering support, both emotionally and physically, is greatly appreciated

I would also like to dedicate a special mention to my dear sweet young sons ***Saden El Amin***, *and* ***Masen Tamim*** *who was born during my Ph.D. research*

You are my inspiration, my source of distraction, and my guiding light. This work is dedicated to you.

Finally, I extend my gratitude and love to all those who have shown me love and support.

Acknowledgments

Prima facie, I am grateful to God for the good health and well-being that were necessary to complete this THESIS.

This thesis, like all scientific endeavors, could not have been completed without the support of many people who I am immensely grateful for having supported me in various ways throughout this rather protracted process of completing a Ph.D. thesis. and would like to thank a few individuals in particular.

First of all, I owe a debt of gratitude to my incredible supervisors: KHIRI Naima, and BENZERKA Saida who guided me throughout my research. I want to thank them for giving me the opportunity to work on this project, providing valuable guidance, and feedback, and challenging me to grow as a scientist. Special thanks to them for their invaluable advice, continuous support, patience, and assistance at every stage of the research project. I am deeply grateful to them for their unwavering unlimited support, belief in me, and unconditional guidance during my Ph.D. journey.

I would like also to express my sincere gratitude to my supervisor in Turkey Mr.Ismail OZDEMIR. Special thanks to him for providing constant encouragement and was always willing and enthusiastic to assist in any way he could throughout the research project. An immense thanks to him for being a wonderful supervisor during my internship in Turkey. Working in his lab has been a huge joy and I am grateful to have the pleasure of working with him.

I must also thank fellow members of the lab: Ms. Ilknur Ozdemir, Ms.Nevin Gürbüz, Ms.Emine Özge Karaca, Mr. Hüseyin Karcı, Mr. Enes Evren, Mr. Murat Kaloğlu and Mr. Sedat Yaşar for creating such a supportive and fun environment. I have learned a lot from all of them and am grateful for their. It has been an amazing experience working between two research groups across different departments, thanks to everyone from the Inonu university groups I've worked with and from whom I've learned so much.

I would also like to show gratitude to my committee, Mrs. Sabrina BICHA, professor at the University of Mentouri Brothers, Constantine1, who serves as the the committee president; Mr. Raouf Boulcina, professor at the University of Batna,; Mrs. Taoues BOUMOUD, professor at the University of Mentouri Brothers, Constantine1; and to Mrs.Narimane segueni, Docteur at Salah Boubnider University, Constantine3.

I am grateful to them for bestowing upon me the privilege of having them as the esteemed evaluators of this research work.

I wish to express my sincere thanks to Mr, DEBACHE Abd el Madjid director of our lab, for providing me with all the necessary facilities for the research. Many thanks to Mr.Houssem BOULBED for supporting me, and for the valuable discussions we had along the road, was always there for discussions about anything that I was unsure about. I am extremely thankful and indebted to him for sharing his expertise and for the sincere and valuable guidance and encouragement extended to me.

I would like to express my deep gratitude to the research team at the Biotechnology Research Center, especially to Mr. Chawki Bensouici, for the valuable assistance and support they provided me during the period of biological research.

My acknowledgments would not be complete without saying a heartfelt thank you to all the academics who helped me get to this stage. I also place on record, my sense of gratitude to one and all, who directly or indirectly, have lent their hand in this venture.

Thank you of course to the team I've worked so closely on this project with Zineeddine ZEBICH, Siraj Khan, and Sara LASMARI it's been great fun working with you all! I will never forget all the work experiences that we shared, coffee breaks, road trips, and the time spent like a family. Particular thanks to Zineb BELHI for all your help, support, and friendship: your inclusivity is appreciated by many.

Finally, but most importantly, none of this could have happened without my family. that offered me her encouragement every day. I must express my very profound gratitude to especially mother and father who have always believed in me and supported my pursuit of education for providing me with unfailing support and continuous encouragement throughout my years of study and through the process of researching and writing this thesis. This accomplishment would not have been possible without them. I would like to thank my family from the bottom of my heart for their constant support, guidance, and encouragement.

Special thanks to my wife from the bottom of my heart for her constant support, guidance, and encouragement. I am incredibly grateful for the endless love and support over the duration of the Ph.D.

General experimental information

Manipulations

- All preparation reactions of the benzimidazolium salts and their Ag(I)-NHC, and Pd(II)-NHC complexes were carried out under argon atmosphere using flame-dried glassware and standard Schlenk techniques, with an argon atmosphere.

Solvent and reagents

- All reagents and solvents were purchased from Sigma-Aldrich, Merck, and Fluka.

Spectroscopy analysis

- All the analytical and spectroscopic work was performed at the Inönü University research center, Malatya-TURKIYE. The measurements were taken at room temperature, and the solutions were freshly prepared.

Nuclear Magnetic Resonance Spectroscopy

- ^{1}H NMR and ^{13}C NMR spectra were recorded with a Varian As 400 Merkur spectrometer operating at 400 MHz (^{1}H), 100 MHz (^{13}C) in $CDCl_3$, and DMSO-d_6
  - The chemical shifts (δ) were expressed in parts per million (ppm) and referred to tetramethylsilane (TMS) as an internal reference.
  - The residual protiated solvents ($CDCl_3$ with δ = 7.26 ppm, and DMSO-*d*6 with δ = 2,50 ppm) were used as a reference for the ^{1}H NMR spectra. The ^{13}C NMR chemical shifts were reported relative to deuterated solvents ($CDCl_3$ with a δ = 77.16 ppm and DMSO-*d*6 with a δ = 39.52 ppm).
- Coupling constants (*J* values) are given in Hertz. NMR multiplicities are abbreviated as follows: *s*: singlet, *d*: doublet, *t*: triplet, and *m*: multiplet signal.

Fourier-transform infrared spectrometer

- The FT-IR measurement was conducted on the Perkin Elmer Spectrum 100 using the Gladi ATR (Attenuated Total Reflection) unit, covering the range of 400-4000 cm^{-1}.

Elemental analyses

- Elemental analyses were performed by LECO CHNS-932 elemental analyzers.

Melting points

- The melting point was determined using the Stuart SMP 40 melting point apparatus Electrothermal-9200, in open capillary tubes

Chromatography

- Column chromatography was performed using silica gel 60 (70-230 mesh).
- The catalytic reactions were monitored using an Agilent 6890 N GC system equipped with an HP-5 column, which had a length of 30 m, diameter of 0.32 mm, and film thickness of 0.25 µm. Detection was performed using GC-FID.

Biological material

- *Candida albicans* (ATCC MYA-2876) and *Candida glabrata* (ATCC 2001), which are pathogenic yeast species, were used in antifungal tests, and *Escherichia coli* (ATCC 25922), *Staphylococcus aureus* (ATCC 29213), and *Pseudomonas aeruginosa* (ATCC 27853) species were used antibacterial tests.
- The bacterial and fungal strains utilized in the study were obtained from the Molecular Genetics Laboratory located at the Turgut Özal Medical Faculty of İnönü University in Battalgazi, Malatya, Turkey.
- The substrates utilized in the reaction, acetylthiocholine iodide and butyrylthiocholine chloride, were obtained from Sigma Chemical Co. (Sigma-Aldrich GmbH, Stern-Heim, Germany)
- The *AChE* (Type-VI-S, EC 3.1.1.7, 425.84 U/mg) from Electrophorus electricus eel and the horse serum butyrylcholinesterase eq *BChE* (EC 3.1.1.8, 11.4 U/mg), which were utilized in the anticholinesterase assay, were both obtained from Sigma-Aldrich
- The enzymatic activity results were evaluated using a quantitative colorimetric assay and were measured and calculated using a PerkinElmer Multimode Plate Reader EnSpire (USA) with a 96-well microplate. The measurements and calculations were performed at the Center of Biotechnology Research located in Ali Mendjli, Constantine, Algeria.

List of Abbreviations

Å	Ångström
Ad	adamantyl [tricyclo[3.3.1.13,7]decyl]
aNHC	Abnormal N-heterocyclic carbene
AChE	Acetylcholinesterase
BChE	Butyrylcholinesterase
CAS	Catalytic anionic site
CAAC	Cyclic alkyl amino carbene
COD	1,5-cyclooctadiene
Cy	Cyclohexyl
°C	Degree Celsius
DMSO	Dimethyl sulfoxide
DAC	Diamidocarbene
Dipp	2,6-diisopropylphenyl
Dppd	1,3-diphenyl-1,3-propanedionate
ESI	Electrospray ionization
eq	Equivalent
GC	Gas Chromatography
Hz	Hertz
h	Hour
IAd	1,3-diadamantyl-2,3-dihydro-1H-imidazol-2-ylidene
ItBu	1,3-di-tert-butyl-2,3-dihydro-1H-imidazol-2-ylidene
IBu	1,3-dibutyl-2,3-dihydro-1H-imidazol-2-ylidene
ICy	1,3-dicyclohexyl-2,3-dihydro-1H-imidazol-2-ylidene
IMe	1,3-dimethylimidazolin-3-ylidene
IMes	1,3-bis(2,4,6-trimethylphenyl)-2,3-dihydro-1H-imidazol-2-ylidene
IiPr	1,3-bis(2,6-diisopropylphenyl)-2,3-dihydro-1H-imidazol-2-ylidene
IPr	1,3-(2,6-diisopropylphenyl)imidazolin-2-ylidene
IPh	1,3-Diphenyl-2,3-dihydro-1H-imidazole
IXy	1,3-bis(2,6-dimethylphenyl)imidazol-2-ylidene
ITol	1,3-bis(4-methylphenyl)imidazol-2-ylidene
IHept	1,3-bis(2-heptyl) imidazol-2-ylidene
IiPr	1,3-diisopropylimidazol-2-ylidene

IMe	1,3-dimethylimidazol-2-ylidene
IMes	1,3-bis(2,4,6-trimethylphenyl)imidazol-2-ylidene
in situ	"In the reaction mixture", without isolation
iPr	Isopropyl
IR	Infrared spectra
LUMO	lowest unoccupied molecular orbital
Mes	Mesityl
MIC	Minimum Inhibitory Concentration
Mes	mesityl [1,3,5-trimethylphenyl]
MCHR1	Melanin Concentrating Hormone Receptor 1
NHC	*N*-Heterocyclic carbene
NMR	Nucleare Magnetic Resonance
PEPPSI	Pyridine-enhanced precatalyst preparation stabilization and initiation
PAS	Peripheral anionic site
***p*-NPP**	*p*-Nitrophenol Palmitate
ppm	Parts per million
Ph	Phenyl
rNHC	Remote N-heterocyclic carbene
SIMes	1,3-bis(2,4,6-trimethylphenyl)-4,5-dihydroimidazol-2-ylidene
SIiPr	1,3-bis(2,6-diisopropylphenyl)-4,5-dihydroimidazol-2-ylidene
SICy	1,3-dicyclohexylimidazolin-2-ylidene
THF	Tetrahydrofurane
THT	Tetrahydrothiophene
TMSCl	Chlorotrimethylsilane
RT	Room temperature
RT	Room temperature
Ref	Reference
T	Temperature
t	Time
tol	Tolyl
UV-vis	Ultraviolet–visible
%V_{Bur}	Percentage of buried volume

Table of contents

General Introduction

Drug discovery is highly challenging for scientists [1]. The development or discovery of effective and inexpensive drugs is one of the main goals of researchers [2]. The chemical makeup of drugs used in human medicine is varied, but many contain heterocyclic structural components. Heterocycles are significant not only for their prevalence in organic chemistry but also for their various chemical, biological, and technological uses. Heterocycles, an important class of organic compounds, constitute more than seventy percent of bioactive and drug molecules presently found in the literature [3]. Among these widespread heterocyclic compounds, those containing oxygen, nitrogen, and sulfur have a unique standing due to their natural abundance and broad biological and pharmaceutical significance. The construction of heterocyclic molecules, due to the prevalence of cyclic motifs in pharmaceuticals and natural products, is a crucial topic in organic synthesis.

Developing effective methods for the synthesis of *N*-containing heterocycles is a fundamental challenge in synthetic chemistry [4]. One of the most important classes of this family is *N*-heterocyclic carbenes (NHCs) which are frequently used as ligands to create new complexes from simple starting materials. Commonly, NHCs derived from imidazolium, benzimidazolium, thiazolium, or triazolium salts have been used successfully for this purpose. In recent years, there has been an increased interest in NHC-catalyzed transformations, leading to the development of many new reactions. At present, metal-*N*-heterocyclic carbene complexes have emerged as a newly emerging field of chemistry and medicinal research, with NHC complexes attached to various metals like copper, gold, and silver showing strong potential as anticancer agents and for the treatment of other diseases [5,6].

Combining different heterocycles offers a new opportunity to create novel multicyclic compounds with improved biological activity. Fusing different heterocycles is a promising approach for generating hybrid molecules with enhanced biological activities. This work aims to merge the fields of organic and inorganic chemistry based on the chemistry of heterocycles, specifically the synthesis of polycyclic molecules for therapeutic purposes. The goal is to prepare new classes of

compounds containing heterocycles units and study their biological properties, as well as determine the structure-activity relationship. The thesis can be divided into two main chapters

The initial chapter of our study is focused on investigating the utilization of benzimidazole-derived *N*-Heterocyclic carbenes as a ligand to create new silver and palladium complexes. The main objective is to discover and develop new metallodrug complexes with the metallopharmaceutical "silver", which plays a significant role in therapeutic and diagnostic medicine. Additionally, we aim to synthesize new NHC complexes with palladium, which can function as pre-catalysts in challenging difficult organic reactions to facilitate and enhance the catalytic processes involved in demanding organic (Figure 1).

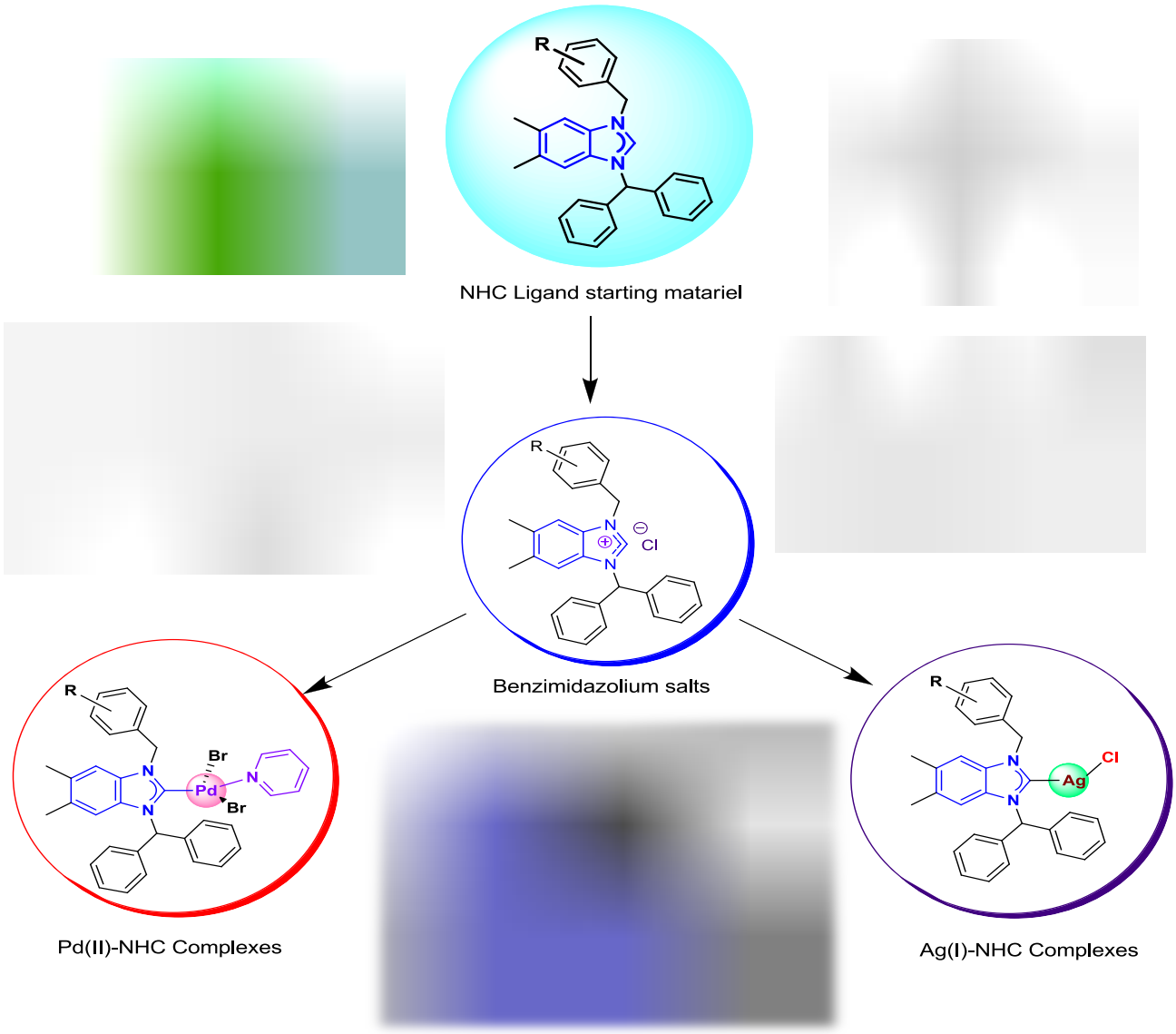

Figure 1. Graphical abstract of Chapter I

The second chapter is focused on the synthesis of some hybrid bioactive heterocycles to create a new polycyclic system with multitarget bioactive effects. Our objective was to use quinoline derivatives, through well-known and straightforward synthetic methods to perform couplings with highly functionalized heterocyclic entities of various structures to create structural analogs of bioactive products.

The overall strategy is fundamentally based on utilizing reactions and procedures that are suitable, simple, efficient, and easy to implement with the aim of advancing heterocyclic chemistry and drug discovery (Figure 2).

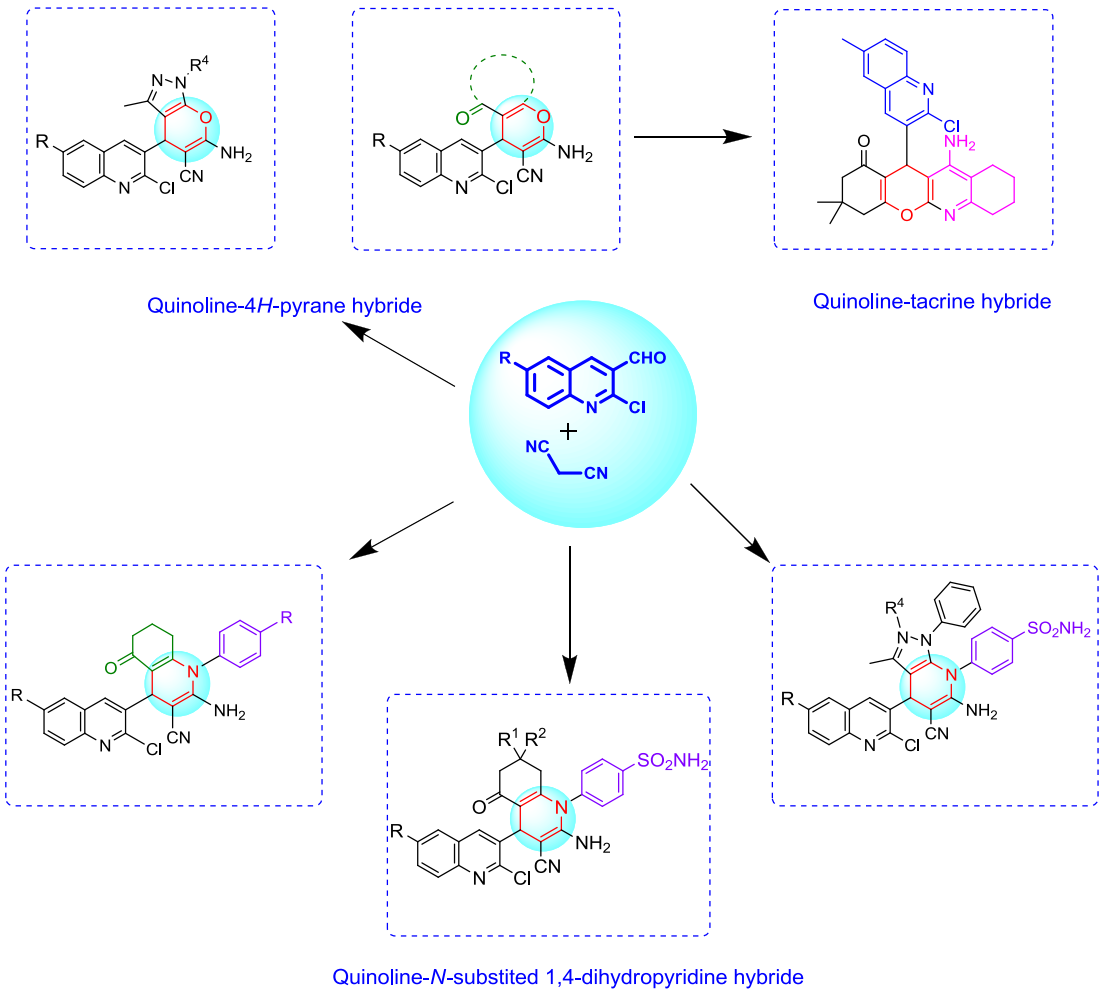

Figure 2. Graphical abstract of Chapter II

Chapter I

Synthesis and applications of metal complexes featuring *N*-Heterocyclic carbene ligands for catalysis capacity, biological interests, and study of their theoretical behavior

I. Bibliographic review

I.1 Introduction

Over the past few decades, stable carbenes have received a great deal of attention from researchers in various fields of chemistry [7]. They were first introduced to organic chemistry in the 1950s by Doering [8] and later to organometallic chemistry in 1964 by Fischer [9]. These unique species have caught the interest of chemists working in organic, inorganic, and theoretical chemistry. *N*-Heterocyclic carbenes are a specific type of carbene that have a carbene located on an *N*-heterocyclic scaffold.

Initially, these species were not commonly used in chemistry, but they are now employed in a wide range of fields, including organometallic chemistry [10] and organocatalysis [11]. *N*-heterocyclic carbenes are versatile building blocks that can be used to connect to a wide variety of coordination compounds [12]. Azole-derived NHCs have found applications in various fields. Researchers have synthesized NHCs that contain different imidazole [13] and benzimidazole heterocycles [14]. This type of ligand is known for its strong σ donor property and is considered stronger than alkyl phosphines ligands. Additionally, azoles, such as imidazole, benzimidazole, and triazole, exhibit diverse biological activities, with benzimidazole specifically being particularly studied in several chemical, biological, and industrial applications [15].

Metal-*N*-heterocyclic carbene complexes represent a rapidly growing area of research in both chemistry and medicine. These complexes, which feature NHC ligands coordinated to various metals including copper, gold, and silver, have demonstrated promising activity as anticancer agents [16] and as potential metallodrugs to fight bacterial infections [17]. The combination of biologically compatible moieties in these compounds, known as M-NHC complexes, enhances their potential as pharmaceuticals.

N-heterocyclic carbenes are also effective ligands that can be used to prepare a wide range of metal complexes and catalysts. They are widely used in organometallic chemistry with new catalytic applications as selective catalysts for a lot of reactions [18]. The coupling with metal pre-catalysts plays a significant role in many organic transformations. Among the most effective transition metals for these reactions are palladium (Pd), ruthenium (Ru), and rhodium (Rh) [19]. Currently, palladium-catalyzed cross-coupling reactions are considered important tools in organic chemistry [20]. One particularly effective type of Pd catalyst is the PEPPSI-type palladium-NHC complex [PdX_2(NHC)(pyridine)] (X/halide), which is easy to synthesize and use [21].

These complexes have shown great success in various carbon-carbon and carbon-heteroatom coupling reactions, and are considered an eco-friendly and economical alternative to traditional methods. They consider the most commonly employed coupling partners for Pd-catalyzed direct arylation reactions [22]. In addition, direct arylation reactions, in which an aryl group is directly added to a molecule, have gained attention as a possible alternative to cross-coupling reactions. The use of Pd-NHC complexes in direct arylation has been particularly successful in the synthesis of a wide variety of arylated heterocycles [23] and has the added benefit of minimizing by-product formation and simplifying organic synthesis.

This chapter provides an overview of *N*-heterocyclic carbenes, including their historical discovery, the latest developments in the field, methods for preparing them, and their characteristics and reactivity. It also explores their uses in chemical and biological research, specifically in organocatalysis. Additionally, the chapter also examines methods for synthesizing new NHCs using benzimidazole as a ligand, and the applications of NHC complexes with silver and palladium in catalysis, biology, and theoretical study.

I.2 Generalities

I.2.1 Historical aspect of *N*-Heterocyclic Carbenes

Chemists have been fascinated with carbenes for over 150 years, trying to create stable versions of these compounds since the 19th century. The search began in 1835 with Dumas [24]. However, his attempt of using dehydrating agents like phosphorous pentoxide failed [25]. Later, Doering and Hoffmann introduced carbenes to organic chemistry in 1954 [8], and in the 1960s, Wanzlick showed that the stability of carbenes could be increased by vicinal amino substituents [26]. Although they failed to isolate any carbenes during that period, they realized that a carbene center in the 2-position of the imidazole ring would be stable due to the electron-donating properties of adjacent nitrogen atoms. This insight laid the foundation for the advancement of carbene chemistry. Exactly in 1964 Fischer and his students introduced carbenes into inorganic and organometallic chemistry, as well as they reported the first stable transition metal complexes bearing carbene ligands, known as so-called Fischer-carbene complexes [27]. In 1988, Bertrand and co-workers isolated the first stable carbene (phosphinosilylcarbene) [28]. Three years later, Arduengo succeeded to isolate the first crystalline cyclic diaminocarbene "IAd", known as an *N*-heterocyclic carbene (NHC) [29]. In 1995, Herrmann *et al*. reported on the first application of NHCs as ligands in transition-metal catalysis [30]. Their research was the starting point for an enormous number of publications on applications of NHCs in reactions [7,31]. Finally, in 1999 Hahn and colleagues announced the discovery and solid-state configuration of the first benzimidazolin-2-ylidene, which marked the culmination of the set of free NHCs [32] (Figure 3).

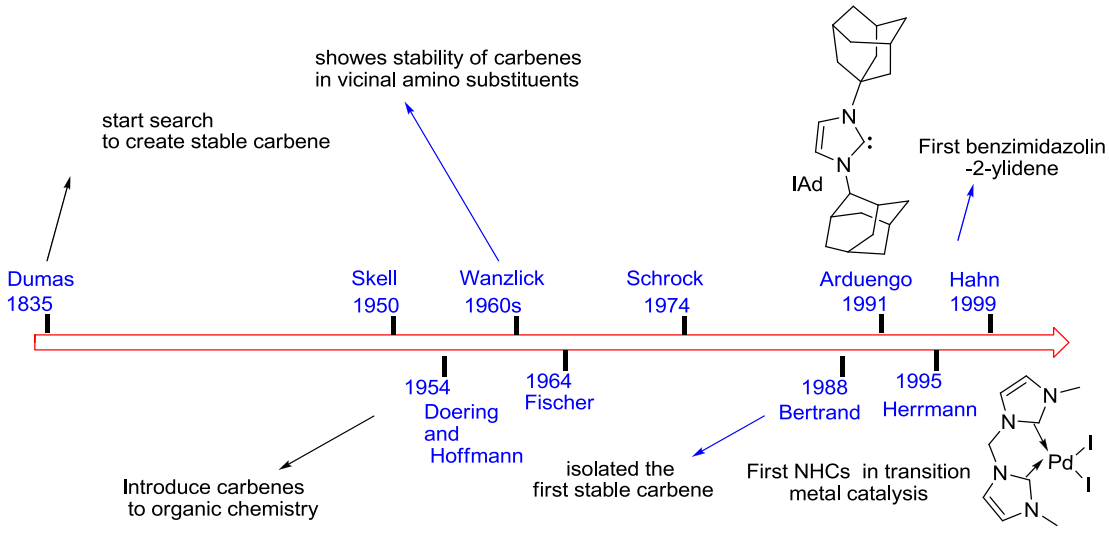

Figure 3. Serial history of discovery *N*-Heterocyclic carbenes

From these beginnings as academic curiosities. Actually, *N*-heterocyclic carbenes are considered the most powerful tools in organic chemistry, with numerous applications in commercially important processes. The dogma that carbenes were only transient species disappeared and a new and exciting field of research unfolded for synthetic chemists (Figure 4)[33].

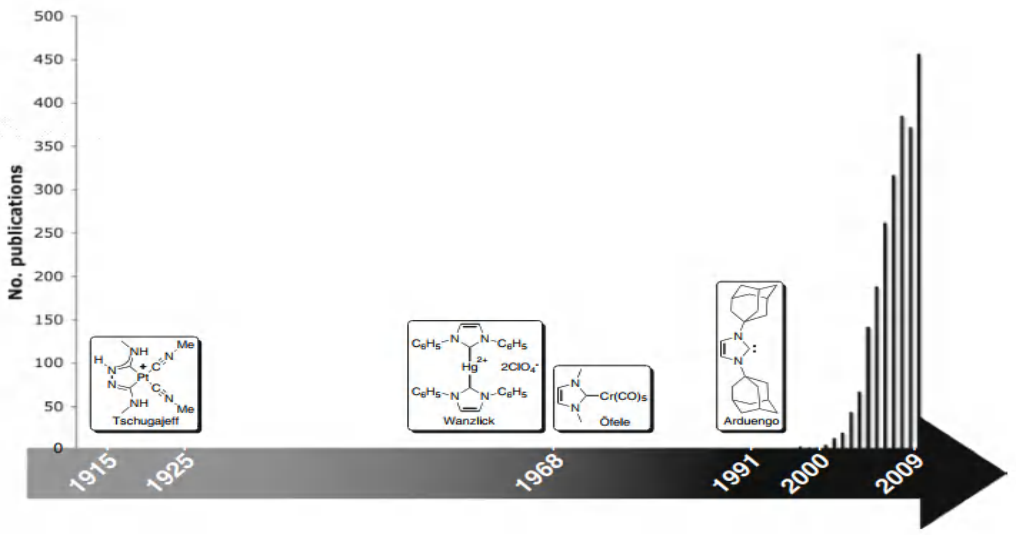

Figure 4. The exponential growth of publications on *N*-heterocyclic carbene as a research topic

I.2.2 Structure and representation of NHC and their NHC-M complexes

I.2.2.1 Representation of N-heterocyclic carbenes Ligants

N-Heterocyclic carbenes (NHCs) are a specific form of carbenes, where the carbene is located on an *N*-heterocyclic scaffold. The definition of NHCs is often subject to different interpretations, and many classes of carbene compounds have been referred to as NHCs in literature. *N*-heterocyclic carbenes [34] are organic compounds with a cyclic structure that incorporates a carbene atom into a heterocyclic ring. As the name suggests, they are neutral and must contain at least one nitrogen atom within the ring. Additionally, they have a divalent carbene atom with a lone pair of electrons. This is the minimum structural requirement for a compound to be considered an NHC (Figure 5).

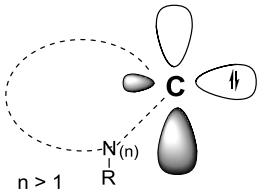

Figure 5. Minimum structural requirement for an *N*-heterocyclic carbine

I.2.2.2 Representation of NHC-Metal Complexes

The way of showing NHC metal complexes in a standardized way has not yet been fully determined, and a number of representations are used in literature. Representation (A) has been abandoned, while others, like representation (B), are used less frequently due to evidence of the carbonic form being more prevalent than ylidic resonance structures [35]. Representation (C and D) are currently the most commonly used. Structure E may be the most accurate representation of the bonding in these species. However, it is the least straightforward to use (Figure 6).

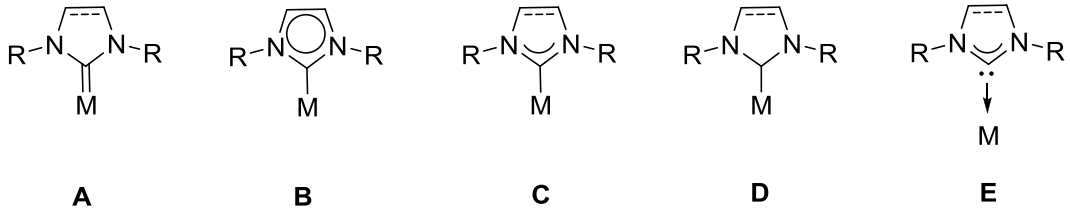

Figure 6. Possible representations of [(NHC)M] complexes

By convention, (Figure 6) typically shows "normal" NHCs, which are carbenes that are coordinated to the metal center through the C2 atom. In contrast, "abnormal" "non-classical" or "unusual" carbenes are those that are bound through the C4 atom. Remote is a term used to describe a carbene that does not have any heteroatom on the α-position to the carbenic carbon [36] (Figure 7).

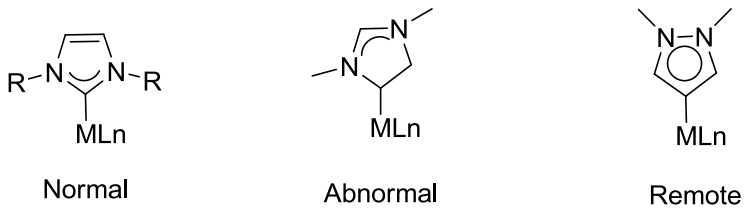

Figure 7. Normal, abnormal (aNHC), and remote (rNHCs).

For the reader's convenience, the general representations used for azolium salts, free NHCs, and NHC-metal complexes are depicted in Figure 8.

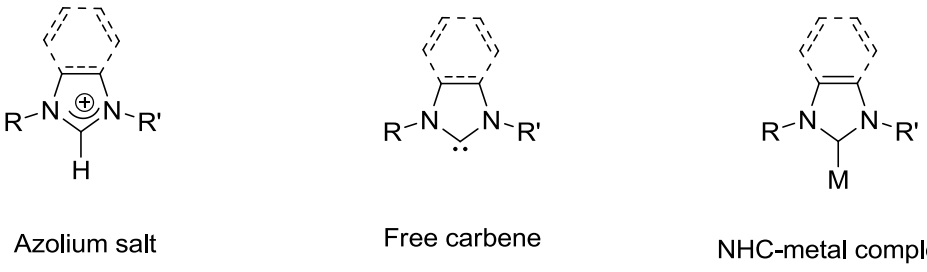

Figure 8. General representations used for azolium salts, free NHCs, and NHC–metal complexes

I.3 The biological interest of NHC Ligands and NHC-Metal Complexes

I.3.1 Biological interest of some benzimidazoles derevatives

Benzimidazole structures are classified under several classes of drugs [37], based on the potential substitutions at different positions of the benzimidazole nucleus, which is a component of benzimidazole structures. Modified nucleosides that contain the benzimidazole ring as a nitrogen base comprise a class of these structures and demonstrate antiviral and antitumor effects. The first halogenated benzimidazole nucleosides were synthesized in 1954 by Tamm *et al.* [38], with 5,6-dichloro-1-beta-D-ribofuranosylbenzimidazole (DRB) exhibiting activity against influenza A and B viruses and other RNA viruses [39] (Figure 9).

Figure 9. Benzimidazoles used as antiviral and antitumoral agents

Benzimidazole derivatives recently attracted medicinal chemists in exploring their potential as anticancer agents. Kumar *et al.* prepared a series of carbomethoxy-substituted benzimidazole derivatives and tested their cytotoxicity against humen breast cancer MCF-7, leukemia HL-60, colorectal adenocarcinoma HT-29, and prostate cancer PC-3 cell lines using Alamar Blue cytotoxicity assays. They discovered that the compound demonstrated cytotoxic effects on the tested cell lines [40] (see Figure 10)

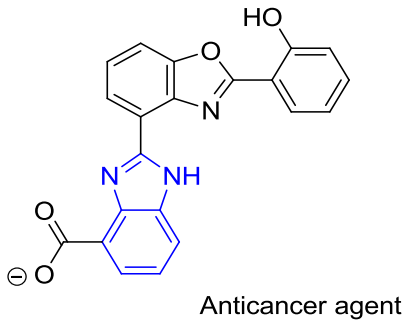

Figure 10. Benzimidazoles used in the treatment of cancer

According to a recent review of the literature, benzimidazole derivatives have emerged as potential candidates for the creation of antibacterial agents. *He et al.* produced 2-piperidin-4-yl-benzimidazole derivatives and evaluated their broad-spectrum antimicrobial efficacy against different strains of microorganisms, such as *Enterococcus, C. albicans,* and *P. aeruginosa*. Their research identified the compound as a promising antibacterial agent [41] (Figure 11).

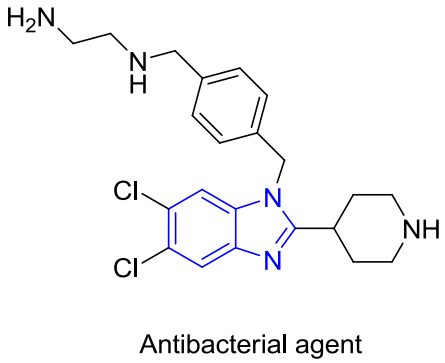

Figure 11. Benzimidazoles used as antibacterial agents

A series of 2-substituted phenyl-1*H*-(5-substituted) benzimidazole were produced and tested *in vitro* against Candida species. The findings from the antimicrobial assessments indicated that cyano-substituted compounds, specifically the compound 1-butyl-2-(4-fluoro-phenyl)-1H-benzimidazole-5-carbonitrile, demonstrated the highest level of activity that was comparable to that of fluconazole [42] (Figure 12).

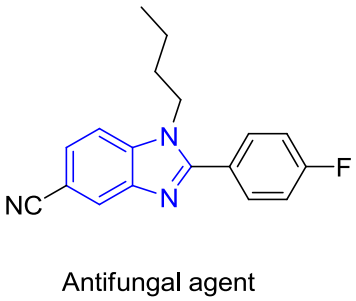

Figure 12. Benzimidazoles used as antifungal agent

Wu *et al.* synthesized novel benzimidazole analogs and tested their effectiveness in blocking MCHR1. They found that two of these compounds were successful in fully inhibiting MCHR1 activity. This suggests that these compounds could potentially be used for treating conditions related to appetite and metabolism [43] (Figure 13).

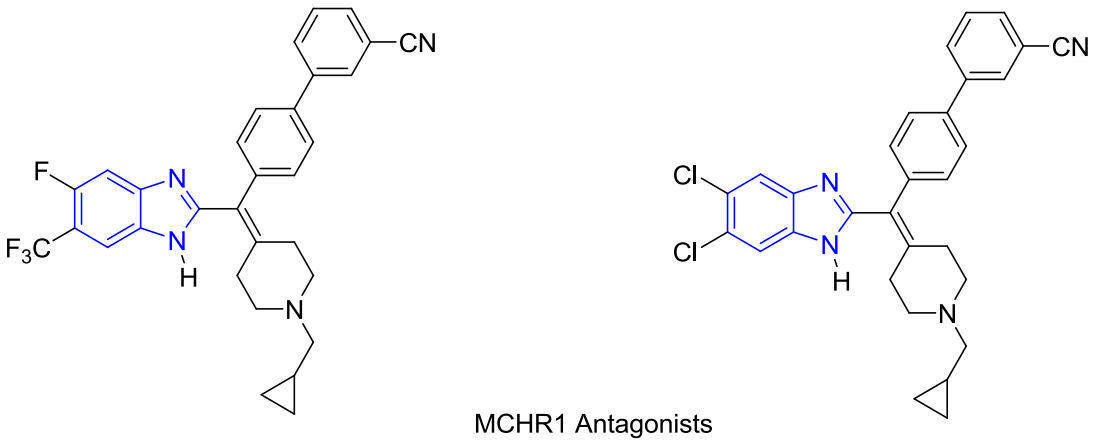

Figure 13. Benzimidazoles in control of obesity

The compound FK614, which is a type of benzimidazole, has been shown to enhance insulin resistance in a mouse model of Type II diabetes called C57BL/KSJ-db/db mice. This effect is due to the activation of a process called PPARc-mediated transcriptional activity, which regulates genes involved in glucose metabolism. These results suggest that FK614 could be a new potential therapy for treating Type II diabetes in humans [44] (Figure 14).

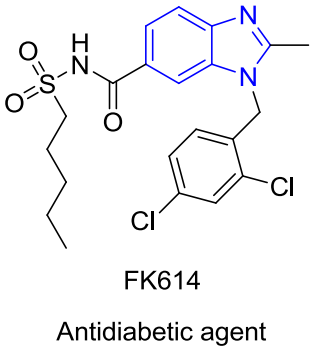

Figure 14. Benzimidazoles as antidiabetic agent

A study was conducted to test 2-(*o*,*p*-substituted phenyl)-1H-benzimidazole derivatives with various 5 and 6-position substituents *in vitro* rat aorta ring test. The study found that two derivatives were particularly effective at reducing blood pressure and showed the strongest antihypertensive activity [45] (Figure 15).

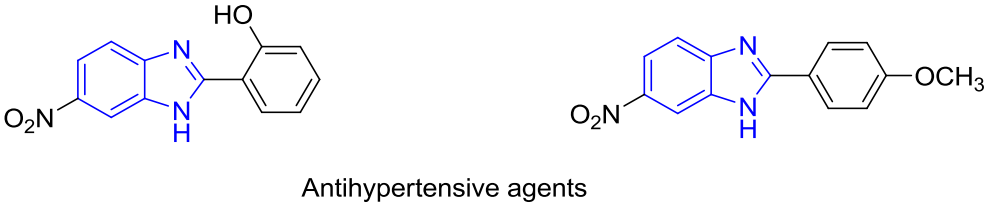

Figure 15. Benzimidazoles as antihypertensive agents

Nokano *et al*. synthesized a series of novel benzimidazole derivatives and evaluated their potential to alleviate allergic reactions by inhibiting *5-lipoxygenase*. The compound exhibited a dose-dependent suppressive action on 48 h homologous passive cutaneous anaphylaxis (PCA) reaction in rats [46] (Figure 16).

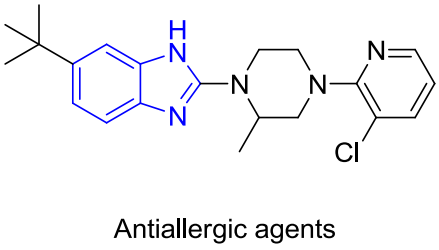

Figure 16. Benzimidazoles used as antiallergic agent

Snow *et al*. in search of a novel class of *kinase* inhibitors synthesized a series of benzimidazole derivatives and evaluated their *anti*-inflammatory potential. From the study, it was evident that the compound possessed a high ITK inhibitory activity [47] (Figure 17).

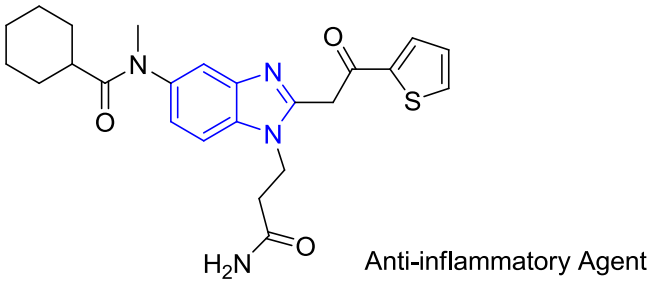

Figure 17. Benzimidazoles as *Anti*-inflammatory Agent

I.3.2 The biological interest of some NHC Ligands

Malhotra and Kumar have demonstrated that a variety of imidazolium salts containing long-chain alkyl substituents are cytotoxic to several types of cancers[48]. Recent work from the Youngs group has shown that the imidazolium salt precursors to the NHC ligands are also cytotoxic to various cancer cell lines (Figure 18) (unpublished work).

The efficacy of the *N*-heterocyclic carbene ligand, in the form of imidazolium salt and benzimidazolium salts, as an anticancer agent was tested against the H460 lung cancer cell line. The study found that the NHC ligand exhibited good toxicity against the cancer cells and its effectiveness was similar to that of cisplatin.

The use of imidazolium salts as anticancer agents instead of silver-NHC complexes significantly reduces the barriers to systemic delivery of the complexes. Without the silver cation, the imidazolium salts can circulate throughout the bloodstream, free of interactions with halides or proteins (Figure 18).

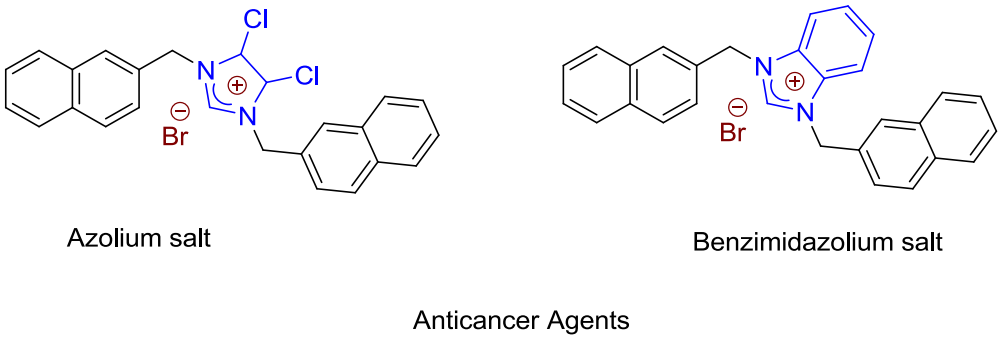

Figure 18. Imidazolium salts and benzimidazolium salts have demonstrated anticancer activity

I.3.3 The biological interest of some Silver-NHC complexes

The Youngs research group first started using silver-NHC complexes as antimicrobial agents through the creation of two specific compounds **1** and **2** [49]. The Youngs group also synthesized a series of compounds **3** and **4** based on imidazole and its derivatives[50]. These silver-NHC complexes also carried the acetate anion as a second ligand and showed high antimicrobial efficacy against the panel of organisms (Figure 19).

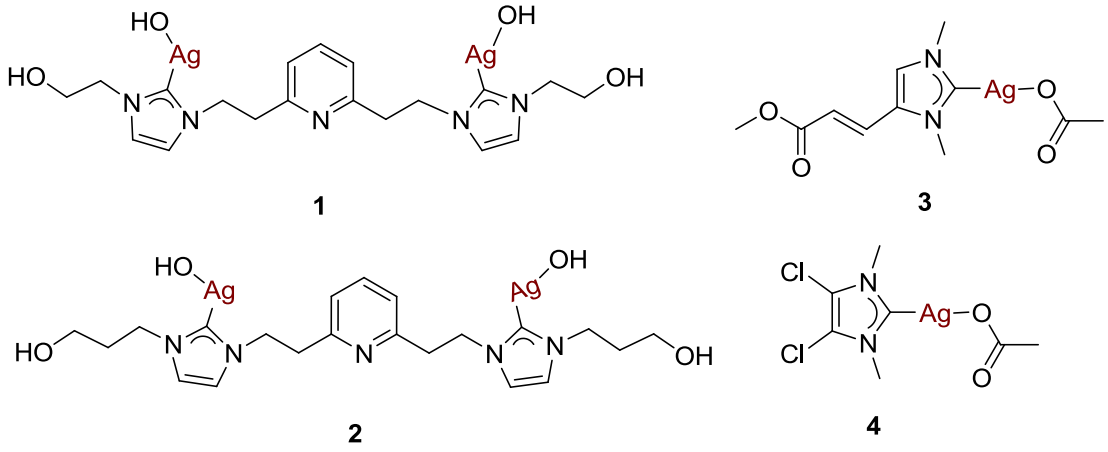

Figure 19. Silver-NHC complexes as antimicrobial agents against the panel of organisms

Through this search, two silver-NHC complexes were created, named **5** and **6**, that are made from xanthine and have an acetate anion as an additional binding agent.

The ability of the two complexes to combat bacteria and fungi, including those that are resistant to treatment and found in the respiratory systems of cystic fibrosis patients, was also evaluated [51] (Figure 20).

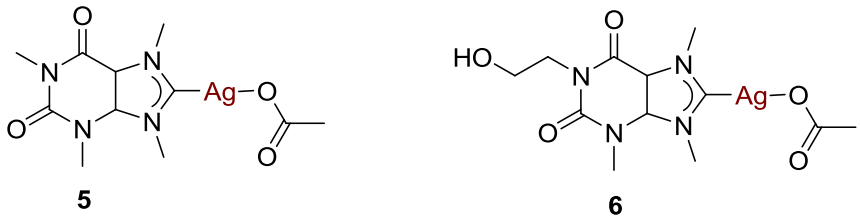

Figure 20. Silver-NHC complexes as antimicrobial agents for bacteria and fungi that are resistant to treatment in the respiratory systems of cystic fibrosis patients.

Another way to deliver silver-NHC complexes is to incorporate them into nanoparticles or nanofibers, which can then be used to create fabrics that have silver impregnated into them. These fabrics can be applied as dressings for wounds that are hard to heal, such as chronic ulcers or severe burns. The silver in these fabrics can act as a barrier against bacterial infections, which are common in these types of injuries. One example of this delivery method is the use of the water-soluble dinuclear silver carbene complex, which is incorporated into a Tecophilic® polymer mat via electrospinning [52] (Figure 21).

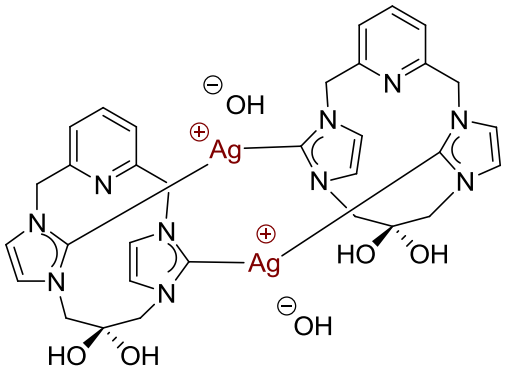

Figure 21. Silver-NHC complexes as a barrier against bacterial infections

Wooley and coworkers developed an alternative NP system for encapsulating silver-NHC using shell-linked knedel-like nanoparticles (SCKs, Figure 22) [53]. They reported the integration of the new compound into the core of SCK NPs. The antimicrobial activity of $AgNO_3$ shell-loaded NPs, Ag-NHC core-loaded NPs, and mixed shell/core-loaded SCK NPs were tested in vitro against CF clinical isolates of *P. aeruginosa* and urinary isolates of *E.coli*.

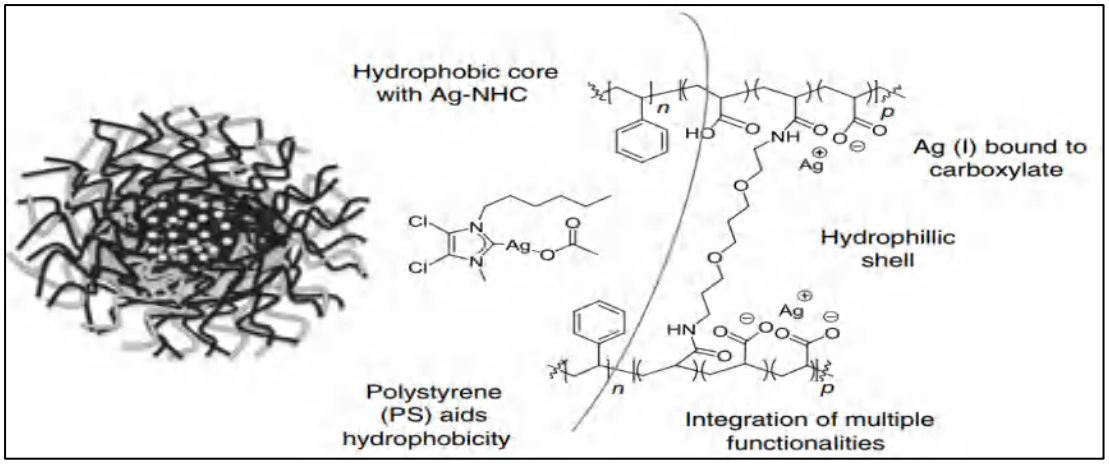

Figure 22. Schematic depicting anti-infective silver-NHC complexes in SCK nanoparticles

The initial report demonstrating the capability of silver-NHC complexes to impede the proliferation of cancer cells was presented by Youngs and colleagues [54]. They tested one such complex, known as **7**, against three different types of human cancer cells and found it to be effective. Since then, other researchers have also found that various silver-NHC complexes have anticancer properties that are comparable to established cancer drugs. Complexes **8**, and **9** were tested against six human cancer cells, including HL60 promyelocytic leukemia, KB-oral carcinoma, HL60R resistant HL60, MCF-7R resistant MCF-7, MCF-7 breast cancer, and T47D breast cancer [55] (Figure 23).

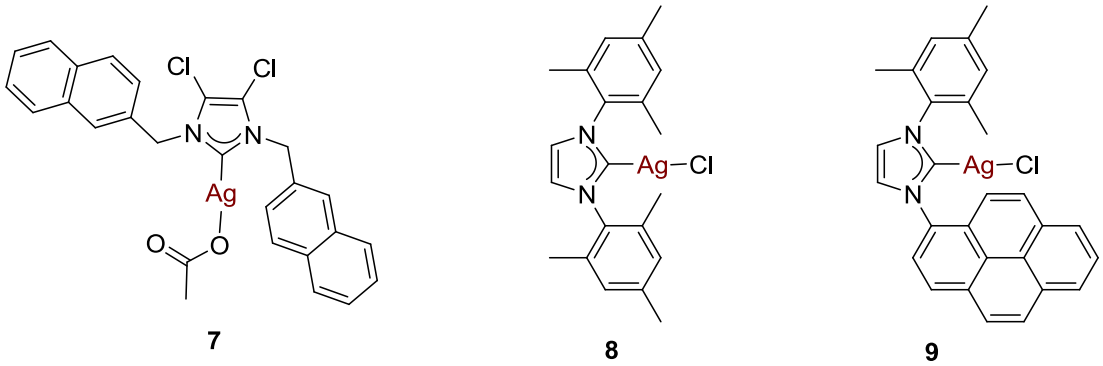

7 **8** **9**

Figure 23. Hydrophobic silver–NHC complexes used as anticancer agents

A diverse series of compounds including chelating and macrocyclic bis(NHC) complexes were synthesized by Willans and coworkers and tested against the MCF-7 breast cancer cell line and the DLD1 colon cancer cell line [56]. Several of the silver-NHC compounds reached cytotoxicity levels on par with or greater than cisplatin. Against the MCF-7 line, the two compounds were slightly higher than cisplatin (Figure 24).

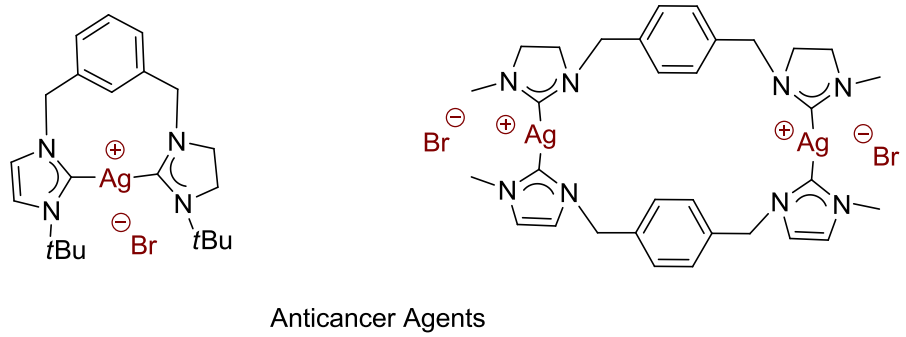

Figure 24. Silver-NHC complexes as Anticancer agents

I.3.4 The biological interest of some Palladium-NHC complexes

Palladium (Pd) has become more prevalent in the field of metallodrugs because of its structural similarities to platinum (Pt) and its high level of cytotoxicity. Additionally, there is growing interested in using complexes containing *N*-heterocyclic carbenes (NHCs) as anticancer agents [55]. One particular Pd complex **10** was found to be more effective than another complex **11** in inhibiting the growth of cervical cancer (HeLa), breast cancer (MCF-7), and colon adenocarcinoma (HCT 116) cells, with even greater efficacy than the standard drug cisplatin [57]. Another Pd complex **12** has an IC_{50} inhibitory that is almost 10 times lower than cisplatin against breast adenocarcinoma (MDA-MB-231) [58] (Figure 25).

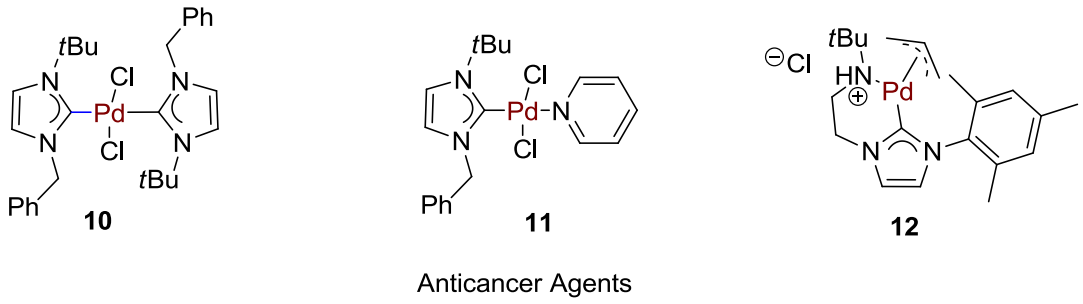

Figure 25. NHC–Pd complexes used against cancer cells

I.4 General Properties of Classical NHCs and Their NHC-M Complexes

Several researchers have used various methods to study the properties and reactivity of free carbenes, in order to synthesize and isolate them. The structural characteristics of NHCs permit independent variations of both electronic and steric properties.

I.4.1 Electronic Properties of NHC

N-heterocyclic carbenes are more electron-rich than even the most basic trialkyl phosphines and have similar levels of electron-donating ability. This is because NHCs only have substituents on the periphery of the ligand, whereas phosphines have different substituents directly attached to the donor atom itself. The electronic properties of NHCs can be adjusted by modifying key structural parameters, as demonstrated in Figure 26.

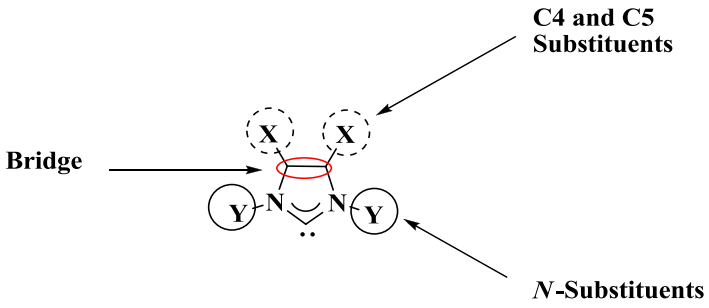

Figure 26. The structural points that can be used to tune the electronic properties of NHC ligands

The electronic properties of NHCs, which have a carbene donor and at least one nitrogen atom within a ring system, can be adjusted by varying the ring substituents and the heterocyclic backbone. Modifying the backbone primarily affects the electronics, although the NCN angles may also be impacted. The most effective way to change the electronics of an NHC is by altering the azole ring. It is believed that the order of electron-donating power increases in the order of benzimidazole < imidazole < imidazoline [59].

I.4.2 Stabilization of NHCs (Push-Pull Effect)

Classical NHCs have a carbene carbon center that is adjacent to two nitrogen atoms, and both nitrogen atoms contribute equally to the combined "push-pull effect." This results in multiple resonance structures, which increases the stability of NHCs. The NCN group in NHCs leads to electron delocalization, resulting in two nearly equal N-C carbene bonds, as shown in Scheme 1.

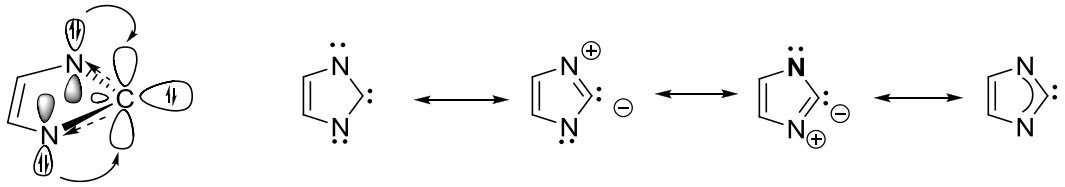

Scheme 1. Combined “Push-pull effect” in imidazole-derived NHCs

The presence of electron delocalization across the NCN moiety in NHCs leads to a "push-pull effect," where the higher electronegativity of the nitrogen atom (-I effect) withdraws electron density from the carbene center, stabilizing the σ orbital. At the same time, the lone pair at the nitrogen atom allows for delocalization and π-donation (+M effect) into the vacant pπ-orbital of the carbene carbon, increasing its electron density. These two effects combine to increase the energy gap between the two frontier orbitals and stabilize the single ground state.

"Traditional" carbenes are typically thought of as lacking electrons, while *N*-heterocyclic carbenes have a surplus of electrons and act as nucleophilic compounds. This is shown by their resonance forms **a** and **c** (Scheme 2).

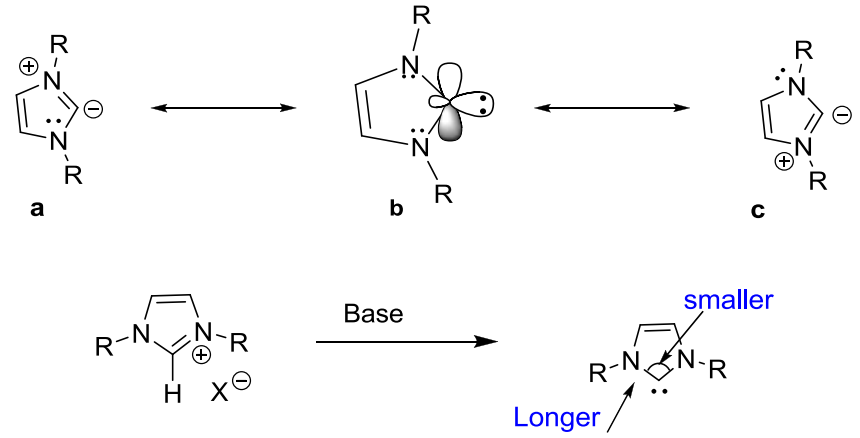

Scheme 2. 1,3-disubstituted imidazolin-2-ylidene

The C2-N bonds are longer in the carbine than in the imidazolium salt and the N-C-N angle is smaller in the carbine state, both findings indicating an increased σ-bond character in (e) and thus the importance of (b)[60].

I.4.3 Steric Impact

The degree of steric bulk that a ligand imposes on the metal complex fragment upon binding is the second important parameter to consider. The steric attributes of a ligand can have a significant impact on the reactivity of its corresponding complexes and often have a greater effect than their electronic effects.

Various steric parameters have been developed based on either experimental or computational data [61]. The most commonly used steric parameter in organometallic chemistry is the Tolman cone angle, which was first introduced by Chadwick Tolman in 1977 for phosphine ligands [62]. The Tolman cone angle is determined using simple 3D space-filling models and is defined as a cone emanating from a center, where the "metal-phosphine" distance is adjusted to 2.28 Å, which encompasses the substituents. This parameter is widely used to quantify the steric influence of a ligand [63]. Furthermore, it is usually observed that the R-substituents of phosphines point away from the metal center. The cone angle (θ) provides an estimate of the amount of "space" that the ligand occupies around the metal center. A bulkier phosphine with larger R-groups would have more widely spread out groups, resulting in a larger cone angle and a higher θ value (refer to Figure 27).

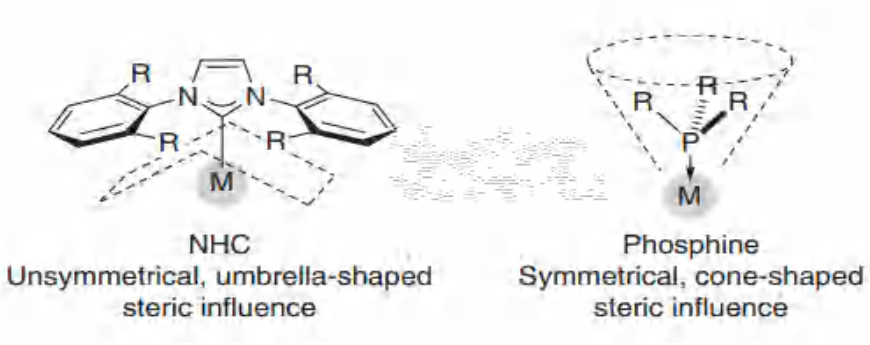

Figure 27. Comparing the steric properties of NHCs and phosphines

Based on the experience with tertiary phosphines, the importance of the steric properties of NHC ligands in determining chemical behavior has been recognized. However, the main problem is that NHC ligands have a local C2 symmetry axis, whereas phosphines have a local C3 symmetry axis. This means that the well-accepted molecular descriptor used to quantify steric properties in phosphines, the Tolman cone angle[62], cannot be applied to NHC ligands. This difference between NHCs and phosphines was acknowledged early, and the so-called fence model was proposed [64].

I.5 Reactivity of N-Heterocyclic Carbenes

The reactivity of NHCs has been studied using various techniques. It is important to understand this aspect of NHCs as it affects their reactivity and the ability to manipulate them through structural modifications. The reactivity of NHCs is determined by their Lewis and Brönsted basicity [65]. Due to their high Lewis basicity, NHCs react with a range of substances including transition metals [7] and organic molecules, forming stable adducts. These interactions can involve reactions with heterocumulenes such as CO_2, CS_2, COS, and other compounds like electron-poor alkenes, alkynes, and carbonyl compounds like aldehydes and esters (Scheme 3).

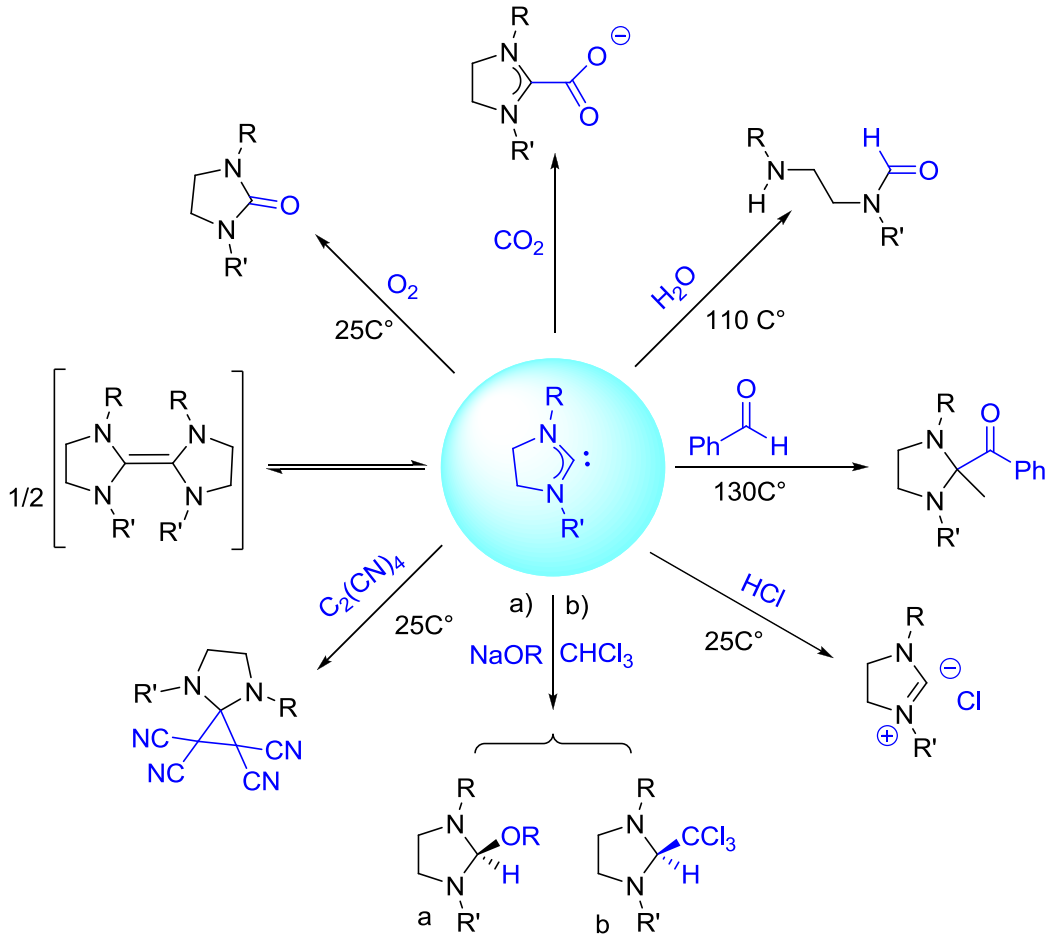

Scheme 3. Reactivity of *N*-Heterocyclic Carbenes

Additionally, NHCs also display some typical reactivity of transient carbenes, such as in dimerization [66] or insertion reactions [67]. Research on the reactivity of NHCs, using techniques such as the thermolysis of dimers, has been conducted since the 1960s by Wanzlick [68]. This research helped to establish the nucleophilic reactivity of these species with various reagents. On the other hand, NHCs are sensitive to air and

moisture, so they need to be handled in an inert atmosphere. They don't react with triplet dioxygen but they are prone to hydrolysis which leads to a ring-opened structure. The reaction of NHCs with HCl yields imidazolium chloride salts. These salts can then be reacted with an alkoxide base, such as sodium methoxide or potassium tert-butoxide, to form the corresponding alcohol adduct [69]. Carboxylate adducts of NHCs can be prepared by exposing the corresponding free carbene species to carbon dioxide, which will then precipitate from the THF solution. These adducts are used in organometallic synthesis and organocatalysis [70].

I.6 General synthetic routes to NHC ligands and NHC-M complexes

I.6.1 Peparation of NHC ligands, azolium salts and free carbenes

Accessing NHCs for use as ligands requires the synthesis of a suitable precursor. As heterocyclic organic molecules, synthetic routes toward Azolium salt have been widely studied in a variety of contexts over many decades. Azolium salts are the precursors used for the generation of *N*-heterocyclic carbenes. Nowadays, there exist many different approaches by which azolium salts can be prepared for all the core ring structures of NHCs [71] (Scheme 4).

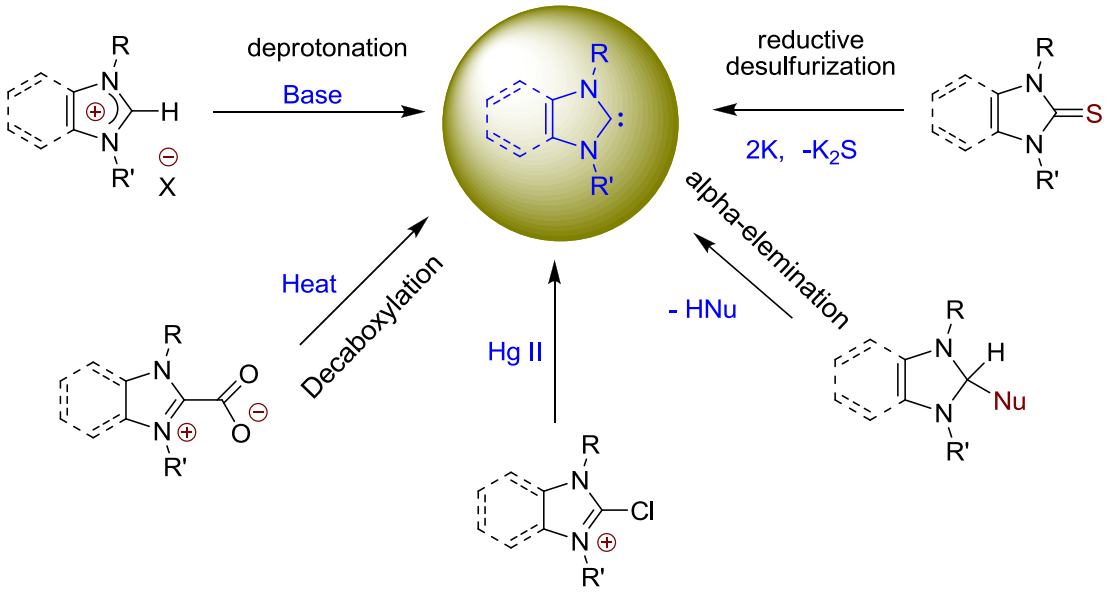

Scheme 4. General routes for the preparation of free *N*-Heterocyclic Carbenes

I.6.1.1 Preparation of some free carbenes

The first successful isolation of stable *N*-heterocyclic carbene was in 1991. Arduengo and colleagues prepared the first free NHC by utilizing NaH and catalytic amounts of DMSO in THF [72]. They used an imidazolium salt as a precursor and proposed that the dimsyl anion, generated in situ by the reaction of NaH with DMSO, was the actual base for the deprotonation step (see Scheme 5). The addition of catalytic amounts of DMSO also aids in the dissolution of NaH, which is otherwise insoluble.

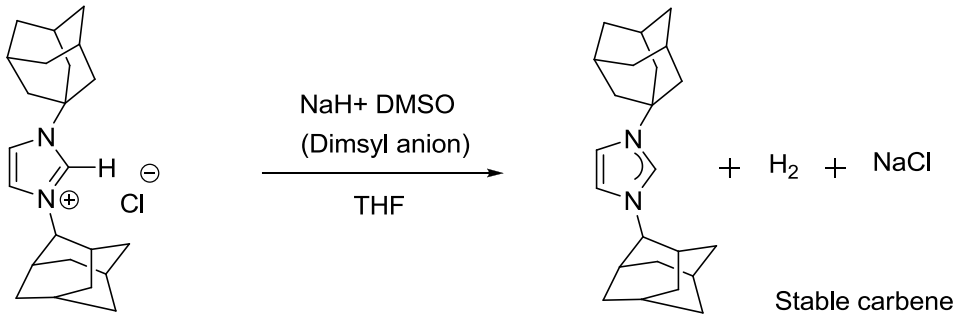

Scheme 5. Preparation of stable free NHC by deprotonation of the corresponding imidazolium salt

The reduction of thiones can also be used to generate free carbenes [73]. The thione compounds can be easily prepared from the corresponding thioureas, by condensation of thioureas with 3-hydroxy-2-butanone in boiling 1-hexanol (Scheme 6).

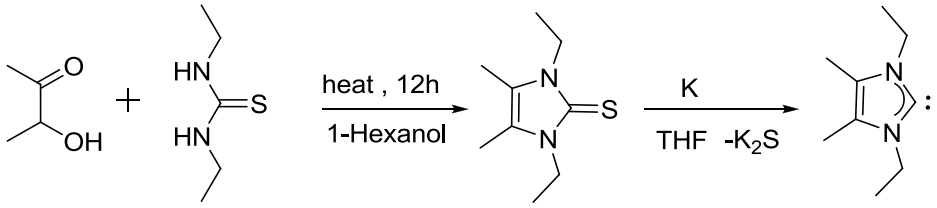

Scheme 6. Preparation of free carbene imidazolin-2-ylidenes by reduction of their thiones

Grubbs and colleagues reported the extension of the alcohol elimination method for the in situ preparation of saturated imidazolidin-2-ylidenes [74]. In this method, the free NHCs are generated by heating the corresponding NHC-alcohol adducts in THF (Scheme 7).

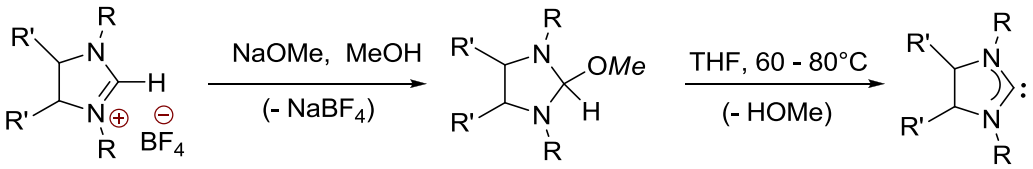

Scheme 7. Preparation of free carbene imidazolidin-2-ylidenes by alcohol elimination

I.6.1.2 Preparation of azolium salts as NHC Precursors

Creating NHCs for use as ligands requires the synthesis of a suitable precursor. Azolium salts, which are heterocyclic organic molecules, have been widely studied for decades in various contexts as precursors for NHCs. Nowadays, there exist many different methods available for preparing azolium salts for all the core ring structures of NHCs [71]. Stepwise *N*-alkylation of parent azoles is one of the most straightforward methods for preparing azolium salts. This method often employs low-cost starting materials and enables the synthesis of 1,3-dialkylazolium compounds. Alkylation of both nitrogen atoms in the heterocycle is required to produce such compounds (Scheme 8).

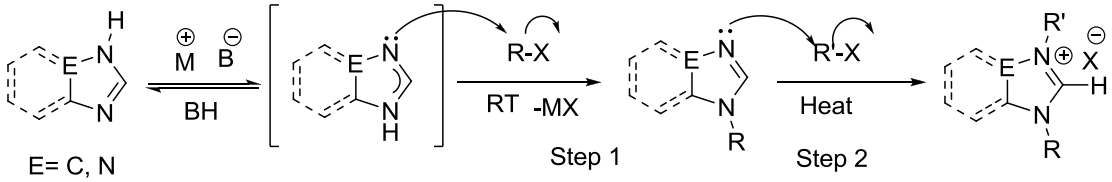

Scheme 8. Synthesis of dialkylazolium salts by stepwise *N*-alkylation of azoles

To perform the first *N*-alkylation in the stepwise *N*-alkylation of parent azoles, a base such as NaOH or K_2CO_3 is often required to deprotonate the N1-H proton. This results in an azolate ion, which is a stronger nucleophile. Once the proton is removed, the negative charge becomes conjugated with the initial "N3=C2 double bond," and the two nitrogen atoms become equivalent due to this delocalization. Following this, nucleophilic substitution with a suitable electrophile R-X, such as an alkyl halide, produces the neutral 1-(R)-substituted azole. The leaving group X typically forms a salt MX with the metal cation of the base. The second nitrogen (N3) still has one lone electron pair available for a second nucleophilic substitution with the same or a different electrophile R-X.

Imidazolium salts can also be obtained through a multi-component condensation reaction that involves a 1,2-dicarbonyl compound such as glyoxal or butane-2,3-diketone, primary amines, and paraformaldehyde, followed by an acidic workup in two steps overall [75]. This process is shown in Scheme 9.

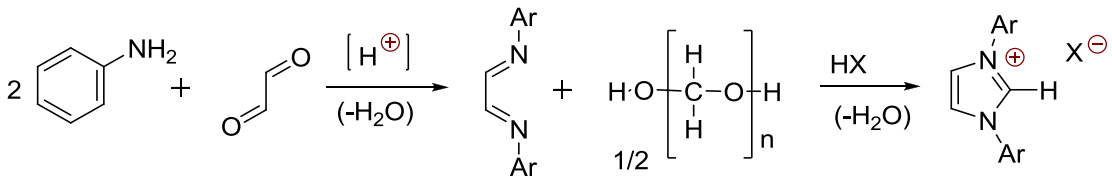

Scheme 9. Two-step synthetic sequence for the preparation of 1,3-diaryl imidazolium salts

The use of trialkyl orthoformate, specifically $HC(OEt)_3$ and $HC(OCH_3)_3$, under acidic conditions allows for the easy cyclization of secondary diamines to produce azolium salts. When *N*,*N*′-disubstituted ethylenediamines are used, this approach leads to the formation of imidazolinium salts with a saturated C4/C5 backbone that can be used as precursors for imidazolidin-2-ylidenes. On the other hand, when ortho-phenylenediamines are used, benzimidazolium salts are produced as precursors for benzimidazolin-2-ylidenes. Therefore, the synthesis of appropriately substituted diamines is a crucial step in this approach (Schema 10).

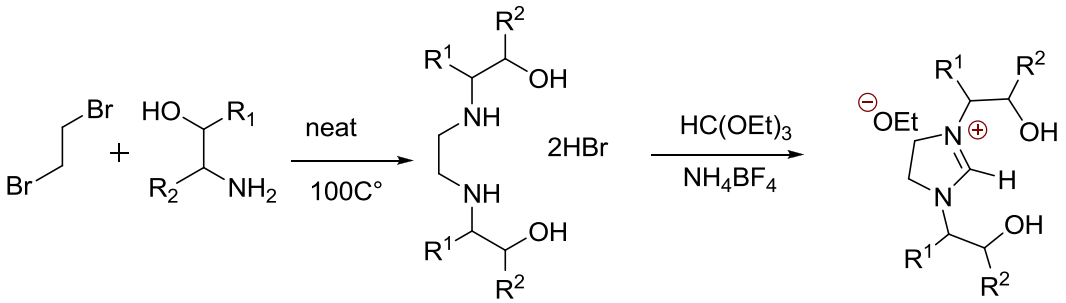

Scheme 10. Preparation of imidazolinium salts from 1,2-dibromoethane and amino alcohols

A different method for obtaining the required diamines for the cyclization process involves reducing diazabutadienes. Diazabutadienes can be obtained by condensing two equivalents of primary amines with glyoxal using standard reducing agents such as $NaBH_4$ or $LiAlH_4$. In the final step, the obtained substituted ethylene diamines undergo ring-closure with trialkyl orthoformate and a proton source to form the corresponding carbene precursors [76] (Scheme 11).

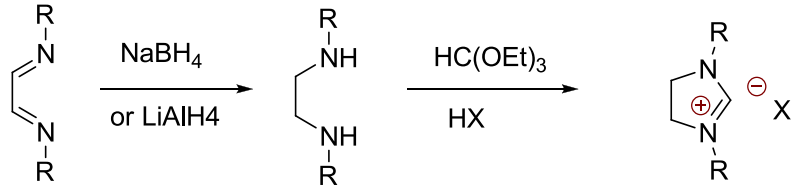

Scheme 11. Diamines *via* reduction of diazabutadienes and subsequent cyclization

I.6.2 General synthetic routes to NHC-Metal Complexes

From today's the most straightforward method for creating carbene complexes is by reacting a ligand with a specific transition metal. Hence, the most effective approaches to synthesizing NHC-metal complexes involve metal-template-directed synthesis or generating free carbenes in situ in the presence of metal ions that can act as traps for the carbenes. Many methods for preparing NHC complexes have been developed, and the most commonly used methods are shown in (Scheme 12) The techniques shown in the scheme are for imidazolidinylidene and imidazolylidene ligands, but they can also be applied to other types of NHCs [77,78].

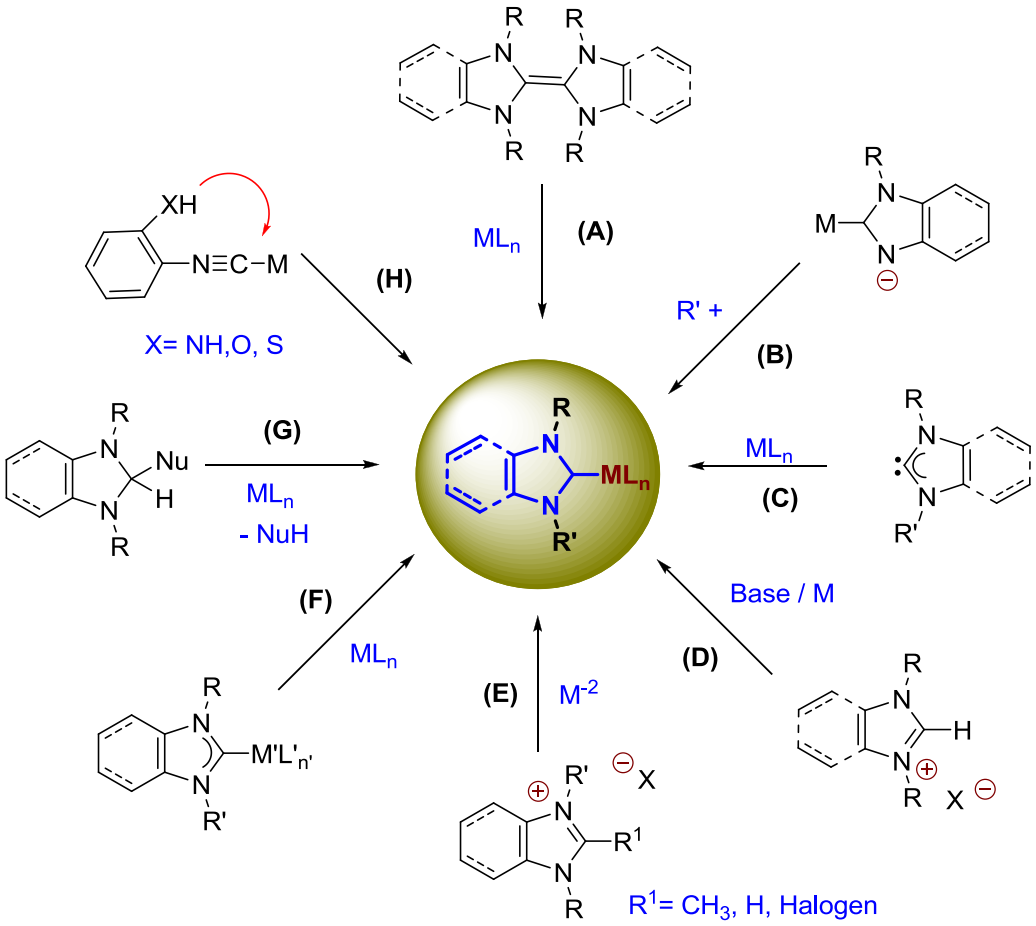

Scheme 12. Major synthetic routes to NHC-Metal complexes

Compared to phosphines, NHCs usually need to be activated before they can coordinate to a metal center. This makes NHC-based complexes less easily accessible than their phosphine counterparts. The methods for creating NHC-metal complexes can be classified based on the type of NHC precursor used and the activation method employed. In this sense, the most widely used strategies are:

(A) Insertion of metal into the C=C bond of bis(imidazolidin-2-ylidene) olefins cleavage of electron-rich entetramines by transition metals; (B) NHC complexes by protonation/alkylation of azolyl complexes; (C) coordination of carbene adducts or "protected" forms of free NHCs ; (D) in *situ* deprotonation of an azolium salt with a base in the presence of transition metals; (E) oxidative addition *via* activation of the C2-R (R= CH_3, halogen, H) of an azolium cation to a low-valent metal complex; (F) metal carbene transfer routes (Transmetallation) from (Ag, Mo, Cu, etc.)-NHC complexes prepared from direct reaction of an imidazolium precursor; (G) NHC complexes by small molecule elimination; and (H) metal-template synthesis using isocyanide complexes as precursors.

I.6.2.1 Synthesis methods of Silver-NHC complexes

Arduengo and colleagues reported the formation of a silver(I)-NHC complex in 1993 [79]. They achieved this by mixing two equivalents of IMes with a silver(I) triflate in tetrahydrofuran, then stirring the mixture at room temperature. This resulted in the formation of the bis(NHC) complex $[Ag(IMes)_2]$ OTf (Scheme 13).

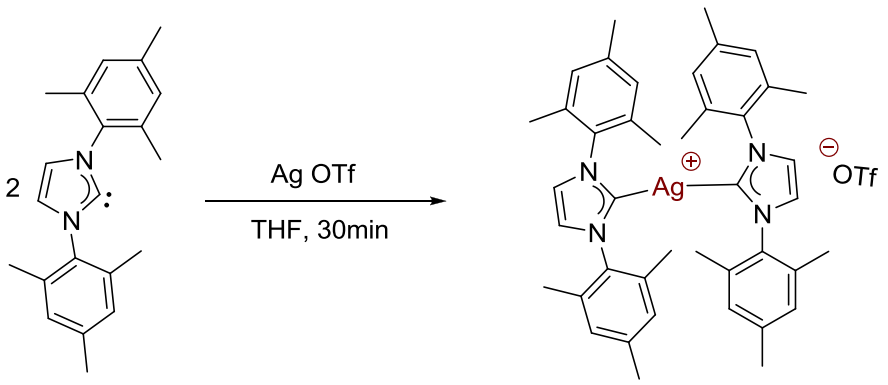

Scheme 13. Formation of silver-NHC complexes by mixing two eq of IMes with a silver(I) triflate

The "free carbene" approach has also been used to synthesize Silver(I)-NHC complexes. In a study by Chung [80], 1,3,4,5-tetramethylimidazolin-2-ylidene was combined with silver (1,3-diphenyl-1,3-propanedionate) in tetrahydrofuran at room temperature using this method. The reaction was finished after one hour, resulting in an air-stable, pale yellow solid of a neutral, three-coordinated silver(I)-complex [Ag(dppd)(IMeMe2)] (dppd = 1,3-diphenyl-1,3 propanedionato) with 80% yield (Scheme 14).

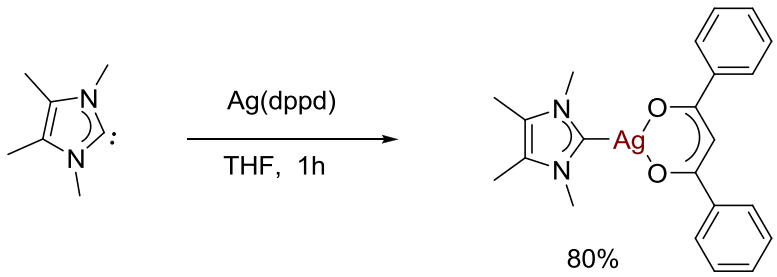

Scheme 14. Preparation of a mixed diketonatocarbene silver(I)-NHC complex *via* free carbene" route

Nolan et al. have reported the successful synthesis of [AgCl(NHC)] complexes through the reaction of two types of imidazolin-2-ylidenes featuring methyl and isopropyl wingtip groups with an excess of silver(I) chloride as stated in Scheme 15 [81].

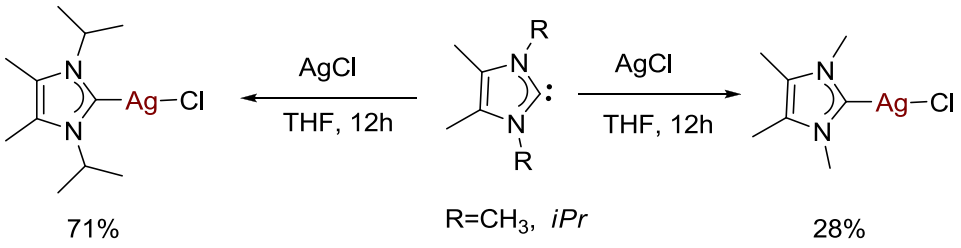

Scheme 15. Preparation of [AgCl(NHC)] complexes using free carbenes

The use of air-sensitive free carbenes in the "free carbene route" for preparing silver(I)-NHC complexes is considered a disadvantage and is now rarely used. Instead, most of these compounds are synthesized through *in situ* deprotonation by exposing azolium salts to basic silver precursors directly. This method is more convenient as it does not require strict inert conditions or additional bases. Typically, basic silver salts such as silver(I) acetate (AgOAc), oxide (Ag_2O), and carbonate (Ag_2CO_3) are used for this purpose.

Bertrand *et al.* first described this method in 1997 [82], where they reacted a dicationic 1,2,4-trialkyltriazolium ditriflate salt with two equivalents of silver(I) acetate in tetrahydrofuran under reflux for two hours. As a result of this reaction, they obtained a unique one-dimensional silver-dicarbene organometallic polymer (Scheme 16).

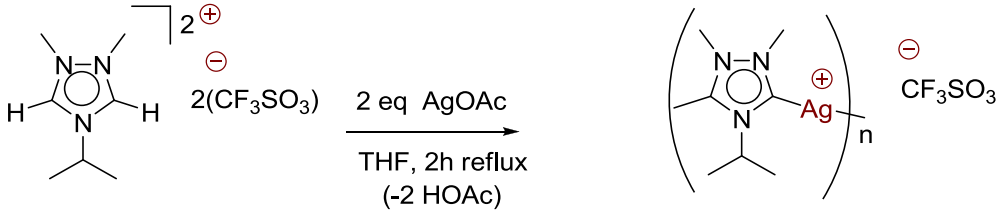

Scheme 16. Preparation of an organometallic silver-carbene polymer with bridging 1,2,4-triazolidin-3,5-diylidene ligands

Azolium salts can be converted into Ag-NHC complexes by using silver compounds like silver oxide (Ag_2O), carbonates (Ag_2CO_3), or acetates (AgOAc) as a basic metal precursor. This process involves two steps in one pot. Lin and Wang discovered a new method for creating silver(I) NHC complexes, which they found to be effective as carbene transfer agents [83]. The discovery was accidental, having occurred when a graduate student mistakenly used silver(I) oxide instead of gold(I) oxide in an experiment. Despite the error, the reaction resulted in excellent yields of silver(I) NHC complexes. This simple method has since become widely used in the field (Scheme 17).

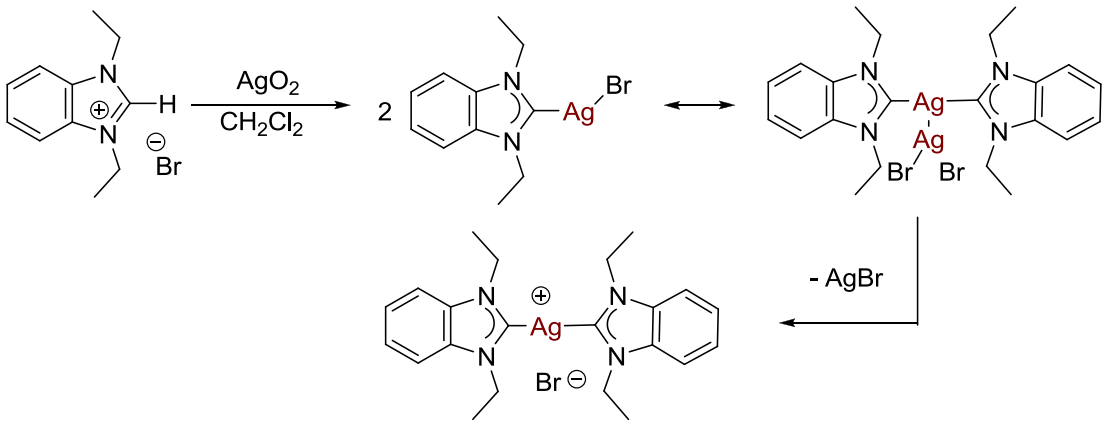

Scheme 17. Formation of silver-NHC complexes *via* silver(I) oxide route and their dynamic behavior

I.6.2.2 Synthesis methods of palladium(II)-NHC complexes

The first example of a palladium(II)-NHC complex had already been prepared using this approach by Lappert *et al*. in 1972 [84]. They heated tetraphenyl enetetramine with the coordinatively unsaturated dipalladium (II) complex $[PdCl_2(PEt_3)]_2$ in xylene at 140°C for one hour. This resulted in the kinetically controlled formation of *trans*-$[PdCl_2(PEt_3)(SIPh)]$ (Scheme 18).

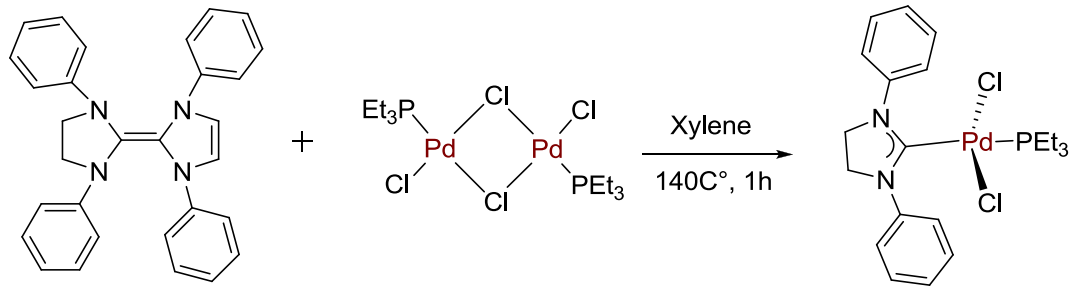

Scheme 18. Preparation of the first palladium(II)-NHC complex *via* insertion of metal into the C=C bond of electron-rich entetramines by transition metals

Hahn and coworkers demonstrated also that room temperature reaction of PdI_2 with a bridged dibenzotetraazafulvalene in THF affords the di(NHC) complex *via* insertion of the PdI_2 moiety[85] (Scheme 19).

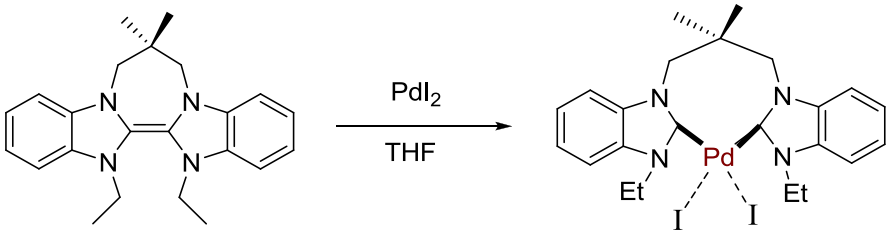

Scheme 19. Synthesis of Pd-NHC complex *via* direct insertion of PdI_2 into dibenzotetraazafulvalene

To avoid isolating air and moisture-sensitive free carbenes in the synthesis of metal-NHC complexes, azolium salts can be in situ deprotonated using an external base. Enders et al. demonstrated this process in 1996 when they created the first chiral imidazolinylidene and triazolinylidene palladium(II) compounds [86]. The procedure involves mixing the azolium perchlorates with KOtBu, NaI, and $Pd(OAc)_2$ in tetrahydrofuran. Stirring the mixture for 1-5 hours at room temperature, followed by column chromatography, resulted in high yields of the palladium(II) carbene complexes. The stoichiometry of the reactants can control the formation of mono- versus bis(carbene) complexes (Scheme 20).

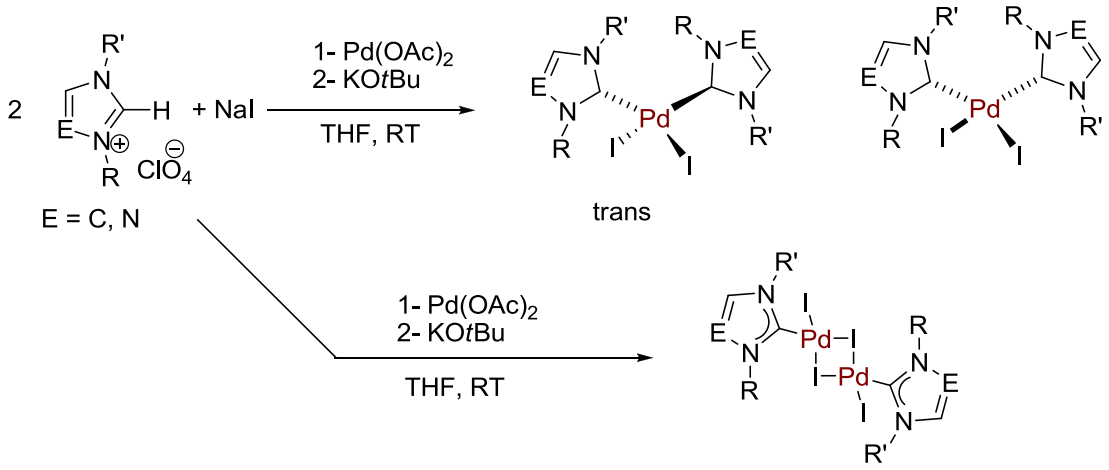

Scheme 20. Preparation of NHC-Pd complexes *via in situ* deprotonation of azolium salts using an external base

Gosh, *et al*. have utilized a much simpler protocol to access bis(triazolin-5-ylidenes) palladium complexes [87] (Scheme 21).

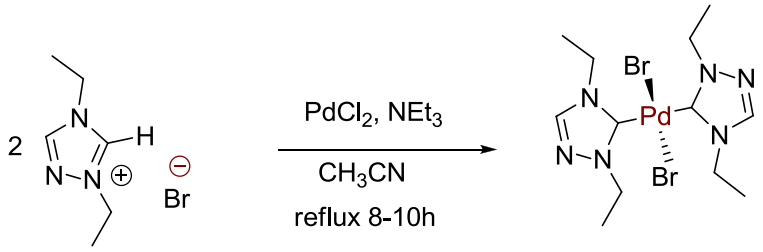

Scheme 21. bis(NHC) Pd(II) complexes *via in situ* generations of free carbenes with a weak base

Another frequent technique for making Pd(II) complexes is by combining palladium salts with isolated or *in situ*-generated NHC ligands. This method is very flexible to create many complexes that have monocarbene, bis-carbene, chelating carbene, and mixed chelating ligands that consist of at least one carbene [88].

In search of synthesizing monocarbene complexes, Nolan et al. reported the reaction of one equivalent of the pre-formed IPr carbene with the dichlorido-bis(benzonitrile) palladium(II) complex [$PdCl_2(NCPh)_2$] [89] (Scheme 22).

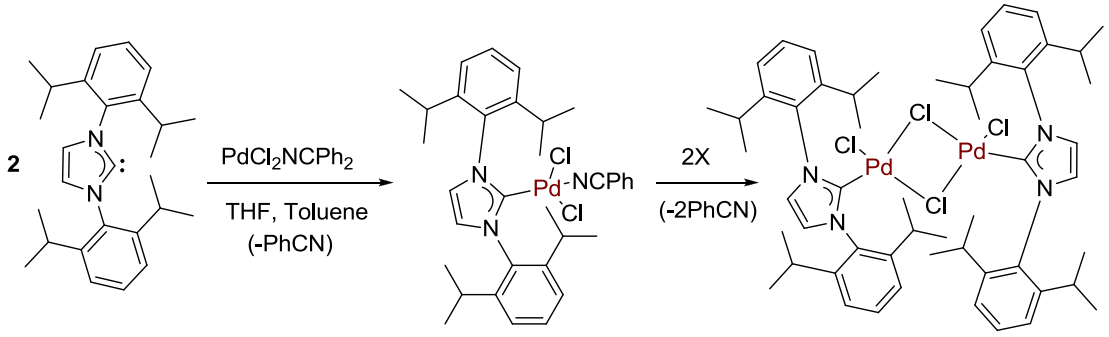

Scheme 22. Formation of a dimeric mono-NHC-Pd complex *via* the "free carbene" route

One more recent example is the one-pot preparation of the so-called PEPPSI-type (**P**yridine **E**nhanced **P**recatalyst **P**reparation **S**tabilization and **I**nitiation) catalysts developed in the group of Mike Organ [90]. The procedure involves heating a mixture of imidazolium salt, $PdCl_2$, and a less strong base (K_2CO_3) in neat 3-chloropyridine. The K_2CO_3 base deprotonates the imidazolium salt to generate the free carbene *in situ*, which can directly coordinate with the PdII center. Notably, 3-chloropyridine acts as a solvent and a source of the co-ligand, which completes the square planar coordination sphere (Scheme 23).

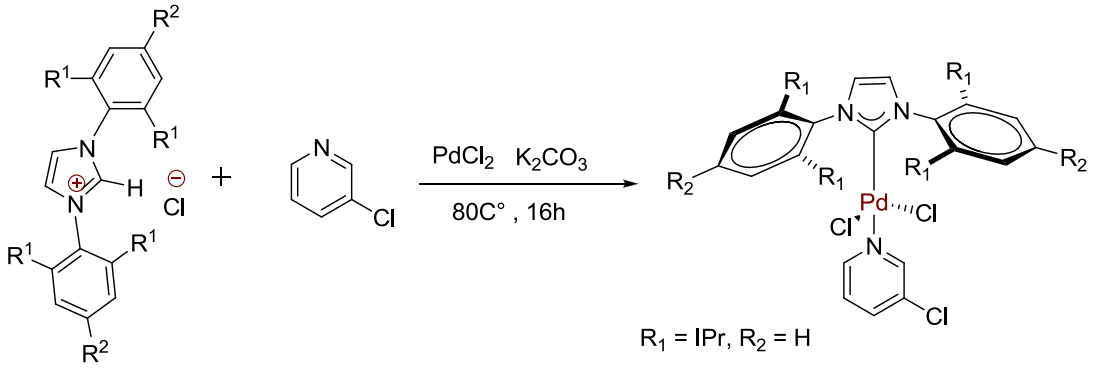

Scheme 23. Preparation of NHC-Pd complex PEPPSI-type *via in situ* deprotonation of an azolium salt with a base in the presence of transition metals

Waymouth and coworkers reported a strategy, which could be applied to prepare palladium(II) NHC complexes. Instead of alcohol adducts of carbenes, they employed 1,3-dimesityl-2-pentafluorophenyl-imidazolidine as an NHC precursor. Heating a solution of the imidazolidine and η3-allylchloridopalladium(II) dimer in toluene afforded a PdII-SIMes complex under bridge-cleavage condition and with the release of pentafluorobenzene [91]. The reaction is driven by the formation of the stable benzene derivative and the saturation of the coordination sites at palladium (Scheme 24)

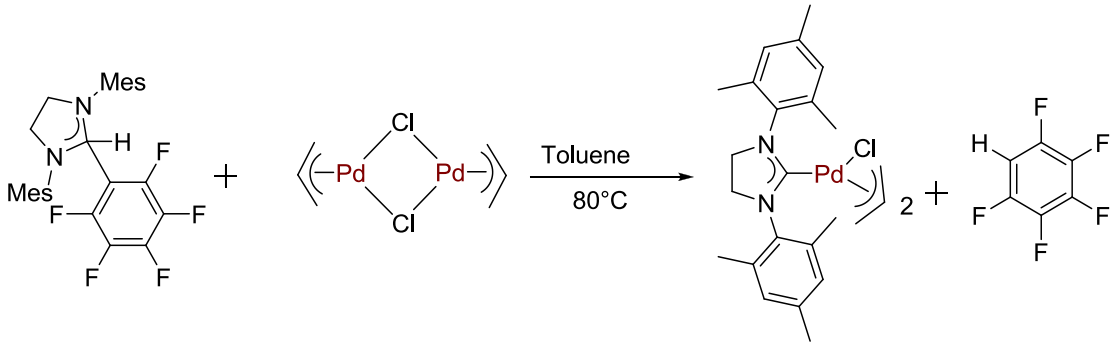

Scheme 24. Preparation of a Pd(II)-NHC complex by α-elimination of pentafluorobenzene

The most commonly applied technique for preparing palladium(II)-NHC complexes involves the pre-generation silver-carbene complexes, which are excellent and highly effective at transferring carbene. In the original procedure reported by Lin and coworkers

The most commonly used technique for preparing palladium(II)-NHC complexes involves the pre-generating of silver-carbene complexes, which are highly effective at transferring carbene. This approach was first reported by Lin and Wang in 1998 [83]. They reported the use of Ag-NHC complexes as carbene transfer reagents

to provide in many cases a convenient way to overcome the difficulties arising from using strong bases, inert atmospheres, and complicated workups. In their work, two benzimidazolylidene complexes of Ag(I) were used as carbene sources to provide NHC complexes of Pd, by reaction with $PdCl_2(NCCH_3)_2$ (Scheme 25).

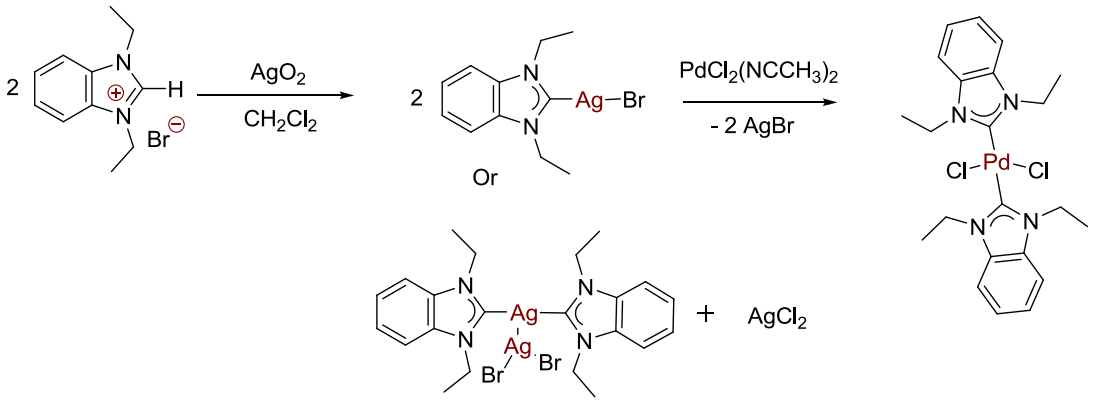

Scheme 25. Synthesis of Pd-NHC complex *via* Stepwise silver(I)-NHC transfer to palladium(II)

Due to the high energy required for the activation of C–alkyl bonds, access to NHC complexes *via* oxidative addition of C2-alkyl azolium salts is uncommon. Nonetheless, Baker and coworkers could activate a special "C2–C2 linked, doubly-bridged" di-imidazolium salt with Pd0 in DMSO at elevated temperatures [92]. This rare example of a concerted C–C activation of a di-imidazolium salt directly led to a cationic dicarbene PdII complex in a single step. The driving force for this reaction is believed to be the relief of ring strain in the precursor salt that occurs upon palladation and dicarbene formation (Scheme 26).

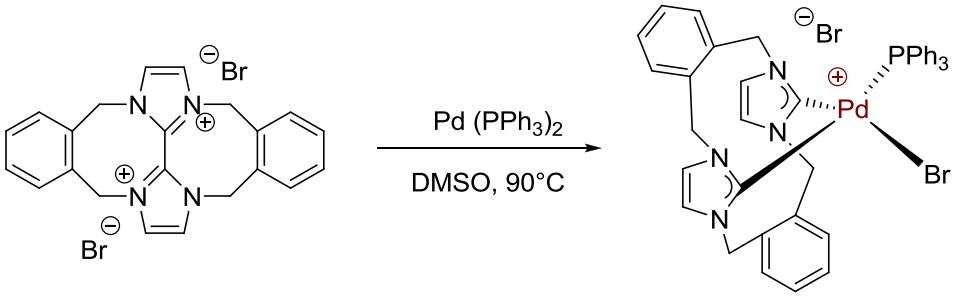

Scheme 26. Synthesis of Pd-NHC complex *via* oxidative addition of strained C2-C2 linked-bridged" di-imidazolium salt with Pd 0

I.7 Application of NHC-metal complexes

Metal complexes containing *N*-heterocyclic carbenes have various applications other than being used in homogeneous catalysis, including use as metallopharmaceuticals [93], and in materials science for self-healing polymers, liquid crystals, metal-organic frameworks [94], and photoactive materials [95]. Additionally, their strong σ-donating properties are being utilized for binding to metal surfaces or nanoparticles [96]. There is a growing trend of industrial companies filing patents for the use of these catalysts in various applications, demonstrating the significant progress made with this ligand family.

Transition metal-catalyzed reactions have emerged as powerful tools for carbon-carbon bond formation [97]. Cross-coupling reactions such as Suzuki-Miyaura, Mizoroki-Heck, and Stille have proven to be dependable, sturdy, and adaptable. Additionally, other catalyzed arylation reactions have been examined and have been found to be highly effective [98]. In recent years, *N*-heterocyclic carbenes complexes have been extensively studied and their use as ligands in transition metal catalysis has led to significant advancements in many reactions [18].

I.7.1 NHC-metal complexes in transfer reactions (Transmetallation)

Certain preformed metal-NHC complexes such as Ag-NHC complexes and Ru-NHC complexes obtained by either one of the other routes can transfer the NHC to another metal (transmetallation). This compound can be used *in situ* if a convenient amount of a metal complex (usually with halide ligands) is added, hence providing the corresponding M-NHC complex (Scheme 27).

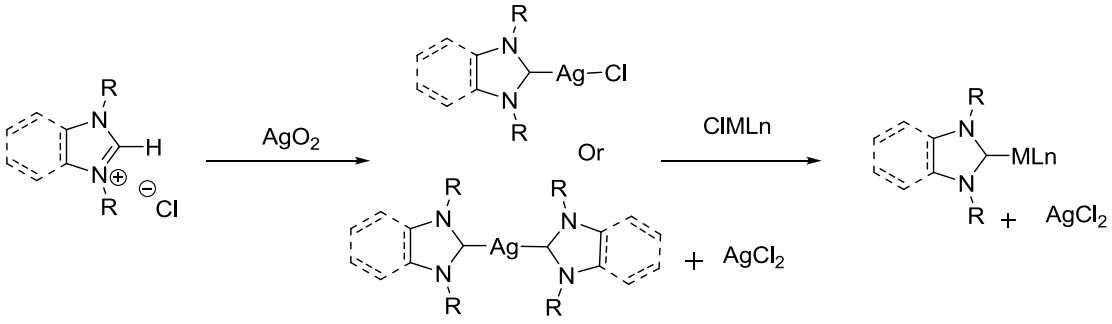

Scheme 27. The use of NHC complexes in transfer reactions (Transmetallation)

I.7.2 NHC-Metal complexes in catalysis

I.7.2.1 Silver–NHC complexes in catalysis

The first known use of NHC-Ag catalyzed reactions was reported in 2005 by Peris and Fernández, who showed the diboration of alkenes using a bis(NHC)-silver complex [99]. Researchers, Zhang and Duan, attempted to improve enantioselectivity by using a cylindrical macrostructure with chiral NHC-Ag complexes, but the results were not successful with enantioselectivity being less than 28% [100]. However, better results were achieved by Lassaletta, Fernández, and co-workers in the 1,3-dipolar cycloaddition of azomethine ylides and acrylates [101] (Scheme 28).

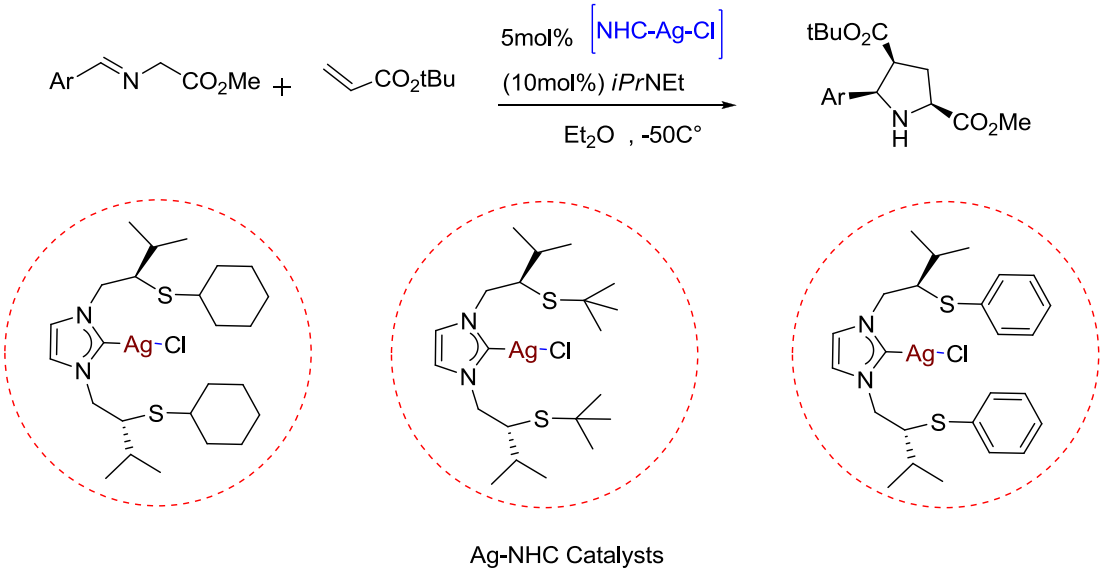

Scheme 28. Ag-NHC complexes catalyzed enantioselective cycloaddition of azomethines and acrylates

In a comparative study encompassing NHC complexes of all three coinage metals, Pérez and Echavarren reported that [(IPr)AgCl] and [(SIPr) AgCl] were able to mediate the cyclopropanation reaction between styrene and phenyldiazoacetate, albeit in lower yields than their copper and gold analogs [102]. Wang and co-workers demonstrated that the [(IPr)AgCl] catalytic system could be used to synthesize epoxides by carbene transfer onto aldehydes [103]. The use of the A^3 (aldehyde–alkyne–amine) coupling reaction represents a benchmark transformation to evaluate the catalytic activity of new NHC–Ag complexes gained a lot of attention since the first examples of this protocol were reported in the early 2000s by Ishii [104], Carreira [105] and Li. [106]. A variety of propargyl amines were efficiently synthesized by this method in the presence of diverse NHC–Ag complexes [107].

Several groups also used NHC–Ag catalysis to enhance the reaction between a terminal alkyne and an electrophile, resulting in Sonogashira couplings and the addition of alkynes to isatins or CO_2. The use of supported NHC-Ag nanoparticles contributed to the efficiency of the process, which was attributed to the activation of the alkyne by the NHC-Ag complex and the activation of CO_2 by a free NHC component in a cooperative manner. The NHC-Ag catalyst was also used to synthesize cyclic carbonates and carbamates from epoxides, propargyl alcohols, or allenyl amines by exploiting CO_2 insertion [108] (Scheme 29).

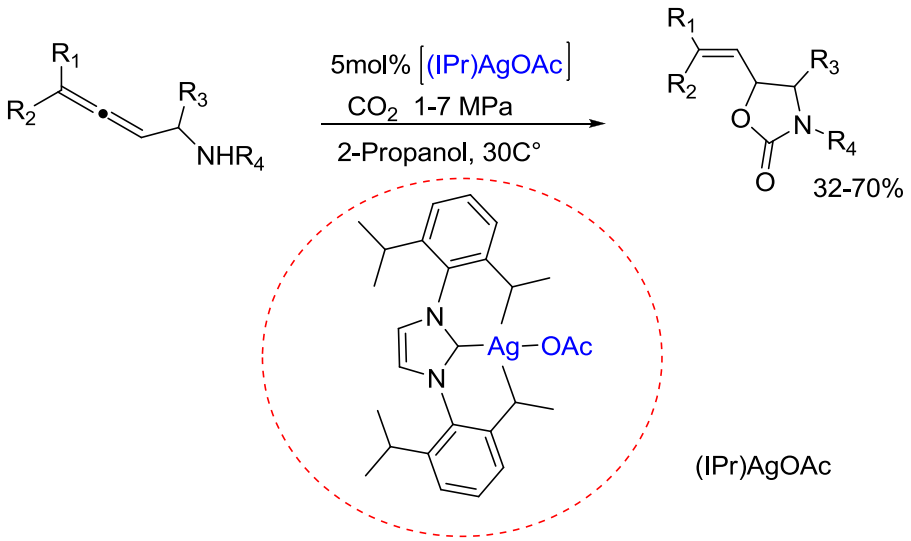

Scheme 29. Ag-NHC complexes enhance the reaction between a terminal alkyne and an electrophile, resulting in Sonogashira couplings

Catalytic diboration of alkenes, a reaction of interest in the synthesis of diols, with an (NHC)Ag complex has been reported by Peris, Fernandez, and coworkers [109]. They have prepared a new silver complex of composition [(mentimid)2Ag] $AgCl_2$ containing the mentimid ligand (1-methyl-3-(+)-methylmenthoxide imidazolidene). This complex catalyzes the reaction of the terminal, as well as internal, alkenes with bis(catecholato)diboron (Scheme 30) to give the corresponding diols after treatment with $NaOH/H_2O_2$, in the first example of a silver-based catalyst for this transformation.

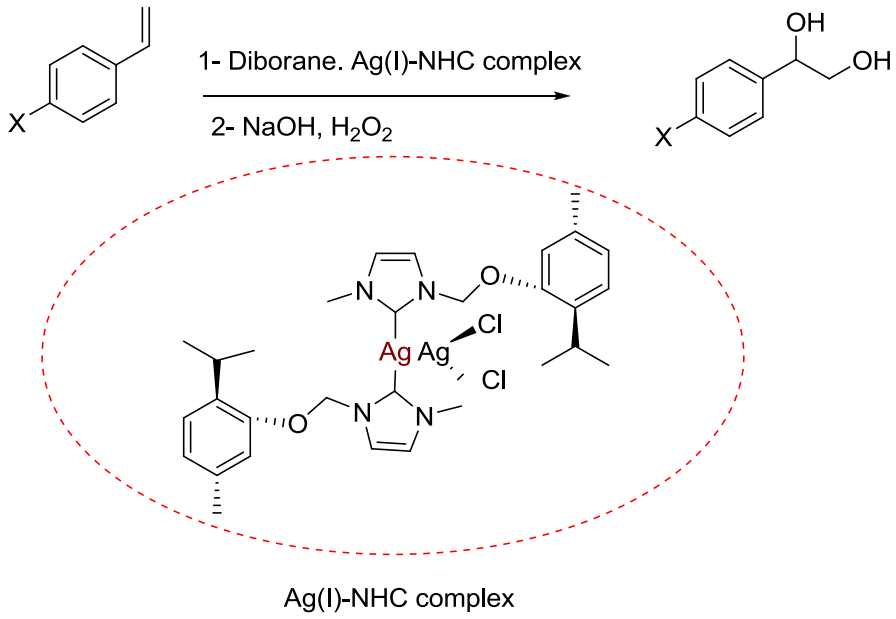

Scheme 30. Catalytic diboration of alkenes with silver NHC complex

I.7.2.2 NHC–Palladium Complexes in Catalysis

Palladium-NHC complexes have been used as catalysts since 1995 [110]. These complexes are particularly active in cross-coupling reactions and are used in large-scale applications such as the Suzuki-Miyaura, Mizoroki-Heck, and Sonogashira coupling reactions. Carbon-carbon cross-coupling reactions are the main application for these complexes, and in recent years there has been a significant amount of research on their use. Researchers such as Herrmann and Hahn have studied the performance of these complexes in various reactions, using a wide range of different well-defined phospha-palladacycle and benzannulated NHC complexes (Scheme 31).

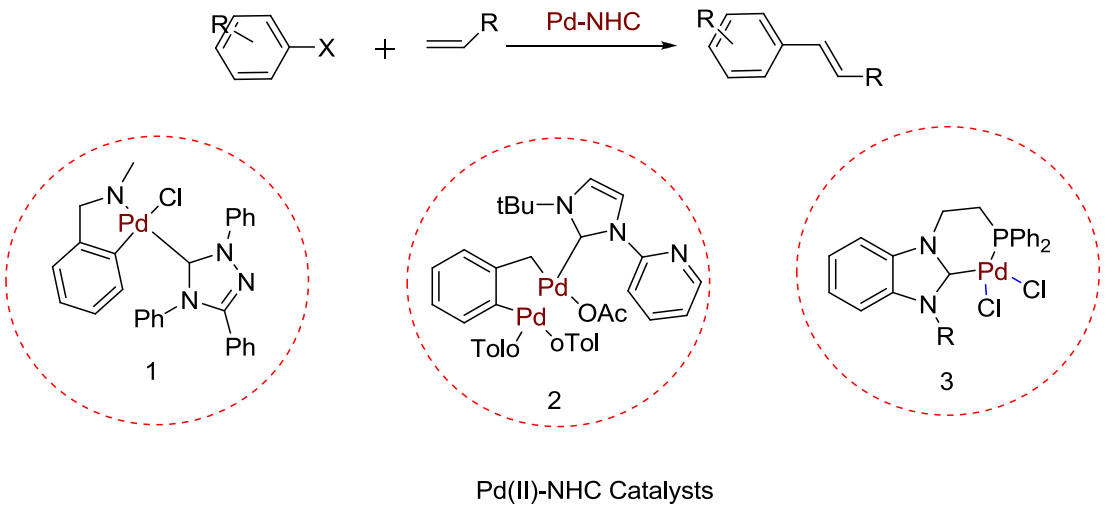

Scheme 31. Pd(II)-NHC complexes for Suzuki reactions

The application of NHC ligands in Suzuki reactions has been widely studied. A series of NHC complexes, which include phosphine and imidazolyl-based palladacycles, were evaluated for their effectiveness in Suzuki couplings in Figure 28.

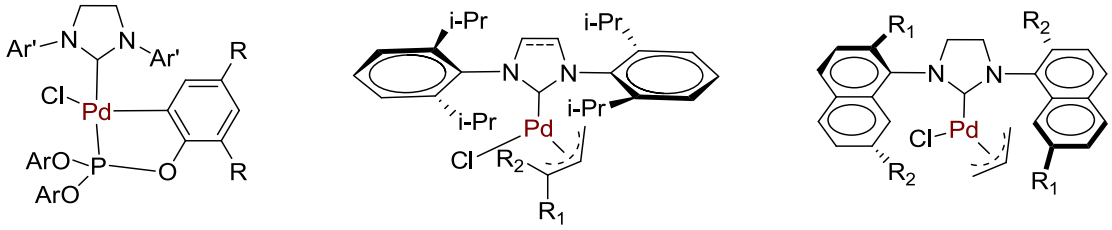

Figure 28. Pd(II)-NHC complexes for Suzuki reactions

In 2006, a group of researchers led by Organ developed a family of NHC-Pd(II) complexes, called NHC-Pd-PEPPSI, that were successful in cross-coupling reactions[90]. They also developed a user-friendly Negishi protocol that could be used to couple a wide range of alkyl and aryl substrates using the complexes [111] (Figure 29).

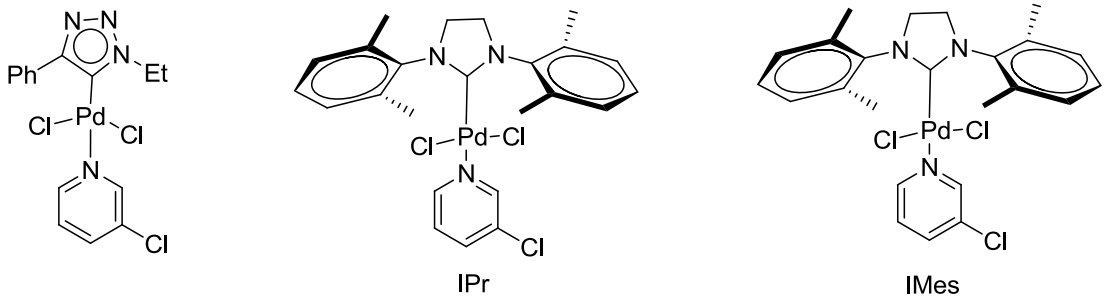

Figure 29. NHC–Pd(II) PEPPSI type complexes for Suzuki reactions

Additionally, in the same year, Glorius and coworkers reported the use of bi-oxazoline-derived NHC ligands as NHC-Pd dimer complex for Sonogashira coupling of alkynes with unactivated secondary alkyl bromides. This was the first example of using NHC-Pd complexes for these types of reactions (Figure 30).

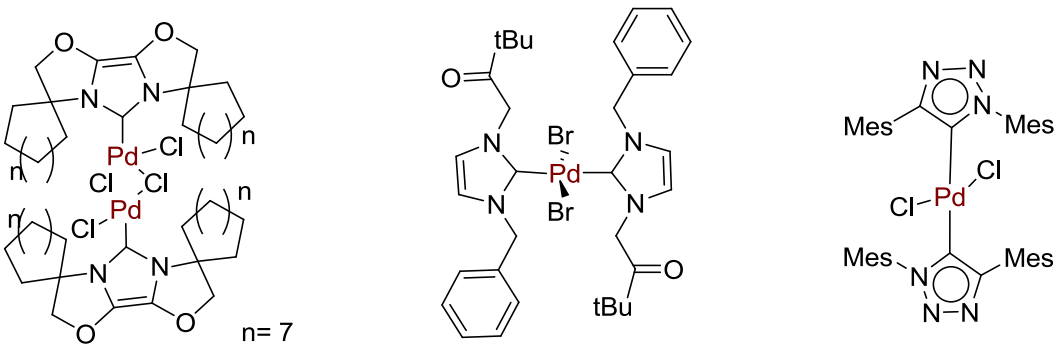

Figure 30. Pd(II)-NHC complexes used in Sonogashira coupling

In 2009, Ghosh and coworkers studied the use of (NHC)–Pd PEPPSI type complexes as catalysts in Hiyama cross-coupling reactions[112]. Later, Lu and colleagues created a 1-methylimidazole analog of these complexes, known as (NHC)Pd(Im)Cl [113]. More recently, Yang and Wang developed four new linear dinuclear NHC-Pd complexes[114]. The results of using these complexes as catalysts in Hiyama coupling reactions showed that complexes with more sterically demanding ligands were more effective, with the complex $[(IPr)PdCl_2]_2$(μ-pyrazine) being the most efficient (Figure 31).

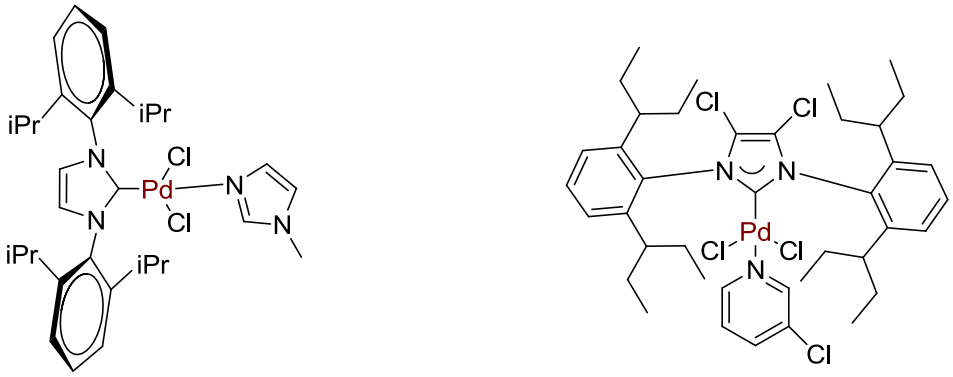

Figure 31. NHC-Pd(II) complexes used in Hiyama Coupling

In 2007, Tandukar and Sen reported the synthesis of the imidazolium-based NHC-Pd complex [115]. As well as Shao and coworkers synthesized a proline-derived complex that was active for Heck reactions of aryl iodides and bromides in water [116] (Figure 32).

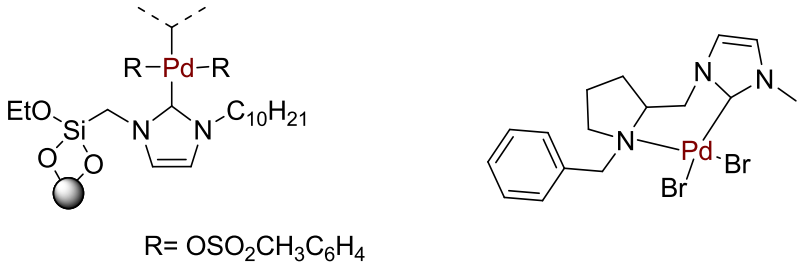

Figure 32. NHC-Pd(II) complexes used in Heck Reaction coupling

The reactions based on direct C–H functionalization, specifically Pd-catalyzed direct arylation, have witnessed extraordinary progress [117]. In 2005, Sames reported the use of several NHC–Pd complexes in the direct arylation of protected heterocycles with aryl halides [118] (Scheme 32).

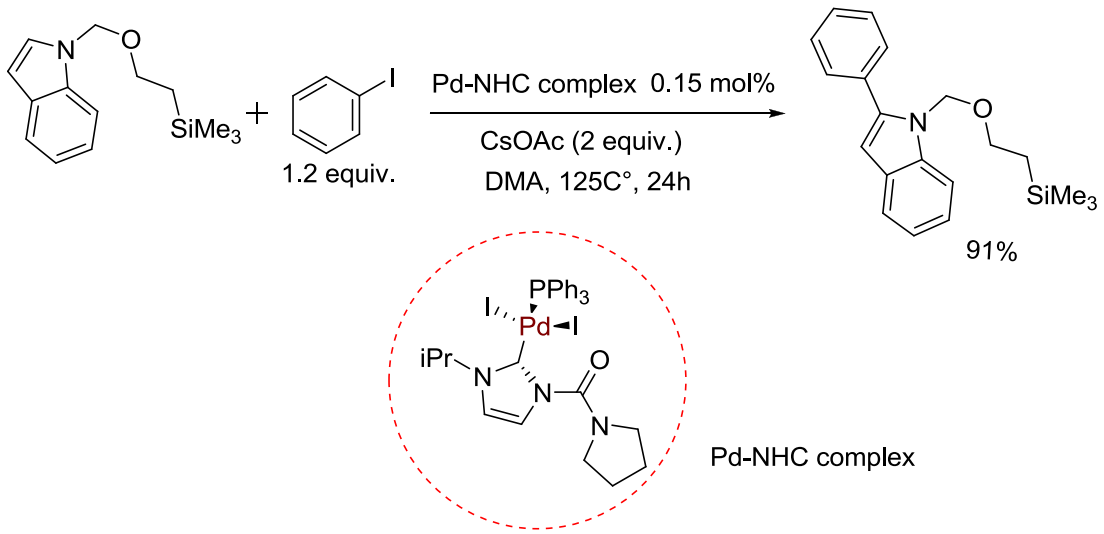

Scheme 32. Direct Arylation by C–H Functionalisation using NHC-Pd complexes

Greaney studied the application of PEPPSI-IPr in the direct arylation of oxazoles. Huynh examined dipalladium Janus-type triazole-based NHC complexes, for the arylation of imidazoles [119] (Figure 33).

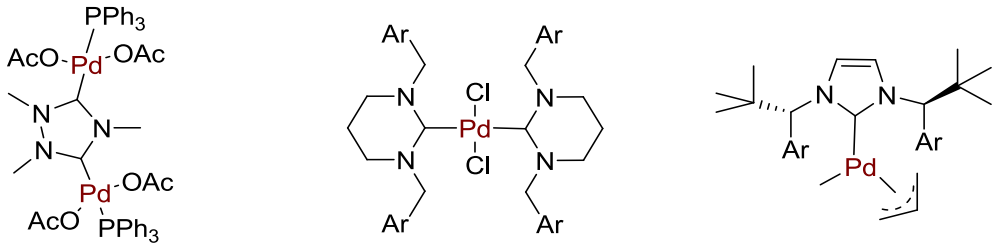

Figure 33. NHC-Pd(II) catalysts used in the direct arylation

The acidity of protons in the α position of carbonyl compounds can be exploited in Pd-catalysed ketone arylation. Using a specific type of molecule called monodentate NHCs has been highly effective in ketone arylation. The groups of Nolan [120] and Bertrand[121] reported a variation of catalysts for this purpose (Figure 34).

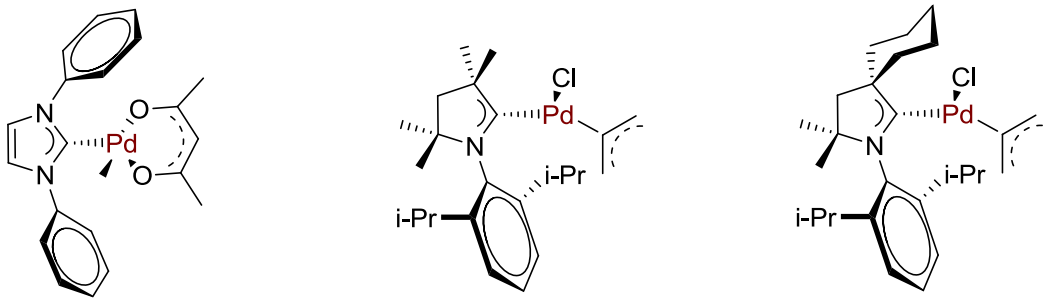

Figure 34. NHC-Pd(II) catalysts used in ketone arylation

Aryl amination, known as Buchwald-Hartwig coupling, is a widely used technique in organic synthesis. Research has focused on using NHC-Pd complexes as catalysts for this reaction. In 2002, Nolan discovered that [(NHC)Pd(π-allyl)Cl] complexes were effective catalysts in cross-coupling reactions, including aryl amination[122] (Figure 35).

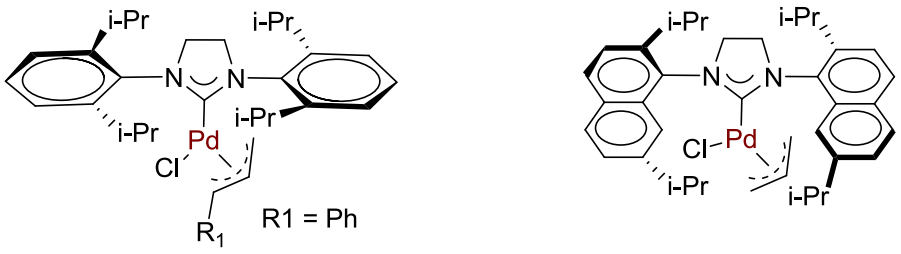

Figure 35. Pd(II)–allyl NHC catalysts for aryl amination

II. Results and Discussion

I.1 Synthesis of 5,6-dimethylbenzimidazolium Salts (2a–f)

The synthesis of benzimidazolium salts was done following a slightly altered method from previous literature methods [123]. The 5,6-dimethylbenzimidazolium salts (**2a-f)** were synthesized through two *N*-alkylation reaction processes as illustrated in scheme 33. Compound (**1)** as a starting material was obtained from the first reaction between 5,6-dimethylbenzimidazole and Bromodiphenylmethane. The second *N*-alkylation reaction produced the six benzimidazolium salts (**2a-f)** by reacting *N*-benzhydryl-5,6-dimethylbenzimidazole (**1)** with different benzylchloride and benzylbromide (Scheme 33).

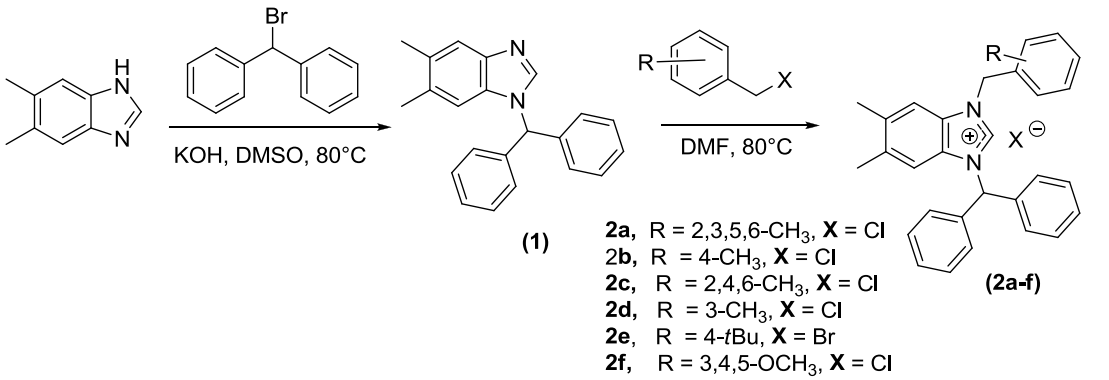

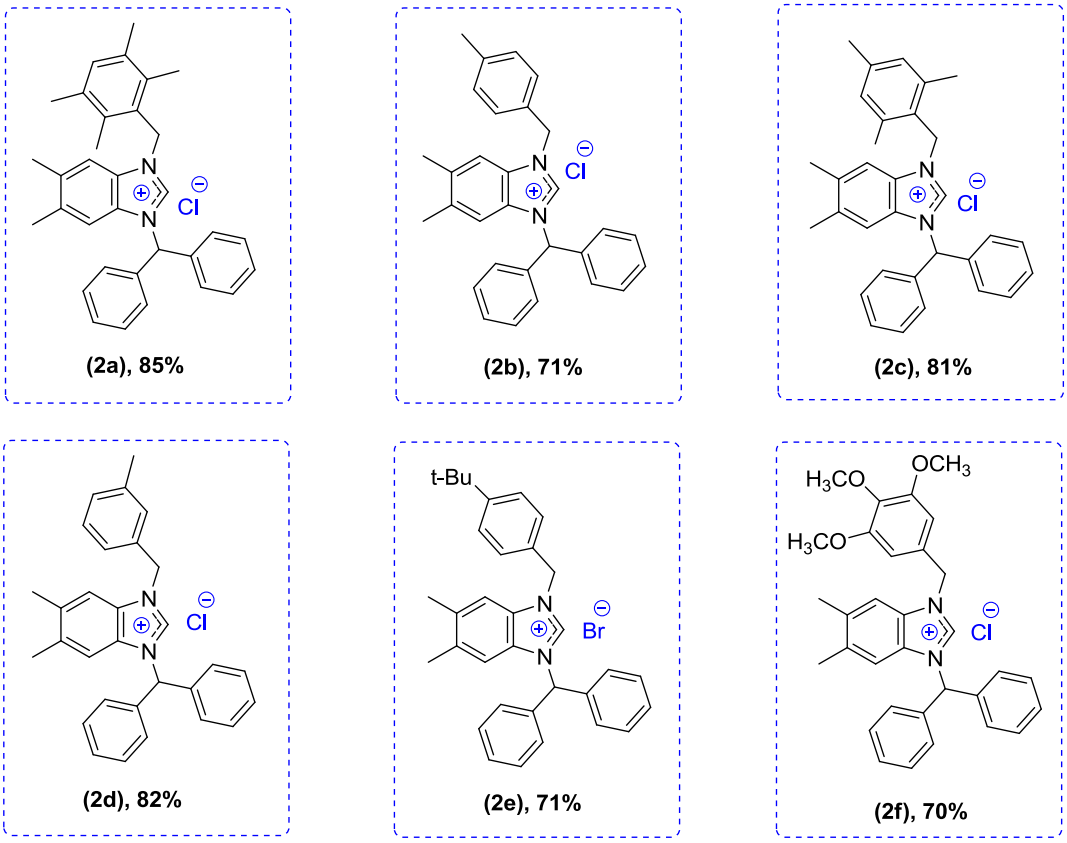

Scheme 33. Synthetic route and the structure of benzimidazolium salts **(2a-f)**

The six new 5,6-dimethylbenzimidazolium salts (**2a-f)** were successfully produced in solid form with good yield. Their spectroscopic data matches what has been reported for other benzimidazolium salts in previous studies [124,125]. A summary of their physical and some spectroscopic data is provided in Table 1.

Table 1. Physical and Spectroscopic data for 5,6-dimethylbenzimidazolium salts (**2a-f)**

Code	Chemical Formula	Molecular Weight (g/mol)	Yield (%)	Melting point °C	^{1}H NMR C*H* (C2) ppm	^{13}C NMR C (C2) ppm	IR *ν*(CN) cm^{-1}
2a	$C_{33}H_{35}ClN_2$	495.10	85	152-153	10.52	142.3	1549
2b	$C_{30}H_{29}ClN_2$	543.02	71	159-160	11.27	142.6	1548
2c	$C_{32}H_{33}ClN_2$	481.07	81	155-156	10.91	142.8	1546
2d	$C_{30}H_{29}ClN_2$	453.02	82	151-152	11.15	142.5	1541
2e	$C_{33}H_{35}BrN_2$	539.55	71	179-180	10.75	141.6	1542
2f	$C_{32}H_{33}ClN_2O_3$	529.08	70	157-158	11.27	142.7	1552

These new 5,6-dimethylbenzimidazolium salts were characterized by different techniques. The FT-IR results showed that 5,6-dimethylbenzimidazolium salts (**2a-f)** had a characteristic $\nu_{(C-N)}$ band typically for all salts around [1541 - 1552] cm^{-1}.

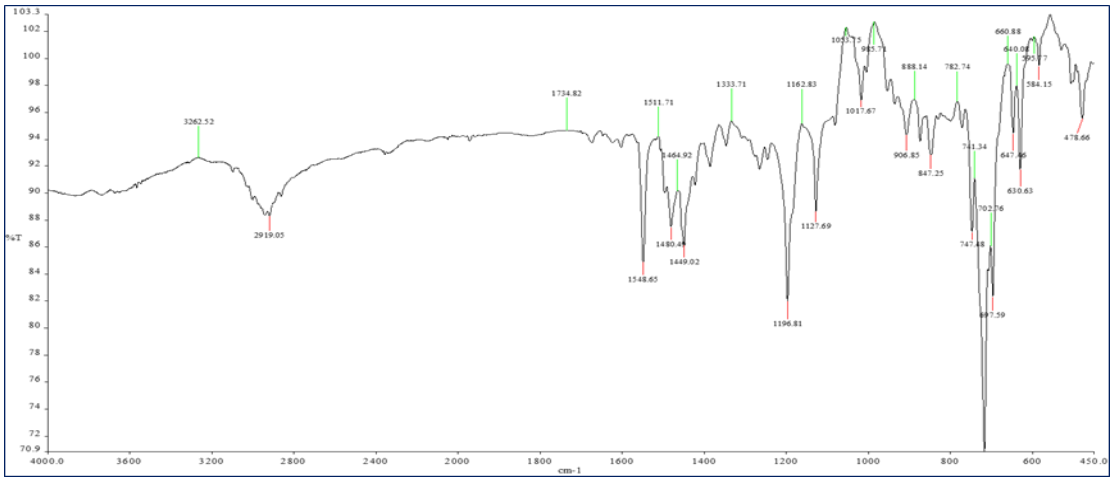

Spectrum 1. IR spectrume of Benzimidazolium salt (**2a)**

The NMR results are presented by chemical shifts in parts per million (ppm) of different protons in a molecule as measured by ^{1}H NMR spectroscopy and ^{13}C NMR spectroscopy. The chemical shifts can be used to identify the chemical environment and multiplicity of each proton, providing insights into the molecular structure.

In ^{1}H NMR, it appears that all new compounds (**2a-f)** do not exhibit significant changes in the chemical shifts of the aromatic protons when compared to the starting

compound, 1-benzhydryl-5,6-dimethyl-1*H*-benzo[d]imidazole. The presence of the acidic proton NCHN was confirmed by the pick of its signal at [10.52-11.27] ppm for all salts (**2a-f)**.

The ^{13}C NMR showed that the carbon NCHN was present as a typical single peak between [141.6-142.8] ppm for all salts (**2a-f)**.

To perform a comprehensive analysis of the new compounds, compound (**2a)** was chosen as a representative sample.

The ^{1}HNMR spectrum of compound (**2a)** showed a peak for the acidic proton NCHN at 10.45 ppm. The spectrum exhibited the expected signals which were observed, around [7.01 - 7.62] ppm, and the peak at 6.93 ppm which is from a proton of CH linked to the two phenyl rings. The peak at 5.90 ppm represents two protons of a methylene group (CH_2) adjacent to a nitrogen atom. Signals at 2.23 and 2.19 correspond to two methyl groups (-CH_3) of benzimidazole. As well as new peaks appearing as two singlets at 2.21 and 2.19 ppm correspond to four different methyl groups (-CH_3) in the benzyl group.

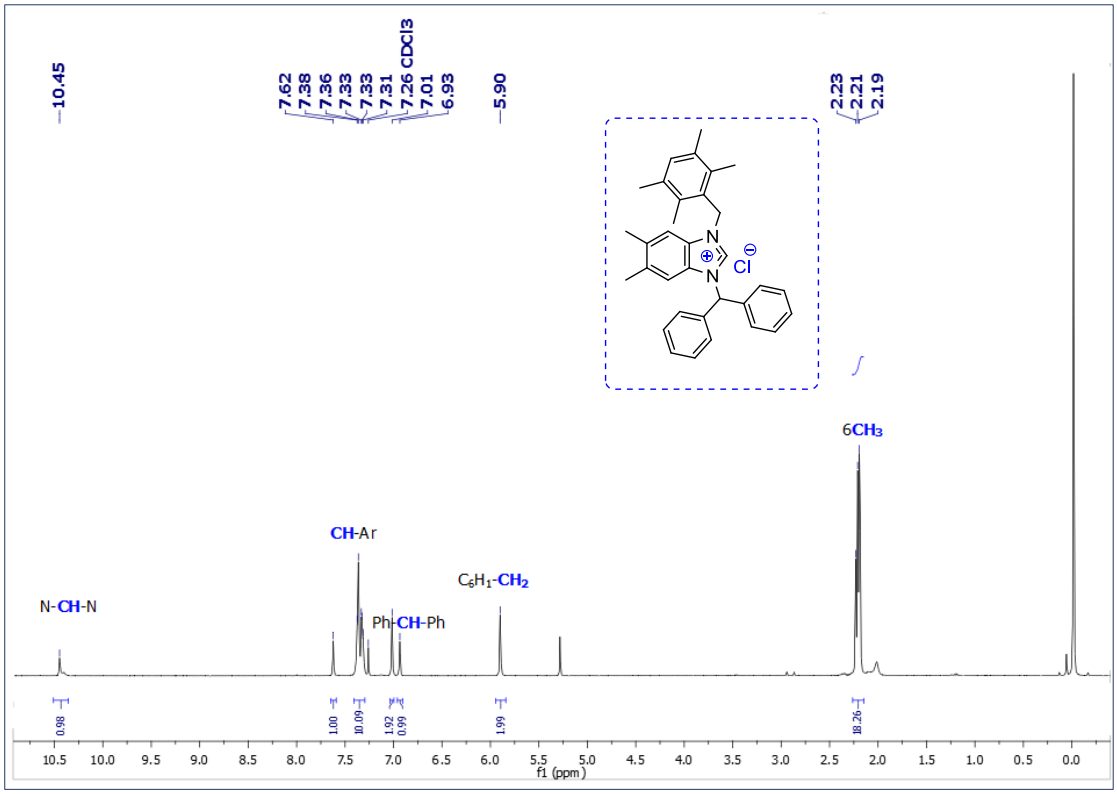

Spectrum 2. ^{1}H NMR spectrume (400 MHz,$CDCl_3$) of Benzimidazolium salt (**2a)**

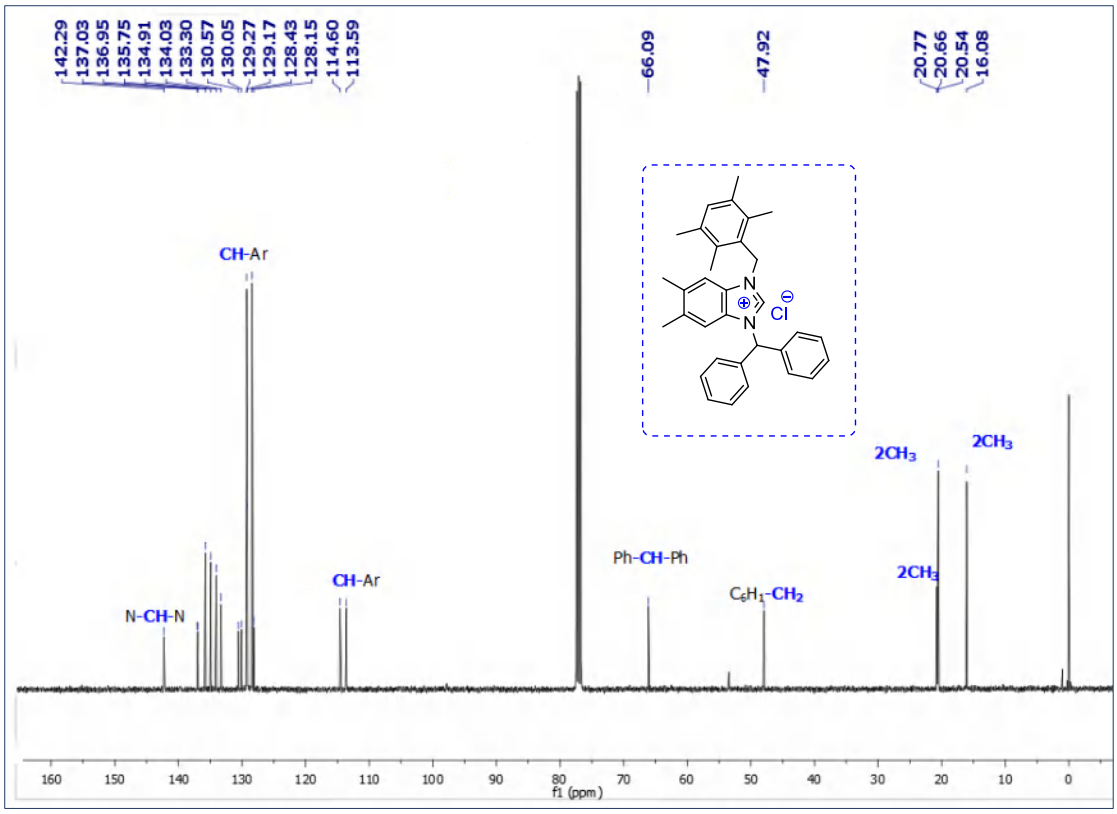

Spectrum 3. ^{13}C NMR spectrum (100 MHz,$CDCl_3$) of Benzimidazolium salt (**2a)**

Based on the information provided, here is a possible interpretation of the ^{13}C NMR spectrum: The spectrum of compound (**2a)** showed a peak at 142.3 ppm corresponding to a carbon atom adjacent to a nitrogen atom (NCHN). The peaks at 137.0 and 133.3 ppm correspond to different types of quaternary carbon atoms with a methyl group (C-CH_3). The peaks at 130.6 and 130.0 ppm correspond to two different types of carbon atoms with a nitrogen atom (Cq, C-N). The peaks between 129.2 and 128.1 ppm correspond to the carbon atoms in an aromatic ring. The peak at 66.1 ppm corresponds to a carbon atom in a phenyl group connected to another phenyl group via a methylene group (Ph-CH-Ph). The peak at 47.9 ppm corresponds to a carbon atom in a methylene group adjacent to a nitrogen atom (N-CH_2). The peaks at 20.8, 20.7, 20.5, and 16.1 ppm correspond to different methyl groups (-CH_3).

The elemental analysis results of the new benzimidazolium salts are in agreement with the proposed molecular formula.

I.2 Synthesis of silver(I)-NHC complexes (3a-f)

Silver(I)-NHC complexes were prepared according to the original procedure reported by Lin and coworkers [83]. All Ag(I)–NHC complexes (**3a-f)** were synthesized *via* the *in situ* deprotonation of 5,6-dimethylbenzimidazolium salts by Silver(I) oxide Ag_2O. Treatment of the benzimidazolium salts with Ag_2O in chloroform at 50°C in dark conditions to generate the desired silver complexes Ag (I)-NHC (**3a-f)** as shown in Scheme 34.

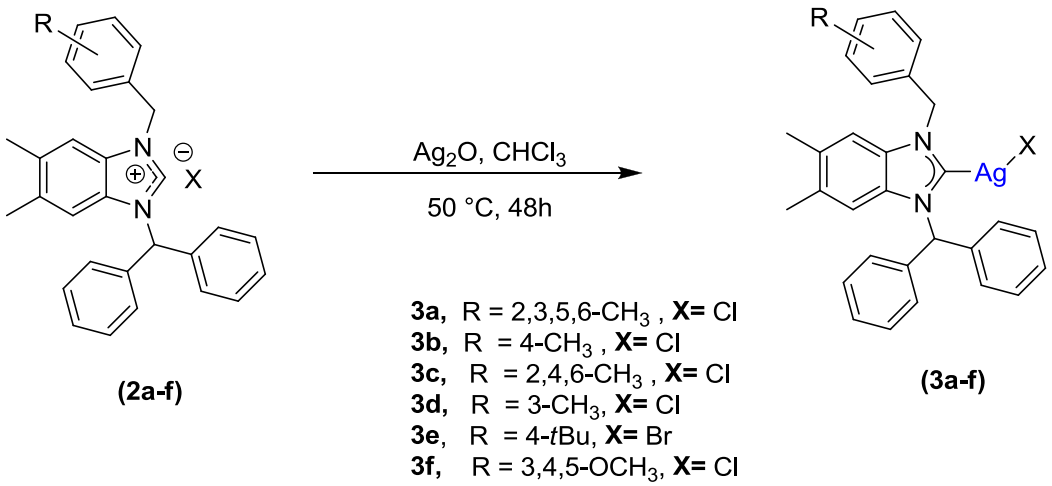

Scheme 34. Synthetic route of Ag(I)–NHC complexes (**3a-f)**

The silver-NHC complexes (**3a-f**) were successfully obtained as white solids in high yields. All the new Ag(I)-NHC complexes (**3a-f)** shown in Scheme 34 were obtained as white solids in good yields, soluble in halogenated solvents. In the air, these complexes are stable but light-sensitive.

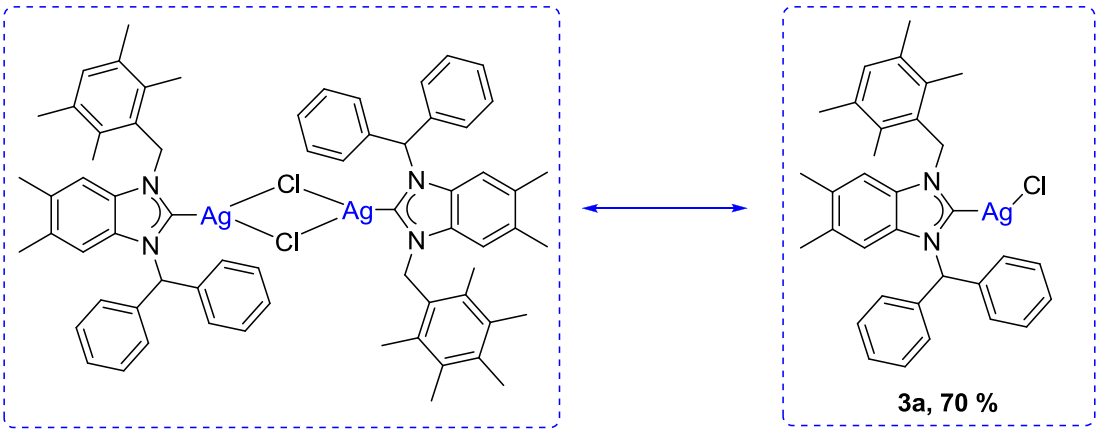

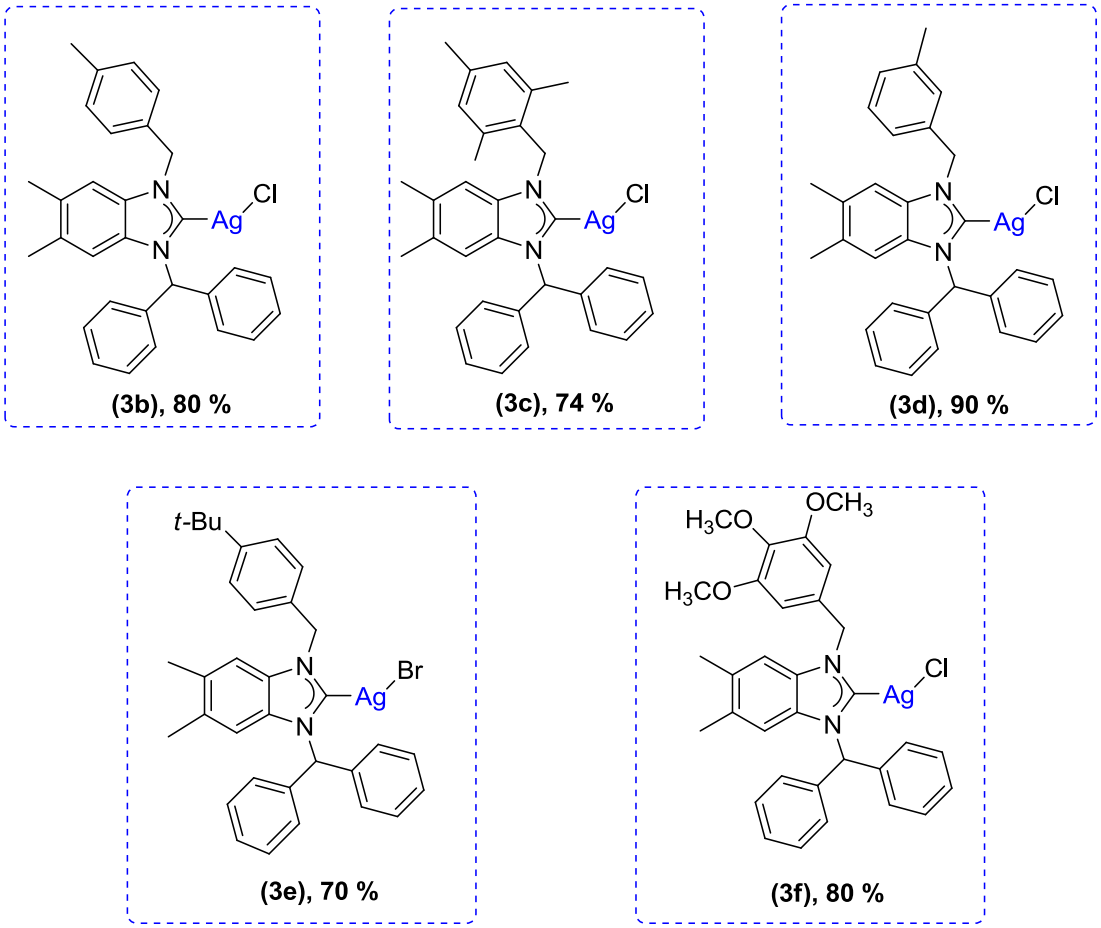

Figure 36. Structures of prepared silver(I)-NHC complexes (**3a–f)**

The spectroscopic data of these complexes aligns with what has been reported for other Ag(I)-NHC complexes in literature [124,126]. A summary of their physical and some spectroscopic data can be found in Table 2.

Table 2. Physical and Spectroscopic data for Ag(I)-NHC complexes[127]

Code	Chemical Formula	Molecular Weight (g/mol)	Yield (%)	Melting point °C	^{1}H NMR C*H* (C2) ppm	^{13}C NMR C (C2) ppm	IR *ν*(CN) cm^{-1}
3a	$C_{32}H_{34}AgClN_2$	601.97	70	245-246	-	-	1471
3b	$C_{30}H_{28}AgClN_2$	559.89	80	144-145	-	-	1484
3c	$C_{32}H_{32}AgClN_2$	584.97	74	200-201	-	-	1496
3d	$C_{30}H_{28}AgClN_2$	559.89	90	222-223	-	-	1485
3e	$C_{33}H_{34}AgBrN_2$	601.96	70	219-220	-	-	1481
3f	$C_{32}H_{33}AgClN_2O_3$	635.93	80	117-118	-	-	1505

These new six Ag(I)-NHC complexes (**3a-f)** were characterized by different techniques. The FT-IR data indicated that Silver(I)-NHC complexes show a characteristic *ν*(CN), band, typically for all complexes (**3a-f)** at 1471, 1484, 1496, 1485, 1481, and 1505 cm^{-1} respectively.

The characteristic proton peak NCHN of the starting benzimidazolium salts was not detected in the ^{1}H NMR spectra of the novel Ag(I)-NHC complexes. This disappearance of the NCHN peak indicates that the reaction has indeed occurred, and the Ag(I)-NHC complexes have been formed. Similarly, in the ^{13}C NMR data, the characteristic signals of carbon NCHN are observed in the starting benzimidazolium salts at around 144 ppm, However, they disappear after the formation of silver NHC complexes, confirming the successful formation of the complexes.

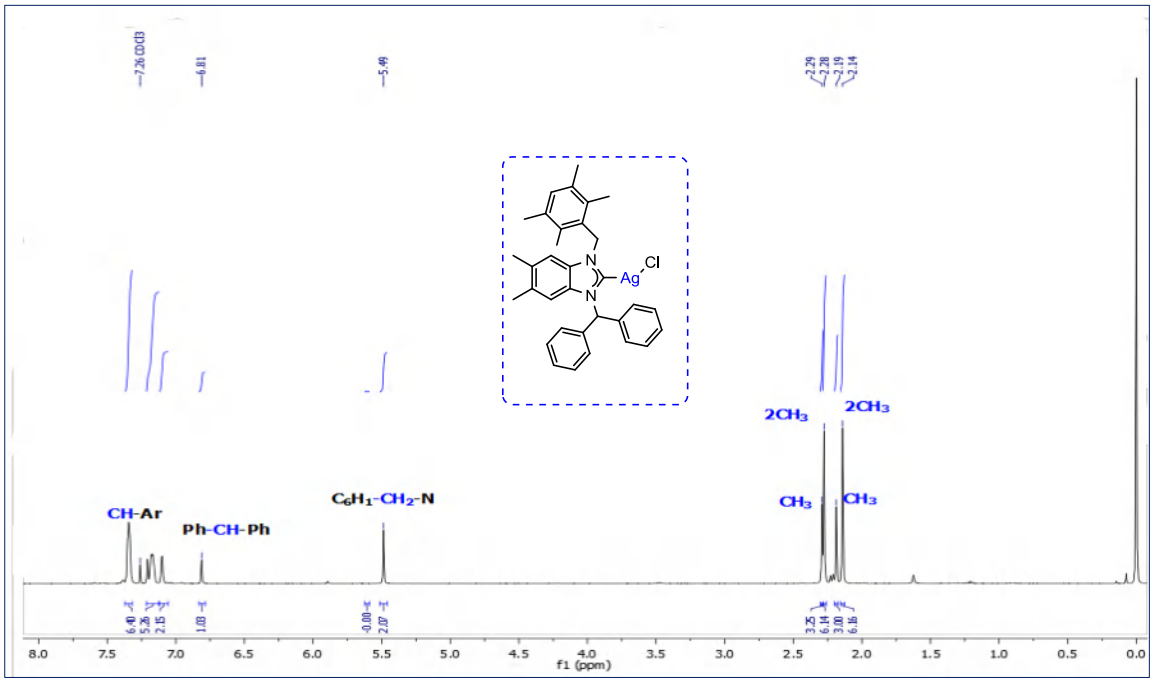

Spectrum 4. ^{1}HNMR spectrum (400 MHz,$CDCl_3$) of Silver(I)-NHC complex (**3a)**

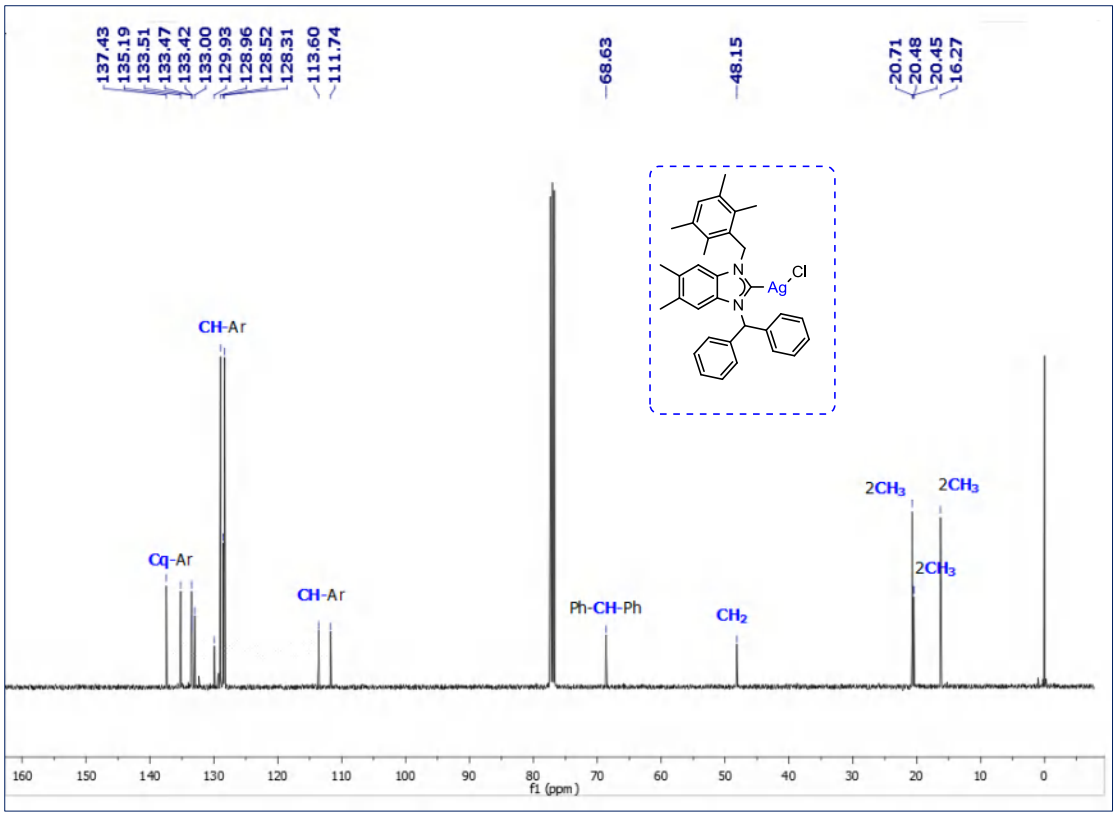

Spectrum 5. ^{13}CNMR spectrum (100 MHz,$CDCl_3$) of silver(I)-NHC complex (**3a)**

I.3 Synthesis of PEPPSI-type palladium–NHC complexes (4a-f)

The Pd(II)-NHC complexes PEPPSI-type (**4a–f)** were synthesized according to procedures described by Organ [90]. The synthesis was done through a simple procedure *via in situ* deprotonation of 5,6-dimethylbenzimidazolium salts (**2a-f)** as a precursor with an external base. The K_2CO_3 base deprotonates the bezimidazolium salt to generate the free carbene *in situ*, which can directly coordinate with the Pd center. The pyridine was used to act as co-ligand, completing the square planar coordination sphere[128,129] (Scheme 35).

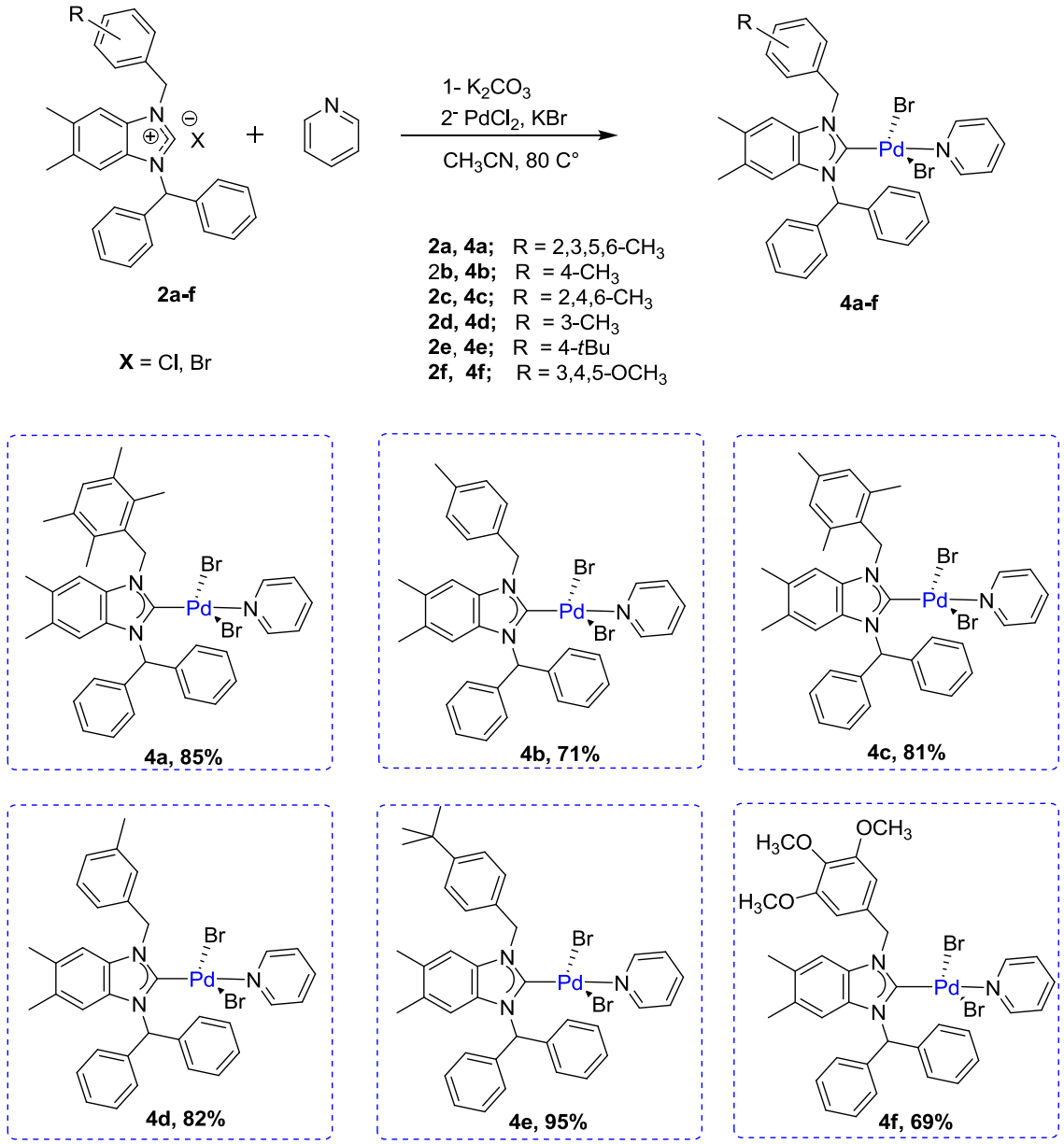

Scheme 35. Synthetic route and the structure of Pd(II)-NHC complexes PEPPSI-type (**4a-f)**

The six newly synthesized Pd(II)-NHC complexes (**4a-f)** exhibit good solubility in most organic solvents such as chloroform, dichloromethane, ethanol, acetonitrile, and dimethylsulfoxide excluding non-polar solvents like pentane and hexane. They are also stable in both solution and solid form against air, light, and moisture, and can be stored at room temperature for several months without affecting their catalytic efficiency. The compounds were confirmed to have formed through spectroscopic techniques such as NMR, FT-IR, and elemental analysis. A summary of their physical and spectroscopic data is provided in Table 3.

Table 3. Physical and some spectroscopic data of Pd(II)-NHC complexes PEPPSI-type (**4a-f)**

Code	**Chemical Formula**	**Molecular Weight (g/mol)**	**Yield (%)**	**Melting point °C**	**^{1}H NMR C*H* (C2) ppm**	**^{13}C NMR (C2) ppm**	**IR *ν*(CN) cm^{-1}**
4a	$C_{38}H_{39}Br_2N_3Pd$	803.98	85	244-245	-	163.1	1400
4b	$C_{35}H_{33}Br_2N_3Pd$	761.90	71	292-293	-	163.3	1400
4c	$C_{37}H_{37}Br_2N_3Pd$	789.95	81	153-154	-	163.1	1400
4d	$C_{35}H_{34}Br_2N_3Pd$	761.88	82	157-158		163.5	1400
4e	$C_{38}H_{40}Br_2N_3Pd$	803.96	95	276-277	-	163.3	1399
4f	$C_{37}H_{38}Br_2N_3O_3Pd$	837.93	69	264-265	-	163.2	1404

The FT-IR spectroscopy data show that the Pd(II)-NHC complexes (**4a-f)** have a recognizable *ν*(CN) band between [1399-1404] cm^{-1}. The creation of carbenes is linked to a change in the ν(CN) vibration, which is shown in the similar absorption bands in the FT-IR spectra of the six complexes. This is due to the transfer of electrons from the carbene ligand to the palladium center, causing a weaker C=N bond and a lower *ν*(CN) stretching frequency.

In the ^{1}H NMR, the downfield resonances of the aromatic hydrogens of the pyridine ring were observed in the range of δ = [7.71-8.99] ppm, indicating that the pyridine ring has formed a PEPPSI-type palladium complex with the palladium center. Also, the characteristic proton peak at the 2-position does not appear as a signal of the acidic proton (NC<u>H</u>N) which confirms the formation of the Pd-carbene bond.

In the ^{13}C NMR, the characteristic Pd–C2-carbene signals of (**4a-f)** complexes appear as a singlet between δ = [163.1-163.3] ppm. The signals of aromatic carbons of the pyridine ring were detected between δ = [124.4-152.8] ppm, for the first two aromatic carbons (**C**N**C**) of the pyridine ring of (**4a-f)** complexes were detected at 152.6, 152.5, 152.6, 152.8, 152.6, and 152.6 ppm, respectively. The second two carbons **C**–CNC–**C** of all Pd-NHC complexes (**4a-f)** were detected at 124.4, 124.4, 124.2, 124.4, 124.5, and 124.4 ppm, respectively. As well as the last carbon for the carbon CH-**C**-CH was detected at δ =137.6, 137.6, 137.7, 138.5, 137.8, and 137.7 ppm, respectively.

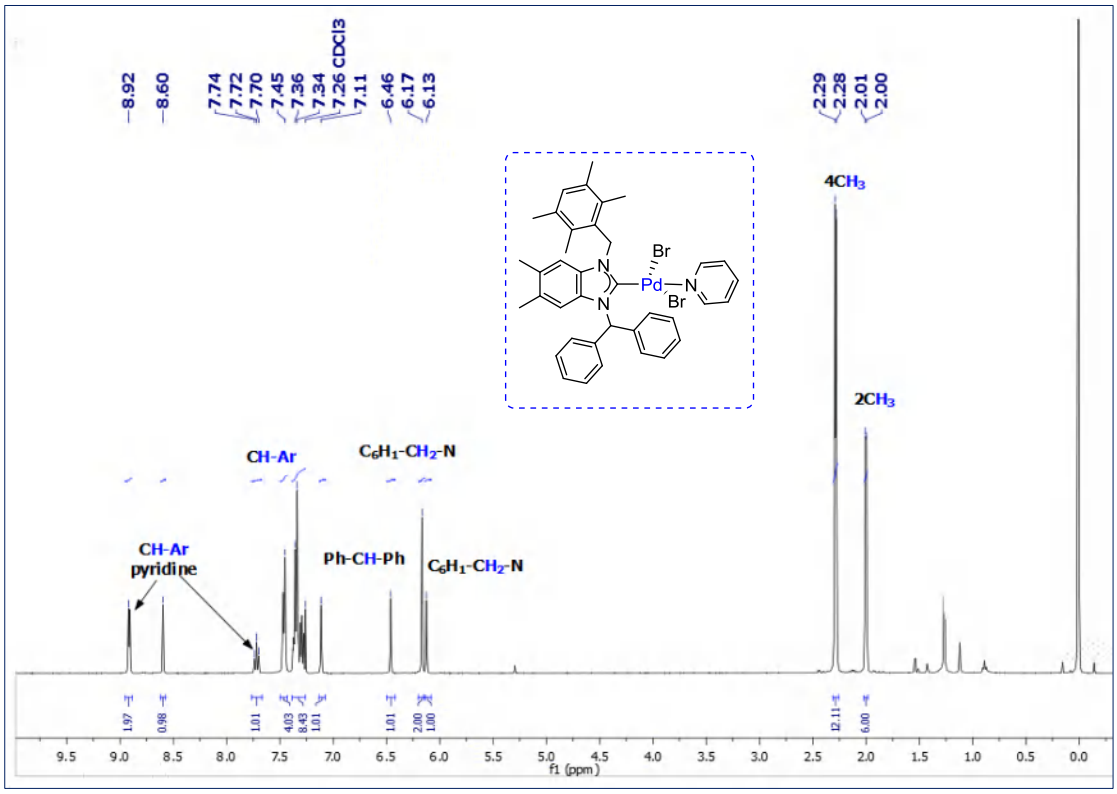

Spectrum 6. ^{1}HNMR spectrum (400 MHz,$CDCl_3$) of Palladium(II)-NHC complex (**4a)**

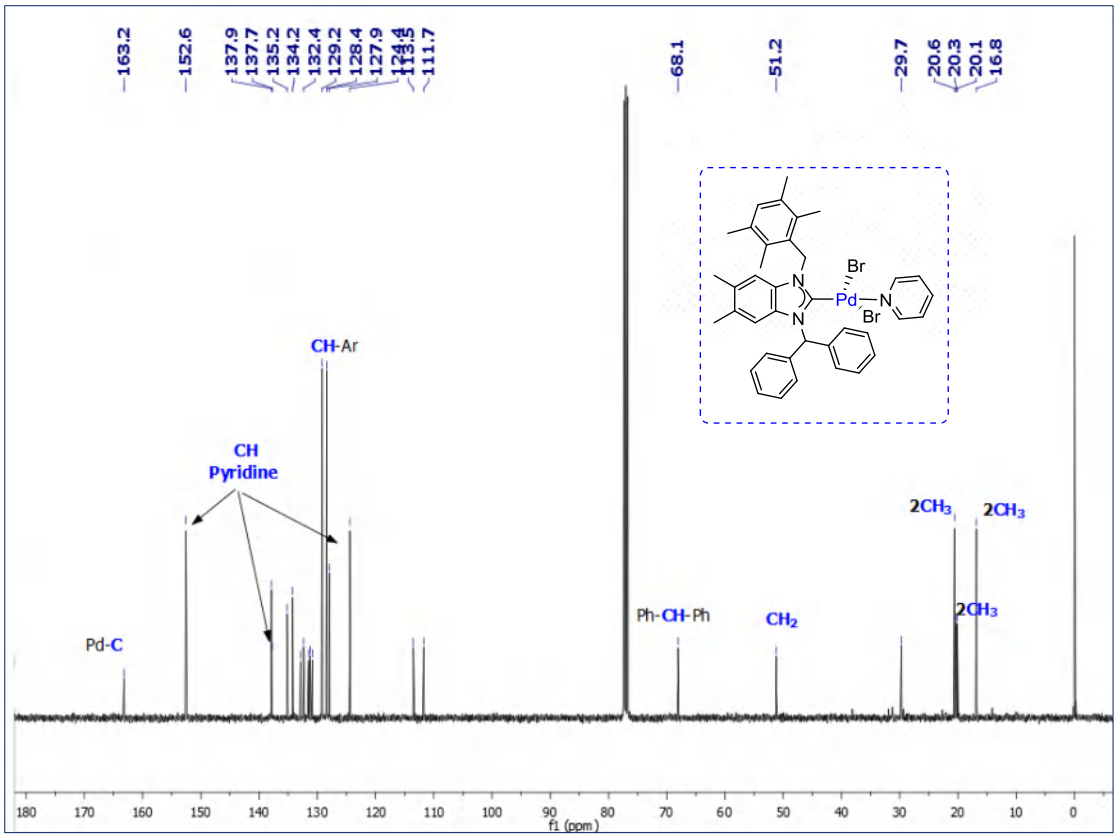

Spectrum 7. ^{13}CNMR spectrum (100 MHz,$CDCl_3$) of Palladium(II)-NHC complex (**4a)** $CDCl_3$

The elemental analysis results of these complexes are in agreement with the proposed molecular formula. These six new complexes show typical spectroscopic signatures, values are in agreement with reported data for similar PEPPSI type Pd(II)-NHC complexes[130,131]

I.4 Crystallography study

I.4.1 Crystal structures of benzimidazolium salts and silver (I)-NHC complexes

The molecular diagrams of (**2c**), (**2f**), and (**3a**) with the adopted atom labeling are shown in (Fig 37-39), while important bond distances and angles are listed in Table 4.

Table 4. Selected geometric parameters for (**2c**), (**2f**), and (**3a**) [127]

Parameters		5,6-Dimethylbenzimidazolium salts		Silver(I)-NHC complex
		2c	**2f**	**3a**
Bond lengths (Å)	Ag1─Cl1	-	-	2.464(2)
	Ag1─Cl1^{i}	-	-	2.629(2)
	Ag1─C1	-	-	2.111(8)
	N1─C1	1.351(7)	1.322(4)	1.342(9)
	N1─C2	1.392(7)	1.392(5)	1.390(9)
	N2─C1	1.341(7)	1.334(5)	1.355(10)
	N2─C9	1.406(8)	1.398(5)	1.391(9)
Bond angles (°)	Cl1─Ag1─C1	-	-	143.2(2)
	Cl1^{i}─Ag1─C1	-	-	124.1(2)
	Cl1─Ag1─Cl1^{i}	-	-	92.66(7)
	Ag1─Cl1─Ag1^{i}	-	-	87.34(7)
	Ag1─C1─N1	-	-	125.7(6)
	Ag1─C1─N2	-	-	127.9(6)
	N1─C1─N2	109.2(6)	110.5(3)	106.2(7)
	C1─N1─C2	109.6(5)	108.4(3)	111.4(7)
	C1─N2─C9	110.1(5)	107.6(3)	110.4(6)

Symmetry code: ^{i} −x+1/2, −y+3/2, −z+1.

I.4.1.1 Description of the structure of the salts 2c and 2f

The 5,6-dimethylbenzimidazolium salts (**2c)** and (**2f)** crystallize in chloroform/diethyl ether as depicted in Figures 37 and 38.

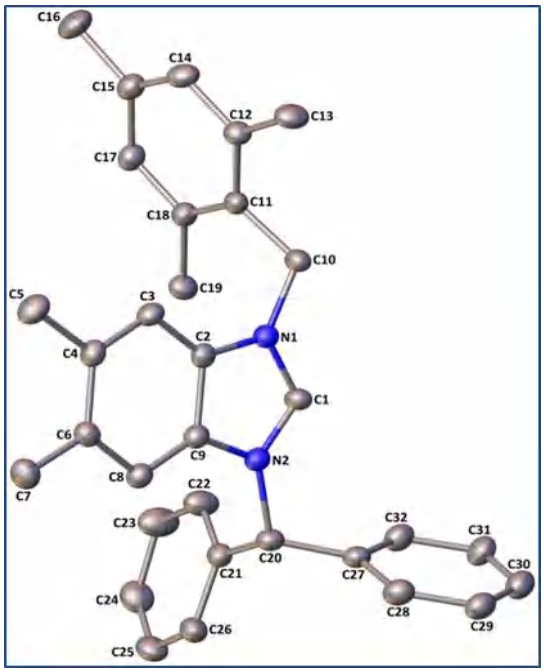

Figure 37. ORTEP structure of the salt **(2c)**

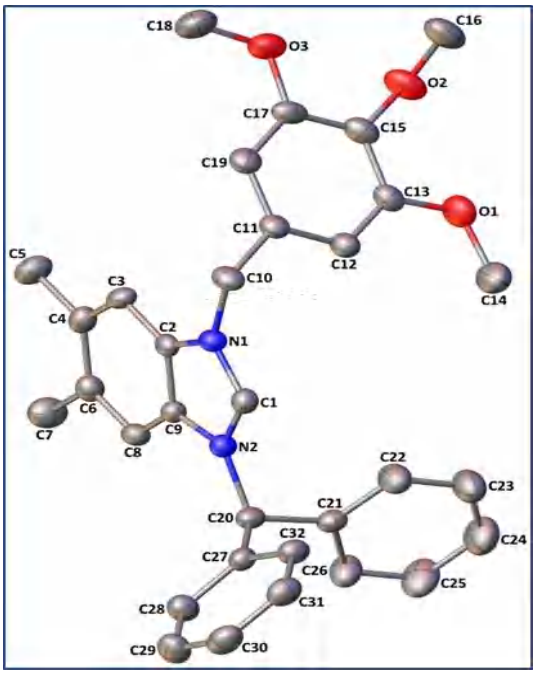

Figure 38. ORTEP structure of salt the **(2f)**

The compounds (**2c)** and (**2f)** crystallize as a salt in which the charge of the NHC cation is neutralized by a chloride anion. Furthermore, in their asymmetric units, (**2c)** contains two solvent water molecules whilst (**2f)** contains one dichloromethane molecule. The bonding within the imidazole rings indicates a pattern of delocalization that extends from atom N1 to atom N2 through atom C1, the N1─C1 and N2─C1 distances being significantly shorter than the N1─C2 and N2─C9 distances. The remaining bond lengths are normal within experimental uncertainty [132].

I.4.1.2 The structure description of the silver complex (3a)

The silver(I)NHC complex (**3a)** crystallizes in chloroform/diethyl ether as depicted in Figure 39. Complex **(3a)** crystallizes as dimers *via* bridging chloride atoms to form an $Ag_2(\mu\text{-}Cl)_2$ quadrangular arrangement which is frequently observed in silver complexes. Because of the inversion center, the Ag_2Cl_2 cluster is strictly planar at the mid-point of the Ag···Ag^{i} line [symmetry code: ^{i} $-x+1/2, -y+3/2, -z+1$], where each silver(I) atom is tri-coordinated with one carbene carbon atom and two chlorine atoms to adopt a distorted trigonal planar geometry. The two (NHC)AgCl moieties are present around an

inversion center with the chlorides asymmetrically bound to the silver center with different Ag─Cl bond lengths of 2.464(2) and 2.629(2) Å.

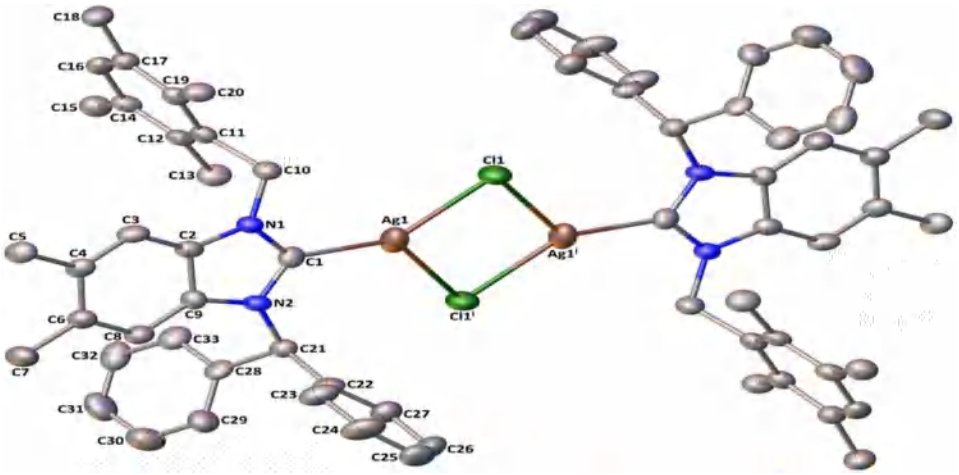

Figure 39. **ORTEP** structure of silver-carbene complexes (**3a)**

The Ag1─C1 distance of 2.111(8) Å falls in the range typical for other silver-carbene complexes[81]. With an angle of 143.2(2)° the C─Ag─Cl vector deviates from linearity as a result of coordination from an additional bridging Cl. The bond angles of the C1─Ag1─$Cl1^{i}$, Ag1─Cl11─$Ag1^{i,}$ and Cl1─Ag1─$Cl1^{i}$ are 124.1(2), 87.34(7), and 92.66(7)°, respectively. The Ag···Ag distance is 3.5186(11) Å, much greater than the sum of two van der Waals radii for Ag (3.44 Å) [133], ruling out the presence of any 'argentophilic' interaction. Due to the coordination of the NHC ligand, the ring's internal angle (N1─C1─N2) is reduced at the carbene center from 109.2(6) to 106.2(7)°. All the aforementioned data are comparable to those reported dinuclear Ag(I)-NHC complexes [58].

I.4.2 The structure description of Palladium NHC complexes

The solid-state structures of (**4a)**, (**4b)**, (**4d),** and (**4f)** with the adopted atom-labeling scheme are shown in Figures 40-43, while important bond distances and angles are listed in Table 05. The palladium complexes are four-coordinated in a square-planar geometry and surrounded by the carbene carbon atom of the NHC ligand, the nitrogen atom of the pyridine ring, and two bromine atoms. The complexes have a slightly distorted square-planar geometry, in which the anion atoms are *trans* to each other. The *cis* angles varying from 85.32(19) to 93.23(17)° and the *trans* angles changing from 173.05(4) to 179.17(14)° deviate from their ideal values of 90 and 180°, respectively. For quantitative

evaluation of the extent of distortion around the metal center, the structural indexes τ_4 τ_4' were employed;

$$\tau_4 = \frac{360° - (\alpha + \beta)}{360° - 2\theta} \qquad \tau_4' = \frac{\beta - \alpha}{360° - \theta} + \frac{180° - \beta}{180° - \theta}$$

where α and β $(\beta > \alpha)$ are the two greatest valence angles and θ is the ideal tetrahedral angle (109.5°). The τ_4 τ_4' values for ideal square-planar and tetrahedral coordination spheres are 0 and 1, respectively. The calculated τ_4 τ_4' geometry indices are 0.07, 0.06 for (**4a)**, both 0.04 for (**4c)** and 0.03, 0.02 for (**4d)**, respectively, pointing out a slightly distorted square-planar geometry.

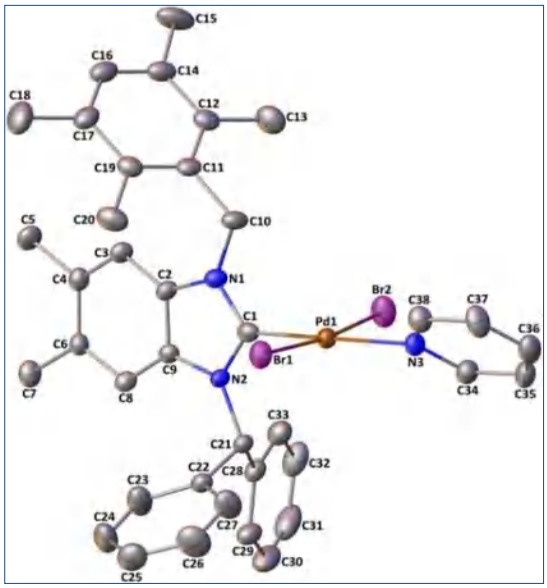

Figure 40. **ORTEP** structure of (**4a)**

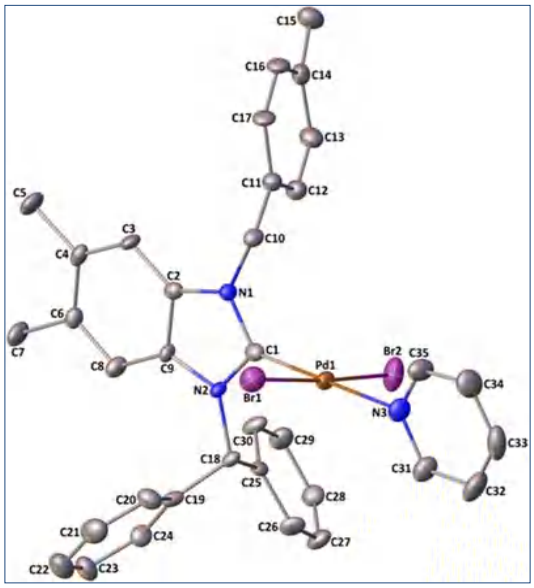

Figure 41. **ORTEP** structure of (**4b)**

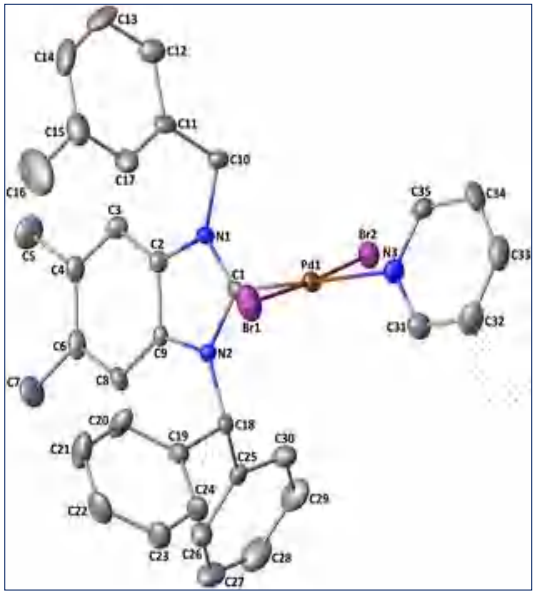

Figure 42. **ORTEP** structure of (**4d)**

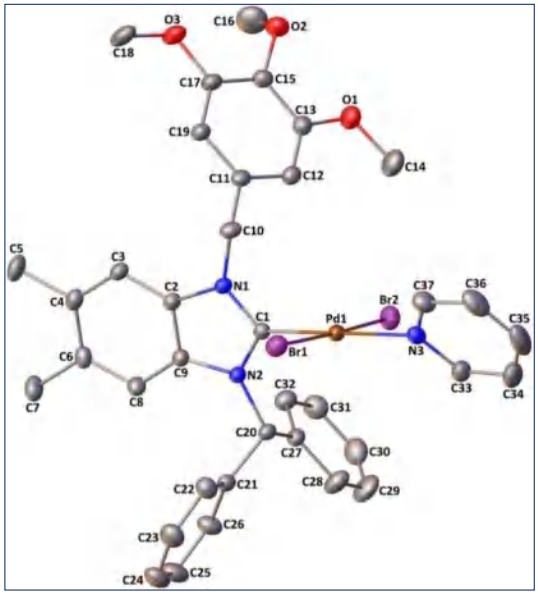

Figure 43. **ORTEP** structure of (**4f)**

Table 5. Selected distances (Å) and angles (°) for (**4a)**, (**4c)**, (**4d)**, and (**4f)** [128]

Parameters		Pd(II)-NHC complexes PEPPSI-Type			
		4a	**4b**	**4d**	**4f**
Bond Distances (Å)	Pd1─Br1	2.4281(9)	2.4182(16)	2.4458(16)	2.4339(5)
	Pd1─Br2	2.4102(10)	2.4352(15)	2.4385(17)	2.4052(5)
	Pd1─N3	2.127(6)	2.078(8)	2.101(9)	2.111(3)
	Pd1─C1	1.965(8)	1.949(9)	1.966(10)	1.964(3)
	N1─C1	1.353(9)	1.350(11)	1.364(12)	1.349(4)
	N2─C1	1.341(9)	1.365(10)	1.362(11)	1.346(5)
Bond Angles (°)	Br1─Pd1─Br2	173.05(4)	175.95(6)	175.41(7)	176.09(2)
	Br1─Pd1─N3	93.23(17)	91.7(2)	90.9(3)	91.91(10)
	Br2─Pd1─N3	91.57(17)	91.1(2)	92.8(3)	91.83(9)
	Br1─Pd1─C1	89.92(19)	90.1(2)	87.3(3)	87.27(10)
	Br2─Pd1─C1	85.32(19)	87.0(2)	89.0(3)	88.99(10)
	N3─Pd1─C1	176.8(2)	178.1(4)	178.1(4)	179.17(14)
	N1─C1─N2	108.5(6)	107.1(7)	107.7(8)	107.6(3)

The average Pd─C_{NHC} bond distance (1.96 Å) is smaller than the sum of the individual covalent radii of the palladium and carbon atoms (2.12 Å), while the average Pd─$N_{pyridine}$ bond distance (2.10 Å) is equal to the sum of the individual covalent radii of the palladium and nitrogen atoms (2.10 Å) [134]. The Pd─Br distances are in the usual range, and the internal N─C─N ring angles at the carbene centers vary from 107.1(7) to 108.5(6)° in the complexes. In sum, these parameters are comparable with those observed for Pd-NHC-pyridine-Br_2 complexes[135,136]. The carbene ring is almost perpendicular to the coordination plane with a dihedral angle of 76.3(3)° in (**4a)**, 89.3(2)° in (**4b),** and 76.07(11)° in (**4d)**, which is typical for NHC complexes to reduce steric congestion. On the other hand, the dihedral angle between the pyridine ring and the coordination plane is 68.7(5)° in (**4a)**, 40.7(4)° in (**4b)**, and 51.8(2)° in (**4d)**.

I.5 Theoretical Results and Discussion

I.5.1 Density functional theory (DFT calculation)

To gain further insights into the geometry of our compounds, the molecular structure and electronic properties of the newly synthesized compounds were studied by determining the molecular geometry of one example molecule, for each benzimidazolium salt (**2d)** ligand and Pd(II)-NHC complex (**4d)**, using DFT calculations at the B3LYP/6-311G(d,p)/LANL2DZ level. The DFT (Density Functional Theory) calculations were carried out using Gaussian 09 software. [137]. The B3LYP (Becke-Lee-Parr hybrid exchange-correlation three-parameter functional) [138] functional in conjunction with LANL2DZ[139] basis set for Palladium atom and 6-311G(d,p) [140] basis set for hydrogen, carbon, nitrogen, and bromine atoms have been used for all calculations. The B3LYP method is effective in predicting molecular structure and electronic properties, offering a good balance of cost and precision[141,142]. The stability of the ground state was confirmed by the absence of imaginary frequencies.

The results were compared to those of X-ray analysis and shown in Figure 44. Some selected experimental and theoretical geometric parameters of complex (**4d)** are reported in Table 06. The predicted molecular geometry was found to be in strong agreement with the experimental results.

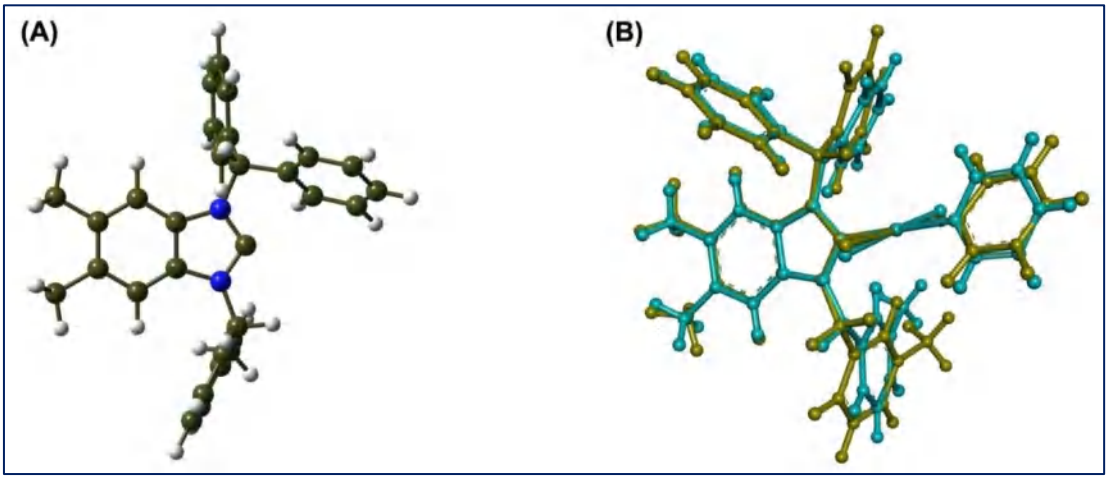

Figure 44. (a) The molecular geometry of the synthesized ligand L and (b) atom-by-atom superimposition of the crystal structure (cyan) and the optimized molecular structure (yellow) of complex (**4d)**.

Table 6. Selected experimental and theoretical geometric parameters of Pd complex (**4d)**.

Complex 4d	**Experimental**	**Calculated**	**Discrepancy**
Bond Distance (Å)			
N3-Pd	2.08	2.11	0.02
C1-Pd	1.95	1.99	0.04
Br1-Pd	2.42	2.53	0.11
Br2-Pd	2.44	2.54	0.1
N2-C1	1.36	1.38	0.01
N1-C1	1.35	1.37	0.02
N2-C19	1.46	1.49	0.03
N2-C10	1.46	1.48	0.02
Bond Angle (°)			
N3-Pd-C1	178.06	179.75	1.69
Br1-Pd-Br2	175.97	176.19	0.22
Br1-Pd-C1	90.15	88.81	-1.34
Br1-Pd-N3	91.14	91.47	0.34
Torsion Angle (°)			
Br1-Pd1-N3-C31	116.57	132.82	16.25
Br1-Pd1-C1-N2	106.45	97.97	-8.48
N2-C18-C25-C26	115.46	112.22	-3.24
N2-C18-C19-C24	162.01	172.57	10.56

The bond lengths between Br1-Pd and Br2-Pd were estimated to be 2.42 Å and 2.44 Å respectively and were in agreement with the experimental values of 2.53 Å and 2.54 Å. The predicted N3-Pd and C1-Pd bond lengths were also close to the observed values, with only small differences of 0.02 Å and 0.04 Å. The predicted angles of Br1-Pd-Br2 and Br1-Pd-N3 were only slightly different from the experimental values, with discrepancies of 0.22° and 0.34° respectively. The largest differences were found in the torsion angles Br1-Pd1-N3-C31 and N2-C18-C19-C24, with deviations of 16.25° and 10.56°.

These results suggest that the DFT method used in the calculation provides accurate predictions of the molecular geometry for complex (**4d)** systems and can be used for future computations.

I.5.2 Frontier molecular orbitals

The term "Frontier Molecular Orbitals" (FMOs) refers to the highest occupied molecular orbital (HOMO) and lowest unoccupied molecular orbital (LUMO) of a molecule, which are important for understanding its chemical reactivity. The energy of the HOMO reflects the ability of the molecule to donate electrons, while the energy of the LUMO reflects its ability to accept electrons.

The shape of FMOs can provide information about areas where electrophilic and nucleophilic reactions occur. The energy and distribution of FMOs extending from HOMO-1 to LUMO+1 have been calculated at the B3LYP/6-311G(d,p)/LANL2DZ level for both a salt ligand and a Pd-NHC complex. Analysis of the data obtained reveals that the HOMO energy of the ligand (-9.16 eV) is significantly lower than that of the Pd complex (-5.85 eV), suggesting that the electron donation capacity of the former is lower than that of the latter. This result is expected because the ligand is a cationic species. The stability of the ligand could also be estimated to be greater than that of the complex, as can be concluded from their energy gap (4.72 and 3.94) eV, respectively.

The complexation process affects the distribution of FMOs, with the HOMO of the ligand mainly localized on the benzimidazole and slightly on the benzene ring, and the HOMO of the complex distributed over the entire molecular structure. The LUMO and LUMO+1 of the ligand are located on the N2-benzene rings and those of the complex on the Pd atom and the benzene rings. These findings HOMO and LUMO electron density distributions clearly show a transfer of electron density from the benzimidazole to the benzene rings for the ligand, but no significant transfer for the complex (Figure 45).

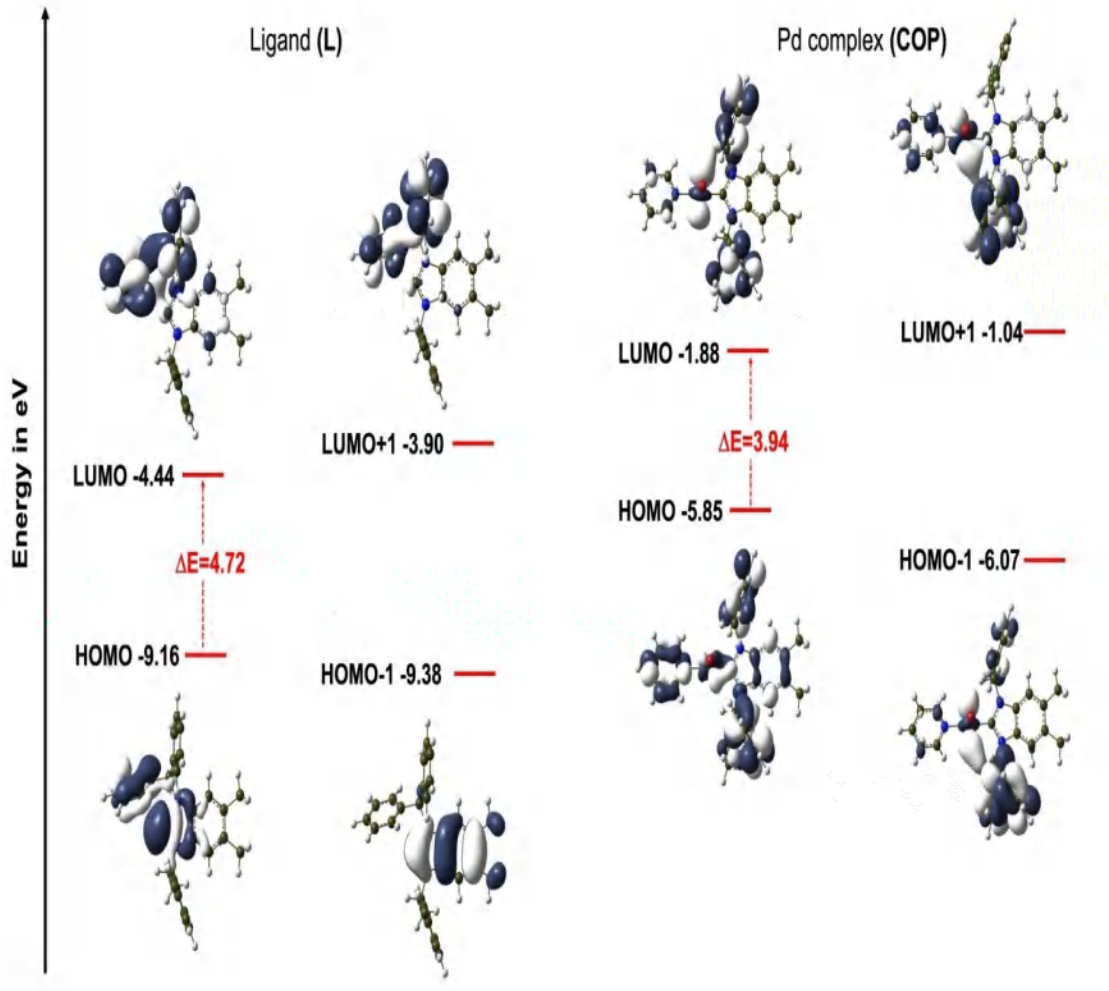

Figure 45. Frontier molecular orbitals energies and distributions of the synthesized ligand (L) and its Pd complex (COP) computed at B3LYP/6-311G(d,p)/LANL2DZ level of theory

I.5.3 Molecular electrostatic potential and atomic polar tensor

The molecular electrostatic potential (MEP) is another useful tool for illustrating the electronic properties and chemical reactivity of molecules. It displays a 3D representation of the charge distribution in a molecule using colors from deep red for electron-rich sites with high electron concentration to deep blue for electron-deficient sites with low electron concentration. The distribution of electronic charges plays a crucial role in determining a molecule's chemical reactivity and electronic properties. The atomic charges of the synthesized ligand and Pd-NHC complex were calculated in the gas phase using the atomic polar tensor (APT) method at the B3LYP/6-311G(d,p)/LANL2DZ level. The results are presented in Figure 46.

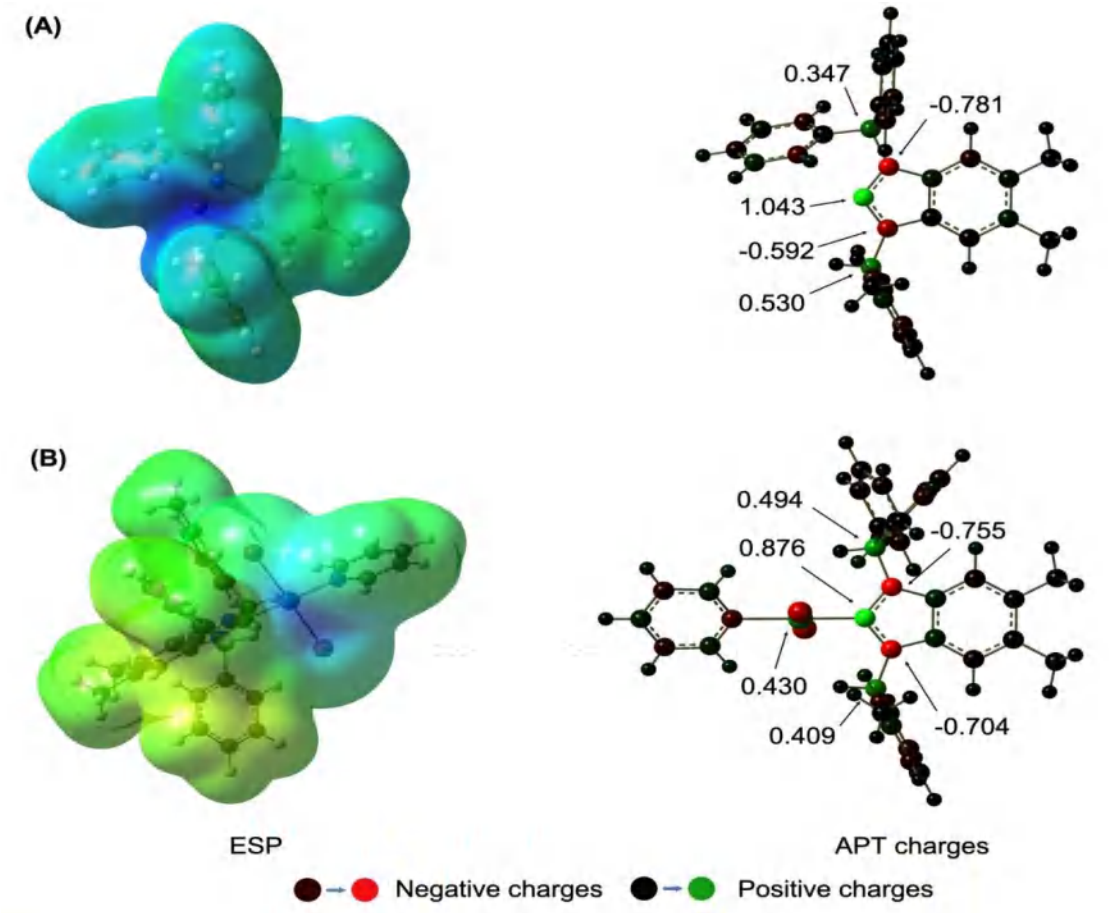

Figure 46. APT charges destitution and molecular electrostatic potential (MEP) of the ligand L (a) and its Pd complex (b) computed at B3LYP/6-311G(d,p)/LANL2DZ level of theory

The analysis showed that the electron density of the carbene's carbon atom increased in the Pd-NHC complex compared to the free ligand, while the electron density of the metal ion decreased. The formal charge of Pd is 2 and 0.430 after complexation, indicating that the charges have shifted from the ligand to the metal ion. Additionally, it was observed that the electronic density of the nitrogen atoms of benzimidazole increased upon complexation. The molecular electrostatic potential of both the L and Pd-NHC complex was computed to show the distribution of electronic charges throughout the molecule, as depicted in Figure 46.

The MEPs reveal that the positive charges (deep blue) in the ligand are largely located near the carbene atom, while in the complex they are spread out over both the carbene and Pd atoms. On the other hand, negative charges (ranging from yellow to red) are spread across the benzene rings for both the complex and the ligand. These observations suggest that the ligand is more polarized than the complex, leading to a higher level of reactivity towards nucleophiles compared to the complex.

I.6 Application of Palladium(II)-NHC complexes

I.6.1 Catalytic evaluation study in direct arylation reaction

The direct arylation of bi(hetero)arenes by C-H bond activation provides an ideal alternative to traditional cross-coupling reactions in the synthesis of bi(hetero)arenes. This process involves the use of a diverse range of arylating reagents, including aryl halides, aryl organometallic reagents, simple arenes, and phenol derivatives such as triflates, mesylates, and arene sulfonyl chlorides. Among these reagents, aryl halides are the most commonly used electrophilic reagents due to their wide availability and substrate diversity. The Pd-catalyzed direct arylation of heteroarenes with aryl halides was first reported by Nakamura in 1982 [143] and Ohta in 1990[144], and has since proven to be a highly effective method for synthesizing a variety of arylated heteroaromatics. To date, Pd-catalyzed direct arylation of (hetero)arenes, especially five-membered heterocycles such as thiophene, furan [145], and thiazole [146] has been largely described by a large number of researchers.

Over the past few years, PEPPSI-type Pd-complexes have gained considerable interest as efficient catalysts for the direct arylation of (hetero)arenes using (pseudo)halides, providing a cost-effective and environmentally friendly alternative to traditional approaches. Direct arylation of heteroarenes is especially appealing due to the prevalence of these groups in biologically active compounds.

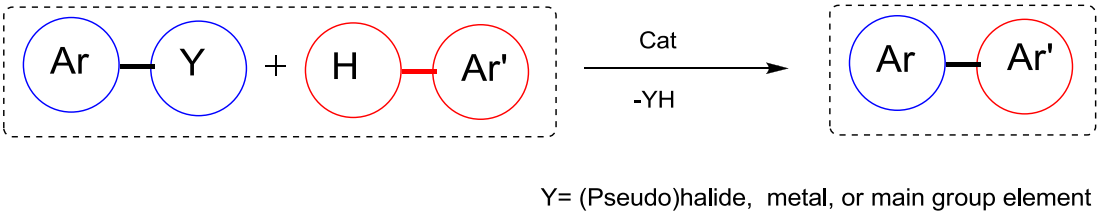

Scheme 36. Direct arylation method

In view of the above information and the increasing attention on the catalytic potential of Pd-NHC complexes in direct arylation to act as an efficient catalyst, in this part, we present the evaluation of the effectiveness of six new Pd-NHC complexes PEPPSI-type (**4a-f)** as a catalyst in direct arylation reaction.

The effectiveness of new Pd(II)-NHC complexes (**4a-f)** as catalysts in intermolecular direct arylation reactions between aryl bromides and substituted furan, and thiophene derivatives were tested. To determine the impact of the catalyst, a control experiment was conducted without Pd-catalyst at 120°C for 24 hours in the presence of Potassium acetate (KOAc) as a base and dimethylacetamide (DMAc) as a solvent. The reaction failed to produce the desired product without the catalyst. However, upon the inclusion of 1 mol% of the Pd-catalyst complex, the successful formation of the desired product was observed (Scheme 37).

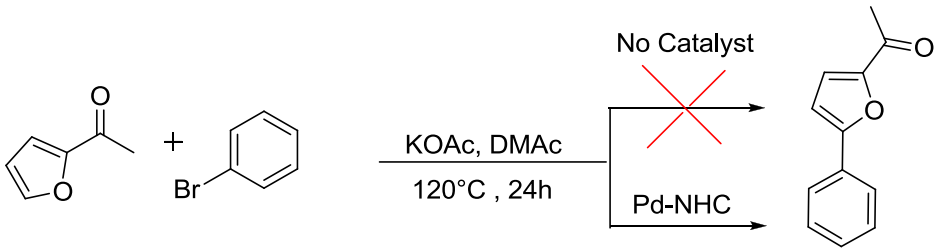

Scheme 37. Direct arylation of five-membered heteroaromatics without catalyst

To find the optimal reaction conditions, the experiment was modified by altering the solvent, base, temperature, and time. In the study, complex (**4a)** was selected as a model test catalyst, 2-acetyl furane (heteroaromatic substrates), and the *p*-bromobenzene as the coupling partner, which was common in the direct arylation of hetero-arenes according to previous studies [147]. In this part, we start selecting dimethylacetamide (DMAc) as a solvent, and potassium acetate (KOAc) as a base. The reaction conditions were varied by changing time (1h, 2h, and 4h) and temperature (80, 100, 120, and 150°C) The reactions were performed under argon. Several solvents and bases were also tested as shown in Scheme 38. The results are summarized in Table 07.

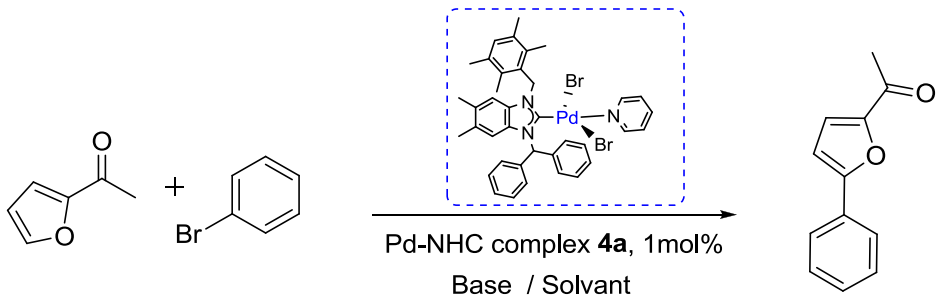

Scheme 38. Influence of the reaction conditions on the Pd-NHC catalyzed direct arylation

Table 7. Optimization of the best conditions for direct arylation reaction [128]

	solvent	Base	Time (h)	Temperature °C	Conversion (%)	Yield (%)
01	DMAc	KOAc	01	80	04	04
02				100	63	23
03				120	95	86
04				150	95	75
05			02	80	04	04
06				100	70	45
07				120	94	80
08				150	96	81
09			04	80	95	82
10				100	80	65
11				120	99	70
12				150	97	82
13	H_2O	KOAc	01	120	06	05
14	EtOH				08	05
15	THF				02	01
16	Toluene				10	09
17	DMF				09	06
18	DMSO				03	02
19	dioxane				04	03
20	DMAc	K_2CO_3	01	120	10	05
21		KOH			14	09
22		TEA			13	07
23		*t*-BuOK			11	06

As shown in Table 07, The preliminary data demonstrated that the reaction displayed the best performance at 120°C temperature, in the presence of KOAc within 1 hour. Further extending the reaction time to 2 or 4 hours resulted in full conversion, but no significant change in yield (Table 07, entries 7 and 11). Increasing the temperature above 120°C had no impact on yield (Table 07, entry 4) while reducing the temperature caused a decrease in yield (Table 07, entries 1 and 2). DMAc was found to be the most effective solvent among the options tested. The evaluation of yield at various temperatures (150, 120, 100, and 80°C) showed the highest yield at 120°C (Table 07, entry 3).

After fixing the reaction conditions (time and temperature) to optimal levels, a variety of solvents and bases were evaluated to determine the best coupling solvent/base choice for the reaction. Tests were run using H_2O, EtOH, THF, Toluene, DMF, DMSO,

and dioxane, with only 1 mol% of the (**4a)** catalyst, but the reaction conversion was low and the yield was below 10 % (Table 07, entries 13-19). Further tests were done using various bases (K_2CO_3, KOH, TEA, and *t*-BuOK) in the presence of a 1 mol% (**4a)** catalyst. The reaction was working but with low conversion and the final product was formed at the lowest yields were 5, 7, 6, and 9% respectively (Table 07, entries 20-23). The best couple solvent/base for the reaction was found to be DMAc and KOAc. In conclusion, the results show that the optimal conditions for the direct arylation reaction using our Pd-catalyst complexes (**4a-f)** are one hour time, 120°C temperature, and DMAc / KOAc solvent/base.

I.6.1.1 Direct arylation of 2-acetylfuran, 2-acetylthiophene, and furaldehyde with aryl bromides

The new palladium(II)-NHC complexes were evaluated by performing a direct arylation of 2-acetylfuran, 2-acetylthiofene, and 2-furaldehyde with aryl-bromide derivatives under the optimal condition. C5-arylated of the three substrates were obtained easily when coupled with eight *p*-substituted aryl bromides. Due to the Pd-catalyst, the reaction was perfect working and the desired products were obtained with moderate to high yield, by using only 1 mol% of catalyst (Scheme 39).

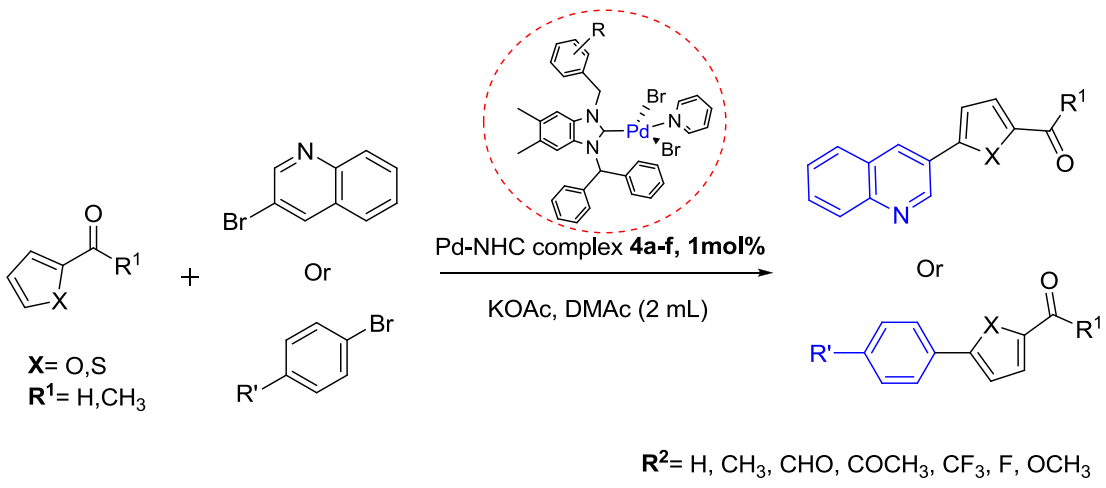

Scheme 39. Pd-catalyzed direct arylation of C2-substituted thiophene and furan with aryl bromides

I.6.1.1.1 Direct arylation of 2-acetylfuran with arylbromides

Firstly, under the optimal condition, an investigation of the reactivity of 2-acetylfuran in Pd-catalyzed direct arylation with various arylbromides was carried out (Scheme 40).

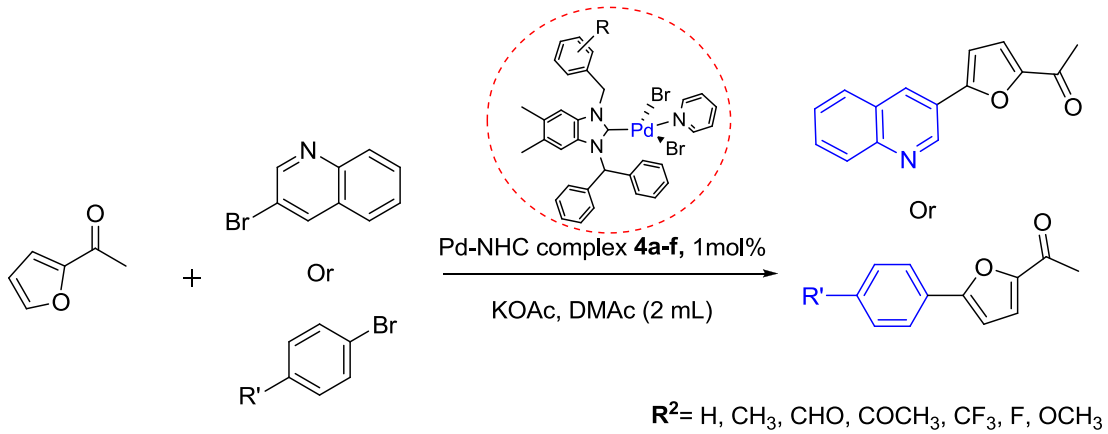

Scheme 40. Direct arylation of 2-acetylfuran with arylbromides

The reaction was successfully working and the desired products were obtained with moderate to high yield. The highest yield was seen with arylbromides that were poor in electrons, such as bromobenzene and *p*-bromotoluene, while the lowest yield was noted with electron-rich arylbromides like *p*-bromoacetophenone and *p*-bromoanisole. The study showed that all Pd(II)-NHC complexes were active. The high yields of the desired products were obtained for most of the reactions, except for the reaction with 3-bromoquinoline which had the lowest yield. The conversion was high for all reactions, ranging from 95-99%. The results are summarized in Table 08.

Table 8. Direct C5-arylation of 2-acetylfurane with aryl bromides by using the new Pd-catalyst [128]

Entry	Aryl Bromide	NHC-Pd catalysts 4a-f	Product	Conversion (%)	Yield (%)
01	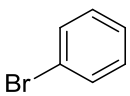	4a	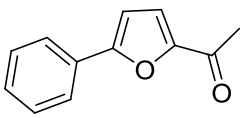	95	67
02		4b		98	78
03		4c		99	44
04		4d		91	51
05		4e		99	64
06		4f		99	72
07	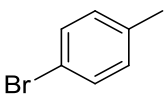	4a	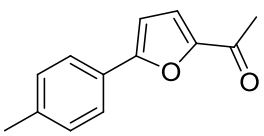	98	73
08		4b		94	85
09		4c		98	74
10		4d		93	76
11		4e		99	78
12		4f		89	67

13	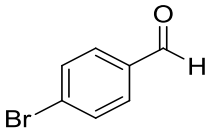	4a	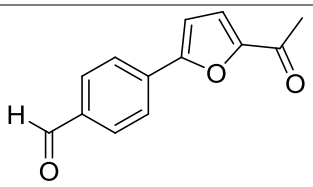	99	64
14		4b		99	75
15		4c		99	88
16		4d		99	81
17		4e		99	91
18		4f		99	85
19	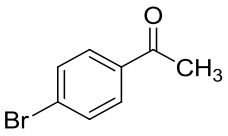	4a	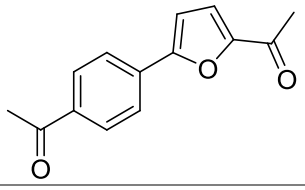	99	71
20		4b		93	80
21		4c		99	82
22		4d		99	79
23		4e		99	73
24		4f		99	72
25	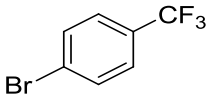	4a	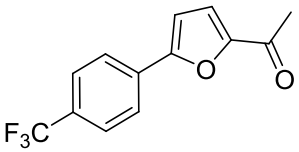	99	70
26		4b		99	80
27		4c		99	80
28		4d		99	86
29		4e		99	78
30		4f		99	82
31	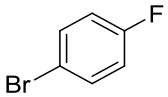	4a	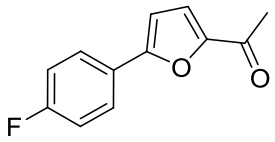	99	74
32		4b		98	76
33		4c		97	85
34		4d		93	80
35		4e		95	75
36		4f		99	76
37	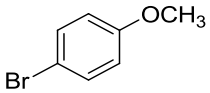	4a	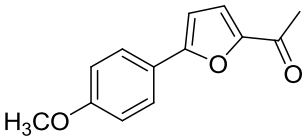	77	62
38		4b		98	77
39		4c		86	69
40		4d		99	70
41		4e		57	39
42		4f		81	43
43	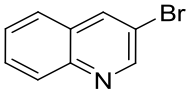	4a	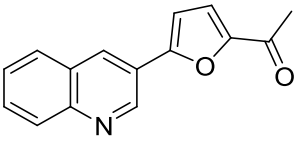	45	42
44		4b		26	20
45		4c		37	34
46		4d		25	18
47		4e		18	16
48		4f		13	08

The reaction conditions: Pd-catalyst (1 mol%), 2-acetylfuran (1.0 mmol), arylbromide (1.0 mmol), KOAc (2 mmol), DMAc (2 mL), 120 °C, and 1 h. GC yields were calculated concerning aryl bromide from the results of GC.

Table 08 shows an excellent conversion and high yield C5 arylated products were obtained in almost all reactions using Pd-NHC catalysts (**4a-f)**. When 2-acetylfurane was reacted with bromobenzene, the product 5-phenyl-2-acetylfurane was obtained at 44-78% yield with 95-99% conversion (Table 08, entries 1-6). The lowest yield was seen with Pd catalyst (**4c)**. When 2-acetylfurane was reacted with *p*-bromotoluene, the desired product was obtained at 67-85% yield with 89-99% conversion (Table 08, entries 7-12). The reaction with *p*-bromobenzaldehyde gave a 64-91% yield with 99% conversion for all Pd-catalysts (Table 08, entries 13-18). The coupling with electron-poor *p*-bromoacetophenone gave a high yield of 71-82% with 99% conversion (Table 08, entries 19-24). The reaction with 1-Bromo-4-(trifluoromethyl)benzene gave 70-86% yield with

99% conversion (Table 08, entries 25-30). The reaction with 1-bromo-4-fluorobenzene gave a high yield of 74-85% with 99% conversion (Table 08, entries 31-36). The coupling with *p*-bromoanisole gave a moderate yield of 39-77% with 57-99% conversion (Table 08, entries 37-42). The lowest yield was seen in the reaction with 3-bromoquinoline with 8-42% yield (Table 08, entries 43-48).

I.6.1.1.2 Direct arylation of 2-acetylthiofene with arylbromides

In the second test, the direct arylation of 2-acetylthiofene was carried out under the same reaction conditions as the first test with different arylbromide derivatives. Using the same range of *p*-substituted aryl bromides (Scheme 41).

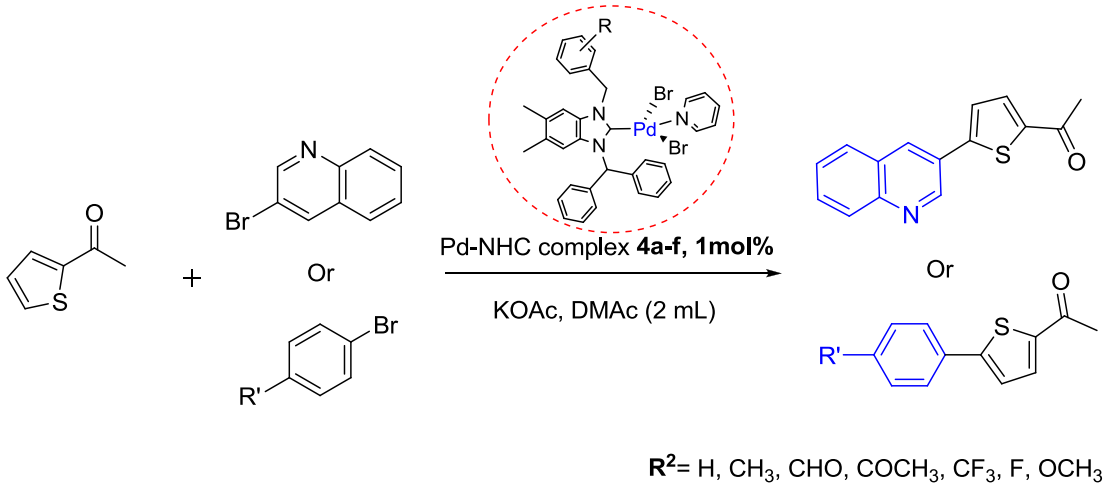

Scheme 41. Direct arylation of 2-acetylthiofene with arylbromides

The reaction worked efficiently with a conversion rate of 98-99% and an average yield of 80% using all Pd-NHC catalysts (**4a-f)**. The best yield was achieved with arylbromides lacking electrons, such as bromobenzene and *p*-bromotoluene. The evaluation showed that all Pd-NHC complexes of the PEPPSI type (**4a-f)** were active catalysts. The results are summarized in Table 09.

Table 9. Direct C5-arylation of 2-acetyl-thiophene with aryl bromides using the new Pd-catalyst [128].

Entry	Aryl Bromide	NHC-Pd catalysts 4a-f	Product	Conversion (%)	Yield (%)
01	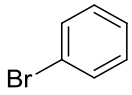	4a	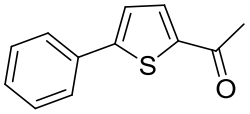	98	93
02		4b		98	78
03		4c		99	93
04		4d		96	77
05		4e		98	93
06		4f		98	92
07	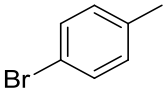	4a	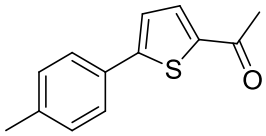	96	92
08		4b		92	86
09		4c		98	84
10		4d		79	73
11		4e		95	89
12		4f		95	89
13	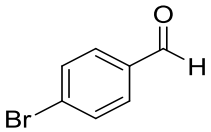	4a	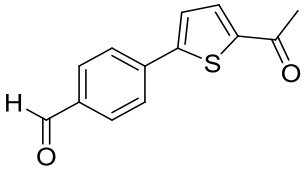	98	75
14		4b		99	70
15		4c		99	81
16		4d		99	74
17		4e		99	81
18		4f		99	80
19	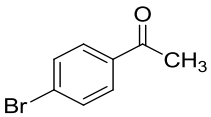	4a	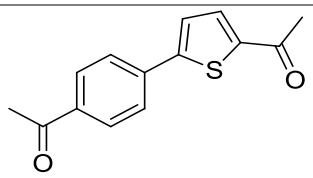	96	84
20		4b		99	77
21		4c		94	75
22		4d		98	76
23		4e		93	73
24		4f		98	82
25	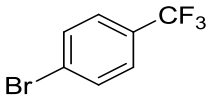	4a	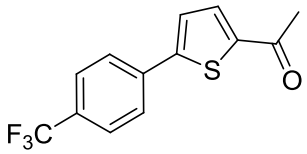	98	94
26		4b		77	75
27		4c		65	60
28		4d		86	77
29		4e		90	85
30		4f		90	85
31	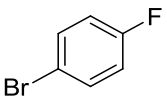	4a	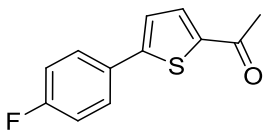	97	93
32		4b		99	95
33		4c		97	94
34		4d		90	80
35		4e		95	86
36		4f		96	90
37	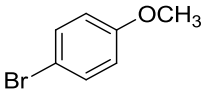	4a	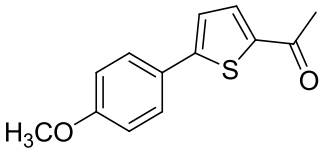	60	56
38		4b		90	80
39		4c		82	74
40		4d		51	48
41		4e		90	82
42		4f		67	60
43	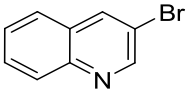	4a	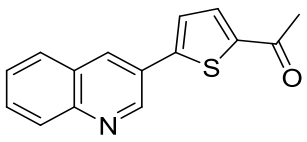	99	80
44		4b		99	79
45		4c		99	80
46		4d		99	80
47		4e		99	80
48		4f		99	79

The reaction conditions: Pd-catalyst (1 mol%), 2-acetylfuran (1.0 mmol), arylbromide (1.0 mmol), KOAc (2 mmol), DMAc (2 mL), 120 °C, and 1 h. GC yields were calculated concerning aryl bromide from the results of GC.

As presented in Table 09, direct C5 arylation reactions had moderate to high yields of desired products with excellent conversion using all Pd-NHC catalysts (**4a-f)**. When 2-acetylthiophene was arylated with bromobenzene, desired products were obtained at 78-93% yields using Pd-NHC complexes (**4a-f)** as a catalyst (Table 09, entries 01-06). The reaction was working in 98% conversion. The same reaction of 2-acetylthiophene with *p*-bromotoluene gave the desired product at 84-92% yield, and a conversion reaction between 92-98% (Table 09, entries 07-12). 2-acetylthiophene with *p*-bromobenzaldehyde gave the expected product with 70-81% yield and 99% conversion with almost Pd-NHC catalysts (Table 09, entries 13-18). The electron-poor *p*-bromoacetophenone coupling produced a high yield at 73-84% with 93-99% conversion (Table 09, entries 19-24). The coupling of 2- acetylthiophene with 1-Bromo-4-(trifluoromethyl)benzene generated the desired product at 60-94% yield and 65-98% conversion (Table 09, entries 25-30). Furthermore, 1-Bromo-4-fluorobenzene was also successfully coupled with 2-acetyl-thiophene to give C5 arylated products in high yields at 86-95% with 95-99% conversion (Table 09, entries 31-36). The reaction using *p*-bromoanisole produced moderate to high yields at 56-82% with 60-90% conversion (Table 09, entries 37-42). When the coupling was done with 3-bromoquinoline, the reaction gave a good C5-arylated product with the same yield (80%) with all Pd-catalysts, as well as the conversion of the reaction was 99 % (Table 09, entries 43-48).

I.6.1.1.3 Direct arylation of 2-furaldehyde with aryl bromides

The last evaluation of the new Pd-catalysts was evaluated by performing a direct arylation of 2-furaldehyde with arylbromide derivatives, similar to the conditions used in the first and second tests (Scheme 42).

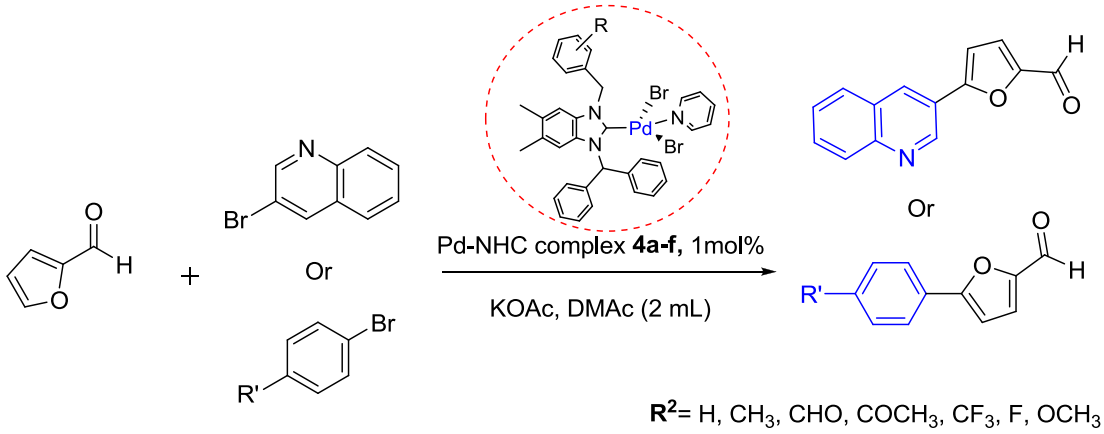

Scheme 42. Direct arylation of 2-furaldehyde with arylbromides

The Pd- NHC catalyst (**4a-f)** worked effectively, yielding the desired product with moderate to high efficiency, except for the arylation with *p*-bromoanisole which showed a lower yield due to its electron-rich nature.

The experiments confirmed that all Pd-NHC complexes (**4a-f)** of the PEPPSI type were catalytically active. A summary of the results can be found in Table 10.

Table 10. Direct C5-arylation of 2-furaldehyde with aryl bromides by using the new Pd-catalyst [128]

Entry	Aryl Bromide	NHC-Pd catalysts 4a-f	Product	Conversion (%)	Yield (%)
01	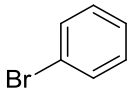	4a	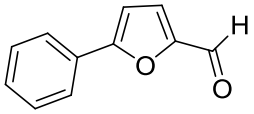	99	90
02		4b		99	86
03		4c		98	76
04		4d		99	81
05		4e		26	22
06		4f		50	46
07	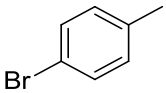	4a	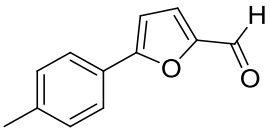	98	79
08		4b		99	76
09		4c		99	82
10		4d		97	90
11		4e		99	82
12		4f		98	51
13	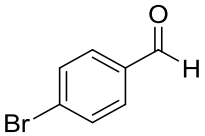	4a	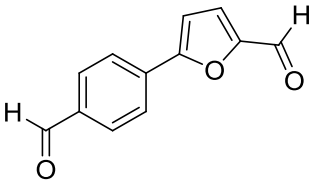	93	63
14		4b		99	65
15		4c		99	65
16		4d		99	62
17		4e		94	63
18		4f		78	53
19	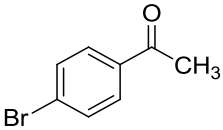	4a	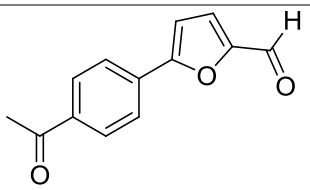	27	23
20		4b		35	27
21		4c		71	46
22		4d		63	46
23		4e		41	28
24		4f		66	47
25	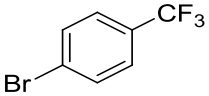	4a	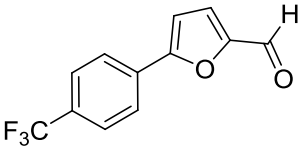	79	59
26		4b		98	75
27		4c		65	50
28		4d		80	55
29		4e		29	26
30		4f		64	47
31	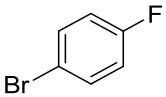	4a	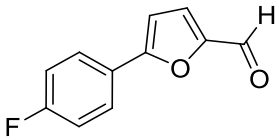	99	85
32		4b		99	82
33		4c		99	72
34		4d		98	72
35		4e		74	55
36		4f		99	70
37	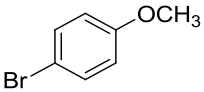	4a	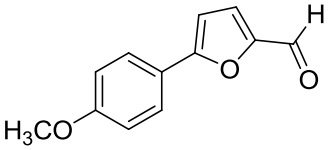	11	09
38		4b		13	09
39		4c		13	10
40		4d		23	19
41		4e		19	16
42		4f		11	10
43		4a		75	48
44		4b		99	74
45		4c		93	77

46	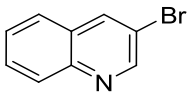	4d	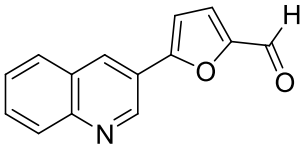	86	64
47		4e		55	37
48		4f		69	47

The reaction conditions: Pd-catalyst (1 mol%), 2-acetylfuran (1.0 mmol), arylbromide (1.0 mmol), KOAc (2 mmol), DMAc (2 mL), 120 °C, and 1 h. GC yields were calculated concerning aryl bromide from the results of GC.

In Table 10, Pd-NHC catalysts produced good results, leading to high to moderate yield C5 arylated products in almost all reactions. When using Pd-NHC complexes (**4a-f)** as a catalyst in the arylation of 2-furaldehyde with bromobenzene, the product 5-phenyl-2-carbaldehyde was obtained at 46-86% yield, with the lowest yield of 22% using Pd-catalyst (**4e)** and the reaction was working in 26-99% conversion (Table 10, entries 01-06). The same reaction with *p*-bromotoluene produced the desired product at 51-82% yield and 99% conversion (Table 10, entries 07-12). The coupling of furaldehyde with *p*-bromobenzaldehyde gave the expected product with moderate yields at 53-65 and with 78-99% conversion (Table 10, entries 13-18). The coupling with electron-poor *p*-bromoacetophenone produced the expected product at 23-48% yield and 27-71% conversion (Table 10, entries 19-24). The reaction of furaldehyde with 1-Bromo-4-(trifluoromethyl)benzene gave the 5-(4-trifluoromethyl)-2-furaldehyde at 47-75% yield and 64-98% conversion, with the lowest yield using Pd-NHC catalyst (**4e)** at 26% (Table 10, entries 25-30). The coupling with 1-Bromo-4-fluorobenzene resulted in a high yield at 55-85% with 77-99% conversion(Table 09, entries 31-36). Relatively low yields were obtained for the coupling of furaldehyde with 4-bromoanisole and 3-bromoquinoline, forming the product at 09-16 % and 37-74% yield respectively (Table 10, entries 37-48). Also as a result of this study, it was observed that the less active catalyst was (**4e)** complex at 22, 28, 26, 55, 16, and 37% yield (Table 10, entries 05,23,29,35,41, and 47).

I.7 Biological Evaluation

I.7.1 Antimicrobial Activity of salts (**2a-f)** and their silver(I)-NHC complexes (**3a-f)**

Investigations have been performed for antibacterial and antifungal activities in vitro against (*E.coli, P.aeruginosa, S.aureus, C.albicans, and C.glabrata*) for all the newly 5,6-dimethylbenzimidazolium salts (**2a-f)** and their related silver(I)-NHC complexes (**3a-f).** The minimum inhibitory concentration (*MIC*) of antifungal and antibacterial compounds was determined using the broth microdilution (BMD) test, following EUCAST for yeasts [148] and CLSI for bacteria [149].

The microplate was incubated at 37°C for 24 hours for yeasts and 16-18 hours for bacteria, then the MIC was determined by measuring the reduction in yeast growth (spectrophotometrically at 530 nm) after incubation in yeasts and by naked eyes in bacteria. *Ampicillin*, *Tetracycline*, *Amphotericin B*, and *Voriconazole* were used as standard control drugs.

The MIC value was measured as the lowest drug concentration causing at least 50 % or more reduction in yeasts' growth compared to the control (no drug) cell group and as the lowest drug concentration without visible growth in bacteria. The (MIC μg/mL) results of the antimicrobial activity of all new compounds are reported in Table 11.

Globally, benzimidazolium salts and silver-NHC complexes showed significant antifungal and antibacterial activity against human pathogenic microorganisms as shown in Table 11. The benzimidazolium salts (**2a-f)** were highly effective against *Candida albicans*, especially the three salts (**2a)**, (**2c)**, and (**2e)**. Silver-NHC complex (**3a-f)** showed high antifungal activity against both *Candida albicans* and *Candida glabrata*, with complex (**3c)** being the most active. All tested benzimidazolium salts (**2a-f)** and silver-NHC complexes (**3a-f)** showed important antibacterial activity against *Escherichia coli*, *Pseudomonas aeruginosa*, and *Staphylococcus aureus* except salt (**2f)**. The benzimidazolium salts (**2a-e)** were effective against *Staphylococcus aureus* and *Escherichia coli*, but not against *Pseudomonas aeruginosa*, especially salts (**2b)** and (**2d)**. The silver-NHC complexes (**3a-f)** showed high antimicrobial activity against *Staphylococcus aureus* and *Escherichia coli*, with the highest activity reported in Ag-NHC complexes (**3b)** and (**3c)**. The lipophilicity of Ag(I)-NHC complexes are believed to contribute to their ability to penetrate cell membranes, and increasing lipophilicity improved their antibacterial activity [150].

Table 11. Antifungal and antibacterial activities of salts (**2a-f)** and their silver(I)-NHC complexes (**3a-f)**

Compounds		*Anti-Fungal* (*MIC* μg/mL)		*Anti-Bacterial* (*MIC* μg/mL)		
		C. albicans [a]	***C. glabrata*** [a]	***E. coli*** [a]	***P. aeruginosa*** [a]	***S. aureus*** [a]
Benzimida-zolium Salts	**2a**	25	100	200	200	200
	2b	200	200	400	800	400
	2c	25	100	200	200	200
	2d	100	200	400	800	400
	2e	12.5	100	200	200	100
	2f	200	400	**NA**	**NA**	**NA**
Silver complexes	**3a**	12.5	12.5	25	50	25
	3b	12.5	12.5	25	25	6.25
	3c	6.25	6.25	25	25	6.25
	3d	12.5	12.5	25	50	12.5
	3e	12.5	12.5	25	25	12.5
	3f	25	12.5	25	50	25
Ampicillin[b]		-	-	12.5	400	3.125
Tetracycline[b]		-	-	0.8	12.5	0.2
Amphotericin B[b]		0.05	0.1	-	-	-
Voriconazole[b]		0.4	0.4	-	-	-

a: *Tested microorganisms.* ***b:*** *Reference drugs.* ***NA:*** *Not Active.*

I.7.2 Enzymatic inhibitory activity assay

This study evaluated the capacity of the novel benzimidazolium salts and silver (I)-NHC complexes as inhibitors of different enzymes. In this context, all compounds were evaluated against a panel of important biological activities such as anticholinesterase, anti-Lipase, and anti-diabetic activities.

The study looked at the ability of benzimidazolium salts (**2a-f)** and their silver(I)NHC complexes (**3a-f)** to inhibit different enzymes such as *AChE*, *BChE*, *Lipase*, and *α-amylase* in vitro at various concentrations. The benzimidazolium salts and their silver complexes showed similar levels of inhibition against *AChE* compared to the reference drug Galantamine, while they all had stronger inhibiting effects against *BChE* than the reference drug. The silver complexes effectively inhibited *lipase*, with an IC_{50} value close to that of the reference drug Orlistat, and showed strong anti-diabetic activity against *α-amylase*. However, the benzimidazolium salts had no activity against either *lipase* or *α-amylase*.

The enzymatic activity was reported similarly to the IC_{50} values shown in Table 12. The IC_{50} values represent the concentration at which 50% inhibition occurs. The ability of the new compound to inhibit enzymes such as *AChE*, *BChE*, *Lipase*, and *α-amylase* was determined by comparing the reaction rates of samples to the control sample. The inhibition was evaluated using spectrophotometric methods, and the low IC_{50} values indicate high inhibition activity

Table 12. Enzymatic inhibitory of benzimidazolium salts (**2a-f)** and their silver(I)-NHC complexes (**3a-f)** [127]

Compound		*Anti-Cholinesterase*		*Anti-Lipase*	*Anti-α-Amylase*
		AChE	*BChE*	*Lipase*	*α-amylase*
		IC_{50}±SD (*μ*M)[a]	IC_{50} ± SD (*μ*M)[a]	IC_{50}±SD (*μ*M)[a]	IC_{50} ± SD (*μ*M)[a]
Benzimid-azolium salts	**2a**	1.33± 0.03	0.96 ± 0.02	NA[c]	NA[c]
	2b	5.56± 0.57	0.72 ± 0.04	NA[c]	NA[c]
	2c	6.17± 0.33	0.70 ± 0.04	NA[c]	NA[c]
	2d	4.19± 0.02	0.15 ± 0.02	NA[c]	NA[c]
	2e	9.06± 0.26	1.08 ± 0.12	NA[c]	NA[c]
	2f	17.97± 0.27	4.29 ± 0.18	NA[c]	NA[c]
Silver(I)-NHC complexes	**3a**	1.60± 0.19	0.88 ± 0.00	33.79 ± 6.17	7.00 ± 0.87
	3b	3.50± 0.52	0.47 ± 0.04	52.25 ± 1.83	70.69 ± 2.69
	3c	5.64± 0.02	0.50 ± 0.03	34.61 ± 2.50	98.57 ± 2.18
	3d	4.21± 0.12	0.61 ± 0.02	40.72 ± 2.47	43.18 ± 2.60
	3e	4.53± 0.13	0.18 ± 0.01	33.15 ± 1.47	65.87 ± 2.66
	3f	4.14± 0.46	3.57 ± 0.15	58.66 ± 1.47	47.55 ± 1.28
Reference	**Galanamine[b]**	4.14± 0.07	20.38±2.10	/	/
	Orlistat [b]			25.07±0.48	
	Acarbose [b]	/	/	/	52.58.±4.69

a: *IC_{50} values represent the means ± SD of three parallel measurements ($p < 0.05$).* ***b:*** *Reference compound.*
c: *Not Active.*

I.7.2.1 In vitro cholinesterases inhibition of benzimidazolium salts and Ag-NHC complexes

The most widely used approach for treating Alzheimer's disease is through the use of inhibitors from the cholinesterase family, targeting acetylcholinesterase (*AChE*) and butyrylcholinesterase (*BChE*) [151,152]. The inhibition of the two enzymes by the new compound was evaluated using the method described by Rhee et al. [153], based on the spectrophotometric method of Ellman's [154] with slight modifications. The capacity of benzimidazolium salts (**2a-f)** and their silver(I)-HNC complexes (**3a-f)** to inhibit

anticholinesterase activity was determined in vitro screening process. The test involved evaluating the effect of these compounds on the two enzymes, which break down acetylthiocholine or butyrylthiocholine. The reaction between the broken-down substrate (thiocholine) and Ellman's reagent (DTNB) produces a detectable product, 2-nitrobenzoic-5-mercaptothiocholine, and 5-thio-2-nitrobenzoate, which can be detected at 412 nm. Galantamine, a commonly used cholinesterase inhibitor in the treatment of mild Alzheimer's disease, was used as a reference point for comparison.

Table 13. The selectivity index for *AChE* over *BChE* and *BChE* over *AChE* with docking score of benzimidazolium salts (**2a-f)** and their silver(I)-NHC complexes (**3a-f)** [127]

Compounds		*AChE*			*BChE*		
		IC_{50}±SD (μM)[a]	**Selectivity index[c]**	**Docking score**	**IC_{50}±SD (μM)[a]**	**Selectivity index[d]**	**Docking score**
Benzimidazolium salts	2a	1.33± 0.03	0.72	59.20	0.96 ± 0.02	1.38	74.74
	2b	5.56± 0.57	0.13	54.43	0.72 ± 0.04	7.72	76.60
	2c	6.17± 0.33	0.11	51.78	0.70 ± 0.04	8.81	76.71
	2d	4.19± 0.02	0.06	56.48	0.15 ± 0.02	14.45	77.60
	2e	9.06± 0.26	0.11	52.73	1.08 ± 0.12	8.39	70.26
	2f	17.97± 0.27	0.23	51.65	4.29 ± 0.18	4.18	68.27
Silver complexes	3a	1.60± 0.19	0.55	59.11	0.88 ± 0.00	1.82	74.98
	3b	3.50± 0.52	0.13	58.43	0.47 ± 0.04	7.44	77.12
	3c	5.64± 0.02	0.08	53.04	0.50 ± 0.03	11.28	76.80
	3d	4.21± 0.12	0.14	56.22	0.61 ± 0.02	30.07	76.58
	3e	4.53± 0.13	0.07	56.87	0.18 ± 0.01	12.94	77.10
	3f	4.14± 0.46	0.86	57.09	3.57 ± 0.15	1.16	70.15
	Galantamine [b]	4.14± 0.07	**4.92**	57.02	20.38±2.10	**0.20**	53.04

c : Selectivity for AChE**:** IC_{50}(BChE)/IC_{50}(AChE). **d:** Selectivity for BChE**:** IC_{50}(AChE)/IC_{50}(BChE)

The data shown in Tables 12 and 13 indicate that depend on the streture the tested compounds exhibit strong inhibition against both *AChE* and *BChE* enzymes with IC_{50} values ranging from (IC_{50}: 1.33 ± 0.3 μM to 17.97 ± 0.27 μM). The best inhibitors of *AChE* among all compounds are (**2a)** for salts with (IC_{50}: 1.33 ± 0.3 μM**)**, and (**3a**)for their silver(I) complexes with (IC_{50}: 1.60 ± 0.19 μM), which are better than Galantamine's (IC_{50}: 4.14 ± 0.07 μM). The least effective *AChE* inhibitor among the salts is (**2f)** with (IC_{50}: 17.97 ± 0.27 μM), while (**3c)** among the silver(I) complexes is the least active with (IC_{50}: 5.64± 0.02 μM**)**. It should be noted that compounds (**2d), (3d), (3e),** and (**3f)** showed IC_{50} values in the same range as the standard Galantamine. Therefore, benzimidazolium

salts and silver (I)-NHC complexes could be potential inhibitors of acetylcholinesterase. According to Taylor et al. [155] the compounds that give a good inhibitory activity of acetylcholinesterase (*AChE*) are more beneficial for human health. The results of the study on the inhibition of *BChE* by the same compounds showed that all compounds had high activity towards *BChE*, with IC_{50} values ranging from (IC_{50}: 0.29 ± 0.04 μM to 4.29 ± 0.18 μM). The most active compounds were (**2d)** benzimidazolium salt with (IC_{50}: 0.15 ± 0.02 μM), and (**3e)** silver (I)-NHC complex with (IC_{50}: 0.18 ± 0.01 μM). On the other hand, (**2f)** and (**3f)** were the least active inhibitors with (IC_{50}: 4.29 ± 0.18 µM) and (IC_{50}: 3.57 ± 0.15µM) respectively. All new compounds were found to be more potent than the standard drug galantamine against *BChE*, and also more selective for *BChE* compared to galantamine. The highest selectivity was seen in compounds (**2c)**, (**2d)**, (**2e)**, (**3c)**, (**3d)**, and (**3e)**, with compound 3d being 30.07 fold more selective for *BChE*. While for *AChE* inhibitors all compounds had a lower affinity for *AChE* compared to galantamine.

I.7.2.2 In vitro cholinesterases inhibition of Pd-NHC complex 4d.

In order to carry on with the investigation in vitro anticholinesterase potential of the new compounds, we turned our attention to evaluating the capacity of palladium-NHC complexes toward anticholinesterase activity. The inhibitory effect of Pd(II)-NHC complex (**4d)** was tested against two enzymes, *AChE*, and *BChE*, at different concentrations. The Pd-NHC complex showed similar levels of inhibition against *AChE* compared to the standard drug Galantamine. However, it was more effective against *BChE* than the standard drug. The compound (**4d)** is less active *AChE* and *BChE* inhibitory compared with benzimidazolium salts and silver(I)-NHC complexes. The results of the new compounds' evaluation, including their selectivity index for *BChE* over *AChE*, are summarized in Table 14.

Table 14. Anti-Cholinesterase activity and the selectivity index for *AChE* over *BChE* and *BChE* over *AChE* of Pd-NHC complex PEPPSI-type (**4d)** [128]

	Enzymes	Pd(II)-NHC complex PEPPSI-type (4d)	Galantamine [b]
AChE	IC_{50}±SD (μM)[a]	19.30± 1.32	4.14± 0.07
	Selectivity index[c]	0.62	4.92
BChE	IC_{50}±SD (μM)[a]	12.06 ± 1.68	20.38±2.10
	Selectivity index[c]	1.60	0.20

a: *IC_{50} values represent the means ± SD of three parallel measurements ($p < 0.05$).* ***b:*** *Reference compound.* ***c:*** *Selectivity for AChE, IC_{50} (BChE) / IC_{50} (AChE).* ***d:*** *Selectivity for BChE, IC_{50} (AChE)/ IC_{50} (BChE)*

Table 14 demonstrates that the test compound effectively inhibits both *AChE* and *BChE* enzymes with (IC_{50}: 19.30 ± 0.62 μM) and (IC_{50}: 12.06 ± 1.68 μM) respectively. This inhibition strength is stronger compared to Galantamine's inhibition of *AChE* with (IC_{50}:4.14 ± 0.07 μM) and *BChE* with (IC_{50}:20.38 ± 2.10 μM). It was observed that the new compound was more specific towards inhibiting *BChE* compared to the commonly used drug Galantamine. This specificity was particularly noticeable for compound (**4d)**, which showed 27.93 times greater selectivity for *BChE*. However, it had a weaker affinity towards inhibiting *AChE* than Galantamine.

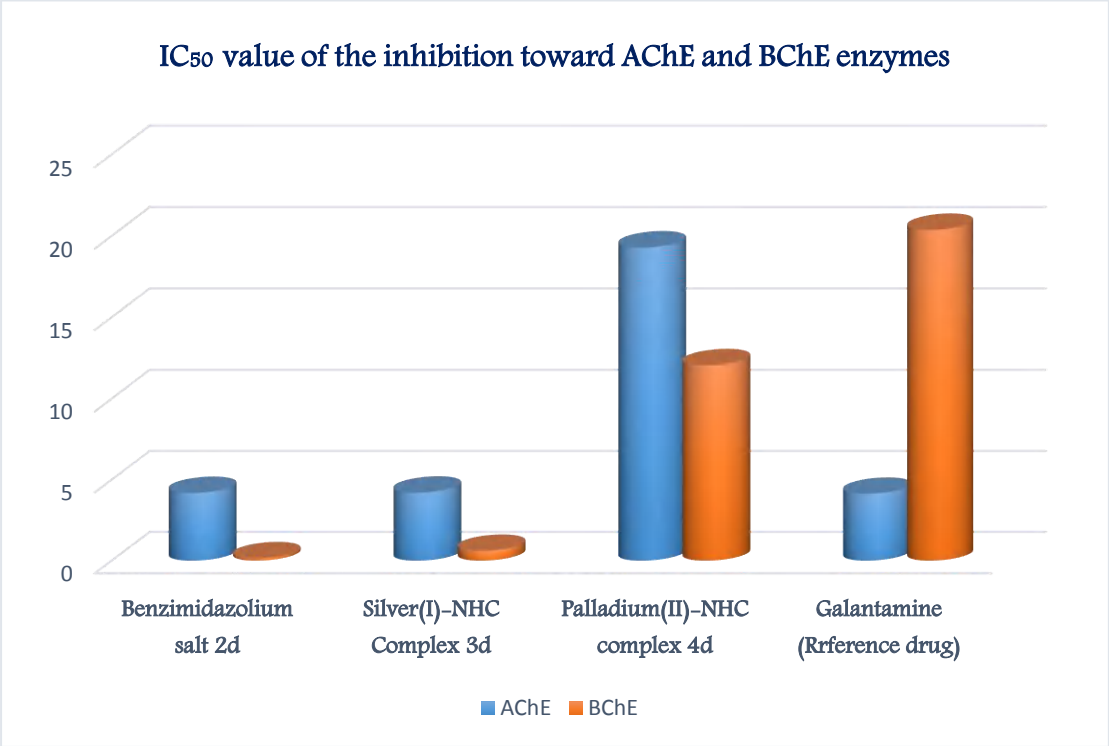

Figure 47. Comparing inhibition values of compounds (**2d)**, (**3d)**, and (**4d)** toward *AChE* and *BChE*

I.7.2.3 Evaluation of Pancreatic Lipase inhibitory capacity (Anti-lipase assay)

The inhibitor of digestive lipase that limits intestinal fat absorption at an initial stage could prove as a proper medication for the treatment of hyperlipidemia and holds great promise as an anti-obesity agent. To identify new inhibitors of pancreatic lipase (*triacylglycerol lipase, EC 3.1.1.3*), a radioactive screening method was used to test the anti-lipase activity of 5,6-dimethylbenzimidazolium salts (**2a-f)** and related silver(I)-NHC complexes (**3a-f)**.

The results, shown in Table 12, demonstrate that all of the silver complexes exhibit significant inhibitory activity against lipase, with (**3a)** and (**3e)** displaying particularly strong anti-lipase activity (IC_{50}: 33.79 ± 6.17 µM and IC50: 33.15 ± 1.47 µM) respectively which found to be very close to the reference drug orlistat (IC_{50} = 25.07 ± 0.48 μM). Conversely, all of the salts (**2a-f)** were inactive against the lipase enzyme. This study confirms that the presence of silver in the compound enhances the complex's anti-lipase activity.

I.7.2.4 Evaluation of α-amylase inhibitory capacity

The evaluation of 5,6-dimethylbenzimidazolium salts and their silver(I)-NHC complexes effect was done using an *α-amylase* inhibitory assay to determine their anti-diabetic activity.

The results, shown in Table 12, indicated that the silver (I)-NHC complexes had greater inhibitory activity compared to acarbose (IC_{50} = 52.58 ± 4.69 µM). The highest α-amylase inhibition was observed in compound (**3a)** with an IC_{50} of 7.00 ± 0.87 µM. However, none of the benzimidazolium salts (**2a-f)** was active against *α-amylase* and displayed no anti-diabetic activity.

I.8 Molecular docking study

Molecular docking studies were carried out to get a better insight into the binding modes and amino acid interactions between synthesized compounds and the active sites of *AChE* and *BChE* enzymes.

Molecular geometries derived from DFT calculations were used for the docking study. The crystal structures of human *AChE* (PDB ID: 4M0E [156] and *BChE* (PDB ID: 2XQF [157]) coordinates were obtained from the Protein Data Bank (PDB) (https://www.rcsb.org). The binding site of the enzymes was defined by selecting residues with a heavy atom within 6 Å of the inhibitor and refined by adding essential residues beyond 6 Å [158].

AChE and *BChE* were prepared in Schrodinger's Protein Preparation Wizard [159] by removing Chain B, water, heteroatoms, and co-factors. Hydrogen and missing atoms were added and bond charges were computed before minimizing the intra-molecular energy and exporting a mol 2 file and used as a starting structure for docking [160]. The compound figures were created in BIOVIA Discovery Studio (https://3dsbiovia.com/), while the others were drawn using the built and LigPrep module implemented in Maestro version 11.3 of the Schrodinger suite [161].

The docking investigation was done using AutoDock Vina (version 1.1.2) [155] for the Pd-NHC complex and GOLD version 5.2.2 for the benzimidazolium salts and Silver(I)-NHC complexes in which the target atoms are fixed and the ligands are flexible. GoldScore scoring function was used to rank the molecules based on their score, which is given as fitness. The best cluster poses were saved and visually examined using PyMol version 2.2.3 [162] and Maestro version 11.3 from the Schrodinger suite [161]. The Discovery Studio software tool (version 2.1) was used to add charges, bond orders, appropriate bonds, and the CHARMm force field.

AutoDockTools (version 1.5.6) was used to add partial charges and hydrogens to the protein and ligand. The search space was created as a 75 Å cube with grid points separated by 1 Å and centered at the middle of the protein, with the coordinates x = 4.76; y = 65.51; z = 56.82 for *AChE* and x = 138.80; y = 123.51; z = 38.60 for *BChE*.

I.8.1 Molecular docking of the benzimidazolium salt (**2a)**, the silver(I)-NHC complex (**3a)**

The results of enzyme inhibitory activity in vitro were consistent with the molecular docking findings. The most effective inhibitors from in vitro tests had the best docking scores against both enzymes. The two most promising compounds (**2a)** for *AChE* and (**2d)** for *BChE*) were further evaluated for their binding mode with their targets. Compound (**2a)** covers both the catalytic anionic site (CAS) and peripheral anionic site (PAS) of *AChE*, resulting in an inhibitory potency three times greater than that of galantamine, which only binds to the catalytic anionic site (Figure 48).

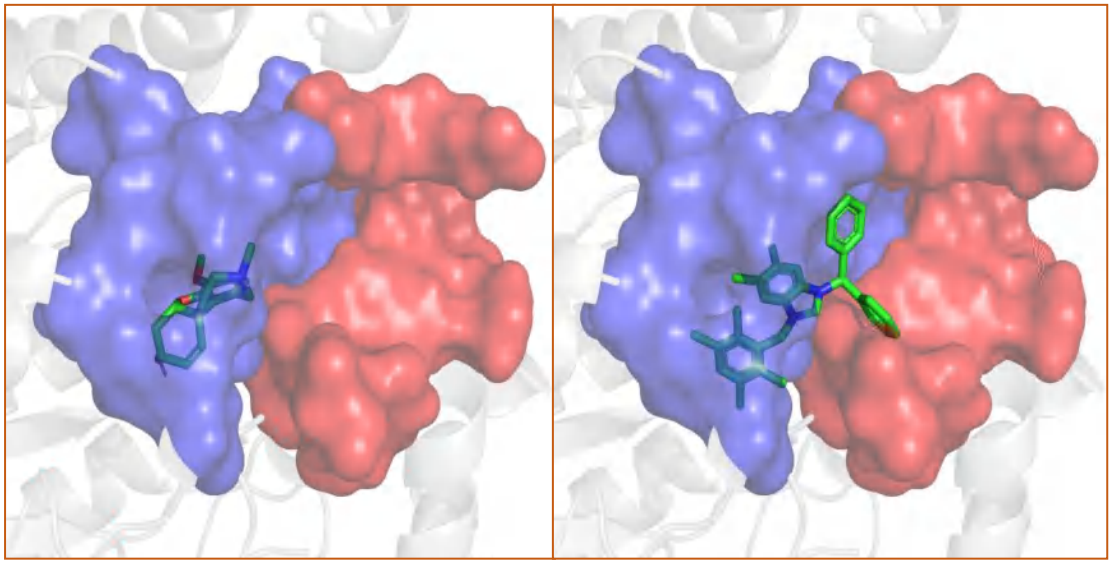

Figure 48. The positioning of galantamine (a) and, (**2a)** (b) in the *AChE* active site

The difference in inhibitory potency between the two compounds is due to the different number of interactions they have with the protein (Figure 49). Compound (**2a)** is involved in eight interactions (six π-π stacking with Trp86, Tyr124, Tyr337, Phe338, Tyr341, and two π-cation interactions with Trp86 and Tyr341), while galantamine is involved in four interactions (two π-cation interactions with Trp86 and Phe338, a hydrogen bond with Gly121 and a π-π stacking with Phe338). The preferred position of each chemical is displayed using results from docking with the software Gold. The amino acid Tyr341, which covers the pocket's ligand, has been left out for clarity. The cavity's active site (CAS) is shown in blue and the pocket (PAS) is shown in red. The ligand components are indicated by color: oxygen is red, carbon is green, and nitrogen is blue. The illustrations were created using PyMol.

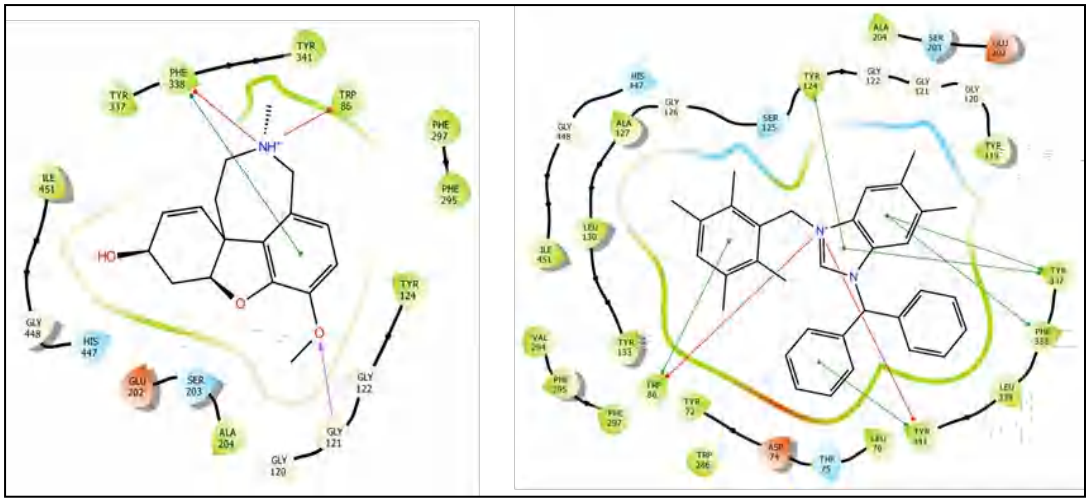

Figure 49. Binding mode prediction of galantamine (a), and compound (**2a)** (b) into the entire *AChE* active pocket.

The images of the hydrogen bonds (purple arrows head from the donor to the acceptor), π-cation interactions (in red), and π-π stacking (in green) were created using the Ligand Interaction Diagram script from Schrödinger Suite. The inhibitory potency of compound (**2d)** is greater than galantamine because it binds to both the CAS and PAS of *BChE* while galantamine only binds to the CAS (Figure 50). Furthermore, (**2d)** has more interactions with the *BChE* active site compared to galantamine (Figure 51). While galantamine only has two interactions (hydrogen bond with Glu197 and π-cation interaction with Trp82), (**2d)** has six interactions including two π-π stackings with His438, which is an important residue for *BChE* activity [163].

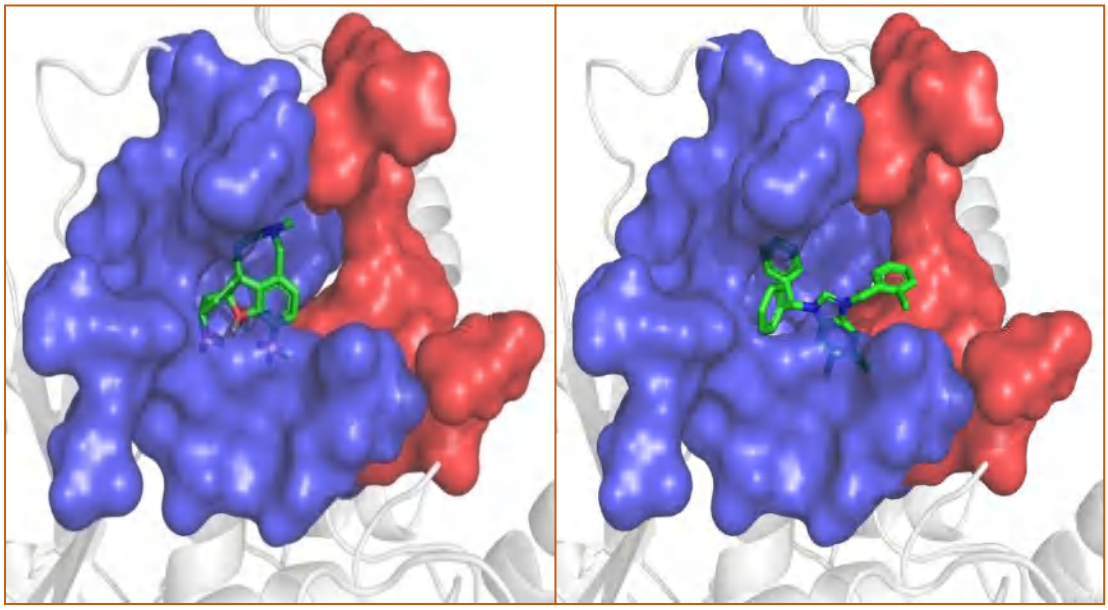

Figure 50. The positioning of galantamine (a), and (**2d)** (b) in the BChE active site.

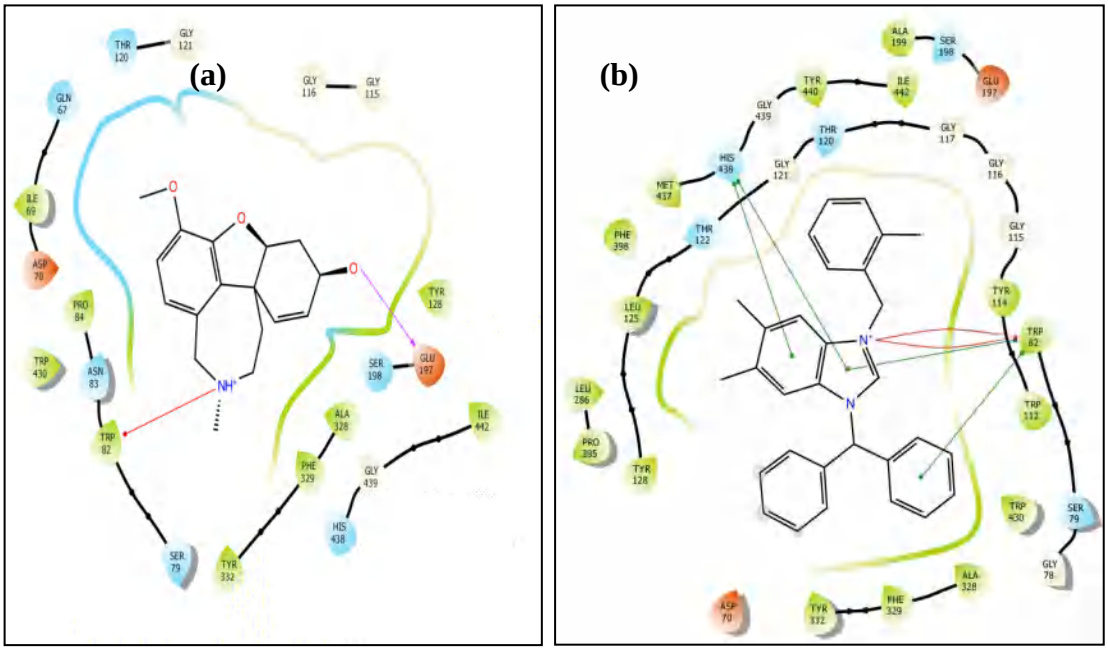

Figure 51. Binding mode prediction of galantamine (a) and compound (**2d)** (b) into the entire *BChE* active pocket.

Salts are more effective than complexes due to the positive nitrogen in the cycle forming π-cation bonds with the enzyme's active site residues (Trp86 in *AChE* and Trp82 in *BChE*), increasing their affinity for (**2a)** and (**2d)** compared to their silver(I)-NHC complex analog (**3a)** and (**3d)** against *AChE* and *BChE* respectively. This results in a greater inhibitory potency compared to their silver(I)-NHC complex counterparts **(3a)** and (**3d)** for *AChE*, and (**3e)** for *BChE*).

Remarkably, the formation of the π-cation interaction between the nitrogen of salts and Trp86 (or Trp82) explains this increase. However, the Ag(I)-NHC complex (**3a)** only forms π-π stackings with three residues of AChE's active site (Tyr124, Tyr341, and His447), and the lack of π-cation interaction with Trp86 decreases its affinity compared to its salt analog (**2a)**. The same is true for the silver(I)-NHC complex (**3e)**, which only forms a π-π stacking with His438 of *BChE's* active site, reducing its affinity compared to its salt analog (Figure 52 (c)).

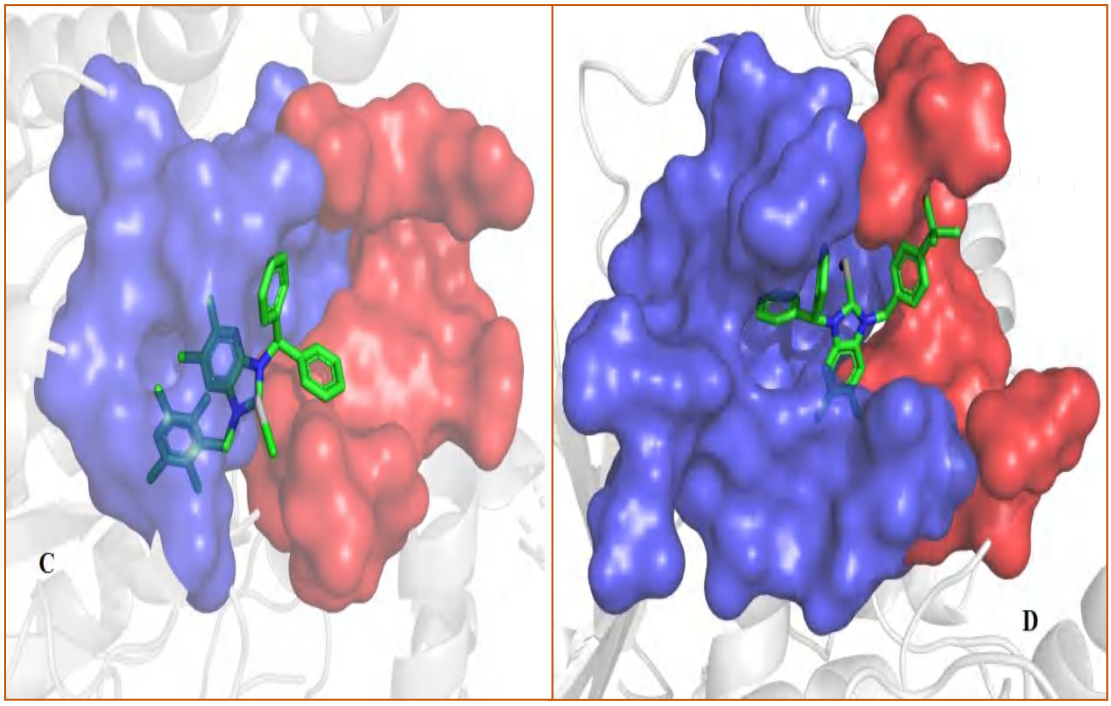

Figure 52. The positioning of complex (**3a)** (c) in *AChE*, and (**3e)** (d) in *BChE* active sites.

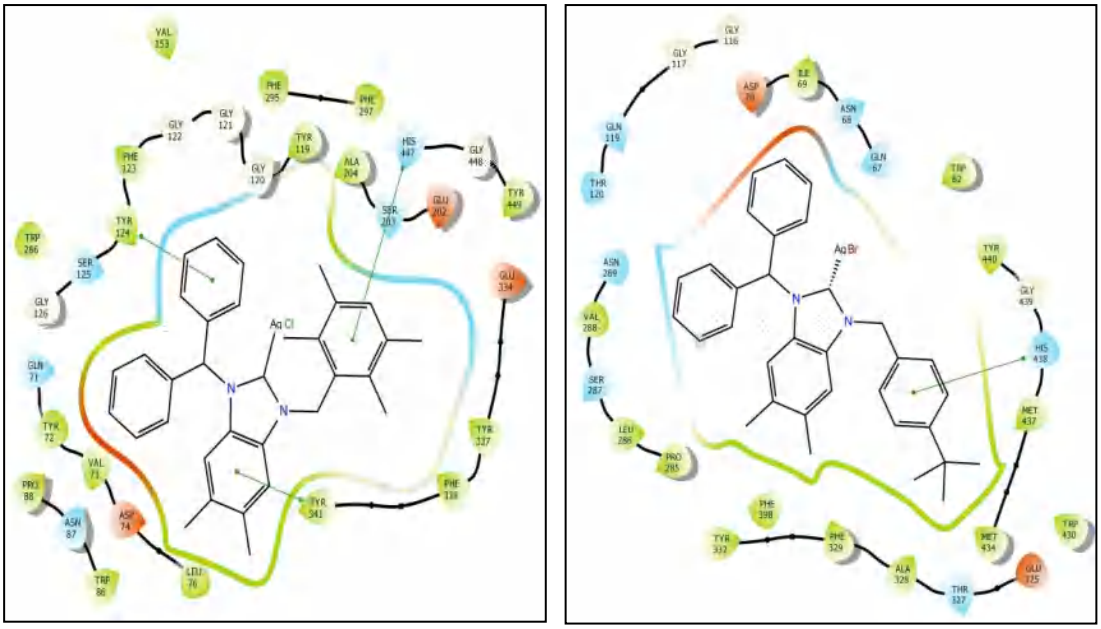

Figure 53. Binding mode prediction of compound (**3a)** (c) and compound (**3e)** (d) into the entire *AChE* and *BChE* active pocket.

I.8.2 Molecular docking of palladium-NHC complex (**4d)**

Additionally, molecular docking experiments were carried out to more closely analyze the way the Pd(II)-NHC compound (**4d)** fits into the active sites of the *AChE* (PDB ID: 1ACJ) and *BChE* (PDB ID: 4BDS) enzymes. Figures 56 and 57 show, respectively, the binding positions of complex (**4d)** in the active sites of *AChE* and *BChE*, as well as the energies of these bindings can be seen in Table 15.

Table 15. Binding energies of Pd-NHC complex (**4d)** and galantamine into the active sites of *AChE* and *BChE*

Compound	**Binding energy (kcal/mol)**	
	AChE	***BChE***
Pd-NHC complex	-4.86	-9.34
Galantamine	-7.83	-6.74

According to the results obtained in vitro assay, the Pd complex (**4d)** is less active than galantamine by about 4.5 times. These results match up with the predictions from molecular modeling. The binding energy of the Pd complex (**4d)** (-4.86 kcal/mol) comparing that of galantamine (-7.83 kcal/mol), meaning the Pd complex (**4d)** is less stable in the active site of the *AChE* enzyme than galantamine. This may explain the observed difference in the inhibitory potential of ligand Pd complex (**4d)** compared to the reference. However, the Pd complex (**4d)** does interact well with certain amino acids in the catalytic site, Trp84, and Phe330, which play a key role in the catalytic function of *AChE* (Figure 54). This could explain its moderate activity despite low binding energy. The Pd complex (**4d)** also forms good hydrophobic interactions with Tyr334 and Tyr121 in the PAS (Figure 54).

In contrast, it showed higher inhibitory activity against the *BChE* enzyme compared to galantamine, with activity 1.8 times higher than that of galantamine. This is because the Pd complex had high binding energies at the active site of *BChE* (-9.34 kcal/mol) (Table 15) and interacted favorably with certain residues in the catalytic site, Trp82 and Phe329, and Val288 and Leu286 in the acyl pocket (Figure 55).

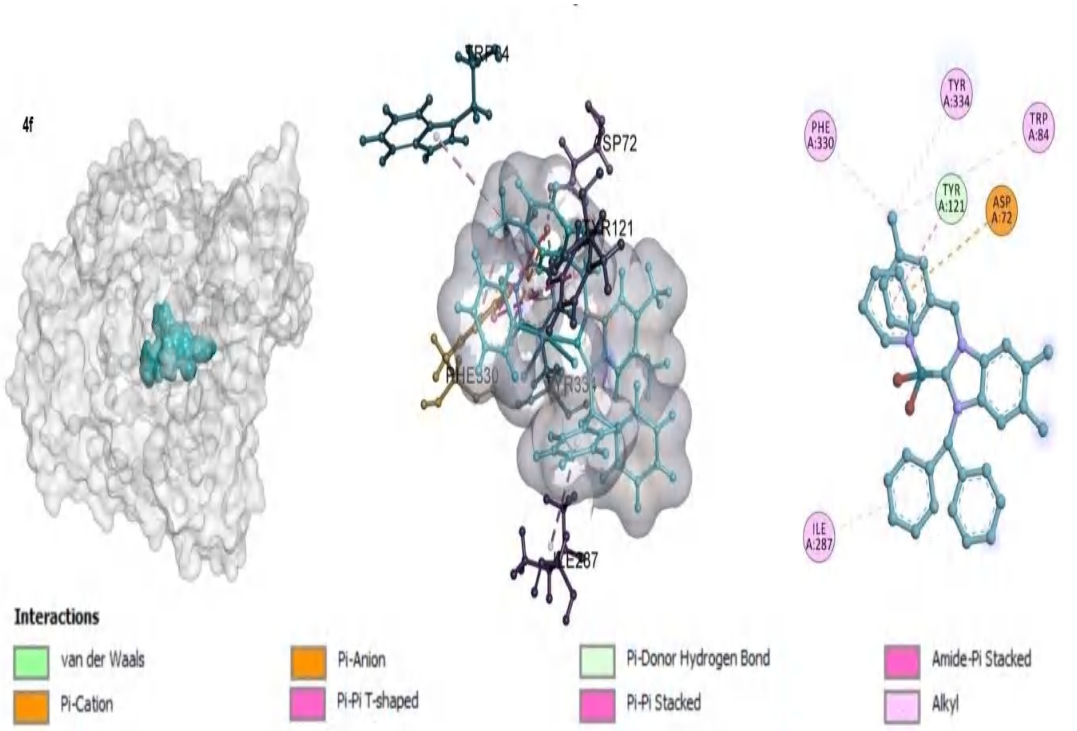

Figure 54. Docking poses of the ligand (a) and Pd complex (**4d)** (b) into the active site of the *AChE* enzyme

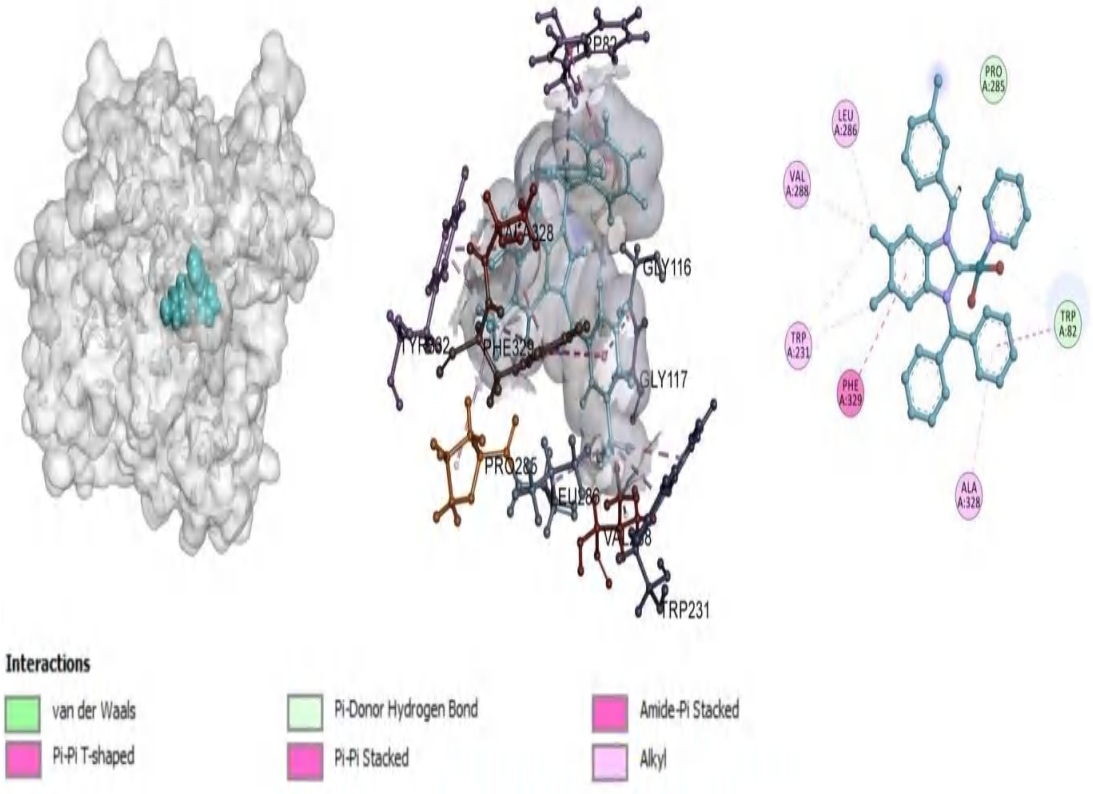

Figure 55. Docking poses of the ligand (a) and Pd complex (**4d)** (b) into the active site of the *BChE* enzyme

I.9 Conclusion

In summary, this research has successfully synthesized and fully characterized six new 5,6-benzimidazolium salts as *N*-heterocyclic carbene precursors, as well as their related new silver(I)-NHC complexes and Pd(II)-NHC complexes PEPPSI-Type. Analytical experimental methods and theoretical calculations were employed to provide a detailed characterization of the molecular structure and electronic properties of the new compounds. Some compounds were determined by a single-crystal X-ray diffraction study, which supports the proposed structures and offered a more detailed structural characterization. As well the result for representative molecule (**3a)** has been confirmed on its electronic, vibrational, and optical properties by means of Density Functional Theory (DFT) calculations.

Additionally, the biological activity of the newly synthesized compounds was evaluated *in vitro*, revealing significant anti-microbial and inhibitory properties against a variety of enzymes, including *AChE*, *BChE*, *α-amylase*, and *lipase*. The study was supported by docking molecular to get a better insight into the binding modes and interactions between synthesized compounds and the active sites of *AChE* and *BChE*. Furthermore, the Pd(II)-NHC complexes **PEPPSI**-Type were found to be effective catalysts in the direct arylation process of five-membered heteroaromatics such as thiophene, furan, and furaldehyde derivatives with various arylbromide derivatives, with a high catalytic activity, achieved using only 1 mol% catalyst for 1 hour. Satisfactory results were obtained as compared with previously reported similar studies.

Overall, these findings contribute to the development of new and potent *N*-heterocyclic carbene complexes with potential applications in both, catalysis and bioactive molecules discovery.

III. Experimental Study

I.1 The general procedure for the preparation of benzimidazolium salts and NHC complexes

The first step in the execution of this procedure was the synthesis of the product (1-benzhydryl-5,6-dimethyl-1*H*-benzo[d]imidazole) as a starting material.

I.1.1 Preparation of 1-benzhydryl-5,6-dimethyl-1*H*-benzo[d]imidazole

Under argon using standard Schlenk, a mixture of 5,6-dimethylbenzimidazol (34 mmol) with bromodiphenylmethane (34 mmol) was heated at 50° C for 10 days in the presence of KOH (0.135 mol) as a basic catalyst. The obtained mixture was cooled at room temperature. After, 45 mL of diethyl ether was added and stirred for 1h, then the product was washed with diethyl ether and filtred to remove the impurities. The product was obtained with high purity.

1-benzhydryl-5,6-dimethyl-1H-benzo[d]imidazole **1**

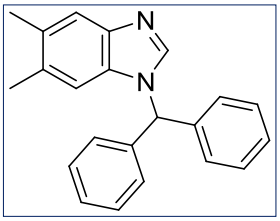

- ✓ ***Chemical Formula:*** $C_{22}H_{20}N_2$
- ✓ ***Molecular Weight:*** 312.10 g/mol
- ✓ ***Yield:*** 45%, (6.5 g); White-solid
- ✓ ***m.p:*** 205.5 °C

^{1}H NMR (400 MHz, $CDCl_3$): δ (ppm) = 7.57 (s, 1H, NC<u>H</u>N); 7.49 (s, 1H, C<u>H</u>); 7.36 (d, *J* = 1.8 Hz, 4H, C<u>H</u>); 7.34 (d, *J* = 1.8 Hz, 2H, C<u>H</u>); 7.13 (dd, *J* = 6.9, 2.3 Hz, 4H, C<u>H</u>); 6.92 (s, 1H, C<u>H</u>); 6.70 (s, 1H, Ph-C<u>H</u>-Ph); 2.34 (s, 3H, C<u>H</u>$_3$); 2.28 (s, 3H, C<u>H</u>$_3$).

^{13}C NMR (100 MHz, $CDCl_3$): δ (ppm) = 142.6 (N<u>C</u>HN); 141.8 (2Cq, <u>C</u>-CH-<u>C</u>); 138.3 (2Cq, <u>C</u>-N); 132.6 (Cq, <u>C</u>-CH$_3$); 132.1 (Cq, <u>C</u>-CH$_3$); 128.9 (4CH, <u>C</u>H-Ar); 128.4 (2CH, <u>C</u>H-Ar); 128.2 (4CH, <u>C</u>H-Ar); 126.5 (2CH, <u>C</u>H-Ar); 120.3 (CH, <u>C</u>H-Ar); 110.7 (CH, <u>C</u>H-Ar); 63.4 (CH, Ph-<u>C</u>H-Ph); 20.5 (C, <u>C</u>H$_3$); 20.2 (C, <u>C</u>H$_3$).

I.1.2 Synthesis of 3,5-dimethylbenzimidazolium Salts (**2a-f)**

Under argon using standard Schlenk, a mixture of 1-benzyl-5,6-dimethylbenzimidazole (1 mmol) and an equivalent amount of alkyl halide derivative (1 mmol), in degassed dimethylformamide, was heated and stirred at 80 °C for 48h. The obtained mixture was cooled at room temperature. After, 45 mL of ether was added and stirred for 1h, then the product was washed with diethyl ether to remove the impurities, and the product was left precipitated. The product was filtered with high purity. After, the crude products were recrystallized in dichloromethane/diethyl ether and dried under a vacuum to provide pure products for experimental analysis.

*I.1.2.1 1-Benzhydryl-5,6-dimethyl-(2,3,5,6-tetramethylbenzyl)benzimidazolium chloride (**2a**)*

A mixture of 1-benzhydryl-5,6-dimethyl-1*H*-benzo[d]imidazole (3.2 mmol, 1g) and 2,3,5,6-tetramethylbenzylchloride (3.2 mmol, 582 mg) gave the desired salt (**2a)**.

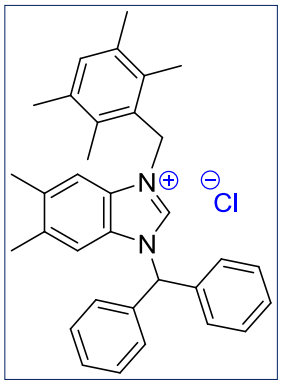

- ✓ ***Chemical Formula:*** $C_{33}H_{35}ClN_2$
- ✓ ***Molecular Weight:*** 495.10 g/mol
- ✓ ***Yield****:* 85%, (1348 mg); White-solid
- ✓ ***m.p****:* 152-153 °C
- ✓ ***FT-IR:*** $\nu_{(C-N)}$ = 1549 cm^{-1}

^{1}H NMR (400 MHz, $CDCl_3$): δ (ppm) = 10.45 (s, 1H, NC<u>H</u>N); 7.62 (s, 1H, $C_6\underline{H}_2(CH_3)_2$); 7.38-7.36 (m, 6H, C<u>H</u>-Ar); 7.34-7.30 (m, 4H, C<u>H</u>-Ar); 7.01 (s, 1H, $C_6\underline{H}_2(CH_3)_2$); 6.93 (s, 1H, Ph-C<u>H</u>-Ph); 5.90 (s, 2H, $C\underline{H}_2N$); 2.23 (s, 3H, $C\underline{H}_3$); 2.21 (s, 6H, $C\underline{H}_3$); 2.19 (s, 9H, $C\underline{H}_3$).

^{13}C NMR (100 MHz, $CDCl_3$): δ (ppm) = 142.3 (N<u>C</u>HN); 137.0 (Cq, C-CH_3); 136.9 (Cq, C-CH_3); 135.7 (2Cq, <u>C</u>-CH-<u>C</u>); 134.9 (2Cq, <u>C</u>-CH_3); 134.0 (2Cq, <u>C</u>-CH_3); 133.3 (Cq, <u>C</u>-CH_2); 130.6 (Cq, <u>C</u>-N); 130.0 (Cq, <u>C</u>-N); 129.3 (4C, <u>C</u>H-Ar); 129.2 (2C, <u>C</u>H-Ar); 128.4 (4C, <u>C</u>H-Ar); 128.2 (C, <u>C</u>H-Ar); 114.6 (<u>C</u>H-Ar); 113.6 (<u>C</u>H-Ar); 66.1 (Ph-<u>C</u>H-Ph); 47.9 (N-$\underline{C}H_2$); 20.8 ($\underline{C}H_3$); 20.7 (CH_3); 20.5 (2$\underline{C}H_3$,); 16.1 (2$\underline{C}H_3$).

Elemental analysis; calcd (%) for $C_{33}H_{35}ClN_2$ (**M.w** = 495.10 g/mol): C 79.89, H 7.31, N 5.65; **found** (%): C 79.83, H 6.78, N 5.35.

*I.1.2.2 1-Benzhydryl -5,6-dimethyl-(4-methylbenzyl)benzimidazolium chloride (**2b**)*

Following the general procedure, a mixture of 1-benzhydryl-5,6-dimethyl-1*H*-benzo[d]imidazole (2.6 mmol, 812 mg) and 4-methylbenzylchloride (2.6 mmol, 340 mg) gave the desired salt (**2b**).

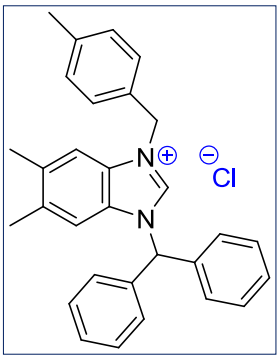

- ✓ ***Chemical Formula:*** $C_{30}H_{29}ClN_2$
- ✓ ***Molecular Weight:*** 453.02 g/mol
- ✓ ***Yield:*** 71%, (1033 mg); White-solid
- ✓ ***m.p:*** 159-160 °C
- ✓ ***FT-IR:*** $\nu_{(C-N)}$ = 1548 cm^{-1}

^{1}H NMR (400 MHz, $CDCl_3$): δ (ppm) = 11.27 (s, 1H, NC<u>H</u>N); 7.37 (d, J = 5.7 Hz, 6H, C<u>H</u>-Ar); 7.34 (s, 3H, C<u>H</u>-Ar); 7.32 (s, 2H, C<u>H</u>-Ar); 7.29 (s, 2H, C<u>H</u>-Ar); 7.11 (d, J = 7.2 Hz, 2H, C<u>H</u>-Ar); 6.97 (s, 1H, Ph-C<u>H</u>-Ph); 5.84 (s, 2H, C<u>H</u>$_2$N); 2.28 (s, 3H, C<u>H</u>$_3$); 2.27 (S, 3H, C<u>H</u>$_3$); 2.20 (s, 3H, C<u>H</u>$_3$).

^{13}C NMR (100 MHz, $CDCl_3$): δ (ppm) = 142.7 (N<u>C</u>HN); 138.9 (Cq, <u>C</u>-CH$_3$); 137.2 (Cq, <u>C</u>-CH$_3$); 137.1 (Cq, <u>C</u>-CH$_3$); 135.5 (2Cq, <u>C</u>-CH-<u>C</u>); 130.3 (Cq, <u>C</u>-N); 130.2 (Cq, <u>C</u>-N); 129.9 (2C, <u>C</u>H-Ar); 129.8 (C, <u>C</u>H-Ar); 129.4 (4C, <u>C</u>H-Ar); 129.3 (2C, <u>C</u>H-Ar); 128.4 (4C, <u>C</u>H-Ar); 128.2 (2C, <u>C</u>H-Ar); 114.5 (C, <u>C</u>H-Ar); 113.4 (C, <u>C</u>H-Ar); 66.4 (Ph-<u>C</u>H-Ph); 51.2 (C, N-<u>C</u>H$_2$); 21.1 (<u>C</u>H$_3$); 20.7 (<u>C</u>H$_3$); 20.7 (<u>C</u>H$_3$).

Elemental analysis; calcd (%) for $C_{30}H_{29}ClN_2$ (**M.w** = 453.02 g/mol): C 79.54, H 6.45, N 6.18; **found** (%): C 79.28, H 6.73, N 5.35.

*I.1.2.3 1-Benzhydryl -5,6-dimethyl-3-(2,4,6-trimethylbenzyl)benzimidazolium chloride (**2c**)*

Following the general procedure, a mixture of 1-benzhydryl-5,6-dimethyl-1*H*-benzo[d]imidazole (2.56 mmol, 800 mg) and 2,4,6-trimethylbenzylchloride (2.56 mmol, 450 mg) gave the desired salt (**2c**).

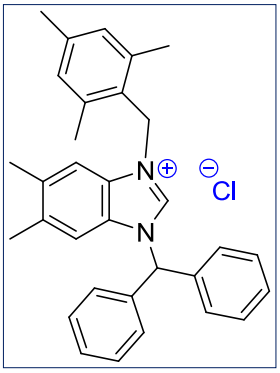

- ✓ ***Chemical Formula:*** $C_{32}H_{33}ClN_2$
- ✓ ***Molecular Weight:*** 481.07 g/mol
- ✓ ***Yield:*** 81%, (1213 mg); White-solid
- ✓ ***m.p:*** 155-156 °C
- ✓ ***FT-IR:*** $\nu_{(C-N)}$ = 1546 cm^{-1}

^{1}H NMR (400 MHz, $CDCl_3$): δ (ppm) = 10.88 (s, 1H, NC<u>H</u>N), 7.50 (s, 1H, $C_6\underline{H}_2(CH_3)_2$), 7.36 (dd, J = 5.3 Hz, 1.6 Hz, 6H, C<u>H</u>-Ar); 7.31 (dd, J = 7.0 Hz, 2.5 Hz, 4H,C<u>H</u>-Ar); 6.94 (s, 1H, CH-Ar); 6.92 (s, 1H, Ph-C<u>H</u>-Ph); 6.86 (s, 2H, C<u>H</u>-Ar); 5.88 (s, 2H, $C\underline{H}_2N$); 2.26 (s, 6H, $C\underline{H}_3$); 2.24 (s, 3H, $C\underline{H}_3$); 2.20 (s, 3H, $C\underline{H}_3$); 2.17 (s, 3H, $C\underline{H}_3$).

^{13}C NMR (100 MHz, $CDCl_3$): δ (ppm) = 142.8 (NCHN); 139.4 (Cq, <u>C</u>-CH_3); 137.9 (2Cq, <u>C</u>-CH_3); 137.1 (Cq, <u>C</u>-CH_3); 137.0 (Cq, <u>C</u>-CH_3); 135.6 (2Cq, <u>C</u>-CH-<u>C</u>); 130.5 (Cq, <u>C</u>-N); 130.0 (Cq, <u>C</u>-N); 129.9 (2C, <u>C</u>H-Ar); 129.3 (4C, <u>C</u>H-Ar); 129.2 (2C, <u>C</u>H-Ar); 128.4 (4C, <u>C</u>H-Ar); 125.6 (Cq, <u>C</u>-CH_2); 114.5 (C, <u>C</u>H-Ar); 113.6 (C, <u>C</u>H-Ar); 66.2 (Ph-<u>C</u>H-Ph); 47.5 (C, N-<u>C</u>H_2); 21.0 (<u>C</u>H_3); 20.7 (<u>C</u>H_3); 20.6 (<u>C</u>H_3); 20.2 (2<u>C</u>H_3).

Elemental analysis; calcd (%) for $C_{32}H_{33}ClN_2$ (**M.w** = 481.07 g/mol): C 79.89, H 6.91, N 5.82; **found** (%): C 79.71, H 6.86, N 6.38.

*I.1.2.4 1-Benzhydryl -5,6-dimethyl-(3-methylbenzyl)benzimidazolium chloride (**2d**)*

Following the general procedure, a mixture of 1-benzhydryl-5,6-dimethyl-1H-benzo[d]imidazole (2.56 mmol, 800 mg) and 3-Methylbenzylchloride (2.56 mmol, 360 mg) gave the desired salt (**2d**).

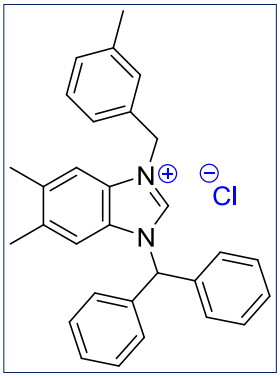

- ✓ ***Chemical Formula:*** $C_{30}H_{29}ClN_2$
- ✓ ***Molecular Weight:*** 453.02 g/mol
- ✓ ***Yield:*** 82%, (1175 mg); White-solid
- ✓ ***m.p:*** 151-152 °C
- ✓ ***FT-IR:*** $\nu_{(C-N)}$ = 1541 cm^{-1}

^{1}H NMR (400 MHz, $CDCl_3$): δ (ppm) = 11.06 (s, 1H, NC<u>H</u>N), 7.39-7.33 (m, 11H, C<u>H</u>-Ar), 7.33 (s, 1H, C<u>H</u>-Ar); 7.21-7.13 (m, 3H, C_6H_4); 7.08 (d, J = 7.2 Hz, 1H, C<u>H</u>-Ar); 6.98 (s, 1H, Ph-C<u>H</u>-Ph); 5.92 (s, 2H, $C\underline{H}_2N$); 2.27 (s, 6H, $C\underline{H}_3$); 2.20 (s, 3H, $C\underline{H}_3$).

^{13}C NMR (100 MHz, $CDCl_3$): δ (ppm) = 142.5 (N<u>C</u>HN); 139.1 (Cq, <u>C</u>-CH_3); 137.3 (Cq, <u>C</u>-CH_3); 137.2 (Cq, <u>C</u>-CH_3); 135.5 (2Cq, <u>C</u>-CH-<u>C</u>); 133.1 (Cq, <u>C</u>-CH_2); 130.4 (Cq, <u>C</u>-N); 129.8 (Cq, <u>C</u>-N); 129,7 (C, <u>C</u>H-Ar); 129.4 (4C, <u>C</u>H-Ar); 129.3 (2C, <u>C</u>H-Ar); 129.1 (C, <u>C</u>H-Ar); 128.6 (C, <u>C</u>H-Ar); 128.4 (4C, <u>C</u>H-Ar); 125.0 (C, <u>C</u>H-Ar); 114.4 (C, <u>C</u>H-Ar); 113.5 (C, <u>C</u>H-Ar); 66.4 (Ph-<u>C</u>H-Ph); 51.4 (C, N-$C\underline{H}_2$); 21.4 ($C\underline{H}_3$); 20.7 ($C\underline{H}_3$); 20.6 ($C\underline{H}_3$).

Elemental analysis; calcd (%) for $C_{30}H_{29}ClN_2$ (**M.w** = 453.02 g/mol): C 79.54, H 6.45, N 6.18; **found** (%): C 79.74, H 6.36, N 6.13.

I.1.2.5 1-Benzhydryl -5,6-dimethyl-(4-tert-butylbenzyl)benzimidazolium bromide (2e)

Following the general procedure, a mixture of 1-benzhydryl-5,6-dimethyl-1*H*-benzo[d]imidazole (2.56 mmol, 800 mg) and 4-*tert*-butylbenzylbromide (2.56 mmol, 544 mg) gave the desired salt (**2e)**.

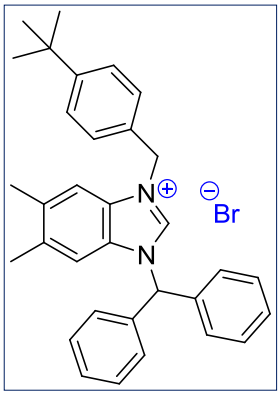

- ✓ ***Chemical Formula:*** $C_{33}H_{35}BrN_2$
- ✓ ***Molecular Weight:*** 539.55 g/mol
- ✓ ***Yield:*** 71%, (980 mg); White-solid
- ✓ ***m.p:*** 179-180 °C
- ✓ ***FT-IR:*** $\nu_{(C-N)}$ = 1542 cm^{-1}

^{1}H NMR (400 MHz, $CDCl_3$): δ (ppm) = 10.73 (s, 1H, NC<u>H</u>N), 7.42-7.37 (m, 11H, C<u>H</u>-Ar); 7.34 (sl, 5H, C<u>H</u>); 7.00 (s, 1H, Ph-C<u>H</u>-Ph); 5.84 (s, 2H, C<u>H</u>$_2$N); 2.31 (s, 3H, C<u>H</u>$_3$); 2.22 (s, 3H, C<u>H</u>$_3$); 1.25 (s, 9H, C<u>H</u>$_3$).

^{13}C NMR (100 MHz, $CDCl_3$): δ (ppm) = 152.1 (Cq, <u>C</u>-(*t*Bu)); 141.6 (N<u>C</u>HN); 137.4 (Cq, <u>C</u>-CH$_3$); 137.2 (Cq, <u>C</u>-CH$_3$); 135.4 (2Cq, <u>C</u>-CH-<u>C</u>); 130.4 (Cq, <u>C</u>-CH$_2$); 130.0 (Cq, <u>C</u>-N); 129.8 (Cq, <u>C</u>-N); 129.5 (4C, <u>C</u>H-Ar); 129.4 (2C, <u>C</u>H-Ar); 128.5 (4C, <u>C</u>H-Ar); 127.9 (2C, <u>C</u>H-Ar); 126.2 (2C, <u>C</u>H-Ar); 114.4 (C, <u>C</u>H-Ar); 113.5 (C, <u>C</u>H-Ar); 66.4 (Ph-<u>C</u>H-Ph); 51.1 (N-<u>C</u>H$_2$); 34.6 (Cq, <u>C</u>-(CH$_3$)$_3$); 31.1 (3<u>C</u>H$_3$); 20.7 (<u>C</u>H$_3$); 20.6 (<u>C</u>H$_3$).

Elemental analysis; calcd (%) for $C_{33}H_{35}BrN_2$ (**M.w** = 539.55 g/mol): C 73.46, H 6.54, N 5.19; **found** (%):C 73.15, H 6.28, N 5.20

I.1.2.6 1-Benzhydryl-5,6-dimethyl-3-(3,4,5-trimethoxybenzyl)benzimidazolium chloride (2f)

Following the general procedure, a mixture of 1-benzhydryl-5,6-dimethyl-1*H*-benzo[d]imidazole (2.56 mmol, 800 mg) and 3,4,5-Trimethoxybenzylchloride (2.56 mmol, 544 mg) gave the desired salt (**2f**).

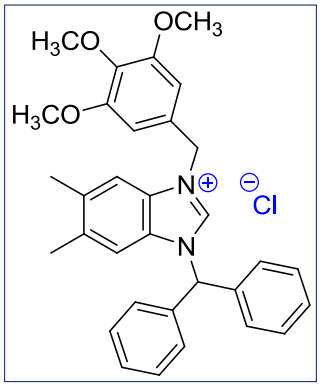

- ✓ ***Chemical Formula:*** $C_{32}H_{33}ClN_2O_3$
- ✓ ***Molecular Weight:*** 529.08 g/mol
- ✓ ***Yield:*** 70%, (950 mg); White-solid
- ✓ ***m.p:*** 157-158 °C
- ✓ ***FT-IR:*** $\nu_{(C-N)}$ = 1552 cm^{-1}

^{1}H NMR (400 MHz, $CDCl_3$): δ (ppm) = 11.25 (s, 1H, NC<u>H</u>N); 7.42-7.32 (m, 12H, C<u>H</u>-Ar), 6.98 (s, 1H, Ph-C<u>H</u>-Ph); 6.76 (s, 2H, $C_6\underline{H}_2$), 5.81 (s, 2H, $C\underline{H}_2N$); 3.79 (s, 6H, $OC\underline{H}_3$); 3.78 (s, 6H, $OC\underline{H}_3$); 2.33 (s, 3H, $C\underline{H}_3$); 2.23 (s, 3H, $C\underline{H}_3$).

^{13}C NMR (100 MHz, $CDCl_3$): δ (ppm) = 153.7 (2Cq, <u>C</u>-OCH_3); 142.7 (N<u>C</u>HN); 138.4 (Cq, <u>C</u>-OCH_3); 137.3 (Cq, <u>C</u>-CH_3); 137.2 (Cq, <u>C</u>-CH_3); 135.50 (2<u>C</u>q, <u>C</u>-CH-<u>C</u>); 130.2 (Cq, C-N); 129.7 (Cq, <u>C</u>-N); 129.4 (4C, <u>C</u>H-Ar); 129.4 (2C, <u>C</u>H-Ar); 128.8 (Cq, <u>C</u>-CH_2); 128.4 (4C, <u>C</u>H-Ar); 114.4 (C, <u>C</u>H-Ar); 113.4 (C, <u>C</u>H-Ar); 105.6 (2C, <u>C</u>H-Ar); 66.5 (Ph-<u>C</u>H-Ph); 60.8 (C, O<u>C</u>H_3); 56.5 (2C, O<u>C</u>H_3); 51.4 (C, N-<u>C</u>H_2); 20.7 (2<u>C</u>H_3).

Elemental analysis; calcd (%) for $C_{32}H_{33}ClN_2O_3$ (**M.w** = 529.08 g/mol): C 72.65, H 6.29, N 5.29; **found** (%): C 72.47, H 6.51, N 5.32

I.1.3 Synthesis of silver(I)-NHC complexes (**3a-f**)

Under argon using standard Schlenk covered with aluminum foil, a solution of 5,6-dimethylbenzimidazolium salts (1 mmol) with Silver(I) oxide Ag_2O (1.5 mmol) in dry chloroform was reacted at 50 °C for 48h in dark conditions. The reaction mixture was filtered through celite, and the solvent was removed under a vacuum to afford the product. The salts were converted to silver(I)-NHC complexes automatically by the reaction, which affords a white solid. The resulting white solid was isolated by filtration then dried in a vacuum, and recrystallized in $CHCl_3/Et_2O$.

*I.1.3.1 Chloro[1-benzhydryl-3-(2,3,5,6-tetramethylbenzyl)-5,6 dimethylbenzimidazole-2-ylidene]silver(I) (**3a**)*

Following the general procedure, the Silver (I)-NHC complex (**3a)** was obtained from a mixture of 1-benzhydryl-5,6-dimethyl-3-(2,3,5,6-tetramethylbenzyl)-1*H*-benzo[d]imidazol-3-ium-chloride (**2a)** (0.5 mmol, 248 mg) and Silver(I) oxide Ag_2O (0.75 mmol, 174 mg).

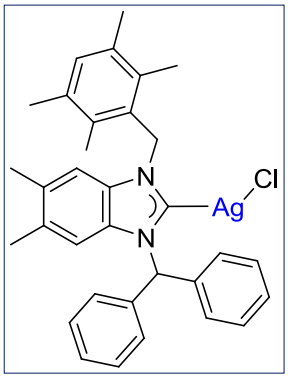

- ✓ ***Chemical Formula:*** $C_{32}H_{34}AgClN_2$
- ✓ ***Molecular Weight:*** 601.97 g/mol
- ✓ ***Yield:*** 70%, (210 mg); White-solid
- ✓ ***m.p:*** 245-246 °C
- ✓ ***FT-IR:*** $\nu_{(C-N)}$ = 1542 cm^{-1}

^{1}H NMR (400 MHz, $CDCl_3$): δ (ppm) = 7.37-7.32 (m, 7H, C<u>H</u>); 7.21 (s, 1H, $C_6\underline{H}_1$); 7.17 (dd, *J* = 6.1 Hz, 2.6 Hz, 4H, C<u>H</u>-Ar); 7.10 (s, 2H, $C_6\underline{H}_2(CH_3)_2$); 6.81 (s, 1H, Ph-C<u>H</u>-Ph); 5.49 (s, 2H, $C\underline{H}_2N$); 2.29 (s, 3H, $C\underline{H}_3$); 2.28 (s, 6H, $C\underline{H}_3$); 2.19 (s, 3H, $C\underline{H}_3$); 2.14 (s, 6H, $C\underline{H}_3$).

^{13}C NMR (100 MHz, $CDCl_3$): δ (ppm) = 137.4 (2Cq, <u>C</u>-CH_3); 135.1 (2Cq, <u>C</u>-CH-<u>C</u>); 133.5 (2Cq, <u>C</u>-CH_3); 133.4 (Cq, <u>C</u>-N); 133.4 (Cq, <u>C</u>-N); 133.0 (2Cq, <u>C</u>-CH_3); 129.9 (C, <u>C</u>H-Ar); 129.0 (4C, <u>C</u>H-Ar); 128.5 (2C, <u>C</u>H-Ar); 128.3 (4C, <u>C</u>H-Ar); 113.6 (C, <u>C</u>H-Ar); 111.7 (C, <u>C</u>H-Ar); 68.6 (Ph-<u>C</u>H-Ph); 48.1 (C, $\underline{C}H_2$-N); 20.7 (2$\underline{C}H_3$); 20.5 ($\underline{C}H_3$); 20.5 ($\underline{C}H_3$); 16.3 (2$\underline{C}H_3$).

Elemental analysis; calcd (%) for $C_{64}H_{68}Ag_2Cl_2N_4$ (**M.w** = 601.97 g/mol): C 65.15, H 5.81, N 4.75; **found** (%): C 66.04, H 5.95, N 4.51

*I.1.3.2 Chloro[1-benzhydryl-3-(4-methylbenzyl)-5,6-dimethylbenzimidazole-2-ylidene]silver(I) **(3b)***

Following the general procedure, the Silver (I)-NHC complex (**3b)** was obtained from a mixture of 1-benzhydryl-5,6-dimethyl-3-(4-Methylbenzyl)-1*H*-benzo[d]imidazol-3-ium-chloride (**2b)** (0.5 mmol, 227 mg) and Silver(I) oxide Ag_2O (0.75 mmol, 174 mg).

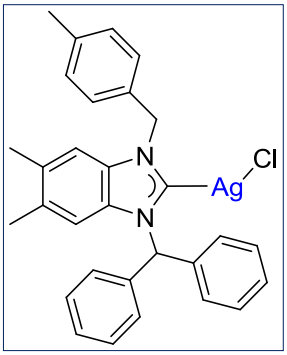

- ✓ ***Chemical Formula:*** $C_{30}H_{28}AgClN_2$
- ✓ ***Molecular Weight:*** 559.89 g/mol
- ✓ ***Yield:*** 80%, (224 mg); White-solid
- ✓ ***m.p:*** 144-145 °C
- ✓ ***FT-IR:*** $\nu_{(C-N)}$ = 1542 cm^{-1}

^{1}H NMR (400 MHz, $CDCl_3$): δ (ppm) = 7.39 (m, 7H, C<u>H</u>-Ar); 7.22 (m, 4H, C<u>H</u>-Ar); 7.14 (s, 1H, N-$C_6\underline{H}_2(CH_3)_2$-N); 7.12 (sl, 4H, $C_6\underline{H}_4$); 7.09 (s, 1H, $C_6\underline{H}_2(CH_3)_2$); 6.92 (s, 1H, Ph-C<u>H</u>-Ph); 5.52 (s, 2H, $C\underline{H}_2N$); 2.31 (s, 3H, $C\underline{H}_3$); 2.26 (s, 3H, $C\underline{H}_3$); 2.20 (s, 3H, $C\underline{H}_3$).

^{13}C NMR (100 MHz, $CDCl_3$): δ (ppm) = 138.2 (Cq, <u>C</u>-CH_3); 137.3 (2Cq, <u>C</u>-CH_3); 133.9 (Cq, <u>C</u>-CH-C); 133.6 (Cq, C-CH-<u>C</u>); 133.0 (<u>C</u>q, C-N); 132.5 (<u>C</u>q, C-N); 132.0 (C, <u>C</u>-CH_2-N); 129.7 (2C, <u>C</u>H-Ar); 129.2 (4C, <u>C</u>H-Ar); 128.8 (2C, <u>C</u>H-Ar); 128.4 (4C, <u>C</u>H-Ar); 127.0 (2C, <u>C</u>H-Ar); 113.0 (C, <u>C</u>H-Ar); 112.3 (C, <u>C</u>H-Ar); 66.9 (Ph-<u>C</u>H-Ph); 53.8 (C, <u>C</u>H_2-N); 21.1 (<u>C</u>H_3); 20.4 (<u>C</u>H_3); 20.4 (<u>C</u>H_3).

Elemental analysis; calcd (%) for $C_{30}H_{28}AgClN_2$ (**M.w** = 559.88 g/mol): C 64.36, H 5.04, N 5.00; **found** (%): C 64.64, H 5.19, N 5.12

*I.1.3.3 Chloro[1-benzhydryl-3-(2,4,6-trimethylbenzyl)-5,6-dimethylbenzimidazole-2-ylidene]silver(I) (**3c**)*

Following the general procedure, the Silver (I)-NHC complex (**3c**) was obtained from a mixture of 1-benzhydryl-5,6-dimethyl-3-(2,4,6-trimethylbenzyl)-1*H*-benzo[d]imidazol-3-ium-chloride (**2c**) (0.5 mmol, 240 mg) and Silver(I) oxide Ag_2O (0.75 mmol, 174 mg).

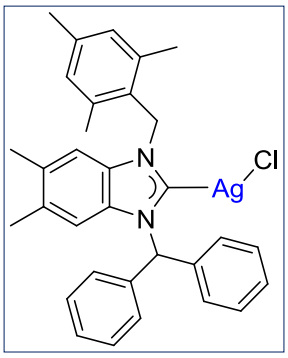

- ✓ ***Chemical Formula:*** $C_{32}H_{32}AgClN_2$
- ✓ ***Molecular Weight:*** 584.97 g/mol
- ✓ ***Yield:*** 74%, (217 mg); White-solid
- ✓ ***m.p:*** 200-201 °C
- ✓ ***FT-IR:*** $\nu_{(C-N)}$= 1542 cm^{-1}

^{1}H NMR (400 MHz, $CDCl_3$): δ (ppm)= 7.36 (m, 7H, C<u>H</u>); 7.19 (m, 5H, C<u>H</u>); 6.94 (s, 2H, $C_6\underline{H}_2$); 6.92 (s, 1H, $C_6\underline{H}_2(CH_3)_2$); 6.84 (s, 1H, Ph-C<u>H</u>-Ph); 5.51 (s, 2H, $C\underline{H}_2N$); 2.32 (s, 3H, $C\underline{H}_3$); 2.23 (s, 9H, $C\underline{H}_3$); 2.18 (s, 3H, $C\underline{H}_3$).

^{13}C NMR (100 MHz, $CDCl_3$): δ (ppm) = 139.2 (Cq, <u>C</u>-CH_3); 137.4 (2Cq, <u>C</u>-CH_3); 137.4 (2Cq, <u>C</u>-CH_3); 133.5 (<u>C</u>q, C-N); 133.4 (<u>C</u>q, C-N); 130.2 (2C, <u>C</u>H-Ar); 129.1 (4C, <u>C</u>H-Ar); 128.6 (2C, <u>C</u>H-Ar); 128.3 (4C, <u>C</u>H-Ar); 127.0 (C, <u>C</u>-CH_2-N); 113.3 (C, <u>C</u>H-Ar); 112.0 (C, <u>C</u>H-Ar); 68.0 (Ph-<u>C</u>H-Ph); 48.8 (C, $\underline{C}H_2$-N); 21.1 ($\underline{C}H_3$); 20.6 ($2\underline{C}H_3$); 20.5 ($\underline{C}H_3$); 20.4 ($\underline{C}H_3$).

Elemental analysis; calcd (%) for $C_{32}H_{32}AgClN_2$ (**M.w** = 559.88 g/mol): C 64.37, H 5.49, N 4.76; **found** (%): C 64.74, H 5.65, N 4.78.

*I.1.3.4 Chloro[1-benzhydryl-3-(3-methylbenzyl)-5,6-dimethylbenzimidazole-2-ylidene]silver(I) (**3d**)*

Following the general procedure, the Silver (I)-NHC complex (**3d**) was obtained from a mixture of 1-benzhydryl-5,6-dimethyl-3-(3-Methylbenzyl)-1*H*-benzo[d]imidazol-3-ium-chloride (**2d**) (0.5 mmol, 227 mg) and Silver(I) oxide Ag_2O (0.75 mmol, 174 mg).

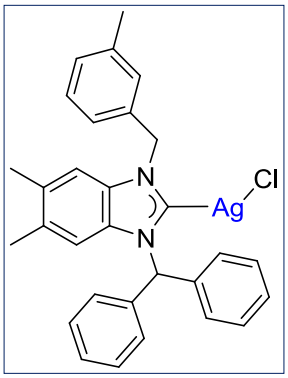

- ✓ ***Chemical Formula:*** $C_{30}H_{28}AgClN_2$
- ✓ ***Molecular Weight:*** 559.89 g/mol
- ✓ ***Yield:*** 90%, (252 mg); White-solid
- ✓ ***m.p:*** 222-223 °C
- ✓ ***FT-IR:*** $\nu_{(C-N)}$ = 1542 cm^{-1}

^{1}H NMR (400 MHz, $CDCl_3$): δ (ppm) = 7.39 (s, 7H, C<u>H</u>-Ar); 7.23 (m, 4H, C<u>H</u>-Ar); 7.20 (s, 1H, C<u>H</u>-Ar); 7.16 (s, 1H, $C_6\underline{H}_2(CH_3)_2$); 7.10 (s, 1H, C<u>H</u>-Ar); 7.08 (s, 1H, C<u>H</u>-Ar); 7.00 (m, 2H, C<u>H</u>-Ar);.6.94 (s, 1H, Ph-C<u>H</u>-Ph); 5.53 (s, 2H, $C\underline{H}_2N$); 2.31 (s, 3H, $C\underline{H}_3$); 2.26 (s, 3H, $C\underline{H}_3$); 2.21 (s, 3H, $C\underline{H}_3$).

^{13}C NMR (100 MHz, $CDCl_3$): δ (ppm) = 138.8 (Cq, <u>C</u>-CH_3); 137.3 (2Cq, <u>C</u>-CH_3); 135.0 (Cq, <u>C</u>-CH-C); 134.0 (Cq, C-CH-<u>C</u>); 133.6 (C, <u>C</u>-CH_2-N); 133.0 (<u>C</u>q, C-N); 132.6 (<u>C</u>q, C-N); 129.2 (4C, <u>C</u>H-Ar); 129.2 (C, <u>C</u>H-Ar); 128.9 (C, <u>C</u>H-Ar); 128.8 (2C, <u>C</u>H-Ar); 128.4 (4C, <u>C</u>H-Ar); 127.5 (C, <u>C</u>H-Ar); 123.9 (C, <u>C</u>H-Ar); 112.9 (C, <u>C</u>H-Ar); 112.3 (C, <u>C</u>H-Ar); 66.9 (Ph-<u>C</u>H-Ph); 53.9 (C, <u>C</u>H_2-N); 21.5 (<u>C</u>H_3); 20.5 (<u>C</u>H_3); 20.4 (<u>C</u>H_3).

Elemental analysis; calcd (%) for $C_{32}H_{32}AgClN_2$ (**M.w** = 559.88 g/mol): C 64.36, H 5.04, N 5.00; **found** (%): C 64.96, H 5.31, N 4.95.

*I.1.3.5 Bromo[1-benzhydryl-3-(4-tert-butylbenzyl)-5,6-dimethylbenzimidazole-2-ylidene]silver(I) (**3e**)*

Following the general procedure, the Silver (I)-NHC complex (**3e**) was obtained from a mixture of 1-benzhydryl-5,6-dimethyl-3-(4-*tert*-butylbenzyl)-1*H*-benzo[d]imidazol-3-ium-bromide (**2e**) (0.5 mmol, 270 mg) and Silver(I) oxide Ag_2O (0.75 mmol, 174 mg).

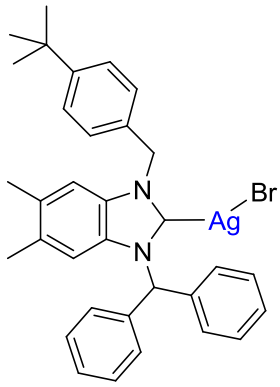

- ✓ ***Chemical Formula:*** $C_{33}H_{34}AgBrN_2$
- ✓ ***Molecular Weight:*** 601.96 g/mol
- ✓ ***Yield:*** 70%, (210 mg); White-solid
- ✓ ***m.p:*** 219-220 °C
- ✓ ***FT-IR:*** $\nu_{(C-N)}$= 1542 cm^{-1}

^{1}H NMR (400 MHz, $CDCl_3$): δ (ppm) = 7.39 (m, 7H, C<u>H</u>-Ar); 7.34 (s, 1H, C<u>H</u>-Ar); 7.32 (s, 1H, $C_6\underline{H}_4$); 7.22 (m, 4H, C<u>H</u>-Ar); 7.17 (s, 1H, $C_6\underline{H}_2(CH_3)_2$); 7.15 (s, 2H, $C_6\underline{H}_4$); 7.12 (s, 1H, $C_6\underline{H}_2(CH_3)_2$); 6.93 (s, 1H, Ph-C<u>H</u>-Ph); 5.54 (s, 2H, $C\underline{H}_2N$); 2.27 (s, 3H, $C\underline{H}_3$); 2.21 (s, 3H, $C\underline{H}_3$); 1.28 (s, 9H, $C\underline{H}_3$ (*t*-Bu)).

^{13}C NMR (100 MHz, $CDCl_3$): δ (ppm) = 151.4 (Cq, <u>C</u>-(*t*Bu)); 137.4 (2Cq, C-CH_3); 133.9 (Cq, <u>C</u>-CH-C); 133.6 (Cq, C-CH-<u>C</u>); 132.9 (Cq, <u>C</u>-N); 132.6 (Cq, <u>C</u>-N); 132.0 (Cq, <u>C</u>-CH_2); 129.2 (4C, <u>C</u>H-Ar); 128.8 (2C, <u>C</u>H-Ar); 128.4 (4C, <u>C</u>H-Ar); 126.7 (2C, <u>C</u>H-Ar); 126.0 (2C, <u>C</u>H-Ar); 113.0 (C, <u>C</u>H-Ar); 112.3 (C, <u>C</u>H-Ar); 67.0 (Ph-<u>C</u>H-Ph); 53.6 ($\underline{C}H_2$-N); 34.6 (Cq, <u>C</u>-$(CH_3)_3$); 31.2 (3$\underline{C}H_3$); 20.4 ($\underline{C}H_3$); 20.4 ($\underline{C}H_3$).

Elemental analysis; calcd (%) for $C_{33}H_{34}AgClN_2$ (**M.w** = 601.96 g/mol): C 65.84, H 5.69, N 4.65; **found** (%): C 65.94, H 5.92, N 4.43.

*I.1.3.6 Chloro[1-benzhydryl-3-(3,4,5-trimethoxybenzyl)-5,6-dimethyl-benzimidazole-2-ylidene] silver(I) (**3f**)*

Following the general procedure, the Silver (I)-NHC complex (**3f**) was obtained from a mixture of 1-benzhydryl-5,6-dimethyl-3-(3,4,5-trimethoxybenzyl)-1*H*-benzo[d]imidazol-3-ium-chloride (**2f**) (0.5 mmol, 265 mg) and Silver(I) oxide Ag_2O (0.75 mmol, 174 mg).

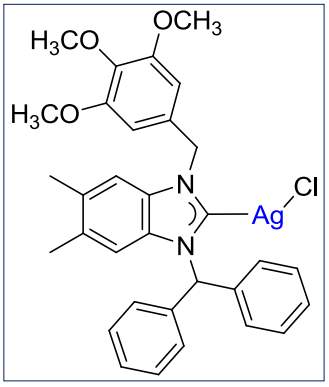

✓***Chemical Formula:*** $C_{32}H_{33}AgClN_2O_3$

✓***Molecular Weight:*** 635.12 g/mol

✓***Yield:*** 80%, (254 mg); White-solid

✓***m.p:*** 117-118 °C

✓***FT-IR:*** $\nu_{(C-N)}$ = 1542 cm^{-1}.

^{1}H NMR (400 MHz, $CDCl_3$): δ (ppm) = 7.38 (m, 7H, C<u>H</u>-Ar); 7.22 (m, 4H, C<u>H</u>-Ar); 7.15 (s, 1H, $C_6\underline{H}_2(CH_3)_2$); 7.14 (s, 1H, $C_6\underline{H}_2(CH_3)_2$); 6.96 (s, 1H, Ph-C<u>H</u>-Ph); 6.43 (S, 2H, C<u>H</u>-Ar), 5.50 (s, 2H, $C\underline{H}_2N$); 3.82 (s, 3H, $OC\underline{H}_3$); 3.77 (s, 6H, $OC\underline{H}_3$); 2.30 (s, 3H, $C\underline{H}_3$); 2.23 (s, 3H, $C\underline{H}_3$).

^{13}C NMR (100 MHz, $CDCl_3$): δ (ppm) = 153.6 (2Cq, <u>C</u>-OCH_3); 137.9 (Cq, <u>C</u>-OCH_3); 137.4 (2Cq, <u>C</u>-CH_3); 134.1 (<u>Cq</u>, <u>C</u>-CH-C); 133.8 (<u>Cq</u>, C-CH-<u>C</u>); 132.9 (Cq, <u>C</u>-N); 132.5 (Cq, <u>C</u>-N); 130.8 (<u>Cq</u>, <u>C</u>-CH_2); 129.4 (<u>Cq</u>-N); 129.2 (4C, <u>C</u>H-Ar); 128.9 (2C, <u>C</u>H-Ar); 128.3 (4C, <u>C</u>H-Ar); 113.0 (C, <u>C</u>H-Ar); 112.1 (C, <u>C</u>H-Ar); 105.7 (2C, <u>C</u>H-Ar); 66.8 (Ph-<u>C</u>H-Ph); 60.9 (C, O<u>C</u>H_3); 56.2 (2C, O<u>C</u>H_3); 53.8 (C, <u>C</u>H_2-N); 20.5 (<u>C</u>H_3); 20.4 (<u>C</u>H_3).

Elemental analysis; calcd (%) for $C_{32}H_{33}AgClN_2O_3$ (**M.w** = 635.12 g/mol): C 60.44, H 5.07, N 4.41; **found** (%): C 60.33, H 5.59, N 3.96.

I.1.4 Synthesis of palladium(II)-NHC complexes (**4a-f**)

Under argon using standard Schlenk, a solution of benzimidazolium salts (1 mmol), Palladium(II) chloride ($PdCl_2$) (1,5 mmol), pyridine (2 mmol), Potassium carbonate K_2CO_3 (5 mmol), and a large excess of Bromure de potassium KBr (10 mmol) were dissolved in 15 mL of acetonitrile (15 mL). The solution was then heated and stirred for 2-3 days at 80°C until it turned black. After the reaction was finished, the solvent was removed under vacuum to afford the product and eliminate excess pyridine then the mixture was washed with hexane three times and the residue was re-dissolved in CH_2Cl_2. The crude product was filtered on a pad of silica covered with Celite, to remove unreacted $PdCl_2$. The product was recrystallized from dichloromethane: hexane (1:4). The final pure product was obtained through chromatography on silica gel as a yellow solid.

*I.1.4.1 Dibromo[1-benzhydryl-5,6-dimethyl-3-(2,3,5,6-tetramethylbenzyl)-benzimedazol-2-ylidene]pyridine palladium (II), (**4a**)*

By following the standard procedure, the Palladium (II)-NHC complex **4a** was obtained from a mixture of 1-benzhydryl-5,6-dimethyl-3-(2,3,5,6-tetramethylbenzyl)-1H-benzo[d]imidazol-3-ium bromide **2a** (0.5 mmol, 250mg), $PdCl_2$ (0.75 mmol, 133 mg), pyridine (1 mmol, 79 mg), K_2CO_3 (2.5 mmol, 345mg), and KBr (5 mmol,595 mg)

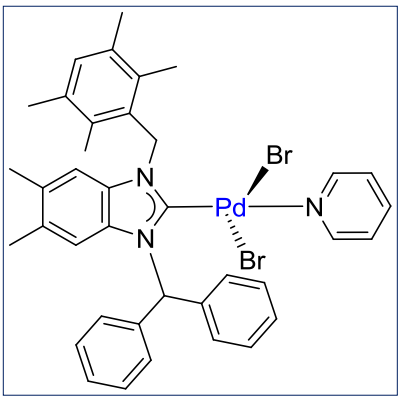

- ✓ ***Chemical Formula:*** $C_{38}H_{39}Br_2N_3Pd$
- ✓ ***Molecular Weight:*** 803.98 g/mol
- ✓ ***Yield:*** 85%, (342 mg); Yellow-solid
- ✓ ***m.p:*** 244-245 °C
- ✓ ***FT-IR:*** $\nu_{(C-N)}$ =1400 cm^{-1}.

^{1}H-NMR (400 MHz, $CDCl_3$): δ(ppm) = 8.91 (d, *J* =5.0 Hz, 2H, $NC_5\underline{H}_5$); 8.60 (s, 1H, $C_6\underline{H}_2(CH_3)_2$); 7.70 (t, *J* =7.6 Hz, 1H, $NC_5\underline{H}_5$); 7.46 (d, *J* =6.7 Hz , 4H, CH-Ar); 7.35 (m, 6H, CH-Ar); 7.29 (t, *J* =7.6 Hz, 2H, $NC_5\underline{H}_5$); 7.10 (s, 1H, $C_6\underline{H}_2(CH_3)_2$); 6.46 (s, 1H, Ph-C$\underline{H}$-Ph); 6.17 (s, 2H, $NC\underline{H}_2$-$C_6H_1(CH_3)_4$); 6.13 (s, 1H, $C_6\underline{H}_1(CH_3)_4$); 2.29 (s, 6H, $C\underline{H}_3$); 2.28 (s, 6H, $C\underline{H}_3$); 2.01 (s, 3H, $C\underline{H}_3$); 2.00 (s, 3H, $C\underline{H}_3$).

^{13}C-NMR (100 MHz, $CDCl_3$): δ(ppm) = 163.2 (Pd-C_{carb}); 152.6 (2C, CH, NC_5H_5); 137.9 (2Cq, C-CH_3); 137.7 (C, CH, NC_5H_5); 135.2 (2Cq, C-CH_3); 134.2 (2Cq, C-CH_3); 132.9 (Cq, C-CH-C); 132.4 (Cq, C-CH-C); 131.5 (Cq, C-N); 131.3 (Cq, C-N); 130.8 (Cq, C-CH_2); 129.1 (4C, CH-Ar); 128.4 (4C, CH-Ar); 127.9 (2C, CH-Ar); 124.2 (2C, CH, NC_5H_5); 113.5 (C, CH-Ar); 111.7 (C, CH-Ar); 68.1 (Ph-CH-Ph); 51.2 (C, CH_2-N); 20.6 ($2CH_3$); 20.3 (CH_3); 20.1 (CH_3); 16.8 ($2CH_3$).

Elemental analysis; calcd (%) for $C_{38}H_{39}Br_2N_3Pd$ (**M.w**.= 803.98 g/mol): C 56.77, H 4.89, N 4.54; **found** (%): C 56.85, H 4.58, N 4.90.

*I.1.4.2 Dibromo[1-benzhydryl-5,6-dimethyl-3-(4-methylbenzyl)benzimedazol-2-ylidene]pyridine palladium (II), (**4b**)*

By following the standard procedure, the Palladium (II)-NHC complex (**4b**) was obtained from a mixture of 1-benzhydryl-5,6-dimethyl-3-(4-Methylbenzyl)-1H-benzo[d]imidazol-3-ium bromide (**2b**) (0.5 mmol, 227mg), $PdCl_2$ (0.75 mmol, 133 mg), pyridine (1 mmol, 79 mg), K_2CO_3 (2.5 mmol, 345 mg), and KBr (5 mmol, 595 mg).

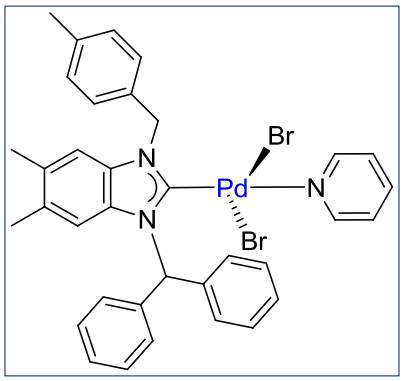

- ✓ ***Chemical Formula:*** $C_{35}H_{33}Br_2N_3Pd$
- ✓ ***Molecular Weight:*** 761.90 g/mol
- ✓ ***Yield:*** 71%, (270 mg); Yellow-solid
- ✓ ***m.p:*** 292-293 °C
- ✓ ***FT-IR:*** $\nu_{(C-N)}$ =1400 cm^{-1}

^{1}H-NMR (400 MHz, $CDCl_3$): δ(ppm) = 8.98 (d, *J* =5.0 Hz, 2H, NC_5H_5); 8.58 (s, 1H, $C_6H_2(CH_3)_2$); 7.72 (t, *J* =7.6 Hz, 1H, C_5H_5); 7.51 (d, *J* =8.1 Hz, 2H, $C_6H_2(CH_3)_2$); 7.48 (d, *J* =8.6 Hz, 4H, CH-Ar); 7.32-7.27 (m, 6H, CH-Ar); 7.18 (d, *J* =8.1 Hz, 2H, N-$C_6H_4(CH_3)$-N); 6.82 (s, 1H, N-$C_6H_2(CH_3)_2$-N); 6.45 (s, 1H, Ph-CH-Ph); 6.14 (s, 2H, NCH_2-$C_6H_4(CH_3)$); 2.34 (s, 3H, CH_3); 2.14 (s, 3H, CH_3); 2.02 (s, 3H, CH_3).

^{13}C-NMR (100 MHz, $CDCl_3$): δ(ppm) = 163.4 (Pd-C_{carb}); 152.7 (2C, CH, NC_5H_5); 137.8 (Cq, C-CH_3); 137.7 (2Cq, C-CH_3); 137.7 (C, CH, NC_5H_5); 133.6 (Cq, C-CH-C); 133.1 (Cq, C-CH-C); 132.0 (Cq, C-N); 132.0 (Cq, C-N); 131.8 (Cq, C-CH_2); 129.5 (2C, CH-Ar); 129.2 (4C, CH-Ar); 128.4 (4C, CH-Ar); 128.0 (2C, CH-Ar); 127.9 (2C, CH-Ar); 124.5 (2C, CH, NC_5H_5); 113.7 (C, CH-Ar); 111.8 (C, CH-Ar); 67,9 (Ph-CH-Ph); 53.4 (CH_2-N); 21.2 (CH_3); 20.2 (CH_3); 20.1 (CH_3).

Elemental analysis; calcd (%) for $C_{35}H_{33}Br_2N_3Pd$ (**M.w**.= 761.90 g/mol): C 55.18, H 4.37, N 5.52; **found** (%): C 54.98, H 4.43, N 5.37.

*I.1.4.3 Dibromo[1-benzhydryl-5,6-dimethyl-3-(2,4,6-trimethylbenzyl)benzimedazol-2-ylidene]pyridine palladium (II), (**4c**)*

By following the standard procedure, the Palladium (II)-NHC complex (**4c)** was obtained from a mixture of 1-benzhydryl-5,6-dimethyl-3-(2,4,6-trimethylbenzyl)-1*H*-benzo[d]imidazol-3-ium bromide (**2c)** (0.5 mmol, 240mg), $PdCl_2$ (0.75 mmol, 133 mg), pyridine (1 mmol, 79 mg), K_2CO_3 (2.5 mmol, 345 mg), and KBr (5 mmol, 595 mg).

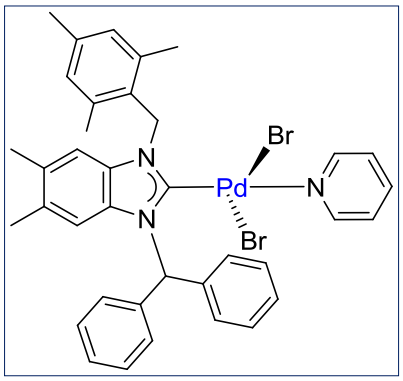

- ✓ ***Chemical Formula:*** $C_{37}H_{37}Br_2N_3Pd$
- ✓ ***Molecular Weight:*** 789.95 g/mol
- ✓ ***Yield:*** 81%, (320 mg); Yellow-solid
- ✓ ***m.p:*** 153-154 °C
- ✓ ***FT-IR*:** $\nu_{(C-N)}$ =1400 cm^{-1}

^{1}H-NMR (400 MHz, $CDCl_3$): δ(ppm) = 8.96 (d, *J* =5.2 Hz, 2H, NC_5H_5); 8.60 (s, 1H, $C_6H_2(CH_3)_2$); 7.72 (t, *J* =7.7 Hz, 1H, NC_5H_5); 7.46 (d, *J* =6.6 Hz, 4H, CH-Ar); 7.36 (m, 6H, CH-Ar); 7.30 (t, *J* =7.6 Hz, 2H, NC_5H_5); 6.95 (s, 2H, $C_6H_2(CH_3)_3$); 6.46 (s, 1H, Ph-CH-Ph); 6.14 (s, 2H, NCH_2-$C_6H_2(CH_3)_3$); 6.13 (s, 1H, $C_6H_2(CH_3)_2$); 2.38 (s, 6H, CH_3); 2.35 (s, 3H, CH_3); 2.00 (s, 3H, CH_3); 1.99 (s, 3H, CH_3).

^{13}C-NMR (100 MHz, $CDCl_3$): δ(ppm) = 163.2 (Pd-C_{carb}); 152.6 (2C, CH, NC_5H_5); 138.9 (C, CH, NC_5H_5); 138.5 (Cq, C-CH_3); 137.8 (2Cq, C-CH_3); 137.7 (2Cq, C-CH_3); 134.1 (Cq, C-CH-C); 132.9 (Cq, C-CH-C); 131.6 (Cq, C-N); 131.3 (Cq, C-CH_2); 129.4 (2C, CH-Ar); 129.1 (4C, CH-Ar); 128.4 (4C, CH-Ar); 127.9 (2C, CH-Ar);

124.4 (2C, CH, NC_5H_5); 113.5 (C, CH-Ar); 111.7 (C, CH-Ar); 68,0 (Ph-CH-Ph); 50.8 (C, CH_2-N); 21.2 (2CH_3); 21.1 (CH_3); 20.3 (CH_3); 20.1 (CH_3).

Elemental analysis; calcd (%) for $C_{37}H_{37}Br_2N_3Pd$ (**M.w** = 789.95 g/mol): C 55.26, H 4.72, N 5.32; **found** (%): C 55.56, H 4.67, N 5.15.

I.1.4.4 Dibromo[1-benzhydryl-5,6-dimethyl-3-(3-methylbenzyl)benzimedazol-2-ylidene]pyridine palladium (II), (4d)

By following the standard procedure, the Palladium (II)-NHC complex (**4d)** was obtained from a mixture of 1-benzhydryl-5,6-dimethyl-3-(3-Methylbenzyl)-1*H*-benzo[d]imidazol-3-ium bromide (**2d)** (0.5 mmol, 227mg), $PdCl_2$ (0.75 mmol, 133 mg), pyridine (1 mmol, 79 mg), K_2CO_3 (2.5 mmol, 345 mg), and KBr (5 mmol, 595 mg)

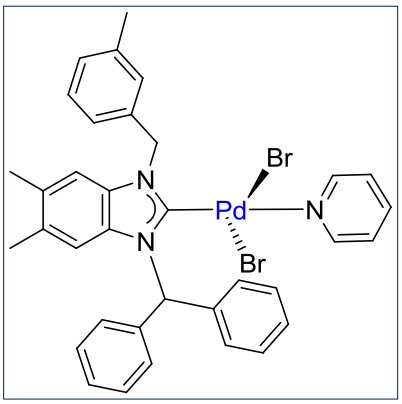

- ✓ ***Chemical Formula:*** $C_{35}H_{33}Br_2N_3Pd$
- ✓ ***Molecular Weight:*** 761.90 g/mol
- ✓ ***Yield:*** 82%, (312 mg); Yellow-solid
- ✓ ***m.p:*** 157-158°C
- ✓ ***FT-IR:*** $\nu_{(C-N)}$ =1400 cm^{-1}

^{1}H-NMR (400 MHz, $CDCl_3$): δ(ppm) = 8.98 (d, 2H, J =5.1 Hz, NC_5H_5); 8.58 (s, 1H, $C_6H_2(CH_3)_2$); 7.72 (t, 1H, *J* =7.6 Hz, N-C_5H_5); 7.52-7.47 (m, 7H, CH-Ar); 7.39-7.34 (m, 5H, CH-Ar); 7.29 (t, 2H, *J* =7.6 Hz, NC_5H_5); 7.18 (d, 2H, *J* =7.4 Hz, N-$C_6H_4(CH_3)$); 6.82 (s, 1H, $C_6H_2(CH_3)_2$); 6.45 (s, 1H, Ph-CH-Ph); 6.14 (s, 2H, NCH_2-$C_6H_4(CH_3)$); 2.34 (s, 3H, CH_3); 2.14 (s, 3H, CH_3); 2.03 (s, 3H, CH_3).

^{13}C-NMR (100 MHz, $CDCl_3$): δ(ppm) = 163.6 (Pd-C_{carb}); 152.6 (2C, CH, NC_5H_5); 152.0 (Cq, C-CH_3); 138.5 (C, CH, NC_5H_5); 137.8 (2Cq, C-CH_3); 135.0 (Cq, C-CH-C); 133.6 (Cq, C-CH-C); 133.2 (Cq, C-CH_2); 132.0 (Cq, C-N); 131.9 (Cq, C-N); 129.2 (4C, CH-Ar); 128.8 (C, CH-Ar); 128.7 (C, CH-Ar); 128.6 (C, CH-Ar); 128.4 (4C, CH-Ar); 128.0 (2C, CH-Ar); 125.1 (C, CH-Ar); 124.4 (2C, CH, NC_5H_5); 113.7 (C, CH-Ar); 111.7 (C, CH-Ar); 68.0 (Ph-CH-Ph); 53.5 (C, CH_2-N); 21.3 (CH_3); 20.3 (CH_3); 20.1 (CH_3).

Elemental analysis; calcd (%) for $C_{35}H_{33}Br_2N_3Pd$ (**M.w** = 761.90 g mol-1): C 55.18, H 4.37, N 5.52; **found** (%): C 55.10, H 4.34, N 5.47.

*I.1.4.5 Dibromo[1-benzhydryl-5,6-dimethyl-3-(4-tert-butylbenzyl)benzimedazol-2-ylidene]pyridine palladium (II), (**4e**)*

By following the standard procedure, the Palladium (II)-NHC complex (**4e**) was obtained from a mixture of 1-benzhydryl-5,6-dimethyl-3-(4-*tert*butylmethylbenzyl)-1H-benzo[d]imidazol-3-ium bromide (**2e**) (0.5 mmol, 270 mg), $PdCl_2$ (0.75 mmol, 133 mg), pyridine (1 mmol, 79 mg), K_2CO_3 (2.5 mmol, 345 mg), and KBr (5 mmol,595 mg)

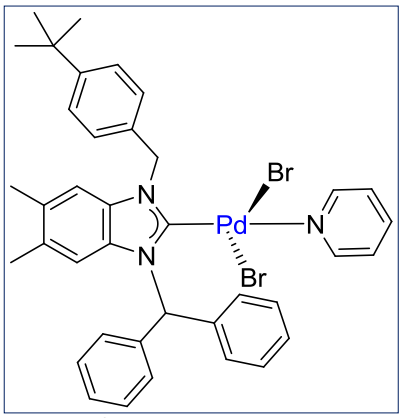

- ✓ ***Chemical Formula:*** $C_{38}H_{39}Br_2N_3Pd$
- ✓ ***Molecular Weight:*** 803.96 g/mol
- ✓ ***Yield:*** 95%, (393 mg); Yellow-solid
- ✓ ***m.p:*** 276-277°C
- ✓ ***FT-IR*:** $\nu_{(C-N)}$ =1399 cm^{-1}

^{1}H-NMR (400 MHz, $CDCl_3$): δ(ppm) = 8.98 (d, *J* =5.1 Hz, 2H, $NC_5\underline{H}_5$); 8.59 (s, 1H, $C_6\underline{H}_2(CH_3)_2$); 7.71 (t, *J* =7.7 Hz, 1H, $NC_5\underline{H}_5$); 7.57 (d, *J* =8.2 Hz, 2H, $C_6\underline{H}_4$-(*t*Bu)); 7.49 (d, *J* =6.7 Hz, 4H, C<u>H</u>-Ar); 7.40 (d, *J* =8.2 Hz, 2H, $C_6\underline{H}_4$-(*t*Bu)); 7.35 (m, 6H, C<u>H</u>-Ar); 7.29 (t, *J* =7.6 Hz, 2H, $NC_5\underline{H}_5$); 6.82 (s, 2H, $C_6\underline{H}_2(CH_3)_2$); 6.45 (s, 1H, Ph-C<u>H</u>-Ph); 6.15 (s, 2H, $NC\underline{H}_2$-C_6H_4(*t*Bu)); 2.14 (s, 3H, $C\underline{H}_3$); 2.03 (s, 3H, $C\underline{H}_3$); 1.31 (s, 9H, $C\underline{H}_3$/(tBu)).

^{13}C-NMR (100 MHz, $CDCl_3$): δ(ppm) = 163.4 (Pd-C_{carb}); 152.6 (2C, <u>C</u>H, NC_5H_5); 150.9 (Cq, <u>C</u>-(*t*Bu)); 137.7 (C, <u>C</u>H, NC_5H_5); 137.7 (2Cq, <u>C</u>-CH_3); 133.6 (Cq, <u>C</u>-CH-C); 133.1 (Cq, C-CH-<u>C</u>); 132.1 (Cq, <u>C</u>-N); 131.9 (Cq, <u>C</u>-N); 131.8 (Cq, C-CH_2); 129.2 (4C, <u>C</u>H-Ar); 128.4 (4C, <u>C</u>H-Ar); 128.0 (2C, <u>C</u>H-Ar); 127.7 (2C, <u>C</u>H-Ar); 125.7 (2C, <u>C</u>H-Ar); 124.4 (2C, <u>C</u>H, NC_5H_5); 113.7 (<u>C</u>H-Ar); 111.8 (<u>C</u>H-Ar); 68,0 (Ph-<u>C</u>H-Ph); 53.4 (C, <u>C</u>H_2-N); 34.6 (<u>C</u>-$(CH_3)_3$); 31.3 (3<u>C</u>H_3); 20.2 (<u>C</u>H_3); 20.1 (<u>C</u>H_3).

Elemental analysis; calcd (%) for $C_{38}H_{39}Br_2N_3Pd$ (**M.w** = 803.98 g/mol): C 56.77, H 4.89, N 5.23; **found** (%): C 56.43, H 4.71, N 5.16.

I.1.4.6 Dibromo[1-benzhydryl-5,6-dimethyl-3-(3,4,5-trimethoxybenzyl)benzimedazol-2-ylidene]pyridine palladium (II), (4f)

By following the standard procedure, the Palladium (II)-NHC complex (**4f)** was obtained from a mixture of 1-benzhydryl-5,6-dimethyl-3-(3,4,5-trimethoxybenzyl)-1*H*-benzo[d]imidazol-3-ium bromide (**2f)** (0.5 mmol, 265 mg), $PdCl_2$ (0.75 mmol, 133 mg), pyridine (1 mmol, 79 mg), K_2CO_3 (2.5 mmol, 345 mg), and KBr (5 mmol, 595 mg)

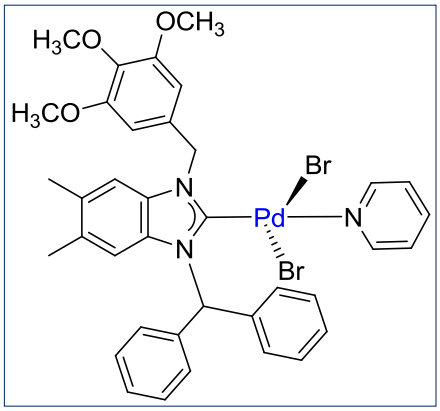

- ✓ ***Chemical Formula:*** $C_{37}H_{37}Br_2N_3O_3Pd$
- ✓ ***Molecular Weight:*** 837.93 g/mol
- ✓ ***Yield:*** 69%, (288 mg); Yellow-solid
- ✓ ***m.p:*** 264-265°C
- ✓ ***FT-IR:*** $\nu_{(C-N)}$ =1404 cm^{-1}

^{1}H-NMR (400 MHz, $CDCl_3$): δ(ppm) = 8.99 (d, *J* =5.2 Hz, 2H, $NC_5\underline{H}_5$); 8.58 (s, 1H, $C_6\underline{H}_2(CH_3)_2$); 7.72 (t, *J* =7.6 Hz, 1H, $NC_5\underline{H}_5$); 7.47 (d, *J* =5.3 Hz, 4H, C<u>H</u>-Ar); 7.35-7.37 (m, 6H, C<u>H</u>-Ar); 7.30 (t, *J* =7.6 Hz, 2H, $NC_5\underline{H}_5$); 6.90 (s, 2H, $C_6\underline{H}_2$-$(OCH_3)_3$); 6.88 (s, 1H, s, 1H, $C_6\underline{H}_2(CH_3)_2$); 6.46 (s, 1H, Ph-C<u>H</u>-Ph); 6.09 (s, 2H, $NC\underline{H}_2$-$C_6H_2(OCH_3)_3$); 3.87 (s, 6H, $OC\underline{H}_3$); 3.84 (s, 3H, $OC\underline{H}_3$); 2.17 (s, 3H, $C\underline{H}_3$); 2.04 (s, 3H, $C\underline{H}_3$).

^{13}C-NMR (100 MHz, $CDCl_3$): δ(ppm) = 163.3 (Pd-C_{carb}); 153.6 (2Cq, <u>C</u>-OCH_3); 152.6 (2C, <u>C</u>H, $N\underline{C}_5H_5$); 137.9 (<u>C</u>q, C-OCH_3); 137.7 (2Cq, <u>C</u>-CH_3); 137.6 (C, <u>C</u>H, $N\underline{C}_5H_5$); 133.5 (Cq, <u>C</u>-CH-C); 133.2 (Cq, C-CH-<u>C</u>); 132.1 (Cq, C-N); 132.0 (Cq, C-N); 130.9 (Cq, <u>C</u>-CH_2); 129.1 (4C, <u>C</u>H-Ar); 128.4 (4C, <u>C</u>H-Ar); 128.1 (2C, <u>C</u>H-Ar); 124.5 (2C, <u>C</u>H, $N\underline{C}_5H_5$); 113.8 (<u>C</u>H-Ar); 111.7 (<u>C</u>H-Ar); 67,9 (Ph-<u>C</u>H-Ph); 60.8 (C, $O\underline{C}H_3$); 56.7 (2C, $O\underline{C}H_3$); 53.8 (C, $\underline{C}H_2$-N); 20.3 ($\underline{C}H_3$); 20.2 ($\underline{C}H_3$).

Elemental analysis; calcd (%) for $C_{37}H_{37}Br_2N_3O_3Pd$ (**M.w** = 837.95 g/mol): C 53.04, H 4.45, N 5.01; **found** (%): C 52.81, H 4.27, N 5.04.

I.2 Catalytic study of Pd(II)-NHC complexes PEPPSI-type

I.2.1 General Procedure for the direct arylation Reaction

A typical standard experiment involved using a 10 mL oven-dried Schlenk tube containing 1% Pd(II)-NHC complexes as catalyst (0.01 mmol), a five-membered heteroaromatic compound derivative (2.0 mmol), (hetero)aryl halide (1.0 mmol), KOAc (2.0 mmol) as a base, and DMAc (2 mL) as a solvent in an argon atmosphere. The mixture was placed in a preheated oil bath at 120°C, stirred for 1 hour, and then vacuum distilled to remove the solvent. The residue was further purified using a micro-silica gel chromatography column with an n-hexane/diethyl ether mixture as eluent. The products were analyzed by GC spectrometry. GC yields and Conversions were calculated by taking into account the conversion of aryl bromides to products from the results of GC spectrometry with dodecane as an internal standard.

I.3 X-Ray crystallographic analysis study

A suitable single crystal of compounds (**2c)**, (**2f)**, (**3a),** (**4a)**, (**4b)**, (**4d)**, and (**4f)** for X-ray diffraction analysis were grown by slow diffusion of diethyl ether in a saturated chloroform solution at room temperature. Crystallographic data were collected using an STOE IPDS II diffractometer with graphite-monochromated Mo Kα radiation by applying the ω-scan method. Data collection and cell refinement were carried out using X-AREA while data reduction was applied using X-RED32 [164]. The crystal structures were determined using the charge-flipping algorithm by SUPERFLIP 2019[165] and refined using the full-matrix least-squares calculations on F^2 with SHELXL-2018[166]. The hydrogen (H) atoms were determined through a geometric calculation and a riding model was utilized during the refinement process. Inserted in idealized positions and treated using a riding model, fixing the bond lengths at 0.93 Å for aromatic CH atoms, 0.98 Å for methine CH atoms, 0.97 Å for CH_2 atoms, and 0.96 Å for CH_3 atoms. The displacement parameters of the H atoms were fixed at $U_{iso}(H) = 1.2U_{eq}$ ($1.5U_{eq}$ for CH_3) of their parent atoms. Molecular graphics were generated by using OLEX2 [167]. The crystallographic data and refinement parameters are collected in Tables 16 and 17.

I.4 General procedures of the biological evaluation

I.4.1 Antimicrobial Activity

The broth micro-dilution technique using a 96-wells microplate was used. The procedure involved diluting the selected compounds in dimethylsulfoxide (DMSO) and adding equal volumes of yeast in SDB (*Sabouraud Dextrose Broth*) medium (1 % peptone, 2 % glucose, pH 5.6) [168] and LB (*Luria-Bertani*) broth medium (1 % tryptone, 1% NaCl, 0.5% yeast extract, pH 7.0) [169] for bacteria. In sterile water, yeast (1-5x10^5 CFU/mL) and bacteria (1x10^6 CFU/mL) cell solutions (inoculums) were prepared and added in equal volumes to wells containing different concentrations of the compounds. The final concentrations of the compounds ranged from 0.8 to 800 mg/L and the cell concentrations were 0.5-2.5x105 CFU/mL for yeasts and 5x105 CFU/mL for bacteria.

The microplate was incubated at 37°C for 24 hours for yeasts and 16-18 hours for bacteria, then the MIC was determined by measuring the reduction in yeast growth (spectrophotometrically at 530 nm) after incubation in yeasts and by naked eyes in bacteria. *Ampicillin*, *Tetracycline*, *Amphotericin B*, and *Voriconazole* were used as standard control drugs.

I.4.2 In vitro cholinesterases inhibition

In this experiment, a reaction volume of 200 µL consisting, of 150 µL of sodium phosphate buffer (100 mM, pH = 8.0), 10 µL of the sample at different concentrations in methanol, and 20 µL of *AChE* or *BChE* solution in buffer was mixed and left to incubate for 15 minutes at 37 °C. Afterward, 10 µL of DTNB (0.5 mM) was added. After that, 10 µL of acetylthiocholine iodide or 10 µL of butyrylthiocholine chloride (0.2 mM) was added to start the reaction. The hydrolysis of these substrates was monitored spectrophotometrically by the formation of yellow 5-thio-2-nitrobenzoate anion as the result of the reaction of DTNB with thiocholine released by the enzymatic hydrolysis of acetylthiocholine iodide or butyrylthiocholine chloride. The absorbance of the solution was measured at 412 nm by using a 96-well microplate reader (Perkin Elmer, Enspire). The measurements were carried out in triplicate, and the results were given as IC_{50} values (µM) corresponding to the 50% inhibition concentration. The percentage of inhibition I (%) was determined using the following formula: Inhibition (I %) = (E-S / S) × 100. Where E is the activity of the enzyme without a test sample, and S is the activity of the

enzyme in the presence of the test sample. Galanthamine was used as a reference compound.

I.4.3 Pancreatic Lipase inhibitory capacity (Anti-lipase assay)

In this experiment, the selected compounds were prepared at the concentration of 4 mM in dimethyl sulfoxide (DMSO). A reaction volume of 200 μL in triplicate consisting, of 50 μL of a sample at different concentrations in DMSO with 100 μL of pancreatic Lipase solution in Tris-HCl buffer (pH = 8) was mixed and incubated for 20 min at 37 °C, Afterwards, The reaction was then initiated by the addition of 50 μL of *p*-Nitrophenol Palmitate (*p*-NPP) after incubation for 2h at 37 °C. A blank with DMSO instead of enzyme solution was prepared. orlistat was used as a positive control. The absorbances of lipase products (*p*-nitrophenol) were measured using a 96-well microplate reader (Perkin Elmer, Enspire) at 410 nm. The findings were expressed as IC_{50} values. (μM) corresponding to the 50 % inhibition concentration. The percent inhibition I (%) of pancreatic lipase was determined using the following equation: I(%)= [(A-a)-(B-b)/(A-a)] ×100. Where **A**: is the absorbance in the absence of the possible inhibitor, which corresponds to the control enzyme assay; **a**: is the absorbance in the absence of the sample and enzyme (blank substrate); **B**: is the absorbance in the presence of the possible inhibitor with the enzyme and substrate; **b**: is the absorbance in the absence of the enzyme.

I.4.4 α-amylase inhibitory capacity

In this experiment, the assay was conducted by mixing 25 μL of the sample at different concentrations in methanol with 50 μL of α amylase solution in 1U of sodium phosphate buffer (*p*H = 6.9 with 6 Mm NaCl) and incubated for 10 min at 37 °C, Afterwards, 50 μL of Amidon (0.1 %), was added. Similarly, by adding sample solution to all reaction reagents, a blank was prepared without enzyme (α-amylase) solution. For 20 minutes, the reaction mixture was incubated at 37 °C. After incubation, The reaction was then stopped by the addition of HCl 25μL (1M), finally, the reaction was initiated by the addition of 100 μL of (IKI) iodine-potassium iodide solution. The absorbance of the solution was measured at 630 nm by the use of a 96-well microplate reader (Perkin Elmer, Enspire).

The results were presented as IC_{50} values (µM) corresponding to 50 % inhibition concentration. The acarbose was used as a reference. The percentage of inhibition I (%) was calculated as follows in the formula: **I % = 1-** [(Ac-Ae)-(As-Ab)/(Ac-Ae)]. **As**=Absorbance [Extrait, Enzyme, Amidon, HCl, IKI]; $\mathbf{A_b}$=Absorbance [Extrait, sodium phosphate buffer, IKI]; $\mathbf{A_e}$=Absorbance [solvant vol Extrait, Enzyme, Amidon, HCl, IKI]; $\mathbf{A_c}$=Absorbance [solvant vol Extrait, sodium phosphate buffer, Amidon, HCl, IKI]

Table 16. Crystal data and structure refinement parameters for **2c**, **2f**, and **3a**.

	3,5-dimethylbenzimidazolium salts		Silver(I)-NHC complex
Parameters	2c	2f	3a
CCDC depository	2058369	2058370	2058371
Color/shape	Colorless/prism	Colorless/plate	Colorless/plate
Chemical formula	$(C_{32}H_{33}N_2)^+ \cdot Cl^- \cdot 2H_2O$	$(C_{32}H_{33}N_2O_3)^+ \cdot Cl^- CH_2Cl_2$	$[Ag_2Cl_2(C_{33}H_{34}N_2)_2]$
Formula weight	517.08	613.98	1203.88
Temperature (K)	296(2)	296(2)	296(2)
Wavelength (Å)	0.71073 Mo Kα	0.71073 Mo Kα	0.71073 Mo Kα
Crystal system	Monoclinic	Triclinic	Monoclinic
Space group	$P2_1/c$ (No. 14)	$P\bar{1}$ (No. 2)	C2/c (No. 15)
Unit cell parameters			
a, b, c (Å)	13.5311(12), 16.4277(17), 14.5904(13)	10.9830(8), 12.0714(8), 12.0148(9)	27.6791(19), 9.3376(7), 22.9241(16)
α, β, γ (°)	90, 116.407(6), 90	85.937(6), 86.665(6), 85.163(6)	90, 106.436(5), 90
Volume ($Å^3$)	2904.8(5)	1581.1(2)	5682.8(7)
Z	4	2	4
$D_{calc.}$ (g/cm^3)	1.182	1.290	1.407
μ (mm^{-1})	0.162	0.325	0.827
Absorption correction	Integration	Integration	Integration
$T_{min.}$, $T_{max.}$	0.9231, 0.9490	0.9128, 0.9867	0.7750, 0.9776
F_{000}	1104	644	2480
Crystal size (mm^3)	0.62 × 0.37 × 0.36	0.49 × 0.19 × 0.06	0.55 × 0.21 × 0.02
Diffractometer/measurement method	STOE IPDS II/ω scans	STOE IPDS II/ω scans	STOE IPDS II/ω scans
Index ranges	$-16 \le h \le 16$, $-19 \le k \le 18$, $-16 \le l \le 16$	$-13 \le h \le 12$, $-14 \le k \le 12$, $-14 \le l \le 14$	$-32 \le h \le 32$, $-11 \le k \le 11$, $-27 \le l \le 27$
θ range for data collection (°)	$1.680 \le \theta \le 25.047$	$2.322 \le \theta \le 25.047$	$1.534 \le \theta \le 25.049$
Reflections collected	15167	14288	24599
Independent/observed reflections	4965/1707	5581/2845	5037/2296
$R_{int.}$	0.1204	0.0781	0.1441
Refinement method	Full-matrix least-squares on F^2	Full-matrix least-squares on F^2	Full-matrix least-squares on F^2
Data/restraints/parameters	4965/0/339	5581/0/378	5037/0/339
Goodness-of-fit on F^2	0.945	1.030	0.984
Final R indices [$I > 2\sigma(I)$]	$R_1 = 0.1148$, $wR_2 = 0.2957$	$R_1 = 0.0734$, $wR_2 = 0.1244$	$R_1 = 0.0764$, $wR_2 = 0.1382$
R indices (all data)	$R_1 = 0.2210$, $wR_2 = 0.3492$	$R_1 = 0.1565$, $wR_2 = 0.1492$	$R_1 = 0.1820$, $wR_2 = 0.1739$
$\Delta\rho_{max.}$, $\Delta\rho_{min.}$ ($e/Å^3$)	0.36, −0.31	0.18, −0.28	0.61, −0.48

Table 17. Crystal data and structure refinement parameters for Pd(II)-NHC complexes PEPPSI-Type **3a**, **3b, 3d**, and **3f**.

Parameters	Pd(II)-NHC complexes PEPPSI-Type			
	3a	3b	3d	3f
CCDC depository	2073777	2073779	2073780	2073778
Color/shape	Yellow/prism	Yellow/prism	Yellow/prism	Yellow/plate
Chemical formula	$[PdBr_2(C_{30}H_{28}N_2)(C_5H_5N)]$	$[PdBr_2(C_{33}H_{34}N_2)(C_5H_5N)]$	[PdBr2(C32H32N2O3)(C5H5N)]	[PdBr2(C30H28N2)(C5H5N)]
Formula weight	761.86	803.94	837.91	761.86
Temperature (K)	296(2)	296(2)	296(2)	296(2)
Wavelength (Å)	0.71073 Mo Kα	0.71073 Mo Kα	0.71073 Mo Kα	0.71073 Mo Kα
Crystal system	Monoclinic	Triclinic	Monoclinic	Monoclinic
Space group	$P2_1/n$ (No. 14)	P−1 (No. 2)	P21/n (No. 14)	P21/c (No. 14)
Unit cell parameters				
a, b, c (Å)	14.9802(13), 11.0510(7), 20.2398(15)	9.3043(7), 11.1447(9), 17.5332(14)	11.9557(9), 16.6440(8), 18.4136(13)	14.3357(5), 10.6693(5), 21.0026(9)
α, β, γ (°)	90, 106.685(6), 90	91.190(6), 104.973(6), 103.026(6)	90, 106.908(6), 90	90, 91.205(3), 90
Volume ($Å^3$)	3209.6(4)	1705.1(2)	3505.7(4)	3211.7(2)
Z	4	2	4	4
$D_{calc.}$ (g/cm^3)	1.577	1.566	1.588	1.576
μ (mm^{-1})	3.096	2.918	2.848	3.094
Absorption correction	Integration	Integration	Integration	Integration
$T_{min.}$, $T_{max.}$	0.5504, 0.8967	0.1567, 0.3154	0.2890, 0.7055	0.4436, 0.9532
F_{000}	1520	808	1680	1520
Crystal size (mm^3)	0.35 × 0.08 × 0.04	0.73 × 0.55 × 0.53	0.48 × 0.45 × 0.11	0.48 × 0.11 × 0.02
Diffractometer/measurement	STOE IPDS II/ω scan	STOE IPDS II/ω scan	STOE IPDS II/ω scan	STOE IPDS II/ω scan
Index ranges	$-19 \le h \le 19, -14 \le k \le 14, -26 \le l \le 26$	$-12 \le h \le 12, -14 \le k \le 14, -22 \le l \le 22$	$-15 \le h \le 15, -21 \le k \le 19, -24 \le l \le 24$	$-18 \le h \le 18, -13 \le k \le 13, -27 \le l \le 27$
θ range for data collection (°)	$1.993 \le \theta \le 27.956$	$1.882 \le \theta \le 27.802$	$1.683 \le \theta \le 27.737$	$1.940 \le \theta \le 27.724$
Reflections collected	36397	21039	54952	26110
Independent/observed reflections	7650/3046	7945/4779	8206/6602	7516/3348
$R_{int.}$	0.2489	0.1482	0.0762	0.1909
Refinement method	Full-matrix least-squares on F^2	Full-matrix least-squares on F^2	Full-matrix least-squares on F2	Full-matrix least-squares on F2
Data/restraints/parameters	7650/0/373	7945/0/403	8206/0/420	7516/0/373
Goodness-of-fit on F^2	0.972	1.036	1.165	0.976
Final R indices [I > 2σ(I)]	$R_1 = 0.0927$, $wR_2 = 0.1253$	$R_1 = 0.0771$, $wR_2 = 0.1750$	R1 = 0.0534, wR2 = 0.0962	R1 = 0.0889, wR2 = 0.1377
R indices (all data)	$R_1 = 0.2310$, $wR_2 = 0.1641$	$R_1 = 0.1301$, $wR_2 = 0.2089$	R1 = 0.0727, wR2 = 0.1022	R1 = 0.1985, wR2 = 0.1708
$\Delta\rho_{max.}$, $\Delta\rho_{min.}$ ($e/Å^3$)	1.06, −0.69	1.17, −1.56	0.70, −0.56	1.15, −0.65

Chapter II.

Synthesis of new hybrid polyfunctionalized heterocyclic compounds bearing quinoline

I. Bibliographic review

I.1 Introduction

In the 20th century, the pharmaceutical industry followed the principle that a single molecule should target a single disease “one molecule, one target, one disease” [170]. This led to the creation of many successful selective drugs. However, for multifactorial diseases, manipulating just one target may not result in effective treatment. Despite the best research efforts[171] thus, it is believed that multitarget drugs should be designed with a more rational and holistic view of the target combination. Hence, there is an increasing interest in developing multi-target drugs, which take a more comprehensive approach to improving therapeutic efficacy and (or) safety[172]. This can be achieved through the use of hybrid molecules which can serve as a "double-edged sword," acting as two separate pharmacophores.

Modern medicinal chemistry focuses on the design and creation of new bioactive compounds for use as drugs, with the primary objective of achieving this goal rapidly and sustainably. However, the traditional methods used for organic synthesis and optimization of synthetic procedures are inefficient in terms of time, cost, waste management, and environmental impact posing a bottleneck in the early stages of drug discovery[173]. To overcome these challenges, scientists are exploring new synthetic techniques in modern organic, bioorganic, and medicinal chemistry[174]. One such technique is molecular hybridization, which involves combining multiple pharmacophores into a single molecule to create a compound with various modes of action[175]. Heterocyclic structures are commonly utilized in the design of potent and specific biologically active agents for a range of targets.

In this scenario, multicomponent reactions (MCRs) have emerged as a powerful tool for medicinal chemists to conduct modern drug discovery[176]. MCRs have been widely used to synthesize bioactive heterocyclic compounds and have become a crucial area of research in organic chemistry, providing a valuable alternative to traditional linear strategies for the synthesis of complex molecule libraries by the combination of two or more reactions in a fewer number of steps, making them an efficient approach for medicinal chemists in the drug discovery process.

Polyfunctionalized heterocyclic compounds have versatile applications in chemistry, biomedicine, and industry, playing a significant role in drug production and biological activity. Oxygen, sulfur, and nitrogen-containing heterocycles are especially

valuable for their medicinal properties. Fused nitrogen-containing heterocycles like quinoline and pyridine are prevalent in bioactive compounds. Dihydropyridines (DHPs) represent an important class with biological applications which have applications in biological systems as useful drugs and pharmaceuticals[177]. Fused quinoline and pyran, which contain oxygen, are crucial for various natural products.

Given these considerations and as part of our ongoing interest on the advancement of heterocyclic chemistry, specifically in the realm of biomolecules which our research team has recently embarked on a new research direction exclusively dedicated to the synthesis and evaluation of the biological activity of novel polycyclic derivatives, with quinoline derivatives as a key component. The objective of this endeavor is to obtain new products that have the potential for therapeutic and biological activity[178–182].

Our attention has been directed towards investigating the feasibility of developing a hybrid structure based on quinoline, incorporating both pyrans and pyridines. Through the modification of this structure using a one-pot multi-component domino approach, we aspire to create novel, biologically active compounds that could have significant pharmacological implications.

This chapter provides an overview of some heterocyclic compounds, including their historical discovery, the latest developments in the field, and some methods for their preparation. It also explores their uses in chemical and biological research. Additionally, the chapter also examines methods for synthesizing new hybrid quinoline-heterocycle and the applications of some of them in biology.

I.2 Generalities

I.2.1 The historical aspect of Quinoline

Quinoline was first discovered by Runge in 1834 in coal tar distillate, who named it "Leukol"[183]. Gerhardt later obtained the base in 1842 by alkaline distillation of quinine, cinchonine, or strychnine, and called it "Chinolein" or "Chinolin"[184]. While Korner was initially credited with proposing the structural formula for quinoline, Dewar suggested in 1871 that quinoline's relationship to pyridine was similar to that of naphthalene to benzene [185]. The structure of quinoline was confirmed through various syntheses.

I.2.2 Structure, interest, and Uses of Quinoline

Quinoline structure is composed of benzene and pyridine rings at two adjacent carbon atoms. Is a heterocyclic aromatic organic compound with the chemical formula C_9H_7N. In quinoline, the nitrogen atom is one atom away from the position at which the rings are fused. The numbering in quinoline commences from the nitrogen atom which is assigned position-1. In an isomer, isoquinoline, the nitrogen atom is positioned two atoms away from the fused ring [186] (Figure 56).

Figure 56. Structure and representation of Quinoline and Isoquinoline

Quinoline-containing compounds have long been used for the treatment of many diseases, beginning with alkaloid quinine isolated as the active ingredient from the crude back of Cinchona trees.

I.3 Biological Activities of Some Quinoline Derivatives

Quinoline and its derivatives constitute an important core among pharmacologically active synthetic and natural compounds with widespread prevalence. Substituted quinolines are historically among the most important antimalarials and their immense use in the 20th century provided well-founded hopes for malaria eradication[187]. Cinchona alkaloids compounds such as quinine and quinidine, which are remarkable members of this family, showed inhibitory activity toward the induction of Epstein–Barr virus early antigen (EBV-EA), and are thus potentially useful as a chemoprotective agent in chemical carcinogenesis[188] (Figure 57).

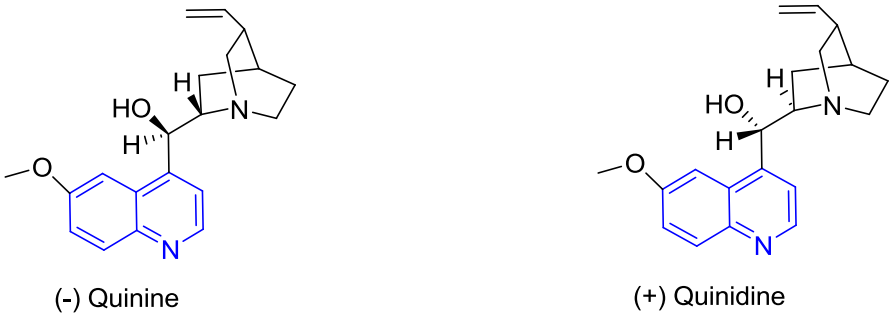

Figure 57. Quinoline alkaloids used as *antimalarial* agents

As far as synthetic quinoline derivatives are concerned, there are a large group of heterocyclic compounds that display interesting medicinal. However, some of the most important examples are the pharmacologically active compounds, including several antimalarial drugs based on the quinine parent, for example, chloroquine, pamaquine[189], and mefloquine[190] (Figure 58).

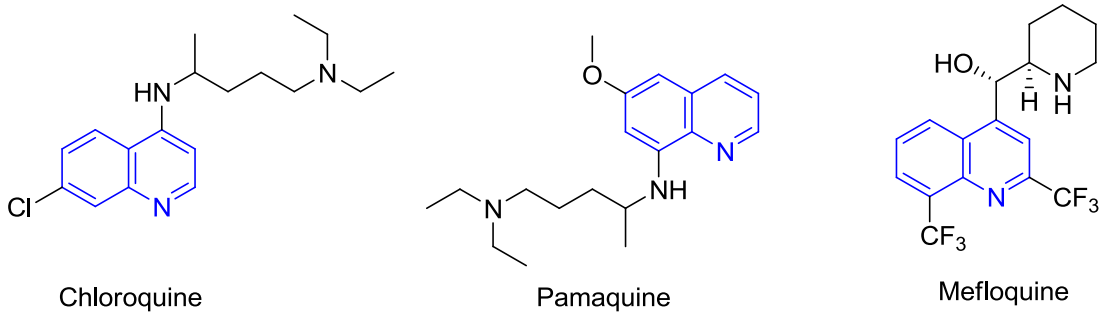

Figure 58. Quinoline derivatives used as *antimalarial* drugs

Pyrroloquinoline-based alkaloids have attracted significant interest due to their intriguing structures and biological activity. Camptothecin is the best-known example, which was isolated from the stem wood of the Chinese tree Camptotheca acuminate in 1966 and elucidation of its structure by Wall and coworkers[191]. This compound has potent antitumor activity and represents a new direction in AIDS chemotherapy (Figure 59).

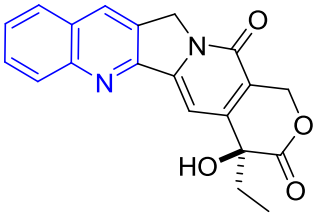

Camptothecin

Figure 59. Quinoline derivatives used as antitumor agent

Pyranoquinoline alkaloids are another important group of quinoline derivatives. Simulenoline, huajiaosimuline, and zanthodioline are representative examples of these natural products isolated from the root bark of *Zanthoxylum simulans*, a shrub found in Taiwan and mainland China. These novel monoterpenoid *pyranoquinolines* are potent inhibitors of platelet aggregation [192] (Figure 60).

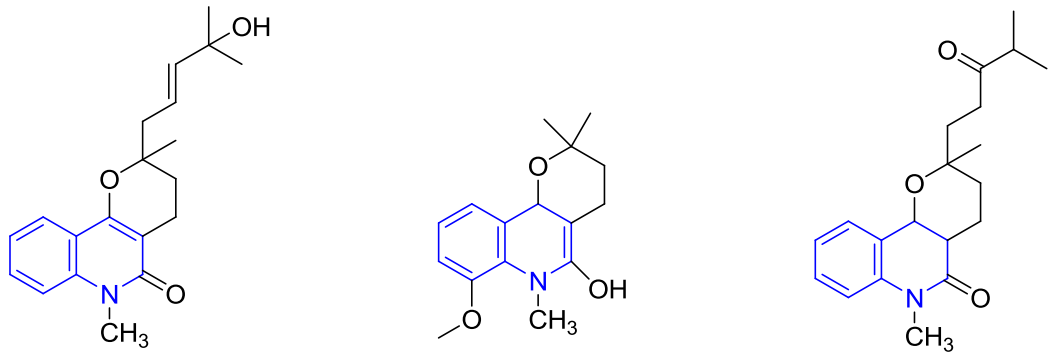

Simulenoline Zanthodioline Huajiaosimuline

Figure 60. Quinoline derivatives have potent inhibitors of platelet aggregation

An alkaloid called *martinelline* was discovered in 1995 by Witherup *et al*. [193] in an extract of Martinella *iquitosensis* roots, exhibits antibacterial activity and also binds to adrenergic, muscarinic, and bradykinin receptors. As well as N-Alkyl-4-quinolone-3-carboxylic acid and related derivatives are components of antibacterial agents, such as nalidixic acid and ciprofloxacin [194], that inhibit gyrase (Figure 61).

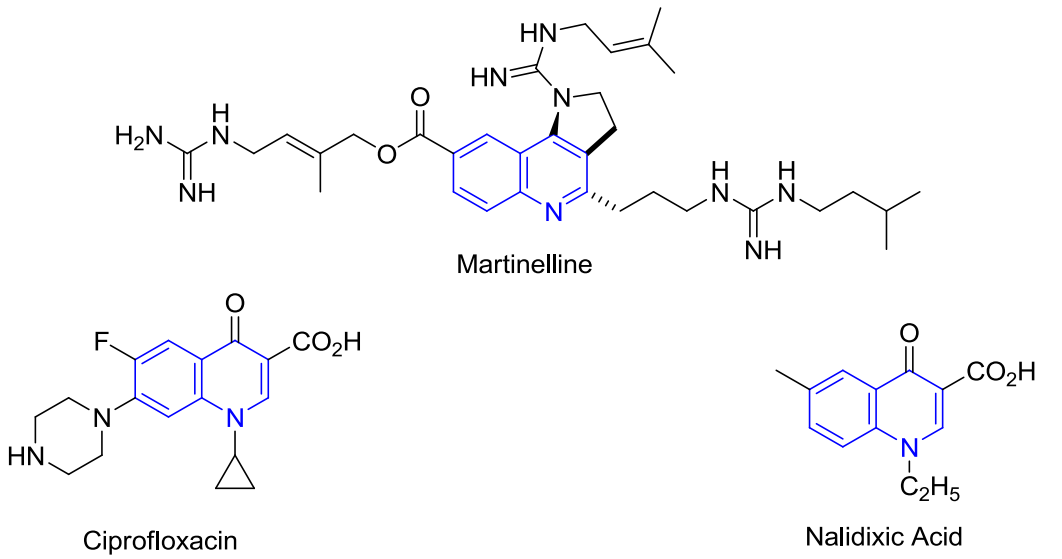

Figure 61. Quinoline dirivaives used as anibacerial agents

In 1996, Maged and colleagues [195] discovered two alkaloids, *cryptotackieine*, and Cryptosanguinolentine, from Cryptolepis *sanguinolenta*, a tropical West African shrub. These compounds exhibit potent antiplasmodial activity against chloroquine-resistant strains of Plasmodium falciparum, as well as several other noteworthy biological properties [196] (Figure 62).

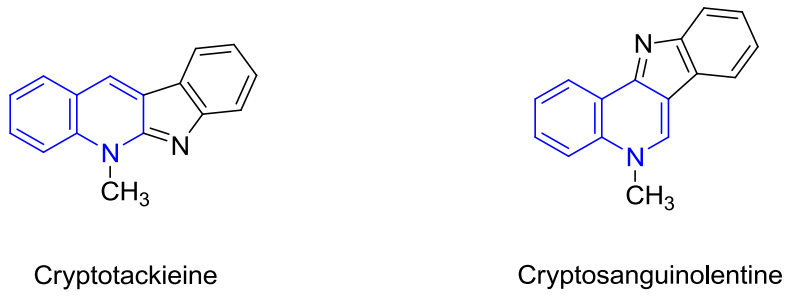

Figure 62. Quinoline derivatives used as an *antiplasmodial* agent

Some derivatives containing the quinoline ring system have been shown to possess useful pharmacological activities, such as Dibucaine hydrochloride is an anesthetic, and Apomorphine is an *anti-perkinosine* (Figure 63).

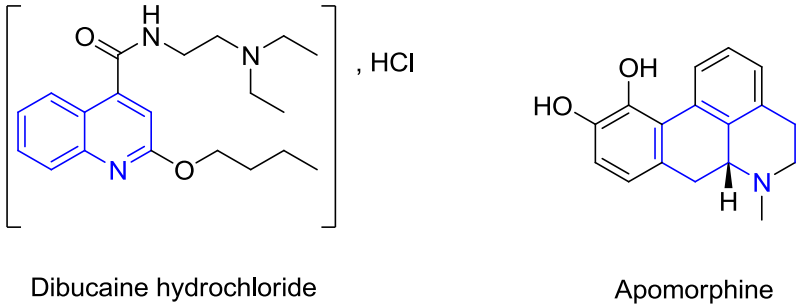

Dibucaine hydrochloride Apomorphine

Figure 63. Clinically used synthetic quinolones as an anesthetic and anti-perkinosine agents

Quinoline derivatives have recently garnered considerable attention for their potential use in the treatment of cancer. Pfizer's Irinotecan is an *anticancer* drug [197], and Merck's L-689,560 is a potent inhibitor of NMDA receptors. The NMDA subtype of excitatory amino acid receptors is implicated in several neurodegenerative disorders, including epilepsy, stroke, and Alzheimer's disease [198] (Figure 64).

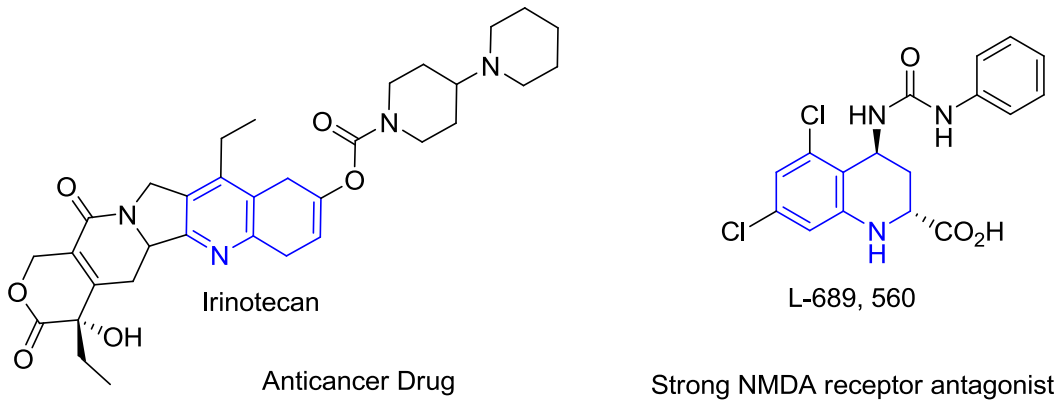

Anticancer Drug Strong NMDA receptor antagonist

Figure 64. Quinoline derivatives used in the treatment of cancer and Alzheimer's disease

The quinoline-8-carboxylic acid derivative, Quinmerac, is utilized as an herbicide for controlling Galium aparine and other broad-leaved weeds. Methoxatin, also called coenzyme PQQ, is a heterotricyclic cofactor for mammalian lysyl oxidase and dopamine β-hydroxylase[199] (Figure 65).

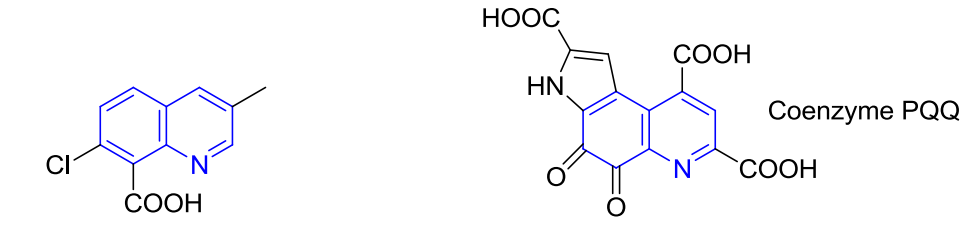

Quinmerac (Herbicide) Methoxatin

Figure 65. Quinoline derivatives used as herbicides

I.4 Some reported synthetic strategies for Quinoline derivatives

The quinoline ring is formed by the *o*-condensation of a benzene ring with pyridine. In recent years, several straightforward and sophisticated methods for the reparation of substituted quinolines have been reported. Although synthetic approaches like the Skraup, Doebner–von Miller, Friedlander, and Combes reactions have been developed for quinoline synthesis, new methods are still being actively explored by researchers owing to the compound's importance [200].

A β-aminoenone can be obtained by condensing arylamine derivatives with a 1,3-dicarbonyl compound, which can then be cyclized by exposure to concentrated acid. The cyclization step occurs *via* an electrophilic substitution by the *O*-protonated β-aminoenone, followed by water elimination, resulting in the formation of the aromatic quinoline derivatives [201] (Scheme 43).

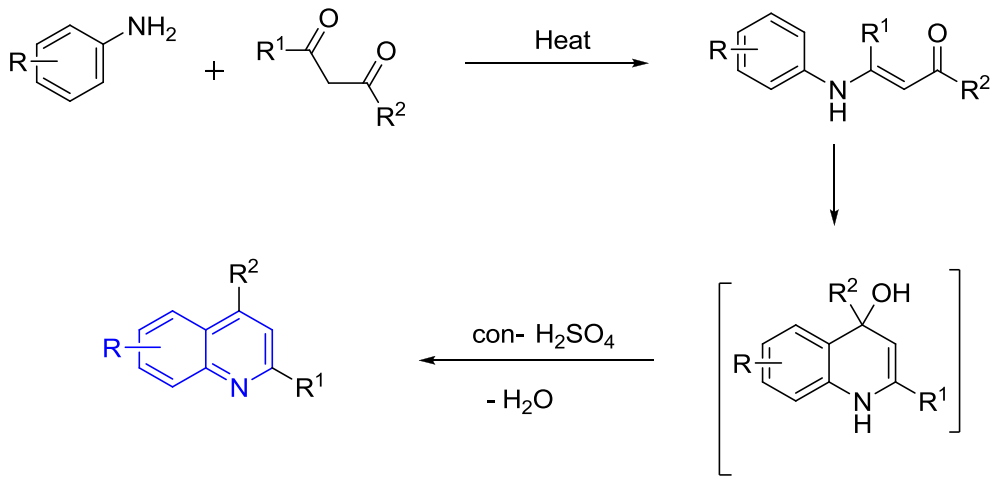

Scheme 43. The Combes synthesis of quinoline

Anilines and β- ketoesters react at lower temperatures to give the kinetic product, a β- aminoacrylate, the cyclization of which gives a 4-quinolone. At higher temperatures, β- ketoacid anilides are formed and cyclization of these affords 2-quinolone (Scheme 44).

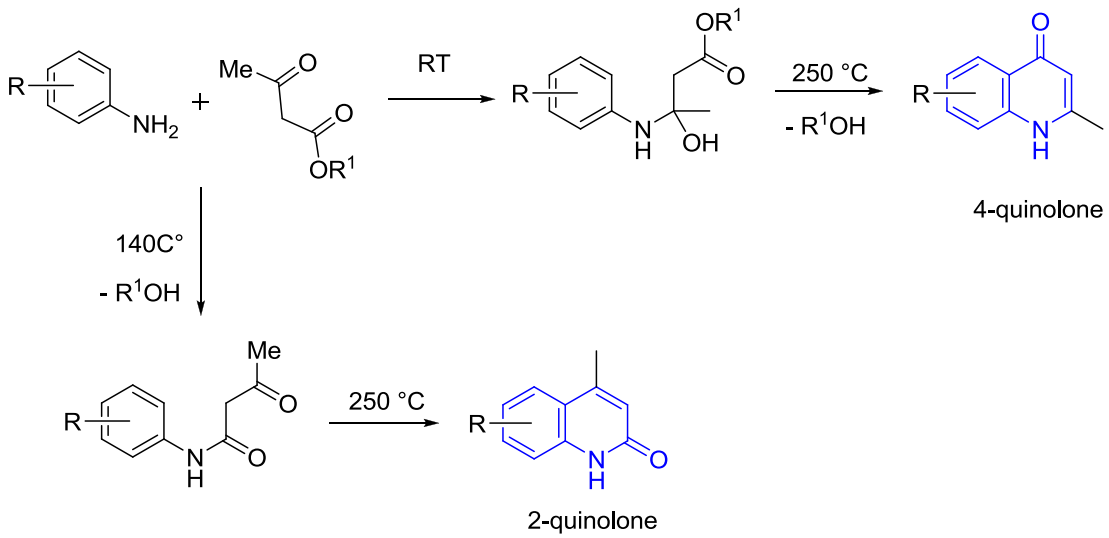

Scheme 44. The Conard-Limpach-Knorr synthesis of quinoline

Arylamines react with an α,β- unsaturated carbonyl compound in the presence of an oxidizing agent to give quinolines. When glycerol is used as an *in situ* source of acrolein, quinolines carrying no substituents on the heterocyclic ring are produced. In the classical Skraup method [202], quinoline is produced when the aromatic amine, in the simplest case aniline, is heated with glycerol, sulfuric acid (which catalyzes the dehydration of glycerol to acrolein), and an oxidizing agent, such as nitrobenzene, which transforms the initially formed 1,2-dihydroquinoline into the fully aromatic heterocycle (Scheme 45).

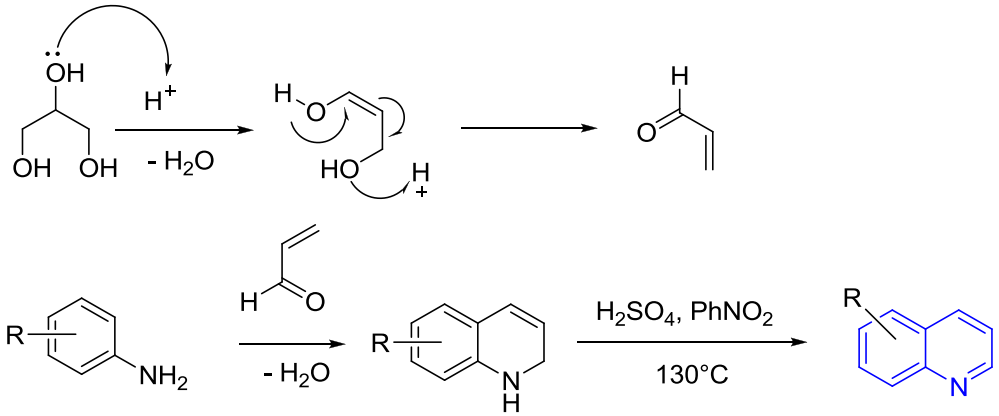

Scheme 45. The Skraup synthesis of quinoline

The use of an enone confirms the mechanism, showing that the interaction of the aniline amino group with the carbonyl group is not the first step, and this variation is known as the Doebner – Miller synthesis. The Doebner–Miller synthesis is the one-

pot chemical reaction of aniline with an aldehyde and pyruvic acid to form quinoline-4-carboxylic acids. The Doebner-von Miller protocol replaced the potentially explosive glycerol with α,β-unsaturated ketone and conducted the reaction by heating with an aromatic amine in the presence of an acid catalyst and iodine to afford the compound (Scheme 46).

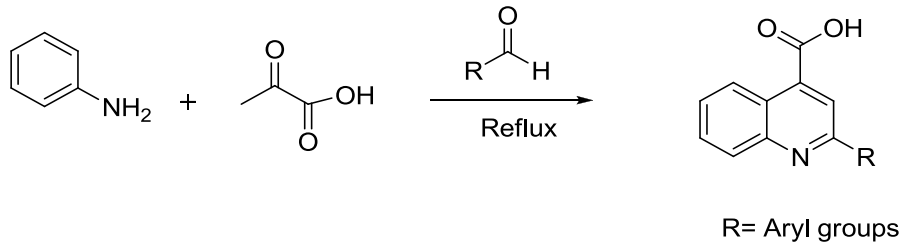

Scheme 46. Doebner-von Miller synthesis of quinolines

The Friedlander reaction is the most simple and straightforward method for the synthesis of quinoline and is also regarded as one of the more common ways and the most convenient routes to synthesize quinoline scaffold, involving condensation followed by cyclodehydration between an aromatic 2-amino aldehyde or ketone (2-aminoacetophenone) with carbonyl derivatives having α-methylene functionality proton(s). Two pathways have been suggested for the Friedlander reaction[203] (Scheme 47).

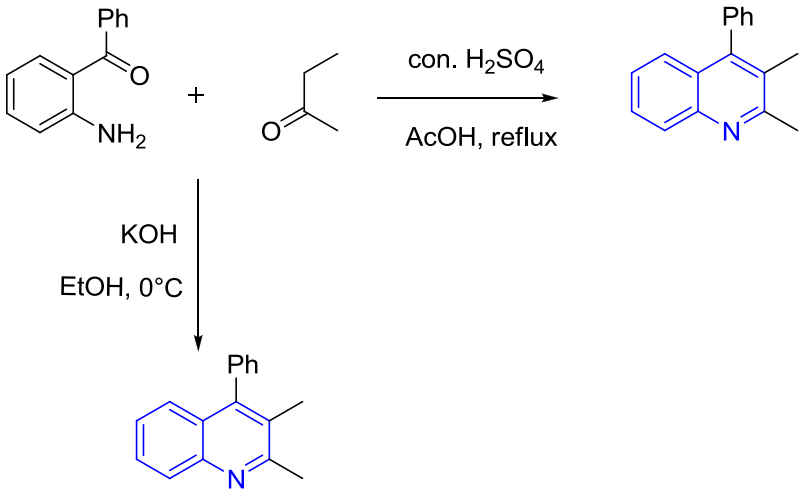

Scheme 47. Friedlander synthesis of quinoline

Recently, Yao and co-workers reported an easy and efficient synthesis of 3-nitroquinoline derivatives from *o*-aminobenzaldehyde and β-nitrostyrenes in the

presence of 1,4-diazabicyclo[2.2.2]octane (DABCO) and silica gel [204]. This one-pot reaction represents an interesting variation in the Friedlander-type quinoline synthesis (Scheme 48).

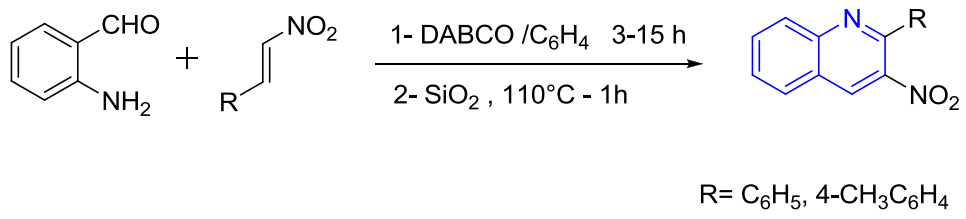

Scheme 48. Friedlander synthesis of substituted quinoline

In 1886, Pfitzinger reported a formal extention of the known Friedlander protocol for the synthesis of quinolinic acid which is known as Pfitzinger synthesis (also known as the Pfitzinger-Borsche reaction) [205] (Scheme 49).

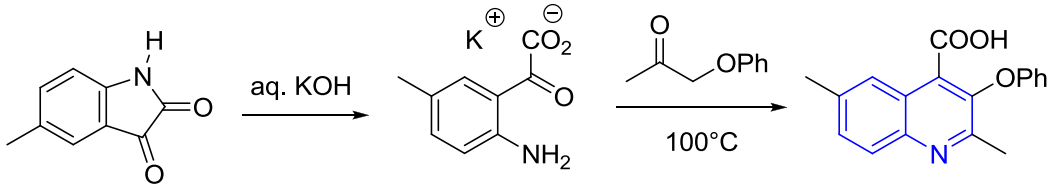

Scheme 49. The Pfitzinger synthesis of quinolines

Vilsmeier-Haack reagent provides a facile entry into a large number of heterocyclic systems. In 1978, the group of Meth-Cohn demonstrated a practically simple procedure in which acetanilide was efficiently converted into 2-chloro-3-quinoline carboxaldehyde. This type of quinoline synthesis was termed the "Vilsmeier Approach" by Meth-Cohn[206] (Scheme 50).

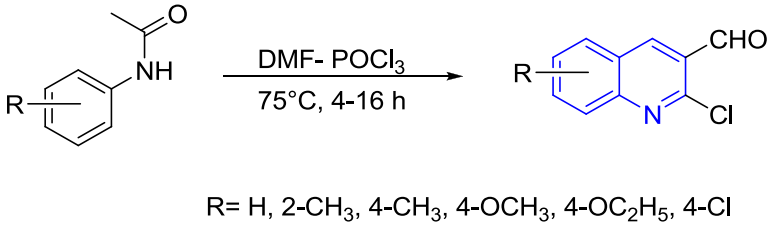

Scheme 50. Vilsmeier Approach" by Meth-Cohn for the synthesis of quinoline

Rajjana *et al*.[207] have demonstrated that acetanilides, particularly deactivated ones (R = Br, Cl, NO_2), undergo rapid cyclization in a micellar medium to afford 2-chloro-3-quinoline carboxaldehyde derivatives. Cyclization in the presence of cetyl trimethyl ammonium bromide (CTAB) under Vilsmeier-Haack conditions afforded 2-

chloro3-quinoline carboxaldehyde in good yield. The same group [208] also demonstrated dramatic enhancements when ultrasonically irradiated Meth-Cohn quinoline syntheses were performed (Scheme 51).

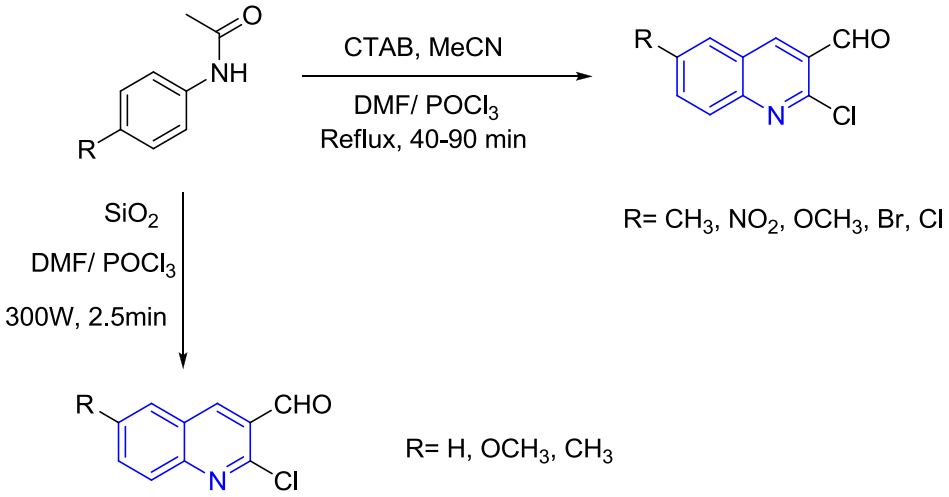

Scheme 51. Synthesis of 2-chloro-3-quinoline carboxaldehyde under Vilsmeier-Haack conditions

The presence of nitrogen in this structure produces an irregular distribution of the electron density in both heterocyclic and carbocyclic rings, a situation that alters the physicochemical properties and reactivity.

I.5 The biological interest of some 4H-pyran derivatives

Pyran and its derivatives are an important class of heterocyclic compounds, which constitute the key core of various natural products [203]. Undoubtedly, the derivatives of 4*H*-pyrans are a crucial group of heterocyclic compounds. They have captured the attention of numerous investigators because of their potential biological activities [204]. The pyrans and pyran-fused motifs, in particular, have been studied for their association with various biological properties, some of them emerged as anticancer [205], antimicrobial [206], molluscicidal [207], cytotoxic [208], anti-HIV [209], antimalarial [210], anti-inflammatory [211], antihyperglycemic, and antidyslipidemic agents [212]. In addition, they possess a potential activity against many neurodegenerative diseases, e.g., Parkinson's disease and Alzheimer's disease [213] (Figure 66).

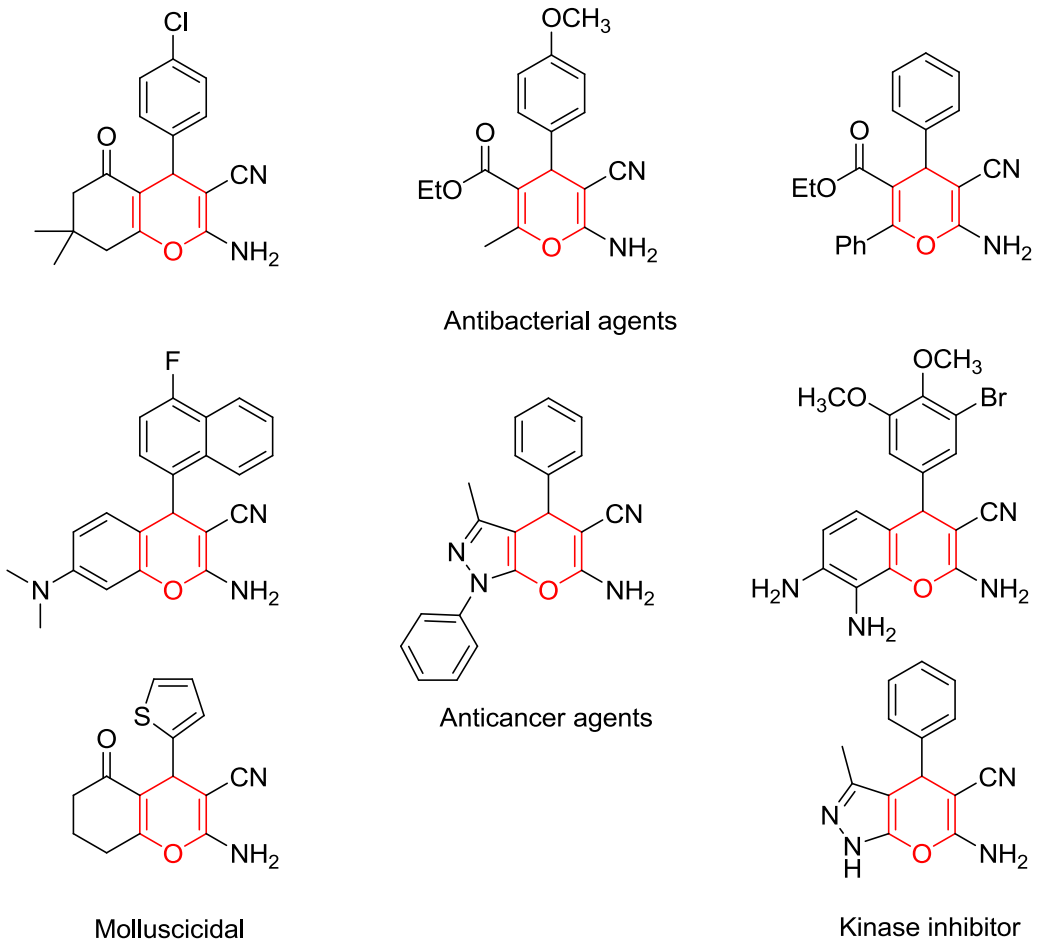

Figure 66. I.5 The biological interest of some 4*H*-pyrans derivatives

In 2012, Harshad and colleagues synthesized pyrano[2,3-c]pyrazole derivatives from indole derivatives [209], which demonstrated antimicrobial activity against Escherichia coli (gram-negative) superior to that of griseofulvin, and against Bacillus subtilis (gram-positive) superior to that of Ampicillin (Figure 67).

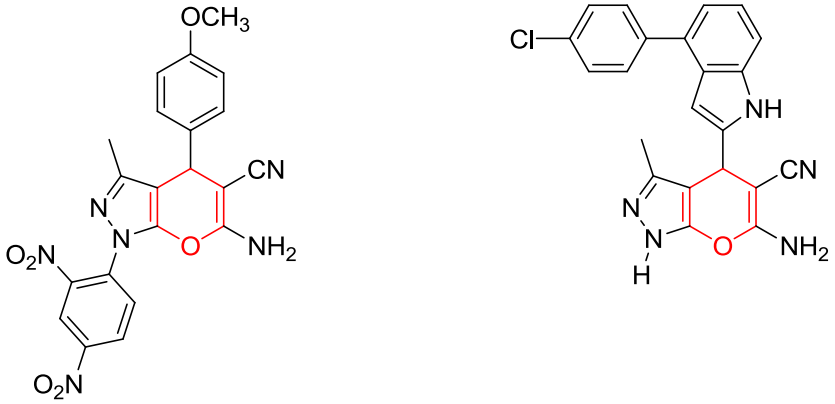

Figure 67. Antibacterial agents

Abidi *et al*. [210] reported the synthesis of a range of 6-amino-4-aryl-3-methyl-2,4-dihydropyrano[2,3-c]pyrazole-5-carbonitriles. These compounds were tested for their in vitro cytotoxic activity against several cancer cell lines (SW48, A549, KB, HepG2). The compounds exhibited significant cytotoxicity compared with that of Doxorubicin, a well-known anti-cancer drug (Figure 68).

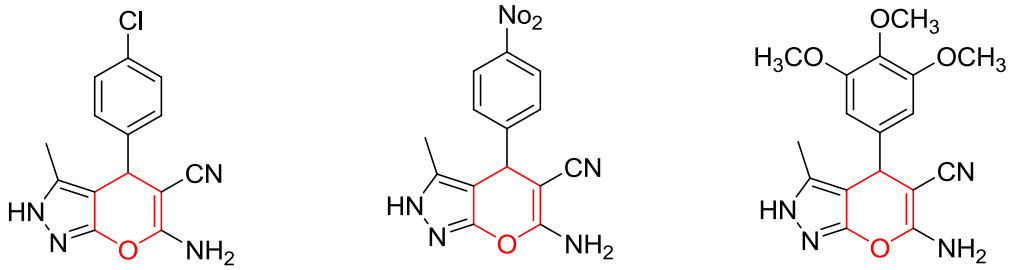

Figure 68. Anti-cancer agents

In 2014, Yang and colleagues [211] created two new sets of compounds, specifically 4*H*-dihydropyrano-[2,3-c]pyrazoles and 2*H*,4*H*-dihydropyrano[2,3-c]pyrazoles from aromatic aldehydes. Their research discovered that incorporating a methoxy group onto the aromatic ring of dihydropyrano[2,3-c]pyrazole had a significant impact on the free radical scavenging properties of these compounds. Additionally, substituents located on N-1 or C-3 in the dihydropyrano[2,3-c]pyrazole ring were found to affect their antioxidant activities (Figure 69).

Figure 69. Antioxydant agents

I.6 Reported synthetic strategies for 4H-pyrans

Synthetic chemists have shown great interest in 4*H*-pyrans and their derivatives as heterocyclic scaffolds in recent years, resulting in the development of various synthetic methods for synthesizing structurally diverse chromenes. One-pot synthesis of chromene derivatives using multicomponent reactions (MCRs) has become

particularly popular among synthetic chemists. MCRs are a versatile tool for creating complex molecules by combining and breaking carbon-carbon and carbon-heteroatom bonds in one step, making them an important tool in combinatorial synthesis.

In 1962 Wiener *et al.* first published that 4-hydroxycoumarin could be cyclized in a two-step procedure through Michael's addition to benzylidene malononitrile in pyridine as a solvent to give a derivative of 2-aminopyrano[3,2-c]benzopyran [212] (Scheme 52).

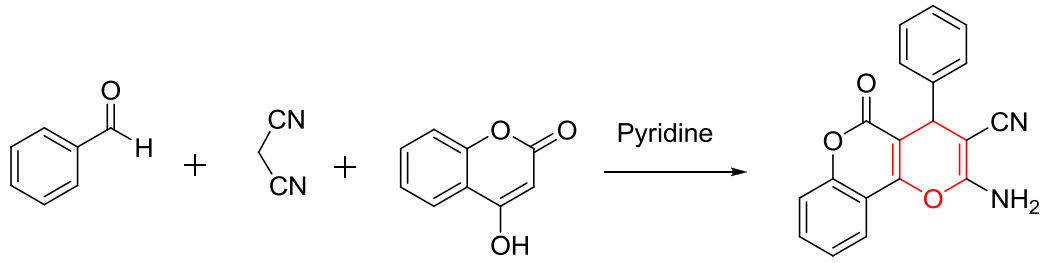

Scheme 52. Two-step synthesis of 2-amino-3-cyano-4*H*-chromenes by Wiener and co-workers

In 2001, Ballini *et al*. reported the three-component synthesis of 4-aryl-4*H*-chromene heterocycles by reacting substituted aryl aldehydes, malononitrile, and substituted phenols (Scheme 53) [213].

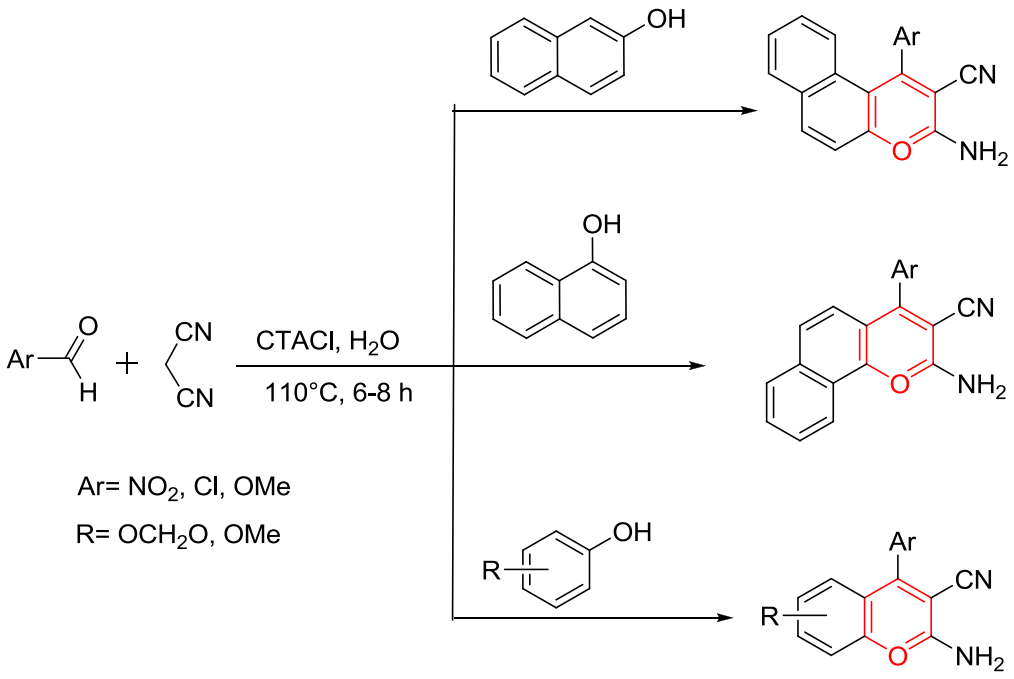

Scheme 53. One-pot synthesis of 4-aryl-4H-chromenes by Ballini

Kidwai *et al*. in 2005 studied the same reaction for synthesizing 2-amino-3-cyano-4Hbenzo[h]chromene heterocycles using aqueous K_2CO_3 basic medium under microwave irradiation[214] (Scheme 54).

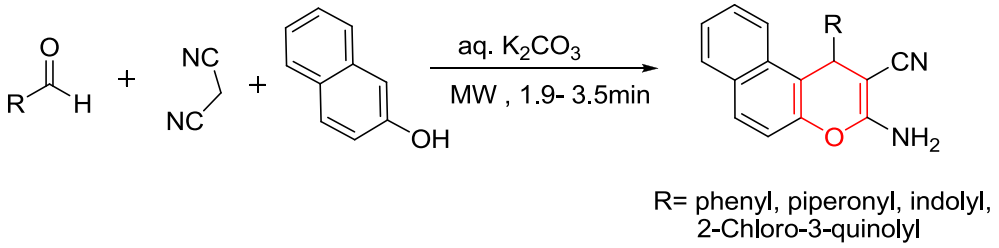

Scheme 54. K_2CO_3-catalyzed one-pot synthesis of 4-aryl-4H-chromenes

In 2008, Magedov *et al*. synthesized two chromene scaffolds, namely pyrano[3,2-c]pyridine and pyrano[3,2-c]quinolone derivatives following multicomponent strategies using a three-component reaction between aryl aldehydes, malononitrile, and 4-hydroxy-1,6-dimethylpyridin-2-(1*H*)-one [215] (Scheme 55).

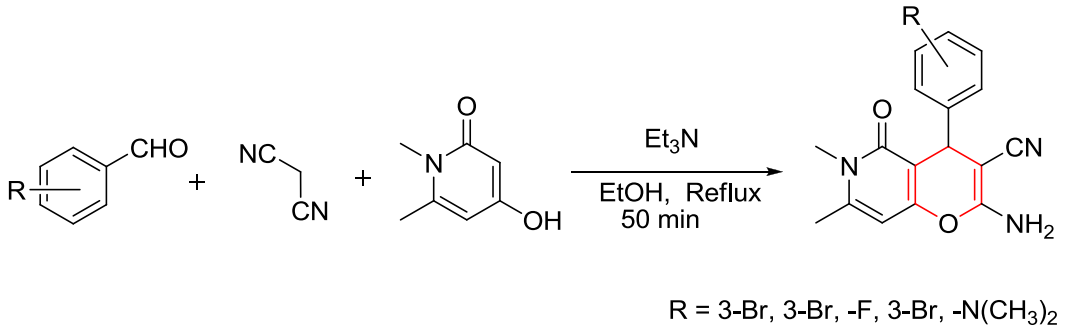

Scheme 55. One-pot synthesis of chromene derivatives by Magedov and co-workers

Multicomponent one-pot synthesis of tetrahydrobenzo[b]pyrans using 10 mol% of tetrabutylammonium fluoride (TBAF) as a catalyst in an aqueous medium under reflux condition was reported by Gao et al.[216] (Scheme 56).

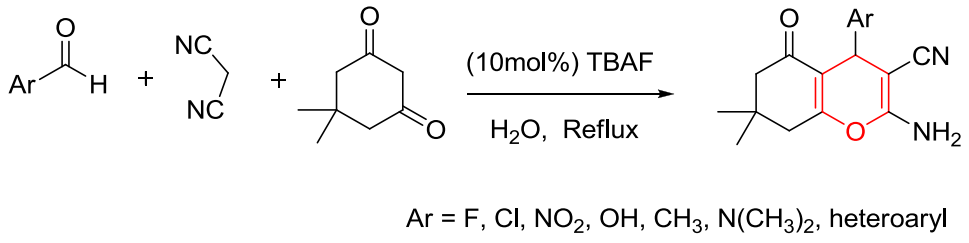

Scheme 56. TBAF catalyzed one-pot synthesis of chromenes

Kumar *et al*. in 2009 developed a multi-component protocol for the synthesis of tetrahydro-4*H*-chromenes and 2-amino-4H-pyrans from the reaction of substituted benzaldehydes, malononitrile, and 1,3 diketone in the presence of MgO as a catalyst [217] (Scheme 57)

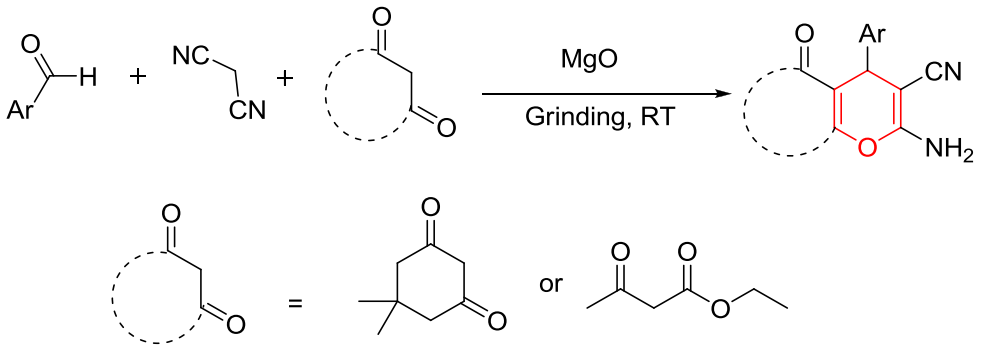

Scheme 57. One-pot synthesis of chromene derivatives by Kumar et al

Magara *et al*. reported the synthesis of 2-amino-4Hchromene derivatives *via* a one-pot reaction of substituted phenols, aldehydes and active methylene compounds using silica gel supported polyamine heterogeneous catalyst under reflux condition in an aqueous ethanolic medium[218] (Scheme 58).

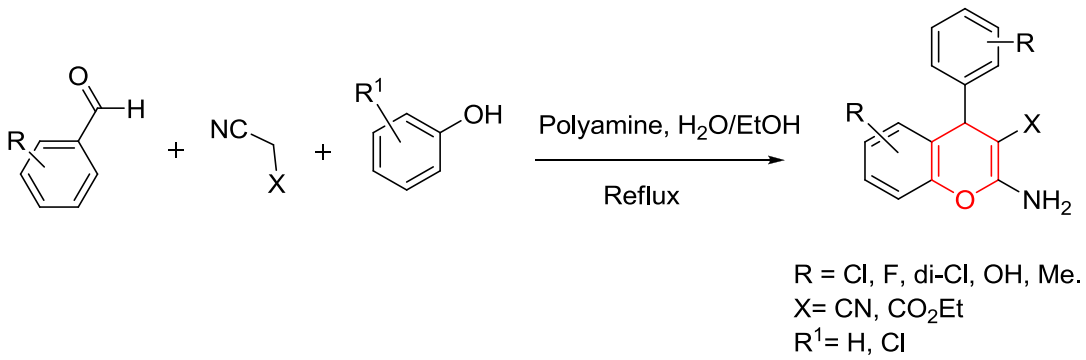

Scheme 58. Polyamine catalyzed one-pot synthesis of 2-amino-4*H*-chromene derivatives

Nano–MgO can efficiently bring this one-pot condensation between resorcinol, aldehydes, and malononitrile at room temperature in water to produce various 4*H*-chromenes in good yields in 25 min [219] (Scheme 59).

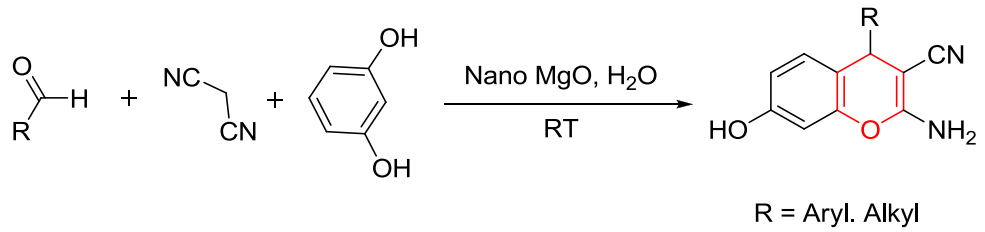

Scheme 59. Nano MgO catalyzed one-pot synthesis of 2-amino-4*H*-chromene derivatives

In 2013, Pradhan *et al*. described the synthesis of a series of chromeno[4,3-b]chromene derivatives by applying a Lewis acid-surfactant-combined catalyst (LASC) [Fe(DS)$_3$] via a three-component reaction of aldehydes, 1,3-diketones, and 4-hydroxycoumarin in aqueous medium under reflux condition [220] (Scheme 60).

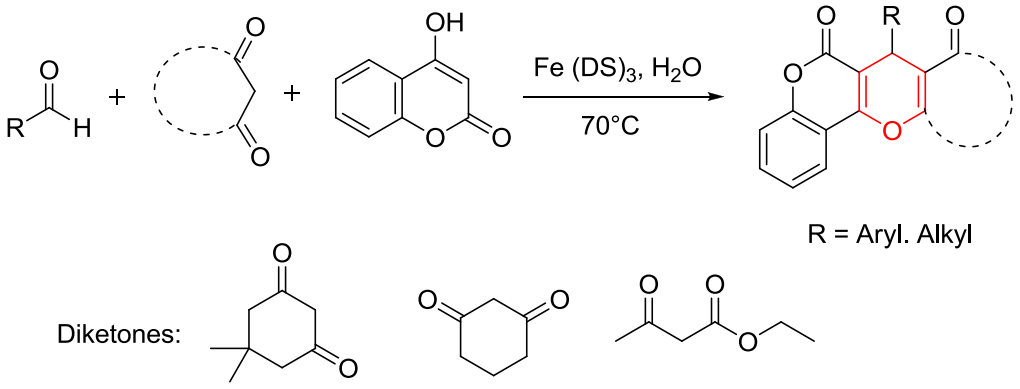

Scheme 60. One-pot synthesis of chromeno[4,3-b]chromene derivatives

In the same year, it was found that CuO–CeO$_2$ nanocomposite can act as an efficient heterogeneous catalyst for one-pot synthesis of 4*H*-benzo[b]pyran derivatives from the reaction of 3-methyl-1-phenyl-2- pyrazoline-5-one, aromatic aldehyde and malononitrile at solid phase under heating condition[219] (Scheme 61).

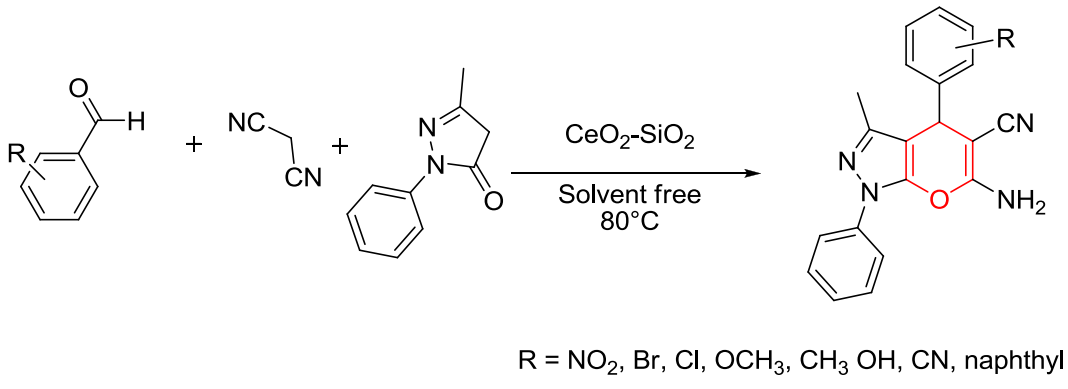

Scheme 61. One-pot synthesis of 4*H*-benzo[b]pyran derivatives

Three-component condensation between aromatic aldehydes, ethyl cyanoacetate or malononitrile, and diverse C–H activated acidic compounds (Z) in the presence of a catalytic amount of 4-(dimethylamino)pyridine (DMAP) in ethanol under reflux conditions could efficiently promote the synthesis of chromenes and analogous heterocycles [221] (Scheme 62).

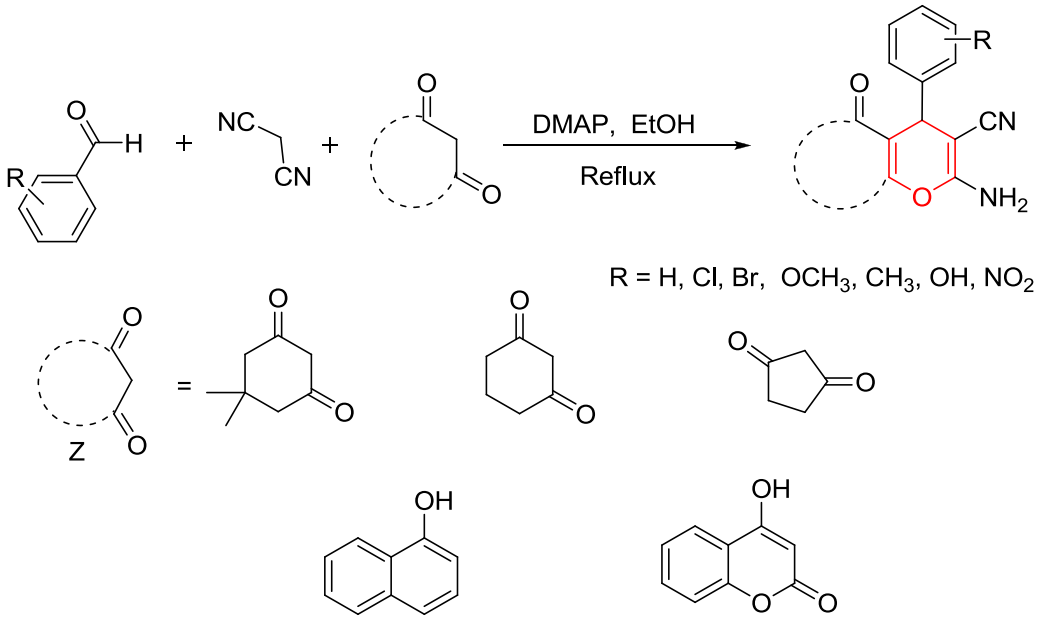

Scheme 62. DMAP catalyzed one-pot synthesis of 2-amino-4*H*-chromenes

In 2009, Shaabani *et al*. reported a room-temperature-based synthesis of benzo[g] and dihydropyrano[2,3-g]chromene derivatives *via* a one-pot multicomponent reaction of aldehyde, malononitrile, and 2-hydroxynaphthalene-1,4-dione or 2,5-dihydroxycyclohexa-2,5-diene-1,4-dione in the presence of a catalytic amount of Et_3N in CH_3CN [222] (Scheme 63).

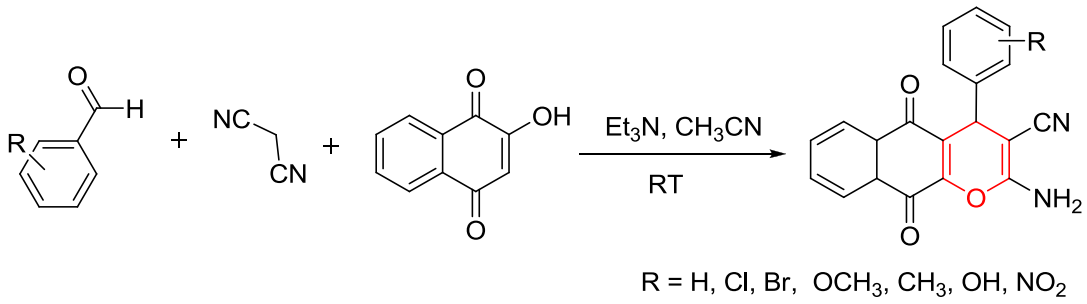

Scheme 63. One-pot synthesis of 4*H*-Pyrano-[2,3-b]naphthoquinone

I.7 The biological interest in pyridine derivatives

Over the last 50 years interest in pyridine derivatives has risen sharply with the discovery of many bioactive compounds containing a pyridine ring. The development of different pyridine drugs has been especially interesting for the pharmaceutical industry, as the existence of over 7000 drugs with a pyridine ring demonstrates[223] Researchers have long been fascinated by the biological activities of 1,4-dihydropyridines (1,4-DHPs) and their derivatives.

The 1,4-Dihydropyridines are a very important class of heterocyclic compounds due to a variety of biological activities. Initially, these compounds were found to be calcium channel modulators and were developed as cardiovascular and antihypertensive drugs. A number of DHP calcium antagonists have been introduced as potential drugs for the treatment of congestive heart failure [224]. DHP drugs, namely nifedipine, nicardipine, and amlodipine, are cardiovascular agents for the treatment of hypertension [225] (Figure 70)

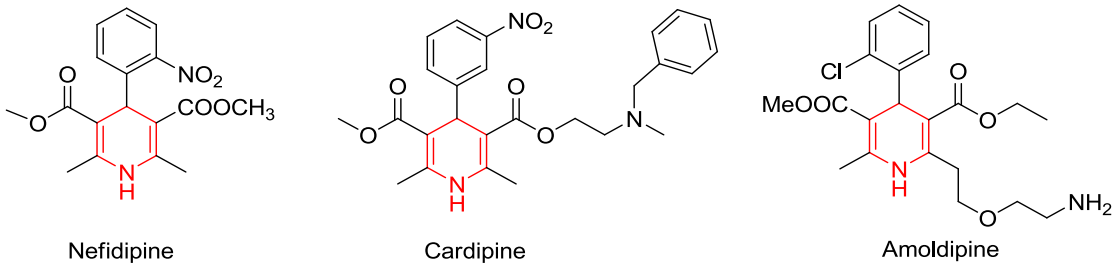

Figure 70. DHP drugs are used as cardiovascular agents for the treatment of hypertension

As a foundation of these early studies, many dihydropyridine derivatives have now been synthesized worldwide and have led to numerous second-generation commercial products such as nimodipine, nisoldipine, nitrendipine, felodipine, isradipine, manidipine, and nilvadipine (Figure 71).

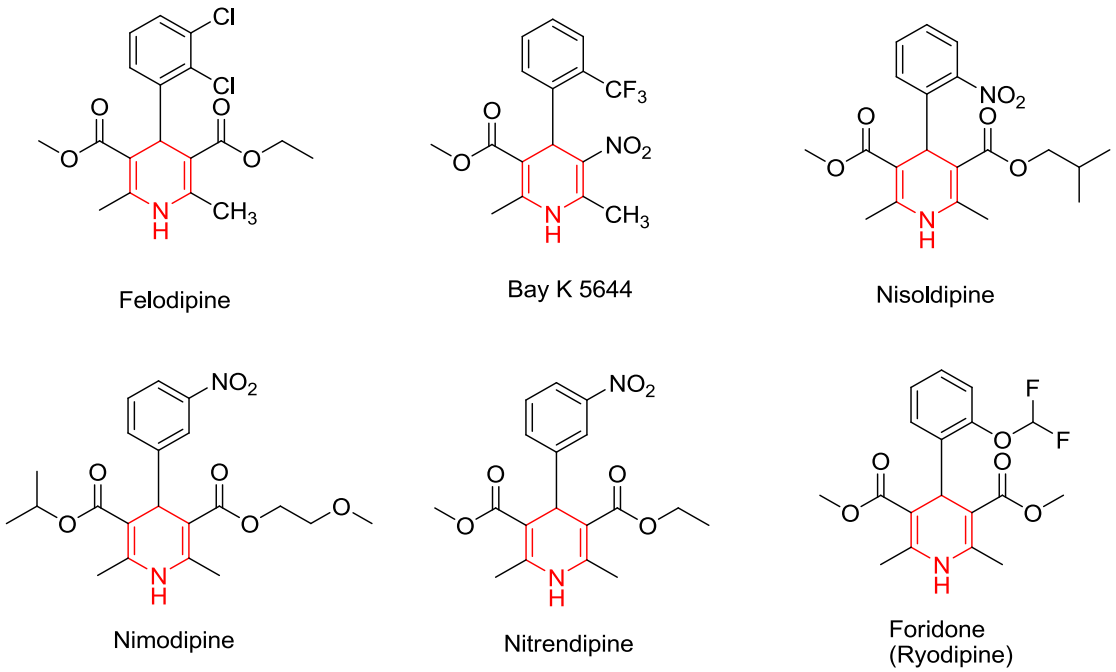

Figure 71. 1,4-DHPs used as clinical drugs

The 4-quinoline-substituted-1,4-dihydropyridines, which have analgesic, morphine agonist, and spasmolytic properties, were described in a Wellcome patent in 1943 (Figure 72).

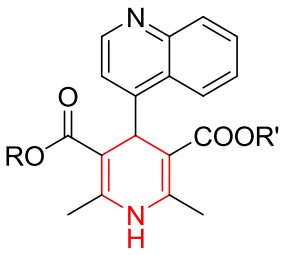

Figure 72.

Some 1,4-dihydropyridine compounds containing benzenesulfonamide groups showed potential for in-vitro cytotoxicity against the EAC cell line. Notably, the compounds with substituted phenyl groups at the 4 position, including Bromo, Chloro, or nitro groups, exhibited the highest levels of in-vitro cytotoxicity when compared to other tested compounds and even to the reference drug Doxorubicin[226] (Figure 73).

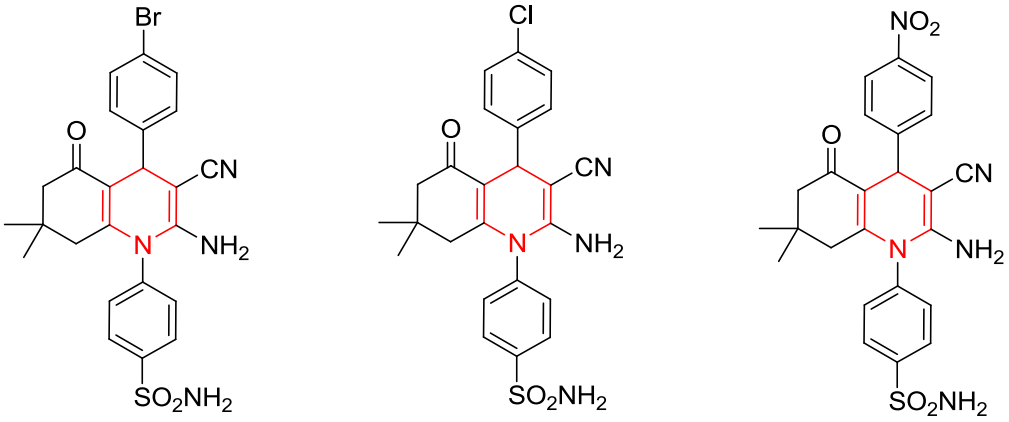

Figure 73. 1,4-Dihydropyridine derivatives had anticancer activity

I.8 Reported synthetic route to 1,4-dihydropyridine derivatives

1,4-Dihydropyridines (DHPs) are one of the most important classes of heterocyclic compounds. They are therefore attractive synthetic targets of organic chemistry. Multicomponent reactions (MCRs) are the most efficient strategies for the synthesis of 1,4-DHPs in terms of providing both sufficient structural diversity and numbers for compound libraries. Following the classical multicomponent synthesis of 1,4-DHPs by the Hantzsch reaction, chemists have developed a large number of new MCRs to access 1,4-DHPs with significantly extended structural diversity. The advances in the synthesis of structurally diversified 1,4-DHPs through new MCRs beyond the classical Hantzsch reaction are reviewed

The Hantzsch synthesis is one of the earliest one-pot multi-component reactions. The reaction was reported for the first time in 1881 by Arthur Rudolf Hantzsch [227]. It represents the most widely used approach for the preparation of dihydropyridine derivatives via a four-component reaction (4CR). The reaction puts a set of an aldehyde, two equivalents of a β-ketoester (activated methylene species), and a source of nitrogen such as ammonium acetate or ammonia without the intervention of any other reagents. These three components combine with each other in a multi-step process to provide a symmetrically substituted 1,4-dihydropyridine (Scheme 64).

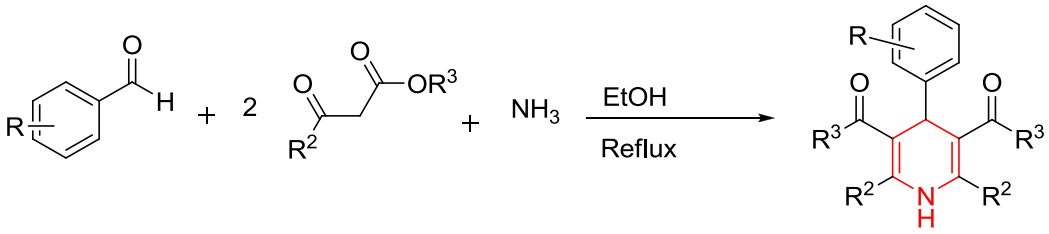

Scheme 64. The general reaction of Hantzsch

Since its inception, several methods have been developed to synthesize this type of molecule, employing various methylene-activated compounds, including acyclic α-diketone (1,4-pentanedione), cyclic (dimedone), or α,β-unsaturated ester, with the aid of a catalyst.

The use of β-dicarbonyl compounds of different structures gives access to unsymmetrical 1,4-dihydropyridine derivatives. Thus the addition of ethyl acetoacetate and dimedone to an aldehyde in NH_4OH medium leads to a poly-substituted 1,4-dihydropyridine asymmetrical [228] (Scheme 65).

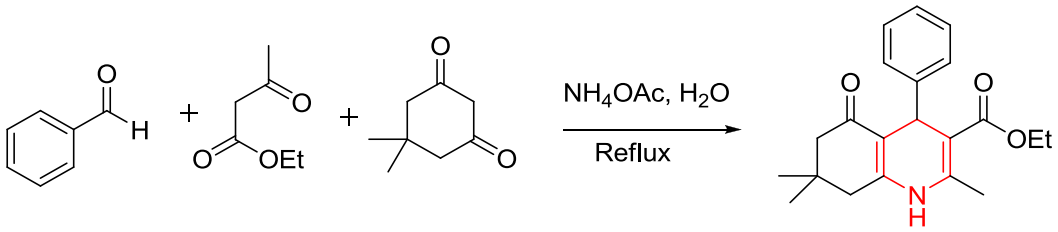

Scheme 65. Synthesis of unsymmetrical 1,4-dihydropyridine derivatives

A whole series of highly functionalized hexahydroquinoline-4-ones has been prepared by Lichitsky *et al.* from benzylidenemalonirile and 3-aminocyclohex-2 en-1-one derivatives in the presence of piperidine as catalyst [228] (Scheme 66).

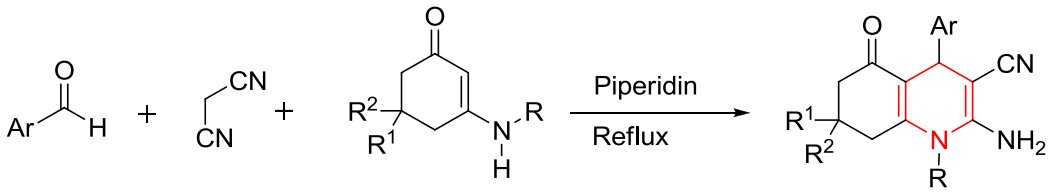

Scheme 66. Synthesis of *N*-substituted-1,4-dihydropyridine derivatives

In their research, Mostafa M. Ghorab and colleagues explored the possible application of 4-(5,5-dimethyl-3-oxo-cyclohex-1-enylamino)benzenesulfonamide in synthesizing 1,4-dihydropyridine derivatives. They achieved this by reacting sulfanilamide with 5,5-dimethyl-1,3-cyclohexandione to form enaminone. The

enaminone was then subjected to a cycloaddition reaction with 2-benzylidene-malononitrile in the presence of triethylamine, leading to the formation of *N*-substituted-1,4-dihydropyridine derivatives [226]. This reaction scheme is depicted in Scheme 67.

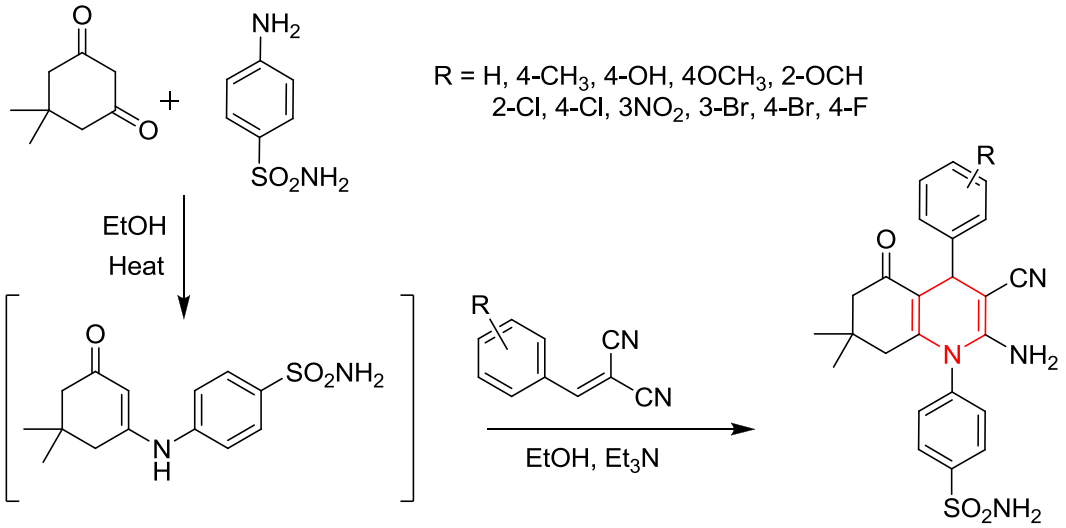

Scheme 67. Synthesis of *N*-sulfanilamide-1,4-dihydropyridine derivatives

Such hypothesis has been confirmed with the fascinating work of Kappe *et al*. [229], where the competitive reaction pathways of the condensation of 5-aminopirazoles, aldehydes, and cyclic 1,3-diketones were analyzed. 5-aminopyrazoles are bifunctional molecules, and at the same time able to act as ammonia or urea source, after adding a base catalyst. (Scheme 68)

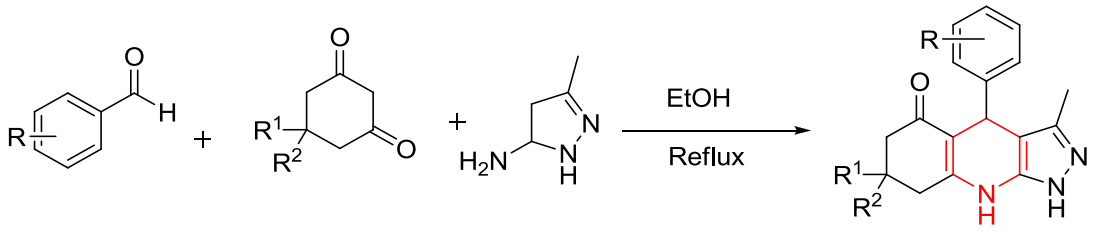

Scheme 68. Synthesis of 1,4-DHPs using cyclic 1,3-diketones

Similar to acyclic 1,3-dicarbonyl compounds, cyclic1,3-dicarbonyl compounds also reacted with aromatic amines, aromatic aldehydes, and dimethyl acetylenedicarboxylate to give the corresponding 1,4-DHPs 22 in a fused structure by employing HOAc as solvent and acid catalyst [230] (Scheme 69).

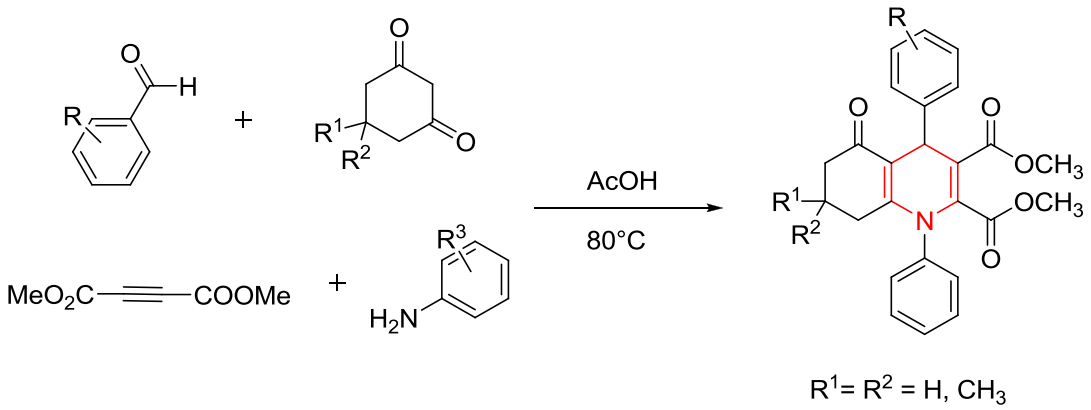

Scheme 69. Synthesis of 1,4-DHPs using cyclic1,3-dicarbonyl compounds

Amines are also favorable amino sources in the devisal of new multicomponent synthesis of 1,4-DHPs. For example, employing α,β-unsaturated aldehydes, 1,3-dicarbonyl compounds, and amines have been found as a very practical approach for the synthesis of unsymmetrical 1,4-DHPs. Renaud et al. conducted tentative investigations on the direct three-component reaction of 1,3-dicarbonyl compounds, amines, and α,β-unsaturated aldehydes to access 1,4- DHPs with Lewis acid catalysis. Moderate to excellent yields have been obtained by performing the reactions in a stepwise manner [231] (Scheme 70).

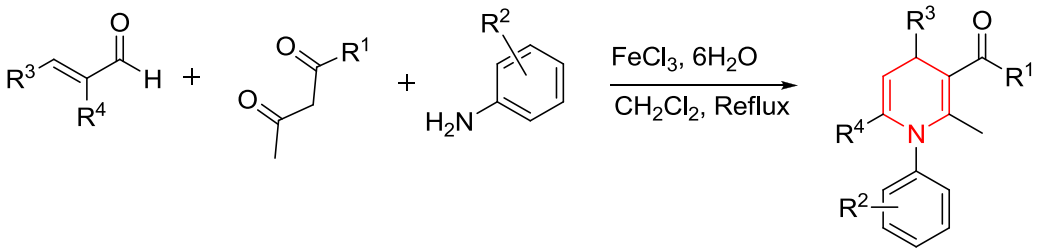

Scheme 70. Three-component stepwise synthesis of *N*-Aryl-1,4-DHPs

A new method for synthesizing NH-free compounds was created by Safari and colleagues[232]. The approach involved using chalcones, ethyl acetoacetate, and ammonia as the three components, and the reaction was catalyzed with cellulose sulfuric acid in refluxing water. The researchers achieved excellent yields of the desired products (Scheme 71).

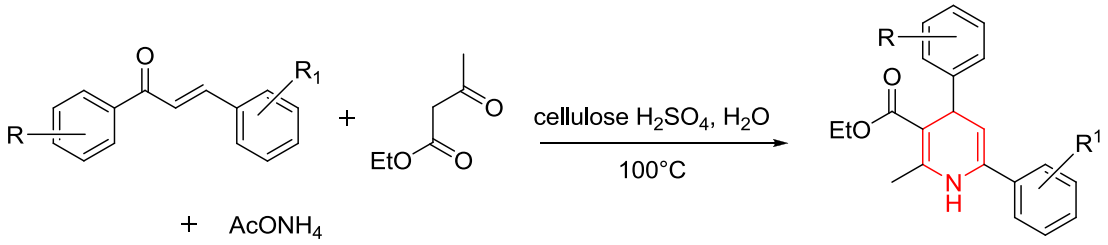

Scheme 71. Chalcone-based three-component 1,4-DHPs synthesis

The multicomponent synthesis of 1,4-DHPs often made use of alkynes as building blocks. In a study by Wang and colleagues [233], a novel approach to this synthesis was developed using TFA as a catalyst to assemble three molecules of E-3 (2-formylphenoxy)propenoates and amines (Scheme 72).

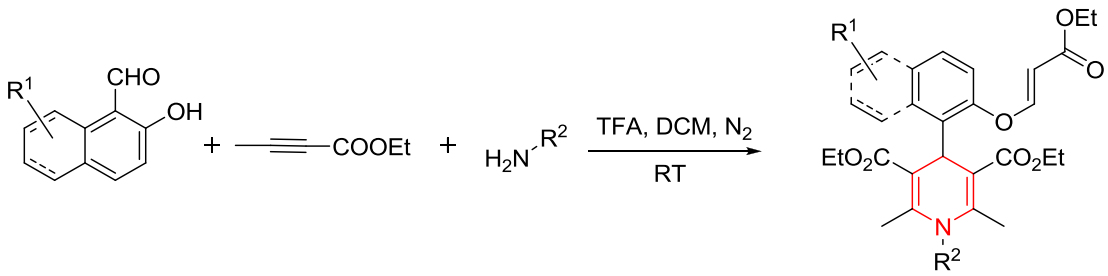

Scheme 72. Three-component synthesis of 1,4-DHPs initiated by E-3-(2- formylphenoxy)propenoates

However, it was later discovered that the direct MCRs of ethyl propiolate, benzaldehyde, and a primary amine were capable of providing corresponding 1,4-DHPs by heating the starting materials in acetic acid. The application scope of this protocol, however, was not defined, as only 4 examples of 1,4-DHPs were prepared for the sake of biological research [234] (Scheme 73).

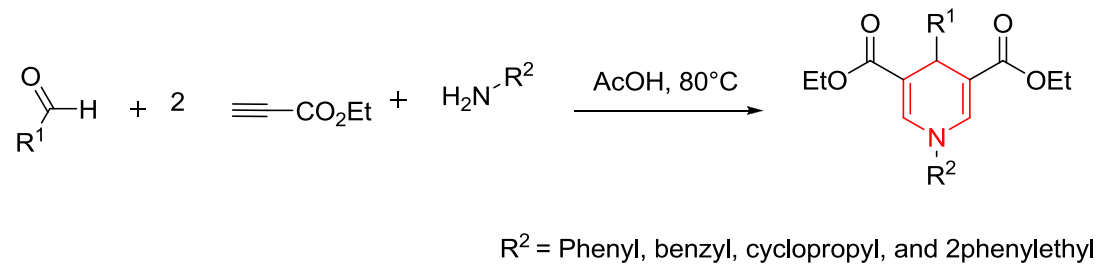

Scheme 73. Direct synthesis of symmetrical 1,4-DHPs from propiolate

Also, Yan et al. established a four-component synthesis of 1,4-DHPs from methyl propiolate, aryl amines, aromatic aldehydes, and acetonitriles. With the catalysis of triethyl amine, the Knoevenagel condensed intermediates incorporated intermediates from an aza Michael addition to providing intermediates that underwent subsequent intramolecular cyclization and tautomerization to 1,4-DHPs as final products. On the other hand, when ethyl 2-cyanoacetate was used as the starting material in place of malononitrile 2-cyanoacetamide, 2-pyridinones were afforded as main or single products in the corresponding entries [235] (Scheme 74).

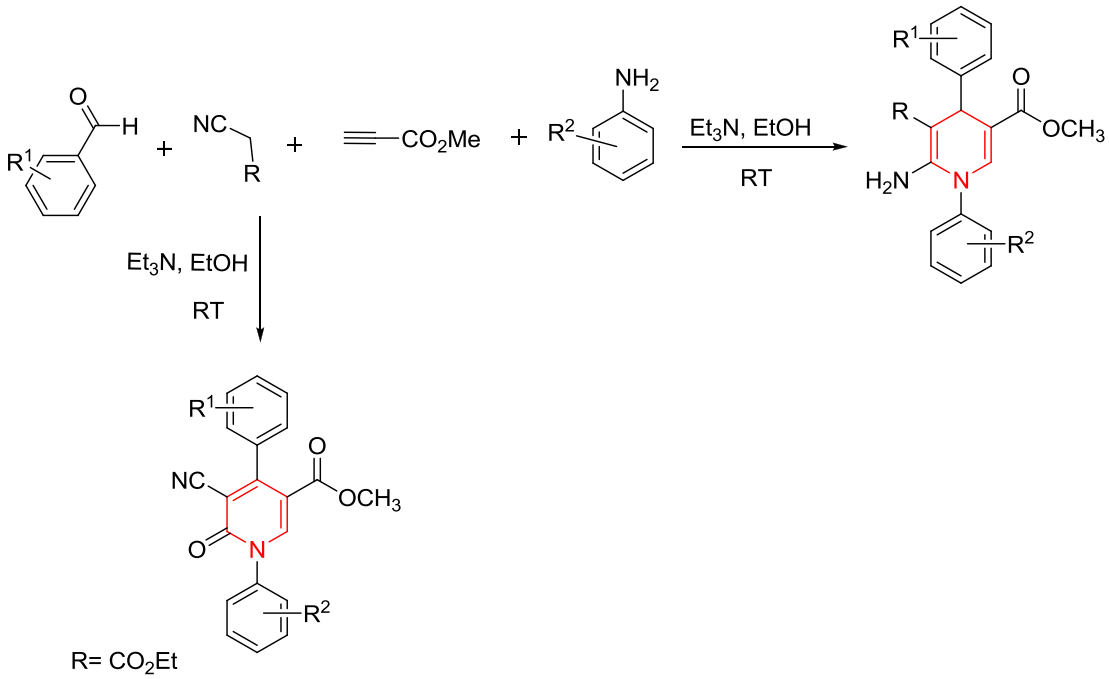

Scheme 74. Four-component synthesis of 1,4-DHPs with aldehyde, amine, propiolate, and nitrile

Recently, Kumar *et al*. discovered that malononitrile or ethyl cyanoacetate was able to efficiently react with diethyl acetylenedicarboxylate, aromatic amines, and aromatic aldehydes to provide 1,4-DHPs of type by a solvent- and catalyst-free grinding protocol. This clean synthetic method proceeded also via enaminoesters and Knoevenagel condensed intermediates [236] (Scheme 75).

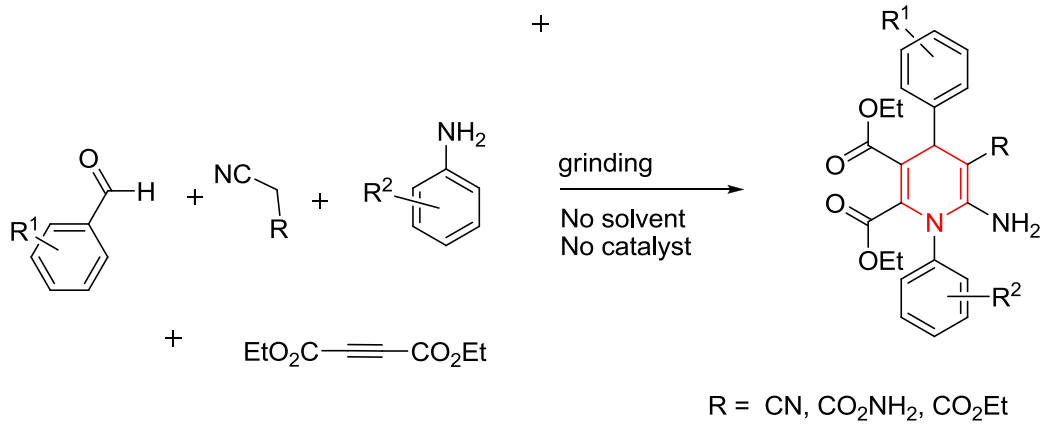

Scheme 75. Solvent- and catalyst-free synthesis of 1,4-DHPs.

In another example, the (2-aryl)methylene malononitriles which were prepared from aldehydes and malononitrile have been successfully employed to react with ethyl acetoacetate and ammonia acetate to provide 1,4-DHPs by grinding under solvent-free conditions[237] (Scheme 76).

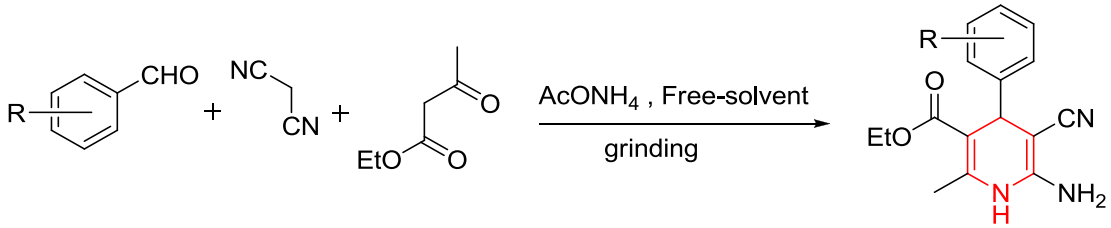

Scheme 76. Three-component synthesis of 1,4-DHPs using malononitriles

Indeed, the interest aroused by this large class of compounds thanks to its broad spectrum of significant biological and pharmaceutical activities, has made the design of new pyran derivatives through the development of new synthetic methods an area of interest major among researchers.

I.9 Tacrine, biological interest, and synthesis

The molecule Tacrine, also known as 9-amino-5,6,7,8-tetrahydroacridine, is made up of three fused rings: a benzene ring (called ring a), a pyridine ring (called ring b) with an amine group, and a cyclohexane ring (called ring c). In the creation of Tacrine analogs (similar molecules), described in the literature, they have mostly made modifications to rings **a** and **c** while leaving the core structure of ring **b** intact, as it is essential for the molecule's activity.

In particular, coupling reactions with other compounds have generally targeted the amine group or the chlorine group (in the case of 9-chloro-5,6,7,8-tetrahydroacridine) (Figure 74).

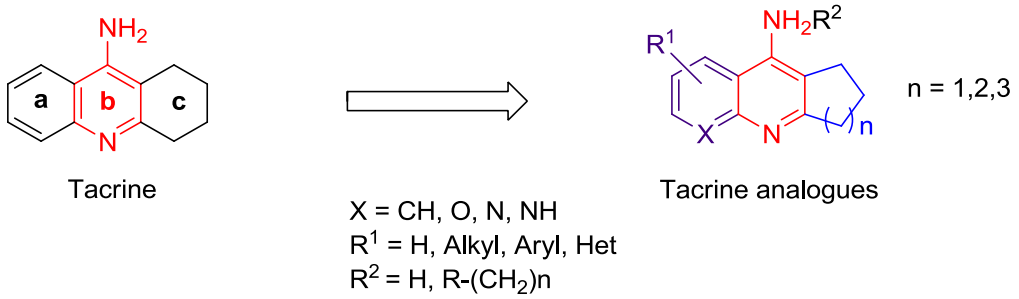

Figure 74. Locations that can undergo structural alterations in Tacrine

I.9.1 The biological interest of some tacrine analogs

Xiaojuan Chao and colleagues have created a fresh collection of hybrid compounds by combining tacrine with caffeic acid. These molecules exhibit antioxidant activity, and one of the compounds, depicted in Figure 75, has an impressive inhibitory effect on acetylcholinesterase (*AChE*) [238].

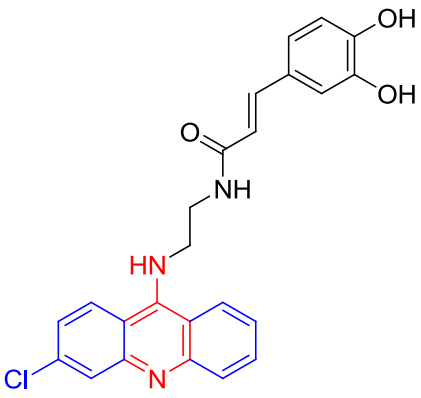

Figure 75. Tacrine analog had an impressive inhibitory effect on acetylcholinesterase

In a recent study by Wang and colleagues [239], they described the creation, testing, and molecular modeling of a fresh set of hybrid compounds by combining tacrine and coumarin (depicted in Figure 76). These compounds were designed to function as inhibitors of multifunctional AChE, which could potentially aid in the treatment of Alzheimer's disease.

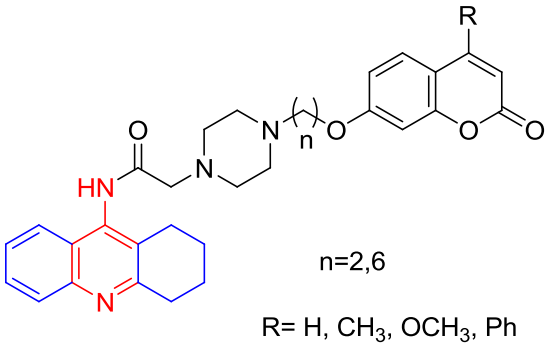

Figure 76. Tacrine analog used in the treatment of Alzheimer's disease

A recent development involves the synthesis of a fresh collection of tacrine-lophine hybrid compounds using a four-component reaction. Some of the resulting hybrid compounds were found to be powerful and selective inhibitors of acetylcholinesterase and butyrylcholinesterase at extremely low concentrations ($IC_{50} \approx 10^{-9}$ M) [240] (Figure 77).

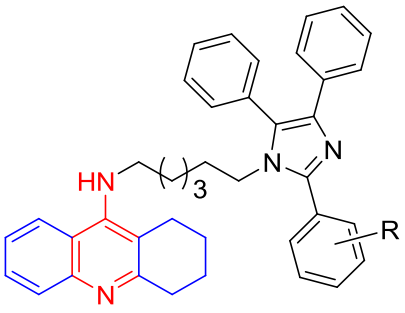

Figure 77. Tacrine analog has *Acetylcholinesterase* and *Butyrylcholinesterase* inhibitory

I.9.2 Reported synthetic route to some tacrine derivatives

Two approaches have been developed for the preparation of Tacrine and similar compounds.

The first method involves producing Tacrine by reacting anthranilonitrile with cyclohexanone through cyclo-dehydration [241]. Afterward, a reaction is performed to attach the desired fragment (usually a brominated derivative) to the aminoacridine structure, forming an N-alkylated Tacrine analog (Scheme 77).

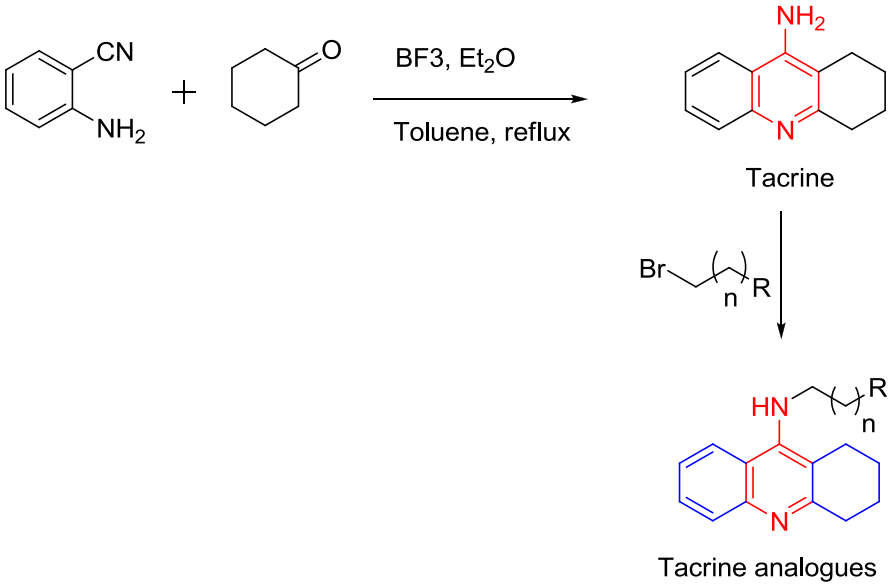

Scheme 77. Tacrine by reacting anthranilonitrile with cyclohexanone

Analogous to the cyclo-dehydration reaction of anthranilonitrile, a key sequence for synthesizing Tacrine analogs involves the condensation reaction of anthranilic acid with cyclohexanone in the presence of $POCl_3$ to yield the chlorine derivative. The addition of alkyl diamine to this intermediate produces the Tacrine analog (Scheme 78).

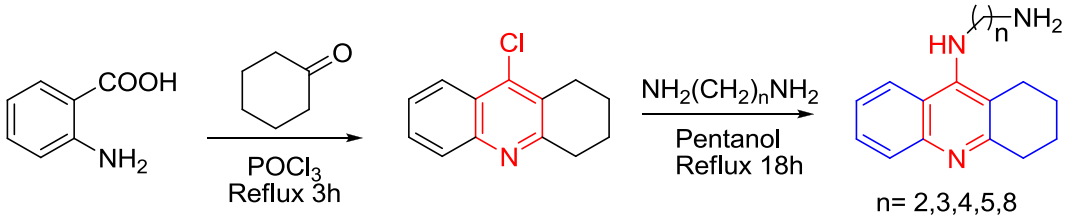

Scheme 78. The cyclo-dehydration reaction of anthranilonitrile for synthesizing Tacrine analogs

The chiral cyclic ketones can also be used in the cyclo-dehydration reaction of anthranonitrile, with $BF_3.Et_2O$ as a catalyst [242] (Scheme 79).

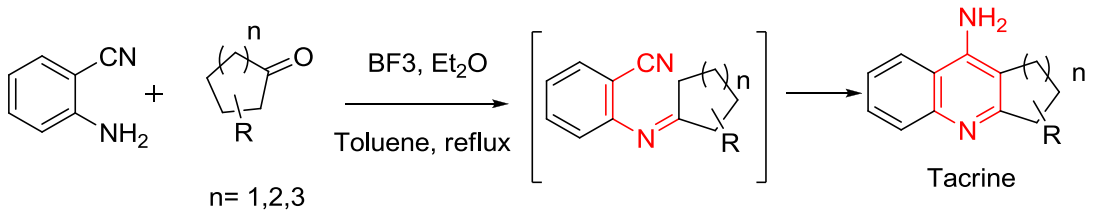

Scheme 79. The cyclo-dehydration reaction using chiral cyclic ketones

The second and most commonly used approach for creating Tacrine analogs involves modifying the structure of the core while keeping the nitrile and amine functions necessary for constructing the Tacrine molecule intact. Previous studies on the reactivity of heterocyclic compounds with various functional groups indicate that selective reactions that target vicinal functional groups such as amines and nitriles, without ring opening, have been observed. Ketone or ester functions are also tolerated in this process. The method is illustrated in Scheme 80.

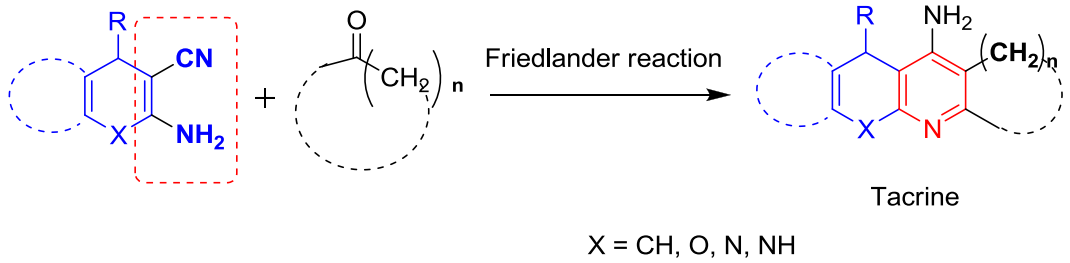

Scheme 80. Friedlander reaction

4*H*-pyran (or 1,4-dihydropyridine or pyridine) is a highly effective precursor for synthesizing Tacrine analogs, as it contains a free amine group at position 2 and a nitrile group at position 3. By incorporating cycloalkanone under typical Friedländer reaction conditions, these precursors have the potential to be converted into a Tacrine derivative.

To carry out this approach, precursor derivatives like 4*H*-pyran are first prepared and then subjected to a Friedländer type reaction [243]. In this reaction, cycloalkanone is added to the 4*H*-pyran derivative in the presence of $AlCl_3$ as a catalyst, and refluxing with 1,2-dichloroethane leads to the formation of the corresponding Tacrine analogs (Scheme 81).

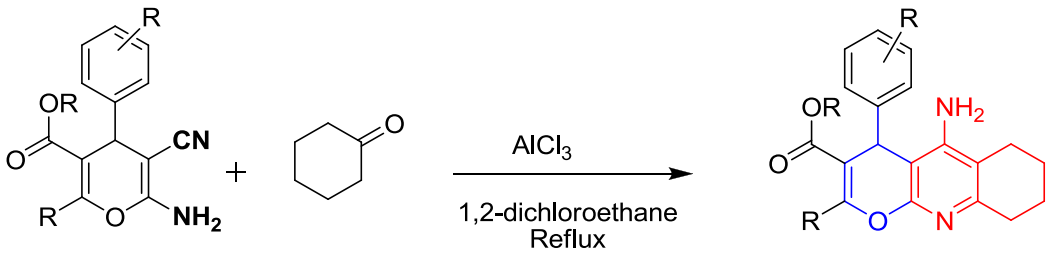

Scheme 81. Synthesis of Tacrine analogs using 4*H*-pyran as a precursor

It's worth noting that $ZnCl_2$ can replace $AlCl_3$ as a catalyst in the Friedländer reaction when refluxing nitrobenzene at a temperature of 120-130°C. However, the use of $AlCl_3$ as a catalyst is preferred due to its greater ease of use in the reaction process.

I.10 Sulfanilamide, interests, and uses

Sulfanilamide was first created in 1908 in Vienna by Paul Gelmo, who was an assistant to Wilhelm Sweden. However, Gelmo did not realize the therapeutic properties of his product. It was not until 1935 that the antibacterial properties of sulfamidochrysoidin, also known as Prontosil, were explored by Jacques and Thérèse Tréfouël, Daniel Bovet, and Federico Nitti at the Institut Pasteur, in Ernest Fourneau's laboratory.

They isolated sulfanilamide, a metabolite of Domagk's drug, and identified it as the active therapeutic agent in sulfamidochrysoidin [244]. Their research marked a turning point by challenging the conventional idea that the antibacterial properties of azo dyes were due to their coloring properties, and instead, it opened up new avenues for sulfonamide therapy.

Sulfanilamide, an aniline derivative of the sulfonamide family is a low-priced drug having chemotherapeutic properties popular in developing countries with serious bacterial resistance problems [245,246]. Sulfanilamide was popularized because of its role in reducing infection rates during 2nd world War [247]

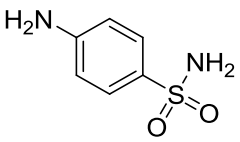

Figure 78. Sulfanilamide

Over the past few years, a considerable amount of research has been dedicated to the discovery of novel compounds possessing biological activity that incorporate the sulphonamide unit R-SO_2-NH_2. The inclusion of this structural motif in heterocyclic molecules can lead to the development of intriguing chemical properties and/or pharmacological effects.

Sulfanilamide and its derivatives have a similar chemical structure to *p*-aminobenzoic acid (PABA) which is a critical component involved in the process of folate synthesis in plants and bacteria. Sulfanilamide functions as an inhibitor of dihydropteroate synthase, an enzyme that catalyzes the fusion of 6-hydroxymethyl-7,8-dihydropteridine pyrophosphate with para acid aminobenzoic acid to create 7,8-dihydropteroate. Sulfanilamide serves as a substrate for dihydropteroate synthase instead of PABA. This "false reaction" between sulfanilamide and the enzyme leads to the formation of an inactive product, which cannot undergo the next metabolic step to create dihydrofolate. This metabolic reaction is normally catalyzed by dihydrofolate synthase.

The chemical structure of sulfanilamide can be found in numerous beneficial compounds, including drugs used in proven therapies. Tolazamide and chlorpropamide are among the oldest drugs utilized in the treatment of diabetes, following insulin. These medications work by stimulating the secretion of insulin in the beta cells of the pancreas, thereby directly increasing the amount of insulin circulating in the blood [248] (Figure 79).

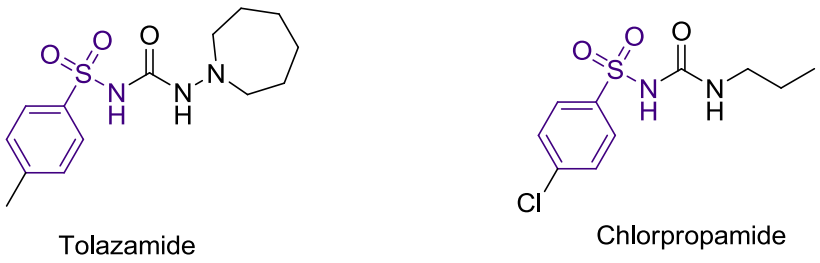

Figure 79. Sulfanilamide derivatives used in the treatment of diabetes

Bactrim® is a medicine in combination with two antibiotics: sulfamethoxazole, from the family of sulfonamides, and trimethoprim, from the family of diaminopyrimidines. It is used in the treatment of various infectious diseases, including

respiratory, ENT, digestive, urinary, or prostate infections. THE (Adiazine®) is used primarily in the prevention and treatment of toxoplasmosis (in combination with another antiparasitic) [249] (Figure 80).

Figure 80. Sulfanilamide derivatives used in the treatment of infectious diseases

Sulfanilamide derivatives are also key intermediates in the synthesis of biologically active substances. The combination of Losartan with hydrochlorothiazide for example is used in the treatment of high blood pressure [250] (Figure 81).

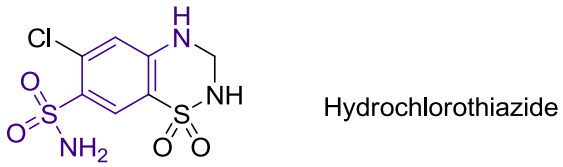

Figure 81. Sulfanilamide derivative used in the treatment of high blood pressure

A range of hybrid pyridazinsulfanilamide derivatives was synthesized by A. Deeb and colleagues, which were then evaluated for their antibacterial activity against *staphylococcus aureus*, *Bacillus subtilis*, *Escherichiacoli*, and *Pseudomonas vulgaris*. The results demonstrated that these compounds exhibited noteworthy antibacterial and fungicidal activity [251] (Figure 82).

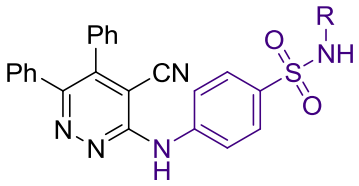

Figure 82. Sulfanilamide derivative used as an antibacterial and fungicidal agent

Celecoxib (Celebrex®) is a potent selective COX-2 inhibitor (the enzyme responsible for inflammation and pain). It also has properties of analgesics and antiarthritics [252] (Figure 83).

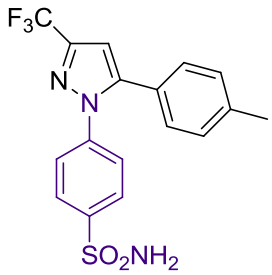

Figure 83. Sulfanilamide derivative used as an anti-inflammatory agent

In 2009, Subudhi et al. screened novel 1,4-dihydropyridines and their mannish bases with sulfanilamide for antiulcer activity and the compounds containing methoxy substitution at C-4 position exhibited good antiulcer activity [253] as depicted in Figure 84.

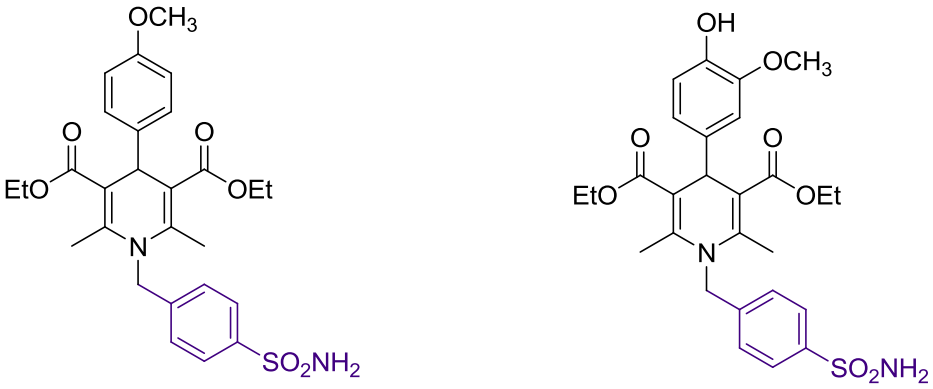

Figure 84. Sulfanilamide derivatives used as anti-ulcer agents

The diverse examples presented demonstrate the significant interest in sulfanilamide derivatives, particularly in the field of therapeutic chemistry. The focus of what follows will mainly be on the synthesis of molecules that incorporate sulfanilamide as a fundamental structure with varying functional groups. Our research efforts can be summarized by the following synthetic diagram.

I.11 Quinoline-heterocycle hybrids

The coupling of the quinoline motif with various heterocyclic entities is a promising approach to improving the pharmacological profile of quinoline derivatives [254]. This approach has led to the preparation of many novel hybrid compounds, which have shown remarkable pharmacological activity. These compounds mainly comprise heterocycles containing nitrogen and/or oxygen atoms, such as pyrazole, oxazole, pyridine, pyrrole, pyran ring, and so on.

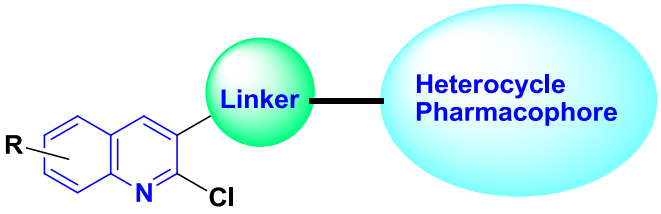

Figure 85. Hybrides (Quinoline)-hétérocycles

The use of nitrogen and/or oxygen heterocycles in the design of hybrid compounds is particularly advantageous because these atoms can form hydrogen bonds and participate in other important interactions with biological targets. These interactions can lead to increased potency and selectivity of the compounds, as well as improved pharmacokinetic properties such as increased solubility, bioavailability, and metabolic stability.

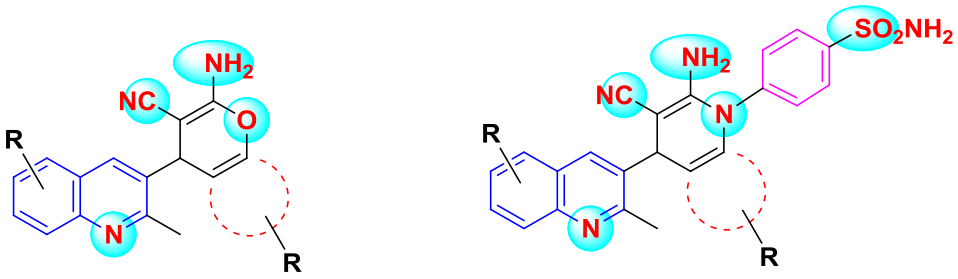

Figure 86.

The literature discusses the combination of a pyran and pyridine motif with the quinoline nucleus. Some hybrid compounds have been reported, and they demonstrate the significance and usefulness of this combination in the field of therapeutics. This highlights the potential of these hybrid compounds for the development of new drugs with multiple therapeutic benefits.

The combination of quinoline and pyridine has also yielded impressive outcomes in the field of chemotherapy. One notable example is Lavendamycin, (Figure 87) a potent antibiotic that exhibits significant antiproliferative properties against various cancer cell lines. This demonstrates the potential of this hybrid compound as a promising candidate for the development of new chemotherapy drugs.

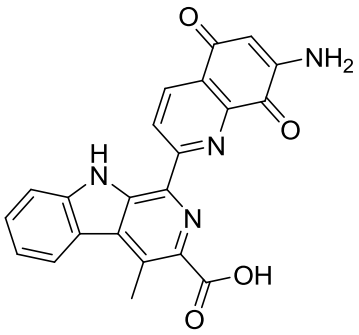

Figure 87. Lavendamycin

II. Results and Discussion

The main objective of this research centers around creating different heterocyclic compounds based on quinoline derivatives. The starting point is to use formyl quinoline derivatives, which is a suitable starting material. This particular compound was chosen as a model for creating precursor compounds due to the presence of favorable chemical sites that can undergo the necessary transformations to produce the desired compounds.

I.1 Preparation of 2-chloro-3-formyl-6-substituted quinoline

The starting materials used during our investigations were the 2-chloro-3-formyl-6-substituted quinoline derivatives (**6a-b)**, which were obtained in two stages according to the method described by *O*. Meth-Cohn [206]. The initial step involved the formation of acetanilide (**5)** through the acylation reaction of the relevant aromatic amine derivatives. The second step involves the treatment of *N*-phenylacetamide derivatives by adding Vilsmeier's reagent ($POCl_3$ and DMF in a 7/3 ratio) which is undoubtedly the key step of the method. The reaction sequence is described in the scheme below (Scheme 82).

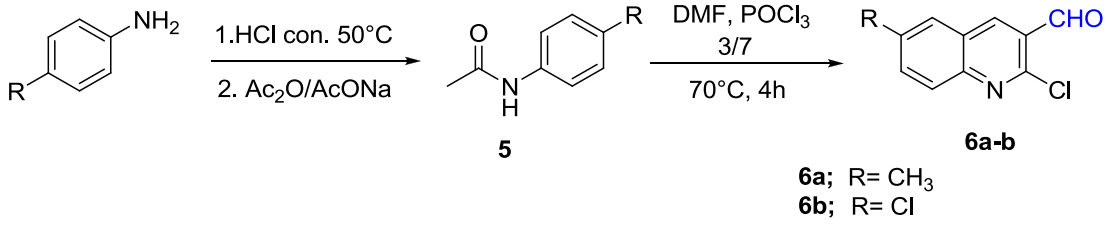

Scheme 82. Synthetic route of 2-Chloroquinolin-3-carbaldehyde **6a-b**

2-chloroquinoline-3-carbaldehyde derivatives (**6a)** and **(6b)** are obtained in good yields (80 and 65%) respectively. The spectroscopic results as well as the physical properties of 2-chloro-3-formyl-6-alkylquinoline **(6a)** and **(6b)** are in good agreement with the proposed structures and confirm those described in the literature [206]. We present in the following a detailed analysis by nuclear magnetic resonance spectroscopy of the proton and carbon-13 of the starting material (**6a)**, which is a known compound, for the purpose of facilitating the understanding and tracking of comments related to the spectroscopic analysis of the various prepared products. The chemical shifts of the quinoline nucleus protons and carbon-13 do not undergo significant changes in the majority of the case (Spectrumes 8 and 9).

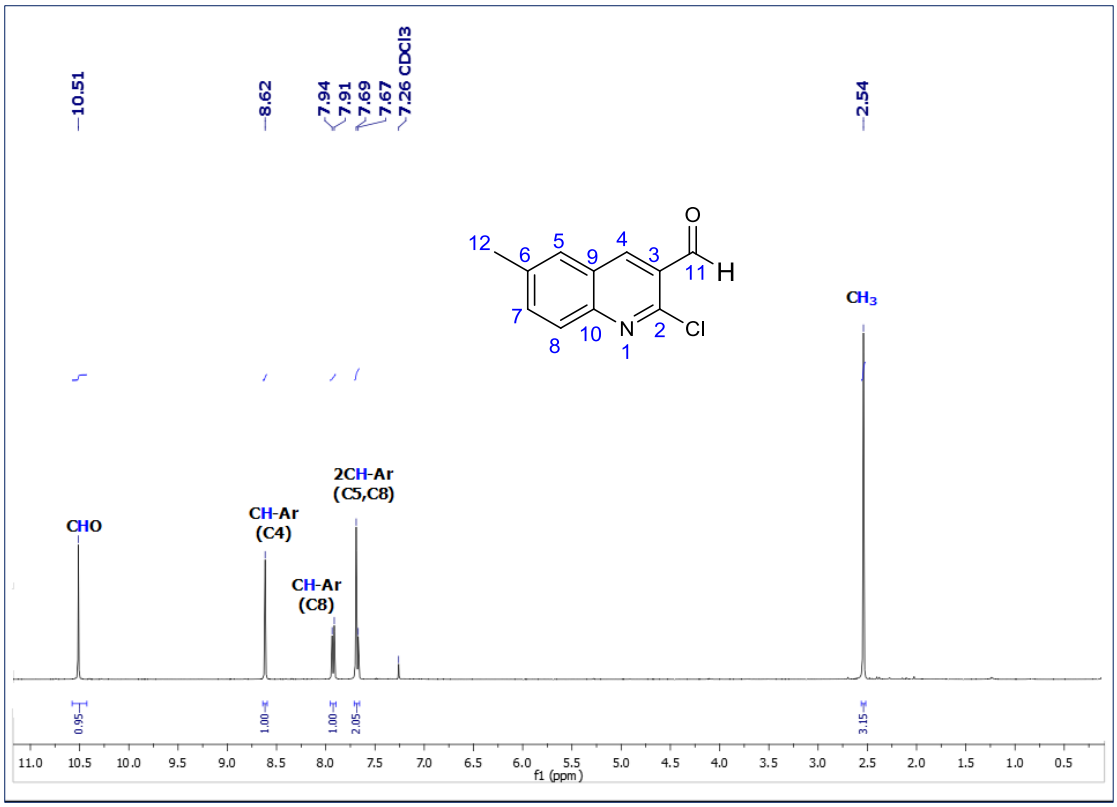

Spectrum 8. ^{1}H NMR spectrum (400 MHz, $CDCl_3$) of 2-chloro-3-formyl-6-methylquinoline (6a)

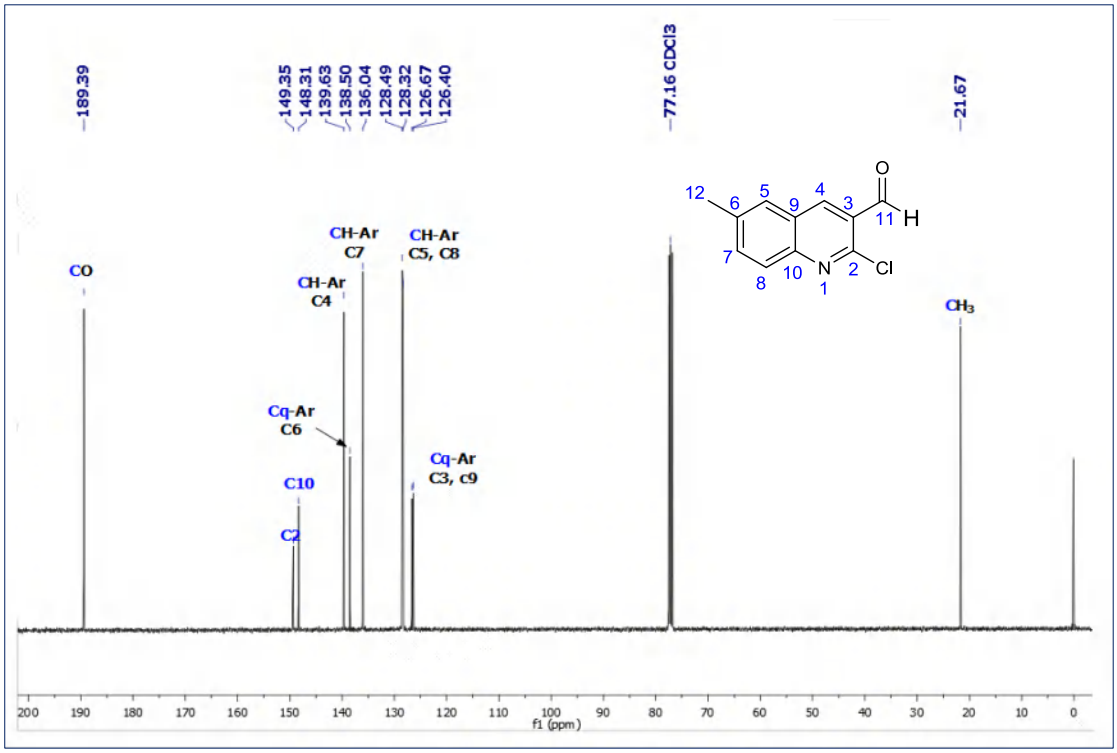

Spectrum 9. ^{13}C NMR spectrum (100 MHz, $CDCl_3$) of 2-chloro-3-formyl-6-methylquinoline (**6a)**

In ^{1}H NMR, the spectral analysis shows a singlet signal at 10.51 ppm, corresponding to the proton of the aldehyde group. The aromatic protons show up as

low-field signals in the expected interval between [7.67-8.62] ppm. The methyl group protons resonate at 2.54 ppm as a 3H integrated singlet.

The ^{13}C NMR shows a signal corresponding to the aldehyde function carbon, which resonates at 189.3 ppm, while the quaternary and tertiary sp^2 and sp hybridized carbons resonate at intermediate fields between [126.2-149.2] ppm, and the sp^3 hybridized methyl group carbon resonates at 21.6 ppm. These results are in good agreement with the proposed structures and are consistent with those described in the literature.

A detailed mechanism of the formation of 2-chloro-3-formylquinoline derivatives is described in the scheme below [206] (Scheme 83).

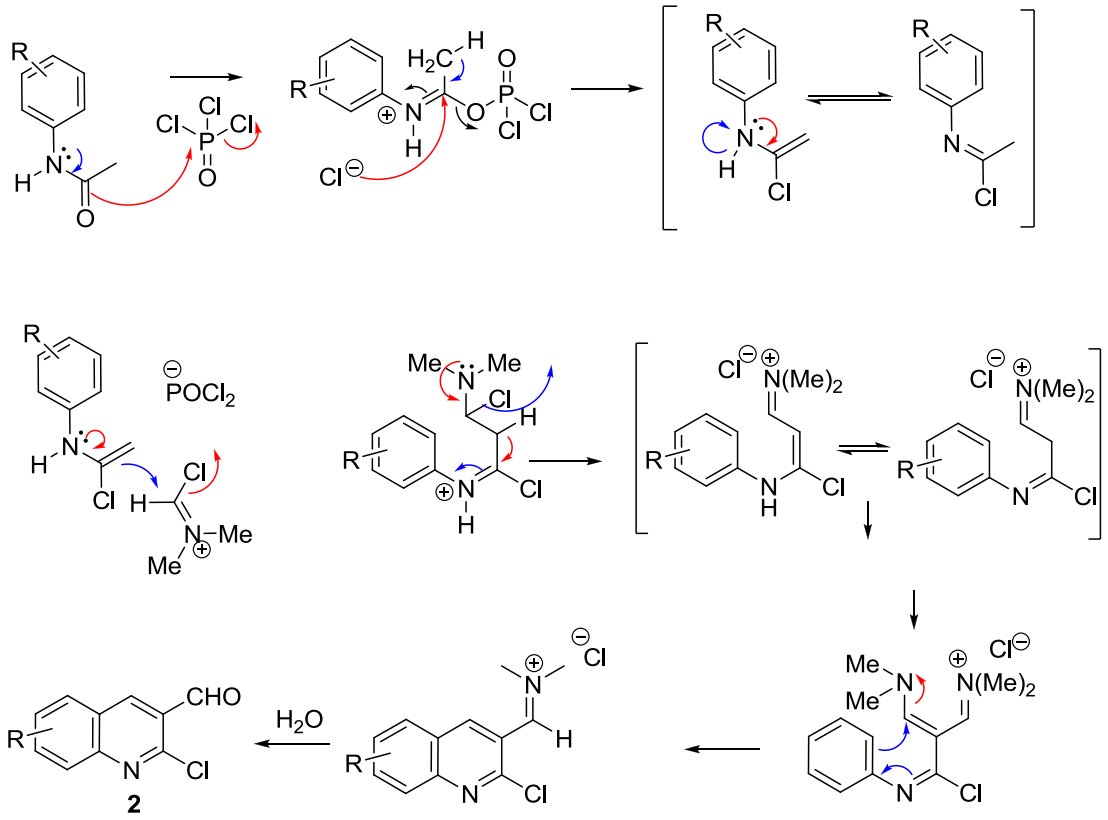

Scheme 83. Proposed mechanism of the formation of 2-chloro-3-formylquinoline derivatives

I.2 Synthesis of new hybrid quinoline-4H-pyran derivatives

The polyheterocycle functionalized 4*H*-pyran derivatives linked at position 4 to the 2-chloro-3-formyl-6-alkylquinoline (**7a-l)** were easily accessible according to the Elnagdi method [255]. The preparation of a diverse range of functionalized 2-amino-3-cyano-4*H*-pyrans and pyran-annulated heterocyclic scaffolds *via* one-pot reaction was achieved from the reaction of three components condensation quinoline aldehyde, malononitrile and a variety of activated methylenes or C−H-activated acids in ethanol using a base as a catalyst. Three series of new compounds were synthesized as shown in Scheme 84.

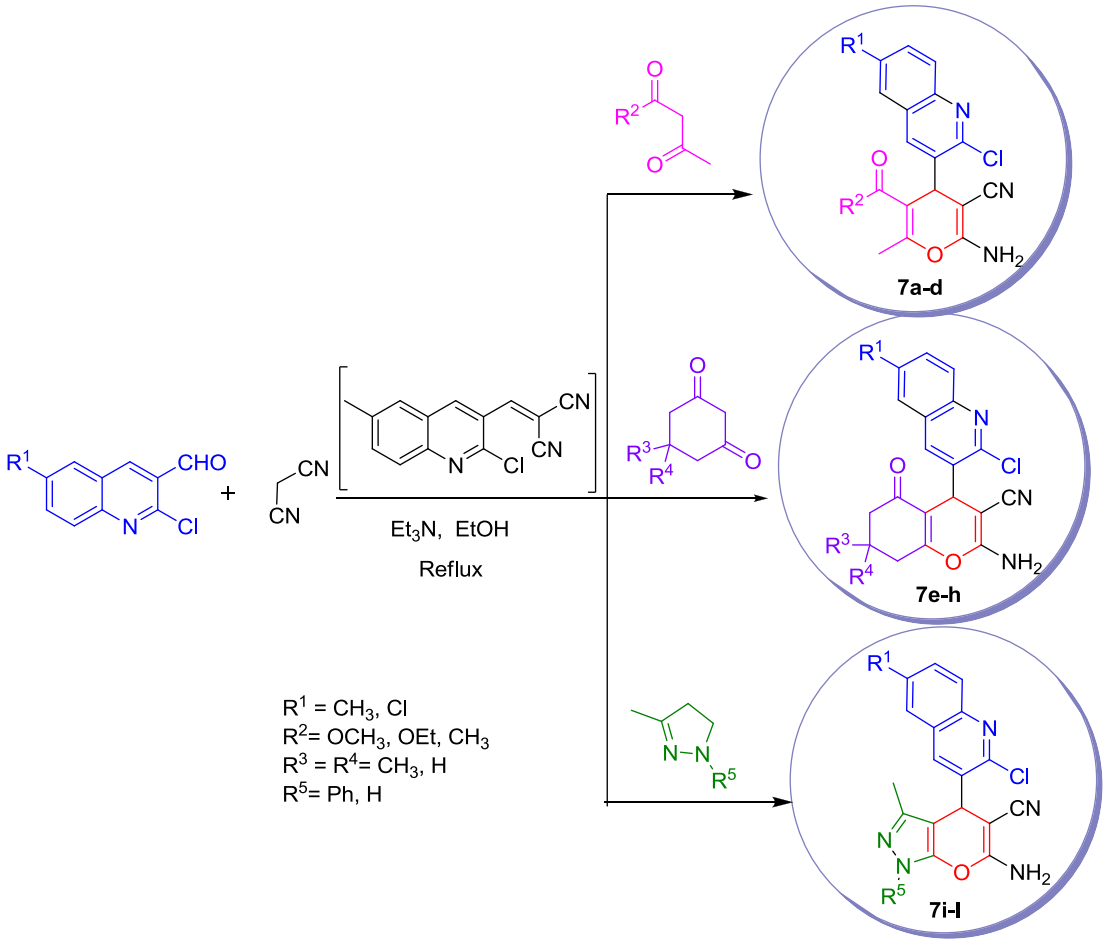

Scheme 84. General synthetic route for the preparation of 4*H*-pyran derivatives (**7a-l)**

I.2.1 Synthesis of new hybrid quinoline-2-amino-3-cyano-4*H*-pyrans (**7a-d)**

Initially, using the approach including one-pot three-component condensation of 2-chloro-3-formyl-6-alkylquinoline (**6a-b)** and malononitrile as model reactants, we attempted the reaction by coupling a linear activated C–H acids alkylacetoacetate compounds such as ethylacetoacetate, methylacetoacetate, and acetylacetone. Delightfully, in all cases, the corresponding functionalized 2-amino-3-cyano-4*H*-pyrans were formed in high to excellent yields within just one hour (Scheme 85).

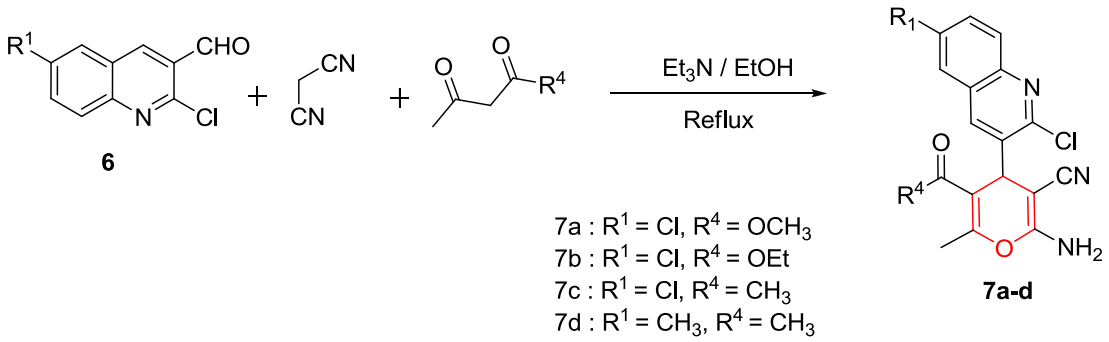

Scheme 85. Synthetic route for the preparation of 2-amino-3-cyano- 4*H*-pyrans-quinoline

During this experiment, it was observed that solid products precipitate out after the addition of cold water in the solution afforded the pale white crude product. After a simple work-up, the corresponding new products were isolated in good pure amounts, just by washing with aqueous ethanol followed by washing with ethylic ether, no tedious chromatographic purification was needed.

All the new 4*H*-pyran derivatives (**7a-d)** showed little solubility in most usual organic solvents, such as chloroform, dichloromethane, ethanol, and methanol, except dimethylsulfoxide which is the best solvent for these compounds. As well as the compounds are not soluble in non-polar solvents, such as pentane and hexane. The corresponding structures and physical data of the new compounds (**7a-d)** are given in Table 18.

Table 18. The structure and physical data of the new 4*H*-pyran derivatives (**7a-d)**

code	Products	Yield (%)	Melting points °C
7a	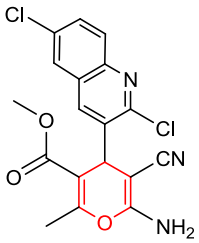	78	269-270
7b	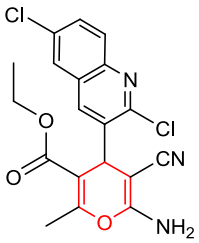	72	267-268
7c	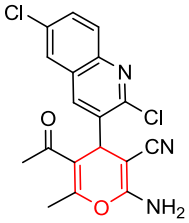	74	265-266
7d	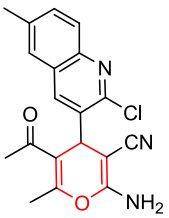	86	209-210

I.2.2 Synthesis of new hybrid quinoline-4*H*-benzo[b]pyran derivatives (**7e-h)**

Prompted by the latter successful results, we expand the series of synthesized compounds using a variety of enolizable C−H activated compounds such as carbonyl compounds possessing a reactive α-methylene group like 5,5-dimethylcyclohexane-1,3-dione and 1,3-cyclohexandione as a cyclic active partner in place of alkylacetoacetates to obtain a new type of compounds 4*H*-benzo[b]pyran (Tetrahydro-4*H*-chromenes). Following the same method as in the first attempt, entirely different

products, tetrahydro-4*H*-chromenes were obtained in high to excellent yields and in a very short reaction time (Scheme 86).

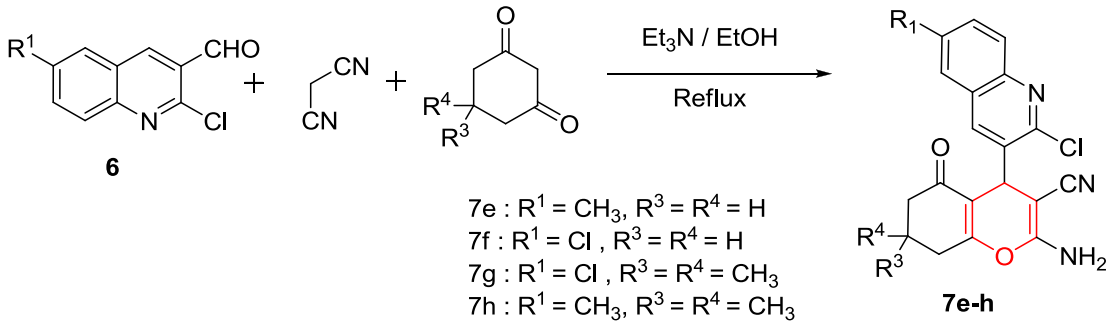

Scheme 86. Synthetic route for the synthesis of 4*H*-benzo[b]pyran-quinoline (**7e-h)**

The corresponding structures and physical data of the new 4*H*-benzo[b]pyran compounds (**7e-h)** are given in Table 19.

Table 19. The structure and physical data of the new 4*H*-benzo[b]pyran compounds (7e-h)

Code	Products	Yield (%)	Melting points °C
7e	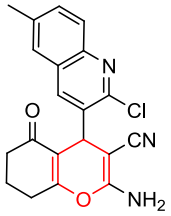	83	267-268
7f	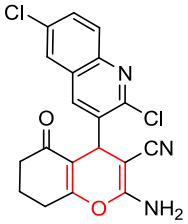	71	>280
7g	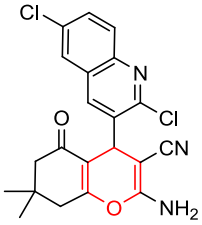	70	257-258
7h	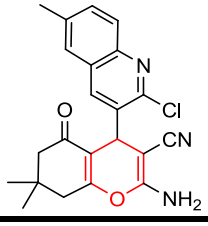	91	265-266

I.2.3 Synthesis of new hybrid quinoline-4*H*-pyrano-pyrazole, 4*H*-pyrano-isoxazole derivatives (**7i-l)**

Encouraged by these results, we attempted to extend the present protocol using pyrazolone derivatives such as 3-methyl-1*H*-pyrazole-5-one, 3-methyl-1-phenyl-2-pyrazole-5-one which is generated *in situ* by the reaction between hydrazine hydrate and ethylacetoacetate and ethyl-3-methyl-5-oxo-4,5-dihydro-1*H*-pyrazole-1-carboxylate to prepare the corresponding pyrano[2,3-c]pyrazole-quinoline derivatives (**7i-k)**, and 3-methylisoxazol-5(4*H*)-one which was generated *in situ* by reacting hydroxylamine and ethylacetoacetate to prepare the corresponding pyrano[3,2-d]isoxazole-5-carbonitrile (**7l)**. All products were obtained with good yields and relatively short reaction times (Scheme 87).

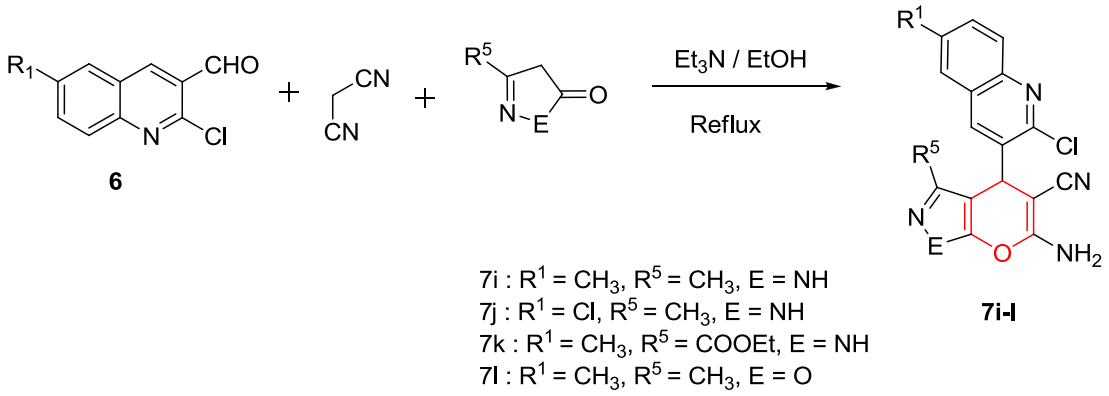

Scheme 87. Synthetic route for the preparation of pyrano[2,3-c]pyrazole-quinoline (**7h-l)**

The corresponding structures and physical data of 4*H*-pyrano-pyrazole derivatives (**7h-l)** are given in Table 20.

Table 20. The structures and physical data of 4*H*-pyrano-pyrazole, and 4*H*-pyrano- isoxazole derivatives (**7h-l)**

code	Products	Yield (%)	Melting points °C
7i	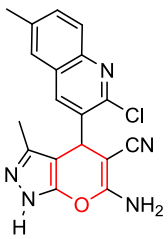	78	268-269

7j	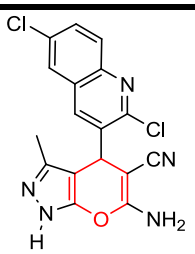	67	279-280
7k	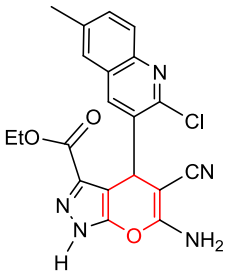	73	274-275
7l	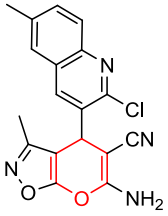	75	>290

The structures of the newly synthesized compounds were confirmed through spectroscopic techniques such as IR, ^{1}H NMR, ^{13}C NMR, mass spectroscopy, and elemental analysis.

The IR spectroscopy showed a peak for the carbonyl group (CO) between [1650-1680] cm^{-1} and a peak for N–H stretching amine between [3318-3461] cm^{-1}, also C-N had an absorption band at [1162-1181] cm^{-1}. Bands for the (CN) group appeared at [2185-2200] cm^{-1}, while a band corresponding to the C-O-C ether function was seen at [1028-1070] cm^{-1}. A specific band for C-Cl was also observed at [739-775] cm^{-1}.

Based on the ^{1}H NMR spectral analysis results, it appears that the majority of the new compounds (**7a-l)** do not exhibit significant changes in the chemical shifts of the aromatic protons in the quinolyl nucleus when compared to the starting compound, 2-Chloro-6-methyl-3-formylquinoline. It's worth noting that in all compounds, there is not only a similar trend observed but also indicated a disappearance of the aldehyde proton. The appearance of a singlet between [4.81-5.04] ppm, assigned to the H-4' proton of the pyranic ring, provided confirmation of the cyclization of the molecules.

A singlet signal appears between [7.03] ppm, which was attributed to the two NH_2 protons.

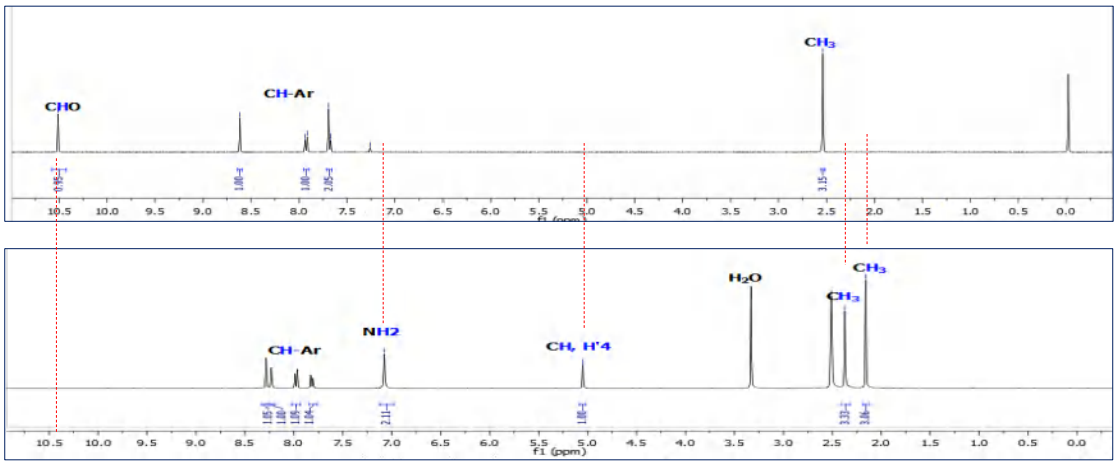

Spectrum 10. The ^{1}H NMR of the compound 7d compared with the starting material

Additionally, the ^{13}C NMR analysis also shows no significant changes in the chemical shifts of the carbons when compared to the starting compound. The signals of the aromatic carbons of the quinoline ring were detected at δ = [126.9-132.2] ppm. The most characteristic signal observed at [30.6- 36.6] ppm indicated methane carbon (C4) of all compounds which confirms the formation of a pyran ring. Signals at [189.2–198] ppm confirm the presence of carbonyl groups. These new compounds show typical spectroscopic signatures, and values are in agreement with reported data for similar 4-*H* pyran (see Experimental section for more details).

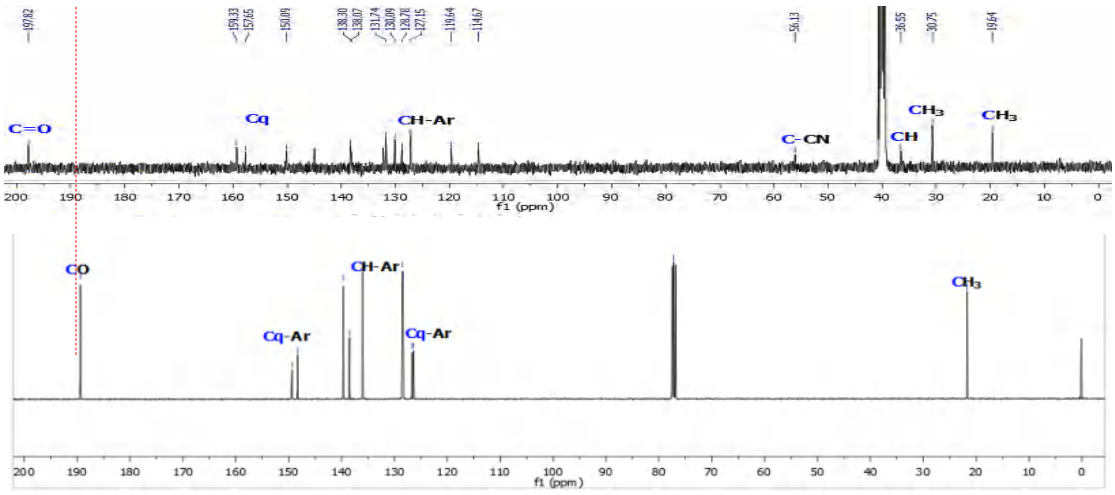

Spectrum 11. The ^{13}C NMR of the compound 7d compared with the starting material

The mass spectrum of compounds showed molecular ion peaks at m/z 390.0376, 404.0533, 374.0428, 354.0924, 418.0827, 386.0426, and 372.0388 for the compounds (**7a)**, (**7b)**,(**7c)**, (**7d)**, (**7f)**, (**7g)**, and (**7i**) respectively.

To conduct a more thorough analytical investigation of the new compounds, compound (**7b)** was selected as an exemplar.

The ^{1}HNMR spectrum of compound (**7b)** exhibited in addition to the expected signals which were observed, at [7.78 and 8.32] ppm. New peaks were observed in the spectral data, appearing as a broad singlet signal between 7.03 ppm, which were attributed to the two NH_2 protons. The appearance of a singlet signal at 4.98 ppm, is assigned to the H-4' proton of the pyranic ring. Two new signals at 3.90 ppm and 0.92 ppm, were assigned to the ethyl groups of the esters (OCH_2 and CH_3). Additionally, a singlet signal was observed at 2.40 ppm for the three protons of the methyl corresponding to the sp^3 hybridized methyl groups(CH_3) of the alkyl chain.

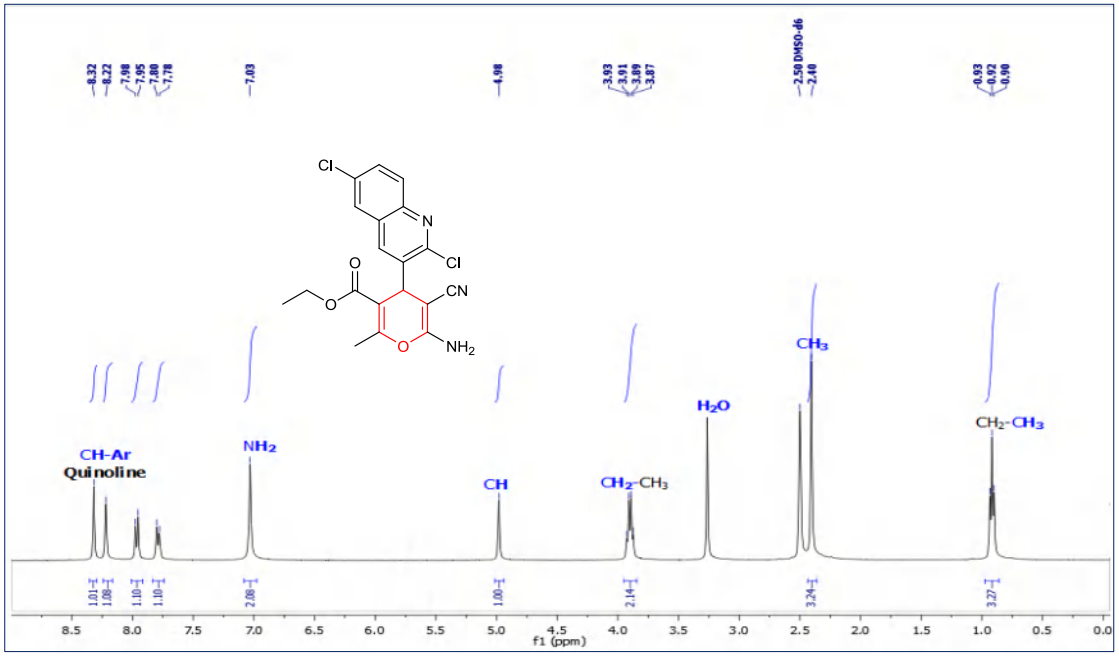

Spectrum 12. ^{1}HNMR spectrum (400 MHz, DMSO-*d6*) of the compound **(7b)**

The ^{13}CNMR spectrum of compound (**7b)** exhibited in addition to the expected signals of the aromatic carbons of the quinoline ring which were observed, at δ = [127.3-136.9]. Two new pics at 65.3 ppm and 14.1 ppm, were assigned to the ethyl groups of the esters (OCH_2 and CH_3) respectively. Additionally, a singlet signal was observed at 18.8 ppm for the carbon of the methyl corresponding methyl groups(CH_3) of the alkyl chain. The most characteristic signal observed at 36.6 ppm indicated methane carbon C4 of the pyranic ring. Signals at 186.7 ppm attributed to the carbonyl group.

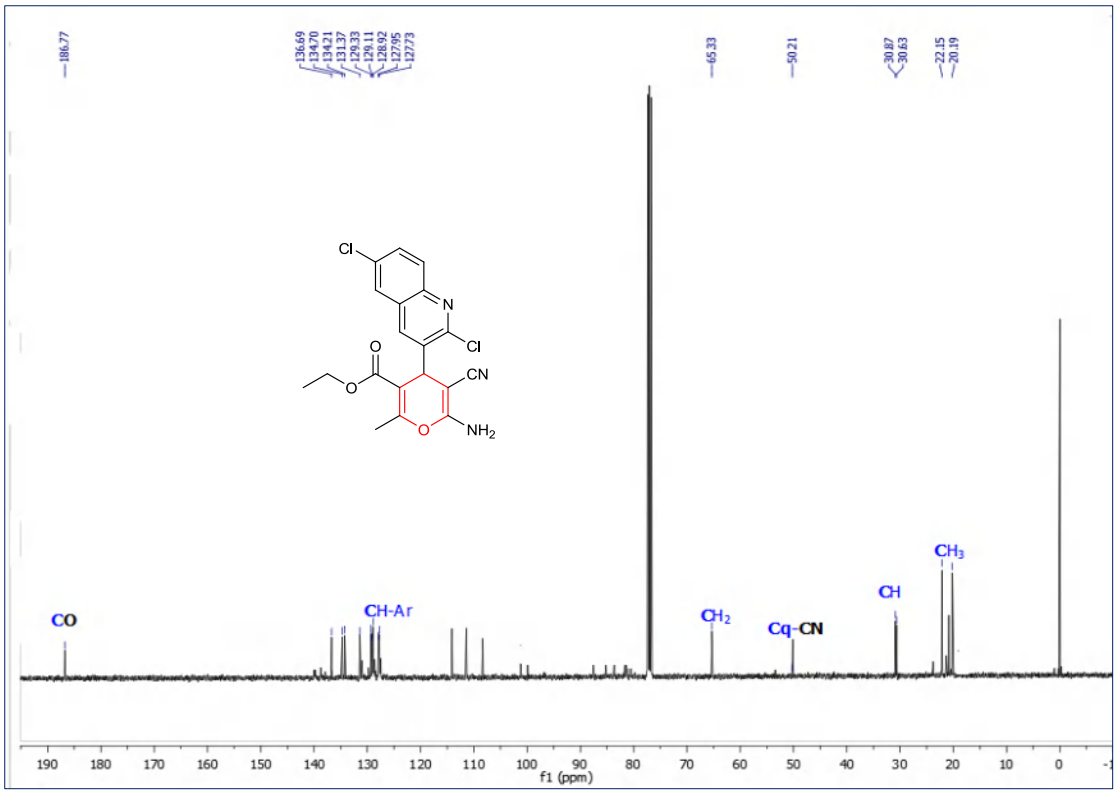

Spectrum 13. ^{13}HNMR spectrum (100 MHz, DMSO-d6) of the compound (**7b)**

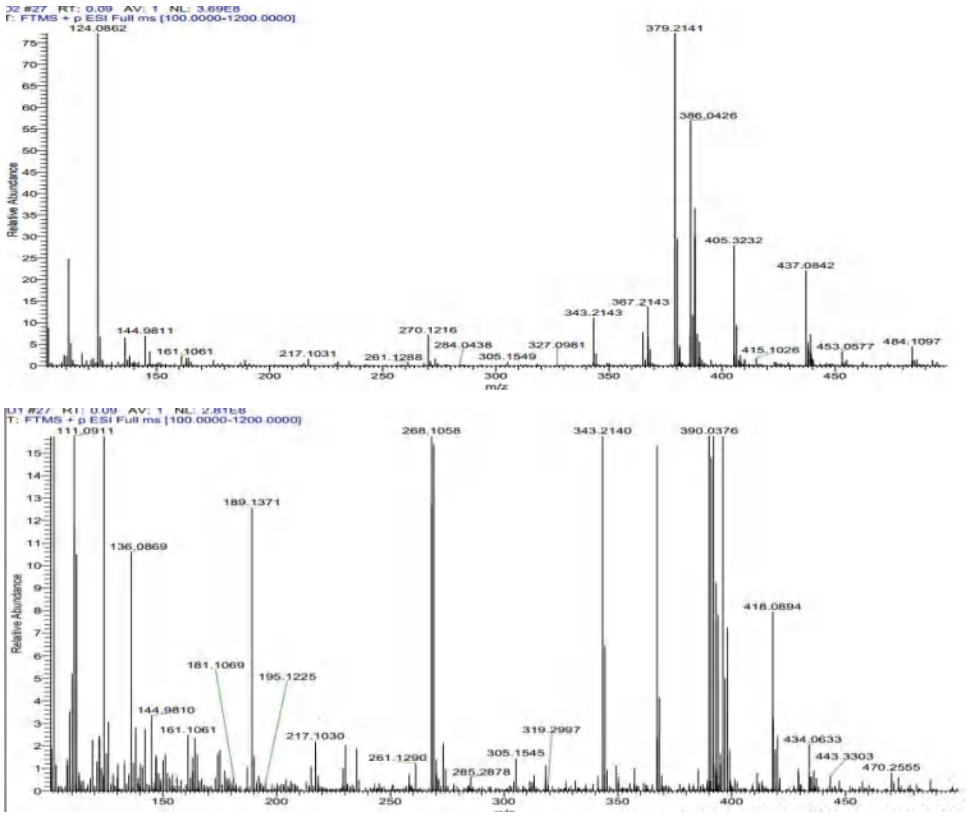

Spectrum 14. Mass spectroscopy of the compounds (**7f)** and (**7g)**

Suggested mechanism

The synthesis of quinoline-based 4*H*-pyran derivatives, tetrahydro-4*H*-chromenes derivatives, and pyrano-pyrazol derivatives has been demonstrated *via* the *one-pot* domino Knoevenagel–Michael cyclo-condensation reaction of quinoline aldehyde, malononitrile, and active methylene. The process involves the addition of malononitrile to the 2-chloro-3-formyl-6-alkylquinoline derivative (**6a-b)**, using triethylamine under Knoevenagel conditions. This results in the creation of an intermediate compound called (quinolylidene methylene malononitrile) (**6'**), which can be isolated. The latter leads, in the presence of α,β-dicarbonyl compound, and an amount catalytic base in ethanol, can undergo a 1,4-type addition reaction (known as a Michael reaction), followed by intramolecular cyclization. This leads to the formation of the 4*H*-pyran derivative through a succession of equilibria. The entire reaction takes place in an ethanol medium. We herein propose a mechanism in Scheme 80 for the formation of pyran-annulated heterocycles (Scheme 88).

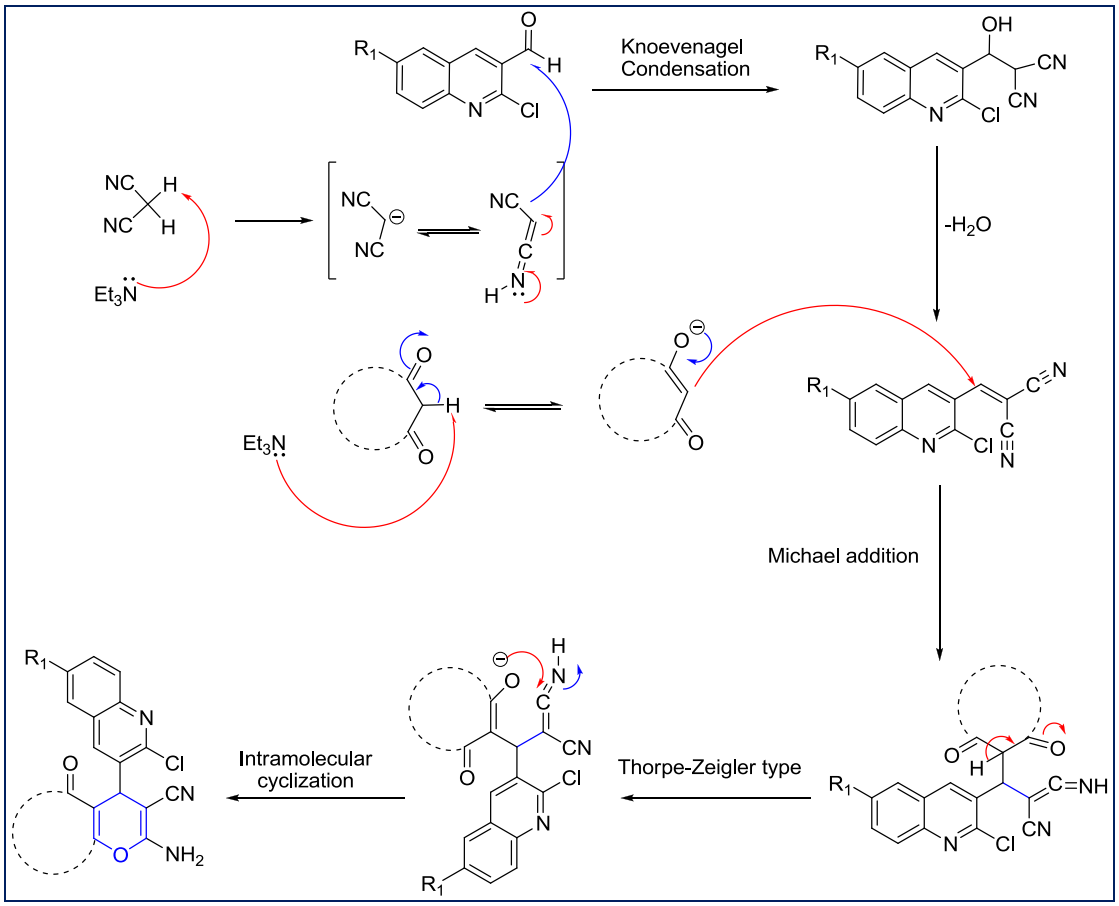

Scheme 88. A suggested mechanism for the reaction

I.3 Synthesis of new hybrid Quinoline-Tacrine derivatives 8a and 8b

One can observe that the 4*H*-pyran precursor derivative has the potential to be converted into a tacrine derivative. A comprehensive review of the literature reveals that derivatives of 4*H*-pyran, 1,4-dihydropyridine, or pyridine that possess a free amine group at position 2 and a nitrile group at position 3, are highly effective precursors in the synthesis of tacrine analogs. This is achieved by incorporating cycloalkanone under typical conditions of the Friedländer reaction [243] (Scheme 89).

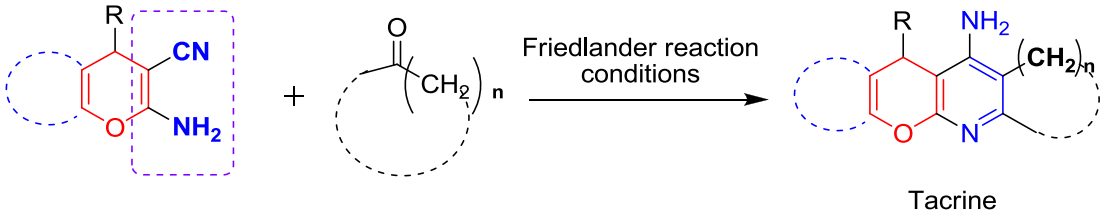

Scheme 89. Friedländer reaction

After the unambiguous characterization of the precursor product, 4*H*-pyran derivatives **7e** and **7h**, it was treated with cyclohexanone using standard Friedländer reaction conditions ($AlCl_3$, 1,2-dichloroethane, reflux). This method resulted in the formation of Tacrine analogs **8a** and **8b** with good yields. The yields of pure products were 69%, and 65% respectively. The reactions are depicted in scheme 90.

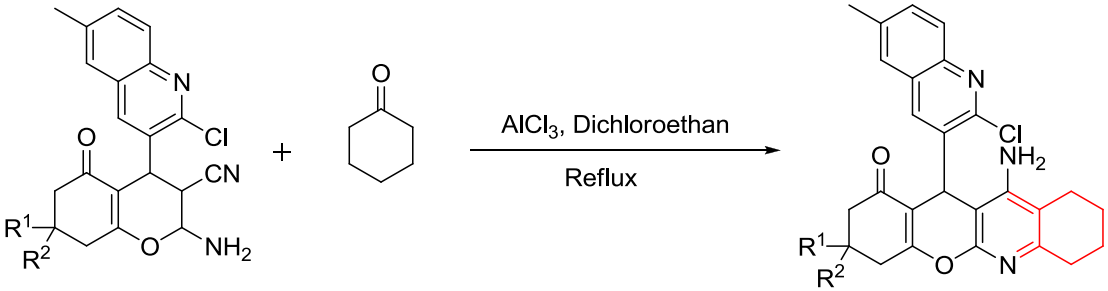

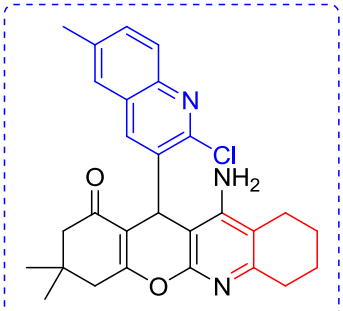

8a, 69%

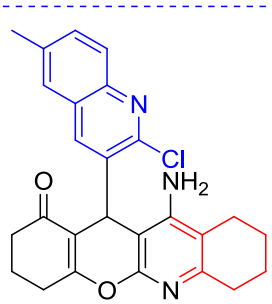

8b, 65%

Scheme 90. Synthetic route and structure of the newly prepared tacrine derivatives

The compounds prepared were characterized using standard spectroscopic methods such as ^{1}H NMR, ^{13}C NMR, and IR, and their structures were found to be consistent with the expected structures. The IR spectra of the Tacrine analogs showed an absorption band corresponding to the carbonyl group of the ester function (ν CO) at around 1628 cm^{-1}, and a band attributed to the amine function beyond 3362 cm^{-1}. No bands characteristic of the nitrile functional group were observed.

Most of the ^{1}H NMR spectral analysis results of these compounds exhibited a singlet signal at 5.32 ppm, which was attributed to the proton H-4 of 4*H*-pyran, along with a broad singlet signal between 4.47 and 4.49 ppm, which was attributed to the protons of the NH_2 group. The protons of the saturated rings were observed as multiplets in the expected range of 2.75 to 1.78 ppm. The NMR spectroscopy of carbon 13, detected a signal at approximately 196 and 191 ppm attributed to the carbonyl group. All new compounds gave analytical and spectroscopic data in good agreement with their structures (Experimental Part)

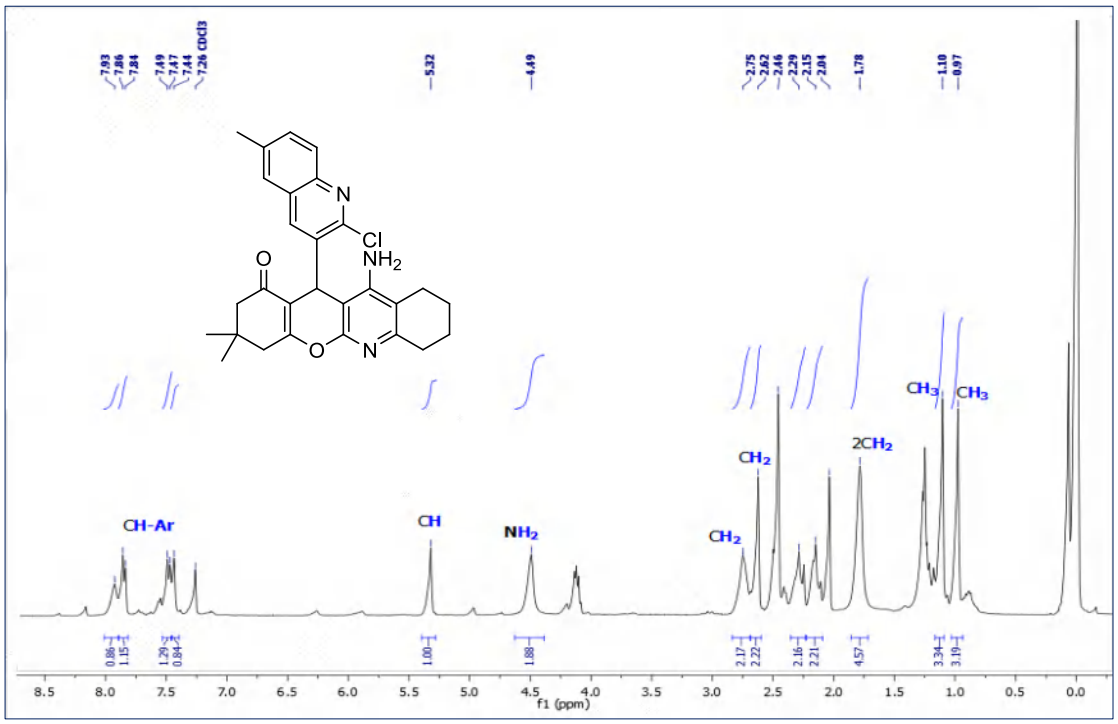

Spectrum 15. ^{1}H NMR spectrum (400 MHz, $CDCl_3$) of the compound **8a**

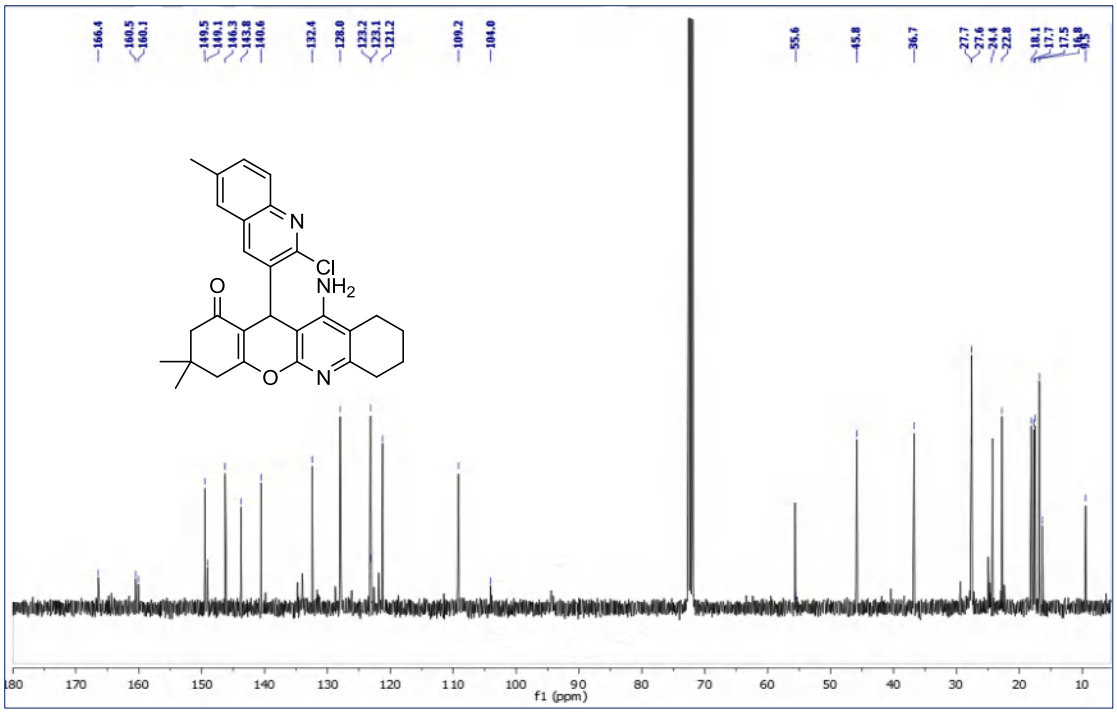

Spectrum 16. ^{13}C NMR spectrum (100 MHz, $CDCl_3$) of the compound 8a

The mass spectrum of compounds showed molecular ion peaks at m/z 474.1852 and 446.1544 for compounds **8a** and **8b** respectively.

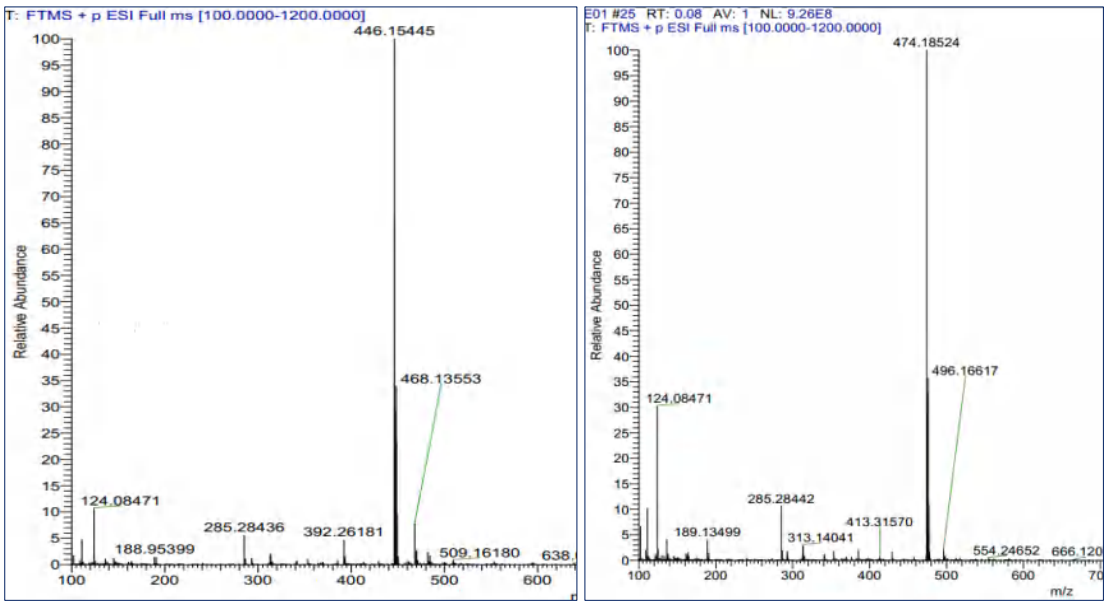

Spectrum 17. Mass spectroscopy of compounds **8a** and **8b**

I.4 Synthesis of new hybrid quinoline-N-substituted-1,4-dihydropyridines

1,4-dihydropyridine are generally synthesized by the classical Hantzsch reaction, which involves the condensation of an aldehyde with an active methylene carbonyl compound and ammonia (or a primary amine or ammonium acetate) in refluxing ethanol or other lower alcohols.

To examine the preparation of new hybrid quinoline-*N*-substituted-1.4-dihydropyridine derivatives, we followed published methods for the synthesis, of fused *N*-substituted-1,4-dihydropyridines by M, Hammouda et all.[256] and B V, Lichitsky, et al.[228] which generally allows restricted variation of substituents at the skeletal *N* atom. The approach involved the preparation of enaminoketones and then reacting them with arylidene derivatives of malononitrile in alcohol, with the addition of a small quantity of a base catalyst, as illustrated in Scheme 91.

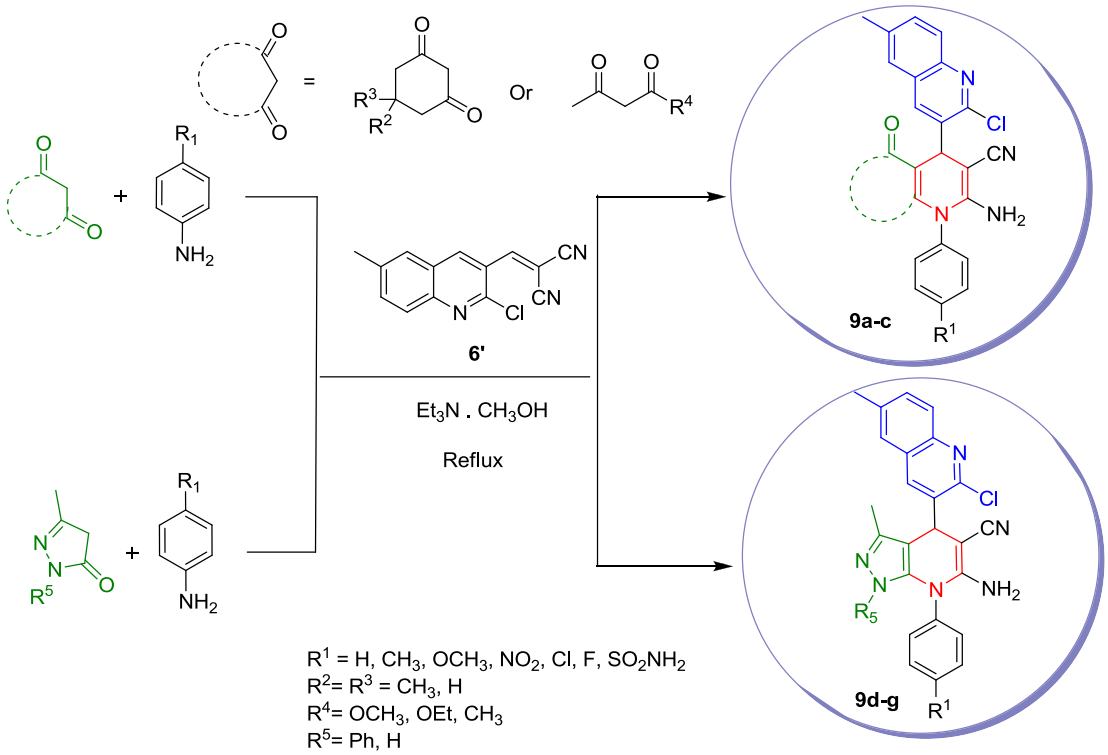

Scheme 91. General synthetic route for the synthesis of hybrid Quinoline- *N*-substituted-1,4-dihydropyridine

The preparation of compounds (**9a-g)** was accomplished by reacting the Knoevenagel isolated product (quinolylidene methylene malononitrile) (**6'**) with the aniline derivatives and a variety of activated methylenes in methanol under reflux. The Knoevenagel product was made by adding malononitrile to 2-Chloro-3-formyl-6-methylquinoline (**6a)**. The reaction between the enamine formed *in situ* and the

Knoevenagel product was catalyzed by triethylamine to form the hybrid quinoline-*N*-substituted-1,4-dihydropyridine compounds (**9a-g)** through a one-pot reaction.

I.4.1 Synthesis of new hybrid quinoline-*N*-aryl-1,4-dihydropyridine derivatives

As an initial attempt, we investigated the possibility of synthesizing hybrid quinoline-*N*-aryl-1,4-dihydropyridine derivatives from the condensation of cyclohexane-1,3-dione, with various aniline derivatives to prepare the cyclic en-aminoketone which react with our isolated intermediate (quinolylidene methylene malononitrile) (**6'**) to give the desired product (**9a-c)** (Scheme 92).

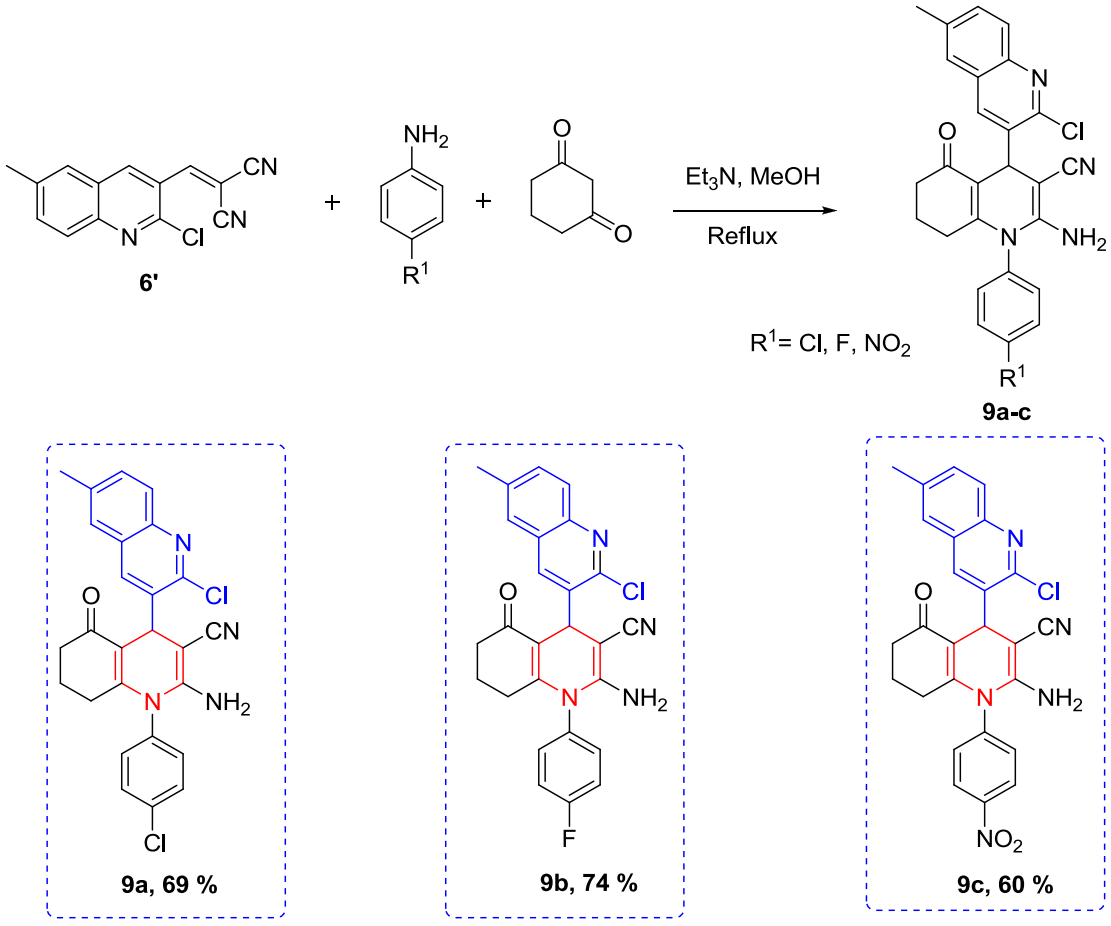

Scheme 92. Synthetic route for the preparation of 1,4-dihydropyridine derivatives (**9a-c)**

During the experiment, it was noticed that solid products formed when cold water was added to the solution, resulting in a pale crude product. The new products were isolated in good quantities by a simple work-up, where they were washed with cold ethylic ether. There was no need for time-consuming chromatographic purification. The new products which were obtained, showed little solubility in most organic solvents like chloroform, dichloromethane, ethanol, and methanol, except for

dimethylsulfoxide, which was found to be the best solvent for these compounds. Moreover, the compounds were not soluble in non-polar solvents such as pentane and hexane.

All products prepared in this way have been identified by the usual spectroscopic analysis including IR, ^{1}H NMR, ^{13}C NMR spectroscopy, mass spectroscopy, and elemental analysis.

The IR spectroscopy showed absorption bands around [1658,–1661] cm^{-1}, which indicates the presence of a carbonyl group (CO). A second band for N–H stretching in the range [3326-3461] cm^{-1}, corresponds to the presence of the amine function (NH2). Bands for the (CN) group appeared at [2185-2200] cm^{-1}, while a band corresponding to the C-O-C ether function was seen at [1028-1070] cm^{-1}. A specific band for C-Cl was also observed at [739-775] cm^{-1}.

The analysis of the spectroscopic results in high-field nuclear magnetic resonance (NMR of proton and carbon 13) shows that these results are in perfect agreement with the proposed structures. The main results of the spectral analysis of compound (**9a)** in ^{1}H NMR, using DMSO-d_6 (Spectrum 17), there was no significant change in the chemical shifts of the aromatic protons of the quinoline nucleus compared to those in the starting product (**6a)**, the characteristic signals for the aromatic protons appeared in the rage of δ = [8.21-7.56] ppm. While the aromatic protons of the aryl group are observed in the downfield region [8.19-7.06] ppm. The NH_2 protons had a broad singlet signal between 5.55 ppm. A singlet signal was observed at 5.09 ppm assigned to the proton H-4' of the pyranic ring which confirms the cyclization of our molecules. A singlet signal was observed at 2.50 ppm for the carbon of the methyl corresponding methyl groups (CH_3). The protons of the three CH_2 were observed as multiplets in the expected range of 2.40 to 1.75 ppm.

The ^{13}HNMR spectrum of compound (**9a)** exhibited a signal at 195.4 ppm confirming the presence of carbonyl groups. The signals of the aromatic carbons of the quinoline ring were detected at [δ =121.4-132.2] ppm. The most characteristic signal observed at 34.8 ppm indicated methane carbon C4 which confirms the formation of a pyran ring.. (see Experimental section for more details).

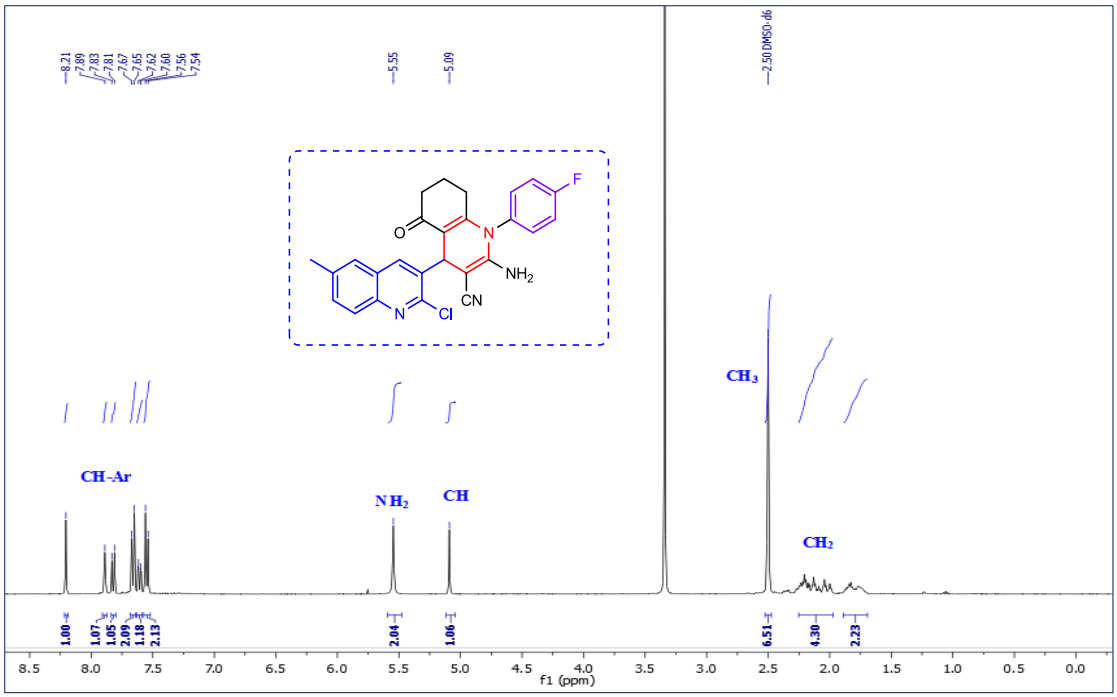

Spectrum 18. ^{1}H NMR spectrum (400 MHz, DMSO-*d6*) of the compound **9a**

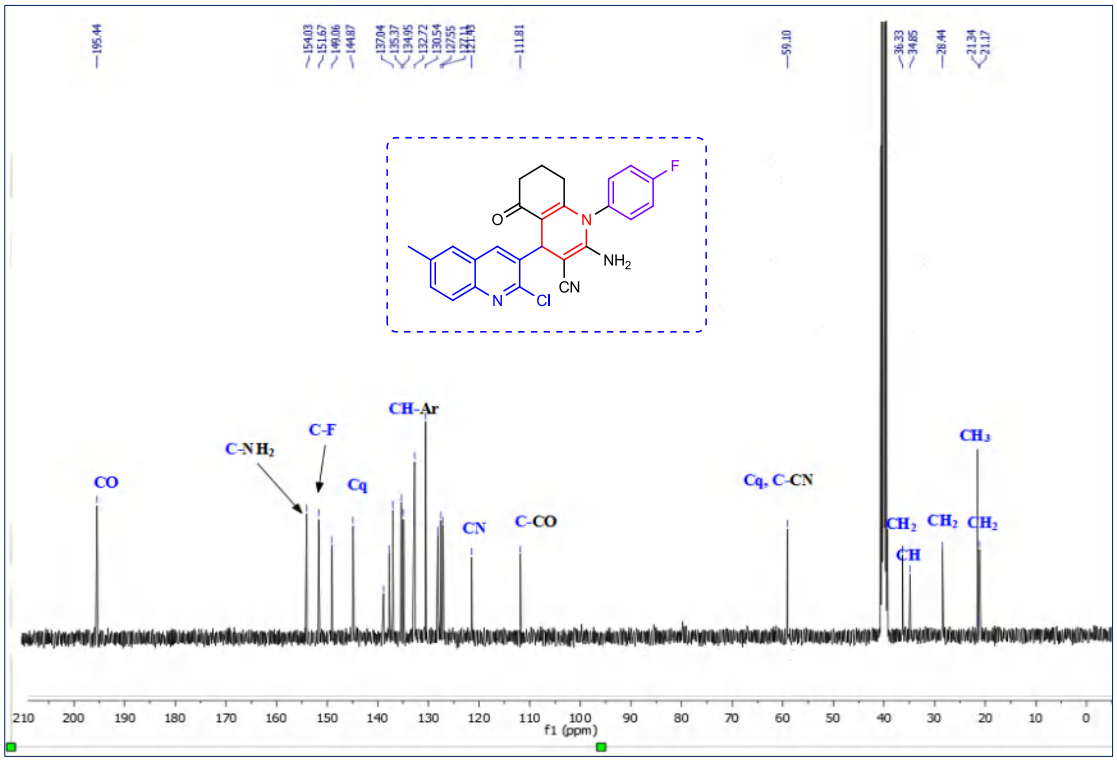

Spectrum 19. ^{13}C NMR spectrum (100 MHz, DMSO-*d6*) of the compound **(9a)**

Mass spectra of titled compounds showed expected molecular ion peak corresponding with proposed molecular mass MS, m/z (%): 459.1299, 475.1022, and 486.1243 for the compounds (**9a-c)** respectively.

I.4.2 Preparation of new hybrid quinoline-*N*-sulfanilamide-1,4-dihydropyridine derivatives (**9d-g)**

To prepare a new series of desired hybrid molecules based on 1,4-dihydropyridine derivatives as the main skeleton, we performed a series of reactions using specific aniline derivatives such as sulfanilamide which has been selected as the most suitable reagents for introducing the NH_2-Ph-SO_2-NH_2 motif. Consequently, we will discuss the significance of certain polycyclic molecules, which include one or more heterocycles, particularly those containing sulfanilamide structures.

In this context, the preparation of hybrids quinoline-*N*-sulfanilamide-1,4-dihydropyridine using the same approach with three components. The synthetic approach was adopted to obtain the target compounds' highly functionalized quinoline-1,4-dihydropyridine associated with the sulfanilamide group. The incorporation of a specific pattern into heterocyclic scaffolds can create fascinating chemical and/or pharmacological features.

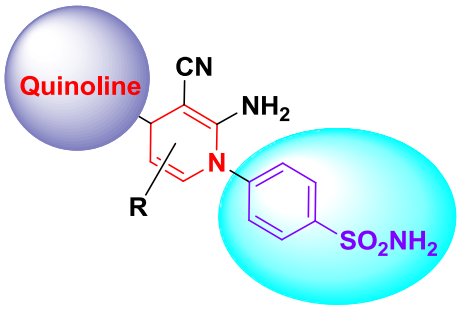

Figure 88. Hybrid quinoline-*N*-sulfanilamide-1,4-dihydropyridine

The initial trial experiment involved combining enolizable C−H activated compounds like carbonyl compounds possessing a reactive α-methylene group (5,5-dimethylcyclohexane-1,3-dione and 1,3-cyclohexandione derivative) with sulfanilamide to generate *in situ* a new cyclic enaminoketone. The reaction was carried out while preserving the same Knoevenagel product (6’), resulting in the creation of new quinoline-1,4-dihydropyridine compounds bearing a sulfonamide (Scheme 93).

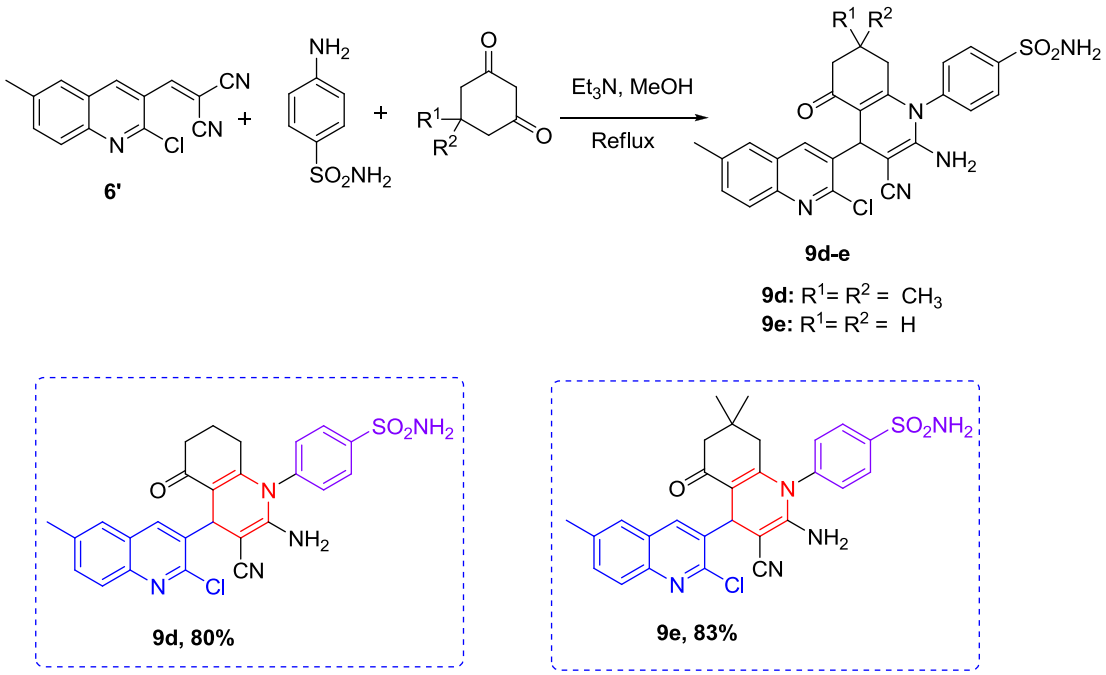

Scheme 93. The synthetic route, and prepared N-sulfanilamide-1,4-dihydropyridine derivatives (**9d-e)**

The new products were isolated in good quantities by a simple work-up, following the same procedure used in the first part. The structures were identified by the usual spectroscopic analysis including IR, ^{1}H NMR, ^{13}C NMR spectroscopy, mass spectroscopy, and elemental analysis.

The IR spectroscopy showed absorption bands around 1661, and 1645 cm^{-1} respectively, which indicates the presence of a carbonyl group (CO). A second band for N–H stretching at 3333, and 3308 cm^{-1} respectively, corresponds to the presence of the amine function (NH_2). Other specific bands for the (CN) group appeared at 1168, and 1189 cm^{-1} respectively for the two compounds (**9d)**, and (**9e)**.

In ^{1}H NMR, DMSO-d_6 (Spectrum 09), the chemical shifts of the aromatic protons of the quinoline nucleus appeared in the range of δ = [8.23-7.61]. The NH_2 protons had a broad singlet signal at 5.67 and 5.60 ppm. A singlet signal was observed at 5.11, and 5.11 ppm assigned to the proton H-4' of the pyranic ring which confirms the cyclization of our molecules. while the aromatic protons of the sulfanilamide group are observed in the region [7.84-7.73] ppm.

Analysis of the ^{13}C NMR spectrum of compound (**9e)** shows the presence of aromatic carbons signals of the quinoline ring which were detected at [δ =121.3-133.0]. The most characteristic positive signal observed at 34.7, and 35.3 ppm indicated

methane carbon C4 which confirms the formation of a pyran ring. Signals at 195.2, and 195.4 ppm attributed to the carbonyl group. (see Experimental for more details).

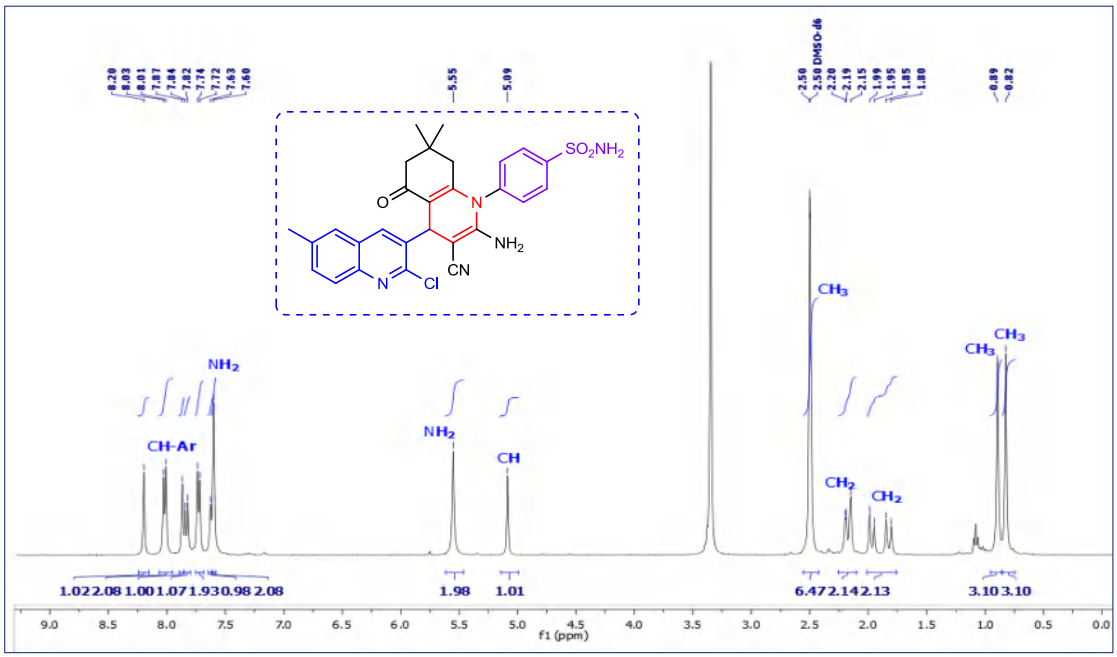

Spectrum 20. ^{1}H NMR spectrum (400 MHz, DMSO-*d6*) of the compound (**9e)**

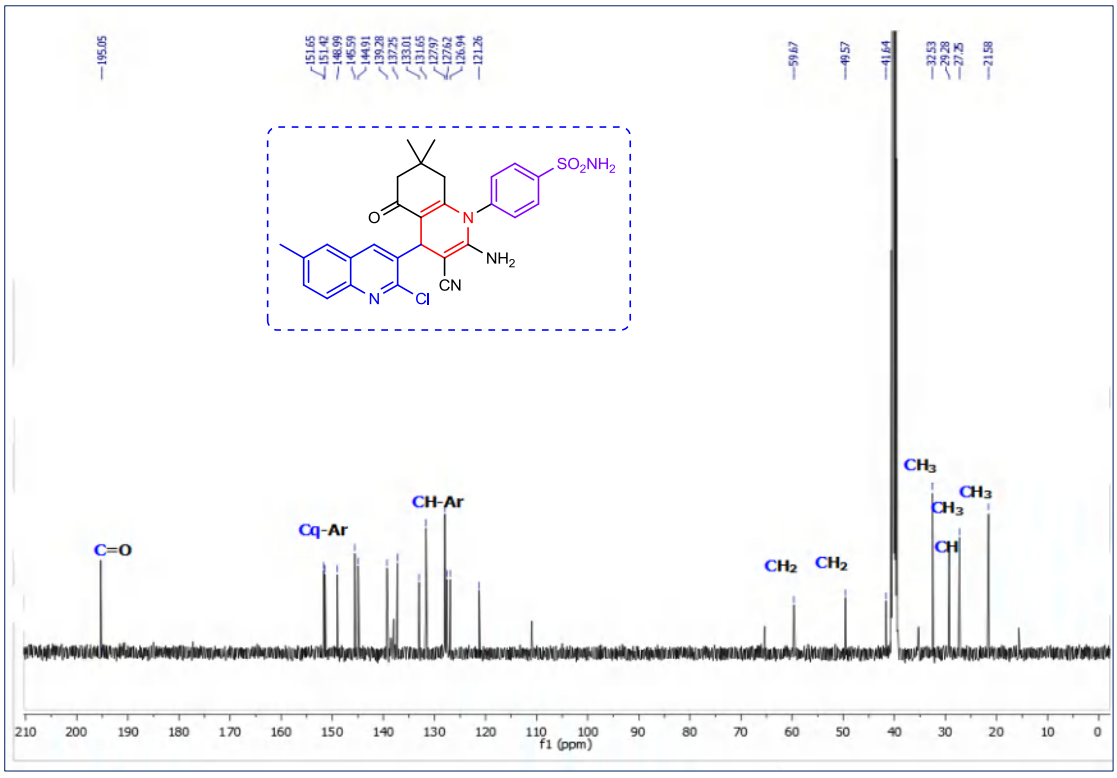

Spectrum 21. ^{13}C NMR spectrum (100 MHz, DMSO-*d6*) of the compound (**9e)**

Mass spectra of title compounds showed expected molecular ion peak corresponding with proposed molecular mass MS, m/z (%): 520,1110, and 548.0242 for the compounds **(9d-e)** respectively

To examine the versatility and extent of this domino reaction, alternative substituted linear 1,3-dicarbonyl compounds such as ethyl acetoacetate, methyl acetoacetate, and acetylacetone were used instead of cyclohexanedione derivatives. Unfortunately, no expected products were observed. As well as the results were unsatisfactory when we use these types of compounds that confirm that this reaction does not apply to the linear 1,3-dicarbonyl under these conditions (Scheme 94).

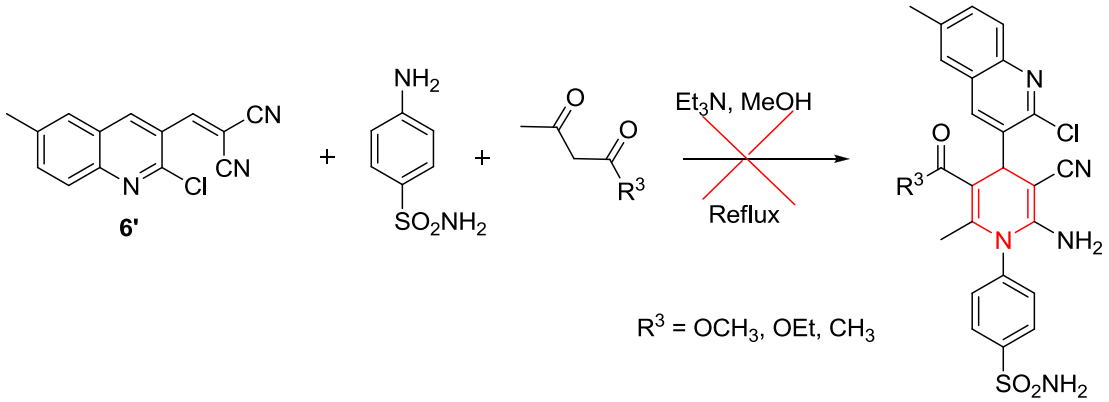

Scheme 94. Failed synthetic route for the preparation of N-sulfanilamide-1,4-dihydropyridine

The last attempt to create the new quinoline-*N*-sulfanilamide-1,4-dihydropyridine compounds was done by keeping the Knoevenagel product constant and experimenting with a new cyclic en-aminoketone using pyrazolone derivatives such as 3-methyl-1*H*-pyrazole-5-one, or 3-methyl-1-phenyl-2-pyrazole-5-one and sulfanilamide group (Scheme 95).

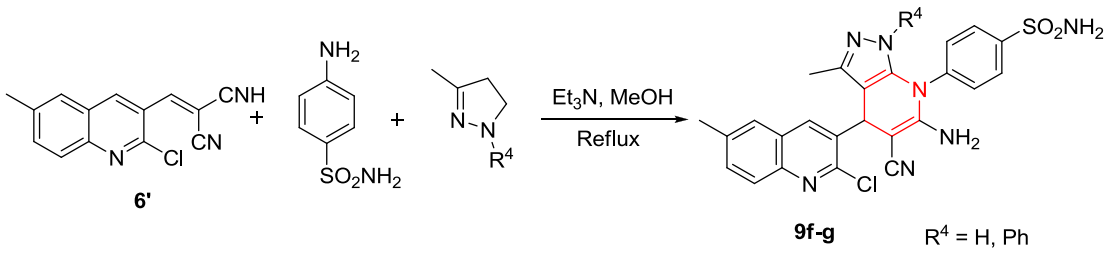

Scheme 95. The synthetic route for the preparation of *N*-sulfanilamide-1,4-dihydropyridine derivatives (**9f-g**)

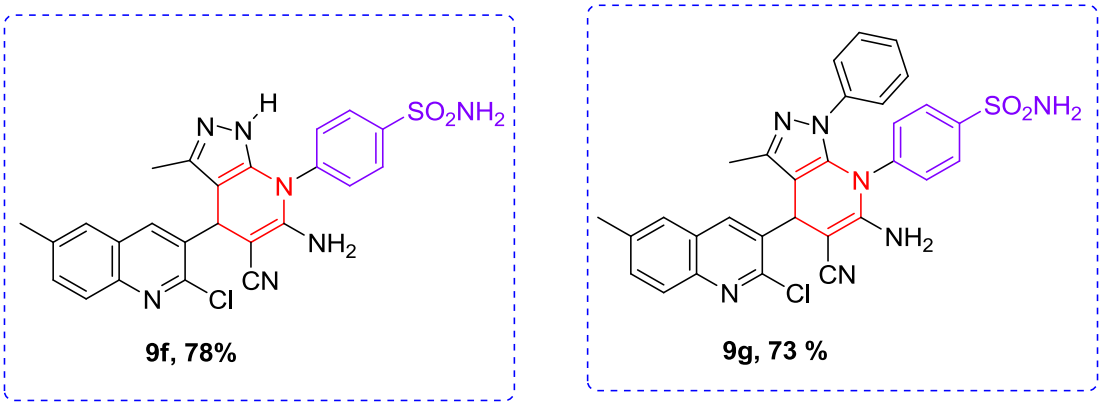

Figure 89. Prepared *N*-sulfanilamide-1,4-dihydropyridine derivatives (**9f-g)**

The new products were isolated in good quantities by a simple work-up, following the same procedure used in the first part. The structures were identified by the usual spectroscopic analysis including IR, ^{1}H NMR, ^{13}C NMR spectroscopy, and elemental analysis.

The structural elucidation of the synthesized compounds (**9f)** and **(9g)** was carried out by FT-IR, ^{1}H NMR, ^{13}C NMR, elemental analysis, and mass spectrometry. IR spectroscopy, the carbonyl group (C=O) had a band at 1656 and 1646 cm^{-1} respectively. N-H bond of amine was observed at 3330 and 3252 cm^{-1} respectively. C-N exhibited an absorption band between 1183-1200 cm^{-1} for the (CN) group.

In the ^{1}H NMR, in addition to previously described characteristic signals of aromatic hydrogens of the quinoline ring. The most characteristic signal peak observed of the proton in C4 (H4) appeared at 5.17, and 5.25 ppm which confirms the formation of a pyridine ring. A signal around 5.55 ppm is assigned to the protons of the amine group. A new signal observed assigned to the two protons of the second amine for the sulfanilamide group appeared at 7.07 and 7.16 ppm. The most characteristic signal observed at 12.18 ppm indicated the proton NH of the pyrazole ring of the compound (**9f)**, while in the spectrum of the compound (**9g)**, we notice that it does not appear in this pic. The signal at 1.76 ppm corresponds to three protons of CH_3 attached to the pyrazole ring for the two compounds (**9f)** and (**9g)**.

In ^{13}C NMR spectra, the signal at 110.9 and 112.60 ppm is assigned to the carbon of carbonitrile. A signal at 151.6 and 153.6 ppm is assigned to the carbon attached to the amine group. The most characteristic signal observed between 34.7 and

35.2 ppm was indicated methane carbon (C4) which confirms the formation of a pyridine ring.

The mass spectrum of compounds showed molecular ion peaks at m/z 506.0865 and 582.2630 for the compounds (**9f)** and (**9g)** respectively.

The obtained elemental analysis values are in consonance with theoretical data. (for details see the experimental part).

I.5 Biological evaluation Structure-activity relationship

An antioxidant is usually defined as a molecule that slows down, prevents, or removes oxidative damage to another molecule is generally referred as an antioxidant [257] Antioxidants counteract oxidative stress by blocking free radicals. An excess of free radicals results in an imbalance between oxidants and antioxidants in the body, leading to oxidative stress, which has been suggested as the underlying cause of aging and various diseases such as cancer, diabetes, stroke, atherosclerosis, and neurodegenerative diseases. The objective of this part is to make a critical study of the various methods of evaluation of the antioxidant activity, and the enzymatic capacity of our new compounds.

I.5.1 In vitro antioxidant activity measurement

To evaluate the antioxidant activities of some of the new hybrid quinoline-4*H*-Pyran compounds several techniques were used and the antioxidant activity was measured in vitro using four complementary tests, **ABTS** free radical scavenging, **Phenolthroline** assay, Cupric-reducing antioxidant capacity (**CUPRAC**) assay, and Galvinoxyl Radical (**GOR**) scavenging. All measurements were taken using a 96-well microplate spectrophotometer and were done in triplicate, with the average value being recorded. Therefore, an approach with multiple assays for evaluating the antioxidant potential of extracts would be more informative and even necessary.

I.5.1.1 ABTS Scavenging assay

According to the antioxidant activities data presented in Table 21, the results for radical scavenging activity were shown in Column 1. A remarkable activity was observed in the $ABTS^{\cdot+}$ assay, for which the best results were obtained with the new compounds. Radical scavenging activity for ABTS ranged from 81.2 to 192.9 μM)). Of the fractions tested (**7j**, **7a**, and **7b**) had the highest ABTS activity, with **7j** showing the greatest radical scavenging activity at (IC_{50}: 81.2 ± 4.72 μM). Conversely, **7g** had the lowest radical scavenging activity among all the samples at (IC50: 192.9 ± 9.8 μM). The $ABTS^{+}$ scavenging abilities of the different extracts were in the following order: BHA > BHT > **7j** > **7a** > **7b** > **7c** > **7f** > **7g**. The result obtained from studying the highest concentration (IC_{50}: 81.2 ± 4.72 μM) showed an excellent high capacity to scavenge the radical $ABTS^{+}$.

I.5.1.2 CUPRAC assay

The CUPRAC assay as a new technique for evaluating antioxidant capacity in vitro was introduced by Phatak and Hendre. The assay was found to be more reliable than other methods such as DPPH and ABTS because the CUPRAC reagent is more stable. The reducing power of a compound is an important factor in its antioxidant abilities, as antioxidants work by breaking free radical chains by donating a hydrogen atom. The assay measures absorbance at 450 nm through the formation of a stable complex between neocuproine and copper (I). In the presence of antioxidant molecules, copper (II) is reduced to copper (I).

The results of using the CUPRAC assay are presented in Column 2 of Table 21, which showed that extracts **7f** and **7g** had the highest reducing power activity, followed by **7c** and **7j**. No reducing power activity was seen in extracts **7a** and **7b**.

I.5.1.3 Galvinoxyl Radical (GOR) scavenging assay

Another approach is the use of the Galvinoxyl free radical scavenging assay. Table 21 showed that the new 4*H*-pyran had the weakest *antioxidant* inhibitory effectiveness with (A0.50 > 400 μM) for the compounds (**7c**, **7f**, **7g**, and **7j**) and no inhibition for the two compounds (**7a)** and (**7b)**.

I.5.1.4 O-Phenanthroline assay

Our research shows also the evaluation of antioxidant activities using *O*-Phenanthroline Activity.

Table 21 shows the ability of 4H-pyran to decrease the Fe3+ ion using the o-phenanthroline method. Similarly, all compounds also exhibited the weakest chelating activity (A0.50 > 200 µM).

Table 21. *Antioxidant* activity of 4H-pyran-quinoline compounds

Compound	ABTS assay IC_{50} ± SD (μM)[a]	CUPRAC assay A0.50 ± SD (µM)[a]	Phenolthroline assay A0.50 ± SD (µM)[a]	Galvinoxyl Radical (GOR) scavenging assay IC_{50} ± SD (µM)[a]
7a	129.5 ± 8,93	**NA**	> 200	**NA**
7b	122.8 ± 7,62	**NA**	> 200	**NA**
7c	169.4 ± 14,25	> 400	> 200	> 800
7f	174.0 ± 3,99	> 200	> 200	> 800
7g	192.9 ± 9,18	> 200	> 200	> 800
7j	81.2 ± 4,72	> 400	> 200	> 400
BHA[b]	1.29±0.30	11.75±0.95	7.32±0.83	21.5±1.67
BHT[b]	1.81±0.10	10.52±0.75	190.32±0.53	30.38±2.04

a*: Values expressed are means±S.D. of three parallel measurements.* ***b:*** *Reference compounds.*
NA*: Not Absorbance*

The results in Table 19 show the antioxidant activity of the new compounds of 4H-Pyran, compared with BHA and BHT. The tests were performed at 100, 200, 400, and 800 µg/mL concentrations. Results were found to be statistically significant when compared with the control. It appears that the values obtained from antioxidant activities are not of the same order of magnitude; the ABTS method gives the highest antioxidant activity followed by the CUPRAC and the Phenolthroline methods. Moreover, the new compounds have low antioxidant activity with Galvinoxyl Radical (GOR) method.

I.5.2 In vitro Cholinesterase Inhibitory Activity evaluation

In order to continue the study of the anticholinesterase potential of the new compounds for potential use in treating Alzheimer's disease, the efficacy of each compound in inhibiting enzyme activity was evaluated. The activity of acetylcholinesterase (*AChE*) and butyrylcholinesterase (*BChE*) was examined using a spectrophotometric method as described by Ellman et al [154]. Galanthamine was used as a reference compound for comparison. The effectiveness of the new compounds was determined by comparing their reaction rates to a blank sample and expressed as the concentration of 50% inhibition (IC_{50}). Lower IC_{50} values indicate higher inhibition activity, and the results are summarized in Table 22.

Table 22*: *Anti-Cholinesterase activity of 4H-pyran-quinoline compounds

Compound	*AChE*	*BChE*
	IC_{50}±SD (μM)[a]	**IC_{50} ± SD (μM)[a]**
7a	11.86 ± 0.41	NA
7b	30.45 ± 0.93	25.00 ± 0.83
7c	118.24 ± 0.95	13.61 ± 0.23
7f	99.67 ± 4.36	1.92 ± 0.09
7g	29.34 ± 1.20	0.78 ± 0.04
7j	82.33 ± 5.04	NA
Galanamine[b]	4.14± 0.07	20.38±2.10

a: *IC_{50} values represent the means ± SD of three parallel measurements ($p < 0.05$).* ***b:*** *Reference compound.*

The results from Table 22 indicate that the new 4*H*-pyran compounds were highly effective in inhibiting the *BChE* enzyme, outperforming Galantamine. When comparing their inhibition of *AChE* to Galanamine, the new compounds showed close percentages of inhibition. The IC_{50} values showed that the new compounds were effective against both acetylcholinesterase and butyrylcholinesterase. Among the new compounds, compound (**7a)** was the most effective against *AChE* with an (IC_{50}: 11.86 ± 0.41 μM**)**, but had no impact on *BChE*. Compounds (**7b)**, (**7c)**, (**7f)**, and (**7g)** showed good inhibition of *BChE* compared to Galantamine's (IC_{50}: 20.38 ± 2.10 μM). It should be noted that both compounds (**7a)** and (**7j)** had the strongest effect on *AChE* but had no effect on *BChE*. In terms of anti-*BChE* activity, the new compounds were more efficient than the anti-*AChE* activity. Additionally, the new compounds were found to be more potent than the standard drug Galantamine against *BChE*.

I.6 Conclusion

In this part, three new series of polyfunctionalized hybrid heterocyclic compounds were prepared *via* a one-pot reaction using 2-chloro-3-formyl-6-alkyl-quinoline as a bioactive starting material, which coupled with different bioactive molecules such as pyran, tacrine, pyridine, and sulfanilamide. The new compounds were successfully characterized via spectroscopic analytical methods. Selected compounds from the first series of 4*H*-pyran were evaluated *in vitro* for their *antioxidant and anti-cholinesterase* activities in search of potent inhibitor compounds.

The results indicated that the majority of compounds displayed moderate levels of antioxidant activity. Furthermore, when assessing their potential to inhibit the enzymes *AChE* and *BChE,* the results were particularly encouraging as they demonstrated promising outcomes in comparison to the reference standard control drug.

The other new polycyclic compounds prepared quinoline-*N*-substituted-1,4-dihydropyridine derivatives will be subjected to an in-depth study of their biological activity as well as a study to determine the structure-activity relationship.

III. Experimental Study

I.1 Preparation of 2-Chloroquinolin-3-carbaldehyde as starting material

A two-necked round bottom flask with a 250 mL capacity, equipped with a thermometer and a mechanical stirrer, was cooled to 0°C. Anhydrous *N*, *N*-dimethylformamide (DMF) (135 mmol, 2.5 eq.) was added. Then, phosphorus oxychloride ($POCl_3$) (378 mmol, 34.8 mL, 7.0 eq.) was slowly added dropwise to the mixture, stirring constantly, while keeping the temperature between 0-10°C. After the addition was complete, the mixture was left at room temperature for 30 minutes. The corresponding acetanilide (54 mmol, 1.0 eq.) was then added, and the mixture was refluxed for 3 to 4 hours at 75°C, monitored by TLC. Once the reaction is complete, the mixture was cooled to room temperature and slowly poured into crushed ice/water (200 mL), and left to stir for 30 minutes at a temperature between 0-10°C. The precipitate that formed was filtered and washed several times with water, then recrystallized from ethyl acetate to produce a light yellow compound (chloroquinoline carbaldehydes).

I.1.1 2-chloro-6-methylquinoline-3-carbaldehyde (**6a)**

Following the general procedure, the desired product (**6a)** was obtained

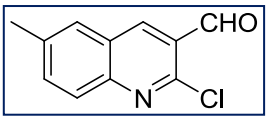

- ✓ ***Chemical Formula:*** $C_{11}H_8ClNO$
- ✓ ***Molecular Weight:*** 205.64 g/mol
  - ✓ ***Yield****:* 66 %, (7.3 g); Yellow-solid
  - ✓ ***m.p****:* 125-126 °C **(lit.)** [258]

I.1.2 2,6-dichloroquinoline-3-carbaldehyde (**6b)**

Following the general procedure, the desired product (**6b)** was obtained

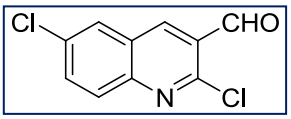

- ✓ ***Chemical Formula:*** $C_{10}H_5Cl_2NO$
- ✓ ***Molecular Weight:*** 226.06 g/mol
  - ✓ ***Yield****:* 58 %, (7.15 mg); Yellow-solid
  - ✓ ***m.p****:* 148-150 °C **(lit.)** [258]

I.2 Synthesis of hybrid quinoline-heterocycle derivatives

I.2.1 Synthesis of 4*H*-pyran derivatives linked to the quinoline motif

In a 100 mL flask, dissolve 1 mmol of the derivative of 2- chloroquinolin-3-carbaldehyde in an adequate volume of ethanol (EtOH 10 mL), then 1.1 eq. of malononitrile and 2-3 drops of triethylamine NEt_3 were added. The mixture is left with stirring at room temperature until the starting product disappears (monitored by TLC). Once the reaction is complete (formation of intermediate), 1.1 eq. activated methylene compound diluted in a minimum of EtOH and a few drops of triethylamine NEt_3 are added. The mixture is left with magnetic stirring at room temperature until the intermediate (Knoevenagel product) has disappeared. The precipitate is filtered, washed with ice-cold and cold ether ethylic, then dried in the open air.

I.2.1.1 Methyl 6-amino-5-cyano-4-(2,6-dichloroquinolin-3-yl)-2-methyl-4H-pyran-3-carboxylate (7a)

According to the standard protocol, the desired 4*H*-pyran derivative (**7a)** was obtained by combining 2-Chloroquinolin-3-carbaldehyde **6b** (1 mmol, 225 mg), malononitrile (1.1 mmol, 73 mg), and methylacetoacetate (1 mmol, 116 mg).

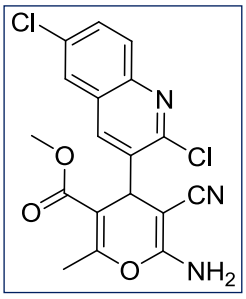

- ✓ ***Chemical Formula:*** $C_{18}H_{13}Cl_2N_3O_3$
- ✓ ***Molecular Weight***: 390.22
- ✓ ***Yield:*** 78%, (304 mg); White solid
- ✓ ***m.p:*** 269-270°C

FT-IR: ν(CO)=1668cm^{-1}, ν(NH)=3461 cm^{-1}, ν(CN)= 1172 cm^{-1}.

^{1}H-NMR (400 MHz, DMSO-*d*$_6$): δ(ppm) = 8.32 (s, 1H, C<u>H</u>-Ar); 8.23 (s, 1H, C<u>H</u>-Ar); 7.96 (d, 1H, *J* = 9,0 Hz, 1H, C<u>H</u>-Ar); 7,80 (d, *J* = 9,0 Hz, 1H, C<u>H</u>-Ar); 7.09 (s, 2H, N<u>H</u>$_2$); 4.97 (s, 1H, C<u>H</u>); 3.47 (s, 3H, O-C<u>H</u>$_3$); 2.40 (s, 3H, C<u>H</u>$_3$).

^{13}C-NMR (100 MHz, DMSO-*d*$_6$): δ(ppm) = 166.0 (C, <u>C</u>O); 159.3 (C, O-<u>C</u>CH$_3$); 159.1 (C, O-<u>C</u>NH$_2$); 150.2 (C, <u>C</u>-Cl); 144.9 (C, <u>C</u>q, CN<u>C</u>-Cl); 138.3 (C, <u>C</u>q, <u>C</u>NC); 132.1 (C, <u>C</u>-Cl); 131.7 (C, <u>C</u>H-Ar); 130.1 (C, <u>C</u>H-Ar); 128.8 (C, <u>C</u>H-Ar); 127.1

(C, CH-Ar); 119.6 (C, CN); 105.6 (C, CCO); 56.0 (C, CCN); 52.1(C, O-CH_3); 36.4 (C, CH); 19.0 (C, CH_3).

Elemental analysis calcd. (%) for $C_{18}H_{13}Cl_2N_3O_3$ (**M.w** = 390.22 g/mol): C 55.40, H 3.36, N 10.77; found (%): C 55.15, H 3.45, N 10.55

I.2.1.2 Ethyl 6-amino-5-cyano-4-(2,6-dichloroquinolin-3-yl)-2-methyl-4H-pyran-3-carboxylate (7b)

According to the standard protocol, the desired 4*H*-pyran derivative **7b** was obtained by combining 2-Chloroquinolin-3-carbaldehyde **6b** (1 mmol, 225 mg), malononitrile (1.1 mmol, 73 mg), and ethylacetoacetate (1 mmol, 130 mg).

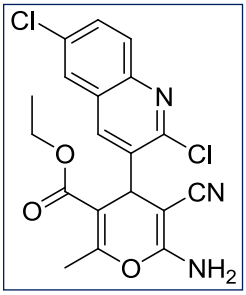

- ✓ ***Chemical Formula***: $C_{19}H_{15}Cl_2N_3O_3$
- ✓ ***Molecular Weight***: 404.25 g/mol
- ✓ ***Yield:*** 72%, (293 mg); White solid
- ✓ ***m.p:*** 267-268 °C

FT-IR: *v*(CO)= 1690 cm^{-1}, *v*(NH)= 3318 cm^{-1}, *v*(CN) = 1181 cm^{-1}.

^{1}H-NMR (400 MHz, DMSO-d_6): δ(ppm) = 8.32 (s, 1H, CH-Ar); 8.22 (s, 1H, CH-Ar); 7.97 (d, 1H, *J*=8,9 Hz, 1H, CH-Ar); 7,79 (d, *J*=8,9 Hz, 1H, CH-Ar); 7.03 (s, 2H, NH_2); 4.98 (s, 1H, CH); 3.90 (q, *J* = 6,9 Hz, 2H, O-CH_2); 2.40 (s, 3H, CH_3); 0.92 (t, *J* = 7.0 Hz, 3H, CH_3).

^{13}C-NMR (100 MHz, DMSO-d_6) : *δ*(ppm) = 165.4 (C, CO) ; 159.3 (C, O-CNH_2); 159.0 (C, O-CCH_3); 150.3 (C, C-Cl); 144.8 (C, Cq, CNC-Cl); 138.3 (C, Cq, CNC); 132.2 (C, C-Cl); 131.6 (C, CH-Ar); 130.1 (C, CH-Ar); 128.75 (C, CH-Ar); 127.6 (C, CH-Ar); 119.5 (C, CN); 105.6 (C, CCO); 60.7 (C, O-CH_2); 55.9 (C, CCN); 36.6 (C, CH); 18.8 (C, CH_3); 14.1 (C, CH_3).

Elemental analysis calcd. (%) for $C_{19}H_{15}Cl_2N_3O_3$ (**M.w** = 404.25 g/mol): C 56.45, H 3.74, N 10.39; found (%): C 56.50, H 3.62, N 10.15.

I.2.1.3 5-acetyl-2-amino-4-(2,6-dichloroquinolin-3-yl)-6-methyl-4H-pyran-3-carbonitrile (7c)

According to the standard protocol, the desired 4*H*-pyran derivative **7c** was obtained by combining 2-Chloroquinolin-3-carbaldehyde **6b** (1 mmol, 225 mg), malononitrile (1.1 mmol, 73 mg), and pentane-2,4-dione (1 mmol, 100 mg).

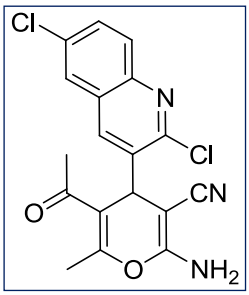

- ✓ ***Chemical Formula:*** $C_{18}H_{13}Cl_2N_3O_2$
- ✓ ***Molecular Weight:*** 374.22 g/mol
- ✓ ***Yield****:* 74%, (277 mg); White solid
- ✓ ***m.p****:* 265-266°C.

FT-IR: ν(CO)=1658 cm^{-1}, ν(NH)= 3455 cm^{-1}, ν(CN)=1168 cm^{-1}.

^{1}H-NMR (400 MHz, DMSO-*d*$_6$): δ (ppm) = 8.27 (s, 1H, C<u>H</u>-Ar); 8.22 (s, 1H, C<u>H</u>-Ar); 7.97 (d, 1H, *J* = 9,0 Hz, 1H, C<u>H</u>-Ar); 7,81 (d, *J* = 9,0 Hz, 1H, C<u>H</u>-Ar); 7.07 (s, 2H, N<u>H</u>$_2$); 5.04 (s, 1H, C<u>H</u>); 2.36 (s, 3H, C<u>H</u>$_3$); 2.15 (s, 3H, C<u>H</u>$_3$).

^{13}C-NMR (100 MHz, DMSO-*d*$_6$): δ (ppm) = 197.8 (C, <u>C</u>O); 159.3 (C, O-<u>C</u>CH$_3$); 157.6 (C, O-<u>C</u>NH$_2$); 150.1 (C, <u>C</u>-Cl); 144.9 (C, <u>C</u>q, CN<u>C</u>-Cl); 138.3 (C, <u>C</u>q, <u>C</u>NC); 132.2 (C, <u>C</u>-Cl); 131.7 (C, <u>C</u>H-Ar); 130.1 (C, <u>C</u>H-Ar); 128.8 (C, <u>C</u>H-Ar); 127.1 (C, <u>C</u>H-Ar); 119.6 (C, <u>C</u>N); 114.7 (C, <u>C</u>CO); 56.1 (C, <u>C</u>CN); 36.5 (C, <u>C</u>H); 30.8 (C, <u>C</u>H$_3$); 19.6 (C, <u>C</u>H$_3$).

Elemental analysis calcd. (%) for $C_{18}H_{13}Cl_2N_3O_2$ (**M.w** = 374.22 g/mol): C 57.77, H 3.50, N 11.23; **found** (%): C 57.46, H 3.25, N 11.02.

I.2.1.4 5-acetyl-2-amino-4-(2-chloro-6-methylquinolin-3-yl)-6-methyl-4H-pyran-3-carbonitrile (7d)

According to the standard protocol, the desired 4*H*-pyran derivative **7d** was obtained by combining 2-Chloroquinolin-3-carbaldehyde **6a** (1 mmol, 205 mg), malononitrile (1.1 mmol, 73 mg), and pentane-2,4-dione (1 mmol, 100 mg).

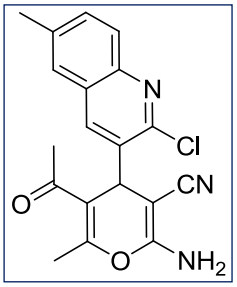

✓ ***Chemical Formula:*** $C_{19}H_{16}ClN_3O_2$

✓ ***Molecular Weight:*** 353.80 g/mol

✓ ***Yield****:* 86%, (330 mg); White yellow solid

✓ ***m.p****:* 209-210°C.

FT-IR: *ν*(CO)=1660 cm^{-1}, *ν*(NH)= 3430 cm^{-1}, *ν*(CN)=1174 cm^{-1}.

^{1}H-NMR (400 MHz, DMSO-*d6*): *δ*(ppm) = 8.15 (s, 1H, C<u>H</u>-Ar); 7.83 (d, *J* = 8.6 Hz, 1H, C<u>H</u>-Ar); 7.80 (s, 1H, C<u>H</u>-Ar); 7.63 (d, *J* = 8.6 Hz, 1H, C<u>H</u>-Ar); 7,02 (s, 1H, C<u>H</u>-Ar); 5.03 (s, 1H, C<u>H</u>); 2.47 (s, 3H, C<u>H</u>$_3$); 2.33 (s, 3H, C<u>H</u>$_3$); 2.12 (s, 3H, C<u>H</u>$_3$).

^{13}C-NMR (100 MHz, DMSO-*d6*): δ(ppm) = 198.0 (C, <u>C</u>O); 159.3 (C, <u>C</u>NH$_2$); 157.1 (C, C=<u>C</u>-O); 148.6 (C, <u>C</u>-Cl); 145.1 (C, <u>C</u>q); 138.4 (C, <u>C</u>q); 137.6 (C, <u>C</u>q); 133.4 (C, <u>C</u>H-Ar); 127.9 (C, <u>C</u>H-Ar); 127.7 (C, <u>C</u>H-Ar); 127.0 (C, <u>C</u>H-Ar); 119.7 (C, <u>C</u>N); 114.6 (C, <u>C</u>CO); 56.3 (C, <u>C</u>CN); 36.6 (C, <u>C</u>H); 30.6 (C, <u>C</u>H$_3$); 21.5 (C, <u>C</u>H$_3$); 19.5 (C, <u>C</u>H$_3$).

Elemental analysis calcd. (%) for $C_{19}H_{16}ClN_3O_2$ (M.w.= 353.80 g/mol): C 65.67, H 4.41, N 11.49; **found** (%): C 65.80, H 4.23, N 11.65.

I.2.1.5 2-Amino-4-(2-chloro-6-methylquinolin-3-yl)-5-oxo-5,6,7,8-tetrahydro-4H-chromene-3-carbonitrile (7e)

According to the standard protocol, the desired 4*H*-benzo[b]pyran derivative **7e** was obtained by combining 2-Chloroquinolin-3-carbaldehyde **6a** (1 mmol, 205 mg), malononitrile (1.1 mmol, 73 mg), and cyclohexane-1,3-dione (1 mmol, 112 mg).

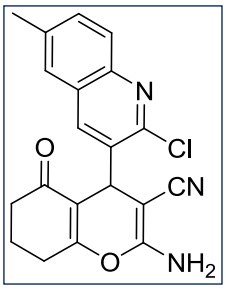

- ✓ ***Chemical Formula:*** $C_{20}H_{16}ClN_3O_2$
- ✓ ***Molecular Weight:*** 365.81 g/mol
- ✓ ***Yield:*** 83%, (304 mg); White yellow solid
- ✓ ***m.p:*** 267-268 °C.

FT-IR: *ν*(CO)=1676 cm^{-1}, *ν*(NH)= 3331 cm^{-1}, *ν*(CN)=1176cm^{-1}.

^{1}H-NMR (400 MHz, DMSO-*d6*): *δ*(ppm) = 8.19 (s, 1H, C<u>H</u>-Ar); 7.81 (d, *J* = 8,6 Hz, 1H, C<u>H</u>-Ar); 7.78 (s, 1H, C<u>H</u>-Ar); 7,61 (d, *J* = 8,6 Hz, 1H, C<u>H</u>-Ar); 7.17 (s, 2H, N<u>H</u>$_2$); 4.79 (s, 1H, C<u>H</u>); 2.72-2.60 (m, 2H, C<u>H</u>$_2$); 2.47 (s, 3H, C<u>H</u>$_3$); 2.36-2.14 (m, 2H, C<u>H</u>$_2$); 2.18-1.68 (m, 2H, C<u>H</u>$_2$).

^{13}C-NMR (100 MHz, DMSO-*d6*): *δ*(ppm) = 196.5 (C, <u>C</u>O); 165.9 (C, <u>C</u>NH$_2$); 159.0 (C, C=<u>C</u>-N); 148.9 (C, <u>C</u>-Cl); 145.0 (C, <u>C</u>q); 137.3 (C, <u>C</u>q); 133.1 (2C, <u>C</u>H-Ar); 127.9 (C, <u>C</u>H-Ar); 127.6 (C, <u>C</u>H-Ar); 126.9 (C, <u>C</u>H-Ar); 119.7 (C, <u>C</u>H-Ar); 112.8 (C, <u>C</u>N); 56.7 (C, <u>C</u>CN); 36.7 (C, <u>C</u>H$_2$); 33.7 (C, <u>C</u>H); 27.1 (C, <u>C</u>H$_2$); 21.6 (C, <u>C</u>H$_3$); 20.3 (C, <u>C</u>H$_2$).

Elemental analysis calcd. (%) for $C_{20}H_{16}ClN_3O_2$ (**M.w** = 365.81 g/mol): C 65.67, H 4.41, N 11.49; **found** (%): C 65.46, H 4.22, N 11.64.

I.2.1.6 2-Amino-4-(2,6-dichloroquinolin-3-yl)-5-oxo-5,6,7,8-tetrahydro-4H-chromene-3-carbonitrile (7f)

According to the standard protocol, the desired 4*H*-benzo[b]pyran derivative **7f** was obtained by combining 2-Chloroquinolin-3-carbaldehyde **6b** (1 mmol, 225 mg), malononitrile (1.1 mmol, 73 mg), and cyclohexane-1,3-dione (1 mmol, 112 mg).

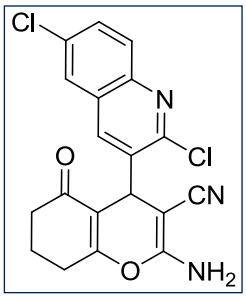

- ✓ ***Chemical Formula:*** $C_{19}H_{13}Cl_2N_3O_2$
- ✓ ***Molecular Weight:*** 386.23 g/mol
- ✓ ***Yield****:* 71%, (275 mg); White yellow solid
- ✓ ***m.p****:* > 280°C.

FT-IR: ν(CO) =1667 cm^{-1}, ν(NH) = 3460 cm^{-1}, ν(CN) = 1170 cm^{-1}.

^{1}H-NMR (400 MHz, DMSO-*d6*): δ(ppm) = 8.31 (s, 1H, C<u>H</u>-Ar); 8.18 (s, 1H, C<u>H</u>-Ar); 7.95 (d, 1H, *J* = 9,0 Hz, 1H, C<u>H</u>-Ar); 7,78 (d, *J* = 9,0 Hz, 1H, C<u>H</u>-Ar); 7.17 (s, 2H, N<u>H</u>$_2$); 4.81 (s, 1H, C<u>H</u>); 2.79-2.53 (m, 2H, C<u>H</u>$_2$); 2.37-2.09 (m, 2H, C<u>H</u>$_2$); 2.12-1.78 (m, 2H, C<u>H</u>$_2$).

^{13}C-NMR (100 MHz, DMSO-*d6*): δ(ppm) = 189.2 (C, <u>C</u>O); 143.9 (C, O-<u>C</u>CH$_2$); 141.6 (C, O-<u>C</u>NH$_2$); 140.4 (C, <u>C</u>-Cl); 139.4 (C, <u>C</u>q, CN<u>C</u>-Cl); 138.2 (C, <u>C</u>q, <u>C</u>NC); 131.7 (C, <u>C</u>-Cl); 131.5 (C, <u>C</u>H-Ar); 129.6 (C, <u>C</u>H-Ar); 128.7 (C, <u>C</u>H-Ar); 127.6 (C, <u>C</u>H-Ar); 120.5 (C, <u>C</u>N); 114.1 (C, <u>C</u>CO); 53.5 (C, <u>C</u>CN); 30.5 (C, <u>C</u>H); 18.9 (C, <u>C</u>H$_2$); 18.2 (C, <u>C</u>H$_2$).

Elemental analysis calcd. (%) for $C_{19}H_{13}Cl_2N_3O_2$ (**M.w** = 386.23 g/mol): C 59.08, H 3.39, N 10.88; found (%): C 58,95 H 3.2, N 10.73

I.2.1.7 2-Amino-4-(2,6-dichloroquinolin-3-yl)-7,7-dimethyl-5-oxo-5,6,7,8-tetrahydro-4H-chromene-3-carbonitrile (7g)

According to the standard protocol, the desired 4*H*-benzo[b]pyran derivative **7g** was obtained by combining 2-Chloroquinolin-3-carbaldehyde **6b** (1 mmol, 225 mg), malononitrile (1.1 mmol, 73 mg), and 5,5-dimethylcyclohexane-1,3-dione (1 mmol, 140 mg).

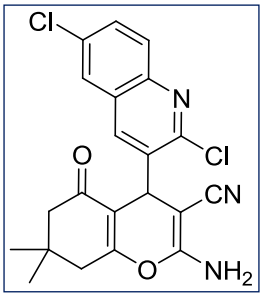

- ✓ ***Chemical Formula:*** $C_{21}H_{17}Cl_2N_3O_2$
- ✓ ***Molecular Weight:*** 414.28 g/mol
- ✓ ***Yield:*** 70%, (291 mg); White yellow solid
- ✓ ***m.p:*** 257-258 °C

FT-IR: ν(CO) = 1667 cm^{-1}, ν(NH)= 3453 cm^{-1}, ν(CN) = 1179 cm^{-1}.

^{1}H-NMR (400 MHz, DMSO-*d6*): δ(ppm) = 8.32 (s, 1H, C<u>H</u>-Ar); 8.19 (s, 1H, C<u>H</u>-Ar); 7.95 (d, *J* = 9.0 Hz, 1H, C<u>H</u>-Ar); 7,79 (d, *J* = 8.9 Hz, 1H, C<u>H</u>-Ar); 7.21 (s, 2H, N<u>H</u>$_2$); 4.81 (s, 1H, C<u>H</u>); 2.56 (s, 2H, C<u>H</u>$_2$); 2.17 (d, *J* = 16.1, 1H, C<u>H</u>$_2$); 2.09 (d, *J* = 16.0, 1H, C<u>H</u>$_2$); 1.05 (s, 3H, CH_3); 1.01 (s, 3H, C<u>H</u>$_3$).

^{13}C-NMR (100 MHz, DMSO-*d6*): δ(ppm) = 196.3 (C, <u>C</u>O); 164.0 (C, <u>C</u>NH$_2$); 159.2 (C, C=<u>C</u>-N); 150.3 (C, <u>C</u>-Cl); 144.8 (C, <u>C</u>q); 132.1 (2C, <u>C</u>H-Ar); 131.6 (C, <u>C</u>H-Ar); 130.0 (C, <u>C</u>H-Ar); 128.7 (C, <u>C</u>H-Ar); 126.9 (C, <u>C</u>H-Ar); 119.6 (C, <u>C</u>N); 56.4 (C, <u>C</u>CN); 50.3 (C, <u>C</u>H$_2$); 32.2 (C, <u>C</u>(CH$_3$)$_2$); 32.2 (C, <u>C</u>H$_2$); 28.70 (C, <u>C</u>H$_3$); 27.6 (C, <u>C</u>H$_3$.).

Elemental analysis calcd. (%) for $C_{21}H_{17}Cl_2N_3O_2$ (**M.w** = 414.28 g/mol): C 60.88, H 4.14, N 10.14; **found** (%): C 60.52, H 4.01, N 10.34

I.2.1.8 2-Amino-4-(2-chloro-6-methylquinolin-3-yl)-7,7-dimethyl-5-oxo-5,6,7,8-tetrahydro-4H-chromene-3-carbonitrile (7h)

According to the standard protocol, the desired 4*H*-benzo[b]pyran derivative **7h** was obtained by combining 2-Chloroquinolin-3-carbaldehyde **6a** (1 mmol, 205 mg), malononitrile (1.1 mmol, 73 mg), and 5,5-dimethylcyclohexane-1,3-dione (1 mmol, 140 mg).

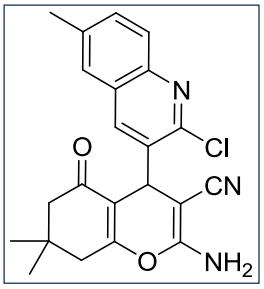

- ✓ ***Chemical Formula***: $C_{22}H_{20}ClN_3O_2$
- ✓ ***Molecular Weight***: 393.78 g/mol
- ✓ ***Yield:*** 91%, (360 mg); White yellow solid
- ✓ ***m.p:*** 265-266 °C.

FT-IR: *ν*(CO) = 1662 cm^{-1}, *ν*(NH)= 3445 cm^{-1}, *ν*(CN) = 1170 cm^{-1}.

^{1}H-NMR (400 MHz, DMSO-*d6*): *δ*(ppm) = 8.21 (s, 1H, C<u>H</u>-Ar); 7,84 (d, *J* = 8.6 Hz, 1H, C<u>H</u>-Ar); 7.81 (s, 1H, C<u>H</u>-Ar); 7.64 (d, *J* = 8.6 Hz, 1H, C<u>H</u>-Ar); 7.19 (s, 2H, N<u>H</u>$_2$); 4.82 (s, 1H, C<u>H</u>); 2.58 (s, 2H, C<u>H</u>$_2$); 2.53 (s, 2H, C<u>H</u>$_2$); 2.50 (s, 3H, CH_3); 1.08 (s, 3H, C<u>H</u>$_3$); 1.04 (s, 3H, C<u>H</u>$_3$).

^{13}C-NMR (100 MHz, DMSO-*d6*): *δ*(ppm) = 21.6 (C, <u>C</u>H$_3$); 27.6 (C, <u>C</u>H$_3$); 28.7 (C, <u>C</u>H$_3$); 32.2 (C, <u>C</u>(CH$_3$)$_2$); 45.6 (C, <u>C</u>H$_2$); 56.4 (C, <u>C</u>CN); 119.7 (C, <u>C</u>N); 126.8 (C, <u>C</u>H-Ar); 127.6 (C, <u>C</u>H-Ar); 127.8 (C, <u>C</u>H-Ar); 133.2 (2C, <u>C</u>H-Ar); 137.4 (C, <u>C</u>q); 145.0 (C, <u>C</u>q); 148.8 (C, <u>C</u>-Cl); 159.2 (C, C=<u>C</u>-N); 163.9 (C, <u>C</u>NH$_2$); 196.3 (C, <u>C</u>O).

Elemental analysis calcd. (%) for $C_{22}H_{20}ClN_3O_2$ (**M.w** = 393.78 g/mol): C 67.09, H 5.12, N 10.67; **found** (%): C 67.18, H 5.03, N 10.54

I.2.1.9 6-Amino-4-(2-chloro-6-methylquinolin-3-yl)-3-methyl-1,4-dihydropyrano[2,3-c]pyrazole-5-carbonitrile (7i)

By following the standard procedure, 4*H*-pyrano-pyrazole derivative **7i** was obtained from a mixture of 2-Chloroquinolin-3-carbaldehyde **6a** (1 mmol, 205 mg), malononitrile (1.1 mmol, 73 mg), hydrazine (1 mmol, 32 mg), and ethylacetoacetat (1 mmol, 140 mg).

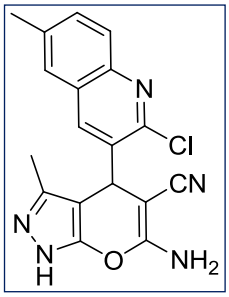

✓ ***Chemical Formula:*** $C_{18}H_{14}ClN_5O$
✓ ***Molecular Weight:*** 351.79 g/mol
✓ ***Yield:*** 78%, (275 mg); White yellow solid
✓ ***m.p:*** 269 °C

FT-IR: *ν*(CO)=1648 cm^{-1}, *ν*(NH)= 3355 cm^{-1}, *ν*(CN)=1162 cm^{-1}.

^{1}H-NMR (400 MHz, DMSO-*d6*): δ(ppm) = 12.18 (s, 1H, NH); 8.25 (s, 1H, CH-Ar); 7.84 (d, *J* = 6.2 Hz, 1H, CH-Ar); 7.81 (s, 1H, CH-Ar); 7.64 (d, *J* = 6.8 Hz, 1H, CH-Ar); 7.07 (s, 2H, NH_2); 5.17 (s, 1H, CH); 2.47 (s, 3H, CH_3); 1.76 (s, 3H, CH_3).

^{13}C-NMR (100 MHz, DMSO-*d6*): δ(ppm) = 158.1 (C, CNH_2); 156.4 (C, O-C-NH); 144.6 (C, C-Cl); 140.6 (C, Cq); 137.8 (C, Cq); 135.9 (C-Cq); 133.9 (C, CH-Ar); 127.5 (C, CH-Ar); 127.1 (C, CH-Ar); 126.1 (C, CH-Ar); 115.4 (C, CN); 113.5 (C, CC=N); 56.5 (C, CCN); 33.4 (C, CH); 21.4 (C, CH_3); 11.0 (C, CH_3).

Elemental analysis calcd. (%) for $C_{18}H_{14}ClN_5O$ (**M.w** = 351.79 g/mol): C 61.46, H 4.01, N 19.91; **found** (%): C 61.32, H 4.10, N 19.72.

I.2.1.10 6-Amino-4-(2,6-dichloroquinolin-3-yl)-3-methyl-1,4-dihydropyrano[2,3-c]pyrazole-5-carbonitrile (7j)

By following the standard procedure, 4*H*-pyrano-pyrazole derivative **7j** was obtained from a mixture of 2-Chloroquinolin-3-carbaldehyde **6b** (1 mmol, 225 mg), malononitrile (1.1 mmol, 73 mg), hydrazine (1 mmol, 32 mg), and ethylacetoacetat (1 mmol, 140 mg).

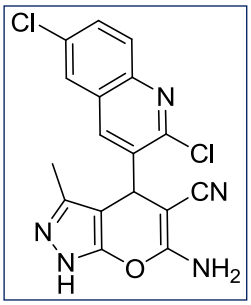

- ✓ ***Chemical Formula:*** $C_{17}H_{11}Cl_2N_5O$
- ✓ ***Molecular Weight:*** 372.21 g/mol
- ✓ ***Yield:*** 67%, (250 mg); White yellow solid
- ✓ ***m.p:*** 279-280 °C

FT-IR: ν(CO)= 1609 cm^{-1}, ν(NH) = 3437 cm^{-1}, ν(CN)=1162 cm^{-1}.

^{1}H-NMR (400 MHz, DMSO-d_6): δ (ppm) = 12.16 (s, 1H, NH); 8.32 (s, 1H, CH-Ar); 8.23 (s, 1H, CH-Ar); 7.97 (d, 1H, *J* = 8,9 Hz, 1H, CH-Ar); 7,81 (d, *J*=8,9 Hz, 1H, CH-Ar); 7.05 (s, 2H, NH_2); 4.98 (s, 1H, CH); 2.40 (s, 3H, CH_3).

^{13}C-NMR (100 MHz, DMSO-d_6): δ (ppm) = 159.3 (C, O-CCH_3); 157.6 (C, O-CNH_2); 150.0 (C, C-Cl); 144.9 (Cq, CNC-Cl); 138.3 (C, Cq, CNC); 132.2 (C, C-Cl); 131.7 (C, CH-Ar); 130.0 (C, CH-Ar); 128.7 (C, CH-Ar); 127.1 (C, CH-Ar); 119.6 (C, CN); 114.6 (C, CCO); 56.1 (C, CCN); 36.5 (C, CH); 30.7 (C, CH_3); 19.6 (C, CH_3).

Elemental analysis calcd. (%) for $C_{17}H_{11}Cl_2N_5O$ (**M.w** = 372.21 g/mol): C 54.56, H 3.50, N 18.71; **found** (%): C 54.75, H 3.25, N 18.54.

I.2.1.11 Ethyl 6-amino-4-(2-chloro-6-methylquinolin-3-yl)-5-cyano-1,4-dihydropyrano[2,3-c]pyrazole-3-carboxylate (7k)

By following the standard procedure, 4*H*-pyrano-pyrazole derivative **7k** was obtained from a mixture of 2-Chloroquinolin-3-carbaldehyde **6a** (1 mmol, 205 mg), malononitrile (1.1 mmol, 73 mg), ethyl 5-oxo-4,5-dihydro-1H-pyrazole-3-carboxylate (1 mmol, 157 mg).

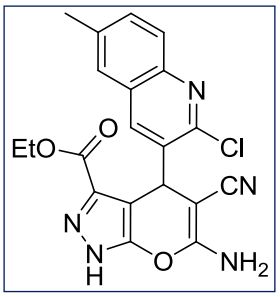

- ✓ ***Chemical Formula:*** $C_{20}H_{16}ClN_5O_3$
- ✓ ***Molecular Weight:*** 409.83 g/mol
- ✓ ***Yield:*** 73%, (300 mg); White yellow solid
- ✓ ***m.p:*** 274-275 °C

FT-IR: *ν*(CO)=1670 cm^{-1}, *ν*(NH)= 3168 cm^{-1}, *ν*(CN)=1153 cm^{-1}.

^{1}H-NMR (400 MHz, DMSO-*d6*): *δ*(ppm) = 8.36 (s, 1H, C<u>H</u>-Ar); 7.90 (s, 1H, C<u>H</u>-Ar); 7.87 (d, *J* = 8,6 Hz, 1H, C<u>H</u>-Ar); 7,66 (d, *J* = 8.6 Hz, 1H, C<u>H</u>-Ar); 7.20 (s, 2H, N<u>H</u>$_2$); 5.12 (s, 1H, C<u>H</u>); 3.71 (q, *J* = 6.9 Hz, 2H, OC<u>H</u>$_2$); 2.50 (s, 3H, C<u>H</u>$_3$); 0.68 (t, *J* = 7,1 Hz, 3H, C<u>H</u>$_3$).

^{13}C-NMR (100 MHz, DMSO-*d6*): δ(ppm) = 165.5 (C, <u>C</u>O); 159.7 (C, <u>C</u>NH$_2$); 156.3 (C, O-<u>C</u>-NH); 148.8 (C, <u>C</u>-Cl); 145.2 (C, <u>C</u>q); 138.9 (C, <u>C</u>q); 137.6 (C, <u>C</u>q); 133.6 (C, <u>C</u>q); 133.4 (C, <u>C</u>q); 130.4 (<u>C</u>-Cq); 129.0 (C, <u>C</u>H-Ar); 128.5 (C, 2<u>C</u>H-Ar); 127.9 (C, 2<u>C</u>H-Ar); 127.7 (C, <u>C</u>H-Ar); 127.1 (C, <u>C</u>H-Ar); 119.7 (C, <u>C</u>N); 107.3 (C, <u>C</u>CH); 60.8 (C, O<u>C</u>H$_2$); 55.6 (C, <u>C</u>N); 37.7 (C, <u>C</u>H); 21.7 (C, <u>C</u>H$_3$); 13.6 (C, <u>C</u>H$_3$).

Elemental analysis calcd. (%) for $C_{20}H_{16}ClN_5O_3$ (**M.w** = 409.83 g/mol): C 58.61, H 3.94, N 17.09; **found** (%): C 58.53, H 4.02, N 17.22.

I.2.1.12 6-Amino-4-(2-chloro-6-methylquinolin-3-yl)-3-methyl-4H-pyrano[3,2-d]isoxazole-5-carbonitrile (7l)

By following the standard procedure, 4*H*-pyrano-isoxazole derivative **7l** was obtained from a mixture of 2-Chloroquinolin-3-carbaldehyde **6a** (1 mmol, 205 mg), malononitrile (1.1 mmol, 73 mg), hydrazine (1 mmol, 32 mg), and hydroxylamine (1 mmol, 33 mg).

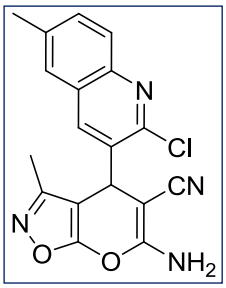

- ✓ ***Chemical Formula:*** $C_{18}H_{13}ClN_4O_2$
- ✓ ***Molecular Weight:*** 352.77 g/mol
- ✓ ***Yield:*** 75%, (264 mg); White solid
- ✓ ***m.p:*** 290 °C

FT-IR: *ν*(CO)=1638 cm^{-1}, *ν*(NH)= 3154 cm^{-1}, *ν*(CN)=1187 cm^{-1}.

^{1}H-NMR (400 MHz, DMSO-*d6*): *δ*(ppm) = 8.17 (s, 1H, C<u>H</u>-Ar); 7.83 (d, *J* = 8.6 Hz, 1H, C<u>H</u>-Ar); 7.80 (s, 1H, C<u>H</u>-Ar); 7,62 (d, *J* = 8.7 Hz, 1H, C<u>H</u>-Ar); 7.19 (s, 2H, N<u>H</u>$_2$); 5.36 (s, 1H, C<u>H</u>); 2.50 (s, 3H, C<u>H</u>$_3$); 2.46 (s, 3H, C<u>H</u>$_3$).

^{13}C-NMR (100 MHz, DMSO-*d6*): δ(ppm) = 158.7 (C, <u>C</u>NH$_2$); 156.2 (C, O-<u>C</u>-NH); 148.7 (C, <u>C</u>-Cl); 145.1 (C, <u>C</u>q); 137.5 (C, <u>C</u>q); 133.3 (C, <u>C</u>q); 129.3 (C, <u>C</u>H-Ar); 127.6 (C, <u>C</u>H-Ar); 127.0 (C, <u>C</u>H-Ar); 120.3 (C, <u>C</u>N); 52.3 (C, <u>C</u>CN); 35.2 (C, <u>C</u>H); 21.5 (C, <u>C</u>H$_3$); 11.8 (C, <u>C</u>H$_3$).

Elemental analysis calcd. (%) for $C_{18}H_{13}ClN_4O_2$ (**M.w** = 352.77 g/mol): C 61.28, H 3.71, N 15.88; **found** (%): C 61.43, H 3.64, N 15.76.

I.2.2 Synthesis of hybrid quinoline tacrine derivatives (8a-b)

To conduct the reaction, we start by introducing 1.7 equivalents of aluminum chloride into a balloon with adequate capacity containing anhydrous 1.2-dichloroethane (0.15M). After stirring the suspension formed at room temperature under nitrogen, we add 1.0 equivalent of a 4*H*-pyran derivative and 1.7 equivalents of cycloalkanone. The reaction mixture is then brought to reflux and stirred until the starting product disappears. The reaction progress is monitored by TLC. Once the reaction is complete, the mixture is allowed to cool to room temperature, and a mixture of THF/H_2O (1:1)

and 10% aqueous solution of sodium hydroxide NaOH is added dropwise until the reaction mixture becomes basic. The mixture is then stirred for 30 minutes, and extracted three times with dichloromethane. The organic phases are combined, washed with a saturated solution of NaCl, dried with anhydrous Na_2SO_4, filtered, and the solvent is evaporated. The resulting solid is then purified using column silica gel chromatography, eluting with an AcOEt/hexane or Et_2O mixture.

I.2.2.1 11-Amino-12-(2-chloro-6-methylquinolin-3-yl)-3,3-dimethyl-2,3,4,7,8,9,10,12-octahydro-1H-chromeno[2,3-b]quinolin-1-one 8b

Following the general procedure, a mixture of 4*H*-pyran derivative (**7h)** (0.5 mmol, 197 mg), aluminum chloride (0.85 mmol, 113 mg), and cyclohexanone (0.85 mmol, 84 mg), gave the desired tacrine analog product (**8a)**.

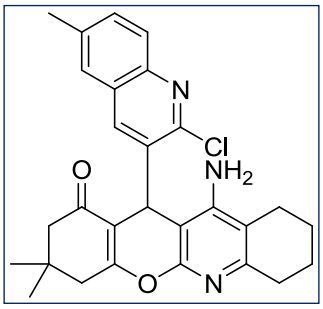

- ✓ ***Chemical Formula***: $C_{28}H_{28}ClN_3O_2$
- ✓ ***Molecular Weight:*** 473.99 g/mol
- ✓ ***Yield****:* 70%, (165 mg); yellow
- ✓ ***m.p****:* 252-253 °C

FT-IR: *ν*(CO) =1628 cm^{-1}, *ν*(NH) = 3362 cm^{-1}.

^{1}H NMR (400 MHz, $CDCl_3$): *δ* (ppm) = 7.93 (s, 1H, C<u>H</u>-Ar); 7.85 (d, *J* = 8.5 Hz, 1H, C<u>H</u>-Ar); 7.48 (d, *J* = 8.7 Hz, 1H, C<u>H</u>-Ar); 7.44 (s, 1H, C<u>H</u>-Ar); 5.32 (s, 1H, C<u>H</u>); 4.49 (s, 2H, NH_2); 2.75 (s, 2H, CH_2); 2.62 (s, 2H, CH_2); 2.46 (s, 3H, CH_3); 2.29 (m, 2H, CH_2); 2.15 (m, 2H, CH_2); 2.01 (m, 2H, CH_2); 1.78 (m, 4H, CH_2); 1.10 (s, 3H, CH_3); 0.97 (s, 3H, CH_3).

^{13}C-NMR (100 MHz, $CDCl_3$): *δ*(ppm) = 191.8 (C, <u>C</u>O); 166.4 (Cq, O-<u>C</u>-N); 160.5 (Cq, O-<u>C</u>-CH_2); 160.1 (C, O-<u>C</u>NH_2); 149.5 (C, <u>C</u>-Cl); 149.1 (Cq, CH_2-<u>C</u>N); 146.3 (Cq, N=<u>C</u>=CH_2); 143.8 (<u>C</u>q, CH-C-N); 140.6 (C, <u>C</u>q); 132.4 (C, <u>C</u>H-Ar); 128.0 (C, <u>C</u>H-Ar); 123.2 (C, <u>C</u>H-Ar); 121.2 (C, <u>C</u>H-Ar); 109.2 (C, <u>C</u>CO); 104.0 (C, <u>C</u>q); 55.6 (C, <u>C</u>H_2); 45.8 (C, <u>C</u>H_2); 36.8 (C, (<u>C</u>CH_3)$_2$); 32.5 (C, <u>C</u>H_2); 27.7 (C, <u>C</u>H); 27.6 (C, <u>C</u>H_2); 24.4 (C, <u>C</u>H_2); 22.8 (C, <u>C</u>H_3); 18.1 (C, <u>C</u>H_2).

Elemental analysis calcd. (%) for $C_{28}H_{28}ClN_3O_2$ (**M.w** = 473.99 g/mol): C 70.95, H 5.95, N 8.87; **found** (%): C 70.78, H 5.82, N 8.96.

I.2.2.2 11-Amino-12-(2-chloro-6-methylquinolin-3-yl)-2,3,4,7,8,9,10,12-octahydro-1H-chromeno[2,3-b]quinolin-1-one

Following the general procedure, a mixture of 4*H*-pyran derivative (**7e)** (0.5 mmol, 182.5 mg), aluminum chloride (0.85 mmol, 113 mg), and cyclohexanone (0.85 mmol, 84 mg), gave the desired tacrine analog product (**8b)**.

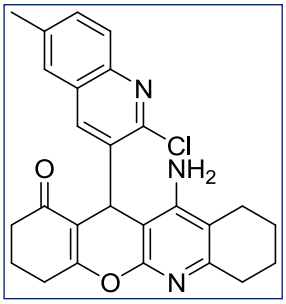

- ✓ ***Chemical Formula:*** $C_{26}H_{24}ClN_3O_2$
- ✓ ***Molecular Weight:*** 445.94 g/mol
- ✓ ***Yield:*** 67%, (150 mg); White Yellow
- ✓ ***m.p:*** > 260 °C

FT-IR: *v* (CO) =1628 cm^{-1}, *v*(NH) = 3362 cm^{-1}.

^{1}H NMR (400 MHz, $CDCl_3$): δ (ppm) = 7.92 (s, 1H, C<u>H</u>-Ar); 7.84 (d, *J* = 8.5 Hz, 1H, C<u>H</u>-Ar); 7.47 (d, *J* = 8.8 Hz, 1H, C<u>H</u>-Ar); 7.45 (s, 1H, C<u>H</u>-Ar); 5.31 (s, 1H); 4.47 (s, 2H, NH_2); 2.83 – 2.70 (m, 4H, CH_2); 2.45 (s, 3H, CH_3); 2.41 – 2.29 (m, 2H, CH_2); 2.29 – 2.09 (m, 2H, CH_2); 2.08-1.93 (m, 4H, CH_2).

^{13}C-NMR (100 MHz, $CDCl_3$): δ(ppm) = 196.6 (C, <u>C</u>O); 166.4 (Cq, O-<u>C</u>-N); 156.2 (Cq, O-<u>C</u>-CH_2); 153.8 (C, O-<u>C</u>NH_2); 151.0 (C, <u>C</u>-Cl); 148.0 (Cq, CH_2-<u>C</u>N); 144.8 (Cq, N=<u>C</u>=CH_2); 140.1 (<u>C</u>q, CH-C-N); 137.1 (C, <u>C</u>H-Ar); 132.7 (C, <u>C</u>H-Ar); 127.9 (C, <u>C</u>H-Ar); 125.1 (C, <u>C</u>H-Ar); 113.9 (C, <u>C</u>CO); 98.8 (C, <u>C</u>q); 36.8 (C, <u>C</u>H_2); 32.5 (C, <u>C</u>H_2); 29.7 (C, <u>C</u>H); 27.9 (C, <u>C</u>H_2); 22.9 (C, <u>C</u>H_2); 22.5 (C, <u>C</u>H_2); 22.3 (C, <u>C</u>H_2); 21.5 (C, <u>C</u>H_3); 20.4 (C, <u>C</u>H_2).

Elemental analysis calcd. (%) for $C_{26}H_{24}ClN_3O_2$ (**M.w** = 445.94 g/mol): C 70.03, H 5.42, N 9.42; **found** (%): C 70.12, H 5.54, N 9.31.

I.2.3 Synthesis of hybrid Quinoline-*N*-substituted-1,4-dihydropyridine derivatives

In a 100 ml round-bottom flask, a solution of arylamine (1.0 mmol), and an isolated intermediate (quinolylidene methylene malononitrile) in 10 mL methanol. The reaction mixture was stirred and heated under reflux until the completion of the reaction as indicated by thin-layer condensation (TLC). The reaction mixture which was initially in a partial liquid state was concentrated to approximately half the volume, cooled, and then poured onto cold water and stirred until the mixture became solid. The product was filtered and washed with small portions of dry ether. The resulting precipitates were collected and the obtained solid product was taken for analysis.

I.2.3.1 2'-Amino-2-chloro-1'-(4-fluorophenyl)-6-methyl-5'-oxo-1',4',5',6',7',8'-hexahydro-3,4'-biquinoline-3'-carbonitrile 9a

Following the general procedure, a mixture of quinolylidene methylene malononitrile (1.0 mmol), cyclohexane-1,3-dione (1.0 mmol), 4-Fluoroaniline (1.0 mmol), and a catalytic amount of trimethylamine. Gave the product **9a**.

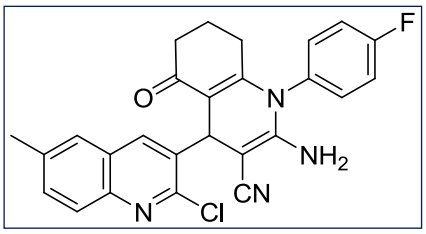

- ✓ ***Chemical Formula***: $C_{26}H_{20}ClFN_4O$
- ✓ ***Molecular Weight***: 458.91 g/mol
- ✓ ***Yield:*** 69%, (316 mg); yellow
- ✓ ***m.p:*** > 260 °C

FT-IR: *ν* (CO) = 1651 cm^{-1}, *ν* (NH) = 3320 cm^{-1}, *ν* (CN) = 1189 cm^{-1}.

^{1}H-NMR (400 MHz, DMSO-d_6): *δ* (ppm) = 8.21 (s, 1H, C<u>H</u>-Ar); 7.89 (s, 1H, C<u>H</u>-Ar); 7.82 (d, *J* = 8.6 Hz, 1H, C<u>H</u>-Ar); 7.66 (d, *J* = 8.6 Hz, 2H, C<u>H</u>-Ar); 7.60 (d, *J* = 6.9 Hz, 1H, C<u>H</u>-Ar); 7.55 (d, *J* = 8.7 Hz, 2H, C<u>H</u>-Ar); 5.55 (s, 2H, N<u>H</u>$_2$); 5.09 (s, 1H, C<u>H</u>); 2.50 (s, 3H, C<u>H</u>$_3$); 2.29-1.64 (m, 6H, CH_2).

^{13}C-NMR (100 MHz, DMSO-d_6): δ (ppm) = 195.4 (C, CO); 154.0 (C, CNH_2); 151.6 (C, C=C-N); 149.0 (C, C-Cl); 144.8 (C, Cq, CN-C); 142.4 (C, Cq); 137.8 (Cq, CNO_2); 137.0 (C, Cq); 133.8 (C, CH-Ar); 132.8 (C, CH-Ar); 132.7 (C, CH-Ar); 132.7 (2C, CH-Ar); 131.5 (2C, CH-Ar); 128.1 (C, CH-Ar); 127.5 (C, CH-Ar); 127.1 (C, CH-Ar); 121.4 (C, CN); 111.8 (Cq, CO-C-CH); 59.1 (C, CCN); 36.3 (C, CH_2); 34.8 (C, CH); 28.4 (C, CH_2); 21.3 (C, CH_3); 21.1 (C, CH_2).

Elemental analysis calcd. (%) for $C_{26}H_{20}ClFN_4O$ (**M.w** = 458.91 g/mol): C 68.05, H 4.39, N 12.21; **found** (%): C 67.90, H 4.50, N 12.05.

I.2.3.2 2'-Amino-2-chloro-1'-(4-chlorophenyl)-6-methyl-5'-oxo-1',4',5',6',7',8'-hexahydro-3,4'-biquinoline-3'-carbonitrile 9b

Following the general procedure, a mixture of quinolylidene methylene malononitrile (1.0 mmol), cyclohexane-1,3-dione (1.0 mmol), 4-Chlororoaniline (1.0 mmol), and a catalytic amount of trimethylamine. Gave the product (**9b)**.

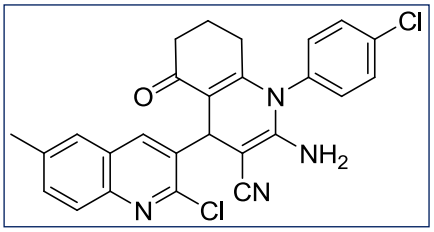

✓***Chemical Formula:*** $C_{26}H_{20}Cl_2N_4O$
✓***Molecular Weight:*** 475.37 g/mol
✓***Yield:*** 74%, (352 mg); White solid
✓***m.p:*** > 260 °C

FT-IR: ν (CO) = 1650 cm^{-1}, ν (NH) = 3201 cm^{-1}, ν (CN) = 1189 cm^{-1}.

^{1}H-NMR (400 MHz, DMSO-d_6): δ (ppm) = 8.20 (s, 1H, CH-Ar); 7.89 (s, 1H, CH-Ar); 7.82 (d, J = 8.6 Hz, 1H, CH-Ar); 7.61 (d, J = 8.6 Hz, 2H, CH-Ar); 7.56 (d, J = 4,9 Hz, 1H, CH-Ar); 7.44 (d, J = 8.7 Hz, 2H, CH-Ar) 5.50 (s, 2H, NH_2); 5.09 (s, 1H, CH); 2.50 (s, 3H, CH_3); 2.32-1.95 (m, 6H, CH_2).

^{13}C-NMR (400 MHz, DMSO-d_6): δ (ppm) = 195.4 (C, CO); 154.2 (C, CNH_2); 151.8 (C, C=C-N); 149.0 (C, C-Cl); 144.8 (C, Cq, CN-C); 138.9 (C, Cq); 137.7 (Cq, CNO_2); 137.0 (C, Cq); 133.8 (C, CH-Ar); 132.8 (C, CH-Ar); 132.7 (C, CH-Ar); 132.7 (2C, CH-Ar); 131.5 (2C, CH-Ar); 128.1 (C, CH-Ar); 127.5 (C, CH-Ar); 127.1 (C, CH-

Ar); 126.3 (C, Cq); 121.4 (C, CN); 111.7 (Cq, CO-C-CH); 59.0 (C, CCN); 36.3 (C, CH_2); 34.8 (C, CH); 28.4 (C, CH_2); 21.5 (C, CH_3); 21.1 (C, CH_2).

Elemental analysis calcd. (%) for $C_{26}H_{20}Cl_2N_4O$ (**M.w** = 475.37 g/mol): C 65.69, H 4.24, N 11.79; **found** (%): C 65.50, H 4.10, N 11.95.

I.2.3.3 2'-Amino-2-chloro-6-methyl-1'-(4-nitrophenyl)-5'-oxo-1',4',5',6',7',8'-hexahydro-3,4'-biquinoline-3'-carbonitrile 9c

Following the general procedure, a mixture of quinolylidene methylene malononitrile (1.0 mmol), cyclohexane-1,3-dione (1.0 mmol), 4-nitroaniline (1.0 mmol), and a catalytic amount of trimethylamine. Gave the product (**9c**).

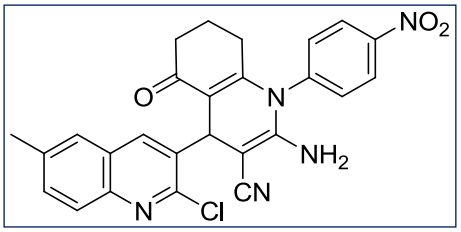

- ✓ ***Chemical Formula***: $C_{26}H_{20}ClN_5O_3$
- ✓ ***Molecular Weight:*** 485.92 g/mol
- ✓ ***Yield****:* 60%, (295 mg); White solid
- ✓ ***m.p****:* > 260 °C

FT-IR: *ν* (CO) = 1657 cm^{-1}, ν (NH) = 3314 cm^{-1}, *ν* (CN) = 1189 cm^{-1}.

^{1}H-NMR (400 MHz, DMSO-*d*$_6$): *δ* (ppm) = 8.42 (d, *J* = 8.8 Hz, 2H, CH-Ar), 8.25 (s, 1H, CH-Ar); 7.94 (d, *J* = 8.8 Hz, 1H, CH-Ar); 7.89 (s, 1H, CH-Ar); 7.83 (d, *J*= 8.9 Hz, 2H, CH-Ar); 7.61 (d, *J*= 8.6 Hz, 1H, CH-Ar); 5.67 (s, 2H, NH_2); 5.09 (s, 1H, CH); 2.50 (s, 3H, CH_3); 2.42-1.84 (m, 6H, CH_2).

^{13}C-NMR (100 MHz, DMSO-*d*$_6$): *δ* (ppm) = 195.4 (C, CO); 157.6 (C, CNH_2); 156.42 (C, C=C-N); 153.3 (C, C-Cl); 151.3(C, Cq, CN-C); 144.8(C, Cq); 142.4 (C, Cq); 137.8 (Cq, CNO_2); 137.0 (C, Cq); 133.8 (C, CH-Ar); 132.8 (C, CH-Ar); 132.7 (C, CH-Ar); 127.5 (C, CH-Ar); 128.1 (C, CH-Ar); 127.1 (C, CH-Ar); 21.4 (C, CH_2); 126.8 (2C, CH-Ar); 126.3 (C, Cq); 125.6 (2C, CH-Ar); 121.2 (C, CN); 112.9 (Cq, CO-C-CH); 59.4 (C, CCN); 36.3 (C, CH_2); 34.9 (C, CH); 28.5 (C, CH_2); 21.5 (C, CH_3).

Elemental analysis calcd. (%) for $C_{26}H_{20}ClN_5O_3$ (**M.w** = 485.92 g/mol): C 64.27, H 4.15, N 14.41; **found** (%): C 64.10, H 4.45, N 14.07

I.2.3.4 4-(2'-amino-2-chloro-3'-cyano-6-methyl-5'-oxo-5',6',7',8'-tetrahydro-3,4'-biquinolin-1'(4'H)-yl)benzenesulfonamide 9d

Following the general procedure, a mixture of quinolylidene methylene malononitrile (1.0 mmol), cyclohexane-1,3-dione (1.0 mmol), sulfanilamide (1.0 mmol), and a catalytic amount of trimethylamine. Gave the product (**9d)**.

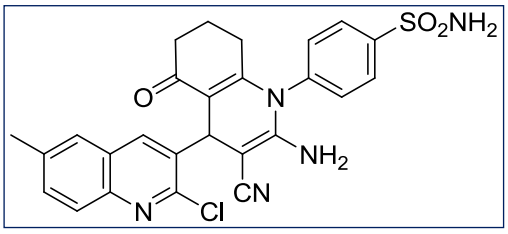

- ✓ ***Chemical Formula***: $C_{26}H_{22}ClN_5O_3S$
- ✓ ***Molecular Weight:*** 520.00 g/mol
- ✓ ***Yield:*** 80%, (415 mg); yellow solid
- ✓ ***m.p****:* 279-280°C

FT-IR: *ν* (CO) = 1661cm^{-1}, ν (NH) = 3389 cm^{-1}, *ν* (CN) = 1170 cm^{-1}.

^{1}H-NMR (400 MHz, DMSO-*d*$_6$): *δ* (ppm) = 8.21 (s, 1H, C<u>H</u>-Ar); 8.01 (d, *J* = 8.5 Hz, 2H, C<u>H</u>-Ar); 7.90 (s, 1H, C<u>H</u>-Ar); 7.83 (d, *J* = 8.6 Hz, 2H, C<u>H</u>-Ar); 7.73 (d, *J* = 8.6 Hz, 2H, C<u>H</u>-Ar); 7,61 (dd, *J* = 8.7, 1H, C<u>H</u>); 7,58 (s, 2H, N<u>H</u>$_2$); 5.54 (s, 2H, N<u>H</u>$_2$); 5.10 (s, 1H, C<u>H</u>); 2.49 (s, 3H, C<u>H</u>$_3$); 2.31-2.16 (m, 2H, CH$_2$); 2.17-2.91 (m, 2H, CH$_2$), 1.90-1.66 (m, 2H, C<u>H</u>$_2$).

^{13}C-NMR (100 MHz, DMSO-*d*$_6$): *δ* (ppm) = 195.5 (C,<u>C</u>O); 153.7 (C,<u>C</u>NH$_2$); 151.5 (C, C=<u>C</u>-N); 149.1 (C, <u>C</u>-Cl); 145.6 (C, <u>C</u>q); 144.9 (C, <u>C</u>q); 139.4 (C, <u>C</u>q); 138.8 (C, <u>C</u>q); 137.7 (C, <u>C</u>q); 132.9 (C, <u>C</u>H-Ar); 131.7 (2C, <u>C</u>H-Ar); 128.2 (C, <u>C</u>H-Ar); 127.8 (2C, <u>C</u>H-Ar); 127.6 (C, <u>C</u>H-Ar); 127.1 (C, <u>C</u>H-Ar); 121.3 (C, <u>C</u>H-Ar); 112.0 (C, <u>C</u>N); 59.7 (C, <u>C</u>-CN); 56.5 (C, <u>C</u>H$_2$-CO); 36.32 (C, <u>C</u>H$_2$); 34.8 (C, <u>C</u>H); 21.6 (C, <u>C</u>H$_3$); 21.1 (C, <u>C</u>H$_2$).

Elemental analysis calcd. (%) for $C_{26}H_{22}ClN_5O_3S$ (**M.w** = 520.00 g/mol): C 60.05, H 4.26, N 13.47; **found** (%): C 60.11, H 4.41, N 13.56

*I.2.3.5 4-(2'-Amino-2-chloro-3'-cyano-6,7',7'-trimethyl-5'-oxo-5',6',7',8'-tetrahydro-3,4'-biquinolin-1'(4'H)-yl)benzenesulfonamide (**9e**)*

Following the general procedure, a mixture of quinolylidene methylene malononitrile (1.0 mmol), 5,5-dimethylcyclohexane-1,3-dione (1.0 mmol), sulfanilamide (1.0 mmol), and a catalytic amount of trimethylamine. Gave the product (**9e**).

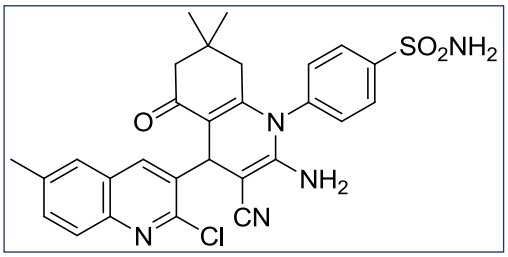

- ✓ ***Chemical Formula:*** $C_{28}H_{26}ClN_5O_3S$
- ✓ ***Molecular Weight:*** 548.06 g/mol
- ✓ ***Yield:*** 83%, (455 mg); yellow solid
- ✓ ***m.p:*** 301-302°C

FT-IR: *ν* (CO) = 1656 cm^{-1}, *ν* (NH) =3330 cm^{-1}, *ν* (CN) = 1170 cm^{-1}.

^{1}H-NMR (400 MHz, DMSO-d_6): δ(ppm) = 8.20 (s, 1H, C<u>H</u>-Ar); 8.02 (d, *J* = 8.0 Hz, 2H, C<u>H</u>-Ar); 7.87 (s, 1H, C<u>H</u>-Ar); 7.83 (d, *J* = 8.6 Hz, 1H, C<u>H</u>-Ar); 7.73 (d, *J* = 8.0 Hz, 2H, C<u>H</u>-Ar); 7,63 (s, 1H, C<u>H</u>); 7,60 (s, 2H, N<u>H</u>$_2$); 5.55 (s, 2H, N<u>H</u>$_2$); 5.09 (s, 1H, C<u>H</u>); 2.50 (s, 3H, C<u>H</u>$_3$); 2.17 (d, *J* = 15.5, 2H, C<u>H</u>$_2$); 1.97 (d, *J* = 16.0 Hz, 1H, C<u>H</u>$_2$), 1.82 (d, *J* = 17.3 Hz, 1H, C<u>H</u>$_2$); 0.89 (s, 3H, C<u>H</u>$_3$); 0.82 (s, 3H, C<u>H</u>$_3$).

^{13}C-NMR (100 MHz, DMSO-d_6): *δ* (ppm) = 195.3 (C, <u>C</u>O); 151.7 (C, <u>C</u>NH$_2$); 151.4 (C, C=<u>C</u>-N); 149.0 (C, <u>C</u>-Cl); 145.6 (C, <u>C</u>q); 144.9 (C, <u>C</u>q); 139.3 (C, <u>C</u>q); 137.3 (C, <u>C</u>q); 133.0 (C, <u>C</u>H-Ar); 131.7 (2C, <u>C</u>H-Ar); 128.0 (2C, <u>C</u>H-Ar); 127.6 (C, <u>C</u>H-Ar); 126.9 (C, <u>C</u>H-Ar); 121.3 (C, <u>C</u>H-Ar); 110.9 (C, <u>C</u>N); 65.4 (C, <u>C</u>CN); 59.7 (C, <u>C</u>H$_2$); 49.6 (C, <u>C</u>H$_2$); 35.3 (C, <u>C</u>H); 29.28 (C, <u>C</u>H$_3$); 27.52 (C, <u>C</u>H$_3$); 21.58 (C, <u>C</u>H$_3$).

Elemental analysis calcd. (%) for $C_{28}H_{26}ClN_5O_3S$ (**M.w** = 548.06 g/mol): C 61.36, H 4.78, N 12.78; **found** (%): C 61.29, H 5.06, N 12.57.

I.2.3.6 4-(6-Amino-4-(2-chloro-6-methylquinolin-3-yl)-5-cyano-3-methyl-1,3a,4,7a-tetrahydro-7H-pyrazolo[3,4-b]pyridin-7-yl)benzenesulfonamide (9f)

Following the general procedure, a mixture of quinolylidene methylene malononitrile (1.0 mmol), 3-methyl-1*H*-pyrazole-5-one (1.0 mmol), sulfanilamide (1.0 mmol), and a catalytic amount of trimethylamine. Gave the product (**9f)**.

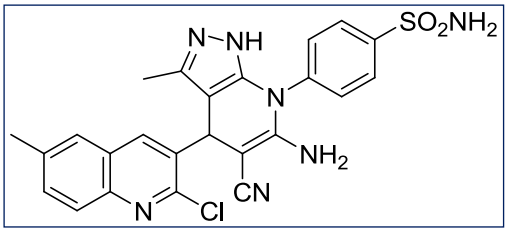

- ✓ ***Chemical Formula:*** $C_{24}H_{20}ClN_7O_2S$
- ✓ ***Molecular Weight:*** 505.98 g/mol
- ✓ ***Yield****:* 78%, (395 mg); Green-solid
- ✓ ***m.p****:* 216-218°C

FT-IR: *ν* (CO) = 1646 cm^{-1}, ν(NH)=3251 cm^{-1}, ν(CN)=1200 cm^{-1}.

^{1}H-NMR (400 MHz, DMSO-*d*$_6$): *δ* (ppm) = 12.18 (s, 1H, NH); 8.26 (s, 1H, CH-Ar); 8.02 (d, *J* = 8.0 Hz, 2H, CH-Ar); 7.85 (d, *J* = 8.6 Hz, 1H, CH-Ar); 7.83 (d, *J* = 8.6 Hz, 2H, CH-Ar); 7.81 (s, 1H, CH-Ar); 7,64 (d, *J* = 8.6 Hz, 1H, CH); 7,07 (s, 2H, NH_2); 5.17 (s, 1H, CH); 2.48 (s, 3H, CH_3); 1.76 (s, 3H, CH_3).

^{13}C-NMR (100 MHz, DMSO-*d*$_6$): *δ* (ppm) = 162.0 (C, CNH_2); 155.6 (C, C=C-N); 148.7 (C, C-Cl); 145.1(C, Cq); 139.3 (C, Cq); 137.7 (C, Cq); 136.0 (C, Cq); 133.4 (C, CH-Ar); 127.7 (2C, CH-Ar); 127.0 (C, CH-Ar); 120.9 (C, CH-Ar); 21.6 (C, CH_3); 10.1 (C, CH_3).

Elemental analysis calcd. (%) for $C_{24}H_{20}ClN_7O_2S$ (**M.w** = 505.98 g/mol): C 56.75, H 4.37, N 19.30; **found** (%): C 56.62, H 4.17, N 19.50

*I.2.3.7 4-(6-Amino-4-(2-chloro-6-methylquinolin-3-yl)-5-cyano-3-methyl-1-phenyl-1,3a,4,7a-tetrahydro-7H-pyrazolo[3,4-b]pyridin-7-yl)benzenesulfonamide (**9g**)*

Following the general procedure, a mixture of quinolylidene methylene malononitrile (1.0 mmol), 3-methyl-1-phenyl-2-pyrazole-5-one (1.0 mmol), sulfanilamide (1.0 mmol), and a catalytic amount of trimethylamine. Gave the product **9g**

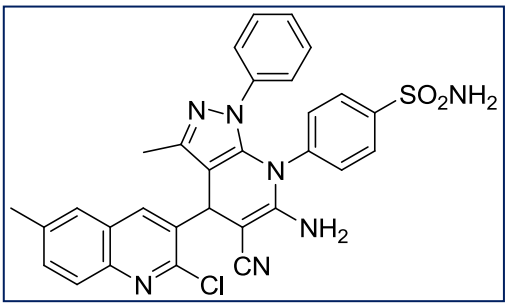

- ✓ ***Chemical Formula:*** $C_{30}H_{24}ClN_7O_2S$
- ✓ ***Molecular Weight:*** 582.08 g/mol
- ✓ ***Yield****:* 73%, (424 mg); White solid
- ✓ ***m.p****:* 199-201°C

FT-IR: *ν* (CO) = 1651 cm^{-1}, *ν* (NH) =3330 cm^{-1}, *ν* (CN) =1183 cm^{-1}.

^{1}H-NMR (400 MHz, DMSO-d_6): *δ* (ppm) = 8.22 (s, 1H, C<u>H</u>-Ar); 7.33-7.86 (M, 12H, C<u>H</u>-Ar); 7,16 (s, 2H, N<u>H</u>$_2$); 5.25 (s, 1H, C<u>H</u>); 2.48 (s, 3H, C<u>H</u>$_3$); 1.76 (s, 3H, C<u>H</u>$_3$).

^{13}C-NMR (100 MHz, DMSO-d_6): *δ* (ppm) = 139.8 (C, <u>C</u>q); 139.6 (C, <u>C</u>q); 127.9 (C, <u>C</u>H-Ar); 127.3 (C, <u>C</u>H-Ar); 127.7 (C, <u>C</u>H-Ar); 127.3 (C, <u>C</u>H-Ar); 127.0 (C, <u>C</u>H-Ar); 126.5 (C, <u>C</u>H-Ar); 120.5 (C, <u>C</u>H-Ar); 118.4 (2C, <u>C</u>H-Ar); 21.4 (C, <u>C</u>H$_3$); 13.0 (C, <u>C</u>H$_3$).

Elemental analysis calcd. (%) for $C_{30}H_{24}ClN_7O_2S$ (**M.w** = 582.08 g/mol): C 61.90, H 4.16, N 16.84; **found** (%): C 61.79, H 4.45, N 16.88.

I.3 General procedures of the biological evaluation

I.3.1 ABTS Scavenging Activity

The evaluation of antioxidant activity was done using the stable $ABTS^{\bullet+}$ (2,2'-azino-bis(3-ethylbenzothiazoline-6-sulfonic acid)) method in 96-well microplates. The ABTS radical cation was produced by mixing 7 mM ABTS with 2.45 mM potassium persulfate in a 2:1 ratio and allowing it to sit for 16 hours in the dark at room temperature to generate the cation $ABTS^{+}$. The stock solution was then diluted with distilled water and mixed with 40 µL of each sample of the compounds in methanol at varying concentrations with 160 µL of the ABTS mixture. The mixture was stored in the dark for 10 minutes and the absorbance was measured at 734 nm. The antioxidant activity was expressed as the IC_{50} value, which is the dose of the extract required to reduce the absorbance by 50%. A lower IC_{50} value indicates a higher antioxidant activity. BHA and BHT were used as reference antioxidants. The inhibition rate was calculated using the following formula: % Inhibition $= \frac{Abs517\ blank - bs517\ blank}{bs517\ blank}\ 100.$

I.3.2 CUPRAC assay

The procedure was done by testing our sample for its reduction capability by adding various concentrations (40 µL) to a reaction mixture consisting of 60 µL CH_3COONH_4 buffer (1 mL, 1 M, pH 7.0), 50 µL CuCl2 (1 mL, 10 mM), and 50 µL Neocuprine (1 mL, 7.5 mM). The mixture was incubated in the dark at room temperature for 1 hour. The absorbance was then measured at 450 nm using a Perkin Elmer Enspire microplate reader in Singapore. An increase in absorbance indicates increased reduction capability, which was expressed as ascorbic acid equivalent (AAE). *BHA* and *BHT* were used as reference antioxidants. The concentration, given an absorbance of 0.5 (A0.5), was calculated from the absorbance curve at different concentrations. A blank sample was also prepared and analyzed without the sample to serve as a reference.

I.3.3 O-Phenanthroline assay

The sample was tested with *O*-Phenanthroline Chelating assay by adding various concentrations (10 µL) to a reaction mixture consisting of 50 µL Ferric chloride $FeCl_3$ (0.2%), 30 µL *O*-Phenanthroline methanol solution (0.5%), and 110 M methanol, and incubated them at room temperature for 20 min before the analysis. An orange-red solution absorbance was detected at 510 nm using a 96-well microplate reader. BHT and BHA were used as the standards.

I.3.4 Galvinoxyl Radical (GOR) scavenging assay

In this experiment, 160 µL of Galvinoxyl methanolic solution at 0.1 mM was mixed with 40 µL of different 4*H*-pyran samples concentrations in methanol. Using a spectrophotometer at 428 nm, the absorbance of the resulting solution was measured after 120 min of incubation at room temperature in darkness. The standards were BHT and BHA. Galvinoxyl's methanolic solution was employed as a control for this test. The inhibition percentage I (%) was expressed as follows: Inhibition (%) = [(A (Control) − A (Sample)/A (Control)] × 100

General conclusion

This thesis is divided into two chapters preceded by a general introduction and followed by a general conclusion. Through our research efforts, we have achieved our main objective by creating and examining a total of 35 novel compounds known as sumurase

The first chapter of the research focuses on creating new complexes of silver and palladium *N*-heterocyclic carbenes. As well as their precursor salts which are based on the benzimidazole heterocycle in order to test on the one hand their biological capacity and on the other hand their catalytic potential in direct arylation reactions.

After a bibliographical overview of biological, propriety, synthesis, and the use of *N*-heterocyclic carbenes, we describe the preparation of the new series of benzimidazolium salts as *N*-heterocyclic carbene precursors and their related Ag-NHCs and the PEPPSI type Pd-NHCs complexes. All the complexes are original and obtained with excellent yields.

The biological activity of the newly synthesized compounds was evaluated *in vitro*, revealing significant *anti-microbial* and inhibitory properties against several enzymes, including *AChE*, *BChE*, *α-amylase*, and *lipase*. Additionally, the experimental results obtained in vitro evaluations were compared to the results obtained through molecular docking. It was observed that the experimental data and the molecular docking results were in perfect agreement, further validating the effectiveness and accuracy of the molecular docking approach used in this study.

On the other hand, the catalytic effect of all Pd-NHC complexes PEPPSI type was evaluated in the direct arylation reaction at the C5 and C2 position from 2-acetyl furan, furfural, and 2-acetyl-thiophene by arylbromides. All palladium complexes gave excellent catalytic effects.

Overall, these findings contribute to the development of new and potent *N*-heterocyclic carbene complexes with potential applications in both, catalysis and bioactive molecule discovery.

In the second chapter, the research centers on the synthesis of novel hybrid quinoline-heterocycle compounds in the aime to create new hybrid heterocycles with multitarget bioactive properties.

After a brief bibliographical overview focusing on the biological interest of some quinoline, 4*H*-pyran, and 1,4-dihydropyridine derivatives, we exposed the most used synthesis methods associated type of compound. The subsequent sections of the chapter focus on the synthesis of new hybrid compounds. Specifically, the synthesis of functionalized rigid system quinoline-4*H*-pyran hybrid derivatives, as well as their related tacrine analogs and quinoline-1,4-dihydropyridine-*N*-substituted hybrid derivatives via the multicomponent reaction. Indeed, some of the new compounds prepared were tested for their biological activity.

All parts are completed by an experimental part where all the procedures implemented are described. The compounds prepared were identified by the usual spectroscopic methods (IR, ^{1}H, and ^{13}C NMR) and for some of them, additional analyzes were carried out (masse spectroscopy, elemental analysis, and/or X-ray diffraction). As well as the result for representative molecules has been confirmed on their electronic, vibrational, thermodynamic, and optical properties by Density Functional Theory (DFT) calculations.

Finally, the results obtained from the synthesis and characterization of these compounds have been presented, commented and discussed in detail on in the results and discussion section. The implications and significance of these results in relation to the research objectives are thoroughly examined and analyzed.

Parts of this thesis have been published in the following journal articles:

- Silver (I)-N-heterocyclic carbene complexes: Synthesis and characterization, biological evaluation of Anti-Cholinesterase, anti-Alpha-amylase, anti-Lipase, and antibacterial activities, and molecular docking study **June 2021, Inorganica Chimica Acta 525(3):120486, DOI: 10.1016/j.ica.2021.120486**

- Synthesis, structures, DFT calculations, and catalytic application in the direct arylation of five-membered heteroarenes with aryl bromides of novel Palladium-N-Heterocyclic carbene complexes PEPPSI-Type **August 2021, New Journal of Chemistry / DOI: 10.1039/D1NJ03388C**

- New benzimidazolium N-heterocyclic carbene precursors and their related Pd-NHC complex PEPPSI-type: Synthesis, structures, DFT calculations, biological activity, docking study, and catalytic application in the direct arylation. **September 2021, Journal of Molecular Structure / DOI: 10.1016/j.molstruc.2021.131504**

References

[1] A.L. Harvey, R. Edrada-Ebel, R.J. Quinn, The re-emergence of natural products for drug discovery in the genomics era, Nature Reviews Drug Discovery. 14 (2015) 111–129.

[2] M. Dickson, J.P. Gagnon, Key factors in the rising cost of new drug discovery and development, Nature Reviews Drug Discovery. 3 (2004) 417–429.

[3] Eicher, S. Hauptmann, The Chemistry of Heterocycles, Wiley VCH, 2003.

[4] B.C.G. Soderberg, Synthesis of heterocycles via intramolecular annulation of nitrene intermediates, Current Organic Chemistry. 4 (2000) 727–764.

[5] İ. Özdemir, S. Demir, S. Günal, İ. Özdemir, C. Arıcı, D. Ülkü, Synthesis, characterization and antimicrobial activity of new silver complexes with N-heterocyclic carbene ligands, Inorganica Chimica Acta. 363 (2010) 3803–3808.

[6] İ. Özdemir, O. Ciftci, E. Evren, N. Gürbüz, N. Kaloğlu, N.B. Türkmen, Ş. Yaşar, E. Üstün, N. Hamdi, L. Mansour, Synthesis, characterization and antitumor properties of novel silver (I) and gold (I) N-heterocyclic carbene complexes, Inorganica Chimica Acta. 506 (2020) 119530.

[7] D. Bourissou, O. Guerret, F.P. Gabbaï, G. Bertrand, Stable Carbenes, Chemical Reviews. 100 (2000) 39–91. https://doi.org/10.1021/cr940472u.

[8] W. von E. Doering, A.K. Hoffmann, The addition of dichlorocarbene to olefins, Journal of the American Chemical Society. 76 (1954) 6162–6165.

[9] E.O. Fischer, A. Maasböl, Zur Frage eines Wolfram-Carbonyl-Carben-Komplexes, Angewandte Chemie. 76 (1964) 645.

[10] S. Diez-Gonzalez, N. Marion, S.P. Nolan, N-heterocyclic carbenes in late transition metal catalysis, Chemical Reviews. 109 (2009) 3612–3676.

[11] D. Enders, O. Niemeier, A. Henseler, Organocatalysis by N-heterocyclic carbenes, Chemical Reviews. 107 (2007) 5606–5655.

[12] R. Kılınçarslan, N. Sadıç, Catalytic activity of N-heterocyclic carbene silver complexes derived from imidazole ligands, Inorganic and Nano-Metal Chemistry. 47 (2017) 462–466. https://doi.org/10.1080/15533174.2016.1186054.

[13] H. Lv, L. Zhu, Y. Tang, J. Lu, Structure–activity relationship of N-heterocyclic carbene–Pd (II)–imidazole complexes in Suzuki–Miyaura coupling between 4-methoxyphenyl chloride and phenylboronic acid, Applied Organometallic Chemistry. 28 (2014) 27–31.

[14] W. Sikorski, W. Zawartka, A.M. Trzeciak, PEPPSI-type complexes with small NHC ligands obtained according to the new method efficiently catalyzed Suzuki-Miyaura reaction, Journal of Organometallic Chemistry. 867 (2018) 323–332.

[15] G. Onar, C. Gürses, M.O. Karataş, S. Balcıoğlu, N. Akbay, N. Özdemir, B. Ateş, B. Alıcı, Palladium (II) and ruthenium (II) complexes of benzotriazole functionalized N-heterocyclic carbenes: Cytotoxicity, antimicrobial, and DNA interaction studies, Journal of Organometallic Chemistry. 886 (2019) 48–56.

[16] A. Gautier, F. Cisnetti, Advances in metal–carbene complexes as potent anti-cancer agents, Metallomics. 4 (2012) 23–32.

[17] M.C. Perry, K. Burgess, Chiral N-heterocyclic carbene-transition metal complexes in asymmetric catalysis, Tetrahedron: Asymmetry. 14 (2003) 951–961.

[18] F. Glorius, N-heterocyclic carbenes in transition metal catalysis, Springer, 2007.

[19] M.G. Organ, G.A. Chass, D.-C. Fang, A.C. Hopkinson, C. Valente, Pd-NHC (PEPPSI) complexes: Synthetic utility and computational studies into their reactivity, Synthesis. 2008 (2008) 2776–2797.

[20] C.C.C. Johansson Seechurn, M.O. Kitching, T.J. Colacot, V. Snieckus, Palladium-catalyzed cross-coupling: a historical contextual perspective to the 2010 Nobel Prize, Angewandte Chemie International Edition. 51 (2012) 5062–5085.

[21] N. Marion, S.P. Nolan, Well-defined N-heterocyclic carbenes− palladium (II) precatalysts for cross-coupling reactions, Accounts of Chemical Research. 41 (2008) 1440–1449.

[22] F. Bellina, R. Rossi, Transition metal-catalyzed direct arylation of substrates with activated sp3-hybridized C− H bonds and some of their synthetic equivalents with aryl halides and pseudohalides, Chemical Reviews. 110 (2010) 1082–1146.

[23] T. Satoh, M. Miura, Catalytic direct arylation of heteroaromatic compounds, Chemistry Letters. 36 (2007) 200–205.

[24] J.-B. Dumas, E.M. Peligot, Mémoire sur l'esprit de bois et sur les divers composés éthérés qui en proviennent, 1835.

[25] A.J. Arduengo III, R. Krafczyk, Auf der Suche nach stabilen Carbenen, Chemie in Unserer Zeit. 32 (1998) 6–14.

[26] H. Wanzlick, Nucleophile Carben-Chemie, Angewandte Chemie. 74 (1962) 129–134.

[27] E.O. Fischer, A. Maasböl, On the existence of a tungsten carbonyl carbene complex, Angewandte Chemie International Edition in English. 3 (1964) 580–581.

[28] A. Igau, H. Grutzmacher, A. Baceiredo, G. Bertrand, Analogous. alpha.,. alpha.'-bis-carbenoid, triply bonded species: synthesis of a stable. lambda. 3-phosphino carbene-. lambda. 5-phosphaacetylene, Journal of the American Chemical Society. 110 (1988) 6463–6466.

[29] A.J. Arduengo III, R.L. Harlow, M. Kline, A stable crystalline carbene, Journal of the American Chemical Society. 113 (1991) 361–363.

[30] W.A. Herrmann, M. Elison, J. Fischer, C. Köcher, G.R.J. Artus, Metallkomplexe heterocyclischer Carbene-ein neues Katalysator-Strukturprinzip in der homogenen Katalyse, Angewandte Chemie. 107 (1995) 2602–2605.

[31] A.J. Arduengo, Looking for stable carbenes: The difficulty in starting anew, Accounts of Chemical Research. 32 (1999) 913–921. https://doi.org/10.1021/ar980126p.

[32] F.E. Hahn, L. Wittenbecher, R. Boese, D. Bläser, N, N′-Bis (2, 2-dimethylpropyl) benzimidazolin-2-ylidene: A Stable Nucleophilic Carbene Derived from Benzimidazole, Chemistry–A European Journal. 5 (1999) 1931–1935.

[33] C.S.J. Cazin, N-Heterocyclic carbenes in transition metal catalysis and organocatalysis, Springer Science & Business Media, 2010.

[34] G.D. Frey, M. Song, J.-B. Bourg, B. Donnadieu, M. Soleilhavoup, G. Bertrand, A persistent P, N-heterocyclic carbene, Chemical Communications. (2008) 4711–4713.

[35] D.A. Dixon, A.J. Arduengo III, Electronic structure of a stable nucleophilic carbene, The Journal of Physical Chemistry. 95 (1991) 4180–4182.

[36] O. Schuster, L. Yang, H.G. Raubenheimer, M. Albrecht, Beyond conventional N-heterocyclic carbenes: abnormal, remote, and other classes of NHC ligands with reduced heteroatom stabilization, Chemical Reviews. 109 (2009) 3445–3478.

[37] J. Velık, V. Baliharova, J. Fink-Gremmels, S. Bull, J. Lamka, L. Skálová, Benzimidazole drugs and modulation of biotransformation enzymes, Research in Veterinary Science. 76 (2004) 95–108.

[38] I. Tamm, K. Folkers, C.H. Shunk, F.L. Horsfall Jr, Inhibition of influenza virus multiplication by N-glycosides of benzimidazoles, The Journal of Experimental Medicine. 99 (1954) 227–250.

[39] J. Raaf, E. Brunstein, O.-G. Issinger, K. Niefind, The CK2α/CK2β interface of human protein kinase CK2 harbors a binding pocket for small molecules, Chemistry & Biology. 15 (2008) 111–117.

[40] D. Kumar, M.R. Jacob, M.B. Reynolds, S.M. Kerwin, Synthesis and evaluation of anticancer benzoxazoles and benzimidazoles related to UK-1, Bioorganic & Medicinal Chemistry. 10 (2002) 3997–4004.

[41] Y. He, B. Wu, J. Yang, D. Robinson, L. Risen, R. Ranken, L. Blyn, S. Sheng, E.E. Swayze, 2-Piperidin-4-yl-benzimidazoles with broad spectrum antibacterial activities, Bioorganic & Medicinal Chemistry Letters. 13 (2003) 3253–3256.

[42] H. Göker, C. Kuş, D.W. Boykin, S. Yildiz, N. Altanlar, Synthesis of some new 2-substituted-phenyl-1H-benzimidazole-5-carbonitriles and their potent activity against Candida species, Bioorganic & Medicinal Chemistry. 10 (2002) 2589–2596.

[43] W.-L. Wu, D.A. Burnett, M.A. Caplen, M.S. Domalski, C. Bennett, W.J. Greenlee, B.E. Hawes, K. O'Neill, B. Weig, D. Weston, Design and synthesis of orally efficacious benzimidazoles as melanin-concentrating hormone receptor 1 antagonists, Bioorganic & Medicinal Chemistry Letters. 16 (2006) 3674–3678.

[44] H. Minoura, S. Takeshita, M. Ita, J. Hirosumi, M. Mabuchi, I. Kawamura, S. Nakajima, O. Nakayama, H. Kayakiri, T. Oku, Pharmacological characteristics of a novel nonthiazolidinedione insulin sensitizer, FK614, European Journal of Pharmacology. 494 (2004) 273–281.

[45] G. Navarrete-Vázquez, H. Moreno-Diaz, F. Aguirre-Crespo, I. León-Rivera, R. Villalobos-Molina, O. Munoz-Muniz, S. Estrada-Soto, Design, microwave-assisted synthesis, and spasmolytic activity of 2-(alkyloxyaryl)-1H-benzimidazole derivatives as constrained stilbene bioisosteres, Bioorganic & Medicinal Chemistry Letters. 16 (2006) 4169–4173.

[46] H. Nakano, T. Inoue, N. Kawasaki, H. Miyataka, H. Matsumoto, T. Taguchi, N. Inagaki, H. Nagai, T. Satoh, Synthesis and biological activities of novel antiallergic agents with 5-lipoxygenase inhibiting action, Bioorganic & Medicinal Chemistry. 8 (2000) 373–380.

[47] R.J. Snow, A. Abeywardane, S. Campbell, J. Lord, M.A. Kashem, H.H. Khine, J. King, J.A. Kowalski, S.S. Pullen, T. Roma, Hit-to-lead studies on benzimidazole inhibitors of ITK: discovery of a novel class of kinase inhibitors, Bioorganic & Medicinal Chemistry Letters. 17 (2007) 3660–3665.

[48] S. V Malhotra, V. Kumar, A profile of the in vitro anti-tumor activity of imidazolium-based ionic liquids, Bioorganic & Medicinal Chemistry Letters. 20 (2010) 581–585.

[49] C. Hemmert, A. Fabié, A. Fabre, F. Benoit-Vical, H. Gornitzka, Synthesis, structures, and antimalarial activities of some silver(I), gold(I) and gold(III) complexes involving N-heterocyclic carbene ligands, European Journal of Medicinal Chemistry. (2013). https://doi.org/10.1016/j.ejmech.2012.11.038.

[50] U.E.I. Horvath, G. Bentivoglio, M. Hummel, H. Schottenberger, K. Wurst, M.J. Nell, C.E.J. van Rensburg, S. Cronje, H.G. Raubenheimer, A cytotoxic bis (carbene) gold (I) complex of ferrocenyl complexes: synthesis and structural characterisation, New Journal of Chemistry. 32 (2008) 533–539.

[51] B. PJ, Baker MV. Berners-Price SJ. Skelton BW, White AH. J. Chem. Soc., Dalton Trans. 1038 (2004).

[52] S.J. Berners-Price, C.K. Mirabelli, R.K. Johnson, M.R. Mattern, F.L. McCabe, L.F. Faucette, C.-M. Sung, S.-M. Mong, P.J. Sadler, S.T. Crooke, In vivo antitumor activity and in vitro cytotoxic properties of bis [1, 2-bis (diphenylphosphino) ethane] gold (I) chloride, Cancer Research. 46 (1986) 5486–5493.

[53] Y. Li, K. Hindi, K.M. Watts, J.B. Taylor, K. Zhang, Z. Li, D.A. Hunstad, C.L. Cannon, W.J. Youngs, K.L. Wooley, Shell crosslinked nanoparticles carrying silver antimicrobials as therapeutics, Chemical Communications. 46 (2010) 121–123.

[54] W.J. Youngs, D.A. Medvetz, K.M. Hindi, M.J. Panzner, A.J. Ditto, Y.H. Yun, Anticancer activity of Ag(I) N-heterocyclic carbene complexes derived from 4,5-dichloro-1H-imidazole, Metal-Based Drugs. (2008). https://doi.org/10.1155/2008/384010.

[55] M.-L. Teyssot, A.-S. Jarrousse, M. Manin, A. Chevry, S. Roche, F. Norre, C. Beaudoin, L. Morel, D. Boyer, R. Mahiou, Metal-NHC complexes: a survey of anti-cancer properties, Dalton Transactions. (2009) 6894–6902.

[56] D.C.F. Monteiro, R.M. Phillips, B.D. Crossley, J. Fielden, C.E. Willans, Enhanced cytotoxicity of silver complexes bearing bidentate N-heterocyclic carbene ligands, Dalton Transactions. 41 (2012) 3720–3725.

[57] S. Ray, R. Mohan, J.K. Singh, M.K. Samantaray, M.M. Shaikh, D. Panda, P. Ghosh, Anticancer and antimicrobial metallopharmaceutical agents based on palladium, gold, and silver N-heterocyclic carbene complexes, Journal of the American Chemical Society. 129 (2007) 15042–15053.

[58] C.-H. Wang, W.-C. Shih, H.C. Chang, Y.-Y. Kuo, W.-C. Hung, T.-G. Ong, W.-S. Li, Preparation and characterization of amino-linked heterocyclic carbene palladium, gold, and silver complexes and their use as anticancer agents that act by triggering apoptotic cell death, Journal of Medicinal Chemistry. 54 (2011) 5245–5249.

[59] L. Perrin, E. Clot, O. Eisenstein, J. Loch, R.H. Crabtree, Computed ligand electronic parameters from quantum chemistry and their relation to Tolman parameters, lever parameters, and Hammett constants, Inorganic Chemistry. 40 (2001) 5806–5811.

[60] W. Kirmse, Stable Singlet Carbenes—Plentiful and Versatile, Angewandte Chemie International Edition. 43 (2004) 1767–1769.

[61] K.C. Harper, E.N. Bess, M.S. Sigman, Multidimensional steric parameters in the analysis of asymmetric catalytic reactions, Nature Chemistry. 4 (2012) 366–374.

[62] C.A. Tolman, Steric effects of phosphorus ligands in organometallic chemistry and homogeneous catalysis, Chemical Reviews. 77 (1977) 313–348.

[63] C.A. Tolman, Phosphorus ligand exchange equilibriums on zerovalent nickel. Dominant role for steric effects, Journal of the American Chemical Society. 92 (1970) 2956–2965.

[64] J. Huang, H.-J. Schanz, E.D. Stevens, S.P. Nolan, Stereoelectronic effects characterizing nucleophilic carbene ligands bound to the Cp* RuCl (Cp*= η5-C5Me5) moiety: A structural and thermochemical investigation, Organometallics. 18 (1999) 2370–2375.

[65] B. Maji, M. Breugst, H. Mayr, N-heterocyclic carbenes: organocatalysts with moderate nucleophilicity but extraordinarily high Lewis basicity, Angewandte Chemie International Edition. 50 (2011) 6915–6919.

[66] R.W. Alder, M.E. Blake, L. Chaker, J.N. Harvey, F. Paolini, J. Schütz, When and how do diaminocarbenes dimerize?, Angewandte Chemie International Edition. 43 (2004) 5896–5911.

[67] A.J. Arduengo III, JC calabrese, F. Davidson, HVR Dias, JR Goerlich, R. Krafczyk, WJ Marshall, M. Tamm, R. Schmutzler, Helv. Chim. Acta. 82 (1999) 2348.

[68] H.W. Wanzlick, Aspects of nucleophilic carbene chemistry, Angewandte Chemie International Edition in English. 1 (1962) 75–80.

[69] T.M. Trnka, J.P. Morgan, M.S. Sanford, T.E. Wilhelm, M. Scholl, T.-L. Choi, S. Ding, M.W. Day, R.H. Grubbs, Synthesis and activity of ruthenium alkylidene complexes coordinated with phosphine and N-heterocyclic carbene ligands, Journal of the American Chemical Society. 125 (2003) 2546–2558.

[70] A.M. Voutchkova, M. Feliz, E. Clot, O. Eisenstein, R.H. Crabtree, Imidazolium carboxylates as versatile and selective N-heterocyclic carbene transfer agents: synthesis, mechanism, and applications, Journal of the American Chemical Society. 129 (2007) 12834–12846.

[71] L. Benhamou, E. Chardon, G. Lavigne, S. Bellemin-Laponnaz, V. Cesar, Synthetic routes to N-heterocyclic carbene precursors, Chemical Reviews. 111 (2011) 2705–2733.

[72] A.J. Arduengo III, H.V.R. Dias, RL Harlow en M. Kline, J. Am. Chem. Soc. 113 (1991) 361–363.

[73] N. Kuhn, T. Kratz, Synthesis of imidazol-2-ylidenes by reduction of imidazole-2 (3H)-thiones, Synthesis. 1993 (1993) 561–562.

[74] M. Scholl, S. Ding, C.W. Lee, R.H. Grubbs, Synthesis and activity of a new generation of ruthenium-based olefin metathesis catalysts coordinated with 1, 3-dimesityl-4, 5-dihydroimidazol-2-ylidene ligands, Organic Letters. 1 (1999) 953–956.

[75] L. Hintermann, Expedient syntheses of the N-heterocyclic carbene precursor imidazolium salts IPr· HCl, IMes· HCl and IXy· HCl, Beilstein Journal of Organic Chemistry. 3 (2007) 22.

[76] A.J. Arduengo III, R. Krafczyk, R. Schmutzler, H.A. Craig, J.R. Goerlich, W.J. Marshall, M. Unverzagt, Imidazolylidenes, imidazolinylidenes and imidazolidines, Tetrahedron. 55 (1999) 14523–14534.

[77] P. de Fremont, N. Marion, S.P. Nolan, Carbenes: Synthesis, properties, and organometallic chemistry, Coordination Chemistry Reviews. 253 (2009) 862–892.

[78] F.E. Hahn, M.C. Jahnke, Heterocyclic carbenes: synthesis and coordination chemistry, Angewandte Chemie International Edition. 47 (2008) 3122–3172.

[79] A.J. Arduengo III, H.V.R. Dias, J.C. Calabrese, F. Davidson, Homoleptic carbene-silver (I) and carbene-copper (I) complexes, Organometallics. 12 (1993) 3405–3409.

[80] C. Ci, H. Yu, S. Wan, J. Liu, C.-C. Sun, ERRATUM Bull. Korean Chem. Soc. 2011, Vol. 32, No. 4, pp 1187~ 1194, BULLETIN OF THE KOREAN CHEMICAL SOCIETY. 32 (2011) 2501–2502.

[81] P. De Fremont, N.M. Scott, E.D. Stevens, T. Ramnial, O.C. Lightbody, C.L.B. Macdonald, J.A.C. Clyburne, C.D. Abernethy, S.P. Nolan, Synthesis of well-defined N-heterocyclic carbene silver (I) complexes, Organometallics. 24 (2005) 6301–6309.

[82] O. Guerret, S. Solé, H. Gornitzka, M. Teichert, G. Trinquier, G. Bertrand, 1, 2, 4-Triazole-3, 5-diylidene: A building block for organometallic polymer synthesis, Journal of the American Chemical Society. 119 (1997) 6668–6669.

[83] H.M.J. Wang, I.J.B. Lin, Facile synthesis of silver (I)− carbene complexes. Useful carbene transfer agents, Organometallics. 17 (1998) 972–975.

[84] D.J. Cardin, B. Cetinkaya, E. Cetinkaya, M.F. Lappert, L.J. Manojlović-Muir, K.W. Muir, trans/cis-isomerism and isomerisation of PdII and PtII carbene complexes; The crystal and molecular structures of cis-and trans-PtCl2 [C (NPhCH2) 2] PEt3, Journal of Organometallic Chemistry. 44 (1972) C59–C62.

[85] F.E. Hahn, T. von Fehren, T. Lügger, The palladium complexes of a C3-bridged di (benzimidazol-2-ylidene) ligand via cleavage of a dibenzotetraazafulvalene, Inorganica Chimica Acta. 358 (2005) 4137–4144.

[86] D. Enders, H. Gielen, G. Raabe, J. Runsink, J.H. Teles, Synthesis and Stereochemistry of the First Chiral (Imidazolinylidene)-and (Triazolinylidene) palladium (ii) Complexes, Chemische Berichte. 129 (1996) 1483–1488.

[87] C. Dash, M.M. Shaikh, R.J. Butcher, P. Ghosh, A comparison between nickel and palladium precatalysts of 1, 2, 4-triazole based N-heterocyclic carbenes in hydroamination of activated olefins, Dalton Transactions. 39 (2010) 2515–2524.

[88] M.S. Viciu, S.P. Nolan, The Use of N-Heterocyclic Carbenes as Ligands in Palladium-Mediated Catalysis, Palladium in Organic Synthesis. (2005) 241–278.

[89] M.S. Viciu, R.M. Kissling, E.D. Stevens, S.P. Nolan, An air-stable palladium/N-heterocyclic carbene complex and its reactivity in aryl amination, Organic Letters. 4 (2002) 2229–2231.

[90] C.J. O'Brien, E.A.B. Kantchev, C. Valente, N. Hadei, G.A. Chass, A. Lough, A.C. Hopkinson, M.G. Organ, Easily prepared air-and moisture-stable Pd–NHC (NHC= N-heterocyclic carbene) complexes: a reliable, user-friendly, highly active palladium precatalyst for the Suzuki–Miyaura reaction, Chemistry–A European Journal. 12 (2006) 4743–4748.

[91] G.W. Nyce, S. Csihony, R.M. Waymouth, J.L. Hedrick, A general and versatile approach to thermally generated N-heterocyclic carbenes, Chemistry–A European Journal. 10 (2004) 4073–4079.

[92] M. V Baker, D.H. Brown, V.J. Hesler, B.W. Skelton, A.H. White, Synthesis of a Bis (N-heterocyclic carbene) palladium Complex via Oxidative Addition of a C− C Bond in a Biimidazolium Ion, Organometallics. 26 (2007) 250–252.

[93] K.M. Hindi, M.J. Panzner, C.A. Tessier, C.L. Cannon, W.J. Youngs, The Medicinal applications of

imidazolium carbene− metal complexes, Chemical Reviews. 109 (2009) 3859–3884.

[94] C.I. Ezugwu, N.A. Kabir, M. Yusubov, F. Verpoort, Metal–organic frameworks containing N-heterocyclic carbenes and their precursors, Coordination Chemistry Reviews. 307 (2016) 188–210.

[95] L. Mercs, M. Albrecht, Beyond catalysis: N-heterocyclic carbene complexes as components for medicinal, luminescent, and functional materials applications, Chemical Society Reviews. 39 (2010) 1903–1912.

[96] A. V Zhukhovitskiy, M.J. MacLeod, J.A. Johnson, Carbene ligands in surface chemistry: from stabilization of discrete elemental allotropes to modification of nanoscale and bulk substrates, Chemical Reviews. 115 (2015) 11503–11532.

[97] C. Bolm, M. Beller, Transition metals for organic synthesis, Wiley-VCH: Weinheim, 2004.

[98] L. Ackermann, Modern arylation methods, Wiley Online Library, 2009.

[99] J. Ramírez, R. Corberán, M. Sanaú, E. Peris, E. Fernandez, Unprecedented use of silver (I) N-heterocyclic carbene complexes for the catalytic preparation of 1, 2-bis (boronate) esters, Chemical Communications. (2005) 3056–3058.

[100] D. Wang, B. Zhang, C. He, P. Wu, C. Duan, A new chiral N-heterocyclic carbene silver (I) cylinder: synthesis, crystal structure and catalytic properties, Chemical Communications. 46 (2010) 4728–4730.

[101] J. Iglesias-Sigüenza, A. Ros, E. Díez, A. Magriz, A. Vázquez, E. Alvarez, R. Fernández, J.M. Lassaletta, C 2-Symmetric S/C/S ligands based on N-heterocyclic carbenes: a new ligand architecture for asymmetric catalysis, Dalton Transactions. (2009) 8485–8488.

[102] A. Prieto, M.R. Fructos, M.M. Díaz-Requejo, P.J. Perez, P. Perez-Galan, N. Delpont, A.M. Echavarren, Gold-catalyzed olefin cyclopropanation, Tetrahedron. 65 (2009) 1790–1793.

[103] Z. Wang, J. Wen, Q.-W. Bi, X.-Q. Xu, Z.-Q. Shen, X.-X. Li, Z. Chen, Oxirane synthesis from diazocarbonyl compounds via NHC-Ag+ catalysis, Tetrahedron Letters. 55 (2014) 2969–2972.

[104] S. Sakaguchi, T. Kubo, Y. Ishii, A Three-Component Coupling Reaction of Aldehydes, Amines, and Alkynes, Angewandte Chemie. 113 (2001) 2602–2604.

[105] C. Fischer, E.M. Carreira, Direct addition of TMS-acetylene to aldimines catalyzed by a simple, commercially available Ir (I) complex, Organic Letters. 3 (2001) 4319–4321.

[106] C. Wei, C.-J. Li, Enantioselective direct-addition of terminal alkynes to imines catalyzed by copper (I) pybox complex in water and in toluene, Journal of the American Chemical Society. 124 (2002) 5638–5639.

[107] M.T. Chen, B. Landers, O. Navarro, Well-defined (N-heterocyclic carbene)-Ag(i) complexes as catalysts for A 3 reactions, Organic and Biomolecular Chemistry. 10 (2012) 2206–2208. https://doi.org/10.1039/c2ob06900h.

[108] X. Tang, C. Qi, H. He, H. Jiang, Y. Ren, G. Yuan, Polystyrene-supported N-heterocyclic carbene–silver complexes as robust and efficient catalysts for the reaction of carbon dioxide and propargylic alcohols, Advanced Synthesis & Catalysis. 355 (2013) 2019–2028.

[109] J. Ramırez, R. Corberán, M. Sanau ú, E. Peris and E. Fernández, Chem. Commun. 3056 (2005).

[110] W.A. Herrmann, M. Elison, J. Fischer, C. Köcher, G.R.J. Artus, Metal complexes of N-heterocyclic carbenes—a new structural principle for catalysts in homogeneous catalysis, Angewandte Chemie International Edition in English. 34 (1995) 2371–2374.

[111] M.G. Organ, S. Avola, I. Dubovyk, N. Hadei, E.A.B. Kantchev, C.J. O'Brien, C. Valente, A user-friendly, all-purpose Pd–NHC (NHC= N-heterocyclic carbene) precatalyst for the Negishi reaction: a step towards a universal cross-coupling catalyst, Chemistry–A European Journal. 12 (2006) 4749–4755.

[112] C. Dash, M.M. Shaikh, P. Ghosh, Fluoride-Free Hiyama and Copper-and Amine-Free Sonogashira Coupling in Air in a Mixed Aqueous Medium by a Series of PEPPSI-Themed Precatalysts, (2009).

[113] Z.-S. Gu, L.-X. Shao, J.-M. Lu, NHC–Pd (II)–Im (NHCá= áN-heterocyclic carbene; Imá= á1-

methylimidazole) complex catalyzed Hiyama reaction of aryl chlorides with aryltrimethoxysilanes, Journal of Organometallic Chemistry. 700 (2012) 132–134.

[114] J. Yang, L. Wang, Synthesis and characterization of dinuclear NHC–palladium complexes and their applications in the Hiyama reactions of aryltrialkyoxysilanes with aryl chlorides, Dalton Transactions. 41 (2012) 12031–12037.

[115] S. Tandukar, A. Sen, N-heterocyclic carbene–palladium complex immobilized on silica nanoparticles: Recyclable catalyst for high yield Suzuki and Heck coupling reactions under mild conditions, Journal of Molecular Catalysis A: Chemical. 268 (2007) 112–119.

[116] Y.-Q. Tang, C.-Y. Chu, L. Zhu, B. Qian, L.-X. Shao, N-Heterocyclic carbene–Pd (II) complex derived from proline for the Mizoroki–Heck reaction in water, Tetrahedron. 67 (2011) 9479–9483.

[117] V. Ritleng, C. Sirlin, M. Pfeffer, Ru-, Rh-, and Pd-catalyzed C− C bond formation involving C− H activation and addition on unsaturated substrates: reactions and mechanistic aspects, Chemical Reviews. 102 (2002) 1731–1770.

[118] B.B. Touré, B.S. Lane, D. Sames, Catalytic C− H arylation of SEM-protected azoles with palladium complexes of NHCs and phosphines, Organic Letters. 8 (2006) 1979–1982.

[119] S. Guo, H.V. Huynh, Dinuclear triazole-derived Janus-type N-heterocyclic carbene complexes of palladium: syntheses, isomerizations, and catalytic studies toward direct C5-arylation of imidazoles, Organometallics. 33 (2014) 2004–2011.

[120] O. Navarro, N. Marion, N.M. Scott, J. González, D. Amoroso, A. Bell, S.P. Nolan, Synthesis of novel (NHC) Pd (acac) Cl complexes (acac= acetylacetonate) and their activity in cross-coupling reactions, Tetrahedron. 61 (2005) 9716–9722.

[121] V. Lavallo, Y. Canac, C. Präsang, B. Donnadieu, G. Bertrand, Stable cyclic (alkyl)(amino) carbenes as rigid or flexible, bulky, electron-rich ligands for transition-metal catalysts: a quaternary carbon atom makes the difference, Angewandte Chemie International Edition. 44 (2005) 5705–5709.

[122] M.S. Viciu, R.F. Germaneau, O. Navarro-Fernandez, E.D. Stevens, S.P. Nolan, Activation and reactivity of (NHC) Pd (allyl) Cl (NHC= N-heterocyclic carbene) complexes in cross-coupling reactions, Organometallics. 21 (2002) 5470–5472.

[123] J.C. Garrison, W.J. Youngs, Ag (I) N-Heterocyclic Carbene Complexes : Synthesis , Structure , and Application, (2005) 3978–4008.

[124] T.J. Siciliano, M.C. Deblock, K.M. Hindi, S. Durmus, M.J. Panzner, C.A. Tessier, W.J. Youngs, Synthesis and anticancer properties of gold (I) and silver (I) N-heterocyclic carbene complexes, Journal of Organometallic Chemistry. 696 (2011) 1066–1071.

[125] N. Şahin, S. Şahin-Bölükbaşı, M.N. Tahir, C. Arıcı, E. Cevik, N. Gürbüz, İ. Özdemir, B.S. Cummings, Synthesis, characterization and anticancer activity of allyl substituted N-Heterocyclic carbene silver (I) complexes, Journal of Molecular Structure. 1179 (2019) 92–99.

[126] I. Slimani, A. Chakchouk-Mtibaa, L. Mellouli, L. Mansour, I. Ozdemir, N. Gürbüz, N. Hamdi, Novel N-Heterocyclic Carbene Silver (I) Complexes: Synthesis, Structural Characterization, Antimicrobial and Cytotoxicity Potential Studies, Journal of the Brazilian Chemical Society. 31 (2020) 2058–2070.

[127] A.E. Sandeli, N. Khiri-meribout, S. Benzerka, N. Gürbüz, Inorganica Chimica Acta Silver (I) - N - heterocyclic carbene complexes : Synthesis and characterization , biological evaluation of Anti-Cholinesterase , anti-alpha-amylase , anti-lipase , and antibacterial activities , and molecular docking study, 525 (2021).

[128] A. el-Krim Sandeli, N. Khiri-Meribout, S. Benzerka, H. Boulebd, N. Gürbüz, N. Özdemir, İ. Özdemir, Synthesis, structures, DFT calculations, and catalytic application in the direct arylation of five-membered heteroarenes with aryl bromides of novel palladium-N-heterocyclic carbene PEPPSI-type complexes, New Journal of Chemistry. 45 (2021) 17878–17892. https://doi.org/10.1039/d1nj03388c.

[129] A.E.K. Sandeli, H. Boulebd, N. Khiri-Meribout, S. Benzerka, C. Bensouici, N. Özdemir, N. Gürbüz, İ. Özdemir, New benzimidazolium N-heterocyclic carbene precursors and their related Pd-NHC complex

PEPPSI-type: Synthesis, structures, DFT calculations, biological activity, docking study, and catalytic application in the direct arylation, Journal of Molecular Structure. 1248 (2022). https://doi.org/10.1016/j.molstruc.2021.131504.

[130] İ. Özdemir, Y. Gök, Ö. Özeroğlu, M. Kaloğlu, H. Doucet, C. Bruneau, N.-H. Carbenes, Useful Ligands for the Palladium-Catalysed Direct C5 Arylation of Heteroaromatics with Aryl Bromides or Electron-Deficient Aryl Chlorides, Eur. J. Inorg. Chem. 12 (2010) 1798.

[131] M. Kaloğlu, İ. Özdemir, V. Dorcet, C. Bruneau, H. Doucet, PEPPSI-Type Palladium–NHC complexes: synthesis, characterization, and catalytic activity in the direct C5-Arylation of 2-substituted thiophene derivatives with aryl halides, European Journal of Inorganic Chemistry. 2017 (2017) 1382–1391.

[132] F.H. Allen, O. Kennard, D.G. Watson, L. Brammer, A.G. Orpen, R. Taylor, Tables of bond lengths determined by X-ray and neutron diffraction. Part 1. Bond lengths in organic compounds, Journal of the Chemical Society, Perkin Transactions 2. (1987) S1–S19.

[133] A. van Bondi, van der Waals volumes and radii, The Journal of Physical Chemistry. 68 (1964) 441–451.

[134] B. Cordero, V. Gómez, A.E. Platero-Prats, M. Revés, J. Echeverría, E. Cremades, F. Barragán, S. Alvarez, Covalent radii revisited, Dalton Transactions. (2008) 2832–2838.

[135] M. Kaloğlu, N. Kaloğlu, İ. Yıldırım, N. Özdemir, İ. Özdemir, Palladium-carbene catalyzed direct arylation of five-membered heteroaromatics, Journal of Molecular Structure. 1206 (2020) 127668.

[136] L. Barbu, M.M. Popa, S. Shova, M. Ferbinteanu, C. Draghici, F. Dumitrascu, New Pd-NHC PEPPSI complexes from benzimidazolium salts with a phenacyl group attached to N3, Inorganica Chimica Acta. 463 (2017) 97–101.

[137] R.A. Gaussian09, 1, mj frisch, gw trucks, hb schlegel, ge scuseria, ma robb, jr cheeseman, g. Scalmani, v. Barone, b. Mennucci, ga petersson et al., gaussian, Inc., Wallingford CT. 121 (2009) 150–166.

[138] A.D. Becke, Density-functional exchange-energy approximation with correct asymptotic behavior, Physical Review A. 38 (1988) 3098.

[139] P.J. Hay, W.R. Wadt, Ab initio effective core potentials for molecular calculations. Potentials for the transition metal atoms Sc to Hg, The Journal of Chemical Physics. 82 (1985) 270–283.

[140] A.D. McLean, G.S. Chandler, Contracted Gaussian basis sets for molecular calculations. I. Second row atoms, Z= 11–18, The Journal of Chemical Physics. 72 (1980) 5639–5648.

[141] J. Tirado-Rives, W.L. Jorgensen, Performance of B3LYP density functional methods for a large set of organic molecules, Journal of Chemical Theory and Computation. 4 (2008) 297–306.

[142] I.A. Khodja, H. Boulebd, C. Bensouici, A. Belfaitah, Design, synthesis, biological evaluation, molecular docking, DFT calculations and in silico ADME analysis of (benz) imidazole-hydrazone derivatives as promising antioxidant, antifungal, and anti-acetylcholinesterase agents, Journal of Molecular Structure. 1218 (2020) 128527.

[143] N. Nakamura, DIRECT PHENYLATION OF ISOXAZOLES USING PALLADIUM CATALYSTS: SYNTHESIS OF 4-PHENYLMUSCIMOL, (1982).

[144] A. Ohta, Y. Akita, T. Ohkuwa, M. Chiba, R. Fukunaga, Palladium-catalyzed arylation of furan, thiophene, benzo [b] furan and benzo [b] thiophene, Heterocycles (Sendai). 31 (1990) 1951–1958.

[145] B. Glover, K.A. Harvey, B. Liu, M.J. Sharp, M.F. Tymoschenko, Regioselective palladium-catalyzed arylation of 3-carboalkoxy furan and thiophene, Organic Letters. 5 (2003) 301–304.

[146] A. Yokooji, T. Okazawa, T. Satoh, M. Miura, M. Nomura, Palladium-catalyzed direct arylation of thiazoles with aryl bromides, Tetrahedron. 59 (2003) 5685–5689.

[147] E.O. Karaca, N. Gurbuz, I. Ozdemir, H. Doucet, O. Sahin, O. Buyukgungor, B. Cetinkaya, Palladium complexes with tetrahydropyrimidin-2-ylidene ligands: Catalytic activity for the direct arylation of furan, thiophene, and thiazole derivatives, Organometallics. 34 (2015) 2487–2493.

[148] M.C. Arendrup, M. Cuenca-Estrella, C. Lass-Flörl, W. Hope, EUCAST-AFST, EUCAST technical note on the EUCAST definitive document EDef 7.2: method for the determination of broth dilution minimum inhibitory concentrations of antifungal agents for yeasts EDef 7.2 (EUCAST-AFST), Clinical Microbiology and Infection. 18 (2012) E246–E247.

[149] C.L.S. INSTITUTE-CLSL, Methods for dilution antimicrobial susceptibility tests for bacteria that grow aerobically; Approved standard–, M07-A9, (2015).

[150] R.A. Haque, S.Y. Choo, S. Budagumpi, A.A.-A. Abdullah, M.B.K. Ahamed, A.M.S.A. Majid, Synthesis, crystal structures, characterization and biological studies of nitrile-functionalized silver (I) N-heterocyclic carbene complexes, Inorganica Chimica Acta. 433 (2015) 35–44.

[151] F. Mao, J. Li, H. Wei, L. Huang, X. Li, Tacrine–propargylamine derivatives with improved acetylcholinesterase inhibitory activity and lower hepatotoxicity as a potential lead compound for the treatment of Alzheimer's disease, Journal of Enzyme Inhibition and Medicinal Chemistry. 30 (2015) 995–1001.

[152] S. Stepankova, K. Komers, Cholinesterases and cholinesterase inhibitors, Current Enzyme Inhibition. 4 (2008) 160–171.

[153] I.K. Rhee, M. van de Meent, K. Ingkaninan, R. Verpoorte, Screening for acetylcholinesterase inhibitors from Amaryllidaceae using silica gel thin-layer chromatography in combination with bioactivity staining, Journal of Chromatography A. 915 (2001) 217–223.

[154] G.L. Ellman, K.D. Courtney, V. Andres Jr, R.M. Featherstone, A new and rapid colorimetric determination of acetylcholinesterase activity, Biochemical Pharmacology. 7 (1961) 88–95.

[155] O. Trott, A.J. Olson, AutoDock Vina: improving the speed and accuracy of docking with a new scoring function, efficient optimization, and multithreading, Journal of Computational Chemistry. 31 (2010) 455–461.

[156] F. Nachon, E. Carletti, C. Ronco, M. Trovaslet, Y. Nicolet, L. Jean, P.-Y. Renard, Crystal structures of human cholinesterases in complex with huprine W and tacrine: elements of specificity for anti-Alzheimer's drugs targeting acetyl-and butyryl-cholinesterase, Biochemical Journal. 453 (2013) 393–399.

[157] M. Wandhammer, E. Carletti, M. Van der Schans, E. Gillon, Y. Nicolet, P. Masson, M. Goeldner, D. Noort, F. Nachon, Structural study of the complex stereoselectivity of human butyrylcholinesterase for the neurotoxic V-agents, Journal of Biological Chemistry. 286 (2011) 16783–16789.

[158] R.G. Demmak, S. Bordage, A. Bensegueni, N. Boutaghane, T. Hennebelle, E.H. Mokrani, S. Sahpaz, Chemical constituents from solenostemma argel and their cholinesterase inhibitory activity, Natural Product Sciences. 25 (2019) 115–121. https://doi.org/10.20307/nps.2019.25.2.115.

[159] P.P. Wizard, Epik version 2.0, Impact version 5.5, Prime version 2.1, New York (NY): Schrödinger, LLC. (2009).

[160] I. Boualia, C. Derabli, R. Boulcina, C. Bensouici, M. Yildirim, A. Birinci Yildirim, E.H. Mokrani, A. Debache, Synthesis, molecular docking studies, and biological evaluation of novel alkyl bis(4-amino-5-cyanopyrimidine) derivatives, Archiv Der Pharmazie. 352 (2019) 1–10. https://doi.org/10.1002/ardp.201900027.

[161] L.L.C. Schrödinger, The PyMOL molecular graphics system, version 1.8, (2015).

[162] L.L.C. Schrodinger, The PyMOL molecular graphics system, Version. 1 (2010) 0.

[163] M. Wandhammer, E. Carletti, M. Van Der Schans, E. Gillon, Y. Nicolet, P. Masson, M. Goeldner, D. Noort, F. Nachon, Structural study of the complex stereoselectivity of human butyrylcholinesterase for the neurotoxic V-agents, Journal of Biological Chemistry. 286 (2011) 16783–16789. https://doi.org/10.1074/jbc.M110.209569.

[164] S. Cie, X-area (version 1.18) and X-red32 (version 1.04), Darmstadt, Germany. (2002).

[165] L. Palatinus, G. Chapuis, SUPERFLIP–a computer program for the solution of crystal structures by charge flipping in arbitrary dimensions, Journal of Applied Crystallography. 40 (2007) 786–790.

[166] D. Kratzert, J.J. Holstein, I. Krossing, DSR: enhanced modelling and refinement of disordered structures with SHELXL, Journal of Applied Crystallography. 48 (2015) 933–938.

[167] O. V Dolomanov, L.J. Bourhis, R.J. Gildea, J. a. K. Howard and H. Puschmann, J. Appl. Crystallogr. 42 (2009) 339–341.

[168] R. Sabouraud, Contribution a l'etude de la trichophytie humaine. Etude clinique, microscopique et bacterioloqique sur la pluralité des trichophytons de l'homme, Ann. Dermatol. Syphil. 3 (1892) 1061–1087.

[169] J. Sambrook, D.W. Russell, Molecular cloning: a laboratory manual. 2001. Cold Spring Harbor Laboratory Press, Cld Spring Harbor, NY. 502 (2001).

[170] J.L. Medina-Franco, M.A. Giulianotti, G.S. Welmaker, R.A. Houghten, Shifting from the single to the multitarget paradigm in drug discovery, Drug Discovery Today. 18 (2013) 495–501.

[171] L. Costantino, D. Barlocco, Designed multiple ligands: basic research vs clinical outcomes, Current Medicinal Chemistry. 19 (2012) 3353–3387.

[172] M. L Bolognesi, Polypharmacology in a single drug: multitarget drugs, Current Medicinal Chemistry. 20 (2013) 1639–1645.

[173] J. Boström, D.G. Brown, R.J. Young, G.M. Keserü, Expanding the medicinal chemistry synthetic toolbox, Nature Reviews Drug Discovery. 17 (2018) 709–727.

[174] A. Nefzi, J.M. Ostresh, R.A. Houghten, The current status of heterocyclic combinatorial libraries, Chemical Reviews. 97 (1997) 449–472.

[175] C. Viegas-Junior, A. Danuello, V. da Silva Bolzani, E.J. Barreiro, C.A.M. Fraga, Molecular hybridization: a useful tool in the design of new drug prototypes, Current Medicinal Chemistry. 14 (2007) 1829–1852.

[176] J.D. Sunderhaus, S.F. Martin, Applications of multicomponent reactions to the synthesis of diverse heterocyclic scaffolds, Chemistry–A European Journal. 15 (2009) 1300–1308.

[177] G.M. Reddy, M. Shiradkar, A.K. Chakravarthy, Chemical and pharmacological significance of 1, 4-dihydropyridines, Current Organic Chemistry. 11 (2007) 847–852.

[178] A. Debache, B. Boumoud, M. Amimour, A. Belfaitah, S. Rhouati, B. Carboni, Phenylboronic acid as a mild and efficient catalyst for Biginelli reaction, Tetrahedron Letters. 47 (2006) 5697–5699.

[179] S. Nemouchi, R. Boulcina, B. Carboni, A. Debache, Phenylboronic acid as an efficient and convenient catalyst for a three-component synthesis of tetrahydrobenzo [b] pyrans, Comptes Rendus Chimie. 15 (2012) 394–397.

[180] A. Ziadi Chibane, A. Dedache, Nouvelles voies de Synthèse des 1, 4-dihydropyranopyrazoles, tétrahydrobenzo [b] pyranes et β-acétamidoacétones., (2018).

[181] A.M. Kedjadja, F.; Debache, A.; Rhouati, S.; Belfaitah, A, Journal de La Societe Algerienne de Chimie. 14 (2004) 225–233.

[182] A. Debache, L. Chouguiat, R. Boulcina, B. Carboni, A one-pot multi-component synthesis of dihydropyrimidinone/thione and dihydropyridine derivatives via Biginelli and Hantzsch condensations using t-BuOK as a catalyst under solvent-free conditions, The Open Organic Chemistry Journal. 6 (2012).

[183] M.J.S. Dewar, P.M. Maitlis, 490. Electrophilic substitution. Part XI. Nitration of some six-membered nitrogen-heterocyclic compounds in sulphuric acid, Journal of the Chemical Society (Resumed). (1957) 2521–2528.

[184] H.E. Jansen, J.P. Wibaut, The bromination of quinoline, isoquinoline, thiazole and benzthiazole in the gaseous phase, Recueil Des Travaux Chimiques Des Pays-Bas. 56 (1937) 699–708.

[185] R.D. Brown, u. RD Harcourt: J. chem. Soc.[London] 1959, 3451. Brown, RD: Austral, J. Chem. 8 (1955) 100.

[186] R.K. Bansal, Text book of heterocyclic chemistry, New Age International Publisher, New Delhi. 389 (2001).

[187] S. Cacchi, The Chemistry of Heterocycles, 2004. https://doi.org/10.1055/s-2004-834452.

[188] J.P. Michael, Quinoline, quinazoline and acridone alkaloids, Natural Product Reports. 24 (2007) 223–246.

[189] A.R. Surrey, H.F. Hammer, Some 7-substituted 4-aminoquinoline derivatives, Journal of the American Chemical Society. 68 (1946) 113–116.

[190] J. Wiesner, R. Ortmann, H. Jomaa, M. Schlitzer, New antimalarial drugs, Angewandte Chemie International Edition. 42 (2003) 5274–5293.

[191] M.E. Wall, M.C. Wani, C.E. Cook, K.H. Palmer, A.T. and McPhail, G.A. Sim, Plant antitumor agents. I. The isolation and structure of camptothecin, a novel alkaloidal leukemia and tumor inhibitor from camptotheca acuminata1, 2, Journal of the American Chemical Society. 88 (1966) 3888–3890.

[192] M.J. McLaughlin, R.P. Hsung, Total syntheses of pyranoquinoline alkaloids: simulenoline, huajiaosimuline, and (±)-7-demethoxyzanthodioline, The Journal of Organic Chemistry. 66 (2001) 1049–1053.

[193] K.M. Witherup, R.W. Ransom, A.C. Graham, A.M. Bernard, M.J. Salvatore, W.C. Lumma, P.S. Anderson, S.M. Pitzenberger, S.L. Varga, Martinelline and martinellic acid, novel G-protein linked receptor antagonists from the tropical plant Martinella iquitosensis (Bignoniaceae), Journal of the American Chemical Society. 117 (1995) 6682–6685.

[194] V.G. Granik, V.A. Makarov, C. Parkanyi, Enamines as Synthons in the Synthesis of Heterocycles, Advances in Heterocyclic Chemistry. 72 (1998) 283–359.

[195] M.H.M. Sharaf, P.L. Schiff Jr, A.N. Tackie, C.H. Phoebe Jr, G.E. Martin, Two new indoloquinoline alkaloids from Cryptolepis sanguinolenta: cryptosanguinolentine and cryptotackieine, Journal of Heterocyclic Chemistry. 33 (1996) 239–243.

[196] P.M. Fresneda, P. Molina, S. Delgado, A novel approach to the indoloquinoline alkaloids cryptotackieine and cryptosanguinolentine by application of cyclization of o-vinylsubstituted arylheterocumulenes, Tetrahedron. 57 (2001) 6197–6202.

[197] J. Duffour, S. Gourgou, F. Desseigne, C. Debrigode, L. Mineur, F. Pinguet, S. Poujol, P. Chalbos, F. Bressole, M. Ychou, Multicentre phase II study using increasing doses of irinotecan combined with a simplified LV5FU2 regimen in metastatic colorectal cancer, Cancer Chemotherapy and Pharmacology. 60 (2007) 383–389.

[198] M. Takamura, K. Funabashi, M. Kanai, M. Shibasaki, Catalytic enantioselective reissert-type reaction: Development and application to the synthesis of a potent NMDA receptor antagonist (−)-L-689,560 using a solid-supported catalyst, Journal of the American Chemical Society. 123 (2001) 6801–6808.

[199] P. Martin, E. Steiner, K. Auer, T. Winkler, Zur Herstellung von PQQ in kg-Mengen, Helvetica Chimica Acta. 76 (1993) 1667–1673.

[200] A.R. Katritzky, M. Arend, A convenient and highly regioselective one-pot synthesis of quinolines by addition of a Vilsmeier-type reagent to N-arylimines, The Journal of Organic Chemistry. 63 (1998) 9989–9991.

[201] R. Long, K. Schofield, 630. Some alkylquinoline-5: 8-quinones, Journal of the Chemical Society (Resumed). (1953) 3161–3167.

[202] R.H.F. Manske, M. Kulka, The S kraup Synthesis of Quinolines, Organic Reactions. 7 (2004) 59–98.

[203] C. Cheng, S. Yan, The F riedländer Synthesis of Quinolines, Organic Reactions. 28 (2004) 37–201.

[204] M.-C. Yan, Z. Tu, C. Lin, S. Ko, J. Hsu, C.-F. Yao, An investigation of the reaction of 2-aminobenzaldehyde derivatives with conjugated nitro-olefins: An easy and efficient synthesis of 3-nitro-1, 2-dihydroquinolines and 3-nitroquinolines, The Journal of Organic Chemistry. 69 (2004) 1565–1570.

[205] P.K. Calaway, H.R. Henze, Utilization of aryloxy ketones in the synthesis of quinolines by the pfitzinger reaction, Journal of the American Chemical Society. 61 (1939) 1355–1358.

[206] O. Meth-Cohn, B. Narine, B. Tarnowski, A versatile new synthesis of quinolines and related fused pyridines, Part 5. The synthesis of 2-chloroquinoline-3-carbaldehydes, Journal of the Chemical Society, Perkin Transactions 1. (1981) 1520–1530.

[207] M.M. Ali, K.C. Tasneem, P.K. Rajanna, An efficient and facile synthesis of 2-chloro-3-formyl quinolines from acetanilides in micellar media by Vilsmeier-Haack cyclisation, Synlett. 2001 (2001) 251–253.

[208] M.M. Ali, S. Sana, Tasneem, K.C. Rajanna, P.K. Saiprakash, Ultrasonically accelerated vilsmeier haack cyclisation and formylation reactions, Synthetic Communications. 32 (2002) 1351–1356.

[209] H.G. Kathrotiya, R.G. Patel, M.P. Patel, Microwave-assisted multi-component synthesis of 3'-indolyl substituted pyrano [2, 3-c] pyrazoles and their antimicrobial activity, Journal of the Serbian Chemical Society. 77 (2012) 983–991.

[210] H. Adibi, L. Hosseinzadeh, S. Farhadi, F. Ahmadi, J. Reports Pharma. Sci. 2013, 2, 116-124. 106) J. Ding; T. Welton; and DW Armstrong, Analytical Chemistry. 76 (2004) 107.

[211] X.-H. Yang, P.-H. Zhang, Z.-M. Wang, F. Jing, Y.-H. Zhou, L.-H. Hu, Synthesis and bioactivity of lignin related high-added-value 2H, 4H-dihydro-pyrano [2, 3-c] pyrazoles and 1H, 4H-dihydro-pyrano [2, 3-c] pyrazoles, Industrial Crops and Products. 52 (2014) 413–419.

[212] C. Wiener, C.H. Schroeder, B.D. West, K.P. Link, Studies on the 4-Hydroxycoumarins. XVIII. 1a 3-[α-(acetamidomethyl) benzyl]-4-hydroxycoumarin and related products1b, The Journal of Organic Chemistry. 27 (1962) 3086–3088.

[213] R. Ballini, G. Bosica, M.L. Conforti, R. Maggi, A. Mazzacani, P. Righi, G. Sartori, Three-component process for the synthesis of 2-amino-2-chromenes in aqueous media, Tetrahedron. 57 (2001) 1395–1398.

[214] M. Kidwai, S. Saxena, M.K.R. Khan, S.S. Thukral, Aqua mediated synthesis of substituted 2-amino-4H-chromenes and in vitro study as antibacterial agents, Bioorganic & Medicinal Chemistry Letters. 15 (2005) 4295–4298.

[215] I. V Magedov, M. Manpadi, M.A. Ogasawara, A.S. Dhawan, S. Rogelj, S. Van Slambrouck, W.F.A. Steelant, N.M. Evdokimov, P.Y. Uglinskii, E.M. Elias, Structural simplification of bioactive natural products with multicomponent synthesis. 2. Antiproliferative and antitubulin activities of pyrano [3, 2-c] pyridones and pyrano [3, 2-c] quinolones, Journal of Medicinal Chemistry. 51 (2008) 2561–2570.

[216] S. Gao, C.H. Tsai, C. Tseng, C.-F. Yao, Fluoride ion catalyzed multicomponent reactions for efficient synthesis of 4H-chromene and N-arylquinoline derivatives in aqueous media, Tetrahedron. 64 (2008) 9143–9149.

[217] D. Kumar, V.B. Reddy, S. Sharad, U. Dube, S. Kapur, A facile one-pot green synthesis and antibacterial activity of 2-amino-4H-pyrans and 2-amino-5-oxo-5, 6, 7, 8-tetrahydro-4H-chromenes, European Journal of Medicinal Chemistry. 44 (2009) 3805–3809.

[218] R.L. Magar, P.B. Thorat, V.B. Jadhav, S.U. Tekale, S.A. Dake, B.R. Patil, R.P. Pawar, Silica gel supported polyamine: a versatile catalyst for one pot synthesis of 2-amino-4H-chromene derivatives, Journal of Molecular Catalysis A: Chemical. 374 (2013) 118–124.

[219] J. Albadi, A. Mansournezhad, Z. Derakhshandeh, CuO–CeO2 nanocomposite: a highly efficient recyclable catalyst for the multicomponent synthesis of 4H-benzo [b] pyran derivatives, Chinese Chemical Letters. 24 (2013) 821–824.

[220] K. Pradhan, S. Paul, A.R. Das, Fe (DS) 3, an efficient Lewis acid-surfactant-combined catalyst (LASC) for the one pot synthesis of chromeno [4, 3-b] chromene derivatives by assembling the basic building blocks, Tetrahedron Letters. 54 (2013) 3105–3110.

[221] A.T. Khan, M. Lal, S. Ali, M.M. Khan, One-pot three-component reaction for the synthesis of pyran annulated heterocyclic compounds using DMAP as a catalyst, Tetrahedron Letters. 52 (2011) 5327–5332.

[222] A. Shaabani, R. Ghadari, S. Ghasemi, M. Pedarpour, A.H. Rezayan, A. Sarvary, S.W. Ng, Novel one-pot three-and pseudo-five-component reactions: synthesis of functionalized benzo [g]-and dihydropyrano [2, 3-g] chromene derivatives, Journal of Combinatorial Chemistry. 11 (2009) 956–959.

[223] H.J. Roth, A. Kleemann, T. Beisswenger, Pharmaceutical chemistry: drug synthesis, Ellis Horwood, 1988.

[224] D. Vo, W.C. Matowe, M. Ramesh, N. Iqbal, M.W. Wolowyk, S.E. Howlett, E.E. Knaus, Syntheses, calcium channel agonist-antagonist modulation activities, and voltage-clamp studies of isopropyl 1, 4-dihydro-2, 6-dimethyl-3-nitro-4-pyridinylpyridine-5-carboxylate racemates and enantiomers, Journal of Medicinal Chemistry. 38 (1995) 2851–2859.

[225] F.R. Bühler, W. Kiowski, Calcium antagonists in hypertension., Journal of Hypertension. Supplement: Official Journal of the International Society of Hypertension. 5 (1987) S3-10.

[226] M.M. Ghorab, F.A. Ragab, E. Noaman, H.I. Heiba, E.M. El-Hossary, Utility of 4-(5,5-Dimethyl-3-oxo-cyclohex-1-enylamino)benzenesulfonamide in the Synthesis of Novel Quinolines as Possible Anticancer and Radioprotective Agents, 2008.

[227] A. Hantzsch, Condensationsprodukte aus Aldehydammoniak und ketonartigen Verbindungen, Berichte Der Deutschen Chemischen Gesellschaft. 14 (1881) 1637–1638.

[228] B. V Lichitsky, V.N. Yarovenko, I. V Zavarzin, M.M. Krayushkin, Reactions of cyclic enhydrazinoketones with arylidene derivatives of malononitrile. Synthesis of fused N-substituted 1, 4-dihydropyridines, Russian Chemical Bulletin. 49 (2000) 1251–1254.

[229] V.A. Chebanov, V.E. Saraev, S.M. Desenko, V.N. Chernenko, I. V Knyazeva, U. Groth, T.N. Glasnov, C.O. Kappe, Tuning of chemo-and regioselectivities in multicomponent condensations of 5-aminopyrazoles, dimedone, and aldehydes, The Journal of Organic Chemistry. 73 (2008) 5110–5118.

[230] J. Sun, Y. Sun, H. Gao, C. Yan, Selective Synthesis of Fused 1, 4-and 1, 2-Dihydropyridines by Domino Reactions of Arylamines, Acetylenedicarboxylate, Aldehydes, and Cyclic 1, 3-Diketones, (2011).

[231] R.K. Vohra, C. Bruneau, J. Renaud, Lewis Acid-Catalyzed Sequential Transformations: Straightforward Preparation of Functional Dihydropyridines, Advanced Synthesis & Catalysis. 348 (2006) 2571–2574.

[232] J. Safari, S.H. Banitaba, S.D. Khalili, Cellulose sulfuric acid catalyzed multicomponent reaction for efficient synthesis of 1, 4-dihydropyridines via unsymmetrical Hantzsch reaction in aqueous media, Journal of Molecular Catalysis A: Chemical. 335 (2011) 46–50.

[233] S.-L. Cui, J. Wang, X.-F. Lin, Y.-G. Wang, Domino reaction of 3-(2-formylphenoxy) propenoates and amines: A novel synthesis of 1, 4-dihydropyridines from salicaldehydes, ethyl propiolate, and amines, The Journal of Organic Chemistry. 72 (2007) 7779–7782.

[234] A. Mai, S. Valente, S. Meade, V. Carafa, M. Tardugno, A. Nebbioso, A. Galmozzi, N. Mitro, E. De Fabiani, L. Altucci, Study of 1, 4-dihydropyridine structural scaffold: discovery of novel sirtuin activators and inhibitors, Journal of Medicinal Chemistry. 52 (2009) 5496–5504.

[235] J. Sun, Y. Sun, E.-Y. Xia, C.-G. Yan, Synthesis of functionalized 2-aminohydropyridines and 2-pyridinones via domino reactions of arylamines, methyl propiolate, aromatic aldehydes, and substituted acetonitriles, ACS Combinatorial Science. 13 (2011) 436–441.

[236] A. Kumar, S. Sharma, A grinding-induced catalyst-and solvent-free synthesis of highly functionalized 1, 4-dihydropyridines via a domino multicomponent reaction, Green Chemistry. 13 (2011) 2017–2020.

[237] A.M. Zonouz, D. Moghani, Synthesis of 1, 4-Dihydropyridine derivatives under solvent-free and grinding conditions, Synthetic Communications. 41 (2011) 2152–2160.

[238] X. Chao, X. He, Y. Yang, X. Zhou, M. Jin, S. Liu, Z. Cheng, P. Liu, Y. Wang, J. Yu, Design, synthesis and pharmacological evaluation of novel tacrine–caffeic acid hybrids as multi-targeted compounds against Alzheimer's disease, Bioorganic & Medicinal Chemistry Letters. 22 (2012) 6498–6502.

[239] S.-S. Xie, X.-B. Wang, J.-Y. Li, L. Yang, L.-Y. Kong, Design, synthesis and evaluation of novel tacrine–coumarin hybrids as multifunctional cholinesterase inhibitors against Alzheimer's disease, European Journal of Medicinal Chemistry. 64 (2013) 540–553.

[240] J.S. da Costa, J.P.B. Lopes, D. Russowsky, C.L. Petzhold, A.C. de Amorim Borges, M.A. Ceschi, E. Konrath, C. Batassini, P.S. Lunardi, C.A.S. Gonçalves, Synthesis of tacrine-lophine hybrids via one-pot four component reaction and biological evaluation as acetyl-and butyrylcholinesterase inhibitors, European

Journal of Medicinal Chemistry. 62 (2013) 556–563.

[241] M.T. McKenna, G.R. Proctor, L.C. Young, A.L. Harvey, Novel tacrine analogues for potential use against Alzheimer's disease: potent and selective acetylcholinesterase inhibitors and 5-HT uptake inhibitors, Journal of Medicinal Chemistry. 40 (1997) 3516–3523.

[242] D. dos Santos Pisoni, J.S. da Costa, D. Gamba, C.L. Petzhold, A.C. de Amorim Borges, M.A. Ceschi, P. Lunardi, C.A.S. Gonçalves, Synthesis and AChE inhibitory activity of new chiral tetrahydroacridine analogues from terpenic cyclanones, European Journal of Medicinal Chemistry. 45 (2010) 526–535.

[243] A. Martínez-Grau, J. Marco, Friedländer reaction on 2-amino-3-cyano-4H-pyrans: Synthesis of derivatives of 4H-pyran [2, 3-b] quinoline, new tacrine analogues, Bioorganic & Medicinal Chemistry Letters. 7 (1997) 3165–3170.

[244] E.M. Suolinna, Metabolism of sulfanilamide and related drugs in isolated rat and rabbit liver cells., Drug Metabolism and Disposition. 8 (1980) 205–207.

[245] J.P. Maskell, A.M. Sefton, L.M. Hall, Mechanism of sulfonamide resistance in clinical isolates of Streptococcus pneumoniae, Antimicrobial Agents and Chemotherapy. 41 (1997) 2121–2126.

[246] M.N. Tahir, M. Khalid, A. Islam, S.M.A. Mashhadi, A.A.C. Braga, Facile synthesis, single crystal analysis, and computational studies of sulfanilamide derivatives, Journal of Molecular Structure. 1127 (2017) 766–776.

[247] H.B. Gray, H.B. Gray, J.D. Simon, W.C. Trogler, Braving the Elements, University Science Books, 1995.

[248] J.H. Barnett, S.M. Barnett, Lichenoid drug reactions to chlorpropamide and tolazamide., Cutis. 34 (1984) 542–544.

[249] J. Buxeraud, S. Faure, Les quinolones et les sulfamides, Actualités Pharmaceutiques. 55 (2016) 17–22.

[250] J.A. Schoenberger, Losartan with hydrochlorothiazide in the treatment of hypertension., Journal of Hypertension. Supplement: Official Journal of the International Society of Hypertension. 13 (1995) S43-7.

[251] D.S. Doğruer, Ş. Urlu, T. Önkol, B. Özçelik, M.F. Şahin, Synthesis of some pyridazine derivatives carrying urea, thiourea, and sulfonamide moieties and their antimicrobial activity, Turkish Journal of Chemistry. 34 (2010) 57–65.

[252] R.R. Ranatunge, R.A. Earl, D.S. Garvey, D.R. Janero, L.G. Letts, A.M. Martino, M.G. Murty, S.K. Richardson, D.J. Schwalb, D. V Young, 3-(2-Methoxytetrahydrofuran-2-yl) pyrazoles: a novel class of potent, selective cyclooxygenase-2 (COX-2) inhibitors, Bioorganic & Medicinal Chemistry Letters. 14 (2004) 6049–6052.

[253] B.B. Subudhi, P.K. Panda, D. Bhatta, Synthesis and antiulcer activity study of 1, 4-dihydropyridines and their Mannich bases with sulfanilamide, (2009).

[254] N. Kaila, K. Janz, S. DeBernardo, P.W. Bedard, R.T. Camphausen, S. Tam, D.H.H. Tsao, J.C. Keith, C. Nickerson-Nutter, A. Shilling, Synthesis and biological evaluation of quinoline salicylic acids as P-selectin antagonists, Journal of Medicinal Chemistry. 50 (2007) 21–39.

[255] M.H. Elnagdi, N.M. Abed, M.R.H. Elmoghayar, D.H. Fleta, REACTIVITY OF α-CYANOCHALCONES AS MICHAEL ACCEPTORS, Chemischer Informationsdienst. 7 (1976) no-no.

[256] M. Hammouda, M.M. Mashaly, E.M. Afsah, Enaminones in heterocyclic syntheses. I: one-pot synthesis of some new quinoline derivatives, Pharmazie. 49 (1994) 365–366.

[257] B. Halliwell, Cellular responses to oxidative stress: adaptation, damage, repair, senescence and death, Free Radicals in Biology and Medicine. (2007) 187–267.

[258] O. Meth-Cohn, B. Narine, B. Tarnowski, R. Hayes, A. Keyzad, S. Rhouati, A. Robinson, A versatile new synthesis of quinolines and related fused pyridines. Part 9. Synthetic application of the 2-chloroquinoline-3-carbaldehydes, Journal of the Chemical Society, Perkin Transactions 1. (1981) 2509–2517. https://doi.org/10.1039/P19810002509.

Resumé

Ce travail décrit une thèse qui est divisée en deux chapitres :

Le premier chapitre concerne la synthèse de nouvelles séries de sels de benzimidazolium en tant que précurseurs de carbène *N*-hétérocycliques et de leurs complexes Ag-NHC et Pd-NHC de type PEPPSI. D'une part, l'évaluation de l'activité biologique des complexes d'argents Ag-NHCs montre que la majorité des complexes ont une activité importante. Les résultats expérimentaux ont montré également un très bon accord avec les résultats du *Docking moléculaire*. D'autre part, l'effet catalytique de tous les complexes de Pd-NHCs de type PEPPSI a été évalué dans la réaction d'arylation directe. Tous les complexes de palladium ont donné un très bon effet catalytique.

Le deuxième chapitre se concentre sur la synthèse de nouveaux composés polycycliques avec des dérivés hybrides quinoléine-4*H*-pyrane à système rigide fonctionnalisés et des dérivés hybrides quinoléine-1,4-dihydropyridine *N*-substitués. Les nouveaux composés polycycliques préparés ont été soumis à une étude approfondie de leur activité biologique ainsi qu'à une étude de détermination de la relation structure-activité.

Mots-clés :

Carbène *N*-hétérocyclique, sels de benzimidazolium, complexes Argent NHC, complexes Palladium NHC type PEPPSI, activités biologiques, catalyse, réaction d'arylation, quinoléine, 4H-pyrane, 1,4-dihydropyridine.

ملخص

يصف هذا العمل أطروحة مقسمة إلى فصلين.

الفصل الأول يناقش تخليق سلسلة جديدة من أملاح البانزيميدازول ذات صلة بالمركبات الحلقية التي تحتوي على كاربين ، والتي بدورها ساهمة في تخليق مركبات الفضة و البالاديوم لنفس النوع.

كل المركبات المنتجة تم تتقييمها في المختبر للتأكد من فعاليتها بيولوجيا ، كما تم التأكد من فعالية مركبات البالاديوم كمحفزات للتفاعلات الكمياءية. تم أيضًا تقييم التأثير التحفيزي لجميع مركبات Pd-NHC في تفاعلات الأريل المباشرة. تؤكد النتائج تطوير مركبات جديدة وفعالة مع تطبيقات محتملة في كل من التحفيز واكتشاف الجزيئات النشطة بيولوجيًا

يركز الفصل الثاني على تخليق مركبات جديدة متعددة الحلقات مع مشتقات هجينة وظيفية من الكينولين-4-هيدروجين بيران الهجين و الكينولين-4،1-ثنائي الهيدروجين بيريدين الهجين عبر التفاعل متعدد المكونات

تم تقييم المركبات من حيث نشاطها البيولوجي ، وخاصة في مضادات الأكسدة ومضادات الكولينستريز ، وتم عرض النتائج ومناقشتها. ستتم دراسة المركبات بشكل أكبر لعلاقتها بالهيكل والنشاط لاحقا.

الكلمة الأساسية المفتاحية :

المركبات الحلقية الكاربينية ، أملاح البانزيميدازول ، مركبات الفضة ، مركبات البالاديوم ، الفعالية البيولوحية ، محفزات، تفاعلarylation ، الكينولين، 4-هيدروجين بيران، 4،1-ثنائي الهيدروجين بيريدين

Abstract

This work describes a thesis that is divided into two chapters.

In the first chapter, a synthesis of novel benzimidazolium salts is presented as *N*-heterocyclic carbene precursors (NHCs), along with the synthesis of their corresponding Ag-NHC and PEPPSI-type Pd-NHC complexes. The antimicrobial and enzyme inhibitory properties of these complexes were evaluated in vitro. Additionally, the catalytic activity of the Pd-NHC complexes was assessed in direct arylation reactions. The results demonstrate the successful development of potent *N*-heterocyclic carbene complexes with promising prospects for applications in catalysis and the discovery of bioactive molecules.

The second chapter focuses on the synthesis of novel polycyclic compounds through a multicomponent reaction, specifically targeting functionalized rigid system quinoline-4*H*-pyran hybrid derivatives and quinoline-1,4-dihydropyridine-*N*-substituted hybrid derivatives. The biological activity of some of these compounds, specifically their antioxidant and anti-cholinesterase activity, was extensively evaluated and the results were comprehensively presented and analyzed. Further investigation will be conducted to explore the relationship between the chemical structures of these compounds and their biological activities, establishing a structure-activity relationship for future studies.

Keyword :

N-heterocyclic carbene, benzimidazolium salts, Silver NHC complexes, Palladium NHC complexes PEPPSI type, biological activities, catalysis, arylation reaction, quinoline, 4*H*-pyran, 1,4-dihydropyridine

List of Figures

List of Schemes

List of Tables

APPENDIX

1-Benzhydryl -5,6-dimethyl-(2,3,5,6-tetramethylbenzyl)benzimidazolium chloride (2a)

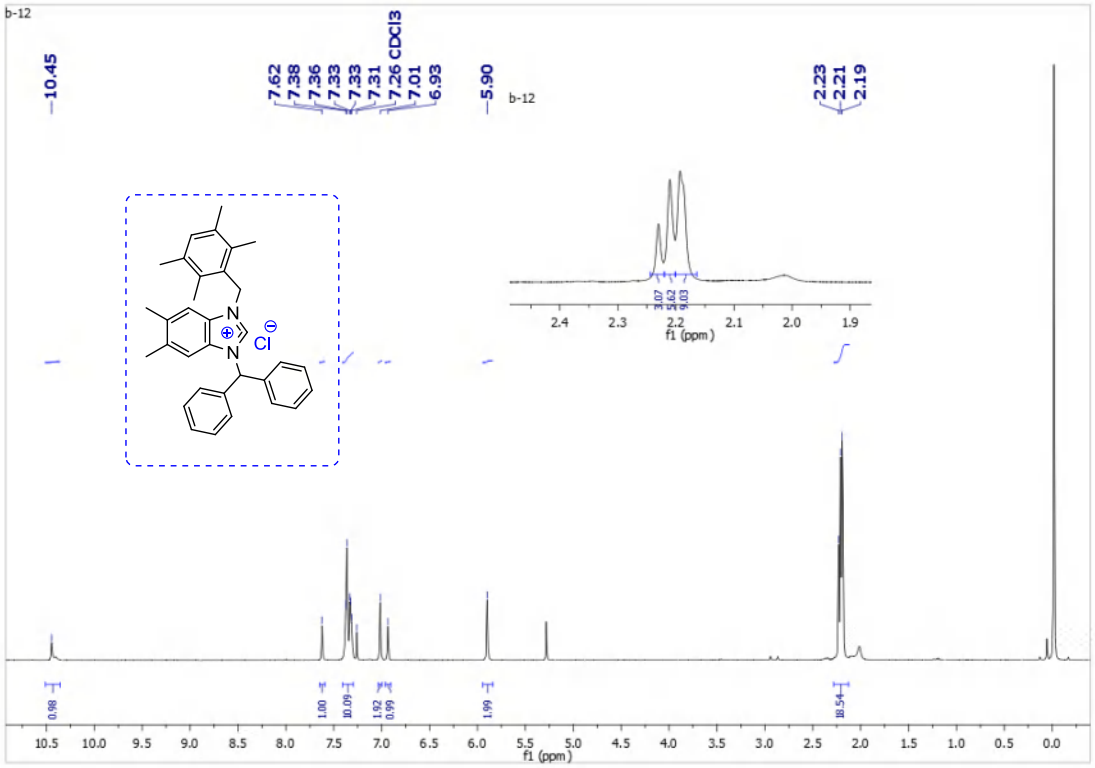

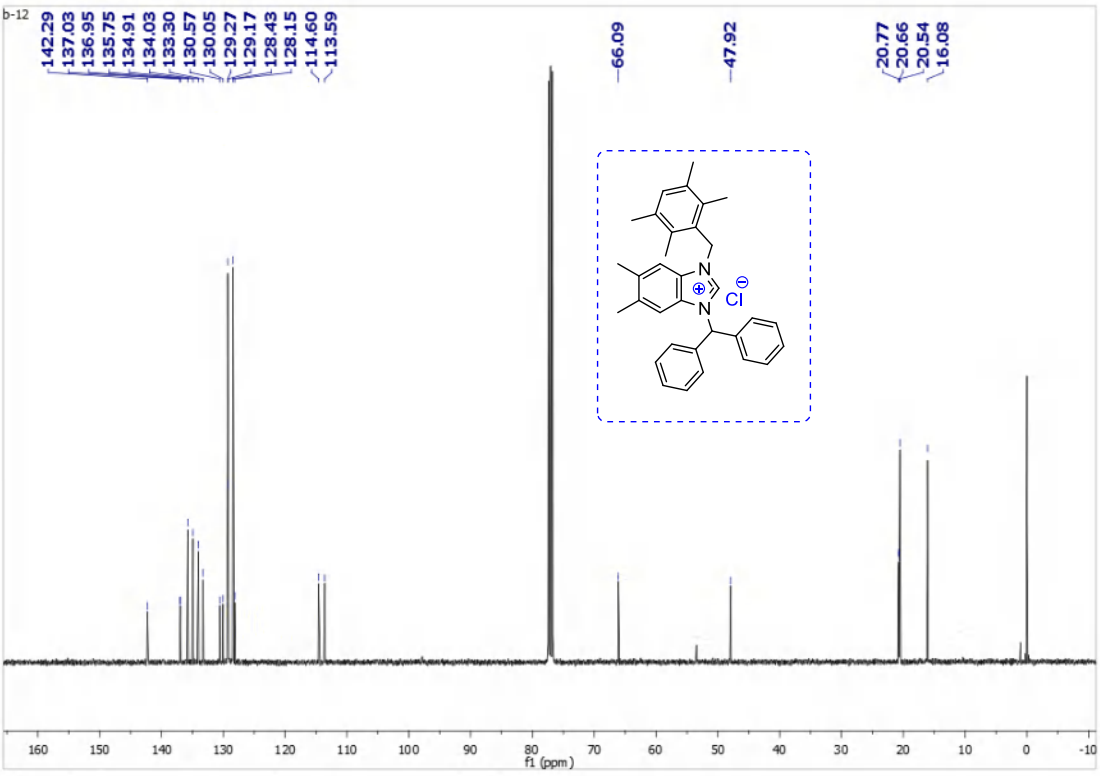

1-Benzhydryl -5,6-dimethyl-(4-methylbenzyl)benzimidazolium chloride (2b)

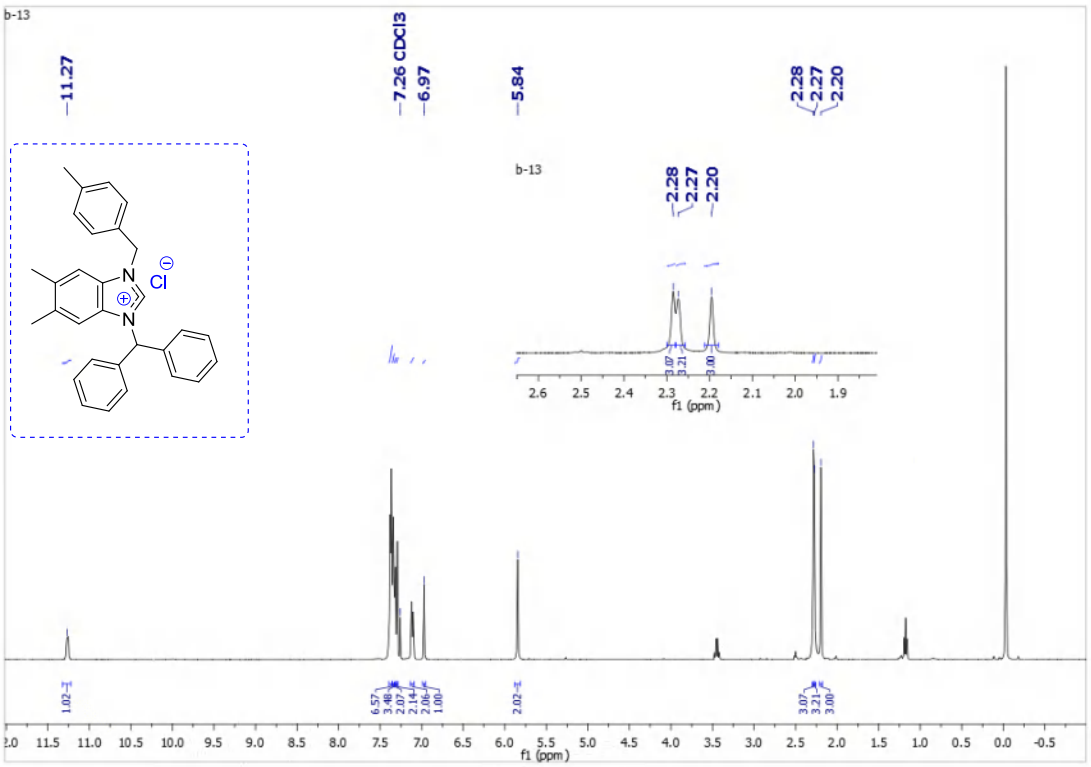

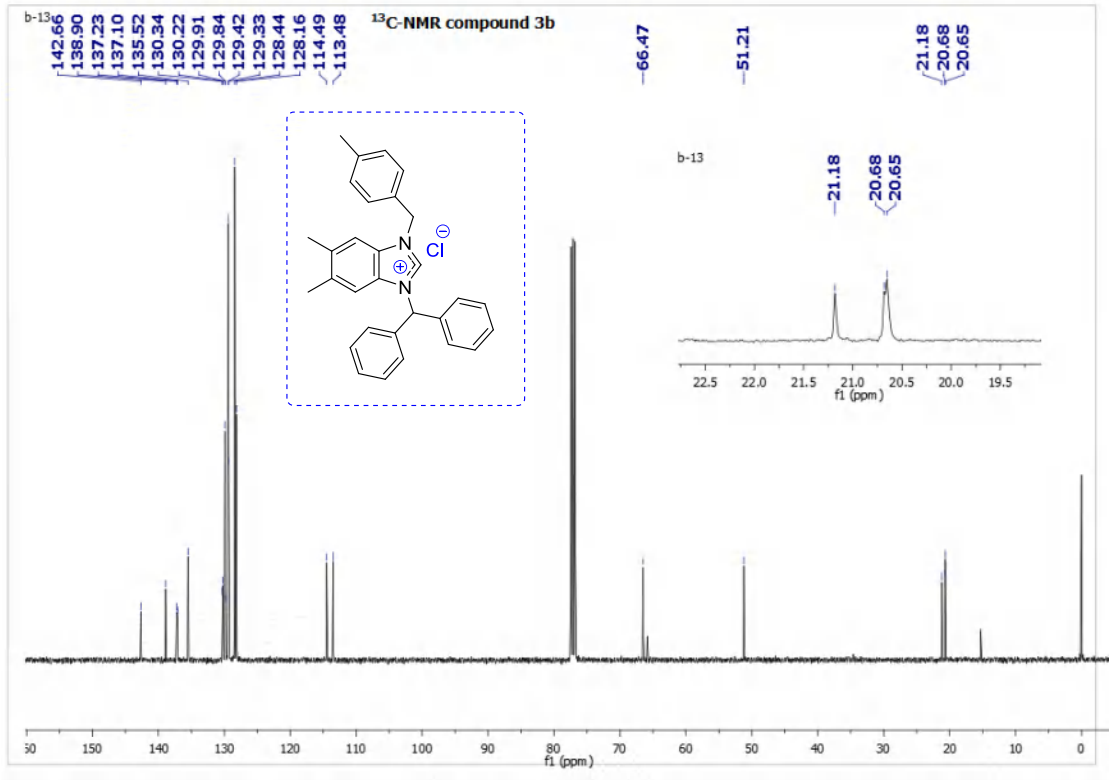

1-Benzhydryl -5,6-dimethyl-3-(2,4,6-trimethylbenzyl)benzimidazolium chloride (2c)

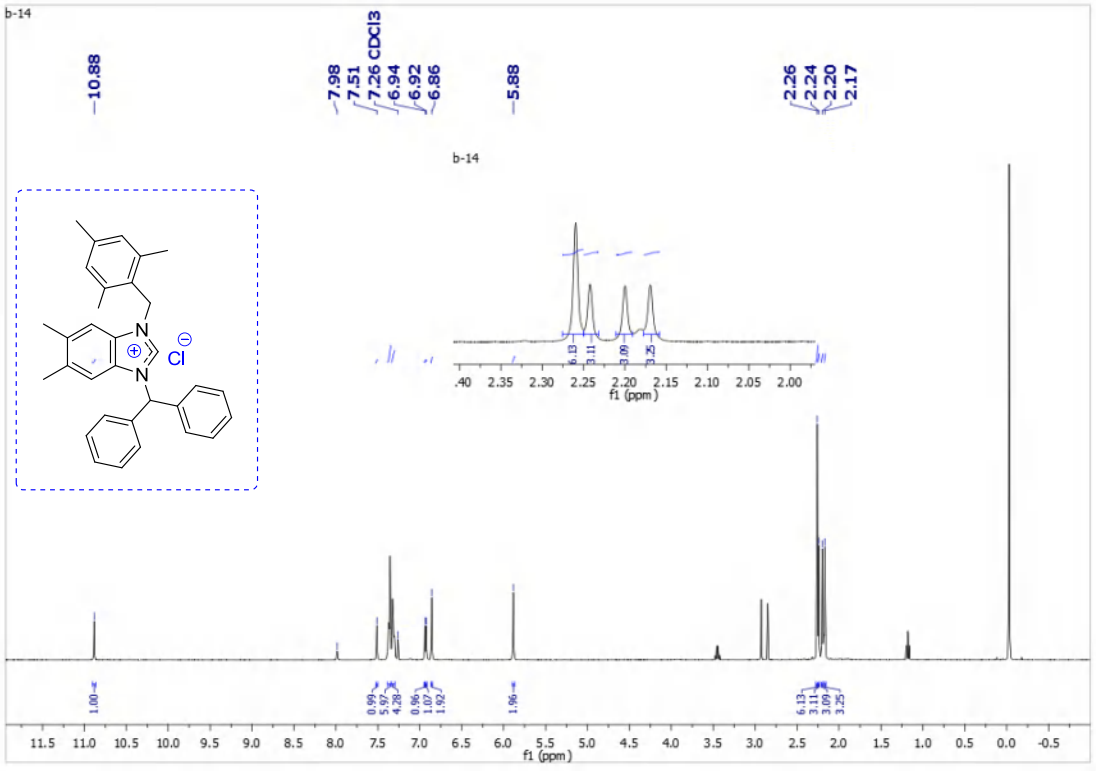

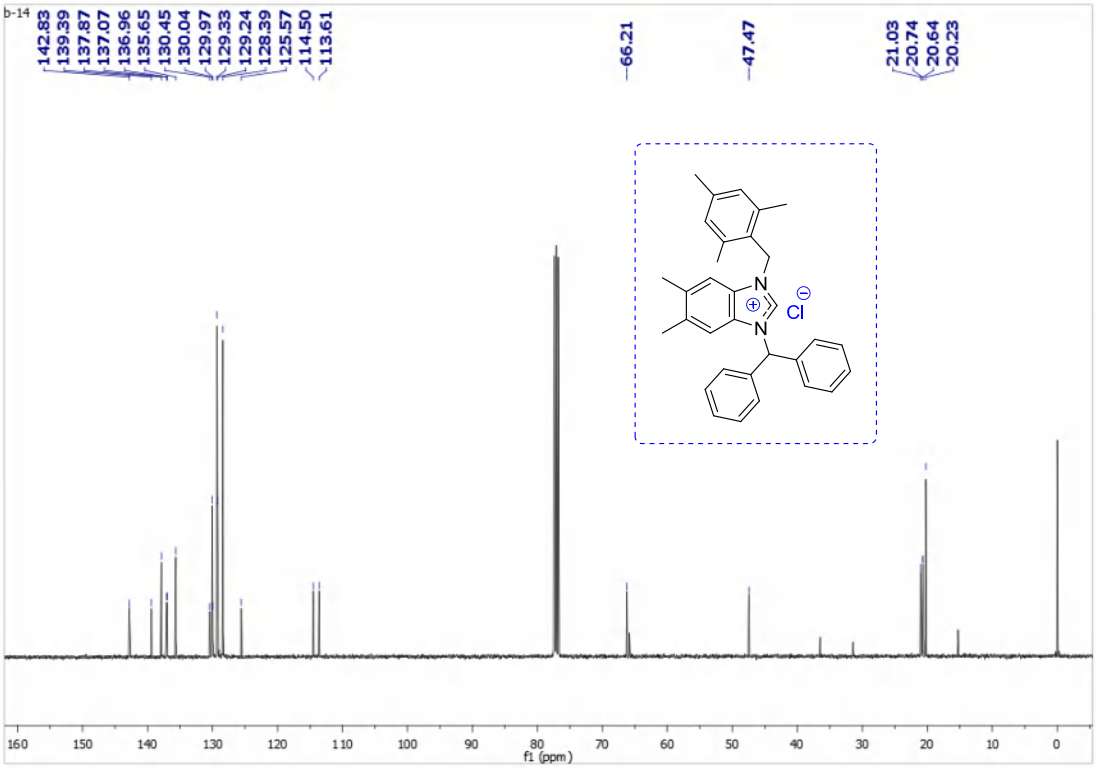

1-Benzhydryl -5,6-dimethyl-(3-methylbenzyl)benzimidazolium chloride (2d)

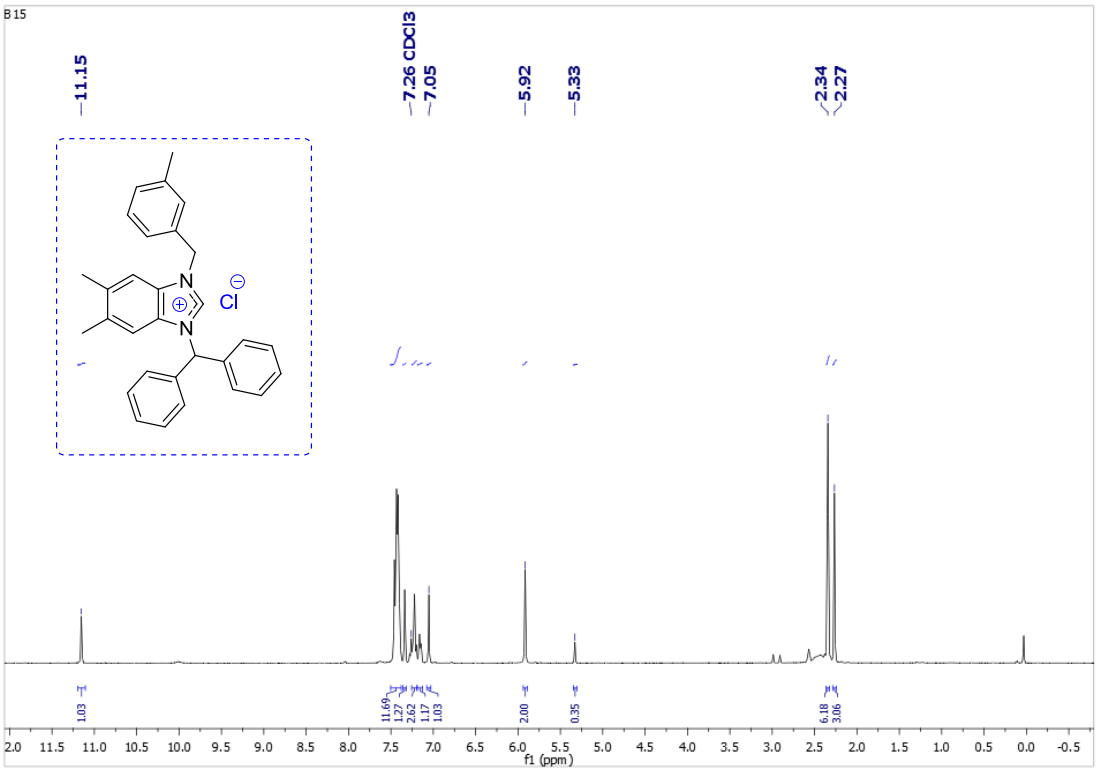

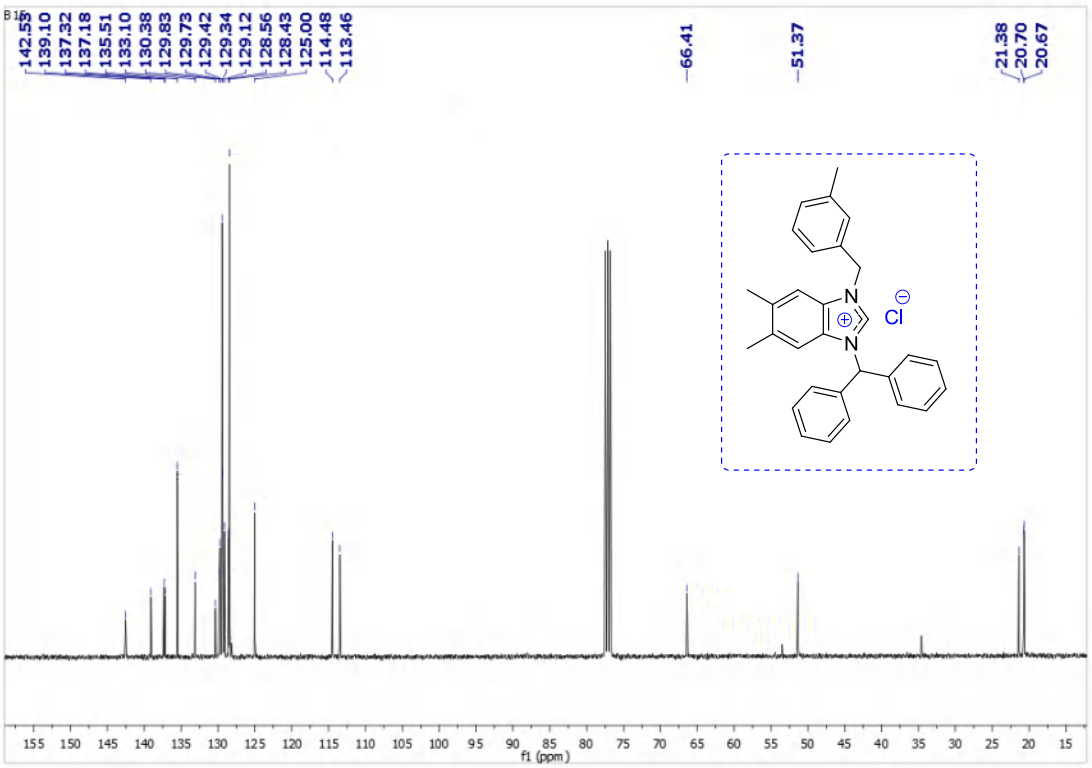

1-Benzhydryl -5,6-dimethyl-(4-tert-butylbenzyl)benzimidazolium bromide (2e)

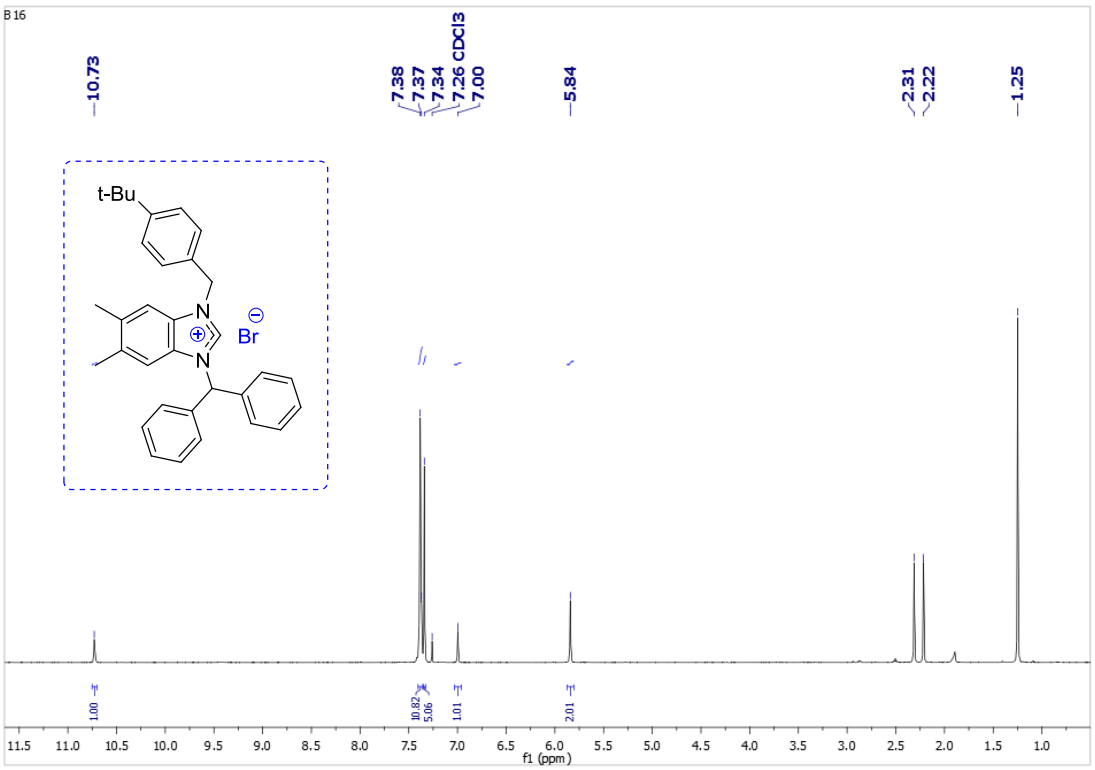

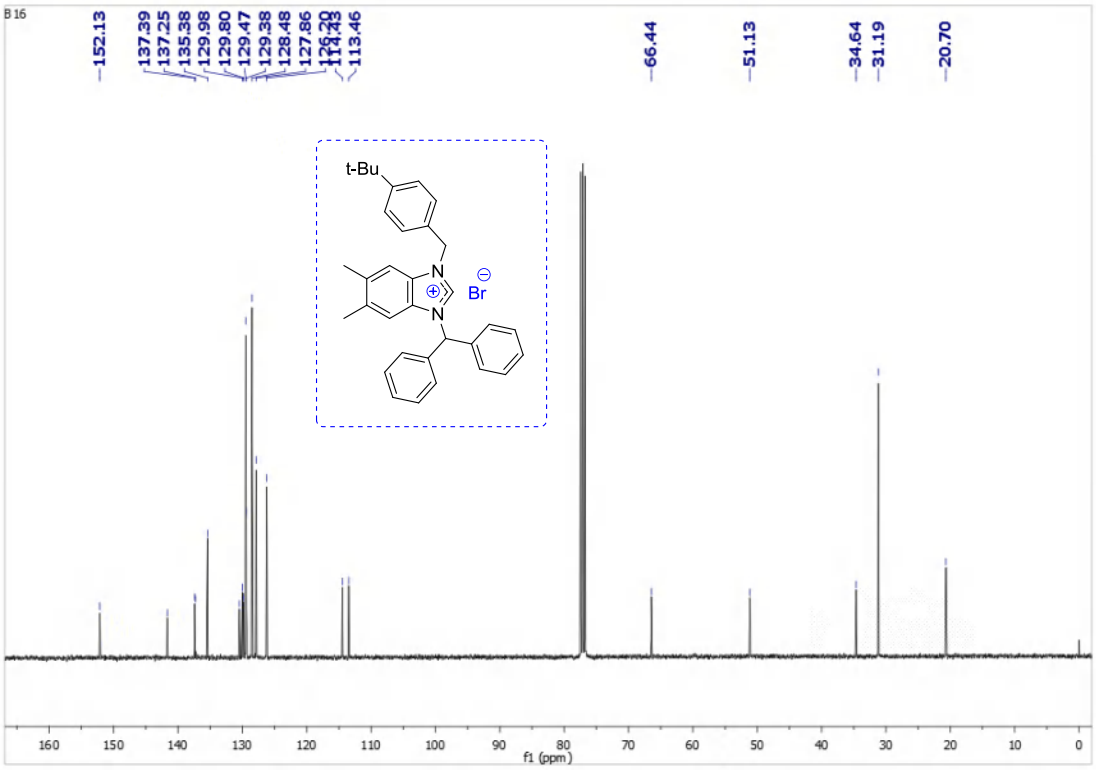

1-Benzhydryl-5,6-dimethyl-3-(3,4,5-trimethoxybenzyl)benzimidazolium chloride (2f)

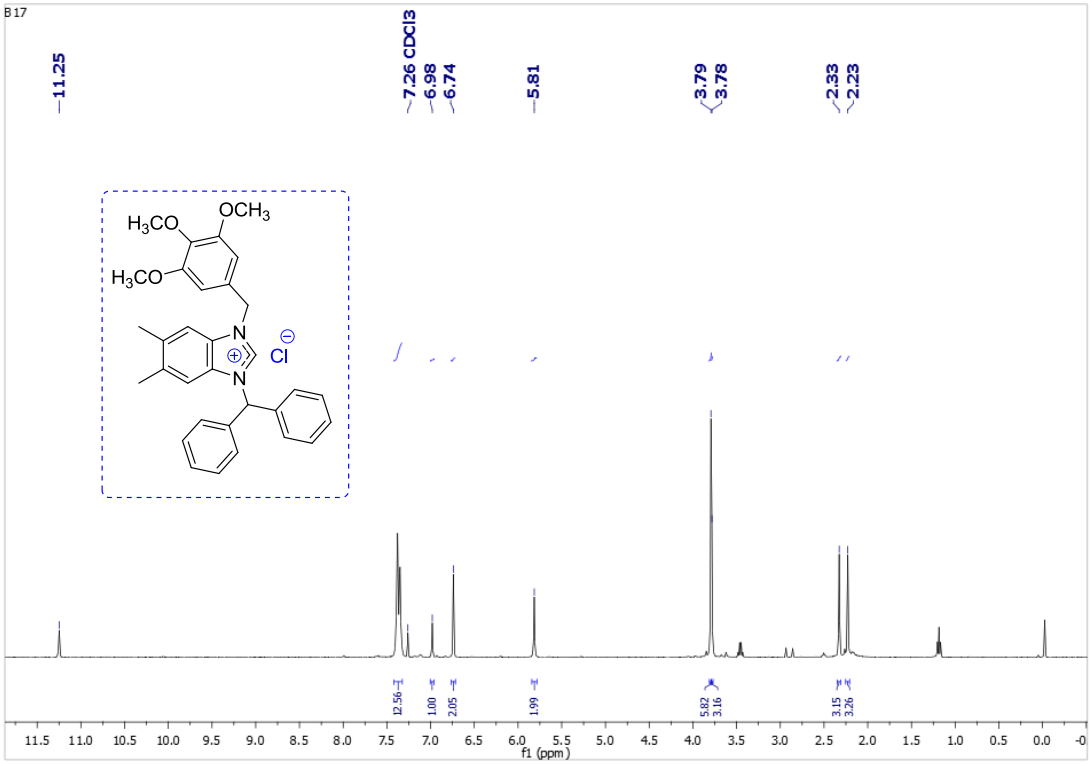

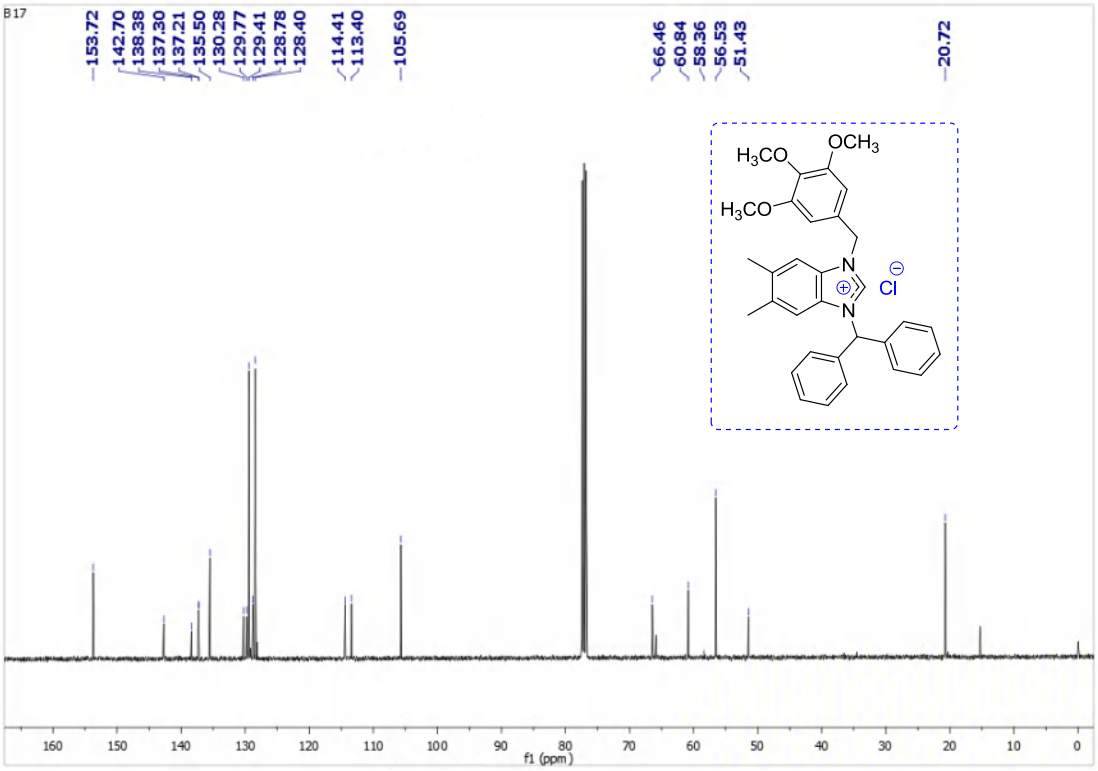

Chloro[1-benzhydryl-3-(2,3,5,6-tetramethylbenzyl)-5,6 dimethylbenzimidazole-2-ylidene]silver(I) (3a)

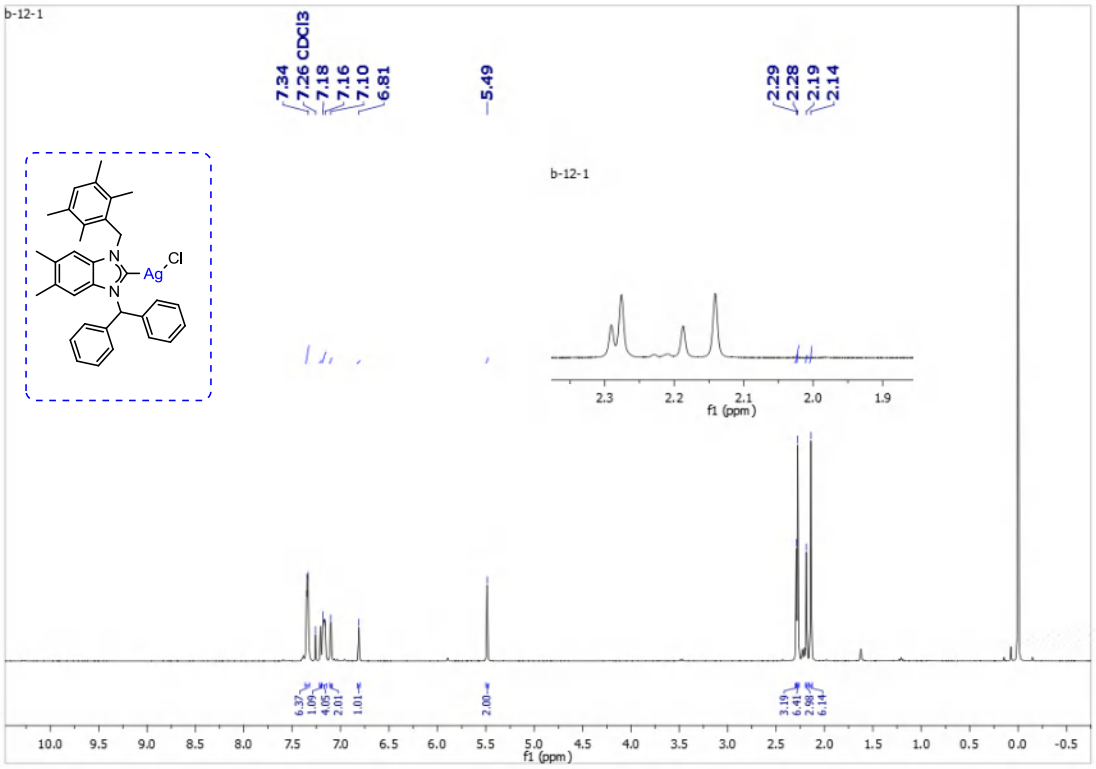

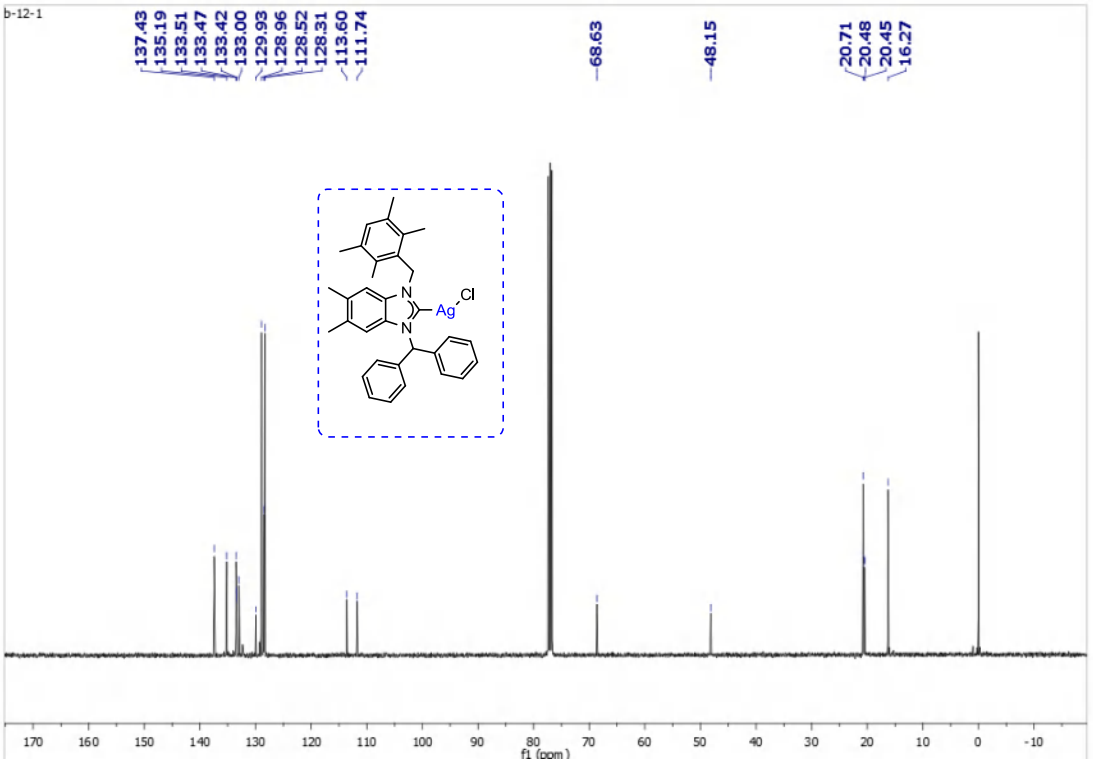

Chloro[1-benzhydryl-3-(4-methylbenzyl)-5,6-dimethylbenzimidazole-2-ylidene]silver(I) (3b)

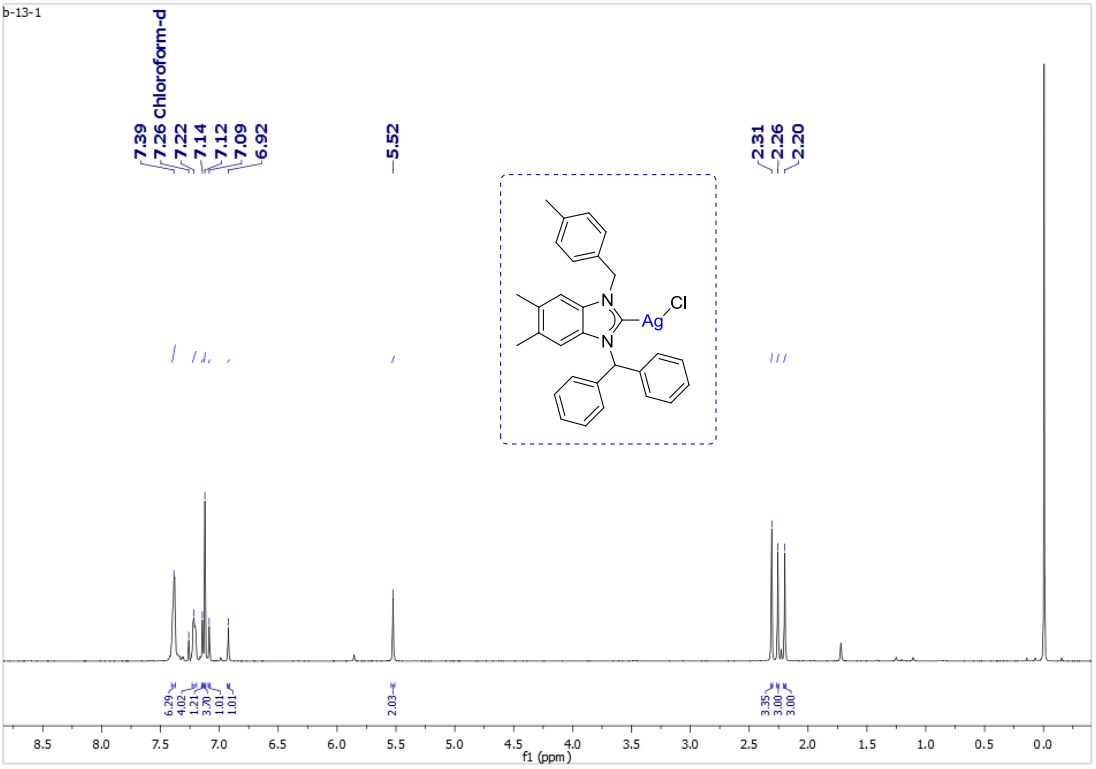

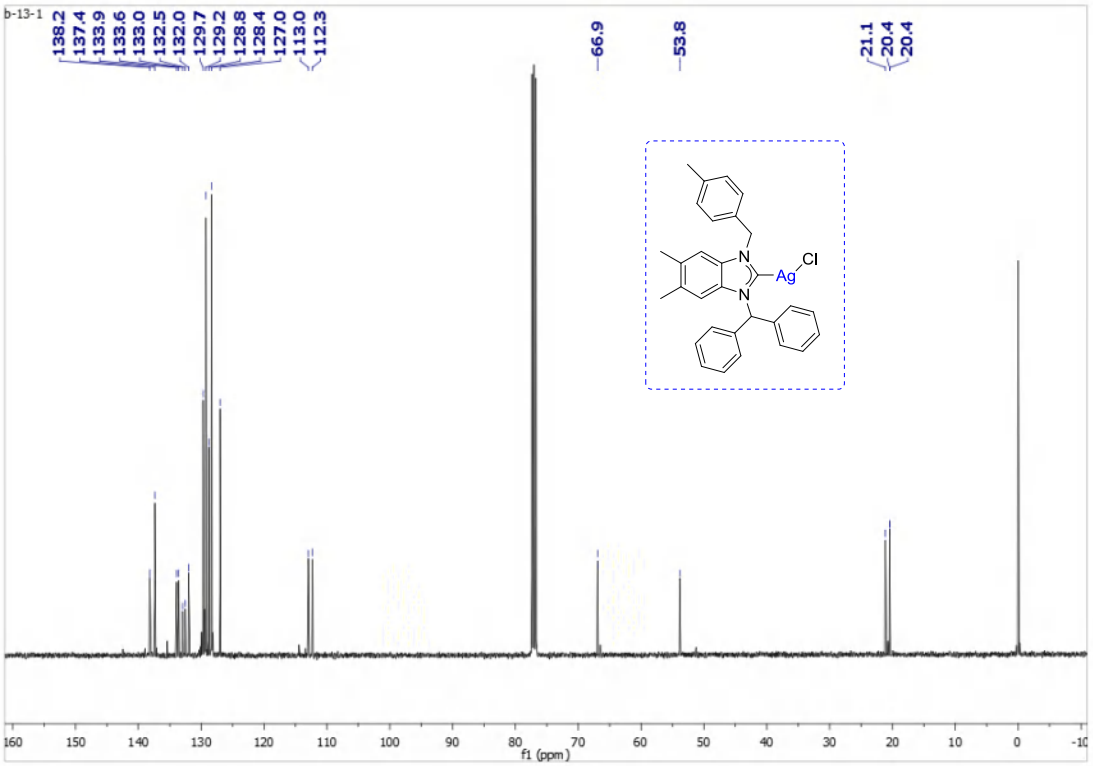

Chloro[1-benzhydryl-3-(2,4,6-trimethylbenzyl)-5,6-dimethylbenzimidazole-2-ylidene]silver(I) (3c)

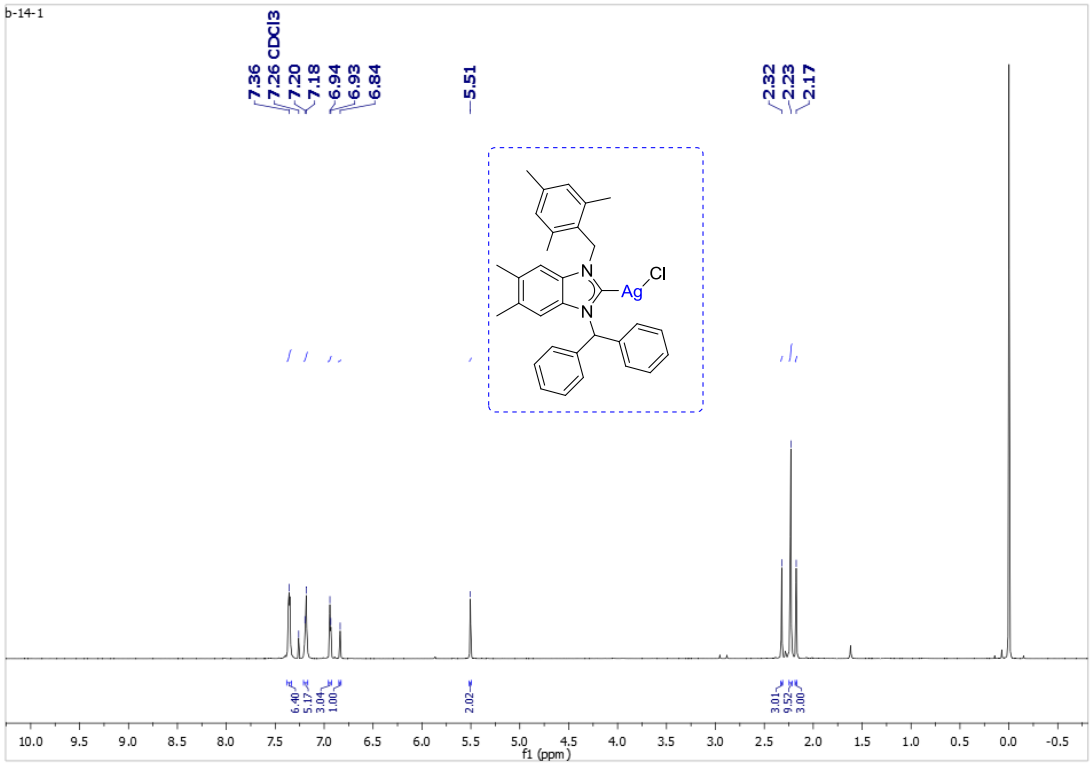

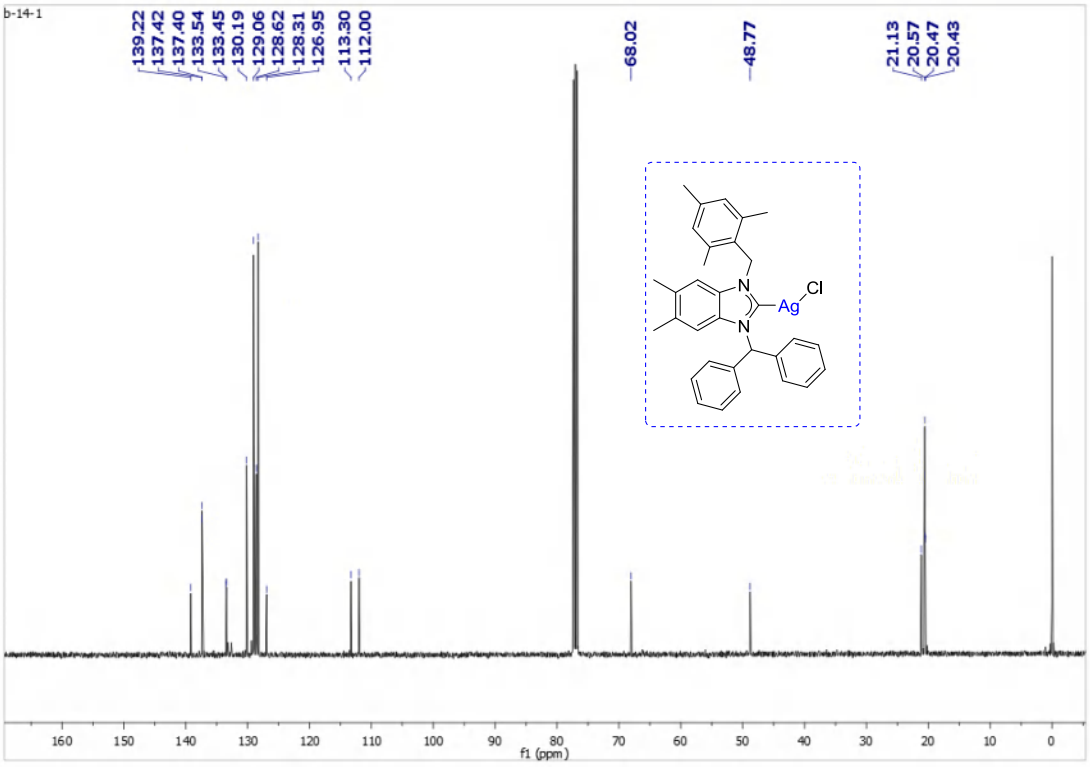

Chloro[1-benzhydryl-3-(3-methylbenzyl)-5,6-dimethylbenzimidazole-2-ylidene]silver(I) (3d)

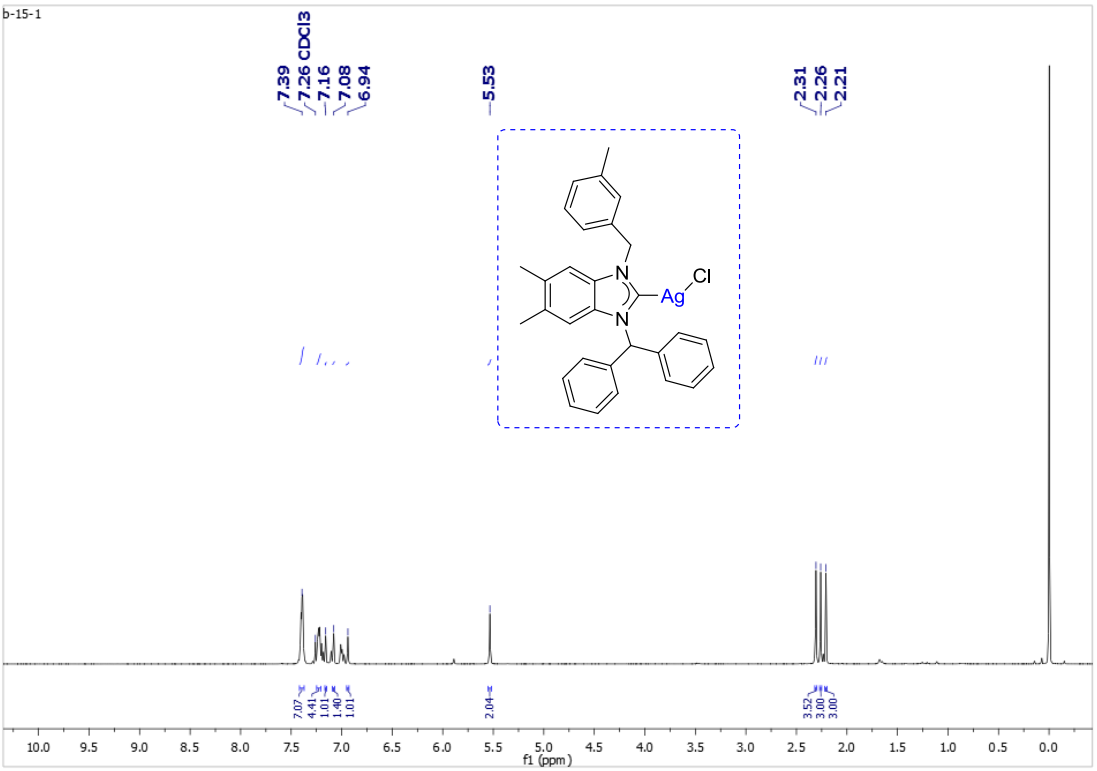

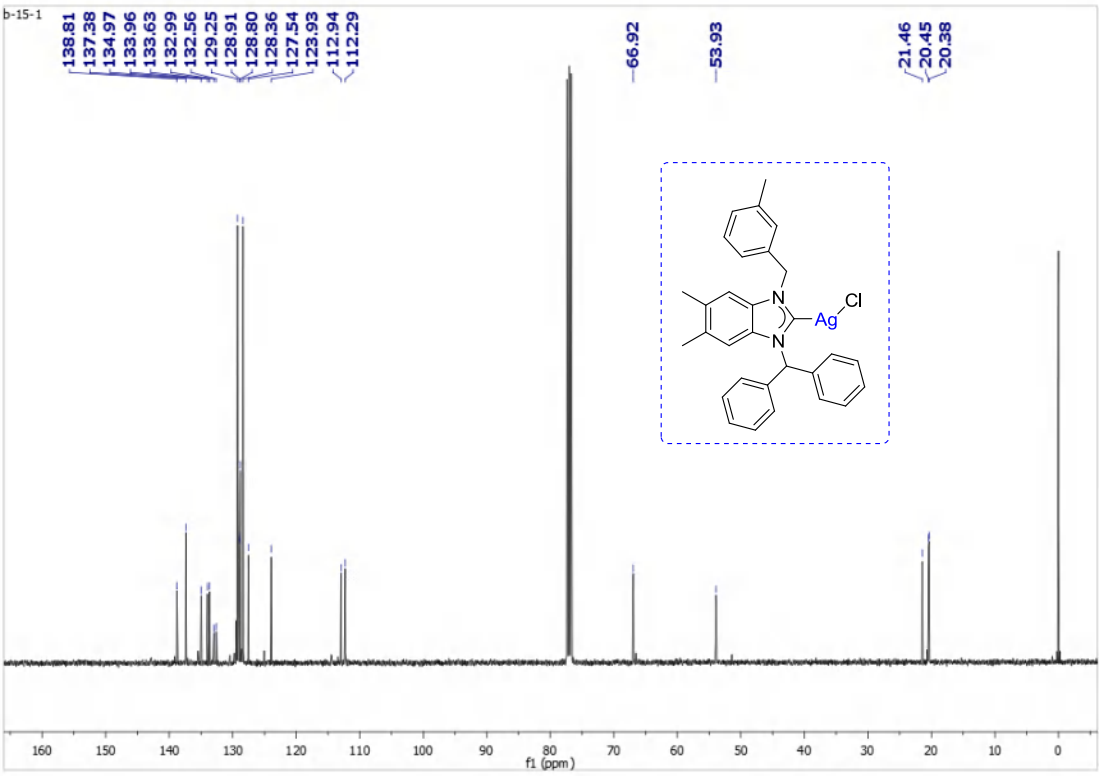

Bromo[1-benzhydryl-3-(4-tert-butylbenzyl)-5,6-dimethylbenzimidazole-2-ylidene]silver(I) (3e)

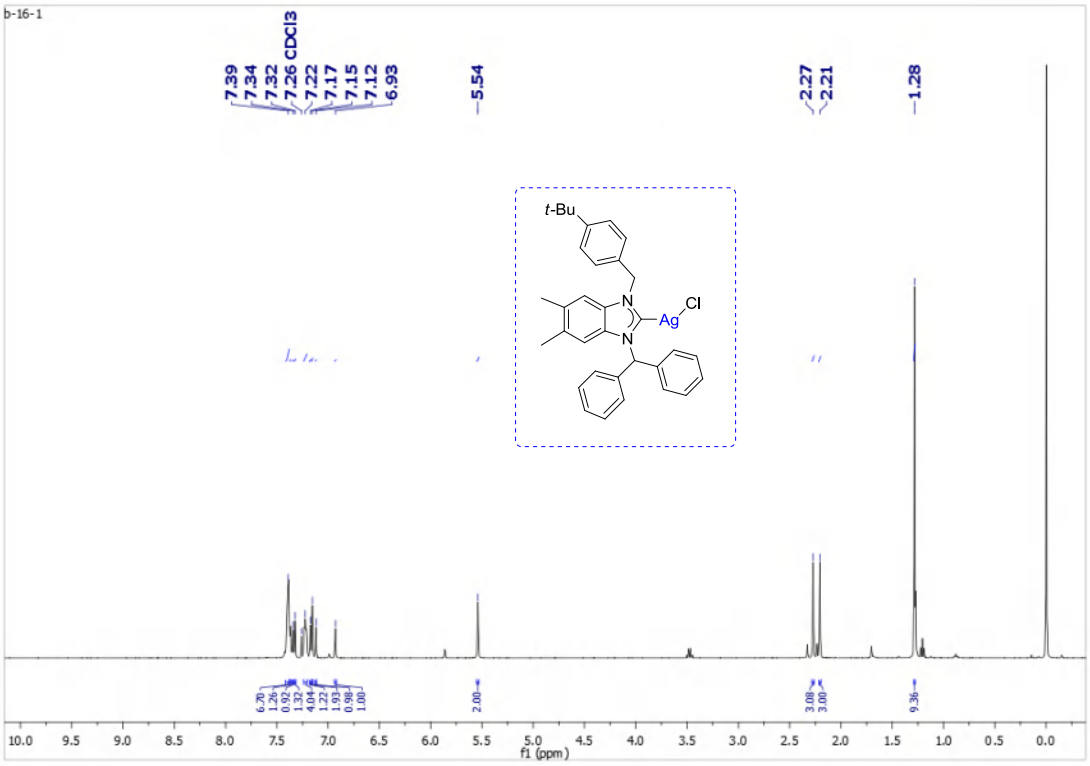

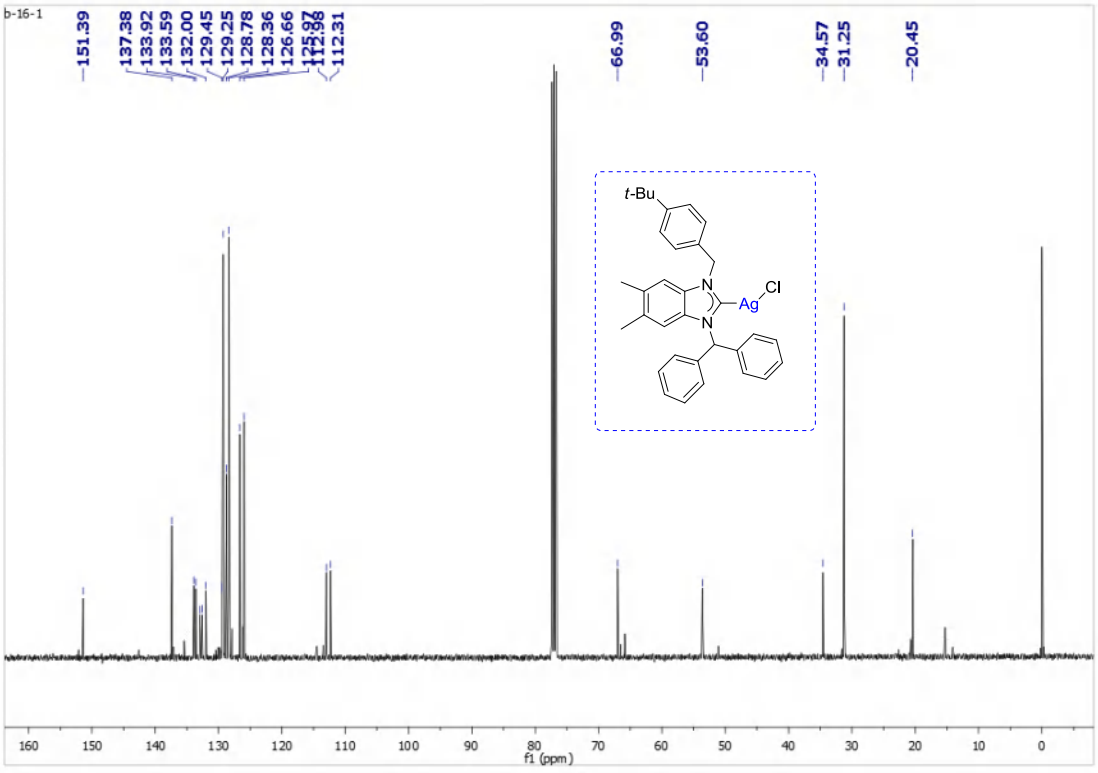

Chloro[1-benzhydryl-3-(3,4,5-trimethoxybenzyl)-5,6-dimethylbenzimidazole-2-ylidene] silver(I) (3f)

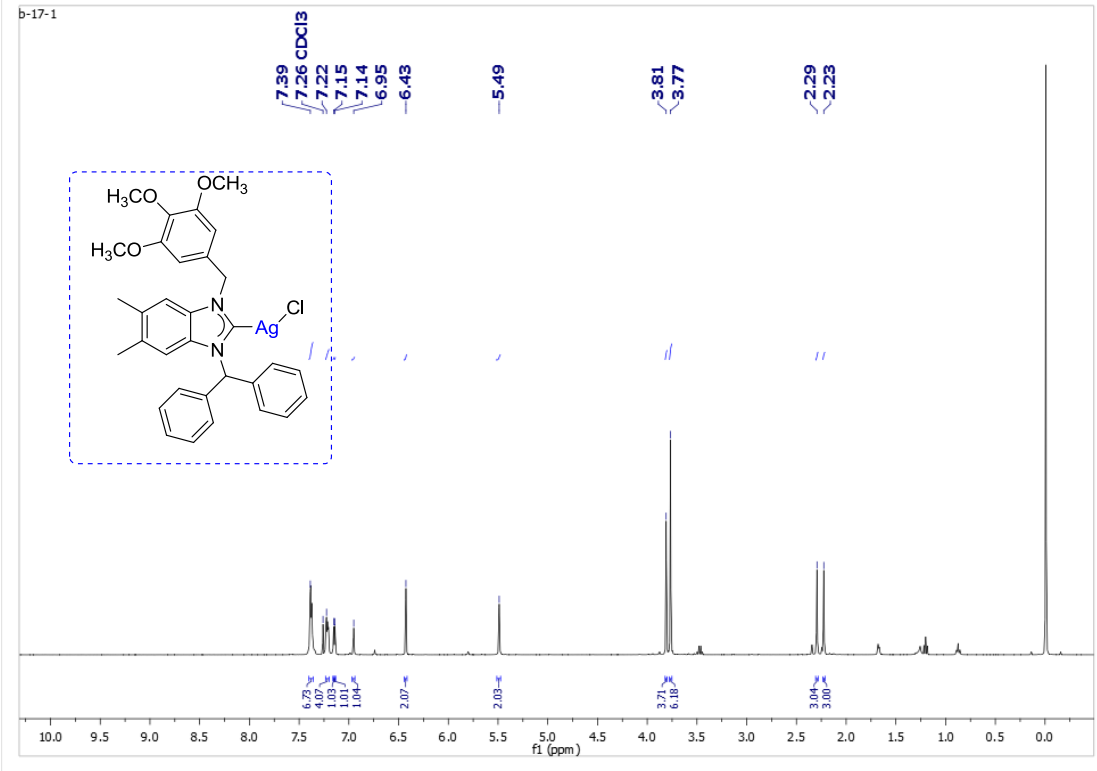

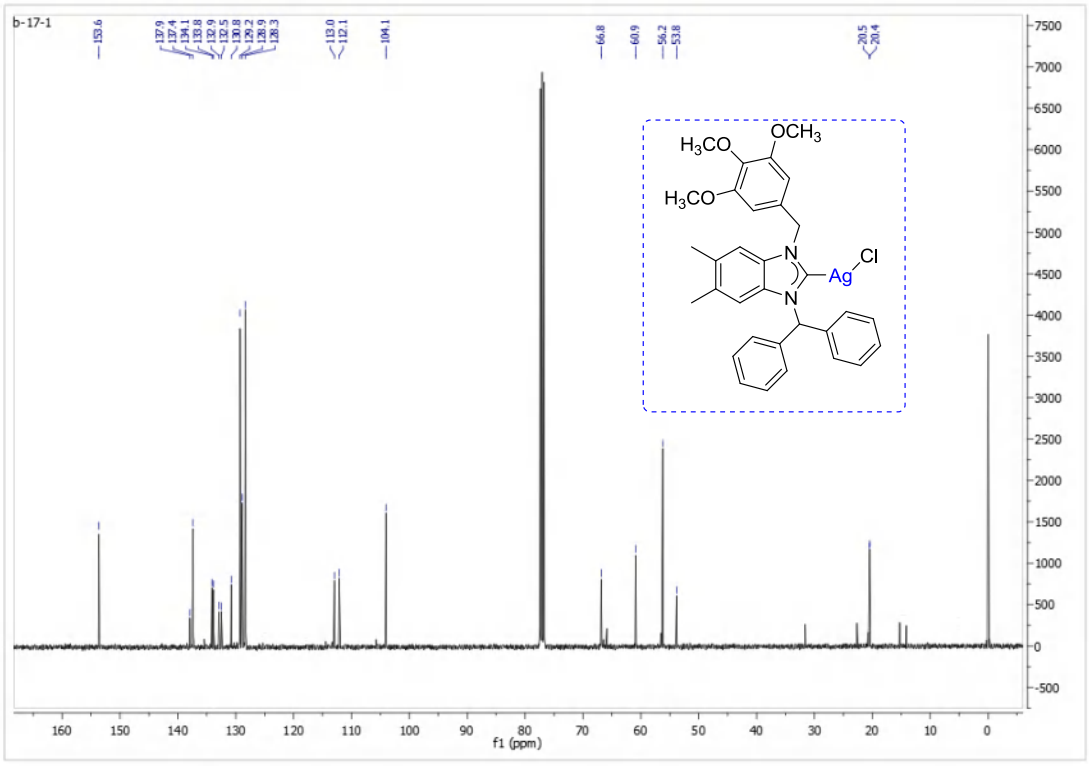

Dibromo[1-benzhydryl-5,6-dimethyl-3-(2,3,5,6-tetramethylbenzyl)-benzimedazol-2-ylidene]pyridine palladium (II), (4a)

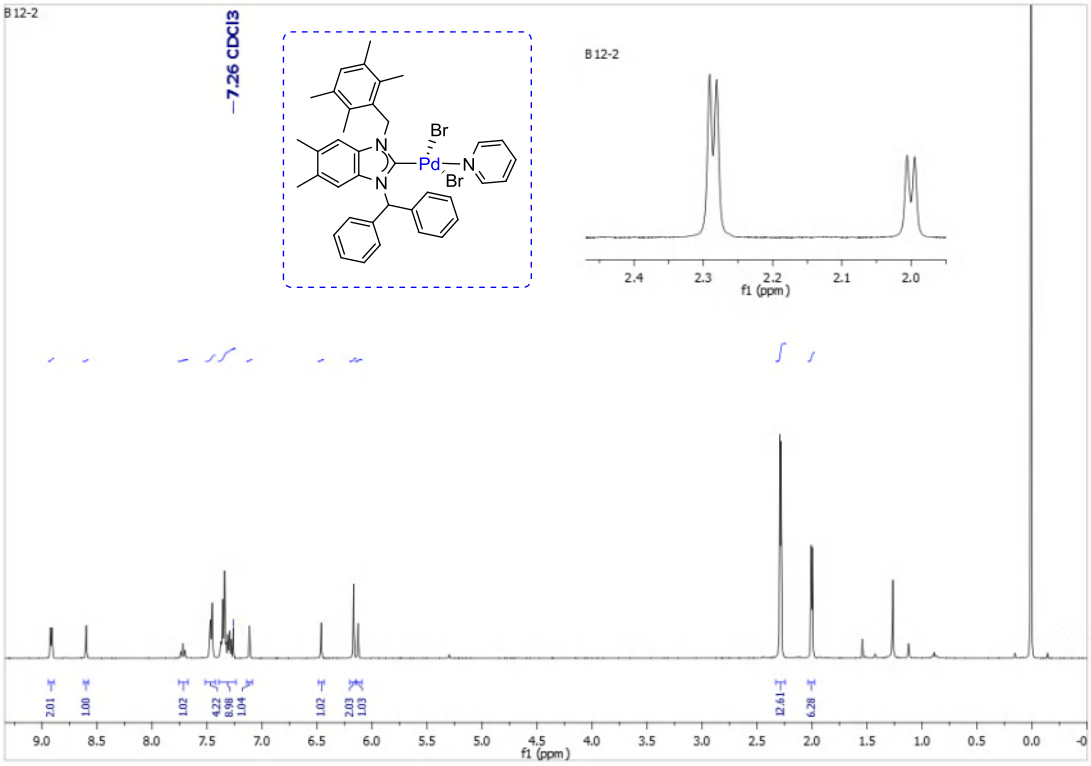

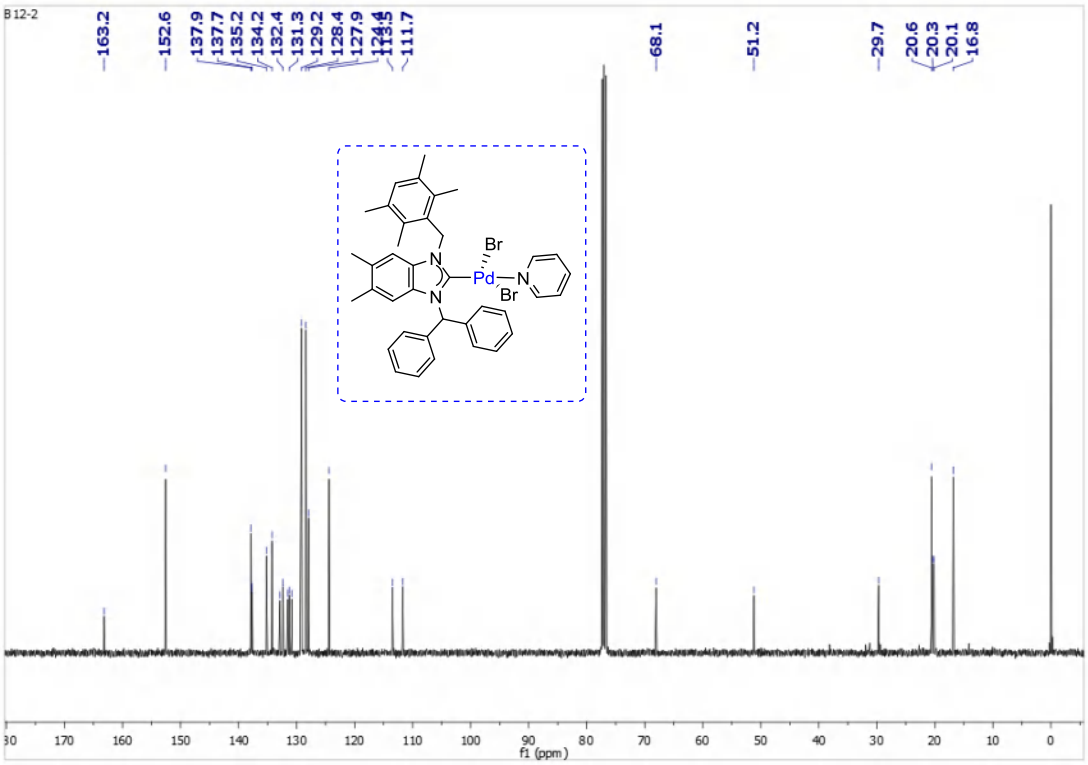

Dibromo[1-benzhydryl-5,6-dimethyl-3-(4-methylbenzyl)benzimedazol-2-ylidene]pyridine palladium (II), (4b)

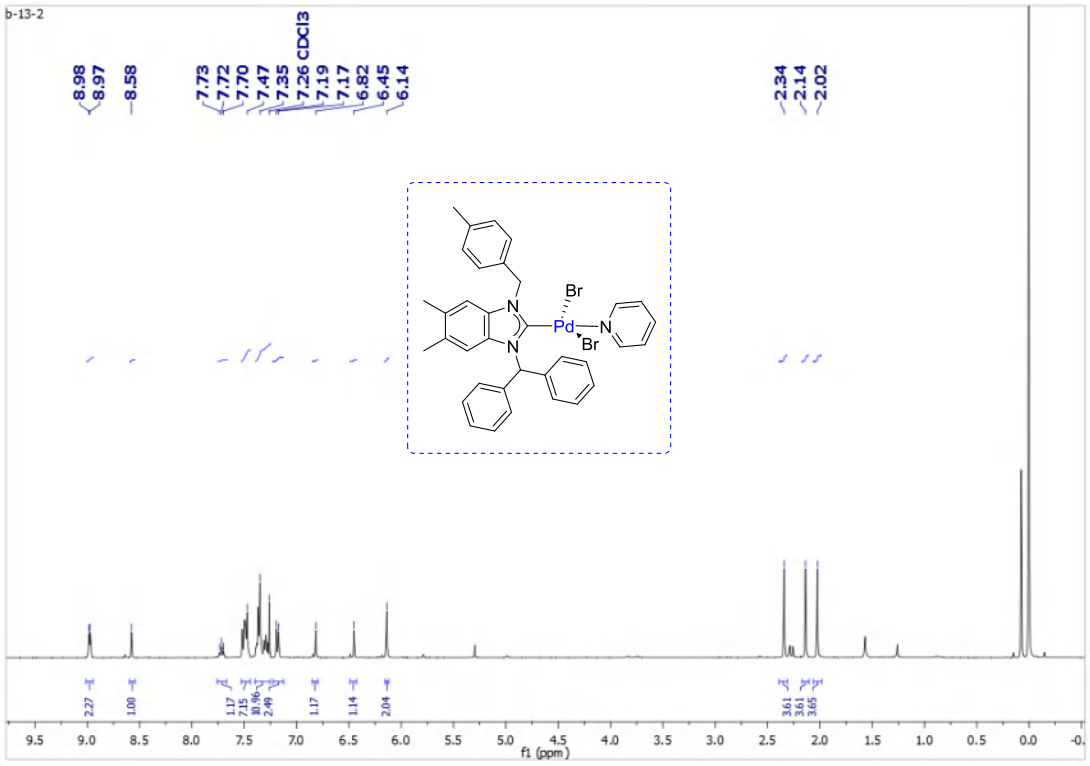

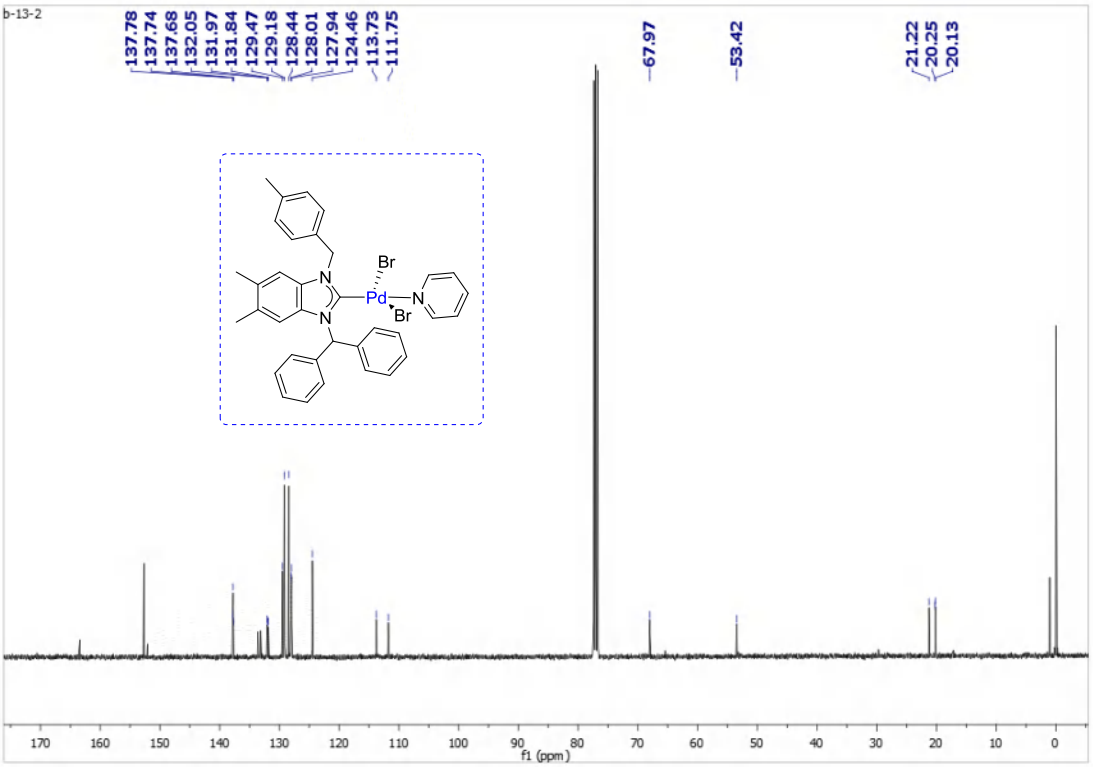

Dibromo[1-benzhydryl-5,6-dimethyl-3-(2,4,6-trimethylbenzyl)benzimedazol-2-ylidene]pyridine palladium (II), (4c)

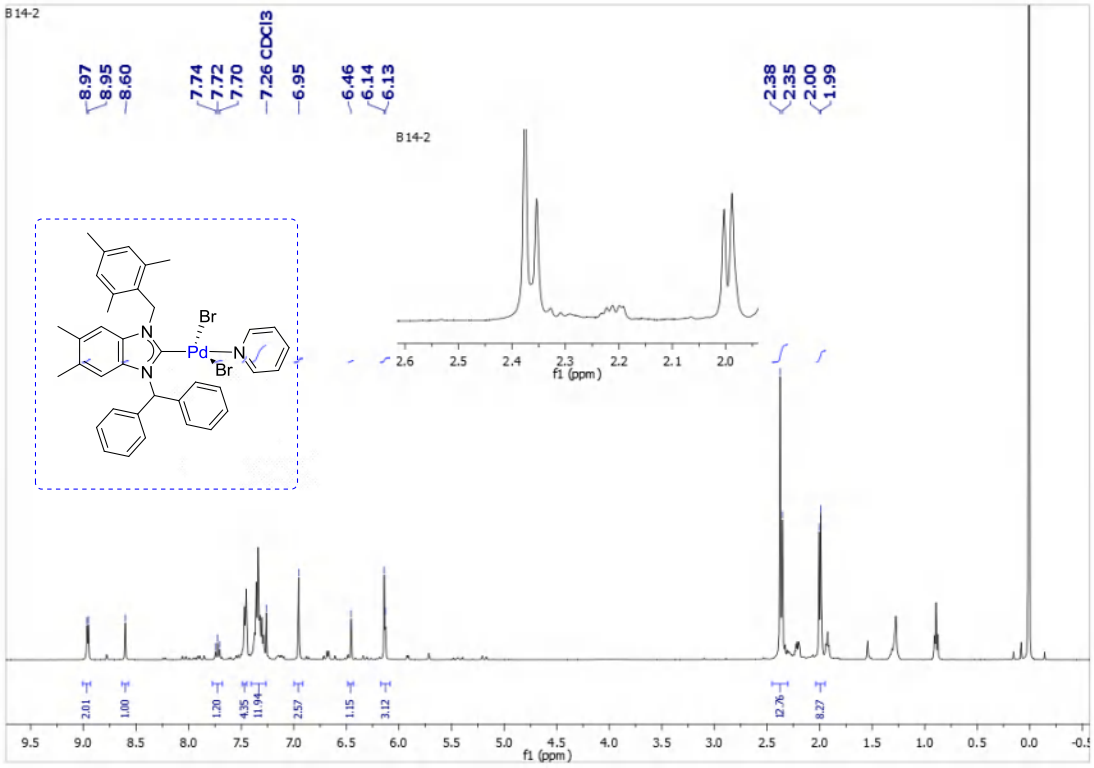

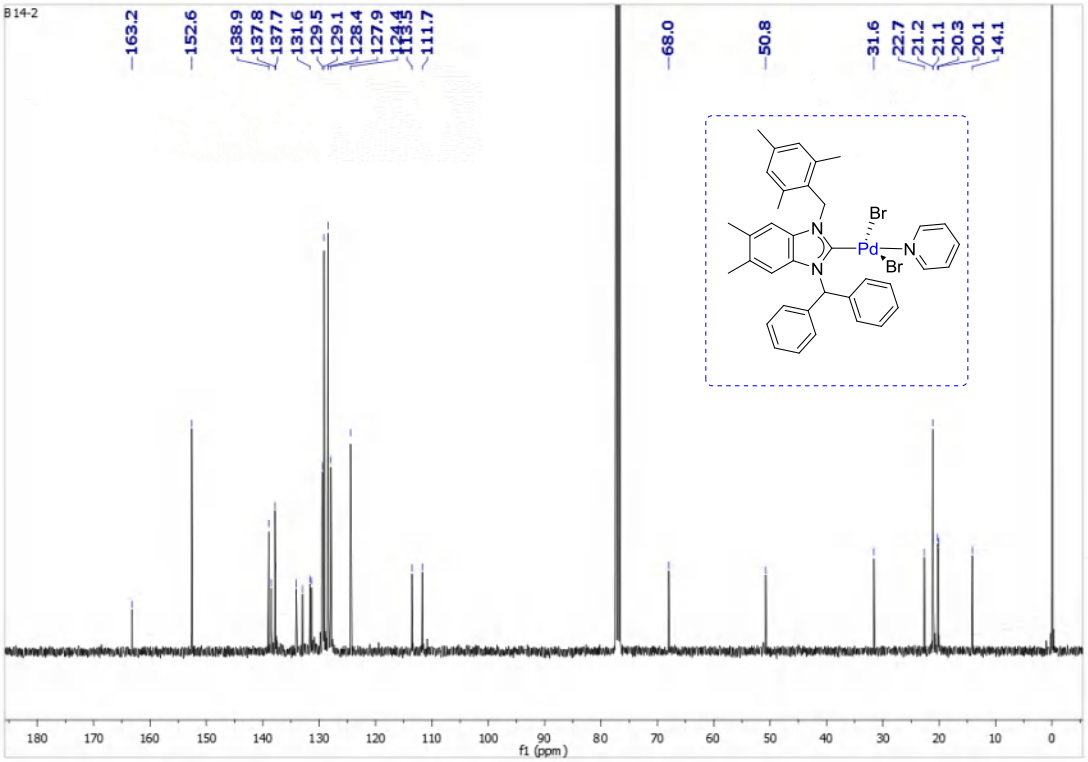

Dibromo[1-benzhydryl-5,6-dimethyl-3-(3-methylbenzyl)benzimedazol-2-ylidene]pyridine palladium (II), (4d)

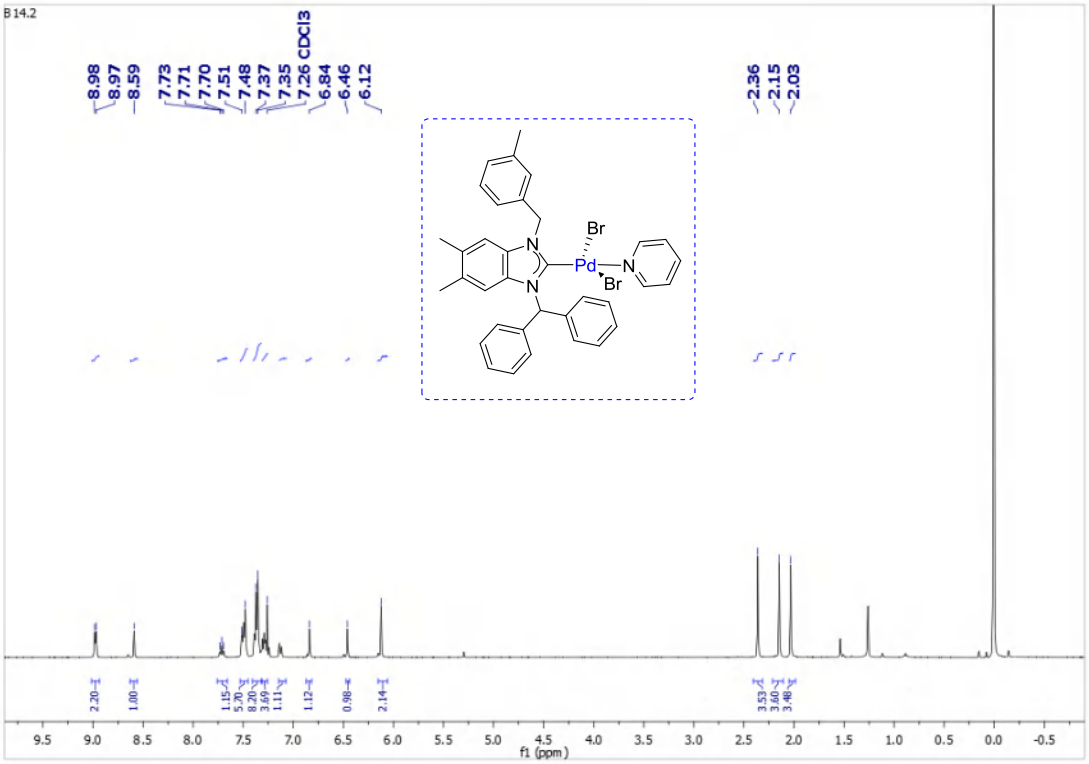

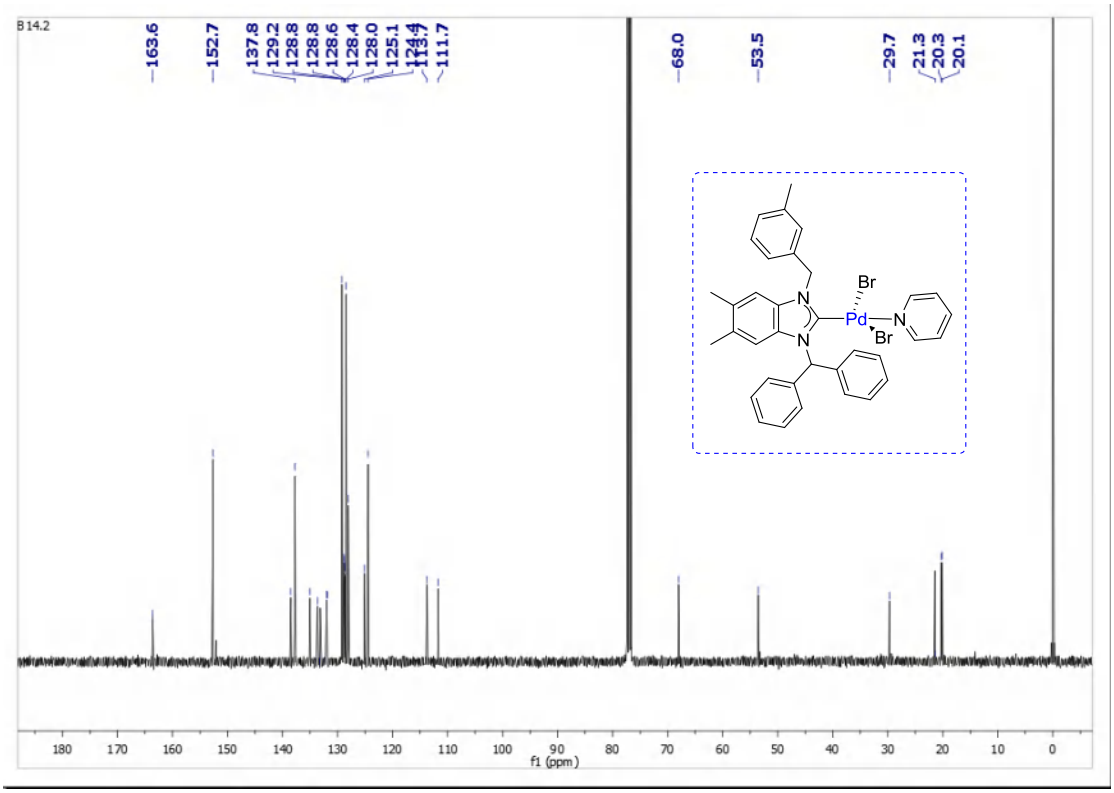

Dibromo[1-benzhydryl-5,6-dimethyl-3-(4-tert-butylbenzyl)benzimedazol-2-ylidene]pyridine palladium (II), (4e)

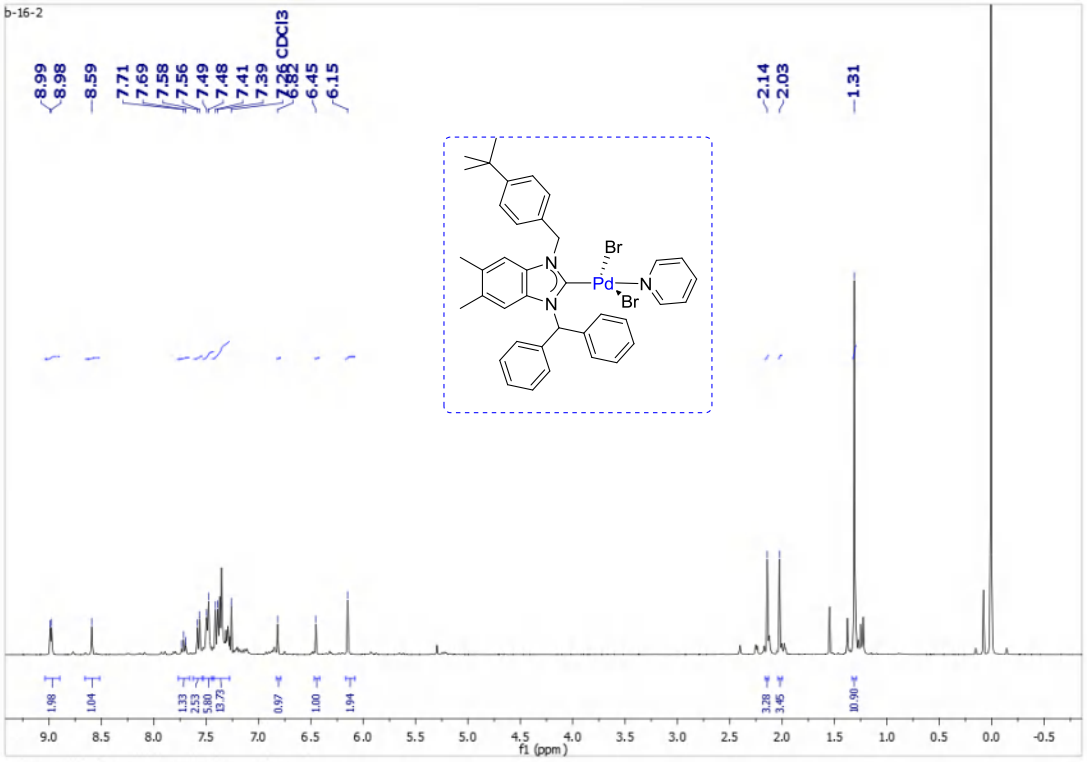

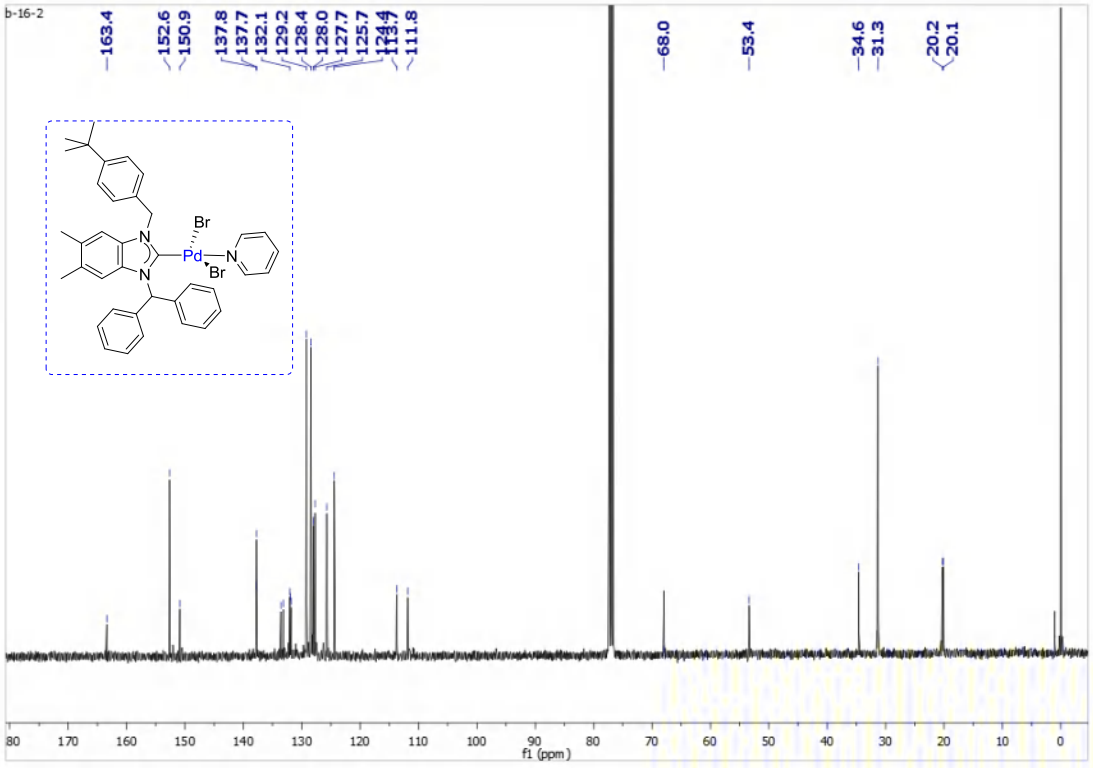

Dibromo[1-benzhydryl-5,6-dimethyl-3-(3,4,5-trimethoxybenzyl)benzimedazol-2-ylidene]pyridine palladium (II), (4f)

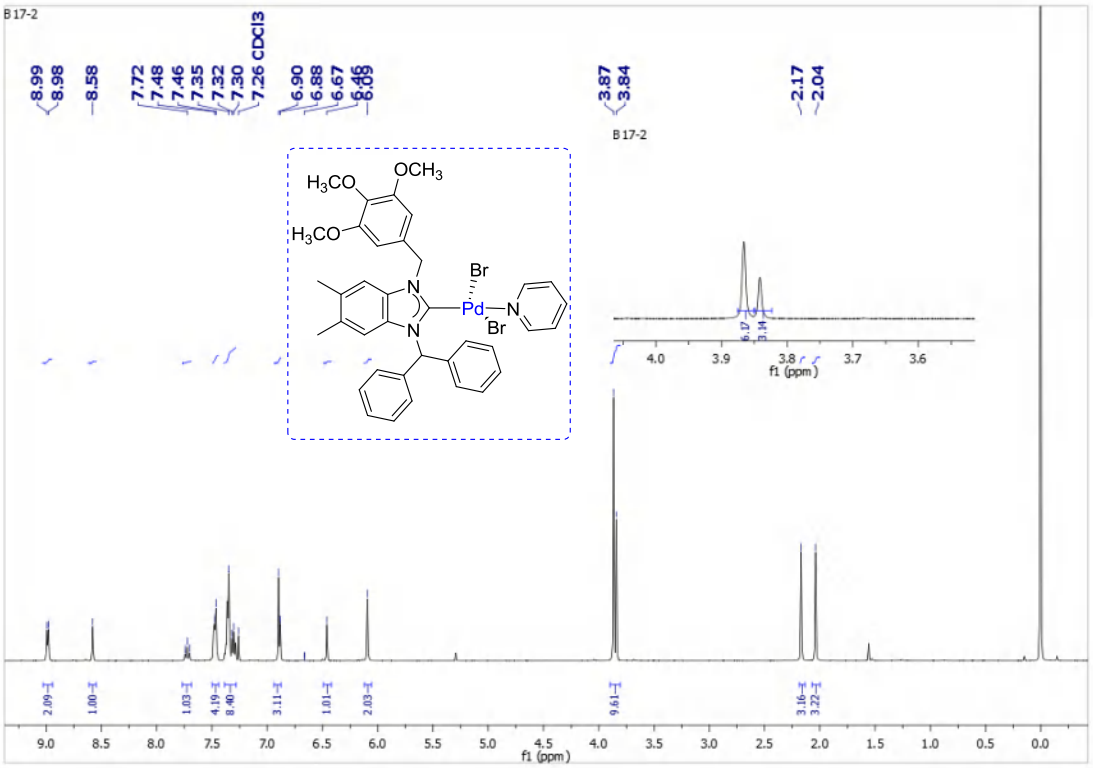

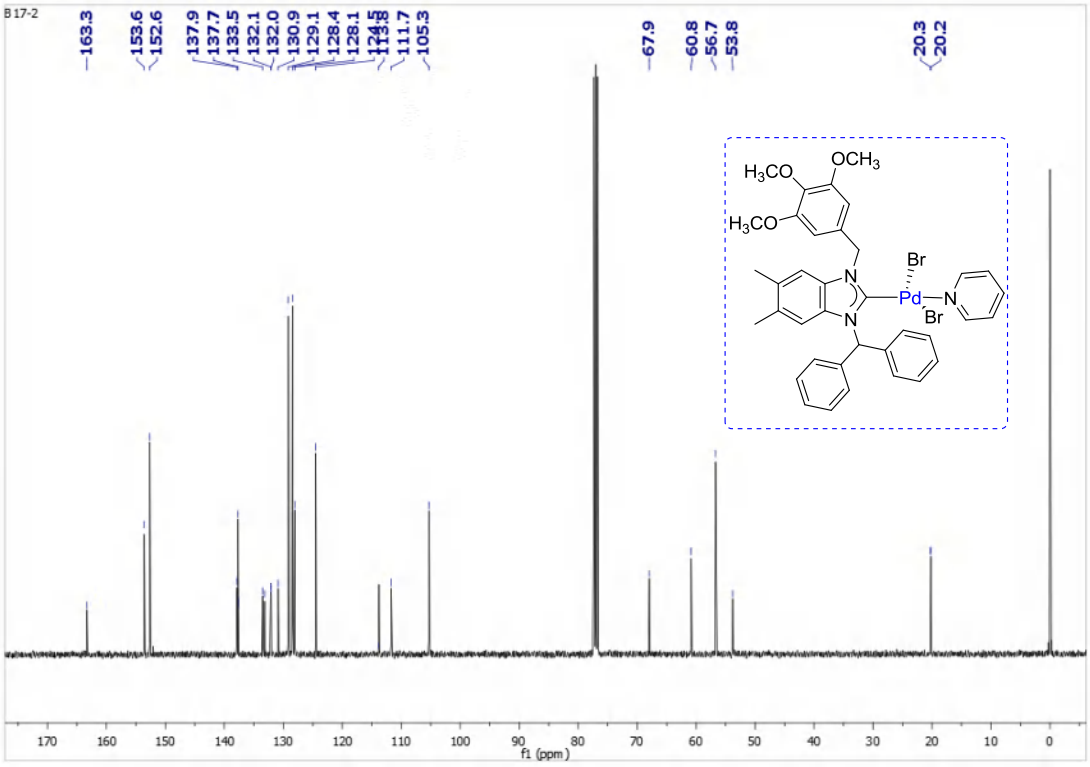

Inorganica Chimica Acta 525 (2021) 120486

Contents lists available at ScienceDirect

Inorganica Chimica Acta

journal homepage: www.elsevier.com/locate/ica

Research paper

Silver (I)-*N*-heterocyclic carbene complexes: Synthesis and characterization, biological evaluation of Anti-Cholinesterase, anti-alpha-amylase, anti-lipase, and antibacterial activities, and molecular docking study

Abd El-Krim Sandeli [a,c], Naima Khiri-Meribout [a,*], Saida Benzerka [a], Nevin Gürbüz [b,c], Muhammed Dündar [d], Hüseyin Karcı [e], Chawki Bensouici [f], El Hassen Mokrani [g], İlknur Özdemir [b], Ahmet Koç [h], Namık Özdemir [i], Abdelmadjid Debache [a], İsmail Özdemir [b,c,*]

[a] *Laboratory of Synthesis of Molecules with Biological Interest, Faculty of Exact Sciences, Brother's Mentouri Constantine 1 University, 25000 Constantine, Algeria*
[b] *Faculty of Science and Art, Department of Chemistry, İnönü University, Malatya, Turkey*
[c] *Catalysis Research and Application Center, İnönü University, 44280 Malatya, Turkey*
[d] *Faculty of Medicine, Department of the Medical Biology and Genetics, İnönü University, Malatya, Turkey*
[e] *Medical School, Department of Medical Biology and Genetics, İnönü University, Battalgazi, Malatya, Turkey*
[f] *National Center for Biotechnologie Research (CRBt), Ali Mendjli New Town, Constantine, Algeria*
[g] *Laboratory of Applied Biochemistry, Department of Biochemistry and Cellular and Molecular Biology, Faculty of Natural and Life Sciences, Brother's Mentouri Constantine 1 University, Constantine, Algeria*
[h] *Inonu University, Medical School, Department Genetics, Battalgazi, Malatya, Turkey*
[i] *Department of Mathematics and Science Education, Faculty of Education, Ondokuz Mayıs University, 55139 Samsun, Turkey*

ARTICLE INFO

Dedicated to Professor Christian Bruneau

Keywords:
Silver(I)–NHC complexes
Antimicrobial
Anticholinesterase activity (*anti*-Alzheimer)
Anti-lipase activity
Anti-diabetic activity
X-Ray
Molecular docking

ABSTRACT

A series of novel silver(I)-*N*-heterocyclic carbene complexes have been prepared and fully characterized by spectroscopic methods and X-ray crystallographic analyses. The biological capacity of the synthesized compounds was evaluated *in vitro* for their anti-microbial, anti-cholinesterase, anti-lipase, anti-diabetic activities in search of potent inhibitors compound. All compounds were tested against two types of fungi and three bacterias. The results proved that most compounds indicated moderate to excellent activity against all types of bacteria and fungi except compound **2f** that didn't show any antibacterial activity. The synthesized compound's capacity to inhibit the enzymes AChE, BChE, Lipase, and α-amylase were evaluated. The results showed that silver(I)–NHC complexes **3a-f** are effective against all types of enzymes. The highest activity was reported toward AChE, BChE, and α-amylase enzymes, and at a lower rate against Lipase enzyme compared to the references drug. In contrast, benzimidazolium salts **2a-f,** which showed significant inhibitory activity against AChE and BChE enzymes, while all salts were not active against both Lipase and α-amylase enzymes. Molecular docking simulations using AutoDock, have been performed of the new compounds as a representative set of our molecules into AChE and BChE enzymes for lead optimization of the binding interaction template of the most active inhibitors docked into the active site of their relevant AChE and BChE enzymes inhibitors.

1. Introduction

The chemistry of *N*-heterocyclic carbenes (NHCs) has appeared as flexible building blocks for the ligation of a large variety of coordination compounds[1]. It has limited to metal coordination compounds derived from benzimidazolium precursors. Recently, *N*-Heterocyclic Carbenes' use in organometallic chemistry as ligands pulled insignificant consideration and became a rapidly growing field with a broad range of

Abbreviations: **NHC**, *N*-Heterocyclic carbine; **NMR**, Nucleare Magnetic Resonance; **IR**, Infrared spectra; **DMSO**, Dimethyl sulfoxide; **Ag_2O**, Silver oxide; **AChE**, Acetylcholinesterase; **BChE**, Butyrylcholinesterase; ***p*-NPP**, *p*-Nitrophenol Palmitate; **MIC**, Minimum Inhibitory Concentration; **CAS**, Catalytic anionic site; **PAS**, Peripheral anionic site.

* Corresponding authors at: Faculty of Science and Art, Department of Chemistry, İnönü University, Malatya, Turkey (İ. Özdemir). Laboratory of Synthesis of Molecules with Biological Interest, Faculty of Exact Sciences, Brother's Mentouri Constantine 1 University, 25000 CONSTANTINE, ALGERIA (N. Khiri-Meribout).

https://doi.org/10.1016/j.ica.2021.120486
Received 23 March 2021; Received in revised form 9 May 2021; Accepted 29 May 2021
Available online 2 June 2021

medicinal applications [2]. Currently, as a new emerging field of chemistry and medicinal research, metal-*N*-heterocycle carbenes (M-NHC) complexes have strongly appeared, where NHC complexes with different metals as (Cu, Au and Ag) proved to be active against several types of diseases as anticancer agents[3-7]. Among different transition metal-*N*-heterocyclic carbene complexes, the use of NHC with silver metal is the more important M-NHC−complexes, it has extraordinary consideration because of their structures, now has been broadly used as sources of different metal complexes in organic chemistry as transfer agents in the reaction of transmetalation due to the effective carbene, that allowed to form other NHC-metal complexes. Besides, the low silver toxicity for humans has attracted the researcher's attention to explore their biological activity and their medical applications, specifically antimicrobial and anticancer [1,8,9]. The synthesis of silver(I) complexes is generally done according to a straightforward procedure listed in the literature, starting from benzimidazolium salts or using directly commercial *N*-heterocycle carbenes [10-14]. In general, the *N*-heterocyclic carbenes (NHCs) could be generated by deprotonation of the related benzimidazolium salts. Our experience led us directly to adopt these types of complexes using 3,5-dimethylbenzimidazolium salts, which consider as very reactive ligands. However, most literature methods showed that the preparation of the silver(I)–NHC complexes have generally based on *N*-alkylation reactions to synthesis benzimidazolium salts as a precursor to nucleophilic carbenes. This type of ligands' characteristic was considered a strong σ donor property, which confirms that benzimidazolium salts are stronger than alkyl phosphines ligand and even the steric properties are also different than phosphines. In many cases, these properties and advantages frequently lead to greater stability of the catalysts[15-17]. On the other hand, benzimidazole salts are an important class that attracted considerable attention in various chemical, biological and industrial areas [18]. Further, the family of *N*-heterocyclic carbenes (NHCs) possessing a wide range of biological activities [3]. The coupling of these two types of compounds generates a pharmaceutically enhanced class of compounds known as M-NHC complexes.

As part of our ongoing research into novel functionalized NHC ligands as supporting a favorable environment for the development and application of metal complexes, Herein, we report the preparation of a new series of silver(I)–NHC complexes that contain 5,6-dimethylbenzimidazole. All the new products are tested against different biological activities such as anti-microbial, anti-Alzheimer, anti-lipase, and anti-diabetic. Also, to recognize and validate the inhibition mechanisms, a molecular docking analysis was carried out.

2. Experimental

2.1. Chemistry

2.1.1. Materials and methods

All reactions for the preparation of the benzimidazolium salts and their complexes Ag(I)–NHC were carried out under argon in flame-dried glassware using standard Schlenk techniques. All reagents were purchased from Sigma-Aldrich, Merck, and Fluka. ^{1}H NMR and ^{13}C NMR spectra were recorded with a Varian As 400 Merkur spectrometer operating at 400 MHz (^{1}H), 100 MHz (^{13}C) in $CDCl_3$ with tetramethylsilane as an internal reference. Coupling constants (*J* values) are given in Hertz. NMR multiplicities are abbreviated as follows: *s* = singlet, *d* = doublet, *t* = triplet, *sept* = septet, *q* = quartet and *m* = multiplet signal. FT-IR spectra were recorded on the ATR unit in the range 400–4000 cm^{-1} on Perkin Elmer Spectrum 100. Melting points were measured in open capillary tubes with Stuart SMP 40 melting point apparatus and uncorrected. Elemental analyses were performed at the İnönü University research center.

2.1.2. General procedure for the preparation of benzimidazolium salts (2a-f)

The benzimidazolium salts can be prepared in analogy to published procedures according to a slightly modified procedure from the literature methods [19]. A mixture of 1-benzyl-5,6-dimethylbenzimidazole (1 mmol) and an equivalent amount of alkyl halide derivative (1 mmol), in degassed dimethylformamide, was heated and stirred at 80 °C for 48 h under argon. The obtained mixture was cooled at room temperature. After 45 mL of ether were added and stirred for 1 h, then the product filtered and washed with diethyl ether to remove the impurities, and the product was left precipitated with high purity. After, the crude products were recrystallized in dichloromethane/diethyl ether and dried under vacuum to provide pure products for experimental analysis.

1-Benzhydryl −5,6-dimethyl-(2,3,5,6-tetramethylbenzyl)benzimidazolium chloride (2a)

Yield 85% (421 mg, white solid); m.p = 152–153 °C; FT-IR $\nu_{(CN)}$ = 1549 cm^{-1} .^{1}H NMR (400 MHz, $CDCl_3$, TMS, 25 °C): δ (ppm) = 10.45 (s, 1H, NC<u>H</u>N); 7.62 (s, 1H, N-$C_6\underline{H}_2(CH_3)_2$-N); 7.38–7.36 (m, 6H, C<u>H</u>-Ar); 7.34–7.30 (m, 4H, C<u>H</u>-Ar); 7.01 (s, 1H, N-$C_6\underline{H}_2(CH_3)_2$-N); 6.93 (s, 1H, Ph-C<u>H</u>-Ph); 5.90 (s, 2H, $C\underline{H}_2$N); 2.23 (s, 3H, $C\underline{H}_3$); 2.21 (s, 6H, $C\underline{H}_3$); 2.19 (s, 9H, $C\underline{H}_3$). ^{13}C NMR (400 MHz, $CDCl_3$, TMS, 25 °C): δ (ppm) = 142.3 (N<u>C</u>HN,C_1); 137.0 (C_4); 136.9 (C_6); 135.7 ($C_{22,28}$); 134.9 ($C_{14,17}$); 134.0 ($C_{12,19}$); 133.3 (C_{11}); 130.6 (C_2); 130.0 (C_9); 129.3 (4<u>C</u>H, $C_{24,26,30,32}$); 129.2 (2<u>C</u>H, $C_{25,31}$); 128.4 (4<u>C</u>H, $C_{23,27,29,33}$); 128.1 (<u>C</u>H, C_{16}); 114.6 (<u>C</u>H, C_3); 113.6 (<u>C</u>H, C_8); 66.1 (<u>C</u>H, C_{21}); 47.9 (N-$C\underline{H}_2$, C_{10}); 20.8 (2$C\underline{H}_3$, $C_{15,18}$); 20.7 (CH_3, C_7); 20.5 ($C\underline{H}_3$, C_5); 16.1 (2$C\underline{H}_3$, $C_{13,20}$). Elemental analysis calcd. (%) for $C_{33}H_{36}ClN_2$ (M.w. = 496.11 g/mol): C 79.89, H 7.31, N 5.65; found (%): C 79.83, H 6.78, N 5.35

1-Benzhydryl −5,6-dimethyl-(4-methylbenzyl)benzimidazolium chloride (2b)

Yield 71% (322 mg, white solid); m.p = 159–160 °C; FT-IR $\nu_{(CN)}$ = 1548 cm^{-1}. ^{1}H NMR (400 MHz, $CDCl_3$, TMS, 25 °C): δ (ppm) = 11.27 (s, 1H, NC<u>H</u>N); 7.37 (d, *J* = 5.7 Hz, 6H, C<u>H</u>-Ar); 7.34 (s, 3H, C<u>H</u>-Ar); 7.32 (s, 2H, C<u>H</u>-Ar); 7.29 (s, 2H, C<u>H</u>-Ar); 7.11 (d, *J* = 7.2 Hz, 2H, C<u>H</u>-Ar); 6.97 (s, 1H, Ph-C<u>H</u>-Ph); 5.84 (s, 2H, $C\underline{H}_2$N); 2.28 (s, 3H, $C\underline{H}_3$); 2.27 (S, 3H, $C\underline{H}_3$); 2.20 (s, 3H, $C\underline{H}_3$). ^{13}C NMR(400 MHz, $CDCl_3$, TMS, 25 °C): δ (ppm) = 142.6 (N<u>C</u>HN,C_1). 138.9 (C_{14}); 137.2 (C_6); 137.1 (C_4); 135.5 ($C_{19,25}$); 130.3 (C_2); 130.2 (C_9); 129.9 (2<u>C</u>H,$C_{12,17}$); 129.8 (C_{11}); 129.4 (4<u>C</u>H, $C_{21,23,27,29}$); 129.3 (2<u>C</u>H, $C_{22,28}$); 128.4 (4<u>C</u>H, $C_{20,24,26,30}$); 128.1 (2<u>C</u>H, $C_{13,16}$); 114.5 (<u>C</u>H, C_3); 113.4 (<u>C</u>H, C_8); 66.4 (<u>C</u>H, C_{18}); 51.2 (N-$C\underline{H}_2$, C_{10}); 21.1 ($C\underline{H}_3$, C_{15}); 20.7 ($C\underline{H}_3$, C_7); 20.6 ($C\underline{H}_3$, C_5). Elemental analysis calcd. (%) for $C_{30}H_{29}ClN_2$ (M.w. = 453.02 g/mol): C 79.54, H 6.45, N 6.18; found (%): C 79.28, H 6.73, N 5.35

1-Benzhydryl −5,6-dimethyl-3-(2,4,6-trimethylbenzyl)benzimidazolium chloride (2c)

Yield 81% (390 mg, white solid); m.p = 155–156 °C; FT-IR $\nu_{(CN)}$ = 1546 cm^{-1}. ^{1}H NMR (400 MHz, $CDCl_3$, TMS, 25 °C): δ (ppm) = 10.88 (s, 1H, NC<u>H</u>N), 7.50 (s, 1H, N-$C_6\underline{H}_2(CH_3)_2$-N), 7.36 (dd, *J* = 5.3 Hz, 1.6 Hz, 6H, C<u>H</u>-Ar); 7.31 (dd, *J* = 7.0 Hz, 2.5 Hz, 4H,C<u>H</u>-Ar); 6.94 (s, 1H, CH-Ar); 6.92 (s, 1H, Ph-C<u>H</u>-Ph); 6.86 (s, 2H, C<u>H</u>-Ar); 5.88 (s, 2H, $C\underline{H}_2$N); 2.26 (s, 6H, $C\underline{H}_3$); 2.24 (s, 3H, $C\underline{H}_3$); 2.20 (s, 3H, $C\underline{H}_3$); 2.17 (s, 3H, $C\underline{H}_3$). ^{13}C NMR (400 MHz, $CDCl_3$, TMS, 25 °C): δ (ppm) = 142.8 (N<u>C</u>HN,C_1); 139.4 (C_{15}); 137.8 ($C_{12,18}$); 137.0 (C_4); 136.9 (C_6); 135.6 ($C_{21,27}$); 130.4 (C_2); 130.0 (2<u>C</u>H, $C_{14,17}$); 129.9 (C_9); 129.3 (4CH $C_{23,25,29,31}$); 129.2 (2<u>C</u>H, $C_{24,30}$); 128.3 (4<u>C</u>H, $C_{22,26,28,32}$); 125.5 (C_{11}); 114.5 (<u>C</u>H, C_3); 113.6 (<u>C</u>H, C_8); 66.2 (<u>C</u>H, C_{20}); 47.4 (N-$C\underline{H}_2$, C_{10}); 21.0 ($C\underline{H}_3$, C_{16}); 20.7 ($C\underline{H}_3$, C_7); 20.6 ($C\underline{H}_3$, C_5); 20.2 (2$C\underline{H}_3$, $C_{13,19}$). Elemental analysis calcd. (%) for $C_{32}H_{33}ClN_2$ (M.w. = 481.08 g/mol): C 79.89, H 6.91, N 5.82; found (%): C 79.71, H 6.86, N 6.38

1-Benzhydryl −5,6-dimethyl-(2-methylbenzyl)benzimidazolium chloride (2d)

Yield 82% (372 mg, white solid); m.p = 151–152 °C; FT-IR $\nu_{(CN)}$ = 1541 cm^{-1}. ^{1}H NMR (400 MHz, $CDCl_3$, TMS, 25 °C): δ (ppm) = 11.06 (s, 1H, NC<u>H</u>N), 7.39–7.33 (m, 11*H*, C<u>H</u>-Ar), 7.33 (s, 1H, C<u>H</u>-Ar); 7.21–7.13 (m, 3H, C_6H_4); 7.08 (d, *J* = 7.2 Hz, 1H, C<u>H</u>-Ar); 6.98 (s, 1H, Ph-C<u>H</u>-Ph); 5.92 (s, 1H, $C\underline{H}_2$N); 2.27 (s, 6H, $C\underline{H}_3$); 2.20 (s, 3H, $C\underline{H}_3$). ^{13}C NMR (400

MHz, $CDCl_3$, TMS, 25 °C): δ (ppm) = 142.5 (NCHN,C_1); 139.1 (C_{12}); 137.3 (C_4); 137.1 (C_6); 135.5 ($C_{19,25}$); 133.1 (C_{11}); 130.3 (C_2); 129.8 (C_9); 129,7 (CH, C_{17}); 129.4 (4CH, $C_{21,23,27,29}$); 129.3 (2CH, $C_{22,28}$); 129.1 (CH, C_{15}); 128.5 (CH, C_{16}); 128.4 (4CH, $C_{20,24,26,30}$); 125.0 (C_{14}); 114.4 (CH, C_3); 113.4 (CH, C_8); 66.4 (CH, C_{18}); 51.3 (N-CH_2, C_{10}); 21.3 (CH_3, C_{13}); 20.7 (CH_3, C_7); 20.6 (CH_3, C_5). Elemental analysis calcd. (%) for $C_{30}H_{29}ClN_2$ (M.w. = 453.02 g/mol): C 79.54, H 6.45, N 6.18; found (%): C 79.74, H 6.36, N 6.13

1-Benzhydryl −5,6-dimethyl-(4-tert-butylbenzyl)benzimidazolium bromide (2e)

Yield 71% (384 mg, white solid); m.p = 179–180 °C; FT-IR $\nu_{(CN)}$ = 1542 cm^{-1}. ^1H NMR (400 MHz, $CDCl_3$, TMS, 25 °C): δ (ppm) = 10.73 (s, 1H, NCHN), 7.42–7.37 (m, 11*H*, CH-Ar); 7.34 (sl, 5H, CH); 7.00 (s, 1H, Ph-CH-Ph); 5.84 (s, 2H, CH_2N); 2.31 (s, 3H, CH_3); 2.22 (s, 3H, CH_3); 1.25 (s, 9H, CH_3). ^{13}C NMR (400 MHz, $CDCl_3$, TMS, 25 °C): δ (ppm) = 152.1 (C_{14}); 141.6 (NCHN,C_1); 137.3 (C_4); 137.2 (C_6); 135.3 ($C_{22,28}$); 130.4 (C_{11}); 129.9 (C_2); 129.8 (C_9); 129.4 (4CH, $C_{24,26,30,32}$); 129.3 (2CH, $C_{25,31}$); 128.4 (4CH, $C_{23,27,29,33}$); 127.8 (2CH, $C_{12,20}$); 126.2 (2CH, $C_{13,19}$); 114.4 (CH, C_3); 113.4 (CH, C_8); 66.4 (CH, C_{21}); 51.1 (N-CH_2, C_{10}); 34.6 (C_{15}); 31.1 (3CH_3, $C_{16,17,18}$); 20.7 (CH_3, C_7); 20.6 (CH_3, C_5). Elemental analysis calcd. (%) for $C_{33}H_{35}BrN_2$ (M.w. = 539.56 g/mol): C 73.46, H 6.54, N 5.19; found (%):C 73.15, H 6.28, N 5.20

1-Benzhydryl-5,6-dimethyl-3-(3,4,5-trimethoxybenzyl)benzimidazolium bromide (2f)

Yield 70% (373 mg, white solid); m.p = 157–158 °C; FT-IR $\nu_{(CN)}$ = 1552 cm^{-1}. ^1H NMR (400 MHz, $CDCl_3$, TMS, 25 °C): δ (ppm) = 11.25 (s, 1H, NCHN); 7.42–7.32 (m, 12H, CH-Ar), 6.98 (s, 1H, Ph-CH-Ph); 6.76 (s, 2H, C_6H_2), 5.81 (s, 2H, CH_2N); 3.79 (s, 6H, OCH_3); 3.78 (s, 6H, OCH_3); 2.33 (s, 3H, CH_3); 2.23 (s, 3H, CH_3). ^{13}C NMR (400 MHz, $CDCl_3$, TMS, 25 °C): δ (ppm) = 153.72 ($C_{13,17}$); 142.70 (NCHN, C_1); 138.38 (C_{15}); 137.30 (C_4); 137.21 (C_6); 135.50 ($C_{21,27}$); 130.28 (C_2); 129.77 (C_2); 128.78 (C_{11}); 129.41 (4CH, $C_{23,25,29,31}$); 129.38 (2CH, $C_{24,30}$); 128.40 (4CH, $C_{22,26,28,32}$); 114.41 (CH, C_3); 113.4 (CH, C_8); 105.69 (2CH, $C_{12,19}$); 66.46 (CH, C_{20}); 60.84 (OCH_3, C_{16}); 56.53 (2OCH_3, $C_{14,18}$); 51.43 (N-CH_2, C_{10}); 20.8 (2CH_3, $C_{5,7}$). Elemental analysis calcd. (%) for $C_{32}H_{33}ClN_2O_3$ (M.w. = 529.07 g/mol): C 72.65, H 6.29, N 5.29; found (%): C 72.47, H 6.51, N 5.32

2.1.3. General procedure for preparation of Ag(I)–NHC complexes (3a-f)

The complexes of silver(I)–NHC were prepared with the method of Organ [20]. According to the use of benzimidazolium salts (1 mmol) with Ag_2O (1.5 mmol) in dry chloroform at 50 °C for 48 h, in dark conditions, under argon and covered with aluminum foil. The reaction mixture was filtered through celite, and the solvent was removed under vacuum to afford the product. The salts were converted to silver(I)–NHC complexes automatically by the reaction, which allowed us to obtain a solution mixture, that affords a white solid as silver(I)–NHC. The resulting white solid was isolated by filtration then dried in a vacuum, and recrystallized in $CHCl_3/Et_2O$.

μ-Dikloro-bis-{[1-benzhydryl-3-(2,3,5,6-tetramethylbenzyl)-5,6-dimethylbenzimidazole-2-ylidene]silver(I) (3a). Yield 70% (0.422 g, white solid); m.p = 245–246 °C; FT-IR $\nu_{(CN)}$ = 1542 cm^{-1}. ^1H NMR (400 MHz, $CDCl_3$, TMS, 25 °C): δ (ppm) = 7.37–7.32 (m, 7H, CH); 7.21 (s, 1H, C_6H_1); 7.17 (dd, *J* = 6.1 Hz, 2.6 Hz, 4H, CH-Ar); 7.10 (s, 2H, N-$C_6H_2(CH_3)_2$-N); 6.81 (s, 1H, Ph-CH-Ph); 5.49 (s, 2H, CH_2N); 2.29 (s, 3H, CH_3); 2.28 (s, 6H, CH_3); 2.19 (s, 3H, CH_3); 2.14 (s, 6H, CH_3). ^{13}C NMR (400 MHz, $CDCl_3$, TMS, 25 °C): δ (ppm) = 137.4 (CH, $C_{22,28}$); 135.1 ($C_{14,17}$); 133.5 ($C_{12,19}$); 133.4 (C_4); 133.4 (C_6); 133.0 (C_{11}); 129.9 (CH, C_{16}); 128.9 (4CH, $C_{24,26,30,32}$); 128.5 (2CH, $C_{25,31}$); 128.31(4CH, $C_{23,27,29,33}$); 113.6 (CH, C_3); 111.7 (CH, C_8); 68.6 (CH, C_{21}); 48.1 (CH_2, C_{10}); 20.7 (2CH_3,$C_{15,18}$); 20.4 (CH_3, C_7); 20.4 (CH_3,C_5); 16.2 (2CH_3, $C_{13,20}$). Elemental analysis calcd. (%) for $C_{64}H_{68}Ag_2Cl_2N_4$ (M.w. = 1179.90 g/mol): C 65.15, H 5.81, N 4.75; found (%): C 66.04, H 5.95, N 4.51

Chloro[1-benzhydryl-3-(4-methylbenzyl)-5,6-dimethylbenzimidazole-2-ylidene]silver(I) (3b). Yield 80% (0.450 g, white solid); m.p = 144–145 °C; FT-IR $\nu_{(CN)}$ = 1542 cm^{-1}. ^1H NMR (400 MHz, $CDCl_3$, TMS, 25 °C): δ (ppm) = 7.39 (m, 7H, CH-Ar); 7.22 (m, 4H, CH-Ar); 7.14 (s, 1H, N-$C_6H_2(CH_3)_2$-N); 7.12 (sl, 4H, C_6H_4); 7.09 (s, 1H, N-$C_6H_2(CH_3)_2$-N); 6.92 (s, 1H, Ph-CH-Ph); 5.52 (s, 2H, CH_2N); 2.31 (s, 3H, CH_3); 2.26 (s, 3H, CH_3); 2.20 (s, 3H, CH_3). ^{13}C NMR (400 MHz, $CDCl_3$, TMS, 25 °C): δ (ppm) = 138.2 (C_{14}); 137.3 ($C_{19,25}$); 133.9 (C_6); 133.6 (C_4); 132.9 (C_2); 132.5 (C_9); 132.0 (C_{11}); 129.7 (2CH, $C_{13,15}$); 129.2 (4CH, $C_{21,23,27,29}$); 128.7 (2CH, $C_{22,28}$); 128.3 (4CH, $C_{20,24,26,30}$); 126.9 (2CH, $C_{12,17}$); 112.9 (CH, C_3); 112.3 (CH, C_8); 66.9 (CH, C_{18}); 53.8 (CH_2, C_{10}); 21.1 (CH_3, C_{15}); 20.4 (CH_3, C_7); 20.3 (CH_3, C_5). Elemental analysis calcd. (%) for $C_{30}H_{28}AgClN_2$ (M.w. = 559.88 g/mol): C 64.36, H 5.04, N 5.00; found (%): C 64.64, H 5.19, N 5.12

Chloro[1-benzhydryl-3-(2,4,6-trimethylbenzyl)-5,6-dimethylbenzimidazole-2-ylidene]silver(I) (3c). Yield 74% (0.435 g, white solid); m.p = 200–201 °C; FT-IR $\nu_{(CN)}$ = 1542 cm^{-1}. ^1H NMR (400 MHz, $CDCl_3$, TMS, 25 °C): δ (ppm) = 7.36 (m, 7H, CH); 7.19 (m, 5H, CH); 6.94 (s, 2H, C_6H_2); 6.92 (s, 1H, N-$C_6H_2(CH_3)_2$-N); 6.84 (s, 1H, Ph-CH-Ph); 5.51 (s, 2H, CH_2N); 2.32 (s, 3H, CH_3); 2.23 (s, 9H, CH_3); 2.18 (s, 3H, CH_3). ^{13}C NMR (400 MHz, $CDCl_3$, TMS, 25 °C): δ (ppm) = 139.2 (C_{15}); 137.4 ($C_{21,27}$); 137.4 ($C_{12,18}$); 133.5 (C_6); 133.4 (C_4); 130.1 ($C_{14,17}$); 129.0 (4CH, $C_{23,25,29,31}$); 128.6 (2CH, $C_{24,30}$); 128.3 (4CH, $C_{22,26,28,32}$); 126.9 (C_{11}); 113.3 (CH, C_3); 112.0 (CH, C_8); 68.0 (CH, C_{20}); 48.7 (N-CH_2, C_{10}); 21.1 (CH_3, C_{16}); 20.5 (2CH_3, $C_{13,19}$); 20.4 (CH_3, C_7); 20.4 (CH_3, C_5). Elemental analysis calcd. (%) for $C_{32}H_{32}AgClN_2$ (M.w. = 559.88 g/mol): C 64.37, H 5.49, N 4.76; found (%): C 64.74, H 5.65, N 4.78

Chloro[1-benzhydryl-3-(2-methylbenzyl)-5,6-dimethylbenzimidazole-2-ylidene]silver(I) (3d). Yield 90% (0.532 g, white solid); m.p = 222–223 °C; FT-IR $\nu_{(CN)}$ = 1542 cm^{-1}. ^1H NMR (400 MHz, $CDCl_3$, TMS, 25 °C) : δ (ppm) = 7.39 (s, 7H, CH-Ar); 7.23 (m, 4H, CH-Ar); 7.20 (s, 1H, CH-Ar); 7.16 (s, 1H, N-$C_6H_2(CH_3)_2$-N); 7.10 (s, 1H, CH-Ar); 7.08 (s, 1H, CH-Ar); 7.00 (m, 2H, CH-Ar);0.6.94 (s, 1H, Ph-CH-Ph); 5.53 (s, 2H, CH_2N); 2.31 (s, 3H, CH_3); 2.26 (s, 3H, CH_3); 2.21 (s, 3H, CH_3). ^{13}C NMR (400 MHz, $CDCl_3$, TMS, 25 °C): δ (ppm) = 138.8 (C_{12}); 137.3 ($C_{19,25}$); 134.9 (C_{11}); 133.9 (CH, C_4); 133.3 (CH, C_6); 132.9 (CH, C_2); 132.5 (CH, C_9); 129.2 (4CH, $C_{21,23,27,29}$); 129.1 (CH, C_{15}); 128.9 (CH, C_{16}); 128.8 (2CH, $C_{22,28}$); 128.3 (4CH, $C_{20,24,26,30}$); 123.9 (C_{17}); 112.9 (CH, C_3); 112.2 (CH, C_8); 66.9 (CH, C_{18}); 53.9 (N-CH_2, C_{10}); 21.4 (CH_3, C_{13}); 20.4 (CH_3, C_7); 20.3 (CH_3, C_5). Elemental analysis calcd. (%) for $C_{32}H_{32}AgClN_2$ (M.w. = 559.88 g/mol): C 64.36, H 5.04, N 5.00; found (%): C 64.96, H 5.31, N 4.95.

Bromo[1-benzhydryl-3-(4-tert-butylbenzyl)-5,6-dimethylbenzimidazole-2-ylidene]silver(I) (3e). Yield 70% (0.433 g, white solid); m.p = 219–220 °C; FT-IR $\nu_{(CN)}$ = 1542 cm^{-1}. ^1H NMR (400 MHz, $CDCl_3$, TMS, 25 °C): δ (ppm) = 7.39 (m, 7H, CH-Ar); 7.34 (s, 1H, CH-Ar); 7.32 (s, 1H, C_6H_4); 7.22 (m, 4H, CH-Ar); 7.17 (s, 1H, N-$C_6H_2(CH_3)_2$-N); 7.15 (s, 2H, C_6H_4); 7.12 (s, 1H, N-$C_6H_2(CH_3)_2$-N); 6.93 (s, 1H, Ph-CH-Ph); 5.54 (s, 2H, CH_2N); 2.27 (s, 3H, CH_3); 2.21 (s, 3H, CH_3); 1.28 (s, 9H, CH_3 (*t*-Bu)). ^{13}C NMR (400 MHz, $CDCl_3$, TMS, 25 °C): δ (ppm) = 151.3 (C_{14}); 137.3 ($C_{22,28}$); 133.9 (C_4); 133.5 (C_6); 132.9 (C_9); 132.6 (C_2); 132.0 (C_{11}); 129.4 (C); 129.2 (4CH, $C_{24,26,30,32}$); 128.7 (2CH, $C_{25,31}$); 128.4 (C); 128.3 (4CH, $C_{23,27,29,33}$); 126.6 (2CH, $C_{13,19}$); 125.9 (2CH, $C_{12,20}$); 114.4 (CH, C_3); 113.5 (CH, C_8); 66.9 (CH, C_{21}); 53.6 (N-CH_2, C_{10}); 34.5 (C_{15}); 31.2 (3CH_3, $C_{16,17,18}$); 20.4 (CH_3, C_7); 20.3 (CH_3, C_5). Elemental analysis calcd. (%) for $C_{33}H_{34}AgClN_2$ (M.w. = 601.96 g/mol): C 65.84, H 5.69, N 4.65; found (%): C 65.94, H 5.92, N 4.43.

Chloro[1-benzhydryl-3-(3,4,5-trimethoxybenzyl)-5,6-dimethylbenzimidazole-2-ylidene] silver(I) (3f). Yield 80% (0.540 g, white solid); m.p = 117–118 °C; FT-IR $\nu_{(CN)}$ = 1542 cm^{-1}. ^1H NMR (400 MHz, $CDCl_3$, TMS, 25 °C): δ (ppm) = 7.38 (m, 7H, CH-Ar); 7.22 (m, 4H, CH-Ar); 7.15 (s, 1H,

Table 1
Crystal data and structure refinement parameters for **2c**, **2f,** and **3a**.

Parameters	3,5-dimethylbenzimidazolium salts		Silver(I)–NHC complex
	2c	**2f**	**3a**
CCDC depository	2,058,369	2,058,370	2,058,371
Color/shape	Colorless/ prism	Colorless/plate	Colorless/plate
Chemical formula	$(C_{32}H_{33}N_2)^+$ Cl^- $2H_2O$	$(C_{32}H_{33}N_2O_3)^+$ $Cl^-CH_2Cl_2$	$[Ag_2Cl_2(C_{33}H_{34}N_2)_2]$
Formula weight	517.08	613.98	1203.88
Temperature (K)	296(2)	296(2)	296(2)
Wavelength (Å)	0.71073 Mo Kα	0.71073 Mo Kα	0.71073 Mo Kα
Crystal system	Monoclinic	Triclinic	Monoclinic
Space group	$P2_1/c$ (No. 14)	P (No. 2)	$C2/c$ (No. 15)
Unit cell parameters			
a, b, c (Å)	13.5311(12), 16.4277(17), 14.5904(13)	10.9830(8), 12.0714 (8),12.0148(9)	27.6791(19), 9.3376 (7), 22.9241(16)
α, β, γ (°)	90, 116.407 (6), 90	85.937(6), 86.665(6), 85.163(6)	90, 106.436(5), 90
Volume ($Å^3$)	2904.8(5)	1581.1(2)	5682.8(7)
Z	4	2	4
$D_{calc.}$ (g/cm^3)	1.182	1.290	1.407
μ (mm^{-1})	0.162	0.325	0.827
Absorption correction	Integration	Integration	Integration
$T_{min.}$, $T_{max.}$	0.9231, 0.9490	0.9128, 0.9867	0.7750, 0.9776
F_{000}	1104	644	2480
Crystal size (mm^3)	0.62 × 0.37 × 0.36	0.49 × 0.19 × 0.06	0.55 × 0.21 × 0.02
Diffractometer/ measurement method	STOE IPDS II/ ω scans	STOE IPDS II/ω scans	STOE IPDS II/ω scans
Index ranges	$-16 \le h \le 16$, $-19 \le k \le 18$, $-16 \le l \le 16$	$-13 \le h \le 12$, $-14 \le k \le 12$, $-14 \le l \le 14$	$-32 \le h \le 32$, $-11 \le k \le 11$, $-27 \le l \le 27$
θ range for data collection (°)	$1.680 \le \theta \le 25.047$	$2.322 \le \theta \le 25.047$	$1.534 \le \theta \le 25.049$
Reflections collected	15,167	14,288	24,599
Independent/ observed reflections	4965/1707	5581/2845	5037/2296
$R_{int.}$	0.1204	0.0781	0.1441
Refinement method	Full-matrix least-squares on F^2	Full-matrix least-squares on F^2	Full-matrix least-squares on F^2
Data/restraints/ parameters	4965/0/339	5581/0/378	5037/0/339
Goodness-of-fit on F^2	0.945	1.030	0.984
Final R indices [$I > 2\sigma(I)$]	$R_1 = 0.1148$, $wR_2 = 0.2957$	$R_1 = 0.0734$, $wR_2 = 0.1244$	$R_1 = 0.0764$, $wR_2 = 0.1382$
R indices (all data)	$R_1 = 0.2210$, $wR_2 = 0.3492$	$R_1 = 0.1565$, $wR_2 = 0.1492$	$R_1 = 0.1820$, $wR_2 = 0.1739$
$\Delta\rho_{max.}$, $\Delta\rho_{min.}$ ($e/Å^3$)	0.36, −0.31	0.18, −0.28	0.61, −0.48

N-$C_6\underline{H}_2$-$(CH_3)_2$-N); 7.14 (s, 1H, N-$C_6\underline{H}_2$-$(CH_3)_2$-N); 6.96 (s, 1H, Ph-C<u>H</u>-Ph); 6.43 (S, 2H, C<u>H</u>-Ar), 5.50 (s, 2H, $C\underline{H}_2$N); 3.82 (s, 3H, $OC\underline{H}_3$); 3.77 (s, 6H, $OC\underline{H}_3$); 2.30 (s, 3H, $C\underline{H}_3$); 2.23 (s, 3H, $C\underline{H}_3$). ^{13}C NMR (400 MHz, $CDCl_3$, TMS, 25 °C): δ (ppm) = 153.6 ($C_{13,17}$); 137.9 (C_{15}); 137.3 ($C_{21,27}$); 134.1 (C_4); 133. (C_6); 130.7 (C_{11}); 129.4 (C_9); 129.2 (4<u>C</u>H, $C_{23,25,29,31}$); 128.8 (2<u>C</u>H, $C_{24,30}$); 128.4 (C_2); 128.3 (4<u>C</u>H, $C_{22,26,28,32}$); 112.9 (<u>C</u>H, C_3); 112.1 (<u>C</u>H, C_8); 105.7 (2CH, $C_{12,19}$); 66.8 (<u>C</u>H, C_{20}); 60.9 ($OC\underline{H}_3$, C_{16}); 56.2 (2$OC\underline{H}_3$, $C_{14,18}$); 53.8 (N-$C\underline{H}_2$, C_{10}); 20.4 ($C\underline{H}_3$, C_7); 20.4 ($C\underline{H}_3$, C_5). Elemental analysis calcd. (%) for $C_{32}H_{33}AgClN_2O_3$ (M. w. = 635.12 g/mol): C 60.44, H 5.07, N 4.41; found (%): C 60.33, H 5.59, N 3.96.

2.2. X-Ray crystallographic analysis study

The structure of 3,5-dimethylbenzimidazolium salts **2c**, **2f**, and Ag-NHC complex **3a** was determined by the X-ray diffraction technique, the obtained results confirmed all the spectroscopic data. A suitable single crystal of complex **2c**, **2f**, and **3a** for X-ray diffraction analysis was were grown by slow diffusion of diethyl ether in a saturated chloroform solution at room temperature. Crystallographic data of **2c**, **2f**, and **3a** were gathered with an STOE IPDS II diffractometer using graphite-monochromated Mo Kα radiation by applying the ω -scan method at room temperature. X-AREA was used for data collection and cell refinement. [21] while data reduction was applied using X-RED32 [21]. The structures were solved using the charge-flipping algorithm by SUPERFLIP [22] and refined using the full-matrix least-squares calculations on F^2 using SHELXL-2018 [23]. The H atoms were calculated geometrically and a riding model was applied during the refinement process. Crystal data, data collection, and structure refinement details are collected in Table 1. Molecular graphics were generated by using OLEX2 [24].

2.3. Biological capacity study

All the synthesized 3.5-dimethylbenzimidazolium salts **2a-f** and their related silver(I)–NHC complexes **3a-f** were tested for antimicrobial, Anti-Cholinesterase **(**anti-Alzheimer**),** anti-Lipase, and anti-Alpha-amylase (anti-Diabetic**)** activities.

2.3.1. Material

Candida albicans (ATCC MYA-2876) and *Candida glabrata* (ATCC 2001), which are pathogenic yeast species, were used in antifungal tests, and *Escherichia coli* (ATCC 25922), *Staphylococcus aureus* (ATCC 29213), and *Pseudomonas aeruginosa* (ATCC 27853) species were used antibacterial tests. All types of bacteria and fungi used in the study were provided by the Molecular Genetics Laboratory of the Department of Genetics at İnönü University Turgut Özal Medical Faculty (Battalgazi, Malatya, Turkey).

The acetylthiocholine iodide, butyrylthiocholine chloride which was employed as substrates of the reaction were obtained from Sigma Chemical Co (Sigma-Aldrich GmbH, Stern-Heim, Germany). The AChE from Electrophorus electricus eel-AChE (Type-VI-S, EC 3.1.1.7, 425.84 U/mg) and horse serum butyrylcholinesterase eq BChE, (EC 3.1.1.8, 11.4 U/mg), which are enzymes that were used in anticholinesterase assay, were obtained from Sigma-Aldrich. All other chemicals and solvents were of analytical grade. The measurements and calculations of the enzymatic activity results were evaluated by using quantitative colorimetric assay, they were carried out on a 96-well microplate reader, (PerkinElmer Multimode Plate Reader EnSpire, USA) at the Center of Biotechnology Research. (Ali Mendjli, Constantine, Algeria)

2.3.2. Methods

2.3.2.1. Antibacterial activity

2.3.2.1.1. Determination of the minimum inhibitory concentration (MIC). Antifungal and antibacterial MIC (Minimal Inhibitory Concentration) analysis was performed using the BMD (Broth Microdilution) test, as described in EUCAST EDef 7.3.2 [25] for yeasts and CLSI M07-A10 [26] for bacteria. Briefly, the broth micro-dilution technique using a 96-wells microplate was used to determine the minimum inhibitory concentration (MIC) (Erdemoglu et al., 2007). The selected compounds (NHCs) were dissolved in dimethylsulfoxide (DMSO), and serial dilutions were made in a flat-bottom sterile 96-well microplate, in SDB (Sabouraud Dextrose Broth) medium (1% peptone, 2% glucose, pH 5.6) [27] for yeasts, and LB (Luria-Bertani) broth medium (1% tryptone, 1% NaCl, 0.5% yeast extract, pH 7.0) [28] for bacteria. In sterile water, yeast (1-5x10^5 CFU/mL) and bacteria (1x10^6 CFU/mL) cell solutions

(inoculums) were prepared and added in equal volumes to wells containing different concentrations of the compounds. After the cell solutions were added, the compounds' final concentrations were between 0.8 and 800 mg/L, and the cell concentrations were 0.5–2.5x10^5 CFU/mL for yeasts and 5x10^5 CFU/mL for bacteria in the final step. Finally, the microplate was covered and incubated at 37 °C for 24 h for yeasts and 16–18 h at 37 °C for bacteria. The MIC was determined spectrophotometrically at 530 nm after incubation in yeasts and by naked eyes in bacteria. The MIC value was measured as the lowest drug concentration causing at least 50% or more reduction in yeasts' growth compared to the control (no drug) cell group, and as the lowest drug concentration without visible growth in bacteria. Ampicillin, Tetracycline, Amphotericin B, and Voriconazole were used as the reference drugs.

2.3.2.2. Enzymatic evaluation. This study evaluated the capacity of the novel benzimidazolium salts and silver (I)–NHC complexes as inhibitors of different enzymes. In this context, all compounds were evaluated against a panel of important biological activities such as anticholinesterase, anti-Lipase, and anti-diabetic activities.

a. Anti-Cholinesterase assay (Anti-Alzheimer)

Cholinesterase family inhibitors of acetylcholinesterase (AChE) and butyrylcholinesterase (BChE) are the most investigated and common strategy used for the treatment of Alzheimer's disease [29–32]. Acetylcholinesterase (AChE) and butyrylcholinesterase (BChE) inhibitory activities of the new compound were done according to the method described by Rhee et *al.* [33]. based on the spectrophotometric method of Ellman's [34] with slight modifications. In this experiment, a reaction volume of 200 μL consisting, 150 μL of sodium phosphate buffer (100 mM, Ph = 8.0), 10 μL of the sample at different concentrations in methanol, and 20 μL of AChE or BChE solution in buffer was mixed and left to incubate for 15 min at 37 °C, Afterwards, 10 μL of DTNB (0.5 mM) were added. After that, 10 μL of acetylthiocholine iodide or 10 μL of butyrylthiocholine chloride (0.2 mM). was added to start the reaction. The hydrolysis of these substrates was monitored spectrophotometrically by the formation of yellow 5-thio-2-nitrobenzoate anion as the result of the reaction of DTNB with thiocholine released by the enzymatic hydrolysis of acetylthiocholine iodide or butyrylthiocholine chloride. The absorbance of the solution was measured at 412 nm by the use of a 96-well microplate reader (Perkin Elmer, Enspire). The results were given as IC_{50} values (μM) corresponding to the 50% inhibition concentration. Percentage of inhibition I (%) was determined using the following formula

$$\text{Inhibition (I \%)} = (\text{E} - \text{S} / \text{S}) \times 100$$

Where E is the activity of the enzyme without a test sample, and S is the activity of the enzyme in the presence of the test sample. The measurements were carried out in triplicate and Galanthamine was used as a reference compound.

b. Anti-lipase assay

The assay to determine the inhibitory capacity against pancreatic lipase was performed according to the method of (Souza, 2009) [35] with minor modification. Briefly, in this experiment the selected compounds were prepared at the concentration of 4 mM in dimethyl sulfoxide (DMSO). A reaction volume of 200 μL in triplicate consisting, 50 μL of a sample at different concentrations in DMSO with 100 μL of pancreatic Lipase solution in Tris-HCl buffer (pH = 8) were mixed and incubated for 20 min at 37 °C, Afterwards, The reaction was then initiated by the addition of 50 μL of *p*-Nitrophenol Palmitate (*p*-NPP) after incubation for 2 h at 37 °C. A blank with DMSO instead of enzyme solution was prepared. orlistat was used as a positive control. The absorbances of lipase products (*p*-nitrophenol) were measured using a 96-well microplate reader (Perkin Elmer, Enspire) at 410 nm. The findings were expressed as IC_{50} values. (μM) corresponding to the 50% inhibition concentration. The percent inhibition I (%) of pancreatic lipase was determined using the following equation [36].

$$\text{I}(\%) = [(\text{A} - \text{a}) - (\text{B} - \text{b})/(\text{A} - \text{a})] \times 100$$

Where **A**: is the absorbance in the absence of the possible inhibitor, which corresponds to the control enzyme assay; **a**: is the absorbance in the absence of the sample and enzyme (blank substrate); **B**: is the absorbance in the presence of the possible inhibitor with the enzyme and substrate; **b**: is the absorbance in the absence of the enzyme.

c. Anti-α-amylase activity

The inhibitory activity of alpha-amylase was tested using the iodine /potassium iodide (IKI) method according to (G. Zengin et al. 2014) [37]. With some modifications. Briefly, in this experiment, the assay was conducted by mixing of 25 μL of the sample at different concentrations in methanol with 50 μL of α amylase solution in 1U of sodium phosphate buffer (*p*H = 6.9 with 6 Mm NaCl) and incubated for 10 min at 37 °C, Afterwards, 50 μL of Amidon (0.1%), was added. Similarly, by adding sample solution to all reaction reagents, a blank was prepared without enzyme (α-amylase) solution. For 20 min, the reaction mixture was incubated at 37 °C. After incubation, The reaction was then stopped by the addition of HCl 25 μL (1 M), finally, the reaction was initiated by the addition of 100 μL of (IKI) iodine-potassium iodide solution. The absorbance of the solution was measured at 630 nm by the use of a 96-well microplate reader (Perkin Elmer, Enspire). The results were presented as IC_{50} values (μM) corresponding to 50% inhibition concentration. The acarbose was used as a reference. The percentage of inhibition I (%) was calculated as follows in the formula:

$$\boldsymbol{I}\ \% = \mathbf{1} - [(\text{Ac} - \text{Ae}) - (\text{As} - \text{Ab})/(\text{Ac} - \text{Ae})]$$

As = Absorbance [Extrait, Enzyme, Amidon, HCl, IKI]; $\mathbf{A_b}$ = Absorbance [Extrait, sodium phosphate buffer, IKI]; $\mathbf{A_e}$ = Absorbance [solvant vol Extrait, Enzyme, Amidon, HCl, IKI]; $\mathbf{A_c}$ = Absorbance [solvant vol Extrait, sodium phosphate buffer, Amidon, HCl, IKI]

2.4. Statistical analysis

All data on activity tests were the averages of triplicate analyses. The data were recorded as means ± standard error meaning. Significant differences between means were determined by Student's *t*-test; p values < 0.05 were regarded as significant.

2.5. Molecular docking study

Molecular modeling studies were accomplished to investigate the possible binding mode of the designed compounds into BChE and AChE active sites. Before docking, the crystal structures of human AChE (PDB ID: 4M0E [38]) and BChE (PDB ID: 2XQF [39]) were downloaded from the Protein Data Bank. The binding site of these enzymes was defined by selecting all the residues with at least one heavy atom within 6 Å from the inhibitor of the crystal structure. This selection was refined by adding every residue beyond 6 Å considered essential for the continuity of the cavity [40]. Then, AChE and BChE were prepared using the Protein Preparation Wizard of Schrodinger [41] by removing their Chain B, water molecules, heteroatoms, and co-factors. Hydrogen and missing atoms were added and bond charges were computed. Finally, the intramolecular energy was minimized and a mol2 file was exported and used as a starting structure for docking [42]. Meanwhile, the synthesized compounds were drawn and prepared using the built and LigPrep module implemented in Maestro version 11.3 of the Schrodinger suite [43]. This preparation was carried out in order to create several structures for each molecule. (up to 32) with different enantiomers (when

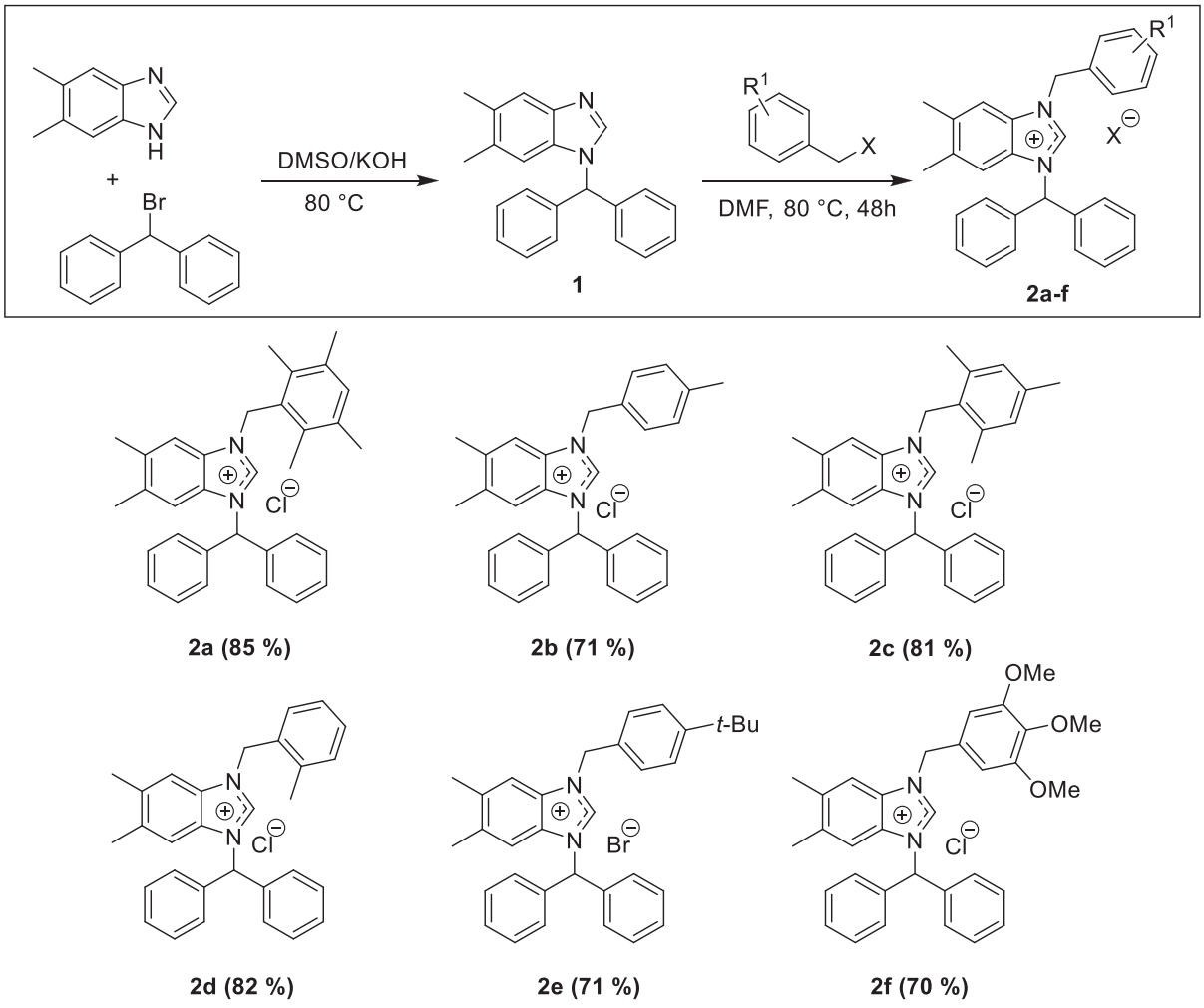

Scheme 1. Synthetic route for the preparation of benzimidazolium salts **2a-f.**

undefined), protonation states at pH = 7.4 ± 1, and tautomers [44]. All the conformations generated were minimized and exported as mol2 files. Molecular docking studies were performed using GOLD version 5.2.2 in which the target atoms are fixed and the ligands are flexible [45]. The GoldScore scoring function was employed for the ranking of molecules according to their score which is given as fitness. Best cluster poses were saved and visually analyzed by PyMol version 2.2.3 [46] and Maestro version 11.3 of the Schrodinger suite [43].

3. Results and discussion

3.1. Chemistry

3.1.1. Preparation of 3,5-dimethylbenzimidazolium salts 2a–f

The 3,5-dimehylbenzimidazolium salts **2a-f** were synthesized *via* two *N*-alkylation reaction processes as illustrated in scheme 1. Compound **1** as a starting material was obtained by the first *N*-alkylation reaction using 5,6-dimethylbenzimidazole with bromodiphenylmethane. The second *N*-alkylation reaction allowed us to prepared six benzimidazolium salts **2a-f** by reacting *N*-benzhydryl-5,6-dimethylbenzimidazole **1** with different benzyl chloride in degassed DMF at 80 °C. All the new 3,5-dimehylbenzimidazolium salts **2a-f** were obtained with good yield, in the solid-state.

All the new 3,5-dimehylbenzimidazolium salts **2a-f** depicted in Scheme 1 were obtained with good yield. The spectroscopic data of 3,5-dimethylbenzimidazolium salts are consistent with the data observed in literature for other benzimidazolium salts [7,9-12]. The physical and some spectroscopic data of 3,5-dimethylbenzimidazolium salts are summarized in Table 2.

These new 5,6-dimethylbenzimidazolium salts were characterized by different techniques. The FT-IR data indicated that 5,6-dimethylbenzimidazolium salts show a characteristic $\nu_{(CN)}$ band typically for all salts **2a-f** at 1549, 1548, 1546, 1541, 1542, and 1552 cm^{-1} respectively. In ^{1}H NMR the important pick for all 3,5-dimethylbenzimidazolium salts is

Table 2
Physical and Spectroscopic data for 3,5-dimethylbenzimidazolium salts **2a-f.**

Code	Chemical Formula	Molecular Weight (g/mol)	Melting point°C	^{1}H NMRCH (C_2) ppm	^{13}C NMR(C_2) ppm	IR$\nu_{(CN)}$
2a	$C_{33}H_{36}ClN_2$	495.11	153	10.52	142.3	1549
2b	$C_{30}H_{29}ClN_2$	453.03	260	11.27	142.6	1548
2c	$C_{32}H_{33}ClN_2$	481.08	156	10.91	142.8	1546
2d	$C_{30}H_{29}ClN_2$	453.03	152	11.15	142.5	1541
2e	$C_{33}H_{35}BrN_2$	539.56	180	10.75	141.6	1542
2f	$C_{32}H_{33}ClN_2O_3$	529.08	158	11.27	142.7	1552

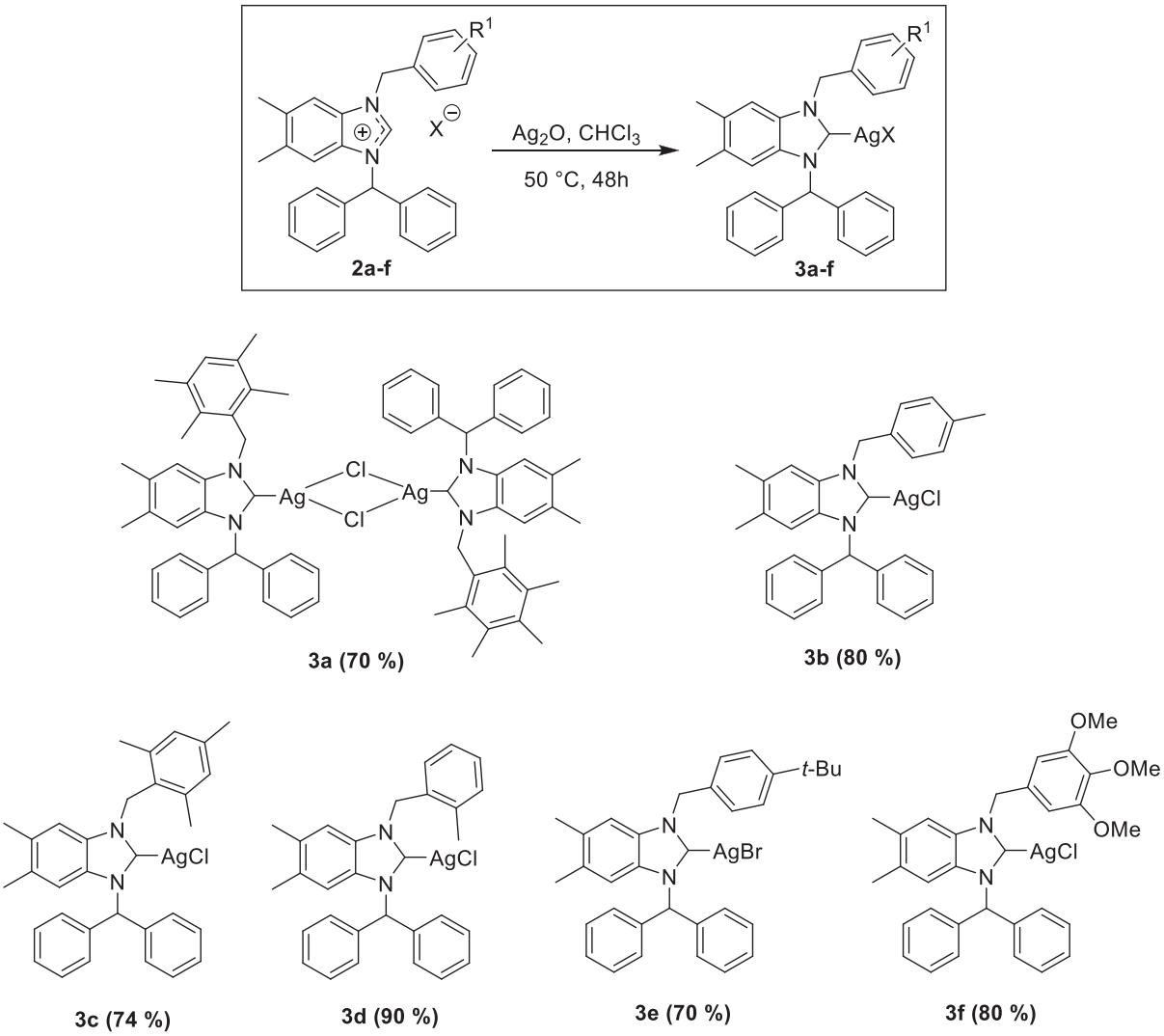

Scheme 2. Synthesis of Ag(I)–NHC complexes **3a-f**.

Table 3
Physical and Spectroscopic data for Ag(I)–NHC complexes.

Code	Chemical Formula	Molecular Weight (g/mol)	Melting point °C	^{1}H NMR*CH* (C_2) ppm	^{13}C NMR (C_2) ppm	IR $\nu_{(CN)}$
3a	$C_{32}H_{34}AgClN_2$	601.97	245–246	–	–	1471
3b	$C_{30}H_{28}AgClN_2$	559.89	144–145	–	–	1484
3c	$C_{32}H_{32}AgClN_2$	584.97	200–201	–	–	1496
3d	$C_{30}H_{28}AgClN_2$	559.89	222–223	–	–	1485
3e	$C_{33}H_{34}AgBrN_2$	646.42	218–219	–	–	1481
3f	$C_{32}H_{33}AgClN_2O_3$	635.94	117–118	–	–	1505

the pick of the acidic proton NC*H*N that confirms the formation of the salt, this pick was detected at 10.52, 11.25, 10.91, 11.08, 10.73, and 11.25 ppm respectively for the salts **2a-f**, as sharp singlets. In ^{13}C NMR the carbon NC*H*N was observed as typical singlets at 142.4, 142.7, 142.8, 142.5, 141.6, and 142.7 ppm respectively for the salts **2a-f**.

3.1.2. Preparation of silver(I)–NHC complexes 3a-f

The Ag(I)–NHC complexes **3a-f** were synthesized *via* the in situ deprotonation of 3,5-dimethylbenzimidazolium salts by Ag_2O. Treatment of the benzimidazolium salts with Ag_2O in dichloromethane at room temperature in the dark afforded the expected silver complexes Ag(I)–NHC **3a-f** (Scheme 2). The silver-NHC complexes **3a-f** were obtained as white solids in high yields, soluble in halogenated solvents. In the air, these complexes are stable but are light-sensitive.

All the new Ag(I)–NHC complexes **3a-f** depicted in Scheme 3 were obtained with good yield. The spectroscopic data of these complexes are consistent with the data observed in literature for other Ag(I)–NHC complexes [9–12]. The physical and some spectroscopic data are summarized in Table 3.

These new six Ag(I)–NHC complexes were characterized by different techniques. The FT-IR data indicated that Silver(I)–NHC complexes show a characteristic $\nu_{(CN)}$ band typically for all complexes **3a-f** at 1471, 1484, 1496, 1485, 1481, and 1505 cm^{-1} respectively. The characteristic proton peak NC*H*N of the starting benzimidazolium was not detected in

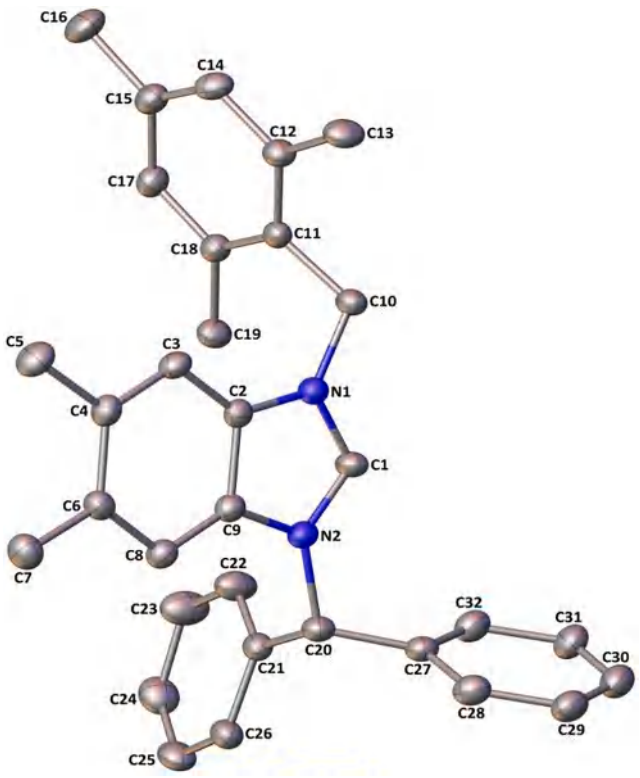

Fig. 1. Molecular structure of salt **2c**.

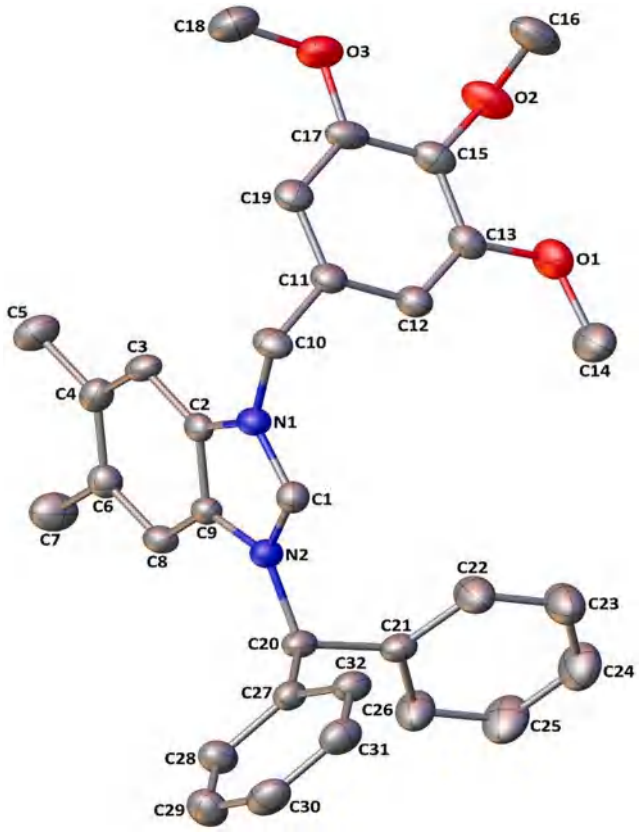

Fig. 2. Molecular structure of salt **2f**.

the ^{1}H NMR spectra of novel Ag(I)–NHC complex that confirmed the formation of the Ag(I)–NHC complexes Table 3. Similarly, in the ^{13}C NMR data, the characteristic signals of carbon NCHN were observed at around 144 ppm for the starting benzimidazolium salts. However, the formation of silver NHC complexes is checked by the disappearance of the signal of NCHN.

3.2. X-ray crystal structures

The molecular diagrams of **2c**, **2f,** and **3a** with the adopted atom-labeling scheme are shown in Figs. 1-3, while important bond distances and angles are listed in Table 4.

3.2.1. Description of the structure of the salts 2c and 2f

The 3,5-dimethylbenzimidazolium salts **2c** and **2f** crystallize in chloroform/diethyl ether as depicted in Figs. 1 and 2.

The compounds **2c** and **2f** crystallize as a salt in which the charge of the NHC cation is neutralized by a chloride anion. Furthermore, in their asymmetric units, **2c** contains two solvent water molecules whilst **2f** contains one dichloromethane molecule. The bonding within the imidazole rings indicates a pattern of delocalization that extends from atom N1 to atom N2 through atom C1, the N1—C1 and N2—C1 distances being significantly shorter than the N1—*C*2 and N2—C9 distances. The remaining bond lengths are normal within experimental uncertainty [47].

3.2.2. The structure description of the silver complex 3a

The silver(I)NHC complex **3a** crystallizes in chloroform/diethyl ether as depicted in Fig. 3.

The silver(I)–NHC complex **3a** crystallizes as dimers *via* bridging chloride atoms to form an $Ag_2(\mu\text{-}Cl)_2$ quadrangular arrangement which is frequently observed in silver complexes (Fig. 3). Because of the inversion center, the Ag_2Cl_2 cluster is strictly planar at the mid-point of the Ag···Ag^{i} line [symmetry code: $^{i} - x + 1/2, -y + 3/2, -z + 1$], where each silver(I) atom is tri-coordinated with one carbene carbon atom and two chlorine atoms to adopt a distorted trigonal planar geometry. The two (NHC)AgCl moieties are present around an inversion center with the chlorides asymmetrically bound to the silver center with different Ag—Cl bond lengths of 2.464(2) and 2.629(2) Å. The Ag1—C1 distance of 2.111(8) Å falls in the range typical for other silver-carbene complexes [48]. With an angle of 143.2(2)° the C—Ag—Cl vector deviates from linearity as a result of coordination from an additional bridging Cl. The bond angles of the C1—Ag1—Cl1^{i}, Ag1—Cl11—Ag1^{i,} and Cl1—Ag1—Cl1^{i} are 124.1(2), 87.34(7), and 92.66(7)°, respectively. The Ag…Ag distance is 3.5186(11) Å, much greater than the sum of two van der Waals radii for Ag (3.44 Å) [49], ruling out the presence of any 'argentophilic' interaction. Due to coordination of the NHC ligand, the ring's internal angle (N1—C1—N2) is reduced at the carbene center from 109.2(6) to 106.2(7)°. All the aforementioned data are comparable to those reported dinuclear Ag(I)–NHC complexes [50–54].

3.3. Evaluation of biological

3.3.1. Evaluation of antibacterial activity

Investigations have been performed for antibacterial and antifungal activities *in vitro* against (E.coli, P.aeruginosa, S.aureus, C.albicans, and C.glabrata) for all the newly 3.5-dimethylbenzimidazolium salts **2a-f** and their related silver(I)–NHC complexes **3a-f,** using AmphotericinB, Voriconazole, Ampicillin, and Tetracycline as a standard control drug. The (MIC μg/mL) results of the antimicrobial activity of all new compounds are reported in Table 5.

Globally, all benzimidazoluim salts and silver-NHC complexes tested showed an important antifungal activity against the human pathogenic microorganisms (*Candida albicans* and *Candida glabrata*) as are presented in Table 4. The benzimidazolium salts **2a-f** showed high antifungal activity against Candida albicans, especially the three salts **2a**, **2c**, and **2e**.

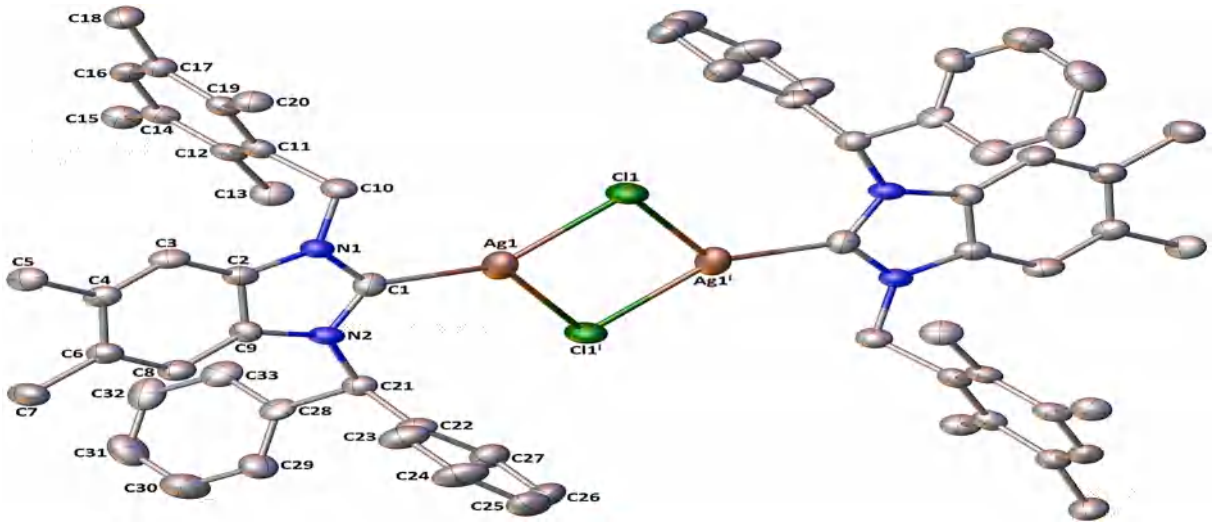

Fig. 3. Molecular structure of silver-carbene complexes **3a**.

Table 4
Selected geometric parameters for **2c**, **2f**, and **3a**.

Parameters		3,5-Dimethylbenzimidazolium salts		Silver(I)–NHC complex
		2c	2f	3a
Bond lengths (Å)	Ag1—Cl1	–	–	2.464(2)
	Ag1—Cl1^{i}	–	–	2.629(2)
	Ag1—C1	–	–	2.111(8)
	N1—C1	1.351(7)	1.322(4)	1.342(9)
	N1—C2	1.392(7)	1.392(5)	1.390(9)
	N2—C1	1.341(7)	1.334(5)	1.355(10)
	N2—C9	1.406(8)	1.398(5)	1.391(9)
Bond angles (°)	Cl1—Ag1—C1	–	–	143.2(2)
	Cl1^{i}—Ag1—C1	–	–	124.1(2)
	Cl1—Ag1—Cl1^{i}	–	–	92.66(7)
	Ag1—Cl1—Ag1^{i}	–	–	87.34(7)
	Ag1—C1—N1	–	–	125.7(6)
	Ag1—C1—N2	–	–	127.9(6)
	N1—C1—N2	109.2(6)	110.5(3)	106.2(7)
	C1—N1—C2	109.6(5)	108.4(3)	111.4(7)
	C1—N2—C9	110.1(5)	107.6(3)	110.4(6)

Symmetry code: $^{i} -x + 1/2, -y + 3/2, -z + 1$.

besides, the silver-NHC complex **3a-f** showed high antifungal activity against *Candida albicans*, and *Candida glabrata*, with almost the same values. Complex **3c** is the more active complex. The antibacterial activity of all benzimidazoluim salts **2a-f** and silver-NHC complexes **3a-f** tested showed an important antibacterial activity against the human pathogenic microorganisms (*Escherichia coli*, *Pseudomonas aeruginosa*, and *Staphylococcus aureus*), except the salt **2f** as are presented in Table 4. All benzimidazolium salts **2a-e** showed good antibacterial activity against *Staphylococcus aureus* and *Escherichia coli,* with almost the same values, but they didn't show high activity against *Pseudomonas aeruginosa* especially for the two salts **2b**, and **2d** the last salt **2f** didn't show any activity against E. coli. In contrast, the silver-NHC complexes **3a-f** showed high antimicrobial activity against Staphylococcus aureus and Escherichia coli. The results revealed that the highest antimicrobial activity was reported in Ag-NHC complexes **3b** and **3c**.

The lipophilicity of Ag(I)–NHC complexes are thought to play a significant role in the ability of these compounds to penetrate cellular membranes, and increased lipophilicity through modification of the NHC wingtip substituents improved the antibacterial activity of compounds [55-57].

3.3.2. *Enzymatic inhibitory activity assay*

The inhibitory effect of all benzimidazolium salts **2a-f** and their silver(I)NHC complexes **3a-f** against different enzymes as AChE, BChE, Lipase, and α-amylase was studied *in vitro* at different concentrations. The benzimidazolium salts and their silver complexes demonstrated close percentages of inhibition against AChE compering with the standard Galanamine, while against BChE, all newly compound inhibited more effectively than the standard drug. The inhibitory effect of silver complexes against lipase showed that all compounds **3a-f** could effectively inhibit lipase with a value of IC_{50} approximates the standard (Orlistat). Also, this series of silver complexes exhibited strong and good anti-diabetic activity against the α-amylase enzyme. Contrary to these results, all benzimidazolium salts didn't show any activity against both lipase and α-amylase enzymes. Enzymatic activity was reported in the same manner as IC_{50} values presented in Table 6. Based on the IC_{50} values, the results were given as a concentration of 50% inhibition (IC_{50}). The inhibition of different enzymes was determined by comparing the reaction rates of samples relative to the blank sample. The capacity of the newly synthesized compound to inhibit the enzymes (AChE, BChE, Lipase, and α-amylase) was evaluated according to the spectrophotometric methods. The low IC_{50} values designated the high inhibition activity.

A. Evaluation of Acetylcholinesterase and Butyrylcholinesterase inhibitory capacity

To find out the capacity of both benzimidazolium salts **2a-f** and their silver(I)–HNC complexes **3a-f** against anticholinesterase activity, all the compounds were screened in an *in vitro* complementary system. Acetylcholinesterase (AChE) and butyrylcholinesterase (BChE) are the enzymes that catalyze the hydrolyses of substrate acetylthiocholine or butyrylthiocholine, respectively. The product thiocholine reacts with Ellman's reagent (DTNB) to produce 2- nitrobenzoic-5-mercaptothiocholine and 5-thio-2-nitrobenzoate which can be detected at 412 nm. For comparison purposes, Galantamine, a medicinal cholinesterase inhibitor used in mild Alzheimer's disease treatment, was used as the positive control.

As can be seen in Table 6, The obtained IC_{50} values revealed that all tested compounds showed a strong inhibitory against both enzymes. (AChE and BChE) with IC_{50} values ranging from (IC_{50}: 1.33 ± 0.3 μM to 17.97 ± 0.27 μM). The best AChE inhibitors between all compounds are **2a** for salts with (IC_{50}: 1.33 ± 0.3 μM), and **3a** for their silver(I) complexes with (IC_{50}: 1.60 ± 0.19 μM) comparing to that of the Galantamine (4.14 ± 0.07 μM). The compound **2f** is the least active AChE inhibitor

Table 5
Antifungal and anti-Bacterial activities (MIC $\mu g/mL$) of benzimidazolium salts **2a-f** and their silver(I)NHC complexes **3a-f.**

Compounds		*Anti-Fungal*		*Anti-Bacterial*		
		C. albicans[a]	C. glabrata[a]	E. coli[a]	P. aeruginosa[a]	S. aureus[a]
Benzimida-zolium Salts	2a	25	100	200	200	200
	2b	200	200	400	800	400
	2c	25	100	200	200	200
	2d	100	200	400	800	400
	2e	12.5	100	200	200	100
	2f	200	400	NA	NA	NA
Silver complexes	3a	12.5	12.5	25	50	25
	3b	12.5	12.5	25	25	6.25
	3c	6.25	6.25	25	25	6.25
	3d	12.5	12.5	25	50	12.5
	3e	12.5	12.5	25	25	12.5
	3f	25	12.5	25	50	25
	Ampicillin[b]	–	–	12.5	400	3.125
	Tetracycline[b]	–	–	0.8	12.5	0.2
	Amphotericin B[b]	0.05	0.1	–	–	–
	Voriconazole[b]	0.4	0.4	–	–	–

a: Tested microorganisms.
b: Reference drugs.
NA: Not Active.

Table 6
Anti-Cholinesterase, anti-Lipase, and Anti-α-Amylase activities of benzimidazolium salts **2a-f** and their silver(I)–NHC complexes **3a-f.**

Compound		Anti-Cholinesterase AChE $IC_{50} \pm SD$ (μM)[a]	Anti-Cholinesterase BChE $IC_{50} \pm SD$ (μM)[a]	Anti-Lipase Lipase $IC_{50} \pm SD$ (μM)[a]	Anti-α-Amylase α-amylase $IC_{50} \pm SD$ (μM)[a]
Benzimidazolium salts	**2a**	1.33 ± 0.03	0.96 ± 0.02	NA[c]	NA[c]
	2b	5.56 ± 0.57	0.72 ± 0.04	NA[c]	NA[c]
	2c	6.17 ± 0.33	0.70 ± 0.04	NA[c]	NA[c]
	2d	4.19 ± 0.02	0.15 ± 0.02	NA[c]	NA[c]
	2e	9.06 ± 0.26	1.08 ± 0.12	NA[c]	NA[c]
	2f	17.97 ± 0.27	4.29 ± 0.18	NA[c]	NA[c]
Silver(I)–NHC complexes	**3a**	1.60 ± 0.19	0.88 ± 0.00	33.79 ± 6.17	7.00 ± 0.87
	3b	3.50 ± 0.52	0.47 ± 0.04	52.25 ± 1.83	70.69 ± 2.69
	3c	5.64 ± 0.02	0.50 ± 0.03	34.61 ± 2.50	98.57 ± 2.18
	3d	4.21 ± 0.12	0.61 ± 0.02	40.72 ± 2.47	43.18 ± 2.60
	3e	4.53 ± 0.13	0.18 ± 0.01	33.15 ± 1.47	65.87 ± 2.66
	3f	4.14 ± 0.46	3.57 ± 0.15	58.66 ± 1.47	47.55 ± 1.28
Reference	**Galanamine**[b]	4.14 ± 0.07	20.38 ± 2.10	/	/
	Orlistat [b]			25.07 ± 0.48	
	Acarbose [b]	/	/	/	5258.02 ± 46.9

a: IC_{50} values represent the means ± SD of three parallel measurements ($p < 0.05$).
b: Reference compound.
c: Not Active.

with (IC_{50}: 17.97 ± 0.27 μM) between all salts. While compound **3c** is the least active AChE inhibitor with (IC_{50}: 5.64 ± 0.02 μM**)** between the silver(I) complexes. It should be noted that compounds **2d, 3d, 3e,** and **3f** showed IC_{50} values in the same range of the standard Galantamine. Accordingly, benzimidazolium salts and silver (I)–NHC complexes could be considered promising acetylcholinesterase inhibitors. According to Taylor et al [58]. The compounds that give a good inhibitory activity of acetylcholinesterase (AChE) are more beneficial for human health.

The data obtained for inhibition of BChE by benzimidazolium salts (**2a-f**) and their silver(I)–NHC complexes (**3a-f**) demonstrated that all compounds had high activity toward BChE. In terms of anti-BChE activity, the inhibitory potencies of all compounds toward BChE with IC_{50} values ranging from (IC_{50}: 0.29 ± 0.04 μM to 4.29 ± 0.18 μM**),** with IC_{50} values ranging from (IC_{50}: 0.29 ± 0.04 μM to 4.29 ± 0.18 μM). The most active benzimidazolium salts were **2d** with (IC_{50}: 0.15 ± 0.02 μM). The most active silver (I)–NHC complexes were **3e** with (IC_{50}: 0.18 ± 0.01 μM). The benzimidazolium salt **2f** and their silver(I) complex **3f** are the least active BChE inhibitor with (4.29 ± 0.18 μM) and (3.57 ± 0.15 μM) respectively. On the other hand, compared with galantamine standard. All-new compounds were more potent than the standard drug galantamine against the BChE enzyme. Generally, the inhibition of BChE by the benzimidazolium salt and their silver(I)–NHC complexes were more efficient than the AChE inhibitor activity. It was also noted that all compounds were more selective for BChE than the standard drug Galantamine. The selectivity was especially pronounced for compounds **2c**, **2d**, **2e**, **3c**, **3d**, and **3e.** The performance for the compound **3d** was 30.07-fold more selective for BChE. While for AChE inhibitors, all compounds had less affinity than Galantamine.

As presented in Table 7, the compounds Ag(II)–NHC complexes **3a-f** are polar molecules, these compounds present high log P values superior to 5 (log P > 5), which means that these compounds are too lipophilic (poor aqueous solubility). The benzimidazolium slats **2a-f** have a good aqueous solubility because of their log P value which included between 0 and 5. The standard (Galantamine**)** has log P values inferior to 3 (log P = -1.42) which has low partition coefficients. This compound is a polar molecule whith a good aqueous solubility.

B. Evaluation of Pancreatic Lipase inhibitory capacity.

The inhibitor of digestive lipase that limits intestinal fat absorption at an initial stage could prove as a proper medication for the treatment of hyperlipidemia and holds great promise as an anti-obesity agent. To find new pancreatic lipase (triacylglycerol lipase, EC 3.1.1.3) inhibitors from these new compounds, all the 3,5-dimethylbenzimidazolium salts **2a-f** and the related silver(I)–NHC complexes **3a-f** were tested for their anti-

Table 7
The selectivity index for AChE over BChE and BChE over AChE with docking score and log P of benzimidazolium salts **2a-f** and their silver(I)–NHC complexes **3a-f.**

Compounds		AChE			BChE			
		$IC_{50} \pm SD$ (μM)[a]	Selectivity index[c]	Docking score	$IC_{50} \pm SD$ (μM)[a]	Selectivity index[d]	Docking score	Log P
Benzimidazolium salts	**2a**	1.33 ± 0.03	0.72	59.20	0.96 ± 0.02	1.38	74.74	5.17
	2b	5.56 ± 0.57	0.13	54.43	0.72 ± 0.04	7.72	76.60	5.04
	2c	6.17 ± 0.33	0.11	51.78	0.70 ± 0.04	8.81	76.71	4.80
	2d	4.19 ± 0.02	0.06	56.48	0.15 ± 0.02	14.45	77.60	4.00
	2e	9.06 ± 0.26	0.11	52.73	1.08 ± 0.12	8.39	70.26	5.30
	2f	17.97 ± 0.27	0.23	51.65	4.29 ± 0.18	4.18	68.27	3.23
Silver complexes	**3a**	1.60 ± 0.19	0.55	59.11	0.88 ± 0.00	1.82	74.98	8.40
	3b	3.50 ± 0.52	0.13	58.43	0.47 ± 0.04	7.44	77.12	7.46
	3c	5.64 ± 0.02	0.08	53.04	0.50 ± 0.03	11.28	76.80	8.19
	3d	4.21 ± 0.12	0.14	56.22	0.61 ± 0.02	30.07	76.58	7.41
	3e	4.53 ± 0.13	0.07	56.87	0.18 ± 0.01	12.94	77.10	8.62
	3f	4.14 ± 0.46	0.86	57.09	3.57 ± 0.15	1.16	70.15	6.64
	Galantamine [b]	4.14 ± 0.07	4.92	57.02	20.38 ± 2.10	0.20	53.04	−1.42

c : Selectivity for AChE: IC_{50}(BChE)/IC_{50}(AChE).
d: Selectivity for BChE: IC_{50}(AChE)/IC_{50}(BChE)

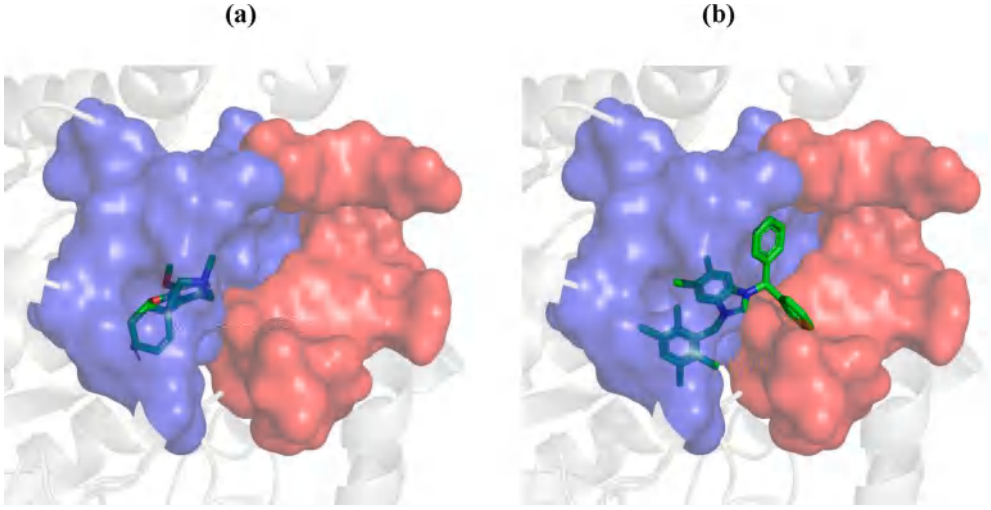

Fig. 4. The positioning of galantamine **(a)** and, **2a (b)** in the AChE active site.

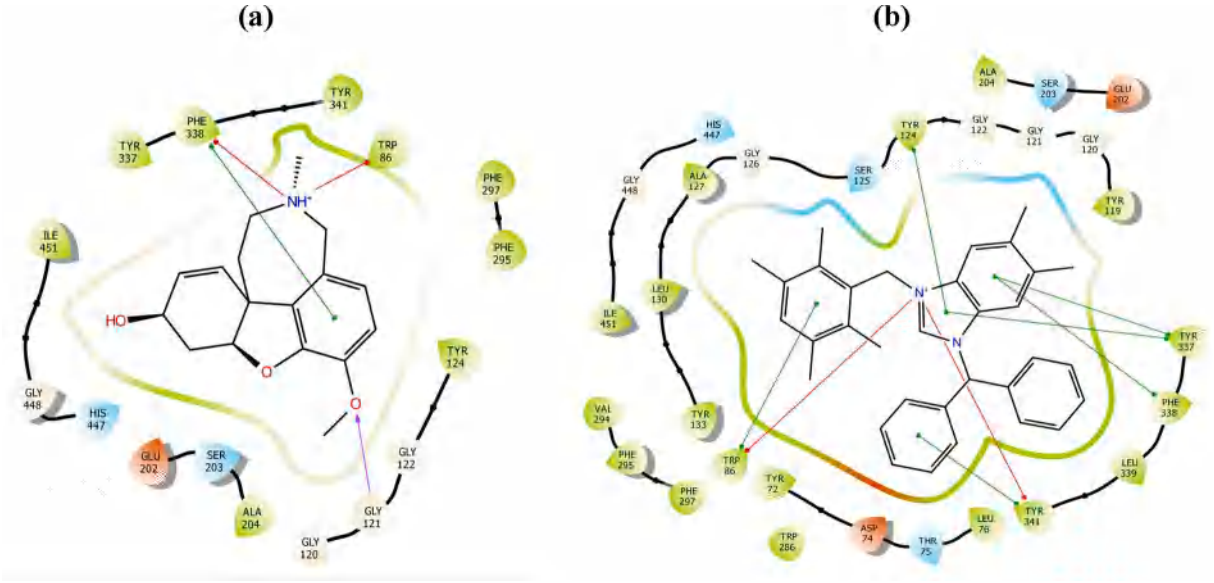

Fig. 5. Binding mode prediction of galantamine **(a),** and compound **2a (b)** into the entire AChE active pocket.

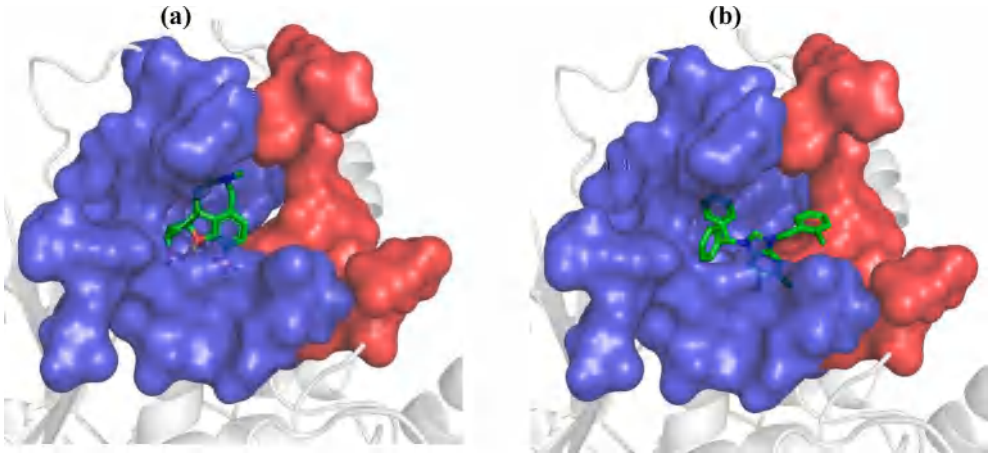

Fig. 6. The positioning of galantamine **(a),** and **2d (b)** in BChE active site.

lipase activity using a radioactive screening method. The results shown in Table 5 represent a significant inhibitory activity against Lipase by all the silver complexes, especially the complexes **3a** and **3e** that displayed remarkable anti-lipase activity with (IC_{50} = 33.79 ± 6.17 μM) and (IC_{50} = 33.15 ± 1.47 μM) respectively, were found to be very close to the reference drug orlistat (IC_{50} = 25.07 ± 0.48 μM). Opposite of that, all salts **2a-f** were not active against the lipase enzyme. This study proved that Ag's presence in the compound gave the capacity for the complexes to had anti-lipase activity.

C. Evaluation of *α*-amylase inhibitory capacity

The evaluation of 3,5-dimethylbenzimidazolium salts and their silver (I)–NHC complexes effect were tested using α-amylase inhibitory assay; the study was investigated the anti-diabetic activity of these new compounds. As shown in table 5. The *α*-amylase inhibitor effects of silver (I)–NHC complexes showed higher inhibitory activity than acarbose (IC_{50} = 5258.02 ± 4.9 μM). The greatest *α*–amylase inhibition activity was obtained in the compound **3a**, with (IC_{50} = 7.00 ± 0.87 μM). While all benzimidazolium salts **2a-f** are not active against *α*–amylase. They didn't show any anti-diabetic activity.

3.4. *Molecular docking study*

Molecular docking studies were carried out to get a better insight into the binding modes and amino acid interactions of the synthesized compounds into AChE and BChE actives sites. Table 7 reveals that the experiment data of enzyme inhibitory activity *in vitro* showed that the molecular docking findings were in good agreement. Indeed, the most potent inhibitors from *in vitro* assays showed the best docking scores against both enzymes. The most promising compounds (compound **2a** for AChE and **2d** for BChE) were chosen to be investigated further of their binding mode with their target. As shown in Fig. 4, compound **2a** covers both the catalytic anionic site (CAS) and the peripheral anionic site (PAS) of AChE, leading to an inhibitory potency 3 fold more than that of galantamine, which binds only to the CAS. Also, The disparity in inhibitory potency between these two compounds may be explained by the different number of interactions between them and the protein (Fig. 5). Indeed, whereas **2a** is involved in eight interactions (six π-π stacking with Trp86, Tyr124, Tyr337, Phe338, Tyr341, and two π-cation interactions with Trp86 and Tyr341), galantamine is involved in only four interactions (two π-cation interactions with Trp86 and Phe338, a hydrogen bond with Gly121 and a π-π stacking with Phe338).

The most plausible pose of each compound is presented as obtained by docking with Gold. Residue Tyr341, which protects the pocket's ligand, is omitted for clarity. The CAS area of the cavity is shown in blue,

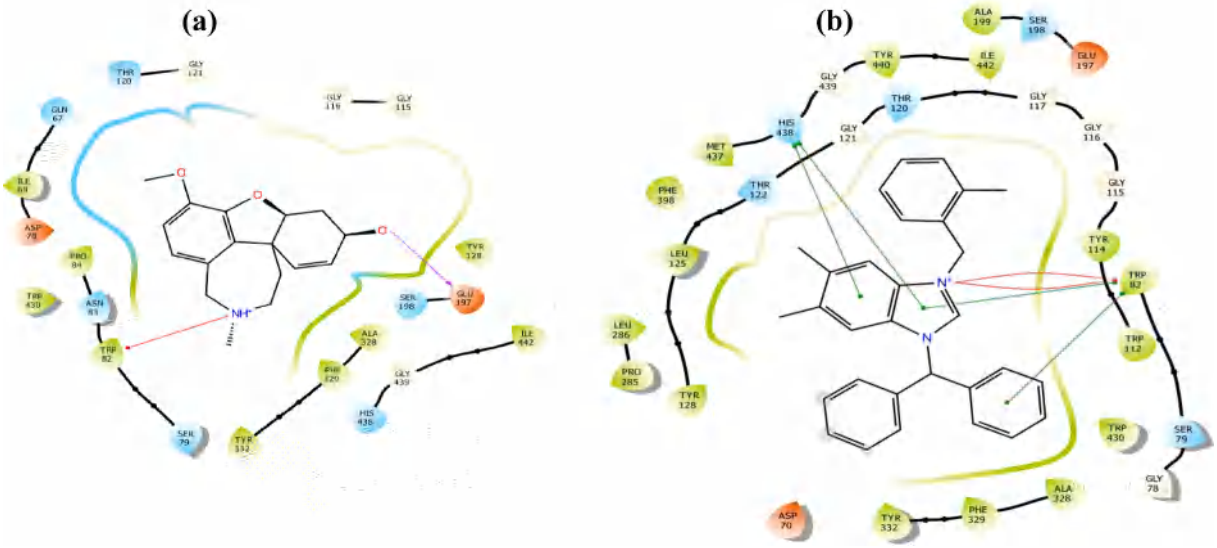

Fig. 7. Binding mode prediction of galantamine **(a)** and compound **2d (b)** into the entire BChE active pocket.

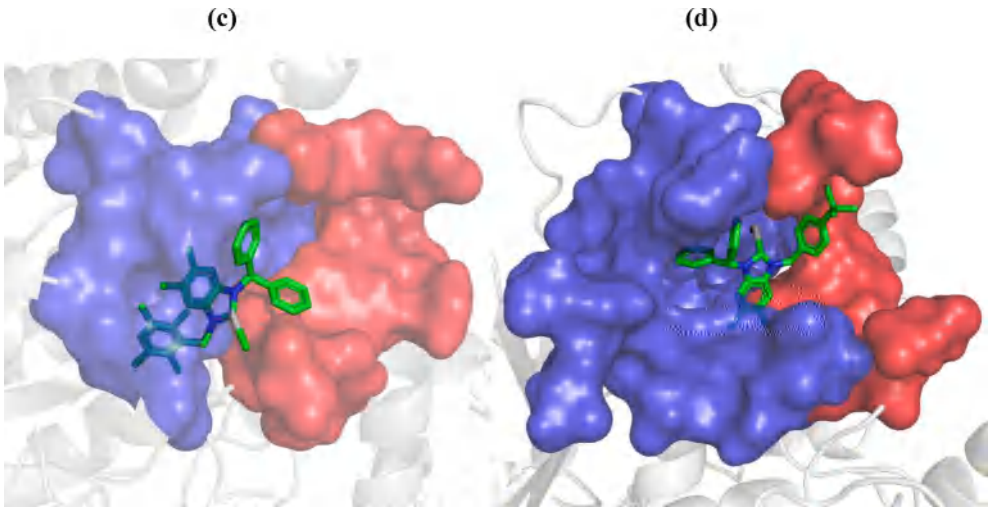

Fig. 8. The positioning of complex **3a (c)** in AChE, and **3e (d)** in BChE active sites.

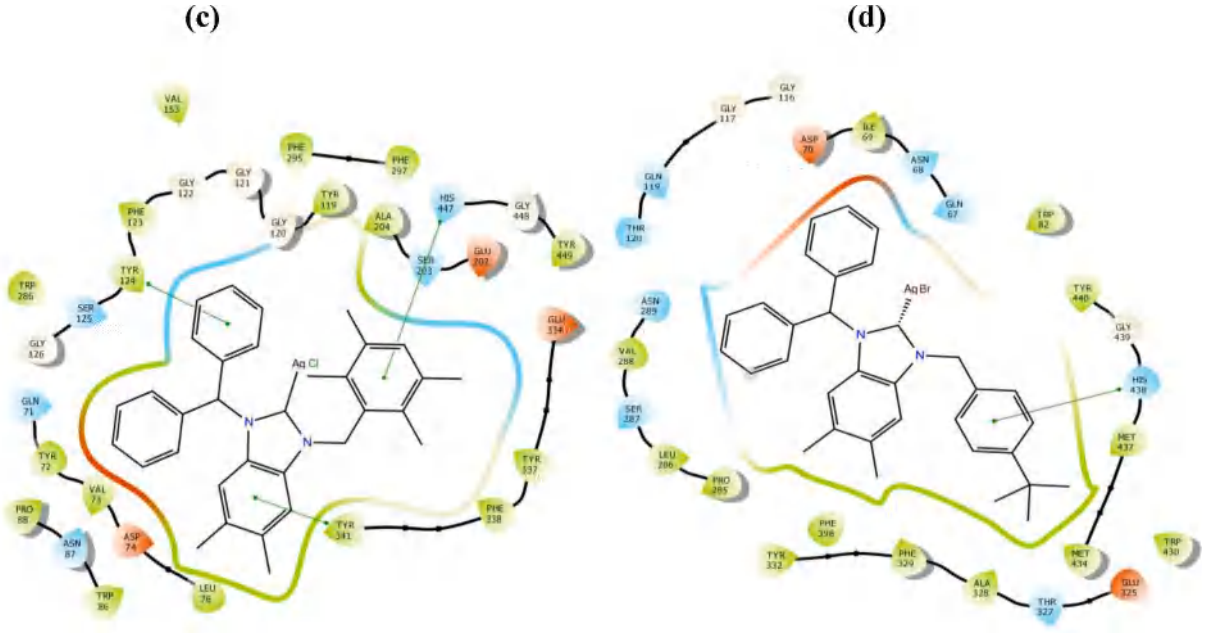

Fig. 9. Binding mode prediction of compound **3a (c)** and compound **3e (d)** into the entire AChE and BChE active pocket.

while the PAS is shown in red. The ligand atoms are color-coded as follows: oxygen in red, carbon in green, and nitrogen in blue. The images were drawn by PyMol.

Purple arrows head from the donor to the acceptor of hydrogen bonds, red lines represent π-cation interactions, and green lines π-π stacking. The images were done with the Ligand Interaction Diagram script from the Schrödinger Suite.

Concerning the BChE, The inhibitory potency of compound **2d** is higher than that of galantamine. because of its rational positioning in this enzyme's binding site. Indeed, compound **2d** binds both the CAS and PAS of BChE in contrary to galantamine which covers only the CAS (Fig. 6). Also, **2d** establishes a higher number of interactions against BChE active site than that of galantamine (Fig. 7). Indeed, whereas galantamine is involved in only two interactions (hydrogen bond with Glu197 and π-cation interaction with Trp82), **2d** is involved in six interactions of which two π-π stackings with His438. This residue was described to play an important role in the BChE activity [39]. Fig. 8. Fig. 9.

Remarkably, salts are more powerful compared to complexes since the positively charged nitrogen of the cycle engages in the formation of π -cation bonds with the residues of the active site of the enzyme (Trp86 in the case of AChE and Trp82 in the case of BChE) which increases the affinity of the salts, as for **2a** and **2d** compared to their silver(I)–NHC complex analog (**3a** and **3d**) against AChE and BChE respectively. This increase of the inhibitory potency may be explained by the formation of a π-cation interaction between the nitrogen of salts, and Trp86 for AChE (Trp82 for BChE). As shown in (Figure 08 (c)) , the Ag(II)NHC complex **3a** forms three π-π stackings with Tyr124, Tyr341 and His447 of AChE active site. The absence of π-cation with Trp86 seems to decrease its affinity compared to its salt analog **2a**. Likewise, the absence of π-cation with Trp82 seems to decrease the affinity of silver(I)–NHC complexes against BChE, as for **3e** establishes a π-π stacking with His438 of BChE active site (Figure 08 (d)).

4. Conclusion

In this research, six benzimidazolium salts and their related silver(I)–NHC complexes have been synthesized and identified with different spectroscopic analysis methods. All selected compounds were tested for their biological capacity using anti-microbial, anti-cholinesterase, anti-α-amylase, and anti-lipase activities. Importantly, our results provide evidence for showing the best results comparing with the reference standard control drug. The silver(I)–NHC complexes showed important anti-microbial activity and significate inhibitory against all types of enzymes, such as AChE, BChE, α-amylase, and lipase. Contrary to this the benzimidazolium salts showed a moderate anti-microbial activity and the inhibition by enzymes was recorded just for AChE and BChE. A great correlation between experimental and theoretical studies for these new compounds was obtained by molecular docking study. Based on our findings, the synthesis of Ag-NHC complexes allowed us to confirm that the use of Ag as a metal with NHCs increase the biological activity, which made silver(I)–NHC complexes considered as metallopharmaceutical compound par excellence to be used in the medicine and pharmaceutical industries, and provide promising starting points for further research to develop new drugs for the treatment of many diseases.

Declaration of Competing Interest

The authors declare that they have no known competing financial interests or personal relationships that could have appeared to influence the work reported in this paper.

Acknowledgments

The authors greatly acknowledge financial support from the İnönü University Research Fund of this work. X-ray analyses were supported by the Scientific Research Projects Unit of Ondokuz Mayıs University (Project No: PYO.FEN.1906.19.001).

Appendix A. Supplementary data

Supplementary data to this article can be found online at https://doi.org/10.1016/j.ica.2021.120486.

References

[1] R. Kılınçarslan, N. Sadıç, Catalytic activity of N-heterocyclic carbene silver complexes derived from imidazole ligands, Inorganic and Nano-Metal Chemistry 47 (3) (2017) 462–466, https://doi.org/10.1080/15533174.2016.1186054.
[2] F.E. Hahn, M. Jahnke, Heterocyclic carbenes: Synthesis and coordination chemistry, Angewandte Chemie - International Edition 47 (17) (2008) 3122–3172, https://doi.org/10.1002/(ISSN)1521-377310.1002/anie.v47:1710.1002/anie.200703883.
[3] R.A. Haque, N. Hasanudin, M.A. Iqbal, A. Ahmad, S. Hashim, A. Abdul Majid, M.B. K. Ahamed, Synthesis, crystal structures, in vitro anticancer, and in vivo acute oral toxicity studies of bis-imidazolium/benzimidazolium salts and respective dinuclear Ag(I)- N -heterocyclic carbene complexes, J. Coord. Chem. 66 (18) (2013) 3211–3228, https://doi.org/10.1080/00958972.2013.831406.
[4] I. Özdemir, S. Demir, S. Günal, I. Özdemir, C. Arici, D. Ülkü, Synthesis, characterization and antimicrobial activity of new silver complexes with N-heterocyclic carbene ligands, Inorg. Chim. Acta 363 (14) (2010) 3803–3808, https://doi.org/10.1016/j.ica.2010.07.034.
[5] İ. Özdemir et al., "Synthesis, characterization and antitumor properties of novel silver(I) and gold(I) N-heterocyclic carbene complexes," Inorganica Chimica Acta, vol. 506, no. February, 2020, doi: 10.1016/j.ica.2020.119530.
[6] M.U.M. Ulu, E. Evren, N. Gürbüz, İ.Ö.İ. Özdemir, N. Hamdi, İ. Özdemir, Rhodium (I) N-heterocyclic carbene Complexes: Synthesis and cytotoxic Properties, New J. Chem. (2021).
[7] N. Şahin, S. Şahin-Bölükbaşı, M.N. Tahir, C. Arıcı, E. Çevik, N. Gürbüz, İ. Özdemir, B.S. Cummings, Synthesis, characterization and anticancer activity of allyl substituted N-Heterocyclic carbene silver(I) complexes, J. Mol. Struct. 1179 (2019) 92–99, https://doi.org/10.1016/j.molstruc.2018.10.094.
[8] E. Meggers, "Targeting proteins with metal complexes," pp. 1001–1010, 2009, doi: 10.1039/b813568a.
[9] T.J. Siciliano, M.C. Deblock, K.M. Hindi, S. Durmus, M.J. Panzner, C.A. Tessier, W. J. Youngs, Synthesis and anticancer properties of gold (I) and silver (I) N-heterocyclic carbene complexes, J. Organomet. Chem. 696 (5) (2011) 1066–1071, https://doi.org/10.1016/j.jorganchem.2010.10.054.
[10] M.T. Chen, B. Landers, O. Navarro, Well-defined (N-heterocyclic carbene)-Ag(i) complexes as catalysts for A 3 reactions, Org. Biomol. Chem. 10 (11) (2012) 2206–2208, https://doi.org/10.1039/c2ob06900h.
[11] S.D. Düşünceli, D. Ayaz, E. Üstün, S. Günal, N. Özdemir, M. Dinçer, İ. Özdemir, Synthesis, antimicrobial properties, and theoretical analysis of benzimidazole-2-ylidene silver(I) complexes, J. Coord. Chem. 73 (13) (2020) 1967–1986, https://doi.org/10.1080/00958972.2020.1812587.
[12] I. Slimani, et al., Novel n-heterocyclic n carbene silver(I) complexes: Synthesis, structural characterization, antimicrobial and cytotoxicity potential studies, J. Braz. Chem. Soc. 31 (10) (2020) 2058–2070, https://doi.org/10.21577/0103-5053.20200107.
[13] M. Kaloğlu, N. Kaloğlu, İ. Özdemir, S. Günal, İ. Özdemir, Novel benzimidazol-2-ylidene carbene precursors and their silver(I) complexes: Potential antimicrobial agents, Bioorg. Med. Chem. 24 (16) (2016) 3649–3656, https://doi.org/10.1016/j.bmc.2016.06.004.
[14] N. Kaloğlu, İ. Özdemir, S. Günal, İ. Özdemir, Synthesis and antimicrobial activity of bulky 3,5-di-tert-butyl substituent-containing silver–N-heterocyclic carbene complexes, Appl. Organomet. Chem. 31 (11) (2017) 1–10, https://doi.org/10.1002/aoc.3803.
[15] D. Bourissou, O. Guerret, F.P. Gabbaï, G. Bertrand, Stable Carbenes, Chem. Rev. 100 (1) (2000) 39–91, https://doi.org/10.1021/cr940472u.
[16] W.A. Herrmann, ChemInform Abstract: N-Heterocyclic Carbenes. Part 31. N-Heterocyclic Carbenes: A New Concept in Organometallic Catalysis, ChemInform 33 (32) (2002) no–no, https://doi.org/10.1002/chin.200232255.
[17] S. Díez-González, S.P. Nolan, Stereoelectronic parameters associated with N-heterocyclic carbene (NHC) ligands: A quest for understanding, Coord. Chem. Rev. 251 (5-6) (2007) 874–883, https://doi.org/10.1016/j.ccr.2006.10.004.
[18] G. Anantharaman, K. Elango, Synthesis of imidazolium/benzimidazolium salts and the preparation of silver(I) complex of bis-benzimidazolium dibromide, Synth. React. Inorg., Met.-Org., Nano-Met. Chem. 37 (9) (2007) 719–723, https://doi.org/10.1080/15533170701674959.
[19] J.C. Garrison, W.J. Youngs, "Ag (I) N-Heterocyclic Carbene Complexes : Synthesis, Structure, and Application", I (2005) 3978–4008.
[20] K.J. OBrien, L. Li (Eds.), Rightful Resistance in Rural China, Cambridge University Press, Cambridge, 2006.
[21] S. Cie, X-area (version 1.18) and X-red32 (version 1.04), Darmstadt, Germany, 2002.
[22] L. Palatinus, G. Chapuis, SUPERFLIP–a computer program for the solution of crystal structures by charge flipping in arbitrary dimensions, J. Appl. Crystallogr. 40 (4) (2007) 786–790.
[23] D. Kratzert, J.J. Holstein, I. Krossing, DSR: enhanced modelling and refinement of disordered structures with SHELXL, J. Appl. Crystallogr. 48 (3) (2015) 933–938.
[24] O.V. Dolomanov, L.J. Bourhis, R.J. Gildea, J. a. K. Howard and H. Puschmann, J. Appl. Crystallogr 42 (2009) 339–341.
[25] M.C. Arendrup, M. Cuenca-Estrella, C. Lass-Flörl, W. Hope, EUCAST-AFST,, EUCAST technical note on the EUCAST definitive document EDef 7.2: method for the determination of broth dilution minimum inhibitory concentrations of antifungal agents for yeasts EDef 7.2 (EUCAST-AFST), Clin. Microbiol. Infect. 18 (7) (2012) E246–E247.
[26] C.L.S. Institute-Clsl, Methods for dilution antimicrobial susceptibility tests for bacteria that grow aerobically; Approved standard–, M07–A9, Clinical and Laboratory Standards Institute Wayne, PA, 2015.
[27] R. Sabouraud, Contribution a l'etude de la trichophytie humaine. Etude clinique, microscopique et bacterioloqique sur la pluralité des trichophytons de l'homme, Ann. Dermatol. Syphil 3 (1892) 1061–1087.
[28] J. Sambrook, D.W. Russell, "Molecular cloning: a laboratory manual., Cold Spring Harbor Laboratory Press", Cld Spring Harbor, NY 502 (2001) 2001.
[29] S. Stepankova, K. Komers, Cholinesterases and cholinesterase inhibitors, Curr. Enzym. Inhib. 4 (4) (2008) 160–171.
[30] F. Mao, J. Li, H. Wei, L. Huang, X. Li, Tacrine–propargylamine derivatives with improved acetylcholinesterase inhibitory activity and lower hepatotoxicity as a potential lead compound for the treatment of Alzheimer's disease, J. Enzyme Inhib. Med. Chem. 30 (6) (2015) 995–1001.
[31] S. Saha, R. Verma, Inhibitory potential of traditional herbs on α-amylase activity, Pharm. Biol. 50 (3) (2012) 326–331.
[32] D. Varma, D. Sen, Role of the unfolded protein response in the pathogenesis of Parkinson's disease, Acta Neurobiol Exp (Wars) 75 (1) (2015) 1–26.
[33] I.K. Rhee, M. van de Meent, K. Ingkaninan, R. Verpoorte, Screening for acetylcholinesterase inhibitors from Amaryllidaceae using silica gel thin-layer chromatography in combination with bioactivity staining, J. Chromatogr. A 915 (1-2) (2001) 217–223.
[34] G.L. Ellman, K.D. Courtney, V. Andres, R.M. Featherstone, A new and rapid colorimetric determination of acetylcholinesterase activity, Biochem. Pharmacol. 7 (2) (1961) 88–95.
[35] S.P. de Souza, L.L.S. Pereira, A.A. Souza, C.D. dos Santos, Inhibition of pancreatic lipase by extracts of baccharis trimera: Evaluation of antinutrients and effect on glycosidases, Brazilian Journal of Pharmacognosy 21 (3) (2011) 450–455, https://doi.org/10.1590/S0102-695X2011005000049.
[36] B.C.S. Santos, A.S. Pires, Célia.H. Yamamoto, M.R.C. Couri, A.G. Taranto, M. S. Alves, A.Lúcia.dos.S.de.M. Araújo, O.V. de Sousa, Methyl chavicol and its synthetic analogue as possible antioxidant and antilipase agents based on the in vitro and in silico assays, Oxid. Med. Cell. Longevity 2018 (2018) 1–11, https://doi.org/10.1155/2018/2189348.

[37] G. Zengin, C. Sarikurkcu, A. Aktumsek, R. Ceylan, O. Ceylan, A comprehensive study on phytochemical characterization of Haplophyllum myrtifolium Boiss. endemic to Turkey and its inhibitory potential against key enzymes involved in Alzheimer, skin diseases and type II diabetes, Ind. Crops Prod. 53 (2014) 244–251.
[38] J. Cheung, E.N. Gary, K. Shiomi, T.L. Rosenberry, Structures of human acetylcholinesterase bound to dihydrotanshinone i and territrem B show peripheral site flexibility, ACS Med. Chem. Lett. 4 (11) (2013) 1091–1096, https://doi.org/10.1021/ml400304w.
[39] M. Wandhammer, E. Carletti, M. Van der Schans, E. Gillon, Y. Nicolet, P. Masson, M. Goeldner, D. Noort, F. Nachon, Structural study of the complex stereoselectivity of human butyrylcholinesterase for the neurotoxic V-agents, J. Biol. Chem. 286 (19) (2011) 16783–16789, https://doi.org/10.1074/jbc.M110.209569.
[40] R.G. Demmak, S. Bordage, A. Bensegueni, N. Boutaghane, T. Hennebelle, E. H. Mokrani, S. Sahpaz, Chemical constituents from solenostemma argel and their cholinesterase inhibitory activity, Nat. Prod. Sci. 25 (2) (2019) 115, https://doi.org/10.20307/nps.2019.25.2.115.
[41] P.P. Wizard, Epik version 2.0, Impact version 5.5, Prime version 2.1, Schrödinger, LLC, New York (NY), 2009.
[42] I. Boualia, C. Derabli, R. Boulcina, C. Bensouici, M. Yildirim, A. Birinci Yildirim, E. H. Mokrani, A. Debache, Synthesis, molecular docking studies, and biological evaluation of novel alkyl bis(4-amino-5-cyanopyrimidine) derivatives, Arch. Pharm. 352 (11) (2019) 1900027, https://doi.org/10.1002/ardp.v352.1110.1002/ardp.201900027.
[43] L. L. C. Schrödinger, "The PyMOL molecular graphics system, version 1.8." November, 2015.
[44] E.H. Mokrani, A. Bensegueni, L. Chaput, C. Beauvineau, H. Djeghim, L. Mouawad, Identification of New Potent Acetylcholinesterase Inhibitors Using Virtual Screening and in vitro Approaches, Mol. Inf. 38 (5) (2019) 1–10, https://doi.org/10.1002/minf.201800118.
[45] G. Jones, P. Willett, R.C. Glen, Molecular recognition of receptor sites using a genetic algorithm with a description of desolvation, J. Mol. Biol. 245 (1) (1995) 43–53.
[46] L.L.C. Schrodinger, The PyMOL molecular graphics system, Version 1 (5) (2010).
[47] F.H. Allen, O. Kennard, D.G. Watson, L. Brammer, A.G. Orpen, R. Taylor, Tables of bond lengths determined by X-ray and neutron diffraction. Part 1. Bond lengths in organic compounds, Journal of the Chemical Society, Perkin Transactions 2 (12) (1987) S1–S19.
[48] P. De Fremont, et al., Synthesis of well-defined N-heterocyclic carbene silver (I) complexes, Organometallics 24 (26) (2005) 6301–6309.
[49] A. Bondi, van der Waals volumes and radii, The Journal of physical chemistry 68 (3) (1964) 441–451.
[50] C. Topf, C. Hirtenlehner, U. Monkowius, Synthesis and characterization of silver (I), gold (I), and gold (III) complexes bearing a bis-dialkylamino functionalized N-heterocyclic carbene, J. Organomet. Chem. 696 (20) (2011) 3274–3278.
[51] Y.-M. Liu, et al., Synthesis and characterization of para-pyridine linked NHC palladium complexes and their studies for the Heck-Mizoroki coupling reaction, Dalton Trans. 41 (24) (2012) 7382–7389.
[52] J. Mormul, M. Steimann, C. Maichle-Mössmer, U. Nagel, Chiral Transition-Metal Complexes of Phenanthro-Annulated N-Heterocyclic Carbenes-Synthesis and Reactivity, Eur. J. Inorg. Chem. 2013 (19) (2013) 3421–3428.
[53] Q. Li, X. Li, J. Yang, H.-B. Song, L.-F. Tang, Synthesis and structural characterization of N-heterocyclic carbene silver complexes derived from N-ferrocenylmethyl-N′-(pyridylmethyl)imidazolium iodides, Polyhedron 59 (2013) 29–37, https://doi.org/10.1016/j.poly.2013.04.032.
[54] Q.-X. Liu, et al., Structures of NHC Hg (II) and Ag (I) complexes and selective recognition of nitrate anion, CrystEngComm 17 (6) (2015) 1358–1373.
[55] R.A. Haque, P.O. Asekunowo, M.R. Razali, "N HC – Silver (I) Complexes as Chemical Nucleases; Synthesis, Crystal Structures, and Antibacterial Studies" 25 (3) (2014) 194–204, https://doi.org/10.1002/hc.
[56] R.A. Haque, S.Y. Choo, S. Budagumpi, A.-A. Abdullah, M.B. Khadeer Ahamed, A.M. S. Abdul Majid, "Synthesis, crystal structures, characterization and biological studies of nitrile- functionalized silver (I) N-heterocyclic carbene complexes The School of Chemical Sciences, Universiti Sains Malaysia, 11800 USM, Penang, Centre for Nano and Material Sciences, Jain University, Jain Global Campus, Bangalore The School of Biological Sciences, Universiti Sains Malaysia, 11800 USM, Penang, EMAN Research and Testing Laboratory, The School of Pharmaceutical Sciences, The School of Chemical Sciences", INORGANICA CHIMICA ACTA, no, I 433 (2015) 35–44, https://doi.org/10.1016/j.ica.2015.04.023.
[57] A. Majid, SC, no. I. Elsevier B.V., 2015.
[58] O. Trott, A.J. Olson, AutoDock Vina: improving the speed and accuracy of docking with a new scoring function, efficient optimization, and multithreading, J. Comput. Chem. 31 (2) (2010) 455–461.

NJC

ROYAL SOCIETY OF CHEMISTRY

PAPER

Cite this: *New J. Chem.*, 2021, 45, 17878

Synthesis, structures, DFT calculations, and catalytic application in the direct arylation of five-membered heteroarenes with aryl bromides of novel palladium-N-heterocyclic carbene PEPPSI-type complexes†‡

Abd el-Krim Sandeli,[ab] Naima Khiri-Meribout,*[ac] Saida Benzerka,[ac] Houssem Boulebd,[ac] Nevin Gürbüz,[bd] Namık Özdemir[e] and İsmail Özdemir*[bd]

A new series of Pd-catalysts based on an N-heterocyclic carbene PEPPSI-type ligand (PEPPSI = pyridine enhanced precatalyst preparation stabilization and initiation) with the general formula [Pd(II)Br2(NHC)(pyridine)] was synthesized and fully characterized *via* spectroscopic analytical methods. Further, the structural characterization of **3a**, **3b**, and **3d** was performed *via* single-crystal X-ray diffraction, which supported the proposed structures and offered a more detailed structural characterization. Additionally, the electronic, vibrational, thermodynamic, and optical properties of **3a**, as a representative molecule, were confirmed utilizing density functional theory (DFT) calculations. The experimental molecular geometry of the ground state of complex **3a** was compared with the minimized structure obtained from DFT calculations. The B3LYP functional in conjunction with the LANL2DZ basis set for the palladium atom and the 6-311G(d,p) basis set for the hydrogen, carbon, nitrogen, and bromine atoms were used for all calculations. The frontier molecular orbitals and molecular electrostatic potential were also analyzed and discussed. Due to the significant interest in halo-substituted arylated heteroarenes in organic chemistry, the catalytic activity of these Pd(II)–NHC PEPPSI–type complexes were evaluated *via* the direct arylation of five-membered heteroaromatics such as thiophene, furan, and thiazole derivatives with various (hetero)aryl bromides in the presence of 1 mol% catalyst. The results showed that all new Pd–NHC complexes are effective catalysts, which exhibited very good catalytic activity and gave C-H activation selectively at the C(5)-position of 2-acetyl furan and 2-acetyl thiophene.

Received 13th July 2021,
Accepted 25th August 2021

DOI: 10.1039/d1nj03388c

rsc.li/njc

Introduction

N-Heterocyclic carbenes (NHCs) are effective ligands that allow the preparation of most metal complexes and chemically acceptable catalysts by altering the substituents on the nitrogen atom.[1] They have become one of the most widely used classes of ligands in organometallic chemistry with new catalytic applications. Due to the activity, stability, and selectivity of metal complexes containing NHC ligands, they are widely used as highly reactive and rather selective catalysts for numerous reactions.[2] Over the last few decades, considerable advances have been achieved in direct arylation methods. Various transition metals such as Pd, Ru, and Rh are effective for direct arylation reactions.[3] However, among them, the Pd-complexes are the most powerful. Today, palladium-catalyzed cross-coupling reactions are highly important synthetic tools in organic chemistry.[4] Due to these features, they have been successfully employed in different applications of organometallic chemistry as a key ligand for metal complexes.[5] The most used Pd–NHC complexes can be categorized into four main classes, *i.e.*, bis-Pd–NHCs, allyl-type Pd–NHCs, pincer-type Pd–NHCs, and **PEPPSI** (**p**yridine **e**nhanced **p**re-catalyst **p**reparation stabilization and **i**nitiation)-type Pd–NHCs.[6,7] Among the most popular catalysts for the above-mentioned reactions are

[a] *Research Laboratory of Synthesis of Molecules with Biological Interest, Mentouri Constantine-1 University, Constantine, Algeria. E-mail: naima.khiri@umc.edu.dz*
[b] *Catalysis Research and Application Center, Inönü University, 44280 Malatya, Turkey. E-mail: ismail.ozdemir@inonu.edu.tr*
[c] *Faculty of Science, Department of Chemistry, Mentouri Constantine-1 University, Constantine, Algeria*
[d] *Faculty of Science and Art, Department of Chemistry, İnönü University, Malatya, Turkey*
[e] *Department of Mathematics and Science Education, Faculty of Education, Ondokuz Mayıs University, 55139 Samsun, Turkey*

† Dedicated to Prof. Christian Bruneau for his outstanding contribution to organometallic chemistryc atalysis.

‡ Electronic supplementary information (ESI) available: All the supplementary data (^{1}H, ^{13}C-NMR, and Crystallographic data) are given in supplementary information. CCDC 2073777, 2073779 and 2073780. For ESI and crystallographic data in CIF or other electronic format see DOI: 10.1039/d1nj03388c

PEPPSI-type palladium–NHC complexes of the type [PdX_2(NHC)(pyridine)] (X/halide), which have gained practical importance in various catalytic processes.

The direct arylation of heteroarenes is particularly attractive given that these moieties are present in many biologically active compounds. In recent years, the Pd-catalyzed direct arylation of (hetero)arenes with (pseudo)halides has received significant attention as an eco-friendly and economic alternative to conventional methods, which are considered as the most commonly employed coupling partners for Pd-catalyzed direct arylation reactions.[8] In 1985–1992, Ohta *et al.* first reported the direct arylation of heteroaromatics with aryl halides using a C–H activation strategy through the cleavage of two C–H bonds, in which $Pd(PPh_3)_4$ was used as the catalyst and dimethylacetamide (DMAc) as the solvent.[9–11] Subsequently, Organ *et al.*[3] reported the synthesis of easily handled, air- and moisture-stable Pd–NHC complexes using the PEPPSI method, which featured Pd(II) species bearing an NHC ligand, two halides, and a labile ligand such as 3-chloropyridine. Following the discovery of Organ's PEPPSI-type Pd-complexes, which are consider a new class of Pd-catalysts that are completely different from other Pd–NHC complexes and easier to synthesize and use,[12] this type of complex has shown remarkable catalytic activities towards various carbon–carbon and carbon–heteroatom coupling reactions. In recent years, some studies on the direct arylation reaction of PEPPSI-type palladium-N-heterocyclic carbene (NHC) complexes have been, published.[13,14] Researchers have synthesized Pd–NHC complexes containing different imidazoles,[15] benzimidazoles[16] and benzotriazoles. In the last two decades, PEPPSI-themed Pd-complexes have been used as effective catalysts in direct arylation and successful results have been obtained.[17] Direct arylation reactions have received great interest as possible alternatives to the most employed cross-coupling reactions. Since then, palladium-catalyzed direct arylation has been successfully applied for the arylation of heteroaryl derivatives with aryl-halides and has proven to be a powerful method for the synthesis of a wide variety of arylated heterocycles.[18–22] Very exciting results have been reported by several groups using thiophenes, furans, pyrroles, thiazoles, oxazoles, imidazoles, and triazoles.[23,24] Azole-derived metal complexes have found application in many fields.[25–27] In particular, nucleophilic N-heterocyclic carbenes (NHCs) have been proven to be useful ligands for transition metal catalysis.[28–30] Alternatively, both thiophene and thiazole derivatives have attracted attention due to their important biological activity, for example, sulfathiazole is an antimicrobial drug, the 2-arylthiophene derivative canagliflozin is a drug used in the treatment of type 2 diabetes, atliprofen is an anti-inflammatory drug, motapizone is used in the treatment against platelet aggregation diabetes, and tiemonium is an antimuscarinic.[31–33] Several thiophene derivatives containing a hydroxyalkyl group at C2 have also been found to be bioactive. Duloxetine is employed against major depressive disorder and penthienate is an antimuscarinic; furthermore, several 2-arylated furans display important biological properties. For example, dantrolene is a muscle relaxant and lapatinib is employed against breast cancer (Fig. 1).

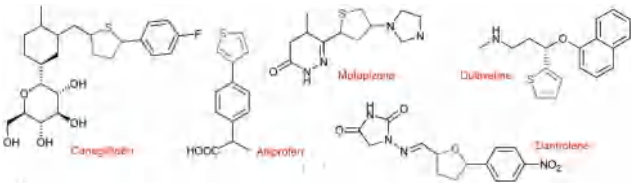

Fig. 1 Examples of bioactive thiazole, thiophene, and furan derivatives.

Considering that they have such important biological activity, the discovery of more direct and selective procedures to synthesize arylated thiophene, thiazole, and furan derivatives is an important topic in synthetic organic chemistry. The use of these functional halo thiophenes for direct arylation would be useful, as they would give simple access to a wide variety of polyfunctionalized thiophenes useful for materials chemistry or pharmaceutical applications. In this context, recently in an attempt to provide a new vision on this topic, herein, we report the successful synthesis of six new PEPPSI-type Pd(II)–NHC complexes (**3a–3e**) with the general formula [PdX2(NHC)(pyridine)], (X = Br; NHC = 1, 3-disubstituted 3,5-dimethylbenzimidazole-2-ylidene). In the present study, we focused our attention on their applications in catalytic processes, paying special attention to the catalytic activity of all these newly synthesized Pd(II)–NHC complexes in direct C5 arylation reactions of a variety of five-membered heteroarenes such as 2-acetylfuran, 2-acetylthiophene, and furaldehyde with several aryl bromides in the presence of 1 mol% catalyst loading.

Experimental

All manipulations were performed in Schlenk-type flasks under an argon atmosphere. The melting point measurements were determined in open capillary tubes with an Electrothermal-9200 melting points apparatus. IR spectra were recorded on a Gladi ATR unit (attenuated total reflection) in the range of 450–4000 cm^{-1} with a PerkinElmer Spectrum 100 Fourier-transform infrared spectrometer. Routine ^1H NMR and ^{13}C NMR spectra were recorded with a Bruker Ascend™ 400 Avance III HD NMR spectrometer with sample solutions prepared in $CDCl_3$. Chemical shifts (d) are reported in parts per million (ppm) relative to tetramethylsilane (TMS) as an internal standard. Coupling constants (*J* values) are given in hertz (Hz). NMR multiplicities are abbreviated as follows: s = singlet, d = doublet, t = triplet, hept = heptet, dd = doublet of doublets, m = multiplet. ^1H NMR spectra are referenced to residual protiated solvents (d = 7.28 ppm for $CDCl_3$) and ^{13}C NMR chemical shifts are reported relative to deuterated solvents (d = 77.16 ppm for $CDCl_3$). The catalytic solutions were analyzed with a Shimadzu GC 2025 equipped with a GC-FID sensor and RX-5 ms column of 30 m length, 0.25 mm diameter and 0.25 mm film thickness. All measurements were performed at room temperature for freshly prepared solutions.

General procedure for the preparation of benzimidazolium salts (2a–e)

A mixture of 1-benzhydryl-5,6-dimethyl-benzimidazole (1 mmol) and an equivalent amount of alkyl halide derivative (1 mmol)

was prepared in degassed dimethylformamide. The reaction mixture was heated and stirred at 80 1C for 48 h under argon. The obtained mixture was cooled at room temperature. After completion of the reaction, 45 mL of ether was added, and stirred for 1 h, and then the product filtered and washed with diethyl ether to remove the impurities, and the product was left to precipitate with high purity. Subsequently, the crude products were recrystallized in dichloromethane and dried under vacuum to provide pure products for experimental analysis. All the benzimidazolium salts (**2a–e**) were isolated as air- and moisture-stable white solids in high yields. The ^{1}H NMR, ^{13}C NMR, and FT-IR spectra of all the benzimidazolium salts were published in our previous study.[34]

General procedure for the preparation of the PEPPSI-type Pd(II)–NHC complexes (3a–e)

The palladium(II)–NHC PEPPSI-type complexes were synthesized *via* the interaction of benzimidazolium salts with $PdCl_2$ (1 mmol) and pyridine in the presence of potassium carbonate K_2CO_3 (5 mmol). After the addition of KBr (10 mmol), the solution was stirred and heated for 48 h at 80 1C. The reactions were carried out in acetonitrile (15 mL) under a nitrogen atmosphere. The solvent was removed under vacuum to afford the product and eliminate pyridine, and then the mixture was washed with hexane three times. The black solid formed was dissolved in DCM (CH_2Cl_2) and purified by flash column chromatography on silica gel, eluting with DCM until the product was completely recovered. DCM was removed under reduced pressure and the pure complex was obtained as a yellow powder solid. Further, the crude product was recrystallized from dichloromethane: hexane (1 : 6) to get pure complexes for analysis and catalysis. The palladium complexes were highly moisture- and air-stable both in solution and solid-state against air, light and moisture.

Dibromo[1-benzhydryl-5,6-dimethyl-3-(4-methylbenzyl)benzimedazole-2-ylidene]pyridine palladium(II), 3a. Yield 71%; 150 mg; m.p: 292–293 1C; yellow-solid(crystal); FT-IR ν(CN) = 1400 cm^{-1}. ^{1}H-NMR (400 MHz, $CDCl_3$, TMS, 25 1C): d(ppm) = 8.98 (d, J = 5.0 Hz, 2H, $NC_5\underline{H}_5$); 8.58 (s, 1H, N-$C_6\underline{H}_2(CH_3)_2$-N); 7.72 (t, J = 7.6 Hz, 1H, $C_5\underline{H}_5$); 7.51 (d, J = 8.1 Hz, 2H, N-$C_6\underline{H}_4(CH_3)$-N); 7.48 (d, J = 8.6 Hz, 4H, C$\underline{H}$-Ar); 7.32–7.27 (m, 6H, C$\underline{H}$-Ar); 7.18 (d, J = 8.1 Hz, 2H, N-$C_6\underline{H}_4(CH_3)$-N); 6.82 (s, 1H, N-$C_6\underline{H}_2(CH_3)_2$-N); 6.45 (s, 1H, Ph-C$\underline{H}$-Ph); 6.14 (s, 2H, NC$\underline{H}_2$-$C_6H_4(CH_3)$); 2.34 (s, 3H, C$\underline{H}_3$); 2.14 (s, 3H, C$\underline{H}_3$); 2.02 (s, 3H, C$\underline{H}_3$). ^{13}C-NMR (400 MHz, $CDCl_3$, TMS, 25 1C): d(ppm) = 20.13 ($\underline{C}H_3$, C_5); 20.25 ($\underline{C}H_3$, C_7); 21.22 ($\underline{C}H_3$, C_{15}); 53.42 (N-$\underline{C}H_2$, C_{10}); 67.97 (Ph-$\underline{C}$H-Ph, C_{18}); 111.75 ($\underline{C}$H, C_8); 113.73 ($\underline{C}$H, C_3); 124.46 ($\underline{C}$H, $N\underline{H}_5H_5$,$C_{32,34}$); 127.94 (2$\underline{C}$H, $C_{22,28}$); 128.01 (2$\underline{C}$H, $C_{13,16}$); 128.44 (4$\underline{C}$H, $C_{20,24,26,30}$); 129.18 (4$\underline{C}$H, $C_{21,23,27,29}$); 129.47 (2$\underline{C}$H, $C_{12,17}$); 131.84 (C_{11}); 131.97 (C_9); 132.05 (C_2); 133.15 (C_6); 133.57 (C_4); 137.68 ($\underline{C}$H, $N\underline{H}_5H_5$, C_{33}); 137.74 ($C_{19,25}$); 137.78 (C_{14}); 152.65 ($N\underline{C}_5H_5$, $C_{31,35}$); 163.38 (Pd-*C*carb, C_1). Elemental analysis calcd (%) for $C_{35}H_{33}Br_2N_3Pd$ (M.w. = 761.90 g mol^{-1}): C 55.18, H 4.37, N 5.52; found (%): C 54.98, H 4.43, N 5.37.

Dibromo[1-benzhydryl-5,6-dimethyl-3-(2,3,5,6-tetramethylbenzyl)-benzimedazole-2-ylidene]pyridine palladium(II), 3b. Yield 85%; 215 mg; m.p: 244–245 1C; yellow-solid(crystal); FT-IR ν(CN) = 1400 cm^{-1}. ^{1}H-NMR (400 MHz, $CDCl_3$, TMS, 25 1C): d(ppm) = 8.91 (d, J = 5.0 Hz, 2H, $NC_5\underline{H}_5$); 8.60 (s, 1H, N-$C_6\underline{H}_2(CH_3)_2$-N); 7.70 (t, J = 7.6 Hz, 1H, $NC_5\underline{H}_5$); 7.46 (d, J = 6.7 Hz, 4H, CH-Ar); 7.35 (m, 6H, CH-Ar); 7.29 (t, J = 7.6 Hz, 2H, $NC_5\underline{H}_5$); 7.10 (s, 1H, N-$C_6\underline{H}_2(CH_3)_2$-N); 6.46 (s, 1H, Ph-C$\underline{H}$-Ph); 6.17 (s, 2H, NC$\underline{H}_2$-$C_6H_1(CH_3)_4$); 6.13 (s, 1H, $C_6\underline{H}_1(CH_3)_4$); 2.29 (s, 6H, C$\underline{H}_3$); 2.28 (s, 6H, C$\underline{H}_3$); 2.01 (s, 3H, C$\underline{H}_3$); 2.00 (s, 3H, C$\underline{H}_3$). ^{13}C-NMR (400 MHz, $CDCl_3$, TMS, 25 1C): d(ppm) = 16.82 (2$\underline{C}H_3$, $C_{13,20}$); 20.13 ($\underline{C}H_3$, C_5); 20.28 ($\underline{C}H_3$, C_7); 20.60 (2$\underline{C}H_3$, $C_{15,18}$); 51.19 (N-$\underline{C}H_2$, C_{10}); 68,05 (Ph-$\underline{C}$H-Ph, C_{21}); 111.74 ($\underline{C}$H, C_8); 113.50 ($\underline{C}$H, C_3); 124.21 ($\underline{C}$H, $N\underline{C}_5H_5$, $C_{35,37}$); 127.91 (2$\underline{C}$H, $C_{25,31}$); 128.40 (4$\underline{C}$H, $C_{23,27,29,33}$); 129.15 (4$\underline{C}$H, $C_{24,26,30,32}$); 130.84 (C_{11}); 131.26 (C_9); 131.50 (C_2); 132.35 (C_6); 132.88 (C_4); 134.23 ($C_{12,19}$); 135.18($C_{14,17}$); 137.69 ($\underline{C}$H, $N\underline{C}_5H_5$,C_{36}); 137.85 (C$\underline{H}$, $C_{22,28}$); 152.56 ($N\underline{C}_5H_5$, $C_{34,38}$); 163.18 (Pd-*C*carb, C_1). Elemental analysis calcd (%) for $C_{38}H_{39}Br_2N3Pd$ (M.w. = 803.98 g mol^{-1}): C 56.77, H 4.89, N 4.54; found (%): C 56.85, H 4.58, N 4.90.

Dibromo[1-benzhydryl-5,6-dimethyl-3-(2,4,6-trimethylbenzyl)benzimedazole-2-ylidene]pyridine palladium(II), 3c. Yield 81%; 130 mg; m.p: 153–154 1C; yellow-solid(crystal); FT-IR ν(CN) = 1400 cm^{-1}. ^{1}H-NMR (400 MHz, $CDCl_3$, TMS, 25 1C): d(ppm) = 8.96 (d, J = 5.2 Hz, 2H, $NC_5\underline{H}_5$); 8.60 (s, 1H, N-$C_6\underline{H}_2(CH_3)_2$-N); 7.72 (t, J = 7.7 Hz, 1H, $NC_5\underline{H}_5$); 7.46 (d, J = 6.6 Hz, 4H, C$\underline{H}$-Ar); 7.36 (m, 6H, C$\underline{H}$-Ar); 7.30 (t, J = 7.6 Hz, 2H, $NC_5\underline{H}_5$); 6.95 (s, 2H, $C_6\underline{H}_2(CH_3)_3$); 6.46 (s, 1H, Ph-C$\underline{H}$-Ph); 6.14 (s, 2H, NC$\underline{H}_2$-$C_6H_2(CH_3)_3$); 6.13 (s, 1H, N-$C_6\underline{H}_2(CH_3)_2$-N); 2.38 (s, 6H, C$\underline{H}_3$); 2.35 (s, 3H, C$\underline{H}_3$); 2.00 (s, 3H, C$\underline{H}_3$); 1.99 (s, 3H, C$\underline{H}_3$). ^{13}C-NMR (400 MHz, $CDCl_3$, TMS, 25 1C): d(ppm) = 20.13 (2C, $\underline{C}H_3$); 20.27 ($\underline{C}H_3$, C_5); 20.28 ($\underline{C}H_3$, C_7); 21.16 (2$\underline{C}H_3$, $C_{13,19}$); 22.66 ($\underline{C}H_3$, C_{16}); 50.79 (N-$\underline{C}H_2$, C_{10}); 68,00 (Ph-$\underline{C}$H-Ph, C_{20}); 111.68 ($\underline{C}$H, C_8); 113.53 ($\underline{C}$H, C_3); 124.44 ($\underline{C}$H, $N\underline{C}_5H_5$, $C_{34,36}$); 127.91(C_{11}); 127.94 (2$\underline{C}$H, $C_{24,30}$); 128.40 (4$\underline{C}$H, $C_{22,26,28,32}$); 129.13 (4$\underline{C}$H, $C_{23,25,29,31}$); 129.45 (2$\underline{C}$H, $C_{14,17}$); 131.36 (C_9); 131.60 (C_2); 132.95 (C_4); 134.05 (C_6); 137.74 ($\underline{C}$H, $N\underline{C}_5H_5$,C_{35}); 137.82 ($C_{21,27}$); 138.48(C_{15}); 138.92($C_{12,18}$); 152.61 ($N\underline{C}_5H_5$, $C_{33,37}$); 163.18 (Pd-*C*carb, C_1). Elemental analysis calcd (%) for $C_{37}H_{37}Br_2N_3Pd$ (M.w. = 789.95 g mol^{-1}): C 55.26, H 4.72, N 5.32; found (%): C 55.56, H 4.67, N 5.15.

Dibromo[1-benzhydryl-5,6-dimethyl-3-(3,4,5-trimethoxybenzyl)-benzimedazol-2-ylidene]pyridine palladium(II), 3d. Yield 69%; 220 mg; m.p: 264–265 1C; yellow-solid(crystal); FT-IR ν(CN) = 1404 cm^{-1}. ^{1}H-NMR (400 MHz, $CDCl_3$, TMS, 25 1C): d(ppm) = 8.99 (d, J = 5.2 Hz, 2H, $NC_5\underline{H}_5$); 8.58 (s, 1H, N-$C_6\underline{H}_2(CH_3)_2$-N); 7.72 (t, J = 7.6 Hz, 1H, $NC_5\underline{H}_5$); 7.47 (d, J = 5.3 Hz, 4H, C$\underline{H}$-Ar); 7.35–7.37 (m, 6H, C$\underline{H}$-Ar); 7.30 (t, J = 7.6 Hz, 2H, $NC_5\underline{H}_5$); 6.90 (s, 2H, $C_6\underline{H}_2$-$(OCH_3)_3$); 6.88 (s, 1H, s, 1H, N-$C_6\underline{H}_2(CH_3)_2$-N); 6.46 (s, 1H, Ph-C$\underline{H}$-Ph); 6.09 (s, 2H, NC$\underline{H}_2$-$C_6H_2(OCH_3)_3$); 3.87 (s, 6H, OC$\underline{H}_3$); 3.84 (s, 3H, OC$\underline{H}_3$); 2.17 (s, 3H, C$\underline{H}_3$); 2.04 (s, 3H, C$\underline{H}_3$). ^{13}C-NMR (400 MHz, $CDCl_3$, TMS, 25 1C): d(ppm) = 20.20 ($\underline{C}H_3$,C_5); 20.27 ($\underline{C}H_3$,C_7); 53.79 (N-$\underline{C}H_2$,C_{10}); 56.69 (2O$\underline{C}H_3$,$C_{14,18}$); 60.85 (O$\underline{C}H_3$, C_{16}); 67,94 (Ph-$\underline{C}$H-Ph, C_{20}); 111.70 ($\underline{C}$H, C_8); 113.78 ($\underline{C}$H, C_3); 124.58 ($\underline{C}$H, $N\underline{C}_5H_5$,$C_{34,36}$); 125.37 (2$\underline{C}$H, $C_{12,19}$); 128.07 (2$\underline{C}$H, $C_{24,30}$); 128.44 (4$\underline{C}$H, $C_{22,26,28,32}$); 129.14 (4$\underline{C}$H, $C_{23,25,29,31}$); 131.83 (C_{11}); 131.94 (C_9); 132.05 (C_2); 133.15 (C_4); 133.58 (C_6); 137.62 (C_{15}); 137.68($C_{21,27}$); 137.85($\underline{C}$H, $N\underline{C}_5H_5$,C_{35}); 150.89 ($C_{13,17}$); 152.65

(NC$_5$H$_5$,C$_{33,37}$); 163.29 (Pd-*C*carb, C$_1$). Elemental analysis calcd (%) for $C_{37}H_{37}Br_2N_3O_3Pd$ (M.w. = 837.95 g mol^{-1}): C 53.04, H 4.45, N 5.01; found (%): C 52.81, H 4.27, N 5.04.

Dibromo[1-benzhydryl-5,6-dimethyl-3-(4-*tert-butylbenzyl*)-benzimedazole-2-ylidene]pyridine palladium(II), 3e. Yield 98%; 100 mg; m.p: 276–277 1C; yellow-solid(crystal); FT-IR ν(CN) = 1399 cm^{-1}. ^{1}H-NMR (400 MHz, CDCl$_3$, TMS, 25 1C): d(ppm) = 8.98 (d, J = 5.1 Hz, 2H, NC$_5$H$_5$); 8.59 (s, 1H, N-C$_6$H$_2$(CH$_3$)$_2$-N); 7.71 (t, J = 7.7 Hz, 1H, NC$_5$H$_5$); 7.57 (d, J = 8.2 Hz, 2H, C$_6$H$_4$-(*t*Bu)); 7.49 (d, J = 6.7 Hz, 4H, CH-Ar); 7.40 (d, J = 8.2 Hz, 2H, C$_6$H$_4$-(*t*Bu)); 7.35 (m, 6H, CH-Ar); 7.29 (t, J = 7.6 Hz, 2H, NC$_5$H$_5$)6.82 (s, 2H, N-C$_6$H$_2$(CH$_3$)$_2$-N); 6.45 (s, 1H, Ph-CH-Ph); 6.15 (s, 2H, NCH$_2$-C$_6$H$_4$(*t*Bu)); 2.14 (s, 3H, CH$_3$); 2.03 (s, 3H, CH$_3$); 1.31 (s, 9H, CH$_3$/(*t*Bu)). ^{13}C-NMR (400 MHz, CDCl$_3$, TMS, 25 1C): d(ppm) = 20.08 (CH$_3$,C$_5$); 20.25 (CH$_3$,C$_7$); 31.33 (3CH$_3$,C$_{16,17,18}$); 34.58 (C-(CH$_3$)$_3$, C$_{15}$); 53.37 (N-CH$_2$,C$_{10}$); 67,95 (Ph-CH-Ph, C$_{21}$); 111.83 (CH, C$_8$); 113.72 (CH, C$_3$); 124.45 (CH, NC$_5$H$_5$,C$_{35,37}$); 125.73 (2CH, C$_{23,19}$); 125.72 (2CH, C$_{24,30}$); 128.01 (2CH, C$_{12,20}$); 128.44 (4CH, C$_{23,27,29,33}$); 129.17 (4CH, C$_{24,26,30,32}$); 131.83 (C$_{11}$); 131.94 (C$_9$); 132.05 (C$_2$); 133.15 (C$_4$); 133.58 (C$_6$); 137.75 (C$_{22,28}$); 137.77 (CH, NC$_5$H$_5$,C$_{36}$); 150.89(C$_{14}$); 152.65 (NC$_5$H$_5$,C$_{34,38}$); 163.39 (Pd-*C*carb, C$_1$). Elemental analysis calcd (%) for $C_{38}H_{39}Br_2N_3Pd$ (M.w. = 803.98 g mol^{-1}): C 56.77, H 4.89, N 5.23; found (%): C 56.43, H 4.71, N 5.16.

X-Ray crystallographic analysis study

The structure of the Pd(II)–NHC complexes **3a**, **3b** and **3d** was determined *via* the X-ray diffraction technique, and the obtained results confirmed all the spectroscopic data. A single suitable crystal of complex **3a**, **3b** and **4d** for X-ray diffraction analysis was grown *via* the slow diffusion of diethyl ether in a saturated chloroform solution at room temperature. Crystallographic data of **3a**, **3b** and **3d** was collected with an STOE IPDS II diffractometer at room temperature using graphite-monochromated Mo Ka radiation by applying the o-scan method. Data collection and cell refinement were carried out using X-AREA while data reduction was applied using X-RED32.[35] The structures were solved by direct methods with SIR2019[36] and refined through full-matrix least-squares calculations on F^2 using SHELXL-2018[37] inserted in idealized positions and treated using a riding model, fixing the bond lengths at 0.93, 0.98, 0.97, and 0.96 Å for the aromatic CH, methine CH, CH$_2$, and CH$_3$ atoms, respectively. The displacement parameters of the H atoms were fixed at U_{iso}(H) = 1.2U_{eq} (1.5U_{eq} for CH$_3$) of their parent atoms. The crystallographic data and

Table 1 Crystal data and structure refinement parameters for **3a**, **3b**, and **3d**

	Pd(II)–NHC PEPPSI-type complexes		
Parameter	**3a**	**3b**	**3d**
CCDC depository	2073777	2073779	2073780
Color/shape	Yellow/prism	Yellow/prism	Yellow/prism
Chemical formula	[PdBr$_2$(C$_{30}$H$_{28}$N$_2$)(C$_5$H$_5$N)]	[PdBr$_2$(C$_{33}$H$_{34}$N$_2$)(C$_5$H$_5$N)]	[PdBr$_2$(C$_{32}$H$_{32}$N$_2$O$_3$)(C$_5$H$_5$N)]
Formula weight	761.86	803.94	837.91
Temperature (K)	296(2)	296(2)	296(2)
Wavelength (Å)	0.71073 Mo Ka	0.71073 Mo Ka	0.71073 Mo Ka
Crystal system	Monoclinic	Triclinic	Monoclinic
Space group	$P2_1/n$ (No. 14)	$P\bar{1}$ (No. 2)	$P\bar{2}_1/n$ (No. 14)
Unit cell parameters			
a, b, c (Å)	14.9802(13), 11.0510(7), 20.2398(15)	9.3043(7), 11.1447(9), 17.5332(14)	11.9557(9), 16.6440(8), 18.4136(13)
a, b, g (1)	90, 106.685(6), 90	91.190(6), 104.973(6), 103.026(6)	90, 106.908(6), 90
Volume (Å^3)	3209.6(4)	1705.1(2)	3505.7(4)
Z	4	2	4
$D_{calc.}$ (g cm^{-3})	1.577	1.566	1.588
m (mm^{-1})	3.096	2.918	2.848
Absorption correction	Integration	Integration	Integration
$T_{min.}$, $T_{max.}$	0.5504, 0.8967	0.1567, 0.3154	0.2890, 0.7055
F_{000}	1520	808	1680
Crystal size (mm^3)	0.35 × 0.08 × 0.04	0.73 × 0.55 × 0.53	0.48 × 0.45 × 0.11
Diffractometer/measurement method	STOE IPDS II/o scan	STOE IPDS II/o scan	STOE IPDS II/o scan
Index ranges	$-19 \le h \le 19$, $-14 \le k \le 14$, $-26 \le l \le 26$	$-12 \le h \le 12$, $-14 \le k \le 14$, $-22 \le l \le 22$	$-15 \le h \le 15$, $-21 \le k \le 19$, $-24 \le l \le 24$
y range for data collection (1)	1.993 ≤ y ≤ 27.956	1.882 ≤ y ≤ 27.802	1.683 ≤ y ≤ 27.737
Reflections collected	36 397	21 039	54 952
Independent/observed reflections	7650/3046	7945/4779	8206/6602
$R_{int.}$	0.2489	0.1482	0.0762
Refinement method	Full-matrix least-squares on F^2	Full-matrix least-squares on F^2	Full-matrix least-squares on F^2
Data/restraints/parameters	7650/0/373	7945/0/403	8206/0/420
Goodness-of-fit on F^2	0.972	1.036	1.165
Final R indices [I 4 2s(I)]	R_1 = 0.0927, wR_2 = 0.1253	R_1 = 0.0771, wR_2 = 0.1750	R_1 = 0.0534, wR_2 = 0.0962
R indices (all data)	R_1 = 0.2310, wR_2 = 0.1641	R_1 = 0.1301, wR_2 = 0.2089	R_1 = 0.0727, wR_2 = 0.1022
Dr$_{max.}$, Dr$_{min.}$ (e Å^{-3})	1.06, −0.69	1.17, −1.56	0.70, −0.56

refinement parameters are summarized in Table 1. Molecular graphics were generated using OLEX2.[38]

Density functional theory (DFT) calculations

Computational details

All DFT (density functional theory) calculations in this work were performed using the Gaussian09 software.[39] The B3LYP (Becke-Lee-Parr hybrid exchange–correlation three-parameter functional) functional[40,41] in conjunction with the LANL2DZ[42] basis set for the palladium atom and 6-311G(d,p)[43] basis set for hydrogen, carbon, nitrogen, and bromine atoms were used for all calculations. The B3LYP method is efficient for the prediction of molecular geometry and electronic properties and also offers a nice balance between cost and precision.[44–46] The ground state was validated by the absence of imaginary frequencies (no imaginary frequency).

Catalytic study of Pd(II)–NHC PEPPSI-type complexes

General procedure for the direct arylation reaction. In 1990, the first examples of the Pd-catalyzed direct arylation of furans and thiophenes were reported by Ohta.[10] In this pioneering work, the direct C(5)-arylation of furan, thiophene, and furaldehyde was carried out with electron-rich or electron-poor aryl bromides using [Pd(II)Br_2(*N*HC)(pyridine)] as the catalyst. In the last two decades, Pd-catalyzed direct arylation has been successfully performed.[47,48] Therefore, in this catalysis study, we selected DMA as the solvent and KOAc as the base according to the methods described in the literature.[49] In a typical experiment, an oven-dried 10 mL Schlenk tube was charged with 1 mol% of Pd(II)–NHC complex (0.01 mmol) as the catalyst, a five-membered heteroaromatic compound derivative (2.0 mmol), (hetero)aryl halide (1.0 mmol), KOAc (2.0 mmol) as the base, and DMAc (dimethylacetamide, 2 mL) as the solvent under an argon atmosphere. The Schlenk tube was placed in a preheated oil bath at 120 1C and the reaction mixture was stirred for 1 h. After completion of the reaction, the solvent was removed under vacuum and the residue was dissolved in CH_2Cl_2 (2 mL) and charged directly onto a micro-silica gel chromatography column. The products were eluted using an *n*-hexane/diethyl ether mixture (5 : 1, v/v) as the eluent to afford the pure product. The chemical characterization of the products was performed *via* gas chromatography-GC spectrometry. The GC yields and conversions were calculated by considering the conversion of aryl bromides to the products from the results of GC spectrometry with dodecane as an internal standard.

Results and discussion

Preparation of PEPPSI-type palladium–NHC complexes 3a–e

The PEPPSI-themed Pd(II)–NHC complexes (**3a–e**) were synthesized according to procedures reported by Organ for other Pd–NHC–PEPPSI complexes.[21] All reactions for the preparation of the palladium complexes were carried out under argon using standard Schlenk techniques. A solution of benzimidazolium salt (1 eq.), $PdCl_2$ (1.5 eq.) in pyridine (2 eq.), K_2CO_3 (5 eq.) and a large excess of KBr (10 eq.) were dissolved in 15 mL of acetonitrile (15 mL) under a nitrogen atmosphere. The reaction was stirred and heated for 2 days at 80 1C until the mixture became black. After the reaction was finished, the solvent was removed under vacuum to afford the product and eliminate pyridine, and then the mixture was washed with hexane three times. After removal of the hexane solvent, the residue was re-dissolved in CH_2Cl_2 and filtered on a pad of silica covered with Celite to remove unreacted $PdCl_2$. The crude product was obtained after evaporating the CH_2Cl_2 solvent. The crude product was recrystallized from dichloromethane : hexane (1 : 4). After chromatography on silica gel, the pure complex was obtained as a yellow Pd(II)–NHC complex (**3a–e**). All the Pd(II)–NHC complexes were prepared in good yields through a simple procedure in three-steps (Scheme 1) from 5, 6-dimethylbenzimidazole and benzhydryl reagents for the preparation of product 1 as the starting material, and then the starting material was reacted with various ligands of chlorobenzyl to obtain 5,6-dimethylbenzimidazoluim salts. These benzimidazolium salts (**2a–e**) were used as a precursor for the synthesis of the Pd(II)–NHC complexes.

All new five Pd(II)–NHC complexes **3a–e** showed good solubility in most organic solvents, such as chloroform, dichloromethane, ethanol, acetonitrile, and dimethylsulfoxide except non-polar ones, as pentane and hexane. They are highly moisture- and air-stable both in solution and in the solid-state against air, light, and moisture, which can be stored at room temperature for months without an obvious decline in catalytic efficiency. The new compounds were successfully characterized *via* spectroscopic techniques such as NMR, FT-IR, and elementary analysis to confirm the formation of the complexes. The physical and some spectroscopic data of the Pd(II)–NHC PEPPSI-type complexes are summarized in Table 2. Firstly, the FT-IR spectroscopy data indicated that the PEPPSI-type Pd(II)–NHC complexes **3a–e** exhibit a characteristic ν(CN) band typically at 1400, 1400, 1400, 1404 and 1399 cm^{-1}, respectively. The formation of carbenes is correlated by the shift in the (CN) vibration. The FT-IR spectra of these five Pd(II)–NHC complexes show similar absorption bands. Due to the flow of electrons from the carbene ligand to the palladium center, the C Q N bond is weakened, and consequently, a decrease in the ν(CN) stretching frequency was observed. Secondly, in the ^{1}H NMR spectra, the characteristic signals of the aromatic hydrogens of the pyridine ring were observed as downfield resonances in the ^{1}H NMR spectra in the range of d = 7.71–8.99 ppm. These signals suggest that the pyridine ring coordinated to the palladium centre to form a PEPPSI-type palladium complex. While in the ^{13}C NMR spectra, the signals of the aromatic carbons of the pyridine ring were detected at d = 152.65, 152.56, 152.61, 152.64, and 152.65 ppm for the first two carbons C̲HNC̲H. The second 2 carbons C̲H–CNC–C̲H were detected at d = 124.46, 124.21, 124.44, 124.58, and 124.45 ppm, and d = 137.68, 137.69, 137.74, 137.85, and 137.77 ppm for the carbon CHC̲HCH. All these data support the formation of the

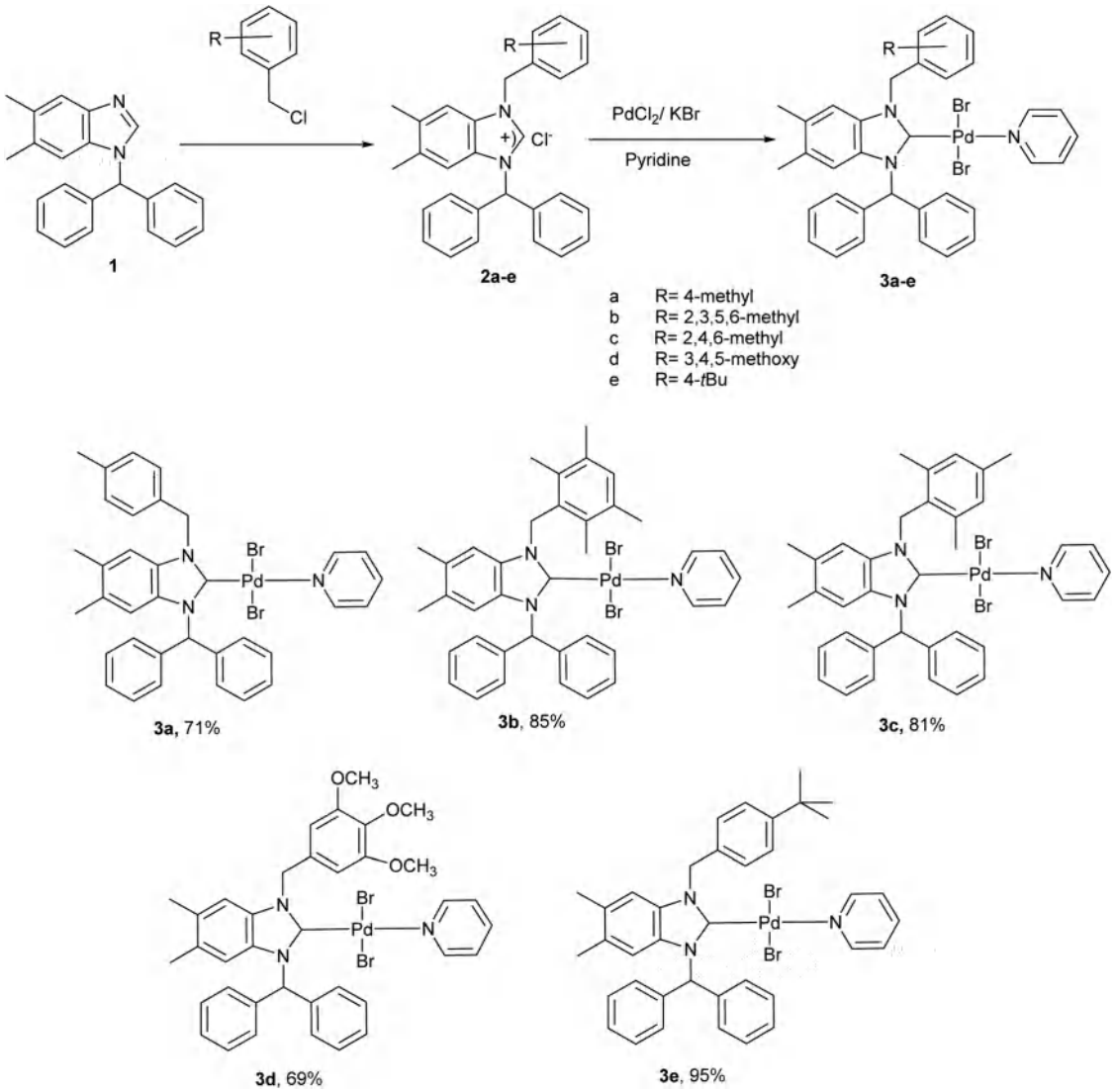

Scheme 1 Synthetic route and structure of Pd(II)–NHC PEPPSI-type complexes (**3a–e**).

Table 2 Physical and some spectroscopic data of the Pd(II)–NHC PEPPSI-type complexes

Code	Chemical formula	Molecular weight (g mol^{-1})	Melting point (1C)	^{13}C NMR (C_2) (ppm)	IR ν(CN)
3a	$C_{35}H_{34}Br_2N_3Pd$	761.90	292–293	163.38	1400
3b	$C_{38}H_{40}Br_2N_3Pd$	803.98	244–245	163.18	1400
3c	$C_{37}H_{38}Br_2N_3Pd$	789.95	153–154	163.18	1400
3d	$C_{37}H_{38}Br_2N_3O_3Pd$	837.95	264–265	163.29	1404
3e	$C_{38}H_{40}Br_2N_3Pd$	803.98	276–277	163.39	1399

PEPPSI-type palladium complex. The PEPPSI Pd–NHC complexes were identified compared to benzimidazolium salts by the characteristic proton peak at the 2-position, which did not appear as a signal of an acidic proton (NCHN) in the ^1H NMR spectra and carbon peak in ^{13}C NMR (NCHN) spectra, where the characteristic signals of the acidic proton and the benzimidazolium salts were not observed, which confirm the formation of a Pd-carbene bond. The characteristic Pd–C_2-carbene signals of the **3a–e** complexes appear as a singlet at d = 163.38, 163.18, 163.18, 163.29 and 163.39 ppm, respectively in their ^{13}C NMR spectra. The elemental analysis results of these complexes are in agreement with the proposed molecular formula. These five new complexes show typical spectroscopic signatures, and their values are in agreement with the reported data for similar PEPPSI type Pd(II)–NHC complexes.[14,49]

X-ray crystal structures

The solid-state structures of **3a**, **3b**, and **3d** with the adopted atom-labeling scheme are shown in Fig. 2, Fig. 3 and 4, respectively, while their important bond distances and angles are listed in Table 3. The palladium complexes are four-coordinated in a square-planar geometry and surrounded by the carbene carbon atom of the NHC ligand, the nitrogen atom of the pyridine ring, and two bromide atoms. The complexes

have a slightly distorted square-planar geometry, in which the anion atoms are *trans* to each other. The *cis* angles vary from 85.32(19) to 93.23(17)1 and the *trans* angles change from 173.05(4) to 179.17(14)1, deviating from their ideal values of 901 and 1801, respectively. For the quantitative evaluation of the extent of distortion around the metal center, the structural indexes t_4[50] and t_4'[51] were employed;

$$t_4 = \frac{360^\circ - (a + b)}{360^\circ - 2y} \quad t_4' = \frac{b - a}{360^\circ - y} + \frac{180^\circ - b}{180^\circ - y}$$

where a and b(b 4 a) are the two greatest valence angles and y is the ideal tetrahedral angle (109.51). The t_4 and t_4' values for the ideal square-planar and tetrahedral coordination spheres are 0 and 1, respectively. The calculated t_4 and t_4' geometry indices are 0.07, 0.06 for **3a**, both 0.04 for **3c**, and 0.03, 0.02 for **3d**, respectively, indicating a slightly distorted square-planar geometry.

The average Pd–C_{NHC} bond distance (1.96 Å) is smaller than the sum of the individual covalent radii of the palladium and carbon atoms (2.12 Å), while the average Pd–$N_{pyridine}$ bond distance (2.10 Å) is equal to the sum of the individual covalent radii of the palladium and nitrogen atoms (2.10 Å).[52] The Pd–Br distances are in the usual range, and the internal N–C–N ring angles at the carbene centers vary from 107.1(7)1 to 108.5(6)1 in the complexes. In summary, these parameters are comparable with that observed for Pd–NHC–pyridine–Br_2 complexes.[53–59] The carbene ring is almost perpendicular to the coordination plane with a dihedral angle of 76.3(3)1 in **3a**, 89.3(2)1 in **3b** and 76.07(11)1 in **3d**, which is typical for NHC complexes to reduce steric congestion. Conversely, the dihedral angle between the pyridine ring and the coordination plane is 68.7(5)1 in **3a**, 40.7(4)1 in **3b**, and 51.8(2)1 in **3d**.

Theoretical investigations

To gain further insights into the molecular structure and electronic properties of the synthesized complexes, DFT calculations at the B3LYP/6-311G(d,p)/LANL2DZ level were performed for complex **3a** as a representative molecule. The obtained molecular geometry by DFT calculations was compared to that from X-ray analysis and the obtained results are shown in Fig. 5. Some selected experimental and theoretical geometric parameters of complex **3a** are also reported in Table 4. As can be seen, the predicted molecular geometry of complex **3a** is strongly in agreement with the experimental results. The calculated Br1–Pb and Br2–Pb bond lengths were found to be 2.441 and 2.434 Å, which are in very good agreement with the experimental values (2.448 and 2.438 Å, respectively). The deviations between the calculated and experimental angles for Br1–Pd–Br2 and Br1–Pd–N9 are only −0.021 and −0.011, respectively. The maximum discrepancies were found for the N8–Pd bond with a deviation of −0.249 Å, and the angles N8–Pd–C1 and Br1–Pd–C1 with deviations of 0.3801 and 0.2591,

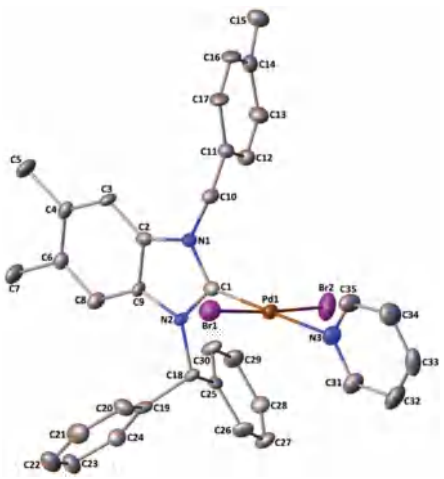

Fig. 2 Molecular structure of **3a** drawn at 20% probability level. H atoms have been omitted for clarity.

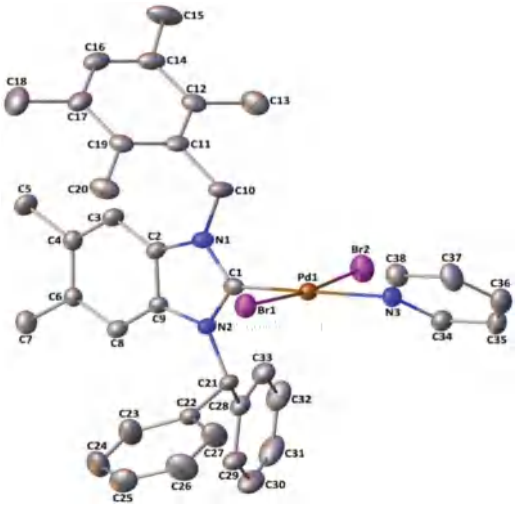

Fig. 3 Molecular structure of 3b drawn at 20% probability level. H atoms have been omitted for clarity.

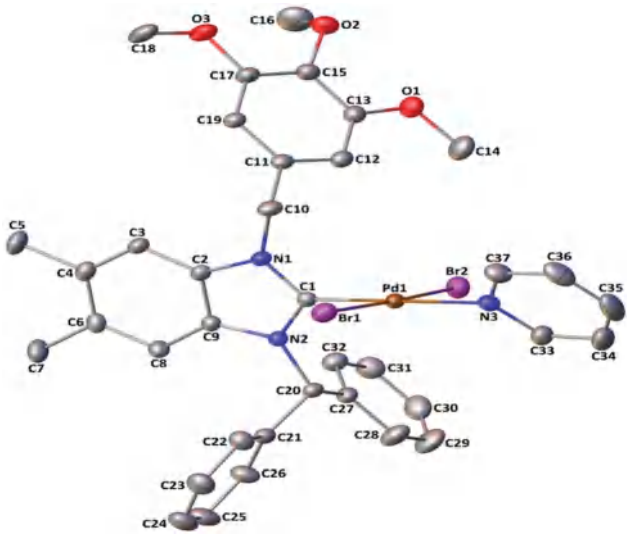

Fig. 4 Molecular structure of 3d drawn at 20% probability level. H atoms have been omitted for clarity.

Table 3 Selected distances (Å) and angles (1) for **3a**, **3c** and **3e**

Parameter		Pd(II)–NHC PEPPSI-type complexes		
		3a	**3c**	**3e**
Bond distances	Pd1–Br1	2.4281(9)	2.4182(16)	2.4339(5)
	Pd1–Br2	2.4102(10)	2.4352(15)	2.4052(5)
	Pd1–N3	2.127(6)	2.078(8)	2.111(3)
	Pd1–C1	1.965(8)	1.949(9)	1.964(3)
	N1–C1	1.353(9)	1.350(11)	1.349(4)
	N2–C1	1.341(9)	1.365(10)	1.346(5)
Bond angles (1)	Br1–Pd1–Br2	173.05(4)	175.95(6)	
	Br1–Pd1–N3	93.23(17)	91.7(2)	176.09(2)
	Br2–Pd1–N3	91.57(17)	91.1(2)	91.91(10)
	Br1–Pd1–C1	89.92(19)	90.1(2)	91.83(9)
	Br2–Pd1–C1	85.32(19)	87.0(2)	87.27(10)
	N3–Pd1–C1	176.8(2)	178.1(4)	88.99(10)
	N1–C1–N2	108.5(6)	107.1(7)	179.17(14)

respectively. These findings indicate that the DFT approach used is sufficiently accurate to predict the molecular geometry of complex **3a**.

The frontier molecular orbitals (FMOs), *i.e.* HOMO (highest occupied molecular orbital) and LUMO (lowest unoccupied molecular orbital), are important parameters that can be used to characterize the stability and chemical reactivity of molecules.[60,61] The energy of the HOMO is related to the electron donation ability, whereas that of the LUMO represents the ability to accept electrons. The shape of FMOs can also give insights into the sites of electrophilic and nucleophilic attack. The energy and distribution of the FMOs, ranging from HOMO−3 to LUMO+3, of complex **3a**, were calculated at the B3LYP/6-311G(d,p)/LANL2DZ level and are reported in Fig. 5 and Table 5, respectively. As illustrated in Table 5, the calculated FMOs energies are in the range of −0.43 to −5.91 eV. The difference between the HOMO and LUMO energy (energy gap) is only 2.26 eV, suggesting the high chemical reactivity of complex **3a**.[62,63] It can also be seen from Fig. 6 that the HOMO and HOMO−1 are mainly distributed on the benzimidazole and the pyridine moieties with very small contributions from the Pd atom. HOMO−2 is located on the benzimidazole, while HOMO−3 is distributed on the benzimidazole, pyridine and Pd

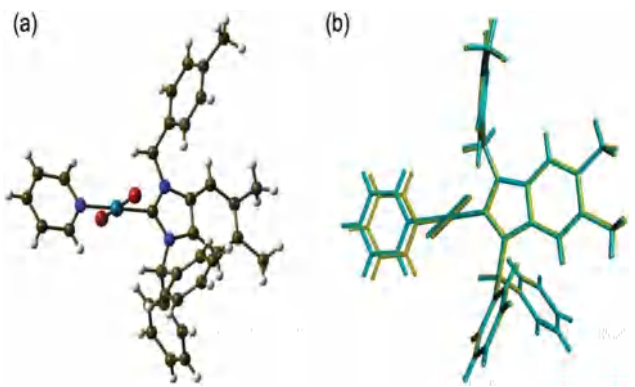

Fig. 5 (a) Optimized molecular structure and (b) atom-by-atom superimposition of the crystal structure (cyan) and optimized molecular structure (yellow) of complex **3a**.

Table 4 Selected experimental and theoretical geometric parameters of complex **3a**

Complex **3a**	Calculated	Experimental	Discrepancy
Bond distance (Å)			
N8–Pd	1.850	2.099	−0.249
Br1–Pb	2.441	2.448	−0.007
Br2–Pb	2.434	2.438	−0.004
C1–Pb	1.838	1.959	−0.121
C1–N1	1.346	1.364	−0.018
C1–N2	1.349	1.368	−0.019
Bond angle (1)			
N8–Pd–C1	178.31	177.93	0.380
Br1–Pd–Br2	175.42	175.44	−0.020
Br1–Pd–C1	87.491	87.231	0.259
Br1–Pd–N9	90.836	90.840	−0.010

atom. These results indicate that the pyridine and the benzimidazole moieties are the most active sites for electron donation. Different from the HOMOs, which have relatively similar distributions, the LUMOs of complex **3a** is different. The LUMO and LUMO+1 are mainly concentrated on the metal center and the benzene ring for LUMO+1. HOMO+2 is located on the pyridine ring, while LUMO+3 is distributed on the benzene rings and slightly on the Pd atom. These distributions of the electron density of the HOMOs and LUMOs clearly show the transfer of the electron density from the benzimidazole and pyridine nucleus to the metal center and other regions of the molecule.

The molecular electrostatic potential (MEP) is another useful tool that can be used to describe the electronic properties and chemical reactivity of molecules.[64,65] MEP represents a 3D view of charge the distributions within a molecule, where color codes ranging from deep red for electron-rich sites to deep blue for electron-deficient sites are used. Fig. 7 shows the MEP of complex **3a** calculated at the B3LYP/6-311G(d,p)/LANL2DZ level in the gas phase. The analysis of the obtained MEP reveals that the most electron-deficient sites of complex **3a** are located on the aromatic rings, in particular on the benzimidazole and pyridine. This suggests that these sites are the most suitable for nucleophilic attacks. Conversely, the positive charges were found distributed on several aromatic hydrogen atoms and the metal center, indicating that these sites are the most electron-deficient and can be considered electrophilic sites.

Catalytic evaluation study

Optimization of the reaction conditions for the direct arylation of heteroaromatics with aryl bromides. The catalytic

Table 5 Energies in eV of the frontier molecular orbitals of complex **3a**

Complex **3a**	Energy in eV
LUMO+3	−0.43
LUMO+2	−0.73
LUMO+1	−0.87
LUMO	−1.22
HOMO	−3.48
HOMO−1	−4.21
HOMO−2	−5.79
HOMO−3	−5.91

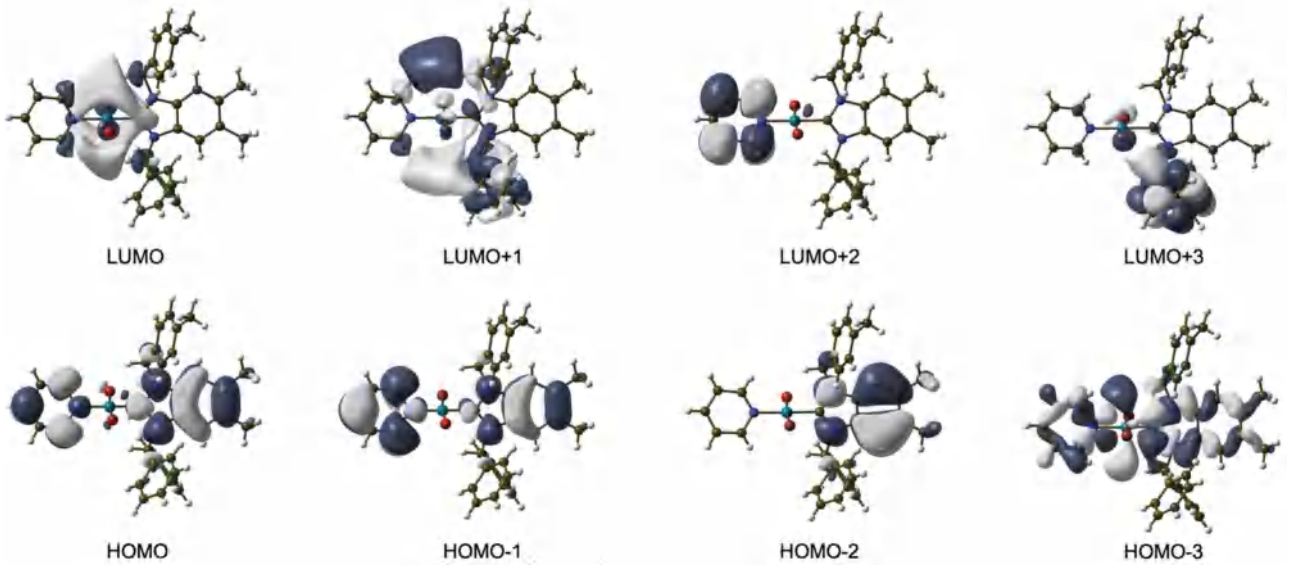

Fig. 6 Frontier molecular orbitals of complex **3a** computed at the B3LYP/6-311G(d,p)/LANL2DZ level of theory.

capacity of the new Pd(II)–NHC complexes **3a–e** in intermolecular direct arylation reactions between aryl bromides and substituted furan and thiophene derivatives were investigated. As an attempt, the first test was carried out at 120 1C for 24 h without Pd-catalyst to examine the effect of the catalyst, and the reaction of 2-acetylfurane with bromobenzene was performed in presence of KOAc as a base and dimethylacetamide (DMAc) as a solvent. This reaction did not work and no desired product was formed. However, under the same conditions in the presence of 1 mol% Pd-catalyst complex, the reaction worked.

To optimize and determine the best reaction conditions for the direct arylation, we studied the reaction by changing the solvent, base, temperature, and time. Complex **3b** was selected as a model test catalyst, 2-acetylfurane as the heteroaromatic substrate, and *p*-bromobenzene as the model coupling partner, which are commonly used for the direct arylation of heteroarene based on previous studies.[66–68] Here, we selected dimethylacetamide DMAc as the solvent and potassium acetate, KOAc, the base. Then we tried changing the time (1 h, 2 h, and 4 h) and temperature (80 1C, 100 1C, 120 1C, 150 1C) of the reaction. However, several attempts were made with many other solvents and bases for this study. The reactions were performed under argon. The results are summarized in Table 6 (Scheme 2).

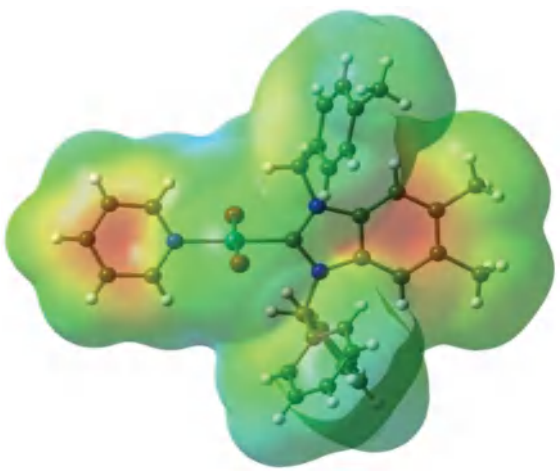

Fig. 7 Molecular electrostatic potential (MEP) of complex 3a computed at the B3LYP/6-311G(d,p)/LANL2DZ level of theory.

As shown in Table 6, the preliminary data demonstrated that the reaction displayed the best performance at the temperature of 120 1C and in a short time (1 h) in the presence of KOAc. When the reaction time was increased to 2 or 4 h, we observed full conversion, but no significant difference in yield (Table 6, entries 7 and 10). When the temperature was increased from 120 1C, no noticeable effect on the yield was observed (Table 6, entry 4). When the temperature was reduced from 120 1C, low yields were observed (Table 6, entries 1 and 2). It was found also that DMAc was the best solvent among the solvents under the conditions tested. The evaluation of the effect of reaction temperature on yield at 150 1C, 120 1C, 100 1C and 80 1C gave the best yield at 120 1C. After fixing the initial conditions of the reaction (time and temperature) with the successful results achieved in the optimization step, the evaluation of the reaction using various solvents and bases was carried out to confirm our coupling solvent/base choice. The test with different solvents such as H_2O, EtOH, THF, toluene, DMF, DMSO and dioxane was performed firstly in the presence of only 1 mol% **3b** catalyst, but the reaction conversion was low with all the solvents used, and the yield dropped to less than 10% (Table 6, entries 12–18). When the test was done with various bases such as K_2CO_3, KOH, TEA, and *t*-BuOK in the presence of only 1 mol% **3b** catalyst, The reaction worked, but with low conversion and the final product was formed at the lowest yields of 5%, 7%, 6%, and 9% (Table 6, entries 19–22), respectively. Therefore, DMAc and KOAc proved to be the best solvent/base pair in this reaction.

Table 6 Optimization of the best conditions for the direct arylation reaction

Entry	Solvent	Time (h)	Base	Temperature (1C)	Conversion (%)	Yield (%)
01				80	04	04
02		1	KOAc	100	63	23
03				120	95	86
04				150	95	75
05				80	04	04
06		2	KOAc	100	70	45
07				120	94	80
08	DMAc			150	96	81
16				80	95	82
09		4	KOAc	100	80	65
10				120	99	70
11				150	97	82
12	H_2O				06	05
13	EtOH				08	05
14	THF				02	01
15	Toluene	1	KOAc	120	10	09
16	DMF				09	06
17	DMSO				03	02
18	Dioxane				04	03
19			K_2CO_3		10	05
20			KOH		14	09
21	DMAc	1	TEA	120	13	07
22			*t*-BuOK		11	06

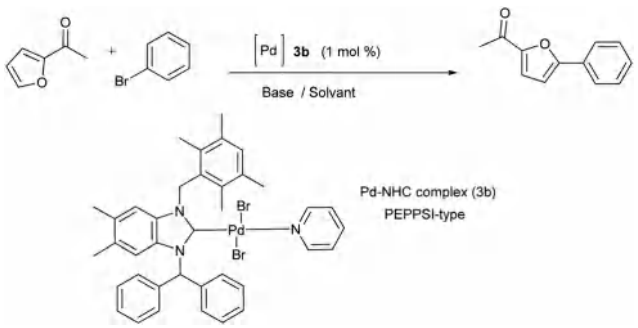

Scheme 2 Influence of the reaction conditions on the Pd-catalyzed direct arylation of five-membered heteroaromatics with *p*-bromobenzene.

As the conclusion of these preliminary studies, it was observed that the best condition for the direct arylation reaction using our Pd-catalyst complexes is 1 h reaction time, 120 1C temperature, and the DMAc/KOAc solvent/base pair.

The direct arylation of 2-acetylfuran, 2-acetylthiophene and furaldehyde with aryl bromides. Firstly, under the optimal conditions, an investigation of the reactivity of 2-acetylfuran in the Pd-catalyzed direct arylation with various (hetero)aryl bromides was carried out, where C(5)-arylated furane derivatives were obtained easily. The substate was coupled with eight *p*-substituted aryl bromides (bromobenzene, *p*-bromotoluene, *p*-bromobenzaldehyde, *p*-bromoacetophenone, *p*-bromoanisole, 1-bromo-4-fluorobenzene, 1-bromo-4-(trifluoromethyl)benzene, and 3-bromoquinoline). Due to the Pd-catalyst, the reaction worked perfectly and the desired products were obtained with moderate to high yield using only 1 mol% Pd-complex (**3a–e**) as the catalyst. The best yield was detected for the arylation with (hetero)aryl bromides, which are electron poor, such as bromobenzene and *p*-bromotoluene. The lowest yield was observed for electron-rich (hetero)aryl bromides such as *p*-bromoacetophenone and *p*-bromoanisole. The preliminary studies showed that all the Pd(II)–NHC complexes were active. The results of our experiments are summarized in Table 7. As shown in Table 7, excellent conversion was observed with all the Pd-catalysts, and depending on the Pd(II) catalyst and the aryl bromide, high-yield C(5)-arylated products were obtained for almost all the reactions. When 2-acetylfurane was arylated with bromobenzene, the product 5-phenyl-2-acetylfurane was obtained in 44–78% yield using Pd-complexes (**3a–e**) as the catalyst (Table 7, entries 1–5, respectively), the lowest yield was observed with Pd catalyst **3c**, where the reaction gave 95–99% conversion. The same reaction of 2-acetylfurane with *p*-bromotoluene gave the desired product in 67–85% yield (Table 7, entries 6–10), and the conversion of the reaction was 89–99%. The reaction of 2-acetylfurane with *p*-bromobenzaldehyde gave the expected product in 64–91 yield (Table 7, entries 11–15), and with 99% conversion with all the Pd-catalysts. The coupling with the electron-poor *p*-bromoacetophenone also gave the expected product with a high yield of 71–82% and 99% conversion (Table 7, entries 16–20).

The reaction of 2-acetylfurane with 1-bromo-4-(trifluoromethyl)benzene generated the 5-(4-trifluoromethyl)-2-acetylfurane in 70–86% yield and 99% conversion (Table 7, entries 21–25). The coupling with 1-bromo-4-fluorobenzene also gave a high yield of 74–85% (Table 7, entries 26–30) with 99% conversion. When the reaction was performed with the *p*-bromoanisole, the obtained product was formed with a moderate yield of 39–77% and conversion between 57–99% (Table 7, entries 31–35). When the coupling was done with 3-bromoquinoline, the reaction gave a lower C5-arylated product with the lowest yield among the reactions, which was between 8% and 42% (Table 7, entries 36–40).

Using the same reaction conditions, the second test was performed for the direct arylation of 2-acetylthiofene with the (hetero)aryl bromides used in the first test, and C(5)-arylated thiophene derivatives were obtained. The arylation of 2-acetylthiophene was tested with a range of para-substituted aryl bromides, which were used in the first test, under the optimized conditions using all the Pd-catalysts. Due to these Pd-catalysts (**3a–e**), the reaction worked perfectly with 98–99% conversion for almost all the reactions tested, and the desired product was obtained at high yield with the average of 80%. The best yield was detected for the arylation with (hetero)aryl bromides, which are electron poor, such as bromobenzene and *p*-bromotoluene. The results of this evaluation showed that the all Pd(II)–NHC PEPPSI-type complexes were active catalysts. The results of these experiments are summarized in Table 8. As presented in Table 8, the direct C5 arylation reactions resulted in moderate to high yields of the desired coupling products. Excellent conversion was observed with all the Pd-catalysts. When 2-acetylthiophene was arylated with bromobenzene, the desired products were obtained in 78–93% yield using the Pd-complexes (**3a–e**) as the catalyst (Table 8, entries 1–5, respectively), with 98% conversion. The same reaction of

Table 7 Direct C5-arylation of 2-acetylfuran with aryl bromides using the new Pd-catalyst

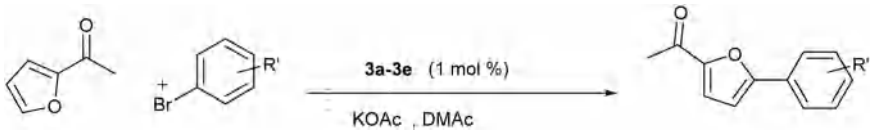

Entry	Aryl bromide	[Pd]	Product	Conversion (%)	Yield (%)
1		**3a**		98	78
2		**3b**		95	67
3		**3c**		99	44
4		**3d**		99	72
5		**3e**		99	64
6		**3a**		94	85
7		**3b**		98	73
8		**3c**		98	74
9		**3d**		89	67
10		**3e**		99	78
11		**3a**		99	75
12		**3b**		99	64
13		**3c**		99	88
14		**3d**		99	85
15		**3e**		99	91
16		**3a**		93	80
17		**3b**		99	71
18		**3c**		99	82
19		**3d**		99	72
20		**3e**		99	73
21		**3a**		99	80
22		**3b**		99	70
23		**3c**		99	80
24		**3d**		99	82
25		**3e**		99	78
26		**3a**		98	76
27		**3b**		99	74
28		**3c**		97	85
29		**3d**		99	76
30		**3e**		95	75
31		**3a**		98	77
32		**3b**		77	62
33		**3c**		86	69
34		**3d**		81	43
35		**3e**		57	39
36		**3a**		95	82
37		**3b**		97	80
38		**3c**		99	86
39		**3d**		93	84
40		**3e**		88	75

The reaction conditions: Pd catalyst (0.01 mmol), 2-acetylfuran (1.0 mmol), aryl bromide (1.0 mmol), KOAc (2 mmol), DMAc (2 mL), 120 1C and 1 h. GC yields were calculated based on aryl bromide from the results of GC.

2-acetylthiophene with p-bromotoluene gave the desired product in 84–92% yield (Table 8, entries 6–10), and the conversion of the reaction was 92–98%. The reaction of 2-acetylthiophene with *p*-bromobenzaldehyde gave the expected product in 70–81 yield (Table 8, entries 11–15), with 99% conversion using the Pd-catalysts. The coupling with the electron-poor p-bromoacetophenone also gave the expected product with a high yield of 73–84% and 93–99% conversion (Table 8, entries 16–20). The reaction of 2-acetylthiophenene with 1-bromo-4-(trifluoromethyl)benzene generated the desired product in 60–94% yield with 65–98% conversion (Table 8, entries 21–55). Furthermore, 1-bromo-4-fluorobenzene was also successfully coupled with 2-acetylthiophene to give C5 arylated products in high yields of 86–95% (Table 8, entries 26–30) with 95–99% conversion. When the reaction was done with the p-bromoanisole, the obtained product was formed in moderate to high yield of 56–82% and conversion between 60–90% (Table 8, entries 31–35). When the coupling was done with 3-bromoquinoline, the reaction gave a good C5-arylated product with the same yield (80%) for all the Pd-catalysts, with the conversion of 99% (Table 8, entries 36–40).

The last evaluation of the new Pd-catalysts was performed under the same conditions for the direct arylation of 2-furaldehyde with the (hetero)aryl bromides that were used in the first and second tests, where C(5)-arylated furaldehyde derivatives were obtained. The arylation of 2-furaldehyde was

Table 8 Direct C5-arylation of 2-acetylthiophene with aryl bromides using the new Pd-catalyst

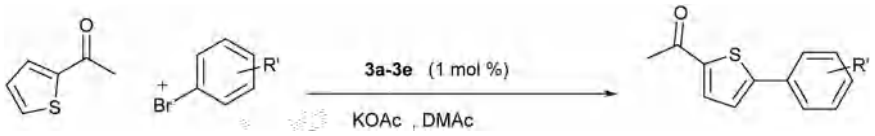

Entry	Aryl bromide	[Pd]	Product	Conversion (%)	Yield (%)
1		**3a**		98	78
2		**3b**		98	93
3		**3c**		99	93
4		**3d**		98	92
5		**3e**		98	93
6		**3a**		92	86
7		**3b**		96	92
8		**3c**		98	84
9		**3d**		95	89
10		**3e**		95	89
11		**3a**		99	70
12		**3b**		98	75
13		**3c**		99	81
14		**3d**		99	80
15		**3e**		99	81
16		**3a**		99	77
17		**3b**		96	84
18		**3c**		94	75
19		**3d**		98	82
20		**3e**		93	73
21		**3a**		77	75
22		**3b**		98	94
23		**3c**		65	60
24		**3d**		90	85
25		**3e**		90	85
26		**3a**		99	95
27		**3b**		97	93
28		**3c**		97	94
29		**3d**		96	90
30		**3e**		95	86
31		**3a**		90	80
32		**3b**		60	56
33		**3c**		82	74
34		**3d**		67	60
35		**3e**		90	82
36		**3a**		99	80
37		**3b**		99	80
38		**3c**		99	80
39		**3d**		99	80
40		**3e**		99	79

Reaction conditions: Pd catalyst (0.01 mmol), 2-acetylthiophene (1.0 mmol), aryl bromide (1.0 mmol), KOAc (2 mmol), DMAc (2 mL), 120 1C and 1 h. GC yields were calculated based on aryl bromide from the results of GC.

carried out using different *p*-substituted aryl bromides, (bromobenzene, *p*-bromotoluene, *p*-bromobenzaldehyde, *p*-bromoacetophenone, *p*-bromoanisole, and 3-bromoquinoline). Due to the Pd-catalyst (**3a–e**), the reaction was worked perfectly and the desired product was obtained with moderate to high yield, where the lowest yield was detected for the arylation with p-bromoanisole, which is electron rich. The results of this test showed that all the Pd(II)–NHC PEPPSI-type complexes were catalytically active. The results of these experiments are summarized in Table 9.

As shown in Table 9, good results were observed with all the Pd-catalysts, and high-to moderate yield C(5)-arylated products were obtained for almost all the reactions. When 2-furaldehyde was arylated with bromobenzene, the product 5-phenyl-2-carbaldehyde was obtained in 46–86% yield using the Pd-complexes (**3a-d**) as the catalyst, while the lowest yield (22%) was observed with the Pd-catalyst **3e** (Table 9, entries 1–5), with 26–99% conversion. The same reaction of furaldehyde with *p*-bromotoluene gave the desired product in 51–82% yield (Table 9, entries 6–10), and the conversion of the reaction was 99%. The reaction of furaldehyde with *p*-bromobenzaldehyde gave the expected product with moderate yields of 53–65% (Table 9, entries 11–15), with 78–99% conversion. The coupling with the electron-poor *p*-bromoacetophenone also gave the expected product with a lower yield of 23–48% and 27–71% conversion (Table 9, entries 16–20). The reaction of furaldehyde with 1-bromo-4-(trifluoromethyl)benzene generated the 5-(4-trifluoromethyl)-2-furaldehyde in 47–75% yield and 64–98% conversion

Table 9 Direct C5-arylation of 2-furaldeyde with aryl bromides using the new Pd-catalyst

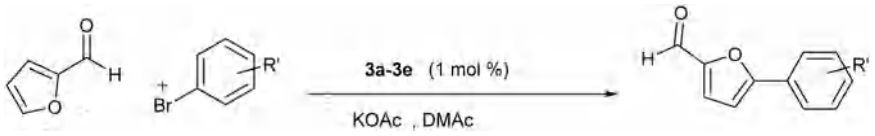

Entry	Aryl bromide	[Pd]	Product	Conversion (%)	Yield (%)
1		**3a**		99	86
2		**3b**		99	90
3		**3c**		98	76
4		**3d**		50	46
5		**3e**		26	22
6		**3a**		99	76
7		**3b**		98	79
8		**3c**		99	82
9		**3d**		98	51
10		**3e**		99	82
11		**3a**		99	65
12		**3b**		93	63
13		**3c**		99	65
14		**3d**		78	53
15		**3e**		94	63
16		**3a**		35	27
17		**3b**		27	23
18		**3c**		71	46
19		**3d**		66	47
20		**3e**		41	28
21		**3a**		98	75
22		**3b**		79	59
23		**3c**		65	50
24		**3d**		64	47
25		**3e**		29	26
26		**3a**		99	82
27		**3b**		99	85
28		**3c**		99	72
29		**3d**		99	70
30		**3e**		74	55
31		**3a**		13	09
32		**3b**		11	09
33		**3c**		13	10
34		**3d**		11	10
35		**3e**		19	16
36		**3a**		99	74
37		**3b**		75	48
38		**3c**		93	77
39		**3d**		69	47
40		**3e**		55	37

Reaction conditions: Pd catalyst (0.01 mmol), 2-furaldeyde (1.0 mmol), aryl bromide (1.0 mmol), KOAc (2 mmol), DMAc (2 mL), 120 1C and 1 h. GC yields were calculated based on aryl bromide from the results of GC.

(Table 9, entries 21–24), while the lowest yield was observed with the Pd-catalyst **3e** at 26%. The coupling with 1-bromo-4-fluorobenzene was also gave a high yield of 55–85% (Table 9, entries 26–30) with 77–99% conversion. Relatively low yields were obtained for the coupling of furaldehyde with 4-bromoanisole, which is an electron-rich aryl bromide, where the obtained product was formed in 9–16% yield (Table 9, entries 31–40). When the coupling was done with 3-bromoquinoline, the reaction gave a good C5-arylated product (Table 9, entries 36–40). Because pyridine derivatives such as quinolines are known to be p-electron deficient heterocycles, the reactivity of these compounds is quite similar to the electron-deficient aryl bromides such as 4-bromoacetophenone.[69] Also as a result of this study, it was observed that the least active catalyst was the **3e** complex, giving yields of 22%, 28%, 26%, 16%, 55%, and 37% (Table 9, entries 5, 10, 15, 20, 25, and 40, respectively).

Conclusions

In summary, a new series of PEPPSI-type palladium-NHC complexes (**3a–e**) based on the benzimidazole group was prepared using 5,6-dimethylbenzimidazolium salts with $PdCl_2$ in pyridine to give new Pd-catalysts. All the Pd(II)–NHC complexes were successfully characterized *via* spectroscopic analytical methods. Further, the crystal structures of the **3a**, **3b**, and **3d** Pd–NHC complexes were also reported. Theoretical calculations using DFT/B3LYP approach were performed to gain

further insights into the molecular structure and electronic properties of complex **3a**. The catalytic activities of these Pd(II)–NHC complexes were investigated in the direct C(5)-arylation of C(2)-blocked heteroarenes such as 2-acetylfuran, 2-acetylthiophene, and 2-furaldehyde. In most cases, high yields were observed using only 1 mol% Pd-catalyst with all the complexes in a very short time (1 h). All these Pd(II)–NHC complexes were found to be suitable for the arylation reaction of aryl bromide with heteroaromatics. Moreover, thiophene and furan derivatives could be efficiently and selectively arylated at the C(5)-position. Satisfactory results were obtained compared with previously reported similar studies. All the new PEPPSI-type palladium-NHC complexes (**3a–e**) proved to be active in the direct arylation reaction. In addition, it was seen that the reaction conditions were more moderate in terms of reaction temperature, time, and quantity of catalyst.

Author contributions

Abd el-Krim Sandeli: investigation; Naima Khiri-Meribout: supervision, writing – review and editing; Saida Benzerka: formal analysis; Houssem Boulebd: formal analysis; Nevin Gürbüz: investigation, visualization; Namık Özdemir: formal analysis; İsmail Özdemir: resources, funding acquisition, writing – review and editing.

Conflicts of interest

There are no conflicts to declare.

Acknowledgements

The authors greatly acknowledge financial support from the İnönü University Research Fund (İÜ-BAP: FBG-2019-1594) of this work. X-ray study was supported by the Scientific Research Projects Unit of Ondokuz Mayıs University (Project No: PYO.FEN.1906.19.001).

Notes and references

1 A. J. Arduengo III, R. L. Harlow and M. Kline, *J. Am. Chem. Soc.*, 1991, **113**, 361–363.
2 F. Glorius, *N-heterocyclic carbenes in transition metal catalysis*, vol. 21. Springer, 2007.
3 M. G. Organ, G. A. Chass, D.-C. Fang, A. C. Hopkinson and C. Valente, *Synthesis*, 2008, 2776–2797.
4 C. C. C. Johansson Seechurn, M. O. Kitching, T. J. Colacot and V. Snieckus, *Angew. Chem., Int. Ed.*, 2012, **51**, 5062–5085.
5 W. A. Herrmann, *Angew. Chem., Int. Ed.*, 2002, **41**, 1290–1309.
6 N. Gürbüz, E. Ö. Karaca, İ. Özdemir and B. Cetinkaya, *Turkish J. Chem*, 2015, **39**, 1115–1157.
7 E. A. B. Kantchev, C. J. O'Brien and M. G. Organ, *Angew. Chem., Int. Ed.*, 2007, **46**, 2768–2813.
8 F. Bellina and R. Rossi, *Chem. Rev.*, 2010, **110**, 1082–1146.
9 Y. Akita, A. Inoue, K. Yamamoto, A. Ohta and T. Kurihara, *Heterocycles*, 1985, **23**, 2327–2333.
10 A. Ohta, Y. Akita, T. Ohkuwa, M. Chiba and R. Fukunaga, *Heterocycles*, 1990, **31**, 1951–1958.
11 Y. Aoyagi, A. Inoue, R. Honma, Y. Akita and A. Ohta, *Heterocycles*, 1992, **33**, 257–272.
12 N. Marion and S. P. Nolan, *Acc. Chem. Res.*, 2008, **41**, 1440–1449.
13 X.-X. He, Y. Li, B.-B. Ma, Z. Ke and F.-S. Liu, *Organometallics*, 2016, **35**, 2655–2663.
14 M. Kaloğlu, İ. Özdemir, V. Dorcet, C. Bruneau and H. Doucet, *Eur. J. Inorg. Chem.*, 2017, 1382–1391.
15 H. Lv, L. Zhu, Y. Tang and J. Lu, *Appl. Organomet. Chem.*, 2014, **28**, 27–31.
16 W. Sikorski, W. Zawartka and A. M. Trzeciak, *J. Organomet. Chem.*, 2018, **867**, 323–332.
17 S. Karthik and T. Gandhi, *Org. Lett.*, 2017, **19**, 5486–5489.
18 M. Ionita, J. Roger and H. Doucet, *ChemSusChem*, 2010, **3**, 367–376.
19 A. L. Gottumukkala and H. Doucet, *Eur. J. Inorg. Chem.*, 2007, 3629–3632.
20 P. Xi, F. Yang, S. Qin, D. Zhao, J. Lan, G. Gao, C. Hu and J. You, *J. Am. Chem. Soc.*, 2010, **132**, 1822–1824.
21 T. Satoh and M. Miura, *Chem. Lett.*, 2007, **36**, 200–205.
22 S. Yang, C. Sun, Z. Fang, B. Li, Y. Li and Z. Shi, *Angew. Chem.*, 2008, **120**, 1495–1498.
23 L. Chen, J. Roger, C. Bruneau, P. H. Dixneuf and H. Doucet, *Chem. Commun.*, 2011, **47**, 1872–1874.
24 M. Nakano, H. Tsurugi, T. Satoh and M. Miura, *Org. Lett.*, 2008, **10**, 1851–1854.
25 E. Üstün, Ş. Koç, S. Demir and İ. Özdemir, *J. Organomet. Chem.*, 2016, **815**, 16–22.
26 E. Üstün, A. Özgür, K. A. Coşkun, S. D. Düşünceli, İ. Özdemir and Y. Tutar, *Trans. Met. Chem.*, 2017, **42**, 331–337.
27 G. Onar, C. Gürses., M. O. Karataş, S. Balcıoğlu, N. Akbay, N. Özdemir, B. Ateş and B. Alıcı, *J. Organomet. Chem.*, 2019, **886**, 48–56.
28 E. Peris and R. H. Crabtree, *Coord. Chem. Rev.*, 2004, **248**, 2239–2246.
29 S. P. Nolan, *N-Heterocyclic carbenes in synthesis*. John Wiley & Sons, 2006.
30 Y. Borguet, G. Zaragoza, A. Demonceau and L. Delaude, *Dalton Trans.*, 2013, **42**, 7287–7296.
31 A. Beladhria, A. L. Gottumukkala, C. Youssef, C. B. Bheeter, H. Ben Ammar, R. Ben Salem and H. Doucet, *Cat. Commun.*, 2013, **41**, 119–122.
32 I. Smari, C. Youssef, H. Ben Ammar, B. Ben Hassine, J.-F. Soulu and H. Doucet, *Tetrahedron*, 2015, **71**, 6586–6593.
33 E. C. Chao, *Drugs Future*, 2011, **36**, 351–357.
34 A.-K. Sandeli, N. Khiri-Meribout, S. Benzerka, N. Gürbüz, M. Dündar, H. Karcı, C. Bensouici, E. H. Mokrani, İ. Özdemir, A. Koç, N. Özdemir, A. Debache and İ. Özdemir, *Inorg. Chim. Acta*, 2021, **525**, 120486–120499.

35 S. Cie, *X-area (version 1.18) and X-red32 (version 1.04)*, Darmstadt, Germany, 2002.
36 L. Palatinus and G. Chapuis, *J. Appl. Crystallogr.*, 2007, **40**, 786–790.
37 D. Kratzert, J. J. Holstein and I. Krossing, *J. Appl. Crystallogr.*, 2015, **48**, 933–938.
38 O. V. Dolomanov, L. J. Bourhis and R. J. Gildea, *J. Appl. Crystallogr.*, 2009, **42**, 339–341.
39 R. A. Gaussian09, *Inc., Wallingford CT*, 2009, **121**, 150–166.
40 P. C. Hariharan and J. A. Pople, *Theor. Chim. Acta*, 1973, **28**, 213–222.
41 A. D. Becke, *Phys. Rev. A: At., Mol., Opt. Phys.*, 1988, **38**, 3098.
42 P. J. Hay and W. R. Wadt, *Int. J. Chem. Phys.*, 1985, **82**, 270–283.
43 A. D. McLean and G. S. Chandler, *Int. J. Chem. Phys.*, 1980, **72**, 5639–5648.
44 J. Tirado-Rives and W. L. Jorgensen, *J. Chem. Theory Comput.*, 2008, **4**, 297–306.
45 I. A. Khodja, H. Boulebd, C. Bensouici and A. Belfaitah, *J. Mol. Struct.*, 2020, **1218**, 128527.
46 I. A. Khodja and H. Boulebd, *Mol. Divers.*, 2020, 1–12.
47 M. Kaloğlu and İ. Özdemir, *Appl. Organomet. Chem.*, 2018, **32**, e4399.
48 H. A. Chiong and O. Daugulis, *Org. Lett.*, 2007, **9**, 1449–1451.
49 İ. Özdemir, Y. Gök, Ö. Özeroğlu, M. Kaloğlu, H. Doucet and C. Bruneau, *Eur. J. Inorg. Chem.*, 2010, 1798–1805.
50 L. Yang, D. R. Powell and R. P. Houser, *Dalton Trans.*, 2007, 955–964.68.
51 A. Okuniewski, D. Rosiak, J. Chojnacki and B. Becker, *Polyhedron*, 2015, **90**, 47–57.
52 B. Cordero, V. Gómez, A. E. Platero-Prats, M. Revés, J. Echeverría, E. Cremades, F. Barragána and S. Alvarez, *Dalton Trans.*, 2008, 2832–2838.
53 Y. Han, H. V. Huynh and G. K. Tan, *Organometallics*, 2007, **26**, 6447–6452.
54 H. V. Huynh, W. Sim and C. F. Chin, *Dalton Trans.*, 2011, **40**, 11690–11692.
55 Y.-C. Lin, H.-H. Hsueh, S. Kanne, L.-K. Chang, F.-C. Liu, I. J. B. Lin, G.-H. Lee and S.-M. Peng, *Organometallics*, 2013, **32**, 3859–3869.
56 L. Barbu, M. M. Popa, S. Shova, M. Ferbinteanu, C. Draghici and F. Dumitrascu, *Inorg. Chim. Acta*, 2017, **463**, 97–101.
57 N. Kaloğlu, M. Kaloğlu, M. N. Tahir, C. Arıcı, C. Bruneau, H. Doucet, P. H. Dixneuf, B. Cetinkaya and İ. Özdemir, *J. Organomet. Chem.*, 2018, **867**, 404–412.
58 M. Kaloğlu, N. Kaloğlu, İ. Yıldırım, N. Özdemir and İ. Özdemir, *J. Mol. Struct.*, 2020, **1206**, 127668–127679.
59 M. Kaloğlu, N. Gürbüz, İ. Yıldırım, N. Özdemir and İ. Özdemir, *Appl. Organomet. Chem.*, 2020, **34**, e5387.
60 H. Boulebd, Y. D. Lahneche, I. A. Khodja, M. Benslimane and A. Belfaitah, *J. Mol. Struct.*, 2019, **1196**, 58–65.
61 A. Nataraj, V. Balachandran and T. Karthick, *J. Mol. Struct.*, 2013, **1038**, 134–144.
62 M. Kumar, M. Kariem, H. N. Sheikh, A. Frontera, S. K. Seth and A. K. Jassal, *Dalton Trans.*, 2018, **47**, 12318–12336.
63 Y.-Y. Cai, L.-Y. Xu, L.-Q. Chai and Y.-X. Li, *J. Mol. Struct.*, 2020, **1204**, 127552–127561.
64 H. Boulebd, *Free Radical Res.*, 2020, **54**, 221–230.
65 H. Boulebd, *Phytochemistry*, 2021, **184**, 112670–112677.
66 E. David, C. Rangheard, S. Pellet-Rostaing and M. Lemaire, *Synlett*, 2006, 2016–2020.
67 E. O. Karaca, N. Gürbüz, İ. Özdemir, H. Doucet, O. Şahin, O. Büyükgüngör and B. Çetinkaya, *Organometallics*, 2015, **34**(11), 2487–2493.
68 E. David, S. Pellet-Rostaing and M. Lemaire, *Tetrahedron*, 2007, **63**, 8999–9006.
69 Y. Fall, C. Reynaud, H. Doucet and M. Santelli, *Eur. J. Org. Chem.*, 2009, 4041–4050.

Journal of Molecular Structure 1248 (2022) 131504

Contents lists available at ScienceDirect

Journal of Molecular Structure

journal homepage: www.elsevier.com/locate/molstr

New benzimidazolium N-heterocyclic carbene precursors and their related Pd-NHC complex PEPPSI-type: Synthesis, structures, DFT calculations, biological activity, docking study, and catalytic application in the direct arylation

Abd El-Krim Sandeli[a,f], Houssem Boulebd[a,b], Naima Khiri-Meribout[a,b,*], Saida Benzerka[a,b], Chawki Bensouici[c], Namık Özdemir[d], Nevin Gürbüz[e,f], İsmail Özdemir[e,f,g,*]

[a] Research Laboratory of Synthesis of Molecules with Biological Interest, Mentouri Constantine-1 University, Constantine 25000, Algeria
[b] Faculty of Science, Department of Chemistry, Mentouri Constantine-1 University, Constantine, Algeria
[c] National Center for Biotechnologie Research (CRBt), Ali Mendjli New Town, Constantine, Algeria
[d] Department of Mathematics and Science Education, Faculty of Education, Ondokuz Mayıs University, Samsun 55139, Turkey
[e] Faculty of Science and Art, Department of Chemistry, İnönü University, Malatya, Turkey
[f] Catalysis Research and Application Center, Inönü University, Malatya 44280, Turkey
[g] Drugs Application and Research Center, Inönü University, Malatya 44280, Turkey

ARTICLE INFO

Article history:
Received 26 July 2021
Revised 9 September 2021
Accepted 14 September 2021
Available online 18 September 2021

Keywords:
N-Heterocyclic carbene
Benzimidazolium salts
Palladium(II)-NHC complexes PEPPSI
DFT calculation
Molecular docking
Direct arylation reaction

ABSTRACT

New benzhydryl-5,6-dimethyl-(3-methylbenzyl)benzimidazolium salt as *N*-heterocyclic carbene precursors and their related new Pd-NHC complex PEPPSI-type with the general formula [$PdBr_2$(NHC)(pyridine)] were prepared and theoretically studied. Quantum chemistry computations at the B3LYP/6-311G(d,p)/LANL2DZ level were used to examine the molecular structure, electronic characteristics, and chemical reactivity of the ligand and its Pd complex. Further, the structural characterization of the complex **(c)** was determined by a single-crystal X-ray diffraction study, which supports the proposed structures and offered a more detailed structural characterization. In addition, their biological activity against. cholinesterase enzymes were also determined. The new compounds were tested against two enzymes (AChE and BChE), furthermore, docking studies were carried out in order to gain a better understanding of the bonding modes of L and COP in the active sites of AChE and BChE enzymes. The new salt and Pd-NHC complex PEPPSI-type were fully characterized by spectroscopic and analytical methods. The new Pd-catalysts based *N*-heterocyclic carbene ligand PEPPSI-Type was applied by the direct arylation process of five-membered heteroaromatics such as thiophene, and furan derivatives with various (hetero)aryl bromides in the presence of 1 mol% catalyst, using KOAc as a co-catalyst. The results showed that the new Pd-NHC complex is an effective catalyst.

1. Introduction

A wide range of *N*-heterocyclic carbenes ligands display a big role in many important organic transformations, when combined with metal pre-catalysts, are now commercially available [1]. Since the isolation of stable NHCs, these ligands have gotten more famous with organometallic chemists. Benzimidazole-based *N*-heterocyclic carbenes are successful effective ligands, and stable systems serving as helpful ligands to construct organometallic complexes. These NHCs are sterically and electronically tunable, strongly binding ligand units in complexes for the search of new materials [2–6]. They have been effectively utilized in various uses of organometallic chemistry [7–9], also, they are a vital ligand for metal complexes. It is important to recognize that benzimidazolium salts are the stable synthetically forms for handling benzimidazole carbenes. Imidazolium salts are always the synthetic pre-stages of NHCs, but benzimidazolium salts, which have two aromatic N1, N2-substituents are rare. More common are benzimidazolium salts possessing two N1, N2- substituents, where one of the N-substituent is an alkyl or benzyl group [10–14] and the other substituent is an aromatic or a benzylic group [15,16]. A synthetic strategy for the preparation of monoaryl benzimidazolium salts starts from the corresponding benzimidazoles possessing a bulky aryl group introducing the other bulky N-substituent by means of

* Corresponding authors.
E-mail addresses: naima.khiri@umc.edu.dz (N. Khiri-Meribout), ismail.ozdemir@inonu.edu.tr (İ. Özdemir).

https://doi.org/10.1016/j.molstruc.2021.131504
0022-2860/

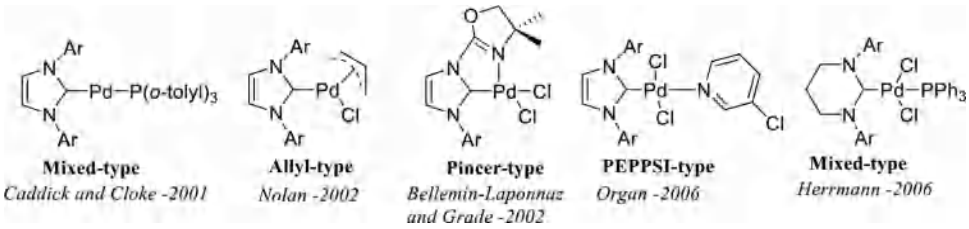

Fig. 1. Commonly Pd-NHC species are used in cross-coupling reactions.

an N-alkylation [17–20]. Indeed benzimidazolium salts that bear N-alkyl or N-alkenyl substituents can be accessed synthetically by simple routes in comparison with those possessing two N-aromatic substituents.

Due to their stability, selectivity, and electronic versatility of *N*-heterocyclic carbene-based ligands, and their metal complexes, have a wide range of uses and applications not just in organometallic chemistry but also in industry and catalysis, they have been used as extremely reactive and selective catalysts for a variety of reactions [21–23]. Strong σ-donation from *N*-heterocyclic carbenes increases the stability of the complexes and gives complexes advantageous properties in catalytic reactions [24,25], based on their electronic properties, σ-donor ability, and π-back donation which can be tuned, they possess great electronic flexibility. Recently, different-type of Pd-*N*-heterocyclic carbenes complexes have been prepared as Pd-NHC mixed-type by Caddick and Cloke [26], Pd-NHC Pincer-type by Bellemin-Laponnaz and Gade [27], Pd-NHC Allyl-type by Nolan [28], Pd-NHC Mixed-type by Herrmann [29], and Pd-NHC PEPPSI-type (PEPPSI = Pyridine Enhanced Precatalyst Preparation Stabilization and Initiation) by Organ [30], (Fig. 1). More recently, metal complexes with *N*HC ligands have been proposed as potential metallodrugs to fight bacterial infections [31,32]. Investigations showed that NHC-Au(I) complexes possibly act as inhibitors of both mammalian and bacterial Thioredoxin reductase (TrxR) and display both antiproliferative and anti-bacterial properties [33].

Pd-NHC complexes PEPPSI-type represent an interesting class of Pd-NHC catalysts that are completely different from other Pd-NHC complexes. Unlike many kinds of Pd-NHC complexes, Pd-NHC complexes PEPPSI-type are the easier ones to synthesize and use [34–36]. These different-type Pd-NHC complexes showed significant and high levels of activity in a variety of cross-coupling reactions. The high action of Pd-NHC complexes PEPPSI-type in catalysis has been founded on the presence of loosely bound throw-away pyridine ligand, which makes way for the incoming substrate [37]. In recent years, Pd-NHC complexes PEPPSI-type have been used as effective catalysts in direct arylation and successful results have been obtained [38–42]. Over the last few decades, extensive advances have been accomplished in direct arylation strategies. Pd, Ru, Rh, and other transition metals have been proven to be effective in direct arylation processes. [43]. However, among all complexes, the Pd-complexes are the most potent. After the discovery of Organ's PEPPSI-type Pd-complexes [44], this type of complex has exhibited great catalytic activities towards various carbon-heteroatom and carbon-carbon coupling reactions. The Pd-NHC complexes were tested as catalysts and tested for direct C2/C5 arylation reaction for a variety of five-membered heteroarenes such as thiophene, thiazole, and furan derivatives with aryl bromides bearing electron-donating and electron-withdrawing groups. Over the most recent twenty years, direct arylation responses have gotten extraordinary interest as possible alternatives to the most employed cross-coupling reactions and there are many reports on the Pd-catalysed direct arylation reactions of heteroaromatic compounds such as thiophenes, pyrroles, azoles, furans, etc. with substituted aryl halides [45–48]. Notably, arylation products up to 99% yields were obtained in the presence of the Pd(II)NHC complexes. More importantly, this method not only minimizes by-product formation but also has an extraordinary benefit to makes natural combinations simpler and a great advantage to makes organic synthesis more easier.

In view of the above information and as part of our ongoing investigation into novel functionalized *N*-heterocyclic carbenes ligands as the supporting environment for metal complexes and their application in catalysis. In the present study, we successfully report the synthesis and structural characterization of new 5,6-dimethylbenzimidazolium chloride salt with the coordination chemistry of these NHC ligands by Palladium. To get their related new complex PEPPSI-type Pd-NHC of the general formula [$PdBr_2$(NHC)(pyridine)]. The structures of these new compounds were characterized by various spectroscopic techniques. such as ^{1}H NMR, ^{13}C NMR, FT-IR, and elemental analysis. The solid-state structure of the Pd-complex was established by a single-crystal X-ray diffraction study. To get more information about these compounds a theoretical DFT calculation with docking study was carried out. The biological capacity for the new compounds also was done as an attempt to test the inhibitions of our compounds against cholinesterase activity. The catalytic application of this complex Pd-carbene has been tested in the direct arylation of five-membered heteroaromatics such as thiophene, and furan with (hetero)aryl bromides in presence of 1 mol% catalyst loading.

2. Experimental

2.1. Chemistry

2.1.1. Materials and measurements

The preparation of these compounds was performed in flame-dried glassware using standard Schlenk techniques under argon gas atmosphere. All solvents and reagents were purchased from Sigma-Aldrich. All of the spectroscopic and analytical work was done at the Inönü University research center, Malatya-TURKIYE. All measurements were taken at room temperature for freshly prepared solutions. Melting points were measured with Stuart SMP 40 melting point apparatus in open capillary tubes. Fourier transform infrared (FT-IR) spectra were recorded in the range 400–4000 cm^{-1} on the ATR unit using Perkin Elmer Spectrum 100. ^{1}H and ^{13}C NMR spectra were registered with a Varian As 400 Merkur spectrometer operating at 400 MHz (^{1}H), (^{13}C) in $CDCl_3$ with tetramethylsilane (TMS) as an internal reference. The chemical shifts (δ) were reported in parts per million (ppm). NMR multiplicities are abbreviated as follows: s = singlet, d = doublet, t = triplet, sept = septet, and m = multiplet signal. Coupling constants (*J* values) are given in Hertz. Catalytic reactions were observed on an Agilent 6890 N GC system by GC-FID.

2.2. Synthesis

2.2.1. Preparation method of 5,6-dimethylbenzimidazolium chloride salt

Benzimidazole-based ligand precursors could be prepared according to the literature [49] with a slight modification. Firstly An equivalent amount of *N*-benzhydryl-5,6-dimethylbenzimidazole (**a**) (0.8 g, 2.56 mmol) and an equivalent amount of 3-methylbenzyl chloride (0.36 g, 2.56 mmol) were dissolved in degassed dimethylformamide. After, the mixture was swirled and heated for three days at 80°C under an argon gas atmosphere. The obtained mixture was cooled at room temperature, after completion of the reaction, 30 mL of ether were added, and stirred for 30 min, then the product was isolated and washed with diethyl ether, and the obtained clear solution was concentrated under vacuum to obtain a high-purity precipitated product. After, the recrystallization of the crude products was done in dichloromethane Finally, to obtain pure products for experimental investigation, they were vacuum-dried.

1-Benzhydryl-5,6-dimethyl-(3-methylbenzyl)benzimidazolium chloride (b). Yield 71 % (322 mg, white solid); m.p = 159-160°C; FT-IR $\nu_{(CN)}$ = 1548 cm^{-1}. ^{1}H NMR (400 MHz, $CDCl_3$, TMS, 25°C): δ (ppm) = 11.27 (s, 1H, NC<u>H</u>N); 7.40 (m, 14H, C<u>H</u>-Ar); 7.11 (d, J = 7.2 Hz, 2H, C<u>H</u>-Ar); 6.97 (s, 1H, Ph-C<u>H</u>-Ph); 5.84 (s, 2H, C<u>H$_2$</u>N); 2.28 (s, 3H, C<u>H$_3$</u>); 2.27 (s, 3H, C<u>H$_3$</u>); 2.20 (s, 3H, C<u>H$_3$</u>). ^{13}C NMR (400 MHz, $CDCl_3$, TMS, 25°C): δ (ppm) = 142.6 (NCHN); 138.9 (C_{Ar}); 137.3 (C_{Ar}); 137.1 (C_{Ar}); 135.6 (C_{Ar}); 130.4 (C_{Ar}); 130.3 (C_{Ar}); 130.0 (CH_{Ar}); 129.9 (C_{Ar}); 129.5 (CH_{Ar}); 129.4 (CH_{Ar}); 128.4 (CH_{Ar}); 128.2 (CH_{Ar}); 114.5 (CH_{Ar}); 113.4 (CH_{Ar}); 66.5 (CH); 51.3 (N-CH_2); 21.2 (CH_3); 20.7 (CH_3); 20.6 (CH_3). Elemental analysis calcd. (%) for $C_{30}H_{29}ClN_2$ (M.w.= 453.02 g mol^{-1}): C 79.54, H 6.45, N 6.18; found (%): C 79.74, H 6.36, N 6.13.

2.2.2. Preparation method of PEPPSI-type Pd(II)-NHC complex

The first PEPPSI type Pd-NHC complex was prepared by Organ and co-workers in 2006 [50]. The Pd(II)-NHC complex PEPPSI-type could be prepared easily with a slight modification by the interaction of benzimidazolium salt with $PdCl_2$ and pyridine. Firstly, a solution of benzimidazolium salt (0.3 g, 0.66 mmol), $PdCl_2$ (0.12 g, 0.66 mmol), and pyridine (0.10 g, 1.32 mmol) was dissolved in acetonitrile (15 mL) in the presence of potassium carbonate K_2CO_3 (0.46 g, 3.31 mmol). Next, after the addition of KBr (0.79 g, 6.62 mmol), the solution was stirred and heated for 48 h at 80°C. The reactions were carried out in acetonitrile (15 mL) under an atmosphere of nitrogen. The solvent was removed under vacuum to afford the product and eliminate pyridine then the mixture was washed with hexane three times. The dark black solid formed was dissolved in dichloromethane. After, by flash column chromatography on silica gel, the product was purified. Then the solvent was removed under reduced pressure. Finally, the crude product was recrystallized from hexane/dichloromethane (4:1), to obtain the pure complex for experimental analysis and catalysis.

Dibromo [1-benzhydryl-5,6-dimethyl-3-(3-methylbenzyl) benzimedazol-2-ylidene]pyridine palladium (II), (c). Yield 81%; 130 mg; M.p: 257-258°C; yellow-solid(crystal); FT-IR ν(CN)=1400cm^{-1} .^{1}H-NMR (400MHz, $CDCl_3$, TMS, 25°C): δ(ppm) = 8.98 (d, 2H, J =5.1 Hz, $NC_5\underline{H}_5$); 8.58 (s, 1H, N-$C_6\underline{H}_2(CH_3)_2$-N); 7.72 (t, 1H, J =7.6 Hz, N-$C_5\underline{H}_5$); 7.52-7.47 (m, 7H, CH-Ar); 7.39-7.34 (m, 5H, C<u>H</u>-Ar); 7.29 (t, 2H, J =7.6 Hz, $NC_5\underline{H}_5$); 7.18 (d, 2H, J =7.4 Hz, N-$C_6\underline{H}_4(CH_3)$); 6.82 (s, 1H, N-$C_6\underline{H}_2(CH_3)_2$-N); 6.45 (s, 1H, Ph-C<u>H</u>-Ph); 6.14 (s, 2H, $NC\underline{H}_2$-$C_6H_4(CH_3)$); 2.34 (s, 3H, C<u>H$_3$</u>); 2.14 (s, 3H, C<u>H$_3$</u>); 2.03 (s, 3H, C<u>H$_3$</u>). ^{13}C-NMR (400MHz, $CDCl_3$, TMS, 25°C): δ(ppm) = 163.5 (N<u>C</u>H); 152.8 (CH_{Ar}); 152.2 (CH_{Ar}); 137.9 (C_{Ar}); 137.8 (C_{Ar}); 137.8 (C_{Ar}); 133.7 (CH_{Ar}); 133.3 (CH_{Ar}); 132.2 (C_{Ar}); 132.1 (C_{Ar}); 132.0 (C_{Ar}); 129.6 (CH_{Ar}); 129.3 (CH_{Ar}); 128.6 (CH_{Ar}); 128.1 (CH_{Ar}); 128.0 (C_{Ar}); 124.6 (CH_{Ar}); 113.9 (CH_{Ar}); 111.9 (CH_{Ar}); 68.1 (CH); 53.6 (N-<u>C</u>H$_2$); 21.4 (CH_3); 20.4 (CH_3); 20.2 (CH_3). Elemental analysis calcd.(%) for C35H33Br$_2$N3Pd (M.w.= 761.90 g mol^{-1}): C 55.18, H 4.37, N 5.52; found (%): C 55.10, H 4.34, N 5.47.

3. X-ray crystallography study

By the X-ray diffraction technique, the structure of the new Pd(II)-NHC complex **(c)**, was determined and, all the spectroscopic data were confirmed by the obtained results. A single suitable crystal of complex **(c)** for X-ray diffraction analysis was grown by slow diffusion of diethyl ether in a saturated chloroform solution at room temperature. X-ray diffraction data of **(c)** were recorded with an STOE IPDS II diffractometer at room temperature using graphite-monochromated Mo Kα radiation by applying the ω-scan method. Data collection and cell refinement were carried out using X-AREA [51]. while data reduction was applied using X-RED32 [51]. The structures were solved by direct methods with SIR2019 [52] and refined through the full-matrix least-squares calculations on F^2 using SHELXL-2018 [53]. inserted in idealized positions and treated using a riding model, fixing the bond lengths at 0.93, 0.98, 0.97, and 0.96 Å for aromatic CH, methine CH, CH_2, and CH_3 atoms, respectively. The displacement parameters of the H atoms were fixed at U_{iso}(H) = 1.2U_{eq} (1.5U_{eq} for CH_3) of their parent atoms. The crystallographic data and refinement parameters are summarized in Table 1. Molecular graphics were generated by using OLEX2 [54].

4. Density functional theory (DFT) calculations

4.1. Computational details

All DFT (density functional theory) calculations of this work have been performed using Gaussian09 software [55]. The B3LYP (Becke-Lee-Parr hybrid exchange-correlation three-parameter functional) functional [56,57] in conjunction with LANL2DZ [58] basis set for Palladium atom and 6-311G(d,p) [59] basis set for hydrogen, carbon, nitrogen, and bromine atoms have been used for all calculations. The B3LYP method is efficient for the prediction of molecular geometry and electronic properties and also offers a nice balance between cost and precision [60–62]. The ground state was validated by the absence of imaginary frequencies (no imaginary frequency).

5. Biological evaluation of the new benzimidazolium chloride (b) and their related Pd-NHC complex PEPPSI-type (c)

5.1. Material

The substrates (butyrylthiocholine chloride and acetylthiocholine iodide) which were used in this evaluation were obtained from (Sigma-Aldrich). The enzymes BChE horse serum butyrylcholinesterase eq(EC 3.1.1.8, 11.4 U/mg) and AChE from Electrophorus electricus eel-AChE (Type-VI-S, EC 3.1.1.7, 425.84 U/mg) were also obtained from Sigma-Aldrich. All other solvents and chemicals reagent were of analytical grade. The estimations and measurements of the inhibition were carried out using quantitative colorimetric assay, on a 96-well microplate reader, (PerkinElmer Multimode Plate Reader EnSpire, USA) at Biotechnology Research Center (Ali Mendjli, Constantine, Algeria)

5.2. Anticholinesterase assay (anti-Alzheimer)

This evaluation study tests the capacity of the new benzimidazolium salt (**b**) and their related Pd(II)-NHC complex (**c**) against anticholinesterase inhibition. The compounds were evaluated as

Table 1
Crystal data and structure refinement parameters for Pd-NHC complex PEPPSI-type.

Parameters	Pd(II)-NHC complex PEPPSI-Type (c)
CCDC depository	2073778
Color/shape	Yellow/plate
Chemical formula	$[PdBr_2(C_{30}H_{28}N_2)(C_5H_5N)]$
Formula weight	761.86
Temperature (K)	296(2)
Wavelength (Å)	0.71073 Mo Kα
Crystal system	Monoclinic
Space group	$P2_1/c$ (No. 14)
Unit cell parameters	
a, b, c (Å)	14.3357(5), 10.6693(5), 21.0026(9)
α, β, γ (°)	90, 91.205(3), 90
Volume (Å^3)	3211.7(2)
Z	4
$D_{calc.}$ (g/cm^3)	1.576
μ (mm^{-1})	3.094
Absorption correction	Integration
$T_{min.}$, $T_{max.}$	0.4436, 0.9532
F_{000}	1520
Crystal size (mm^3)	0.48 × 0.11 × 0.02
Diffractometer/measurement method	STOE IPDS II/ω scan
Index ranges	$-18 \le h \le 18$, $-13 \le k \le 13$, $-27 \le l \le 27$
θ range for data collection (°)	$1.940 \le \theta \le 27.724$
Reflections collected	26110
Independent/observed reflections	7516/3348
$R_{int.}$	0.1909
Refinement method	Full-matrix least-squares on F^2
Data/restraints/parameters	7516/0/373
Goodness-of-fit on F^2	0.976
Final R indices [$I > 2\sigma(I)$]	$R_1 = 0.0889$, $wR_2 = 0.1377$
R indices (all data)	$R_1 = 0.1985$, $wR_2 = 0.1708$
$\Delta\rho_{max.}$, $\Delta\rho_{min.}$ (e/Å^3)	1.15, −0.65

inhibitors of butyrylcholinesterase (BChE) and acetylcholinesterase (AChE) enzymes. According to the method described by Rhee et *al.* [63], And based on the spectrophotometric technique reported by Ellman's [64] the study was done with slight modifications. In this experiment, Galantamine was used as a reference drug. A reaction volume of 200 μL containing, 150 μL of sodium phosphate buffer (pH = 8.0, 100 mM), 10 μL of the sample at different concentrations in methanol, and 20 μL of AChE or BChE solution in buffer was mixed and left to incubate for 15 minutes at 37°C, Afterwards, 10 μL of DTNB (0.5 mM) were added. After that, to start the reaction 10 μL of acetylthiocholine iodide or 10 μL of butyrylthiocholine chloride (0.2 mM) was added. The formation of yellow color as the result of the reaction of DTNB with thiocholine confirmed the hydrolysis of substrates (butyrylthiocholine chloride and acetylthiocholine iodide). The absorbance of the solution was measured at 412 nm by the use of a 96-well microplate reader (Perkin Elmer, Enspire). The measurements were carried out in triplicate, and the results were presented as IC_{50} values (μM) corresponding to the 50% inhibition concentration. The percentage of inhibition I (%) was determined using the following formula: Inhibition (I %) = (E-S / S) × 100.

E is the activity of the enzyme without a test sample.

S is the activity of the enzyme in the presence of the test sample.

6. Docking study

A molecular docking study was performed to gain insight into the potential binding mode of the synthesized ligand **L** and its Pd complex **COP** into the active sites of AChE and BChE enzymes. Molecular geometries derived from DFT calculations were used for the docking study. *Tetronarce californica* acetylcholinesterase (PDB ID: 1ACJ) [65] and human butyrylcholinesterase (PDB ID: 4BDS) [66] coordinates were obtained from the Protein Data Bank (PDB) (https://www.rcsb.org). The proteins were stripped of their ligand, all water molecules, heteroatoms, and co-crystallized solvent. The Discovery Studio software tool (v.2.1) was used to apply charges, hybridization, bond orders, appropriate bonds, and the CHARMm force field. AutoDockTools (v. 1.5.6) was used to add partial charges and hydrogens to both the protein and the ligand. The search space has been constructed as a cube of 75 Å with grid points separated 1 Å, which centered at the middle of the protein: x = 4.765; y = 65.514; z = 56.823 for AChE and x = 138.802; y = 123.517; z = 38.605 for BChE. The docking investigation was carried out using AutoDock Vina (v. 1.1.2) [67]. Except for num_modes (set to 40), all the parameters have been left as default values. Figures were drawn using the BIOVIA Discovery Studio (https://3dsbiovia.com/). The docking procedure was validated by comparing crystallographic and theoretical data of the native ligand tacrine (RMSD values < 0.82, see Figure S1 in Supplementary Meterial).

7. Catalytic study of new Pd-NHC complex PEPPSI-type(c) in direct arylation reaction

In the last two decades, Pd-catalyzed direct arylation was successfully performed [68,69].In this work, the direct C(5)-arylation of furan, thiophene, and furaldehyde was carried using Pd-NHC complex PEPPSI-type **(c)** as a catalyst. Therefore, in this catalysis study, we selected DMA as the solvent, and KOAc as the base according to the methods described in the literature [70]. In a typical experiment an oven-dried 10 mL Schlenk tube was charged with 1 mol% of Pd(II)-NHC complexes (0.01 mmol) as catalyst, five-membered heteroaromatic compound derivative (2.0 mmol), (hetero)aryl halide (1.0 mmol), KOAc (2.0 mmol) as a base, and DMAc (dimethylacetamide, 2 mL) as solvent under argon atmosphere. The Schlenk tube was placed in a preheated oil bath at 120°C, and the reaction mixture was stirred for 1h. After completion of the reaction, the solvent was removed under vacuum and the residue

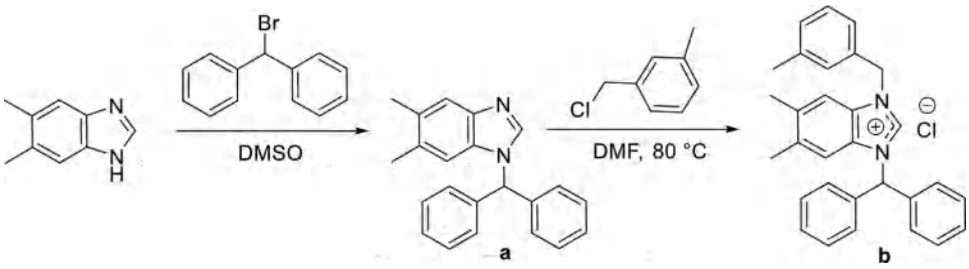

Scheme 1. Synthetic route and structure of benzimidazolium chloride (**b**).

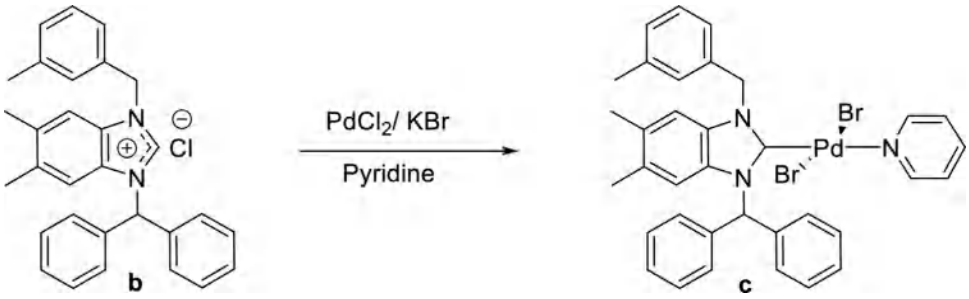

Scheme 2. Synthetic route and structure of Pd(II)-NHC complexes PEPPSI-type (**c**).

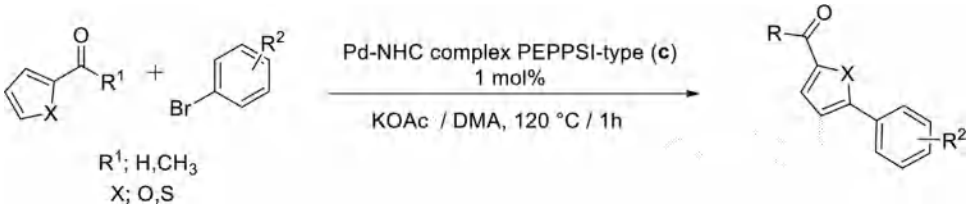

Scheme 3. The reaction conditions on the Pd-catalyzed direct arylation of five-membered heteroaromatics with aryl bromides.

was solved with CH_2Cl_2 (2 mL) and charged directly onto a micro-silica gel chromatography column. The products were eluted by using *n*-hexane/diethyl ether mixture (5:1, v/v) as eluent to afford the pure product. The chemical characterizations of the products were checked by gas chromatography GC. The yields and Conversions were calculated by taking into account the conversion of aryl bromides to products from the results of GC.

8. Results and discussion

8.1. Chemistry

8.1.1. Preparation of 1-Benzhydryl-5,6-dimethyl-(3-methylbenzyl) benzimidazolium chloride (b)

N-alkylation reaction using 5,6-dimethylbenzimidazole (1 mmol) with bromodiphenylmethane (1 mmol) was carried out in DMSO at 90°C to prepare the starting material *N*-benzhydryl-5,6-dimethylbenzimidazole **(a).** The precursor **(b)** was synthesized by the quaternization of the intermediate (**a**) with a 3-methylbenzyl chloride (1 mmol) in degassed dimethylformamide at 80°C (Scheme 1). The new 3,5dimethylbenzmidazolium chloride salt was obtained and isolated as air- and moisture-stable white solid in high yield (Scheme 2 and 3).

8.2. Preparation of PEPPSI-type palladium–NHC complex (c)

According to procedures reported by Organ [21], the Palladium(II)-NHC complex PEPPSI-themed (**c**) was synthesized. The reaction was carried out under an argon gas atmosphere of nitrogen, using standard Schlenk techniques. In 15 mL of acetonitrile a solution of benzimidazolium salt (1 equiv.), $PdCl_2$ (1 equiv.), pyridine (2 equiv.), K_2CO_3 (5 equiv.), and excess of KBr (10 equiv.) were dissolved. The reaction was heated and stirred for 72h at 80°C until the mixture became black. After to afford the product and eliminate pyridine, the solvent was removed under vacuum and the mixture was washed three times with hexane. When the hexane solvent was removed, the residue was re-dissolved in dichloromethane and filtered on a pad of silica covered with Celite, to remove unreacted $PdCl_2$. After evaporating the CH_2Cl_2 solvent, the crude product was obtained, and recrystallized from dichloromethane: hexane (1:4). The pure complex was obtained as a yellow powder solid Pd(II)-NHC complex (**c**).

The new compounds, salt (**b**) and complex (**c)** were showed good solubility in most organic solvents, such as chloroform, dichloromethane, methanol, ethanol, acetonitrile, and dimethylsulfoxide except non-polar ones, as pentane and hexane. The new compound could be stored at room temperature for months. They are highly moisture- and air-stable both in solution and in solid-state against air, light, and moisture. The structure of the new compounds was successfully characterized by spectroscopic techniques such as NMR(^{1}H and ^{13}C) in $CDCl_3$, FT-IR, and elementary analysis to confirm the formation of the complex.

Firstly, the melting point°C detected for the salt was 150-152°C while for their Pd-NHCcomplex **(b)** was 157-158°C. FT-IR spectroscopy data indicated that the benzimidazolium salt shows a characteristic ν(CN) band at 1541 cm^{-1}, whilst the PEPPSI-type Pd(II)-NHC complex (**c**) exhibit a characteristic ν(CN) band typically at 1400 cm^{-1}. The decrease in the ν(CN) stretching frequency was observed compared with the salt due to the flow of electrons from carbene ligand to the palladium center, this causes a C=N

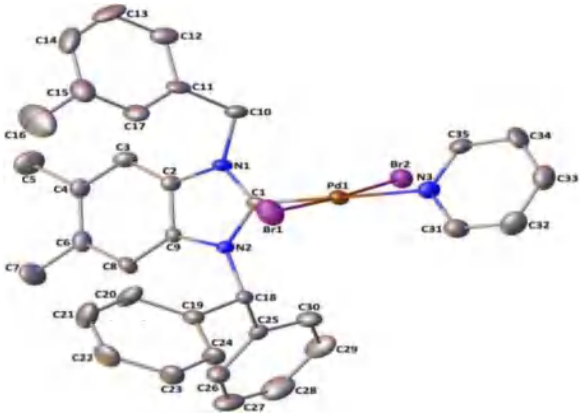

Fig. 2. Molecular structure of Pd(II)-NHC complex **(c)** drawn at 20% probability level. H atoms have been omitted for clarity.

Table 2
Selected distances (Å) and angles (°) for **Pd(II)-NHC complex PEPPSI-type (c)**.

Parameters		Pd(II)-NHC complexes PEPPSI-type(c)
Bond distances	**Pd1–Br1**	2.4458(16)
	Pd1–Br2	2.4385(17)
	Pd1–N3	2.101(9)
	Pd1–C1	1.966(10)
	N1–C1	1.364(12)
	N2–C1	1.362(11)
Bond angles (°)	**Br1–Pd1–Br2**	175.41(7)
	Br1–Pd1–N3	90.9(3)
	Br2–Pd1–N3	92.8(3)
	Br1–Pd1–C1	87.3(3)
	Br2–Pd1–C1	89.0(3)
	N3–Pd1–C1	178.1(4)
	N1–C1–N2	107.7(8)

bond to weak. Secondly, in the ^{1}H NMR, the important pick is the acidic pick NC*H*N which confirms the formation of the salt while his disappearance is evidence of the formation of their Pd-NHC complex (**c**). This pick was detected for the benzimidazolium salt at 11.27 ppm and in ^{13}C NMR the carbon (N*C*HN) was detected as a typical pick at 142.6. Contrary to this, the signal of the acidic proton(NC *H*N) has not appeared for their related Pd-NHC complex in ^{1}H NMR and similarly for the carbon peak (N*C*HN) in ^{13}C NMR spectra. This result, confirms the formation of the Pd-carbene bond. The characteristic signals of aromatic hydrogens of pyridine ring were observed in the ^{1}H NMR spectra at δ = 8.98, 7.71, 7.29 ppm. These signals suggest that the pyridine ring coordinated to the palladium center to form a PEPPSI-type palladium complex. In ^{13}C NMR the signals of the aromatic carbons of the pyridine ring were detected at δ =152.8, 152.2, 128.1 ppm. The characteristic Pd–C_2-carbene signals of Pd-complex (**c**) appear as a singlet at δ = 163.5 ppm in ^{13}C NMR spectra. The elemental analysis results of these two compounds are in agreement with the proposed molecular formula.

9. X-ray crystal structures

9.1. Description of the structure of Pd(II)-NHC complex (c)

The solid-state structure of compound (**c**) with the adopted atom-labeling scheme is shown in Fig. 2, while important bond distances and angles are listed in Table 2. The complex is four-coordinated in a square-planar geometry and surrounded by the carbene carbon atom of the NHC ligand, the nitrogen atom of the pyridine ring, and two bromine atoms. The complex has a slightly distorted square-planar geometry, in which the anion atoms are *trans* to each other. The *cis* angles varying from 87.3(3) to 92.8(3)° and the *trans* angles changing from 175.41(7) to 178.1(4)° deviate from their ideal values of 90 and 180°, respectively. For quantitative evaluation of the extent of distortion around the metal center, the structural indexes τ_4 [71] and τ_4' [72] were employed;

$$\tau_4 = \frac{360^\circ - (\alpha + \beta)}{360^\circ - 2\theta}$$

$$\tau_4' = \frac{\beta - \alpha}{360^\circ - \theta} + \frac{180^\circ - \beta}{180^\circ - \theta}$$

Where α and β ($\beta > \alpha$) are the two greatest valence angles and θ is the ideal tetrahedral angle (109.5°). The τ_4 and τ_4' values for ideal square-planar and tetrahedral coordination spheres are 0 and 1, respectively. The calculated τ_4 and τ_4' geometry indices 0.05 and 0.04, respectively, pointing out a slightly distorted square-planar geometry.

The Pd–C_{NHC} bond distance [1.966(10) Å] is smaller than the sum of the individual covalent radii of the palladium and carbon atoms (2.12 Å), while the Pd–$N_{pyridine}$ bond distance [2.101(9) Å] is equal to the sum of the individual covalent radii of the palladium and nitrogen atoms (2.10 Å) [73]. The Pd–Br distances are in the usual range, and the internal N–C–N ring angle at the carbene center is 107.7(8)°. In sum, these parameters are comparable with those observed for Pd-NHC-pyridine-Br_2 complexes [74–80]. The carbene ring is almost perpendicular to the coordination plane with a dihedral angle of 76.0(3)°, which is typical for NHC complexes to reduce steric congestion. On the other hand, the dihedral angle between the pyridine ring and the coordination plane is 65.8(4)°.

Table 3
Selected experimental and theoretical geometric parameters of Pd complex **COP**.

Complex COP	Experimental	Calculated	Discrepancy
Bond Distance (Å)			
N8-Pd	2.08	2.11	0.02
C1-Pd	1.95	1.99	0.04
Br1-Pd	2.42	2.53	0.11
Br2-Pd	2.44	2.54	0.1
N2-C1	1.36	1.38	0.01
N1-C1	1.35	1.37	0.02
N2-C19	1.46	1.49	0.03
N2-C10	1.46	1.48	0.02
Bond Angle (°)			
N8-Pd-C1	178.06	179.75	1.69
Br1-Pd-Br2	175.97	176.19	0.22
Br1-Pd-C1	90.15	88.81	-1.34
Br1-Pd-N3	91.14	91.47	0.34
Torsion Angle (°)			
Br1-Pd1-N3-C31	116.57	132.82	16.25
Br1-Pd1-C1-N2	106.45	97.97	-8.48
N2-C18-C25-C26	115.46	112.22	-3.24
N2-C18-C19-C24	162.01	172.57	10.56

10. DFT calculations

The molecular geometry of the synthesized ligand **L** and its Pd complex **COP** has been determined using DFT calculations at B3LYP/6-311G(d,p)/LANL2DZ level in order to get insights into the electronic properties and chemical reactivity. The resulting molecular geometry using DFT calculations for the Pd complex was compared to that of X-ray analysis, and the findings are presented in Fig. 3. Table 3 also includes some selected experimental and theoretical geometric characteristics of the Pd complex. As can be observed, the predicted molecular geometry of **COP** closely matches the experimental data. The predicted Br1-Pb and Br2-Pb

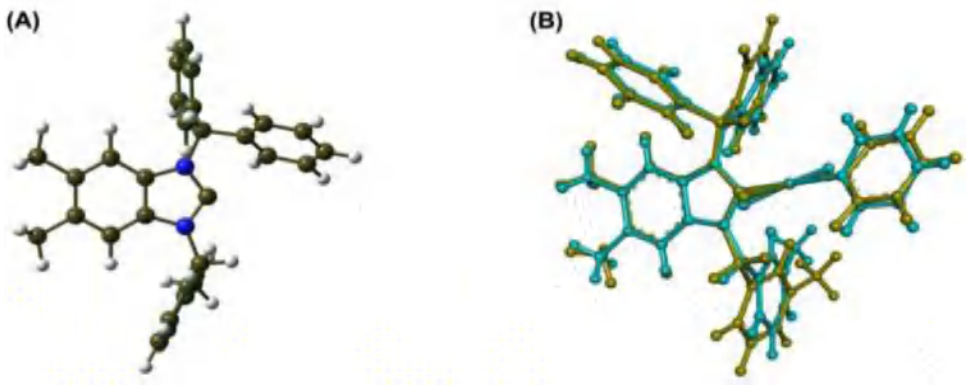

Fig. 3. (a) The molecular geometry of the synthesized ligand **L** and (b) atom-by-atom superimposition of the crystal structure (cyan) and the optimized molecular structure (yellow) of complex **COP**.

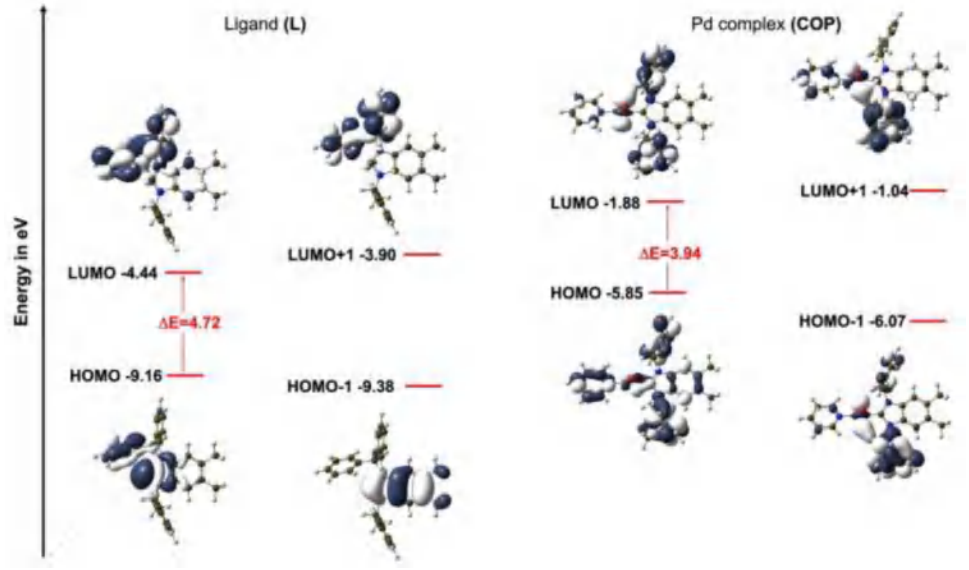

Fig. 4. Frontier molecular orbitals energies and distributions of the synthesized ligand (**L**) and its Pd complex (**COP**) computed at B3LYP/6-311G(d,p)/LANL2DZ level of theory.

bond lengths were 2.42 Å and 2.44 Å, respectively, which correspond well with the experimental values (2.53 Å and 2.54 Å). The predicted and observed N8-Pd and C1-Pd bond lengths were also found to be quite close, with discrepancies of 0.02 Å and 0.04 Å, respectively. For Br1-Pd-Br2 and Br1-Pd-N9, the discrepancies between predicted and experimental angles are only 0.22° and 0.34°, respectively. Torsion angles Br1-Pd1-N3-C31 and N2-C18-C19-C24 had the largest variances, with deviations of 16.25° and 10.56°, respectively. These results indicate that the DFT method applied is precise enough to estimate the molecular geometry of complex **COP** and can thus be used for future computations.

Frontier molecular orbitals (FMOs), also known as HOMO (Highest occupied molecular orbital) and LUMO (Lowest unoccupied molecular orbital), are essential characteristics that may be utilized to describe a molecule's chemical reactivity [81,82]. The energy of HOMO is connected to the capacity to donate electrons, whereas that of LUMO reflects the ability to accept electrons [14]. The shape of FMOs may potentially provide information about the regions of electrophilic and nucleophilic reactions. The energy and distribution of FMOs, extending from HOMO-1 to LUMO+1, of both ligand **L** and Pd complex **COP,** have been computed at the B3LYP/6-311G(d,p)/LANL2DZ level and are shown in Fig. 4. Analysis of the data obtained reveals that the HOMO energy of the ligand (-9.16 eV) is significantly [83] lower than that of the Pd complex (-5.85 eV), suggesting that the electron donation capacity of the former is lower than that of the latter. This result is expected because the ligand is a cationic species. The stability of the ligand could also be estimated to be greater than that of the complex, as can be concluded from their energy gap (4.72 and 3.94 eV, respectively) [84,85]. Upon complexation, the FMO distribution is considerably modified. It can be seen in Fig. 4 that the HOMO of the ligand is mainly localized on the benzimidazole and slightly on the benzene ring, where that of the complex is mainly distributed over the whole of the molecular structure. The LUMOs (LUMO and LUMO+1) of the ligand are located on the N2-benzene rings and those of the complex on the Pd atom as well as the benzene rings. These HOMO and LUMO electron density distributions clearly show the transfer of electron density from benzimidazole to benzene rings for the ligand, while there is no significant electron transfer for the complex.

The distribution of electronic charges is an essential characteristic that influences the chemical reactivity and electronic properties of molecules [86,87]. Atomic charge distributions on atoms of the synthesized ligand and the Pd complex were computed in the gas phase using the atomic polar tensor (APT) method at B3LYP/6-311G(d,p)/LANL2DZ level. The acquired data are depicted in Fig. 5 and Table S1 in the Supplementary Material. The charge distribution findings of the Pd complex's near-neighboring atom revealed

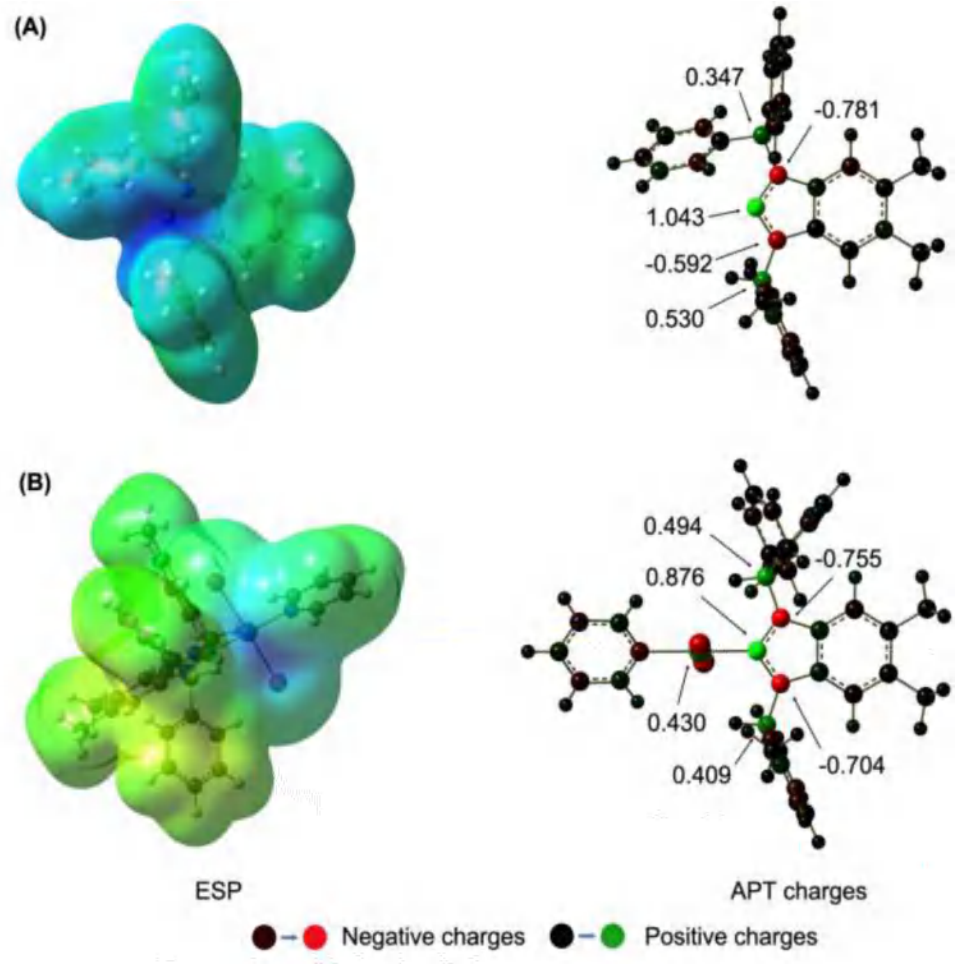

Fig. 5. APT charges destitution and molecular electrostatic potential (MEP) of the ligand **L** (a) and its Pd complex (b) computed at B3LYP/6-311G(d,p)/LANL2DZ level of theory.

that the electron density of the carbene's C atom increased in comparison to the free ligand, while the metal ion's electron density dropped. The formal charge of Pd is 2, while the charge of the metal center after complexation is 0.430, showing that charges move from **L** to metal ions. It can also be seen that the electronic density on the N atoms of benzimidazole increased during complexation. The distribution of electronic charges within the entire molecule, visualized as MEP (Molecular electrostatic potential), was calculated for both **L** and **COP**, as shown in Fig. 5. It can be observed from the MEPs obtained that the positive charges (deep blue) are mainly localized around the carbene atom for the ligand, while they are distributed on both the carbene and Pd atoms for the complex. Negative charges (yellow to red), on the other hand, are distributed over the benzene rings for the complex and the ligand. These findings imply that the ligand is more polarized than the complex and, as a result, should be more reactive towards nucleophiles than the complex.

11. *In vitro* cholinesterases inhibition evaluation

In order to carry on with the investigation in vitro anticholinesterase potential of the new compounds salt and Pd-NHC complex, we focused our attention on evaluating the capacity of this family of *N*-heterocyclic carbene toward anticholinesterase activity that used as a control and treatment to fight against Alzheimer's disease. In fact, the anti-cholinesterase activity of the two compounds was assessed in vitro against AChE and BChE according to the spectrophotometric method of Ellman et al [64]. For comparison purposes, Galanthamine was used as reference compounds. The inhibitory effect of the new benzimidazolium salt **(b)** and their corresponding Pd(II)-NHC complex **(c)** against two enzymes (AChE, and BChE) was tested at different concentrations. The new compounds demonstrated close percentages of inhibition against AChE compering with the standard Galanamine, while against BChE, the two compounds inhibited more effectively than the standard drug. The inhibition of AChE and BChE enzymes was determined by comparing the reaction rates of samples relative to the blank sample. Based on the IC50 values, the results were given as a concentration of 50% inhibition (IC50). The low IC50 values designated the high inhibition activity. The results of this evaluation for the new compounds and their selectivity index for BChE over AChE were summarized in Table 4.

As can be seen in Table 4, the obtained IC50 values revealed that the tested compounds showed a strong inhibitory against both enzymes (AChE and BChE). The benzimidazolium chloride salt was exhibited the highest inhibitory effect against AChE and BChE with (IC50: 4.19 $\pm$ 0.02 μM**)**, and (IC50: 0.15 $\pm$ 0.02 μM**)** respectively. Whilst their Pd(II)-NHC complex was exhibited AChE and BChE with (IC50: 19.30 $\pm$ 0.62 μM) and (IC50: 12.06 $\pm$ 1.68 μM). Comparing to that of the Galantamine against AChE (IC50:4.14 $\pm$ 0.07 μM) and BChE (IC50:20.38 $\pm$ 2.10 μM). The compound (**b**) is more active AChE and BChE inhibitory than their Pd(II)-NHC complex PEPPSI-type **(c)**. The results are consistent with the data observed in the literature of anticholinesterase evaluation for other benzim-

Table 4
Anti-Cholinesterase activity and the selectivity index for AChE over BChE and BChE over AChE of benzimidazolium salt **(b)** and their Pd-NHC complex PEPPSI-type **(c)**.

Enzymes		1,3-benzimidazolium Salt (b)	Pd(II)-NHC complex PEPPSI-type (c)	Galantamine [b]
AChE	IC_{50}±SD (μM)[a]	4.19± 0.02	19.30± 1.32	4.14± 0.07
	Selectivity index[c]	0.03	0.62	4.92
BChE	IC_{50}±SD (μM)[a]	0.15 ± 0.02	12.06 ± 1.68	20.38±2.10
	Selectivity index[c]	27.93	1.60	0.20

[a] **IC50** values represent the means ± SD of three parallel measurements ($p < 0.05$).
[b] Reference compound.
[c] **Selectivity for AChE:** IC_{50}(BChE)/IC_{50}(AChE).d**Selectivity for BChE:** IC_{50}(AChE)/IC_{50}(BChE).

Table 5
Binding energies in kcal/mol of the ligand **L**, Pd complex **COP**, and the native ligand galantamine into the active sites of AChE (PDB ID: 1ACJ) and BChE (PDB ID: 4BDS).

Compound	Binding energy (kcal/mol) AChE	BChE
L	-8.01	-7.82
COP	-4.86	-9.34
Galantamine	-7.83	-6.74

idazolium salts which were very similar to our scaffolds [88] and which gave results very close to those obtained in our study. It should be noted that the inhibition of BChE by the new compounds **b** and **c** demonstrated that the two compounds had high activity toward BChE. In terms of anti-BChE activity, its were more efficient than the AChE inhibitor activity. Accordingly, benzimidazolium salt and their related Palladium(II)-NHC complex PEPPSI-type could be considered promising acetylcholinesterase inhibitors.

On the other hand, compared with galantamine standard. The new compounds were more potent than the standard drug galantamine against the BChE enzyme. It was also noted that the new compounds were more selective for BChE than the standard drug Galantamine. The selectivity was especially pronounced for compounds. The performance for compound **b** was 27.93-fold more selective for BChE. While for AChE inhibitors, the new compounds had less affinity than Galantamine

NB. The low IC50 values assigned the high inhibition.

12. Molecular docking studies

Molecular docking studies were performed to further examine the binding mode of the synthesized ligand (**L**) and its Pd complex (**COP**) into the active sites of AChE (PDB ID: 1ACJ) and BChE (PDB ID: 4BDS) enzymes. Figs. 5 and 6 illustrate, respectively, the docking poses of the ligand and complex into the active sites of AChE and BChE enzymes, and their binding energies are reported in Table 5.

As indicated by the *in vitro* assay, the ligand **L** is significantly more reactive than the Pd complex towards the AChE enzyme, and its inhibitory potential is comparable to that of the native ligand galantamine. However, the Pd complex is about 4.5 times less active than galantamine. These results are in good agreement with the predictions of molecular modeling. As shown in Table 5, the binding energy of ligand **L** (-8.01 kcal/mol) is higher than that obtained for the Pd complex (-4.86 kcal/mol) and comparable to that of galantamine (-7.83 kcal/mol), indicating that the ligand **L** is more stable in the active site of the AChE enzyme than its Pd complex. This may explain the observed difference in the inhibitory potential of ligand **L** compared to its Pd complex. On the other hand, **L** and **COP** interact favorably with the amino acid residues of the catalytic site, Trp84, and Phe330, which are essential amino acids for the catalytic action of the AChE enzyme (Fig. 5). This may explain the moderate activity of the Pd complex even though it shows low binding energy. From Fig. 5, it can also be seen that both compounds form favorable hydrophobic interactions with residues Tyr334 and Tyr121 of the PAS. Unlike the AChE enzyme, both **L** and **COP** showed high inhibitory activity against the BChE enzyme in the experimental when compared to galantamine. The activity of the ligand and Pd complex is approximately 81.5 and 1.8 times higher than that of galantamine, respectively. This good inhibitory activity could be explained by the molecular docking study. Both compounds were shown high boding energies at the active site of BChE of -7.82 and -9.34 kcal/mol for **L** and **COP**, respectively (Table 5). Furthermore, both compounds interact favorably with the residues of the catalytic site, Trp82, and Phe329 as well as Val288 and Leu286 of the acyl pocket (Fig. 6). However, molecular docking does not explain why the ligand is so much more active than the complex or galantamine. This might be attributed to the enzyme ligands' high stability with regard to the enzyme-complex. Molecular dynamics simulations should be performed to validate this hypothesis (Fig. 7).

13. Catalytic evaluation study

13.1. Optimization of the reaction conditions for the direct arylation of heteroaromatics with aryl bromides

In the last two decades, Pd-catalyzed direct arylation was successfully performed using special conditions. As commonly used for the direct arylation of hetero-arenes, based on previous studies [89–91]. The catalytic capacity of the new Pd(II)-NHC complex (c) in intermolecular direct arylation reactions between aryl bromides and substituted furan, and thiophene derivatives was performed. Therefore, for this evaluation, we performed these reactions using DMA as a solvent, KOAc as a base, at 120°C in 1h, and 1 mol% of Pd catalyst as reaction conditions. In order to evaluate the scope and limitations of our new Pd-NHC complex PEPPSI-type for the direct arylation of 2-acetylfurane, 2-acethylthiophene, and furaldehyde with different *p*-substituted aryl bromides. All reactions performed for this purpose worked perfectly to give the desired C(5)-arylated furane and thiophene derivatives products in moderate to high yields. The results are summarized in Table 6.

Firstly as shown in Table 6, under the conditions of the direct arylation reaction, the reactivity of 2-acetylfuran, 2-acetylthiophene, and furaldehyde with aryl bromides was examined and the C(5)-arylated furan and thiophene derivatives were obtained with an excellent conversion using the only 1mol% of our Pd-NHC complex PEPPSI-type **(c)**, depending on the aryl bromides. The GC yields of C(5)- arylated products obtained were good for almost all reactions. The coupling of 2-acetylfurane with bromobenzene and 3-bromoquinoline gave the desired products at 44 and 81 % GC yields (Table 6, entries 1 and 8), While, when the reaction was done with *p*-bromobenzaldehyde, *p*-bromoacetophenone, *p*-bromoanisole, and

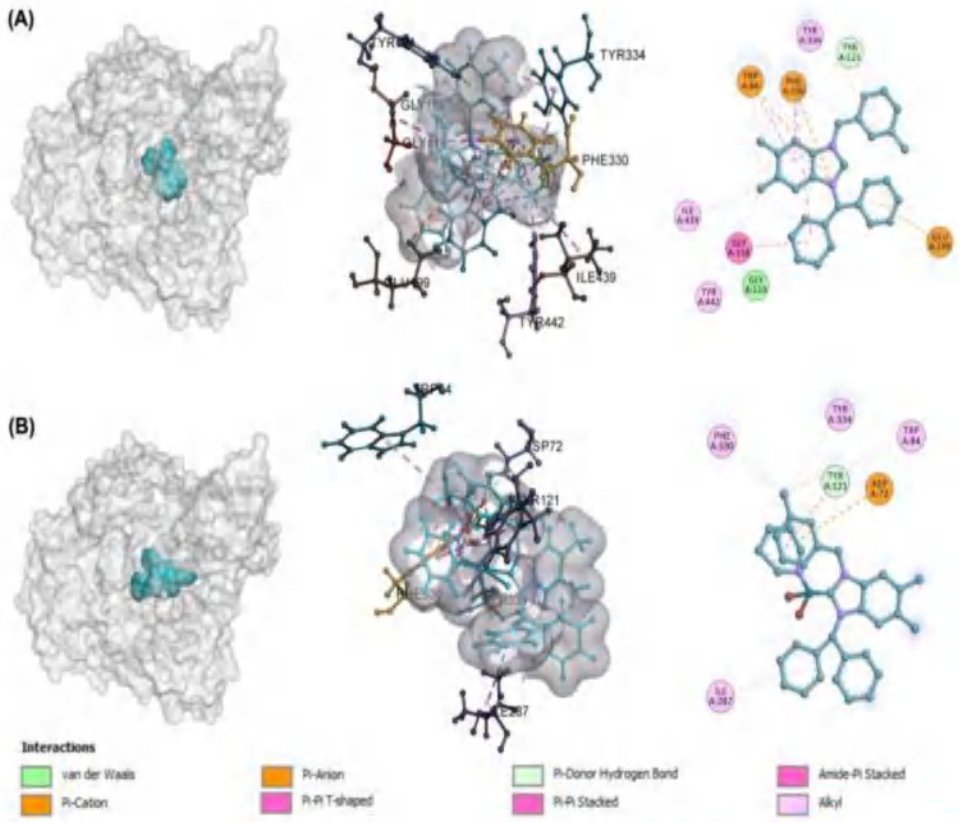

Fig. 6. Docking poses of the ligand (a) and Pd complex (b) into the active site of the AChE enzyme.

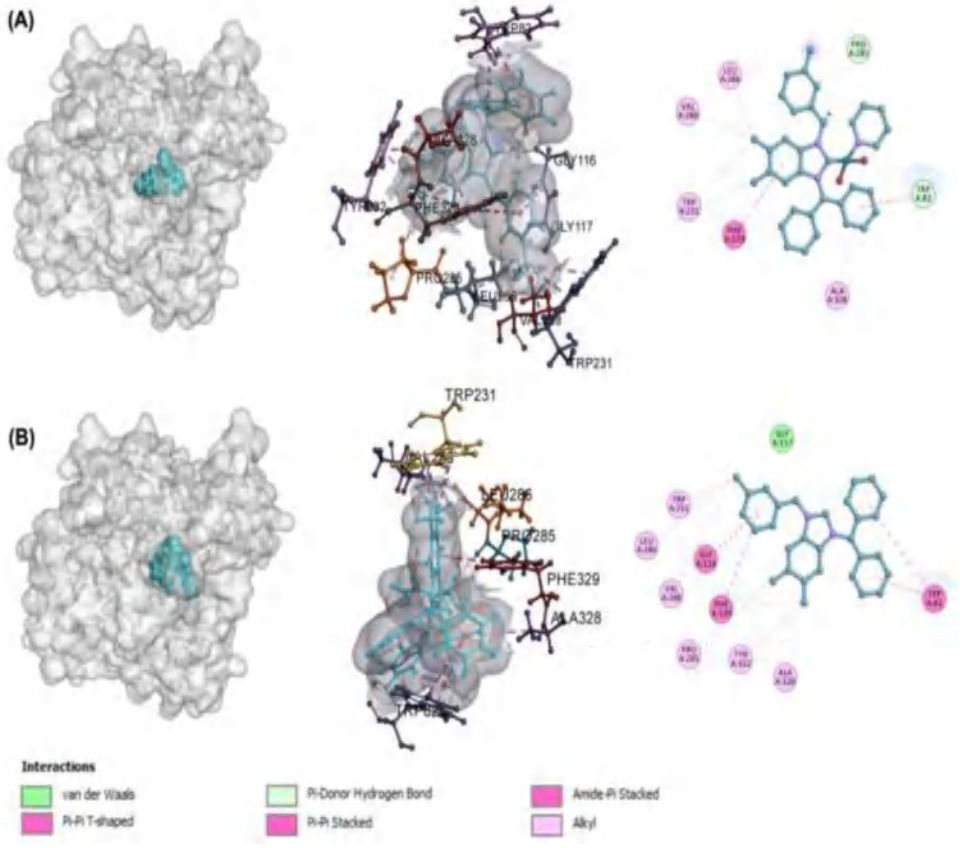

Fig. 7. Docking poses of the ligand (a) and Pd complex (b) into the active site of the BChE enzyme.

Table 6
Direct C5-arylation of 2-acetylfurane, 2-acetylthiophene, and furaldehyde with aryl bromides by using the new Pd-catalyst PEPPSI-type (c).

Entry	Aryl Bromide	Substrates	Conversion (%)	Yield (%)
01	bromobenzene	2-acetylfurane	99	44
02	*p*-bromotoluene	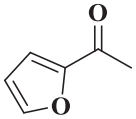	98	74
03	*p*-bromobenzaldehyde		99	88
04	*p*-bromoacetophenone		99	82
05	*p*- bromoanisole		99	80
06	1-bromo-4-fluorobenzene		97	85
07	1-bromo-4-(trifluoromethyl)benzene		86	69
08	3-bromoquinoline		93	81
09	bromobenzene	2-acetylthiophene	99	93
10	*p*-bromotoluene	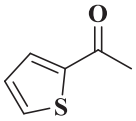	98	84
11	*p*-bromobenzaldehyde		99	81
12	*p*-bromoacetophenone		94	75
13	*p*- bromoanisole		65	59
14	1-bromo-4-fluorobenzene		97	94
15	1-bromo-4-(trifluoromethyl)benzene		82	74
16	3-bromoquinoline		99	80
17	bromobenzene	Furaldehyde	98	76
18	*p*-bromotoluene	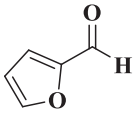	99	82
19	*p*-bromobenzaldehyde		99	65
20	*p*-bromoacetophenone		71	46
21	*p*- bromoanisole		65	50
22	1-bromo-4-fluorobenzene		99	72
23	1-bromo-4-(trifluoromethyl)benzene		13	10
24	3-bromoquinoline		93	77

1-Bromo-4-fluorobenzene, the best yields were observed with Pd catalyst (**c**), and the obtained product formed at 88, 82, 80, and 85% GC yields with conversion between 97-99% (Table 6, entries 3-6). The same reaction of 2-acetylfurane with *p*-bromotoluene, and 1-bromo-4-(trifluoromethyl)benzene, gave the desired product with a moderate GC yield at 74 and 69 % yields. Next, when the reaction was investigated with 2-acethylthiophene, C(5)-arylated 2-acethylthiophene with bromobenzene and 1-Bromo-4-fluorobenzene were obtained at 93 and 94 % GC yields with full conversion (Table 6, entries 9 and 14). However, when the reaction was done with *p*-bromotoluene, *p*-bromobenzaldehyde, *p*-bromoacetophenone, 1-Bromo-4 (trifluoromethyl)benzene, and 3-bromoquinoline good yields were observed for the obtained product formed at 84, 81, 75, 79, and 80% yields respectively, with a high conversion between 97-99% (Table 6, entries 10, 11, 12, 15, and 16). The lowest yield was observed for the coupling with *p*-bromoanisole, in which the obtained product formed at 59 % GC yield (Table 6, entry 13). Finally, the coupling of 2-furaldehyde with bromobenzene, *p*-bromobenzaldehyde, 1-bromo-4-fluorobenzene, and 3-bromoquinoline generated the desired products at 76, 65, 72, and 77 % GC yields (Table 6, entries 20 and 21), The best yield was observed for the coupling with *p*-bromotoluene in which the obtained product formed at 82 % GC yield with full conversion 99% (Table 6, entry 18). Whilst the lowest yield was observed for the coupling with 1-bromo-4-(trifluoromethyl)benzene, in which the GC yield for the obtained product formed was the lowest one at 10 % GC yield, and with a 13 % conversion. (Table 6, entry 23).

Through this study, the catalytic activity of the new Pd-NHC complex PEPPSI-type was investigated in the direct C(5)-arylation of furan and thiophene. Satisfactory results were obtained, 1 mol% loading of the Pd-catalyst PEPPSI-type was used, and the reaction time was shortened to 1 h. Moreover, furan and thiophene derivatives can be efficiently and selectively arylated at the C(5)-position. In most cases, high yields were observed. Surprisingly, similar conversions were obtained for the coupling of each aryl bromide.

The reaction conditions: Pd catalyst (0.02 mmol), 2-acetylfuran, aryl bromide (1.0 mmol), KOAc (2 mmol), DMAc (2 mL), 120°C and 1 h. GC yields were calculated concerning aryl bromide from the results of GC

14. Conclusion

In summary, we presented the synthesis, theoretical DFT calculation, catalytic and biological activities with docking study of new benzimidazolium salt, and their corresponding Pd-NHC complex. The new NHC benzimidazolium salt N-substituents as carbine precursors allowed us to prepare corresponding new Pd-NHC complex PEPPSI-type by simple synthesis route. The new compounds salt and their related Pd(II)-NHC complex PEPPSI-type were designed and structurally characterized using spectroscopic and analytical methods, as NMR (^{1}H and ^{13}C), FT-IR spectra, and elemental analysis. The structure of the new Pd(II)-NHC complex PEPPSI type was determined by X-ray crystallography. The experimental molecular geometry of the ground state of the complex COP was found to be almost identical to the minimized structure obtained from the DFT calculations. Calculations of FMO, ATP charges, and MEP indicated that the chemical reactivity and electronic properties of the ligand were significantly altered during complexation. Docking studies at the active sites of AChE and BChE enzymes have shown that **L** and **COP** are moderate to good cholinesterase inhibitors and their activity may be due to their favorable interactions with essential amino acid residues such as Trp84 and Phe330 as well as Trp82 and Phe329. The new Pd-NHC complex PEPPSI–type was investigated as Pd-catalysts for the direct arylation of 2-acetylfurane, 2-acetylthiophene, and furaldehyde with various aryl bromides. High catalytic activity for arylation was seen reaction using only 1 mol% catalyst for 1 h.

Declaration of Competing Interest

The authors declare that they have no known competing financial interests or personal relationships that could have appeared to influence the work reported in this paper.

CRediT authorship contribution statement

Abd El-Krim Sandeli: Investigation, Writing – original draft. **Houssem Boulebd:** Investigation, Visualization. **Naima Khiri-Meribout:** Supervision, Writing – review & editing, Visualization.

Saida Benzerka: Supervision. **Chawki Bensouici:** Software, Validation. **Namık Özdemir:** Investigation. **Nevin Gürbüz:** Project administration. **İsmail Özdemir:** Conceptualization, Methodology, Software, Supervision, Funding acquisition.

Acknowledgment

The authors greatly acknowledge financial support from the İnönü University Research Fund (FBG-2021-2562) of this work. X-ray study was supported by the Scientific Research Projects Unit of Ondokuz Mayıs University (Project No: PYO.FEN.1906.19.001).

Supplementary materials

Supplementary material associated with this article can be found, in the online version, at doi:10.1016/j.molstruc.2021.131504.

References

[1] S. Lee and J. F. Hartwig, "Improved Catalysts for the palladium-catalyzed synthesis of oxindoles by amide r-arylation. Rate acceleration, use of aryl chloride substrates, and a new carbene ligand for asymmetric transformations," no. 22, pp. 3402–3415, 2001.
[2] A. T. Biju, K. Hirano, R. Frçhlich, and F. Glorius, "Switching the electron-donor properties of N-heterocyclic carbenes by a facile deprotonation strategy," vol. 1, no. 6 mL, pp. 1786–1789, 2009, doi:10.1002/asia.200900410.
[3] R. Article, "Chem Soc Rev photoluminescence and applications †," pp. 3551–3574, 2014, doi:10.1039/c3cs60466g.
[4] F. Lazreg and C. S. J. Cazin, "Medical applications of NHC – gold and – copper complexes," 2014.
[5] O. Schuster, L. Mercs, and M. Albrecht, "The potential of N-heterocyclic carbene complexes as components for electronically active materials," vol. 64, no. 3, pp. 184–187, 2010, doi:10.2533/chimia.2010.184.
[6] M. Sawamoto, "Precision control of radical polymerization via transition metal catalysis : from dormant species to designed catalysts," vol. 41, no. 9, 2008.
[7] D. Preysing, S. K. Schneider, W. A. Herrmann, and O. Karl, "Phospha-palladacycles and N -heterocyclic carbene palladium complexes : efficient catalysts for CC-coupling reactions," vol. 687, 2003, doi:10.1016/j.jorganchem.2003.07.028.
[8] U. Christmann and R. Vilar, "Minireviews palladium catalysts monoligated palladium species as catalysts in cross- coupling reactions," pp. 366–374, 2005, doi:10.1002/anie.200461189.
[9] W.A. Herrmann, ChemInform abstract: N-heterocyclic carbenes. Part 31. N-heterocyclic carbenes: a new concept in organometallic catalysis, ChemInform 33 (32) (2010) p. no-no, doi:10.1002/chin.200232255.
[10] K. Hirano, A. T. Biju, and F. Glorius, "Copper-catalyzed synthesis of 2-unsubstituted, N -substituted benzimidazoles," pp. 9570–9572, 2009, doi:10.1021/jo902160y.
[11] J. Izquierdo, A. Orue, and K. A. Scheidt, "A dual Lewis base activation strategy for enantioselective carbene- catalyzed annulations," pp. 10634–10637, 2013.
[12] A. Chan and K. A. Scheidt, "Highly stereoselective formal [3 + 3] cycloaddition of enals and azomethine imines catalyzed by N-heterocyclic carbenes analytical services laboratory has been furnished in part by the," no. entry 8, pp. 5334–5335, 2007.
[13] H. V. Huynh, L. R. Wong, and P. S. Ng, "Anagostic interactions and catalytic activities of sterically bulky benzannulated n-heterocyclic carbene complexes of nickel (II)," no. II, pp. 2231–2237, 2008.
[14] R. Kishore, S.K. Das, Synthesis, structural characterization and properties of new N - heterocyclic carbene Ag (I) complexes, J. Mol. Struct. (2013) I, doi:10.1016/j.molstruc.2013.08.051.
[15] J. Li et al., "One-pot synthesis of 7,9-dialkylpurin-8-one analogues: broad substrate scope," no. entry 18, 2013.
[16] H. M. Lima and C. J. Lovely, "Synthesis of 2-imidazolones and," no. Figure 1, pp. 14–17, 2011.
[17] W. Fang, J. Jiang, Y. Xu, J. Zhou, T. Tu, Novel robust benzimidazolylidene palladium complexes : synthesis, structure, and catalytic applications in amination of chloroarenes, Tetrahedron 69 (2) (2013) 673–679, doi:10.1016/j.tet.2012.11.003.
[18] N. Gürbüz, S. Yas, and Ö. Özcan, "transfer hydrogenation of ketones by ruthenium complexes bearing benzimidazol-2-ylidene ligands ˙ smail özdemir,* [a] and," pp. 3051–3056, 2010, doi:10.4225/23/5ad043ff9a033.
[19] H. Türkmen, T. Pape, F. E. Hahn, and B. Çetinkaya, "Palladium (II) complexes with benzimidazolin-2-ylidene and phosphane ligands and their catalytic activity in mizoroki – heck coupling reactions," no. Ii, pp. 285–294, 2009, doi:10.1002/ejic.200800948.
[20] P. C. B. Page et al., "A new paradigm in N -heterocyclic carbenoid ligands," vol. 690, pp. 6210–6216, 2005, doi:10.1016/j.jorganchem.2005.09.015.
[21] F. Glorius, N-Heterocyclic Carbenes in Transition Metal Catalysis, 21, Springer, 2007.
[22] S.P. Nolan, N-Heterocyclic Carbenes: Effective Tools for Organometallic Synthesis, John Wiley & Sons, 2014.
[23] S. Díez-González, N-Heterocycliccarbenes: from Laboratory to Curiosities to Efficient Synthetic Tools, 27, Royal Society of Chemistry, 2016.
[24] A. J. Arduengo, M. Kline, J. C. Calabrese, F. Davidson, and N. M. R. Hi, "{'hi 57.79," vol. 11, no. 4, pp. 9704–9705, 1991.
[25] M. C. Perry and K. Burgess, "Chiral N -heterocyclic carbene-transition metal complexes in asymmetric catalysis," vol. 14, no. 56, pp. 951–961, 2003.
[26] L.R. Titcomb, S. Caddick, F.G.N. Cloke, D.J. Wilson, D. McKerrecher, Unexpected reactivity of two-coordinate palladium-carbene complexes; synthetic and catalytic implications, Chem. Commun. (15) (2001) 1388–1389.
[27] V. César, S. Bellemin-Laponnaz, L.H. Gade, Direct coupling of oxazolines and N-Heterocyclic carbenes: A modular approach to a new class of c– n donor ligands for homogeneous catalysis, Organometallics 21 (24) (2002) 5204–5208.
[28] M.S. Viciu, R.F. Germaneau, O. Navarro-Fernandez, E.D. Stevens, S.P. Nolan, Activation and reactivity of (NHC) Pd (allyl) Cl (NHC= N-heterocyclic carbene) complexes in cross-coupling reactions, Organometallics 21 (25) (2002) 5470–5472.
[29] S. K. Schneider, W. A. Herrmann, E. Herdtweck, Active catalysts for the Suzuki coupling: Palladium complexes of tetrahydropyrimid-2-ylidenes, Journal of molecular catalysis A: chemical 245 (1) (2006) 248–254.
[30] C.J. O'Brien, et al., Easily prepared air-and moisture-stable Pd–NHC (NHC= N-heterocyclic carbene) complexes: a reliable, user-friendly, highly active palladium precatalyst for the Suzuki–Miyaura reaction, Chem. – Eur. J. 12 (18) (2006) 4743–4748.
[31] R.H. Crabtree, C.R. Chimie, Recent homogeneous catalytic applications of chelate and pincer N-heterocyclic carbenes, Coord. Chem. Rev. 248 (2004) 2239.
[32] M.C. Perry, K. Burgess, Chiral N-heterocyclic carbene-transition metal complexes in asymmetric catalysis, Tetrahedron Asymmetry 14 (8) (2003) 951–961.
[33] A.J. Arduengo III, R.L. Harlow, M. Kline, A stable crystalline carbene, J. Am. Chem. Soc. 113 (1) (1991) 361–363.
[34] S.P. Nolan, N-Heterocyclic Carbenes in Synthesis, John Wiley & Sons, 2006.
[35] G.C. Fortman, S.P. Nolan, N-Heterocyclic carbene (NHC) ligands and palladium in homogeneous cross-coupling catalysis: a perfect union, Chem. Soc. Rev. 40 (10) (2011) 5151–5169.
[36] F. Glorius, "N-heterocyclic carbenes in catalysis—an introduction," 2006.
[37] C. Valente, C. Selåuk, K. H. Hoi, D. Mallik, M. Sayah, and M. G. Organ, "The development of bulky palladium NHC complexes for the most-challenging cross-coupling reactions," pp. 3314–3332, 2012, doi:10.1002/anie.201106131.
[38] X.-X. He, Y. Li, B.-B. Ma, Z. Ke, F.-S. Liu, Sterically encumbered tetraarylimidazolium carbene Pd-PEPPSI complexes: highly efficient direct arylation of imidazoles with aryl bromides under aerobic conditions, Organometallics 35 (16) (2016) 2655–2663.
[39] S. Karthik, T. Gandhi, Palladium (II)/N-heterocyclic carbene-catalyzed direct C–H acylation of heteroarenes with N-acylsaccharins, Org. Lett. 19 (19) (2017) 5486–5489.
[40] R.D. Froese, J. Lombardi C, M. Pompeo, RP. Rucker, Organ MG, Acc. Chem. Res 50 (2017) 2244.
[41] H. Li, R. Maitra, Y. Kuo, J. Chen, C. Hu, H.M. Lee, A tridentate CNO-donor palladium (II) complex as efficient catalyst for direct C–H arylation: Application in preparation of imidazole-based push–pull chromophores, Appl. Organomet. Chem. 32 (1) (2018) e3956.
[42] W. Chen, J. Yang, Synthesis of N-heterocyclic carbene-PdCl-[(2-Pyridyl) alkyl carboxylate] complexes and their catalytic activities towards arylation of (benzo) oxazoles with aryl bromides, J. Organomet. Chem. 872 (2018) 24–30.
[43] E.J. Yoo, S. Ma, T.-S. Mei, K.S.L. Chan, J.-Q. Yu, Pd-catalyzed intermolecular C–H amination with alkylamines, J. Am. Chem. Soc. 133 (20) (2011) 7652–7655.
[44] C. Valente, S. Baglione, D. Candito, C. J. O. Brien, and M. G. Organ, "High yielding alkylations of unactivated sp 3 and sp 2 centres with alkyl- 9-BBN reagents using an NHC-based catalyst : Pd-PEPPSI-IPr {," no. entry 8, pp. 735–737, 2008, doi:10.1039/b715081d.
[45] D. Alberico, M. E. Scott, and M. Lautens, "Aryl – aryl bond formation by transition-metal-catalyzed direct arylation," pp. 174–238, 2007.
[46] H. Review, "Catalytic direct arylation of heteroaromatic compounds," vol. 36, no. 2, pp. 200–205, 2007, doi:10.1246/cl.2007.200.
[47] J. Roger, A. L. Gottumukkala, and H. Doucet, "Palladium-catalyzed C3 or C4 direct arylation of heteroaromatic compounds with aryl halides by C À H bond activation," pp. 20–40, 2010, doi:10.1002/cctc.200900074.
[48] C. B. Bheeter, L. Chen, J. Soulé, and H. Doucet, "Catalysis science & technology arylation of 5-membered ring heteroaromatics," pp. 2005–2049, 2016, doi:10.4225/23/5ad043ff9a033.
[49] I.J.B. Lin, C.S. Vasam, Preparation and application of N-heterocyclic carbene complexes of Ag(I), Coord. Chem. Rev. 251 (5–6) (2007) 642–670, doi:10.1016/j.ccr.2006.09.004.
[50] C.J. O'Brien, et al., Cover picture: easily prepared air-and moisture-stable Pd–NHC (NHC= N-heterocyclic carbene) complexes: a reliable, user-friendly, highly active palladium precatalyst for the Suzuki–Miyaura reaction/a user-friendly, all-purpose Pd–NHC (NHC= N-heterocyclic carbene) precatalyst for the negishi reaction: a step towards a universal cross-coupling catalyst (Chem. Eur. J. 18/2006),", Chem. –Eur. J. 12 (18) (2006) 4711.
[51] S. Cie, X-area (version 1.18) and X-red32 (version 1.04)," *Darmstadt*, Germany (2002).
[52] L. Palatinus, G. Chapuis, SUPERFLIP–a computer program for the solution of crystal structures by charge flipping in arbitrary dimensions, J. Appl. Crystallogr. 40 (4) (2007) 786–790.

[53] D. Kratzert, J.J. Holstein, I. Krossing, DSR: enhanced modelling and refinement of disordered structures with SHELXL, J. Appl. Crystallogr. 48 (3) (2015) 933–938.
[54] O.V Dolomanov, L.J. Bourhis, R.J. Gildea, J. a. K. Howard and H. Puschmann, J. Appl. Crystallogr 42 (2009) 339–341.
[55] R.A. Gaussian09, 1, mj frisch, gw trucks, hb schlegel, ge scuseria, ma robb, jr cheeseman, g. Scalmani, v. Barone, b. Mennucci, ga petersson et al., gaussian,, Inc., Wallingford CT 121 (2009) 150–166.
[56] P.C. Hariharan, J.A. Pople, The influence of polarization functions on molecular orbital hydrogenation energies, Theor. Chim. Acta 28 (3) (1973) 213–222.
[57] A.D. Becke, Density-functional exchange-energy approximation with correct asymptotic behavior, Phys. Rev. A 38 (6) (1988) 3098.
[58] P.J. Hay, W.R. Wadt, Ab initio effective core potentials for molecular calculations. Potentials for the transition metal atoms Sc to Hg, J. Chem. Phys. 82 (1) (1985) 270–283.
[59] A.D. McLean, G.S. Chandler, Contracted Gaussian basis sets for molecular calculations. I. Second row atoms, Z= 11–18, J. Chem. Phys. 72 (10) (1980) 5639–5648.
[60] J. Tirado-Rives, W.L. Jorgensen, Performance of B3LYP density functional methods for a large set of organic molecules, J. Chem. Theory Comput. 4 (2) (2008) 297–306.
[61] I.A. Khodja, H. Boulebd, C. Bensouici, A. Belfaitah, Design, synthesis, biological evaluation, molecular docking, DFT calculations and in silico ADME analysis of (benz) imidazole-hydrazone derivatives as promising antioxidant, antifungal, and anti-acetylcholinesterase agents, J. Mol. Struct. 1218 (2020) 128527.
[62] I.A. Khodja, H. Boulebd, Synthesis, biological evaluation, theoretical investigations, docking study and ADME parameters of some 1, 4-bisphenylhydrazone derivatives as potent antioxidant agents and acetylcholinesterase inhibitors, Mol. Divers. 25 (1) (2021) 279–290.
[63] I.K. Rhee, M. van de Meent, K. Ingkaninan, R. Verpoorte, Screening for acetylcholinesterase inhibitors from Amaryllidaceae using silica gel thin-layer chromatography in combination with bioactivity staining, J. Chromatogr. A 915 (1–2) (2001) 217–223.
[64] G.L. Ellman, K.D. Courtney, V. Andres Jr, R.M. Featherstone, A new and rapid colorimetric determination of acetylcholinesterase activity, Biochem. Pharmacol. 7 (2) (1961) 88–95.
[65] M. Harel, et al., Quaternary ligand binding to aromatic residues in the active-site gorge of acetylcholinesterase, Proc. Natl. Acad. Sci. 90 (19) (1993) 9031–9035.
[66] F. Nachon, et al., Crystal structures of human cholinesterases in complex with huprine W and tacrine: elements of specificity for anti-Alzheimer's drugs targeting acetyl-and butyryl-cholinesterase, Biochem. J. 453 (3) (2013) 393–399.
[67] O. Trott, A.J. Olson, AutoDock Vina: improving the speed and accuracy of docking with a new scoring function, efficient optimization, and multithreading, J. Comput. Chem. 31 (2) (2010) 455–461.
[68] M. Kaloğlu, İ. Özdemir, Palladium (II)-N-heterocyclic carbene complexes: efficient catalysts for the direct C-H bond arylation of furans with aryl halides, Appl. Organomet. Chem. 32 (7) (2018) e4399.
[69] H.A. Chiong, O. Daugulis, Palladium-catalyzed arylation of electron-rich heterocycles with aryl chlorides, Org. Lett. 9 (8) (2007) 1449–1451.
[70] İ. Özdemir, et al., Useful ligands for the palladium-catalysed direct C5 arylation of heteroaromatics with aryl bromides or electron-deficient aryl chlorides, Eur. J. Inorg. Chem 12 (2010) 1798.
[71] L. Yang, D.R. Powell, R.P. Houser, Structural variation in copper (I) complexes with pyridylmethylamide ligands: structural analysis with a new four-coordinate geometry index, τ 4, Dalton Trans. (9) (2007) 955–964.
[72] A. Okuniewski, D. Rosiak, J. Chojnacki, B. Becker, Coordination polymers and molecular structures among complexes of mercury (II) halides with selected 1-benzoylthioureas, Polyhedron 90 (2015) 47–57.
[73] B. Cordero, et al., Covalent radii revisited, Dalton Trans. (21) (2008) 2832–2838.
[74] Y. Han, H.V. Huynh, G.K. Tan, Syntheses and characterizations of Pd (II) complexes incorporating a N-heterocyclic carbene and aromatic N-heterocycles, Organometallics 26 (25) (2007) 6447–6452.
[75] H.V. Huynh, W. Sim, C.F. Chin, [2]Rotaxanes with Palladium (II)-NHC stoppers, Dalton Trans. 40 (44) (2011) 11690–11692.
[76] Y.-C. Lin, et al., Efficient PEPPSI-themed palladium n-heterocyclic carbene precatalysts for the mizoroki–heck reaction, Organometallics 32 (14) (2013) 3859–3869.
[77] L. Barbu, M.M. Popa, S. Shova, M. Ferbinteanu, C. Draghici, F. Dumitrascu, New Pd-NHC PEPPSI complexes from benzimidazolium salts with a phenacyl group attached to N3, Inorg. Chim. Acta 463 (2017) 97–101.
[78] N. Kaloğlu, et al., Synthesis of N-heterocyclic carbene-palladium-PEPPSI complexes and their catalytic activity in the direct CH bond activation, J. Organomet. Chem. 867 (2018) 404–412.
[79] M. Kaloğlu, N. Kaloğlu, İ. Yıldırım, N. Özdemir, İ. Özdemir, Palladium-carbene catalyzed direct arylation of five-membered heteroaromatics, J. Mol. Struct. 1206 (2020) 127668.
[80] M. Kaloğlu, N. Gürbüz, İ. Yıldırım, N. Özdemir, İ. Özdemir, Well-defined PEPPSI-themed palladium–NHC complexes: synthesis, and catalytic application in the direct arylation of heteroarenes, Appl. Organomet. Chem. 34 (2) (2020) e5387.
[81] A. Nataraj, V. Balachandran, T. Karthick, Molecular structure, vibrational spectra, first hyperpolarizability and HOMO–LUMO analysis of p-acetylbenzonitrile using quantum chemical calculation, J. Mol. Struct. 1038 (2013) 134–144.
[82] H. Boulebd, Y.D. Lahneche, I.A. Khodja, M. Benslimane, A. Belfaitah, New Schiff bases derived from benzimidazole as efficient mercury-complexing agents in aqueous medium, J. Mol. Struct. 1196 (2019) 58–65.
[83] H. Boulebd, Structure-activity relationship of antioxidant prenylated (iso) flavonoid-type compounds: quantum chemistry and molecular docking studies, J. Biomol. Struct. Dyn. (2021) 1–10.
[84] M. Kumar, M. Kariem, H.N. Sheikh, A. Frontera, S.K. Seth, A.K. Jassal, A series of 3D lanthanide coordination polymers decorated with a rigid 3, 5-pyridinedicarboxylic acid linker: syntheses, structural diversity, DFT study, Hirshfeld surface analysis, luminescence and magnetic properties, Dalton Trans. 47 (35) (2018) 12318–12336.
[85] Y.-Y. Cai, L.-Y. Xu, L.-Q. Chai, Y.-X. Li, Synthesis, crystal structure, TD/DFT calculations and Hirshfeld surface analysis of 1-(4-((Benzo) dioxol-5-ylmethyleneamino) phenyl) ethanone oxime, J. Mol. Struct. 1204 (2020) 127552.
[86] H. Boulebd, Are thymol, rosefuran, terpinolene and umbelliferone good scavengers of peroxyl radicals? Phytochemistry 184 (2021) 112670.
[87] H. Boulebd, Theoretical insights into the antioxidant activity of moracin T, Free Radic. Res. 54 (4) (2020) 221–230.
[88] A.E. Sandeli, N. Khiri-meribout, S. Benzerka, N. Gürbüz, Silver (I) - N -heterocyclic carbene complexes : Synthesis and characterization, biological evaluation of Anti-Cholinesterase, anti-alpha-amylase, anti-lipase, and antibacterial activities, and molecular docking study, Inorg. Chim. Acta 525 (2021) 120486.
[89] E. David, C. Rangheard, S. Pellet-Rostaing, M. Lemaire, Synthesis of benz [c] benzothiopheno [2, 3-e] azepines via heck-type coupling and pictet-spengler reaction, Synlett 2006 (13) (2006) 2016–2020.
[90] E.O. Karaca, et al., Palladium complexes with tetrahydropyrimidin-2-ylidene ligands: catalytic activity for the direct arylation of furan, thiophene, and thiazole derivatives, Organometallics 34 (11) (2015) 2487–2493.
[91] E. David, S. Pellet-Rostaing, M. Lemaire, Heck-like coupling and Pictet–Spengler reaction for the synthesis of benzothieno [3, 2-c] quinolines, Tetrahedron 63 (36) (2007) 8999–9006.